

Progress in Molecular and Subcellular Biology
Marine Molecular Biotechnology

Werner E.G. Müller
Heinz C. Schröder
Xiaohong Wang *Editors*

Blue Biotechnology

From Gene to Bioactive Product

 Springer

Progress in Molecular and Subcellular Biology

Marine Molecular Biotechnology

Volume 55

Series editor

Werner E.G. Müller, Mainz, Germany

More information about this series at <http://www.springer.com/series/7234>

Werner E.G. Müller · Heinz C. Schröder
Xiaohong Wang
Editors

Blue Biotechnology

From Gene to Bioactive Product

 Springer

Editors

Werner E.G. Müller
ERC Advanced Investigator Group, Institute
for Physiological Chemistry
University Medical Center of the Johannes
Gutenberg-University Mainz
Mainz
Germany

Xiaohong Wang
ERC Advanced Investigator Group, Institute
for Physiological Chemistry
University Medical Center of the Johannes
Gutenberg-University Mainz
Mainz
Germany

Heinz C. Schröder
ERC Advanced Investigator Group, Institute
for Physiological Chemistry
University Medical Center of the Johannes
Gutenberg-University Mainz
Mainz
Germany

ISSN 0079-6484 ISSN 2197-8484 (electronic)
Progress in Molecular and Subcellular Biology
ISSN 1611-6119
Marine Molecular Biotechnology
ISBN 978-3-319-51282-2 ISBN 978-3-319-51284-6 (eBook)
DOI 10.1007/978-3-319-51284-6

Library of Congress Control Number: 2016961268

© Springer International Publishing AG 2017

This work is subject to copyright. All rights are reserved by the Publisher, whether the whole or part of the material is concerned, specifically the rights of translation, reprinting, reuse of illustrations, recitation, broadcasting, reproduction on microfilms or in any other physical way, and transmission or information storage and retrieval, electronic adaptation, computer software, or by similar or dissimilar methodology now known or hereafter developed.

The use of general descriptive names, registered names, trademarks, service marks, etc. in this publication does not imply, even in the absence of a specific statement, that such names are exempt from the relevant protective laws and regulations and therefore free for general use.

The publisher, the authors and the editors are safe to assume that the advice and information in this book are believed to be true and accurate at the date of publication. Neither the publisher nor the authors or the editors give a warranty, express or implied, with respect to the material contained herein or for any errors or omissions that may have been made. The publisher remains neutral with regard to jurisdictional claims in published maps and institutional affiliations.

Printed on acid-free paper

This Springer imprint is published by Springer Nature
The registered company is Springer International Publishing AG
The registered company address is: Gewerbestrasse 11, 6330 Cham, Switzerland

Preface

Marine invertebrates like sponges and sponge-associated microorganisms are some of the richest sources of novel bioactive molecules and lead compounds for therapeutical and biotechnological applications. However, the sustainable exploitation of marine natural products is limited due to the supply problem. The only likely way to tackle this problem is to isolate and express the genes encoding the enzymes/proteins involved in biosynthesis of these products to obtain the active molecules in sufficient amounts. The aim of this book is to describe new approaches combining the present knowledge in marine genomics and advanced natural products chemistry for the sustainable production of novel secondary metabolites (lead compounds), as well as pharmacologically active peptides/proteins, with antimicrobial, neuroprotective, anti-osteoporotic, anti-protozoan/anti-plasmodial, anti-ageing and immune-modulating activities, using molecular-biology-based approaches and advanced chemical techniques, to obtain and to select candidate compounds for pre-clinical and clinical studies. The authors of this book include European or worldwide leaders in marine genomics and marine natural product chemistry/structure elucidation, as well as leading researchers from high-tech enterprises with special interest in biotechnology and bringing marine biotechnology products to the market. This book also comprises chapters describing the discovery and sustainable exploitation of molecules from hitherto unexploited extreme marine environments, advanced biosynthetic prediction techniques and methods in computer-aided drug discovery, combinatorial biosynthesis methods, as well as strategies in drug discovery and development of marine-derived compounds of biomedical and biotechnological interest. This book also summarizes main results of the European Union Framework Programme FP7 project “BlueGenics—From gene to bioactive product: Exploiting marine genomics for an innovative and sustainable European blue biotechnology industry” (project No. 311848; 2012–2016); Fig. 1. Our intention is to demonstrate that the application of innovative

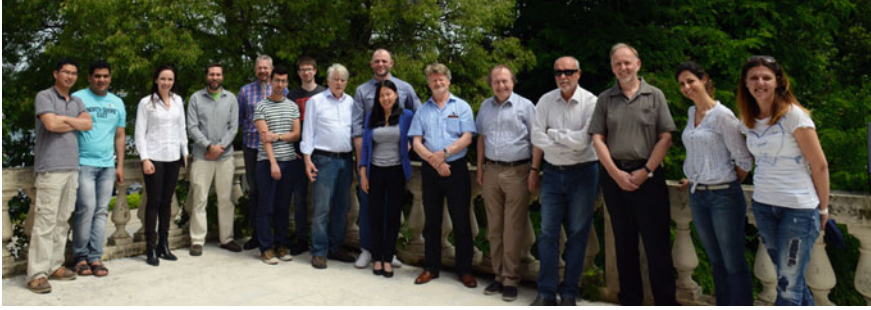


Fig. 1 Group photo of the European Union FP7 project “BlueGenics” team during the summer school 2016 in Rovinj, Croatia

molecular biological approaches is the only way to sustainably exploit the enormous economic potential of the marine molecular biodiversity—for the future of blue biotechnology industry and human benefit.

Mainz, Germany

Werner E.G. Müller
Heinz C. Schröder
Xiaohong Wang

Contents

35 Years of Marine Natural Product Research in Sweden: Cool Molecules and Models from Cold Waters	1
Lars Bohlin, Paco Cárdenas, Anders Backlund and Ulf Göransson	
Major Antimicrobial Representatives from Marine Sponges and/or Their Associated Bacteria	35
Fei He, Linh H. Mai, Johan Gardères, Amjad Hussain, Vesna Erakovic Haber and Marie-Lise Bourguet-Kondracki	
Discovery and Development of Novel Drugs	91
Vesna Erakovic Haber and Radan Spaventi	
Computer-Aided Drug Discovery from Marine Compounds: Identification of the Three-Dimensional Structural Features Responsible for Antimalarial Activity	105
Caterina Fattorusso, Francesca Rondinelli, Marco Persico, Nausicaa Orteca and Antonio Di Dato	
Bluegenics: Bioactive Natural Products of Medicinal Relevance and Approaches to Their Diversification	159
Joseph S. Zarins-Tutt, Emily R. Abraham, Christopher S. Bailey and Rebecca J.M. Goss	
New Target Sites for Treatment of Osteoporosis	187
Werner E.G. Müller, Xiaohong Wang and Heinz C. Schröder	
Biocalcite and Carbonic Acid Activators	221
Xiaohong Wang, Meik Neufurth, Emad Tolba, Shunfeng Wang, Heinz C. Schröder and Werner E.G. Müller	

Electrospinning of Bioactive Wound-Healing Nets 259
Heinz C. Schröder, Emad Tolba, Bärbel Diehl-Seifert, Xiaohong Wang
and Werner E.G. Müller

**Entotheonella Bacteria as Source of Sponge-Derived Natural
Products: Opportunities for Biotechnological Production 291**
Agneya Bhushan, Eike E. Peters and Jörn Piel

Contributors

Emily R. Abraham School of Chemistry, University of St Andrews, St Andrews, Scotland, UK

Anders Backlund Division of Pharmacognosy, Department of Medicinal Chemistry, Biomedical Center, Uppsala University, Uppsala, Sweden

Christopher S. Bailey School of Chemistry, University of St Andrews, St Andrews, Scotland, UK

Agneya Bhushan Institute of Microbiology, Eidgenössische Technische Hochschule (ETH) Zurich, Zurich, Switzerland

Lars Bohlin Division of Pharmacognosy, Department of Medicinal Chemistry, Biomedical Center, Uppsala University, Uppsala, Sweden

Marie-Lise Bourguet-Kondracki Laboratoire Molécules de Communication et Adaptation des Micro-organismes, UMR 7245 MNHN-CNRS, Muséum National d'Histoire Naturelle, Paris, France

Paco Cárdenas Division of Pharmacognosy, Department of Medicinal Chemistry, Biomedical Center, Uppsala University, Uppsala, Sweden

Antonio Di Dato Department of Pharmacy, University of Napoli “Federico II”, Naples, Italy

Bärbel Diehl-Seifert ERC Advanced Investigator Group, Institute for Physiological Chemistry, University Medical Center of the Johannes Gutenberg University, Mainz, Germany; NanotecMARIN GmbH, Mainz, Germany

Vesna Erakovic Haber Fidelta d.o.o., Zagreb, Croatia

Caterina Fattorusso Department of Pharmacy, University of Napoli “Federico II”, Naples, Italy

Johan Gardères Laboratoire Molécules de Communication et Adaptation des Micro-organismes, UMR 7245 MNHN-CNRS, Muséum National d'Histoire Naturelle, Paris, France

Rebecca J.M. Goss School of Chemistry, University of St Andrews, St Andrews, Scotland, UK

Ulf Göransson Division of Pharmacognosy, Department of Medicinal Chemistry, Biomedical Center, Uppsala University, Uppsala, Sweden

Fei He Laboratoire Molécules de Communication et Adaptation des Micro-organismes, UMR 7245 MNHN-CNRS, Muséum National d'Histoire Naturelle, Paris, France

Amjad Hussain Laboratoire Molécules de Communication et Adaptation des Micro-organismes, UMR 7245 MNHN-CNRS, Muséum National d'Histoire Naturelle, Paris, France

Linh H. Mai Laboratoire Molécules de Communication et Adaptation des Micro-organismes, UMR 7245 MNHN-CNRS, Muséum National d'Histoire Naturelle, Paris, France

Werner E.G. Müller ERC Advanced Investigator Group, Institute for Physiological Chemistry, University Medical Center of the Johannes Gutenberg University, Mainz, Germany; NanotecMARIN GmbH, Mainz, Germany

Meik Neufurth ERC Advanced Investigator Group, Institute for Physiological Chemistry, University Medical Center of the Johannes Gutenberg University, Mainz, Germany

Nausicaa Orteca Department of Pharmacy, University of Napoli "Federico II", Naples, Italy

Marco Persico Department of Pharmacy, University of Napoli "Federico II", Naples, Italy

Eike E. Peters Institute of Microbiology, Eidgenössische Technische Hochschule (ETH) Zurich, Zurich, Switzerland

Jörn Piel Institute of Microbiology, Eidgenössische Technische Hochschule (ETH) Zurich, Zurich, Switzerland

Francesca Rondinelli Department of Pharmacy, University of Napoli "Federico II", Naples, Italy

Heinz C. Schröder ERC Advanced Investigator Group, Institute for Physiological Chemistry, University Medical Center of the Johannes Gutenberg University, Mainz, Germany; NanotecMARIN GmbH, Mainz, Germany

Radan Spaventi Triadelta Partners d.o.o., Zagreb, Croatia

Emad Tolba ERC Advanced Investigator Group, Institute for Physiological Chemistry, University Medical Center of the Johannes Gutenberg University, Mainz, Germany

Shunfeng Wang ERC Advanced Investigator Group, Institute for Physiological Chemistry, University Medical Center of the Johannes Gutenberg University, Mainz, Germany

Xiaohong Wang ERC Advanced Investigator Group, Institute for Physiological Chemistry, University Medical Center of the Johannes Gutenberg University, Mainz, Germany; NanotecMARIN GmbH, Mainz, Germany

Joseph S. Zarins-Tutt School of Chemistry, University of St Andrews, St Andrews, Scotland, UK

35 Years of Marine Natural Product Research in Sweden: Cool Molecules and Models from Cold Waters

Lars Bohlin, Paco Cárdenas, Anders Backlund and Ulf Göransson

Abstract Currents efforts in marine biodiscovery have essentially focused on temperate to tropical shallow water organisms. With more than 6000 species of marine plants and animals, the Kosterfjord area has the richest marine biodiversity in Swedish waters, but it remains understudied. The overall objective of our marine pharmacognosy research is to explore and reveal the pharmacological potential of organisms from this poorly explored region. More generally, we wish to understand aspects of structure–activity relationships of chemical interactions in cold-water marine environment (shallow and deep). Our strategy is based on ecologically guided search for compounds through studies of physiology and organism interactions coupled to identification of bioactive molecules guided by especially *in vivo* assays. The research programme originated in the beginning of the 1980s with a broad screening of Swedish marine organisms using both *in vitro* and *in vivo* assays, resulting in isolation and identification of several different bioactive molecules. Two congenerous cyclopeptides, *i.e.* baretin and 8,9-dihydrobaretin, were isolated from the deep-sea sponge *Geodia barretti*, and structurally elucidated, guided by their antifouling activity and their affinity to a selection of human serotonin receptors. To optimize the activity a number of analogues of baretin were synthesized and tested for antifouling activity. Within the EU project BlueGenics, two larger homologous peptides, barrettides A and B, were isolated from *G. barretti*. Also, metabolic fingerprinting combined with sponge systematics was used to further study deep-sea natural product diversity in the genus *Geodia*. Finally, the chemical property space model ‘ChemGPS-NP’ has been developed and used in our research group, enabling a more efficient use of obtained compounds and exploration of possible biological activities and targets. Another approach is the broad application of phylogenetic frameworks, which can be used in prediction of where—in which organisms—to search for novel molecules or better sources of

L. Bohlin (✉) · P. Cárdenas · A. Backlund · U. Göransson (✉)
Division of Pharmacognosy, Department of Medicinal Chemistry,
Biomedical Center, Uppsala University, Box 574, 751 23 Uppsala, Sweden
e-mail: lars.bohlin@fkog.uu.se

U. Göransson
e-mail: ulf.goransson@fkog.uu.se

known molecules in marine organisms. In a further perspective, the deeper understanding of evolution and development of life on Earth can also provide answers to why marine organisms produce specific molecules.

1 Natural Product Research

Nature has for a long time been a source of cures against different diseases. Ethnopharmacological observations, that is observations of how people in different cultures have used plants to treat diseases, have been a major source of bioactive molecules subsequently developed into important drugs (Heinrich and Gibbons 2001). The discovery of morphine, quinine, vincristin and artemisinin are some examples that have revolutionized medicine. Fungi have also been of utmost importance for the development of antibiotics, with penicillin, cyclosporin, avermectin and cephalosporin as typical examples. Microorganisms have become more and more the focus of natural product research due to the development of cultivation techniques, but also due to the increasing use and development of molecular biology tools to discover the real producers of bioactive secondary metabolites (Demain and Sanchez 2009; Gerwick and Fenner 2013).

2 Marine Natural Product Research, a Field on the Rise

Historically, the marine environment has always been more difficult to access for humans and therefore limited knowledge of the use of marine organisms can be found in older literature. Instead, ecological and toxicological observations of terrestrial organisms have been and still are the starting points for many research projects. In comparison to the fields of chemistry and biology of terrestrial plants and microorganisms, marine natural product research is very young. Paul J. Scheuer (1915–2003) was one of the pioneers in the field, when he started serious marine natural product research only six decades ago, at the University of Hawaii at Manoa. Since then, more than 25,700 marine compounds have been discovered, and the field is steadily growing with 1378 new marine natural products in 459 papers for 2014 (there were only 332 new marine compounds reported in 1984) (Blunt et al. 2016). However, so far only a handful of marine compounds have been developed into commercial drugs. Recent examples are Prialt[®] (ω -conotoxin MVIIA), based on a toxic peptide isolated from a tropical snail of the genus *Conus*, and used against neuropathic pain; Yondelis[®] (ET-743/trabectedin), an anticancer drug resulting from research on the Caribbean tunicate *Ecteinascidia turbinata*, and Halaven[®] (eribulin), another anticancer drug derived from halichondrin B, originally isolated from the Japanese sponge *Halichondria okadai* (Molinski et al. 2009; Montaser and Luesch 2011; Newman and Cragg 2016).

3 Cold Waters, from the Shallow to the Deep

The field of marine pharmacognosy has mainly explored easily accessible shallow waters in tropical to temperate regions, where the marine biodiversity is the highest (Chaudhary et al. 2016; Leal et al. 2012) believing that this could lead to higher chemical diversity. In comparison, cold-water organisms have not attracted as much interest, at least not in the early days of this field. Cold waters include not only the boreoarctic waters but also the deep sea, from arctic to tropical regions, which offer a wide array of different habitats and a biodiversity still poorly known. Deep-sea ‘cold waters’ bring other parameters than temperature to take into account, such as depth, permeability for light (at different wavelengths), ice coverage, oxygen saturation depending on temperature in surface layers, and even the water currents distributing nutrients in the vertical sections. In recent years, we note an increasing number of studies on organisms from shallow European cold waters (e.g. from Norway, Spitsbergen, or even the Swedish West Coast) (Blunt et al. 2016) but the number of studies on deep-sea natural products is still very low. Less than 2% of over 25,700 marine natural products described these last 50 years come from deep-sea organisms, and a third of those have only been described these last years (Skropeta 2008; Skropeta and Wei 2014). Among these deep-sea organisms, we note that sponges, just like in shallow waters, represent the main source of new marine natural products (Skropeta 2008; Leal et al. 2012). Indeed, with 200 new sponge metabolites discovered each year and already more than 5300 reported (Ebada and Proksch 2012), sponges are unquestionably the leading source of new marine compounds. However, when we reviewed the cold-water sponge marine natural products from the boreoarctic Atlantic region (including Canada, Greenland, Iceland, Svalbard and Scandinavian waters), we found a meagre 48 compounds (not counting amino acids, fatty acids and sterols) in 27 species investigated (Table 2). These 48 compounds only represent 0.9% of all sponge compounds ever reported, while the 27 species may be compared with the 161 species from the Swedish coast, or even with the estimated 305 species living in Norwegian waters (www.artsdatabanken.no, Norwegian Biodiversity Information Centre, accessed 28-07-2016). Of the 27 species studies, more than half (16) were from the deep sea (>100 m depth). We believe these numbers illustrate how neglected cold waters still are in the field of marine pharmacognosy, but also how much remains to be explored and discovered.

4 Swedish Cold Waters

Sweden is entirely situated north of latitude 55°, and has a 3218 km long coastline with a climate changing rather dramatically during the different seasons of the year. Because the Baltic Sea is essentially brackish water (salinity of 5–15‰), the only true marine environment (with a salinity of 30–35‰) can be found on the West Coast of Sweden, and includes two areas: the Skagerrak strait, which is linked to

the North Sea and Norwegian Sea, and the Kattegat (between Sweden and Denmark) linked to the Baltic Sea. The fieldwork and material described in this chapter originate from the north-eastern part of the Skagerrak: the Kosterfjord area ($58^{\circ}58'–58^{\circ}43'N$). With more than 6000 species of marine plants and animals, the Kosterfjord area has the richest marine biodiversity in Swedish waters (which is one reason why this area has now been declared a marine national park). One reason for this high biodiversity lies in the deepest parts of the Kosterfjord, a deep and narrow trench (up to 247 m deep) known as Kosterrännan (Fig. 1). This deep environment is connected to the deep Norwegian trench, and is characterized by strong currents, absence of light in its deepest parts, high salinity (34–35‰) and low temperatures (5–7 °C). These conditions attract a typical deep-sea oceanic fauna. The latest marine inventory by the Swedish Taxonomy Initiative (2006–2009) recorded a total



Fig. 1 Map over the Kosterfjord area showing the deep-water trench connecting the Kosterrännan with Atlantic deep-water areas. Map made by Hans Sjögren and used with his permission. The red dot indicates the position of the Tjärnö Marine Biological Laboratory

Table 1 Ranking of the five main producers of new marine natural products worldwide (Leal et al. 2012) along with the diversity of these main producers in Swedish waters

Ranking	Phyla	Number of species recorded in Sweden	New species for Sweden since 2004
1	Porifera	161	3
2	Cnidaria	240	7
3	Echinodermata	82	3
4	Chordata (subphyla Tunicata)	63	0
5	Mollusca	720	4

Source www.dyntaxa.se, accessed on 28-07-2016

of 1203 invertebrates of which 30 species were new to science and an additional 43 new to Sweden (Table 1) (Karlsson et al. 2014). Swedish marine waters also host 1084 species of macroalgae and many more unicellular algae (www.dyntaxa.se, Swedish Taxonomic Database, accessed 28-07-2016). Only a handful of these cold-water marine macroorganisms have been investigated for natural products and bioactivity (Table 2).

5 The Emergence of Marine Pharmacognosy in Sweden

The long history of marine biology in Sweden is tightly linked to the marine stations along the Swedish coastline. However, in the beginning of 1980s none of this research was focusing on chemistry and pharmacology of Swedish marine organisms. Based on a postdoctorate experience in the USA, one of the authors (LB) decided to start in 1981 a research programme in Sweden named ‘Marine Pharmacognosy’. Contact was taken with the Director of Tjärnö Marine Biological Laboratory, situated strategically by the Kosterfjord (Figs. 1 and 2). The researchers in this modern marine station had access to a unique marine flora and fauna and a long experience of the biology of the marine organisms in cold waters.

The aim of our studies was to evaluate the potential for isolation of novel pharmacologically active natural products from a selection of marine organisms collected in the Kosterfjord, guided by several *in vivo* and *in vitro* bioassays. No ethnopharmacological data existed for any of these marine organisms and only limited toxicological data was known, e.g. for the well-known lion’s mane jellyfish *Cyanea capillata*. However, ecological observations helped to select some species, for example the ability of some sponges to avoid overgrowth of settling organisms. In the end, the main criteria for collection were (i) the availability of the organisms and (ii) sampling organisms from different phyla: red and brown algae, bryozoans, echinoderms, soft corals, polychaetes, bivalves, brachiopods, tunicates and sponges. The collection was performed using scuba diving down to 25 m (Fig. 2b) and, at larger depths, using a dredge towed after a research vessel.

Table 2 A review of cold-water sponge natural products in the Atlantic boreoarctic region: Canada, Greenland, Iceland, Svalbard and Scandinavian waters

Order	Species	Locality (shallow, S, deep, D)	Extraction solvent(s) (References)	Compound (compound family)	Bioactivities (References)
Homosclerophorida	<i>Plakortis</i> sp.	Norway (D)	1:1 MeOH/DCM (Holzwarth et al. 2005)	Cyclic peroxide 2	No antitumoral activity (Holzwarth et al. 2005)
Verongida	<i>Hexadella debritifera</i>	Norway, Svalbard (D)	1:1 MeOH/DCM (Holzwarth et al. 2005) 1:1 MeOH/DCM (Hanssen et al. 2012), Ethanol (Cárdenas 2016), Acetonitrile 60% (Cárdenas 2016)	Cyclic peroxide 3 Ianthelline (bromotyrosine derivative)	Antitumoral (Holzwarth et al. 2005) Antitumoral (Hanssen et al. 2012) Antifouling (Hanssen et al. 2014)
Dictyoceratida	<i>Dysidea fragilis</i>	France (S)	DCM (Amade et al. 1982)	–	Antibacterial (Amade et al. 1982), Antifungal (Amade et al. 1982)
			Ethanol (Amade et al. 1982)	–	No antibacterial/antifungal activity (Amade et al. 1982)
Haplosclerida	<i>Haliciona (Rhizotera) viscosa</i>	Svalbard (S)	100% MeOH + 1:1 MeOH/DCM + 100% DCM (Lippert et al. 2003)	–	Antibacterial (Lippert et al. 2003)
			1:1 MeOH/DCM + 100% DCM (Köck et al. 2013)	Halclamines C-H (3-alkylpiperidine)	Antibacterial (Köck et al. 2013)
			1:1 MeOH/DCM (Köck et al. 2013)	Halicyclic C, F (3-alkylpyridinium)	–
			?	Cyclostellamine C (3-alkylpyridinium)	–
			1:1 MeOH/DCM (Köck et al. 2013)	Viscosamine (3-alkylpyridinium)	–
			1:1 MeOH/DCM (Köck et al. 2013)	Viscosalines C, B, E (3-alkylpyridinium)	–

(continued)

Table 2 (continued)

Order	Species	Locality (shallow, S, deep, D)	Extraction solvent(s) (References)	Compound (compound family)	Bioactivities (References)
	<i>Haliclona</i> (<i>Rhizotiera</i>) <i>rosea</i>	S/valhard (S)	100% MeOH + 1:1 MeOH/DCM + 100% DCM (Lippert et al. 2003)	–	No antibacterial activity (Lippert et al. 2003)
		Norway (S)	Acetonitrile 60% (Tadesse et al. 2008)	–	Antibacterial/antifungal activity (Tadesse et al. 2008)
	<i>Haliclona</i> sp.	Norway (D)	1/8 trimethylchlorosilane/MeOH (Thiel et al. 2002)	Fatty acids composition (Thiel et al. 2002)	–
	<i>Haliclona</i> sp. 1	Norway (S)	Acetonitrile 60% (Tadesse et al. 2008)	–	Antibacterial/antifungal activity (Tadesse et al. 2008)
	<i>Haliclona</i> sp. 2	Norway (S)	Acetonitrile 60% (Tadesse et al. 2008)	–	Antibacterial/antifungal activity (Tadesse et al. 2008)
	<i>Petrosia crassa</i>	Norway (D)	1/8 trimethylchlorosilane/MeOH (Thiel et al. 2002)	Fatty acids composition (Thiel et al. 2002)	–
	<i>Hemigellius arcofer</i>	Off Labrador (D)	Acetone (Kingston et al. 1979)	Sterols (Kingston et al. 1979)	–
Tetractinellida	<i>Geodia barretti</i>	Sweden (D)	H ₂ O, petroleum ether, chloroform, MeOH (Andersson et al. 1983)	–	Hippocratic screening (Andersson et al. 1983) Guinea-pig ileum activity (Andersson et al. 1983) Antibacterial, antiviral (Andersson et al. 1983)
			H ₂ O (Andersson et al. 1986)	–	No lectin-like activity (Andersson et al. 1986)

(continued)

Table 2 (continued)

Order	Species	Locality (shallow, S, deep, D)	Extraction solvent(s) (References)	Compound (compound family)	Bioactivities (References)
		Sweden, Norway (D)	MeOH (Lidgren et al. 1986) Acetone (Sölter et al. 2002) Ethanol 50% (Sjögren et al. 2004b) H ₂ O + MeOH/DCM (Lind et al. 2013)	Baretin (diketopiperazine)	Antifouling (Sjögren et al. 2004b) Selective 5-HT ligands (Hedner et al. 2006) Antioxidant (Lind et al. 2013) Anti-inflammatory (Lind et al. 2013, 2015) No antitumoral activity (Lind et al. 2013) Inhibitor of electric eel acetylcholinesterase (Olsen et al. 2016a)
			Ethanol 50% (Sjögren et al. 2004b) H ₂ O + MeOH/DCM (Olsen et al. 2016a)	8,9-dihydrobaretin (diketopiperazine)	Antifouling (Sjögren et al. 2004b) Selective 5-HT ligands (Hedner et al. 2006) Inhibitor of electric eel acetylcholinesterase (Olsen et al. 2016a)
			Acetonitrile 15% (Hedner et al. 2008)	Bromobenzisoxalone (diketopiperazine)	Antifouling (Hedner et al. 2008)
			Ethanol (Lidgren et al. 1988)	3-methylcytidine, 3-methyl-2'-deoxycytidine, 3-methyl-2'-deoxyuridine (nucleosides)	Contractile activity (Lidgren et al. 1988) (3-mCyd, 3-mdCyd) No contractile activity (Lidgren et al. 1988) (3-mdUrd)
			Ethanol (Lidgren et al. 1988)	Histamine (histidine derivative)	Contractile activity (Lidgren et al. 1988)

(continued)

Table 2 (continued)

Order	Species	Locality (shallow, S, deep, D)	Extraction solvent(s) (References)	Compound (compound family)	Bioactivities (References)
			Acetonitrile (Carstens et al. 2015)	Barrettides A-B (peptides)	Antifouling (Carstens et al. 2015) No antibacterial activity (Carstens et al. 2015)
		Norway (D)	Acetonitrile 60% (Tadesse et al. 2008)	–	Antibacterial/antifungal activity (Tadesse et al. 2008)
			H ₂ O + MeOH/DCM (Olsen et al. 2016a)	6-bromoconicamin (indole)	Inhibitor of electric eel acetylcholinesterase (Olsen et al. 2016a)
			H ₂ O + MeOH/DCM (Olsen et al. 2016a)	Compound#4 (indole)	No inhibition of electric eel acetylcholinesterase (Olsen et al. 2016a)
			H ₂ O + MeOH/DCM (Olsen et al. 2016a)	2-O-acetyl-1-O-hexadecylglycero-3-phosphocholine	Anitumoral (Olsen et al. 2016a)
		Faroe Islands (D)	0.05 N HCl (Hougaard et al. 1991)	Free amino acids	–
		Faroe Islands, Sweden (D)	Ethyl acetate (Hougaard et al. 1991)	Sterols	–
		Norway (D)	1/8 trimethylchlorosilane/MeOH (Thiel et al. 2002)	Fatty acids composition (Thiel et al. 2002)	–
	<i>Geodia macandrewii</i>	Norway (D)	H ₂ O + MeOH/DCM (Olsen et al. 2016a)	Geodiataurine (fatty acid amide)	Anitumoral (Olsen et al. 2016a)
			H ₂ O + MeOH/DCM (Olsen et al. 2016a)	Barettin (diketopiperazine)	Cf. above
			H ₂ O + MeOH/DCM (Olsen et al. 2016a)	8,9-dihydrobarettin (diketopiperazine)	Cf. above

(continued)

Table 2 (continued)

Order	Species	Locality (shallow, S, deep, D)	Extraction solvent(s) (References)	Compound (compound family)	Bioactivities (References)
		Faroe Islands (D)	0.05 N HCl (Hougaard et al. 1991)	Free amino acids	–
			Ethyl acetate (Hougaard et al. 1991)	Sterols	–
		Off Labrador (D)	Acetone (Kingston et al. 1979)	Sterols	–
	<i>Geodia atlantica</i>	Faroe Islands (D)	0.05 N HCl (Hougaard et al. 1991)	Free amino acids	–
			Ethyl acetate (Hougaard et al. 1991)	Sterols	–
	<i>Geodia phlegraei</i>	Faroe Islands (D)	0.05 N HCl (Hougaard et al. 1991)	Free amino acids	–
			Ethyl acetate (Hougaard et al. 1991)	Sterols	–
	<i>Stryphnus fortis</i>	Faroe Islands (D)	0.05 N HCl (Hougaard et al. 1991)	Free amino acids	–
			Ethyl acetate (Hougaard et al. 1991)	Sterols	–
Polymastida	<i>Polymastia boletiformis</i>	Norway (S)	MeOH (Kong and Andersen 1993, 1996)	Polymastiamides A-F (Steroid amino-acid conjugate)	Antibacterial/antifungal activity (Kong and Andersen 1993)
	<i>Polymastia</i> sp.	Norway (S)	Acetonitrile 60% (Tadesse et al. 2008)	–	Antibacterial/antifungal activity (Tadesse et al. 2008)
Clionaida	<i>Cliona celata</i>	France (S)	DCM (Amade et al. 1982)	–	Antifungal (Lippert et al. 2003), no antibacterial activity (Amade et al. 1982)

(continued)

Table 2 (continued)

Order	Species	Locality (shallow, S, deep, D)	Extraction solvent(s) (References)	Compound (compound family)	Bioactivities (References)
			Ethanol (Amade et al. 1982)	–	No antibacterial/anti-fungal activity (Amade et al. 1982)
Suberitida	<i>Pseudosuberites</i> aff. <i>hyalinus</i>	Faroe Islands (D)	1:10 MeOH/DCM (Rasmussen et al. 1993)	6-bromoindolyl-3-acetonitrile	–
			1:10 MeOH/DCM (Rasmussen et al. 1993)	6-bromoindolyl-3-acetamide	–
			1:10 MeOH/DCM (Rasmussen et al. 1993)	6-bromoindolyl-3-acetate	–
			1:10 MeOH/DCM (Rasmussen et al. 1993)	6-bromoindolyl-3-carboxylic	–
			1:10 MeOH/DCM (Rasmussen et al. 1993)	6-bromoindolyl-3-carbaldehyde	–
	<i>Suberites ficus</i>	Svalbard (S)	1:1 MeOH/DCM (Lippert et al. 2003)	–	No antibacterial activity (Lippert et al. 2003)
	<i>Halichondria</i> (<i>Halichondria</i>) <i>panicea</i>	Sweden (S)	H ₂ O, petroleum ether, chloroform, MeOH (Andersson et al. 1983)	–	Hippocratic screening (Andersson et al. 1983) Guinea-pig ileum activity (H ₂ O extract) (Andersson et al. 1983) No antibacterial/anti-viral activity (Andersson et al. 1983)
			H ₂ O (Andersson et al. 1986)	–	Weak lectin-like activity (Andersson et al. 1986)

(continued)

Table 2 (continued)

Order	Species	Locality (shallow, S, deep, D)	Extraction solvent(s) (References)	Compound (compound family)	Bioactivities (References)
	<i>Halichondria (Halichondria) bowerbanki</i>	Sweden (S)	H ₂ O, petroleum ether, chloroform, MeOH (Andersson et al. 1983)	–	Hippocratic screening (Andersson et al. 1983) Guinea-pig ileum activity (all extracts) (Andersson et al. 1983) No antibacterial/anti viral activity (Andersson et al. 1983)
	<i>Halichondria (Halichondria) genitrix</i>	Svalbard (S)	1:1 MeOH/DCM (Lippert et al. 2003)	–	No antibacterial activity (Lippert et al. 2003)
		Norway (D)	1/8 trimethylchlorosilane/methanol (Blumenberg and Michaelis 2007)	Fatty acids composition (Blumenberg and Michaelis 2007)	–
Bubarida	<i>Phakellia ventilabrum</i>	Sweden (D)	H ₂ O, petroleum ether, chloroform, MeOH (Andersson et al. 1983)	–	Hippocratic screening (Andersson et al. 1983) Guinea-pig ileum activity (H ₂ O, methanol) (Andersson et al. 1983) antibacterial activity (Andersson est al. 1983)
			H ₂ O (Andersson et al. 1986)	–	No lectin-like activity (Andersson et al. 1986)
		France (D)	C ₆ H ₁₂ (Amade et al. 1982)	–	Antibacterial/Antifunga (Amade et al. 1982)
			–	Sesquiterpene isonitrile	Antibacterial/Antifungal (Amade et al. 1982)

(continued)

Table 2 (continued)

Order	Species	Locality (shallow, S, deep, D)	Extraction solvent(s) (References)	Compound (compound family)	Bioactivities (References)
			Ethanol (Amade et al. 1982)	–	No antibacterial/antifungal activity (Amade et al. 1982)
		Norway (D)	1/8 trimethylchlorosilane/MeOH (Thiel et al. 2002), (Blumenberg and Michaelis 2007)	Fatty acids composition (Thiel et al. 2002; Blumenberg and Michaelis 2007)	–
	<i>Phaeothrix robusta</i>	Sweden (D)	H ₂ O, petroleum ether, chloroform, MeOH (Andersson et al. 1983)	–	Hippocratic screening (Andersson et al. 1983) Guinea-pig ileum activity (H ₂ O, chloroform, methanol) (Andersson et al. 1983) antibacterial activity (Andersson et al. 1983)
			H ₂ O (Andersson et al. 1986)	–	Weak lectin-like activity (Andersson et al. 1986)
		Norway (D)	1/8 trimethylchlorosilane/methanol (Blumenberg and Michaelis 2007)	Fatty acids composition (Blumenberg and Michaelis 2007)	–
Axinellida	<i>Axinella infundibuliformis</i>	Norway (D)	1/8 trimethylchlorosilane/MeOH (Thiel et al. 2002), (Blumenberg and Michaelis 2007)	Fatty acids composition (Thiel et al. 2002; Blumenberg and Michaelis 2007)	–

(continued)

Table 2 (continued)

Order	Species	Locality (shallow, S, deep, D)	Extraction solvent(s) (References)	Compound (compound family)	Bioactivities (References)
	<i>Avinella rugosa</i>	Sweden (D)	H ₂ O, petroleum ether, chloroform, MeOH (Andersson et al. 1983)	–	Hippocratic screening (Andersson et al. 1983) Guinea-pig ileum activity (H ₂ O, methanol) (Andersson et al. 1983) antibacterial activity (Andersson et al. 1983)
			H ₂ O (Andersson et al. 1986)	–	No lectin-like activity (Andersson et al. 1986)
		Norway (D)	1/8 trimethylchlorosilane/MeOH (Blumenberg and Michaelis 2007)	Fatty acids composition (Blumenberg and Michaelis 2007)	–
Poecilosclerida	<i>Myxilla incrustans</i>	Norway (S)	Acetonitrile 60% (Tadesse et al. 2008)	–	Antibacterial/antifungal activity (Tadesse et al. 2008)
		Iceland (S)	MeOH/DCM (Einarsdottir et al. 2016)	Myxillin A, B, C (N-acyl dopamine glycosides)	Immunomodulating activity (Einarsdottir et al. 2016)
	<i>Microsphaeropsis</i> sp. (associated fungi from <i>Myxilla incrustans</i>)	Germany (S)	Ethyl Acetate (Höfle et al. 1999)	Microsphaeropsisin (eremophilane derivative)	Antibacterial (Höfle et al. 1999)
			Ethyl Acetate (Höfle et al. 1999)	(R)-mellein	Antibacterial (Höfle et al. 1999)
			Ethyl Acetate (Höfle et al. 1999)	(3R,4S)-hydroxymellein	Antibacteria (Höfle et al. 1999)

(continued)

Table 2 (continued)

Order	Species	Locality (shallow, S, deep, D)	Extraction solvent(s) (References)	Compound (compound family)	Bioactivities (References)
			Ethyl Acetate (Höfle et al. 1999)	(3R,4R)-hydroxymellein	Antibacterial (Höfle et al. 1999)
			Ethyl Acetate (Höfle et al. 1999)	4,8-dihydroxy-3,4-dihydro-2H-naphthalen-1-one	Antibacterial (Höfle et al. 1999)

Some of these species were sometimes investigated in other areas: France (Brittany), off Newfoundland, Germany (Helgoland). (S), shallow water, (D) deep water >100 m; – means bioactivity not tested



Fig. 2 **a** Lars Afzelius (1936–2001), Director of Tjärnö Marine Biological Laboratory, in 1982. **b** Lars Bohlin (*left*) and Göran Lidgren (*right*) collecting marine organisms at Tjärnö in 1982. **c** The Sven Lovén Center Tjärnö by the Kosterfjord, opened in 1963 (photo taken in 2016); the research vessel *Nereus* is at the dock. **d** A remote-operated vehicle (ROV) is bringing back sponge samples in a net, on the deck of the vessel *Nereus* (on the picture: captain Roger Johansson and Christin Appelqvist). **e** Frame grab from the ROV showing a large *Geodia barretti* at 82 m depth in the Kosterfjord; the two laser points are set 55 mm apart. **f** Sampling of *G. barretti* specimen on deck for natural product and genomic research (picture authorship: A: L. Bohlin; B: L. Andersson; C-F: P. Cárdenas)

The identified species collected were frozen and homogenized. After centrifugation and lyophilisation the material was extracted with petroleum ether, chloroform and methanol. Together with the water extract, four different extracts with different polarity were introduced into a broad screening programme, using Hippocratic screening in mice *in vivo*, guinea-pig ileum preparations, but also tests for antibacterial and antiviral activity. A number of 142 extracts from 36 marine organisms were tested, and resulted in the first bioactivity profile of Swedish marine organisms. The results from these studies were published between 1983 and 1986

(Andersson et al. 1983, 1986; Lidgren et al. 1985). These evaluations showed that about 50% of the tested organisms showed significant biological activity in at least one of the assays. To date, such an ambitious bioactivity screening programme on Swedish marine organisms has never been repeated. However, similar screening studies have been made in nearby cold waters. Some 15 years later, antimicrobial activity was screened in Spitsbergen (sub-Arctic) shallow water marine invertebrates (Lippert et al. 2003). This study included ascidians, mollusks (gastropods and nudibranchs), bryozoans, cnidarians and sponges; none of these species had been included in the previous Swedish investigation by Andersson et al. (1983). Interestingly, the antimicrobial activity tested was against sympatric bacteria and not pathogenic bacteria. Lippert et al. (2003) concluded that 6 out of 18 crude extracts had antimicrobial activity on sympatric bacteria. The most potent extract came from the haplosclerid sponge *Haliclona (Rhizoniera) viscosa*. Five years later, another screening study investigated antibacterial and antifungal activities against pathogenic strains in Norwegian marine benthic invertebrates (Tadesse et al. 2008). This study targeted common ascidians, sponges and a soft coral from the shallow waters of northern Norway. Three species (*Geodia barretti*, *Ciona intestinalis* and *Alcyonium digitatum*) were common to the Swedish screening programme (Andersson et al. 1983). In contrast to Andersson et al. (1983), Tadesse et al. (2008) detected some antibacterial activities in extracts of the ascidian *Ciona intestinalis* and the soft coral *Alcyonium digitatum*. Overall, Tadesse et al. (2008) concluded that all these marine organisms were active against all bacteria and fungal strains tested; the colonial ascidian *Synoicum pulmonaria* had the most potent extract.

Later in the Swedish marine pharmacognosy programme, the guinea-pig ileum, with a large number of receptors and a capacity to discover a broad range of bioactivity, was selected to guide the isolation of bioactive principles from the extracts (Andersson et al. 1986). This resulted in novel steroidal glycosides from the common sunstar *Crossaster papposus* (Andersson et al. 1985), indole alkaloids from the moss animal *Flustra foliacea* (Sjöblom et al. 1983) and several different compounds from the deep-sea sponge *Geodia barretti* (Lidgren et al. 1986, 1988). Extracts from *G. barretti* showed an especially strong activity in all of the bioassays, which raised several scientific questions about the rationale for this activity. Furthermore, the conspicuous fouling free surface of *G. barretti* (Fig. 2e–f) sparked us to continue our studies on this remarkable sponge.

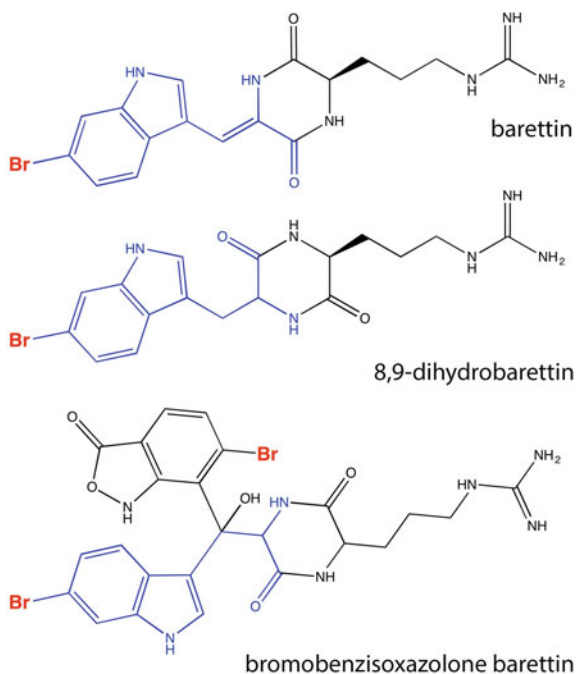
6 Discovery of the Baretins from the Deep-Sea Sponge *Geodia barretti*

Biofouling is a severe problem in the sea for benthic sessile organisms due to unwanted growth of other sessile organisms. The settlement of this type of organisms occurs also on other surfaces, which are exposed in the marine environment. In the case of boat hulls, this leads to a surface with higher friction and

higher fuel consumption to keep the same speed. To avoid biofouling several methods are used, notably antifouling coatings. Traditional heavy-metal-based coatings contained copper or tin oxides, e.g. TBTO (tributyltin oxide), which are very effective to keep the surface free from biofouling but are extremely toxic for the environment and benthic organisms when released into the water (e.g. Evans et al. 1996). In an environment where marine benthic organisms compete for space, light or nutrients in the water current, limiting foreign overgrowth is a decisive advantage in evolution. Several organisms have therefore developed different morphological or chemical antifouling strategies against other sessile organisms (e.g. barnacles, bivalves, sponges, algae). Our research has been aiming at isolating antifouling compounds from these types of organisms.

To evaluate the antifouling activity of *G. barretti*, the barnacle larvae settlement assay was used. The nauplius larvae of the bay barnacle (*Amphibalanus improvisus*) were collected from spawning adults and kept aerated in fresh seawater. After 6–7 days the moulted cyprid larvae were washed and used in the settlement experiments (Sjögren et al. 2004b). The assay was used to guide the fractionation and isolation procedure of an aqueous ethanol extract of *G. barretti*, which showed inhibition of the cyprid settlement. This resulted in identification of two cyclic dipeptides, named baretin (Lidgren et al. 1986) and 8,9-dihydrobaretin (Sjögren et al. 2004b). They both consist of one brominated tryptophane residue and one arginine residue forming a diketopiperazine type of cyclic peptide (Fig. 3). However, the initial structure was for sometime a matter of discussion (Sölter et al. 2002)

Fig. 3 The three baretins extracted from the deep-sea sponge *Geodia barretti* from the Swedish West Coast. The bromine (Br) is in red; the tryptophane residue is in blue



but the definite structure was confirmed by NMR (Sjögren et al. 2004b) and later by total synthesis (Johnson et al. 2004).

Barettin and 8,9-dihydrobarettin showed dose-response inhibition of the cyprids at respective EC_{50} values of 0.9 and 7.9 μM (Sjögren et al. 2004b). Structure–activity studies revealed that the complete structure of barettin including the double bond was necessary for the shown activity. Further LC-MS analysis of seawater, either incubated with undamaged living sponges or in situ, showed the presence of barettin and also strong inhibition of settlement (Sjögren et al. 2004b, 2011). None of the compounds showed any significant activity on larval mortality. When the cyprids were transferred to a control Petri dish with fresh seawater they displayed a normal swimming and settlement behaviour (Sjögren et al. 2004b).

To gain an increased understanding of the relationships between chemical structure and shown biological activity, a number of analogues were synthesized based on the barettin skeleton. For comparison, a dipodazine skeleton was used where arginine is replaced by the amino-acid glycine. Several of the analogues showed significant inhibition of settlement of the cyprids where benzo[g]dipodazine was even more potent than barettin ($EC_{50} = 0.034 \mu\text{M}$) (Sjögren et al. 2006). Later, an even more potent barettin was extracted from *G. barretti*: bromobenzisoxazolone barettin (Fig. 3) had an EC_{50} value of 15 nM (Hedner et al. 2008).

To further understand the mode of action and molecular target of the barettins, we studied their affinity to human serotonin receptors. The selection of receptors was based on the finding that the cyprid larvae contain serotonin receptors but also the structural similarities between the barettins and ligands with affinity to serotonin receptors, such as the drug Tegaserod (Beglinger 2002). Representatives from all subfamilies of human serotonin receptors were used. They were transfected into membranes of embryonic kidney cells. Barettin showed specific activity to 5-HT_{2A}, 5-HT_{2C} and 5-HT₄ at concentrations close to endogenous serotonin, while 8,9-dihydrobarettin had a weaker interaction with 5-HT_{2C} (Hedner et al. 2006).

As mentioned earlier the biofouling of sessile organisms in the marine environment like barnacles but also algae, mussels, ascidians and hydroids is a severe problem for boats and aquaculture equipment (Wahl 1989). Based on the antifouling results for the barettins, their effect in field conditions included in commercially used non-toxic paints was tested to find out their ability to inhibit settlement of cyprids. A significantly reduced recruitment of both larvae from barnacles and blue mussels was observed (Sjögren et al. 2004a).

7 *Geodia barretti*—A Sponge Model for Sponge Ground Investigations

While chemists were studying the barettins, marine biologists started to investigate the morphological/molecular evolution, the biogeography and the phylogenetic relationships of boreoarctic *Geodia* species (Cárdenas 2010; Cárdenas et al. 2010,

2011; Cárdenas and Rapp 2013) which led to a large revision of the six boreoarctic species, including *G. barretti*, gathering basic knowledge on its biology (cultivation, reproduction, microbial community and associated macrofauna) (Cárdenas et al. 2013 and references within). *G. barretti* has a very wide bathymetric range: it can be found from 30 to 2000 m depth (Cárdenas et al. 2013). It is the most common and widespread *Geodia* species across the North Atlantic, recorded from fjords to continental shelf and slopes, and even from the mid-Atlantic ridge (Cárdenas and Rapp 2015; Cárdenas et al. 2013). It is particularly common on the European continental shelf from Spistbergen to the entire Norwegian coastline, and down to the Swedish West Coast. In Sweden, *G. barretti* is quite common in the Kosterfjord, where we now collect it with a remote operated vehicle (ROV) (Fig. 2d). It has never been recorded south of the Kosterfjord, even in the closeby Gullmarfjord (58°15'N) (Théel 1908; P. Cárdenas and M. Tholleson personal observations) which is shallower (42–118 m deep) and probably most importantly, not connected to the deep Norwegian trench.

When one of the authors (PC) joined the BlueGenics project at the Division of Pharmacognosy at Uppsala University in 2014, he brought his knowledge on sponge systematics notably to look for *Geodia* chemical markers, using untargeted and targeted metabolic fingerprinting, a promising tool for sponge chemosystematics (Cárdenas et al. 2012). In order to be able to compare the sponge metabolic fingerprints, it is absolutely necessary to have a solid taxonomical and ecological knowledge of the species extracted, a requirement sometimes too lightly overlooked in the field of natural products (Leal et al. 2016; Cárdenas 2016). Especially since molecular phylogenetic studies have considerably shaken the traditional demosponge classification (Morrow and Cárdenas 2015). This promising study is still in progress but preliminary targeted metabolic results suggest that it will be difficult to find shared compounds by all boreoarctic *Geodia* species, let alone for the *Geodia* genus, since known compounds seem to be species-specific. For instance, baretin has been found in most *G. barretti* specimens investigated, and seldom in other species [e.g. an independent study reported baretin from *Geodia macandrewii* (Olsen et al. 2016b)]. Furthermore, our current metabolic fingerprint database suggests some metabolic variability between *G. barretti* populations across the North Atlantic.

Another important feature of *G. barretti* is that it is one of the key species of deep-sea boreal sponge grounds (i.e. sponge-dominated communities), which occur across the North Atlantic (Klitgaard and Tendal 2004; Murillo et al. 2012). Sponge grounds are among the most diverse, ecologically and biologically important marine ecosystems of the deep sea, and yet they have so far received very little research attention. *G. barretti* dominates these boreal habitats in terms of size and biomass and is therefore one of the main structures forming species. One of the authors (PC) is now part of a large EU funded H2020 consortium to investigate these sponge grounds further: the main goal of the project SponGES (www.deepseasponges.org) is to develop an integrated ecosystem-based approach to

preserve and sustainably use deep-sea sponge ecosystems of the North Atlantic. One of the challenges of SponGES will be to further explore the metabolic diversity of the main sponges from North Atlantic sponge grounds, notably *G. barretti*, combined this time with genomic and metagenomic data. With so much knowledge and data at hand, we are aiming to propose *G. barretti* as a sponge model for the discovery and production of new marine compounds in the deep sea, as well as for the study of their biological role.

8 Cold-Water Temperatures Still Produce Cool Chemistry

The interest for proteins and peptides as bioactive compounds in the fields of pharmacognosy and natural products chemistry has increased during the last decades. Some classes of families and organisms that have never been studied before are now in focus, and they reveal new chemistry and biochemistry of importance for drug discovery, biotechnology and our understanding of ecology and physiology. Reasons for this renewed interest are explained by several factors, including technical developments in nucleotide sequencing, mass spectrometry and the combination into proteomics/peptidomics, but also by the general trend moving towards peptide and proteins in the area of drug development. For the natural product chemists, this change brings changes in methodology, for example moving from mainly working with extractions using organic solvents to aqueous solvents, and the use of big data and data mining for structure elucidation.

Still, with one prominent exemption, the field of ribosomally produced natural products from the marine environment is vastly underexplored. The exemption is the conotoxins, which comprise a very large group of peptide toxins from the Conidae family of marine gastropods, see www.conoserver.org for more information and reviews (e.g. Akondi et al. 2014; Durek and Craik 2015). These peptides are characterized by the presence of disulfide bonds that confine their conserved structural folds. Recently, other marine mollusks have been shown to express similar mixtures of peptides (Verdes et al. 2016). However, considering the fact that peptides are water-soluble compounds and appear ideal also for communication between species, the comparison to the role of volatile compounds for communication between terrestrial organisms is intriguing, where also surprisingly few examples of ribosomally produced peptides have been described. This is true also for sponges, which are as earlier mentioned, one of the—if not *the*—main targets for marine biodiscovery.

Some larger proteins have been described in sponges (e.g. O’Keefe 2001), together with a handful of peptides. The latter includes asteropine A, isolated from a shallow water *Asteropus* from Japan (Takada et al. 2006). This 36 amino-acid residue long peptide comprises six cysteines arranged in a so-called cystine knot

motif, in which the first Cys residue is connected by a disulfide bond to the fourth Cys residue, the second to the fifth and the third to the sixth Cys residue. This motif is shared with many other peptides from all kingdoms of life, but asteropine distinguishes itself by being highly negatively charged. Asteropine A is a potent inhibitor of bacterial sialidase enzyme, but if and how this activity is coupled to its role in nature is unclear. Some years later, further cystine knot peptides, the asteropsins A–G, were reported in a different shallow water species of *Asteropus*, from South Korea (Su et al. 2016; Li et al. 2013, 2014). In analogy to asteropine, their natural functions are unclear.

In the BlueGenics project, our aim was to explore the peptide content of *G. barretti*, sparked by our history of studying the chemistry of this cold-water marine organism, combined with our interest in peptide natural products in general (Burman et al. 2014). We had observed high molecular weight compounds by mass spectrometry (MS) analyses in an extract of *G. barretti*, triggering our interest further. In short, we then successfully isolated two homologous peptides from the aqueous acetonitrile extract of the sponge using a combination of reverse phase and size exclusion chromatography. Two additional peptides were observed by mass spectrometry, but they could not be obtained in sufficient amounts for attempting sequence analyses. Sequencing of the peptides were done by combining quantitative amino-acid analyses and MS/MS peptide sequencing, after first reducing and alkylating possible cysteines. It was clear from the latter experiment that these peptides, which we named barrettides A and B, contained four cysteines engaged in two disulfide bonds. The full sequences were revealed after combining MS/MS data from digests of the peptides using different enzymes. The N-terminal part of these peptides proved to be less than straightforward to sequence by MS/MS because of the presence of multiple acidic residues. However, corroborating evidence was provided by a sequence found in the metatranscriptome of *G. barretti* (Radax et al. 2012). The final sequences of barrettide A and B could thus be determined (Fig. 4). No homologues to these peptides could be found when searching the NCBI databases for similar sequences (Carstens et al. 2015). The three-dimensional structure in solution of barrettide A was determined using NMR. The peptides adopt a long β -hairpin-fold cross-braced by the two disulfide bonds. Both peptides—they differ only with a valine to leucine substitution—are amphipathic in nature: the hydrophobic and charged residues cluster on separate faces of the molecule. Both peptides show antifouling activity against bay barnacles, but it is unlikely that this is the natural function.

From the metatranscriptome, it is clear that the barrettides are ribosomally produced peptides. Most likely, this is the case also for the asteropsins and asteropine; and they all contain the common amino acids found in proteins (although the N-terminal Glu is posttranslationally modified into pyroGlu at the N-terminal in some of the asteropsins). Other smaller sponge peptidic natural products described (Blunt et al. 2016) appear to originate from non-ribosomal peptide synthesis.

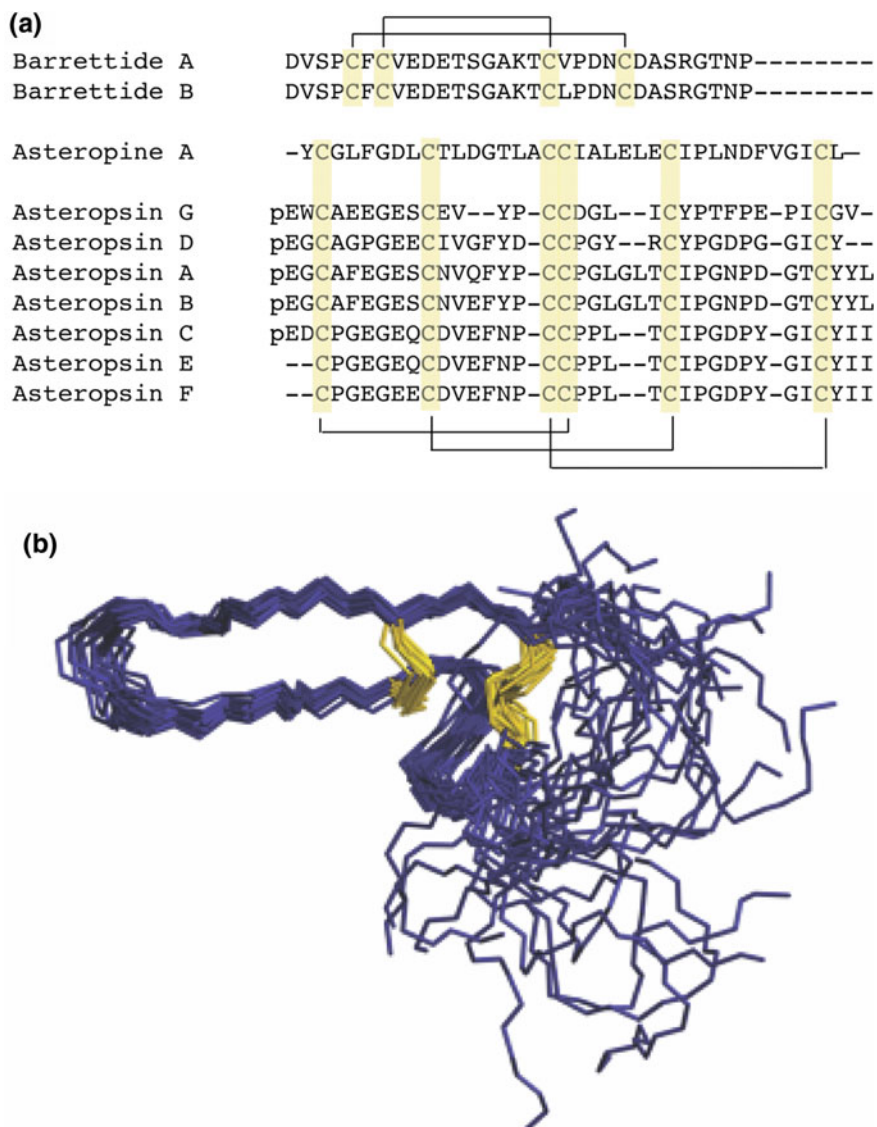


Fig. 4 **a** Sequence alignment of barrettides, asteropine A and asteropsins. Cysteines and disulfide bond configurations are in *yellow*: barrettides A and B contain two disulfide bonds in a ladder arrangement, other peptides are cystine knots. Note that asteropsins G, D, A, B and C contain pyroGlu at their N-terminal. **b** Three-dimensional structure of barrettide A, represented by the overlay of the 20 best structures after NMR. The termini are flexible, whereas the sequence between cysteines adopt a well-defined β -sheet

9 Interpretation, Prediction and Selection

ChemGPS-NP. The tangible diversity of small carbon-based molecules is unfathomably huge, such that already conservative estimates as those by Bohacek and co-authors in the mid-1990s (Bohacek et al. 1996) were pointing to 10^{60} . More recent attempts to address the issue reach far beyond this, and from simple connectivity estimates suggest 10^{240} —or even more—tangible molecules (Lipinski and Hopkins 2004). As 10^{60} is already a number larger than the estimated number of atoms in the known universe, the specific upper border becomes less important. What we can conclude, however, is that there is an immense potential for chemical diversity in nature. In order to navigate this vast ocean of potential diversity, a tool to provide bearing and distance is required. There has been several attempts to provide such devices, until Larsson et al. (2007) proposed a global map of chemical space based on extensive principal component analyses (PCA) of physical chemical properties called the ChemGPS-NP. This is a further development of an initial model suggested by Oprea and Gottfries (2001).

The physical–chemical property map. From the chemical structure of a compound, there are today numerous ways to estimate physical–chemical properties. These can consist of molecular weight, number of nitrogen atoms, degree of aromaticity, lipophilicity, etc. All of these properties will make up an array, which is very well suited for PCA. In the process of PCA, the main purpose is to reduce the complexity, or dimensionality, of the analyzed data, by identifying so-called principal components which can be seen as ways of defining observed covariation in the analyzed data. These principal components, all perpendicular to each other, will define the rules governing the space to navigate—and frequently turning out to be more complex than the physical space in which we live. On an ordinary geographical map of Earth, we can suffice with only three dimensions to pinpoint any position on the surface of Earth, and generously adding the fourth dimension cherished by physicists, time, we can also cater for geological processes changing the face of Earth. In the chemical property space defined by ChemGPS-NP, however, we will need eight dimensions to navigate chemical diversity in an adequate way. The actual mathematics to do this has been in place for more than 100 years (Pearson 1901).

Tool for interpretation, prediction and selection. So, what would then be the purpose of such hyperdimensional frivolities? As such, the visualization of chemical property space becomes an intuitive and fast method of grouping compounds, summarizing their properties for overview, and observing patterns in character distribution. Patterns may be compared to and interpreted in the light of other complex processes—one such being the evolution of life on Earth.

Where life started. Already from the oldest written sources, there has been a conceptualized sequence in which life as we know it emerged. This understanding developed further from the eighteenth century with the appreciation of stratified fossil finds, and continued into modern day with our more finely tuned methods of investigation. In the publications by Darwin (1859) and Haeckel (1866) from the mid nineteenth century one finds the earliest examples of phylogenetic trees,

providing an explicit hypothesis of the order in which these evolutionary events supposedly took place.

Evolutionary perspectives. When attempting to grasp the width and impact of these processes, it is of crucial importance to retain a proper, evolutionary perspective. We have now strong reasons to believe that all life on Earth was not created—albeit sequentially—during the course of 6 days, and we also know that novel breeds of humanoids do not turn up at the rate and divergent forms as in the popular comics about the X-Men featured by Marvel (Lee and Kirby 1963). Evolution takes time, proceeding by numerous small (and some larger) mutations to the genomes of living organisms, complemented by the occasional lateral gene transfer, and subsequently evaluated by the process of natural selection as eloquently described by Darwin (1859).

When did things happen? At the international botanic congress in St. Louis 1999, Prof. Kåre Bremer proposed in a plenary talk, that the most important challenge for the years to come would be not to add further support and resolution to the phylogenies presented, but to start putting dates to the evolutionary events implied. During the 1980s the theory of neutral evolution (Kimura 1983) rendered some support to the idea that differences in DNA sequences, i.e. mutations, between two species accumulated over time and that the observed number of such mutations would stand in proportion to the time between the evolutionary events. This created the first versions of the ‘molecular clock’ interpretation, which gave us some initial hints on the timescales at work. However, comparing these early molecular clocks to other and partly contradictory evidence from fossil data, geological events, and some interpretable transition series, where the change of specific features could be followed in a group of organisms, indicated that this application of the appealing theory had some flaws. In two papers from the 1990s (Albert et al. 1994a, b) these issues were addressed making use of, at that time, comprehensible sets of DNA sequence data. The firm conclusion was that even though a molecular clock appeared to be at hand, it was a sloppy clock, requiring repeated adjustments to perform in an acceptable way. These adjustments or calibration points were provided from fossil data, and as described in the works by Anderson et al. (2005) combining these approaches can provide well-supported and coherent hypotheses about not only the sequence of evolutionary events but also about their dating.

Which order and why? Large parts of the early hypotheses in this field were performed on plants, which exhibit a number of appealing properties. One was that a large joint effort was made at an early stage to produce comparable sets of data focusing on a few molecular markers—which turned out to be very well selected. Another reason is that plants, because of their rigid cell walls, to a larger extent than animals tend to leave interpretable fossils—this includes also the abundant microfossils such as pollen grains. There are examples of fossils from higher plants that are preserved in such detail that the number of cell layers in the anther walls can be counted (Friis 1990). From these and other data, there is strong evidence that all major groups of modern higher plants were already present +100 Mya, at the geological break-up of Gondwanaland (Anderson et al. 2005). Similar data has since been presented both for other evolutionary lineages such as animals, but also

for much more ancient groups of organisms (e.g. Goloboff et al. 2009). This opens exciting opportunities also in the fields of natural products chemistry and drug discovery.

Occurrence of receptor systems. With the available, and rapidly growing, DNA sequence data depositories, and readily accessible phylogenies or tools to estimate such, we now have the possibility to interpret evolutionary events on a much finer scale. These opportunities can be employed to investigate and determine not only how, e.g. members of a specific receptor system have evolved, but also infinitely more exciting to address the question of when these receptors occurred and in some cases also why and from where. As receptor systems and their ligands coevolve through time, so does also other compounds that might affect these receptors. The processes of evolution put selective pressure on the fine-tuning and adaption of ligands and at the same time provide us with a window through which we can follow these adaptations.

The issue of sequential order. Following these conclusions, it becomes evident that evolutionary adaptations such as enzymatic systems, and their related abilities or features, develop sequentially one after the other building on previous advances. This is the normal Darwinian mode of ‘vertical inheritance’, but during the last decades it has become increasingly evident that there are additional competing evolutionary trends, e.g. ‘lateral gene transfer’, ‘secondary losses’ and ‘convergent evolution’ that can in some cases obscure the picture. Nevertheless, in either case, there is a logic to the sequence in which enzymatic systems turn up in the history of life, even if the occasional enzyme or enzymatic system might originate from another source such as in the examples described in some detail by Strese et al. (2014) and Vikeved et al. (2016).

Sea of ancestry. Life on Earth originated in the seas, and persisted during the first 2 billion years under the water surface. It was not until the development of photosynthetic organisms, and substantial production of oxygen (and hence ozon) that a radiation filter protecting from harmful UV radiation from the Sun enabled life to colonize terrestrial environments. At this point in time, several evolutionary lineages had already developed multicellular life forms. Considering this, in the light of the minimum age for many of the early evolutionary lineages among animals [in several cases indicated to predate ‘the cambrian explosion’ with more than 100 million years (Erwin et al. 2011)], and the demonstrated chemical diversity of zoanths, gorgonians and sponges, there is strong support that a large number of the enzymatic systems still present today first occurred and developed for life in a marine environment and then subsequently been adapted to function also in a terrestrial environment.

Transcending the surface. When life transcended the water surface and begun colonizing the terrestrial environment, a number of important ecology-related chemical factors became fundamentally altered. The most obvious is of course that when no longer living submerged in water, the issue of dilution becomes far less important, and while organisms in the sea constantly have to keep this aspect under consideration that is much less of an issue above surface. Related to this follows

degree of solubility or lipophilicity, access to halogens for biosynthetic purposes, and the apparent conflict between molecular size and biological availability.

Terrestrial and marine chemistry. In a study by Muigg et al. (2013) the first chemical property space map of marine natural products was presented. From these preliminary analyses, complemented and refined in the present study (Fig. 5), it was clearly demonstrated that there are fundamental differences between natural products found in marine and terrestrial organisms. These differences became more pronounced when the molecules grew larger, providing access to a wide variety of chemical properties.

Methods for interpretation. There are several ways to interpret the map of chemical property space. One of the most frequently used—and maybe most intuitive—is based on the central dogma in medicinal chemistry that ‘similar compounds have similar functions’. In this case the concept of similarity can be quantified by estimating the Euclidean distance between the positions of two

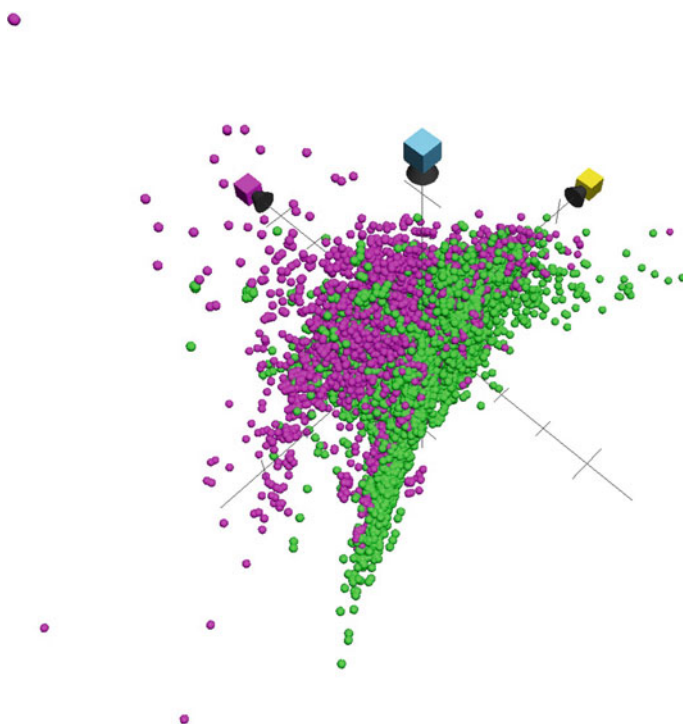


Fig. 5 Plot of compounds from entirely marine lineages (*magenta*) and terrestrial lineages (*green*) in ChemGPS-NP chemical property space. The three dimensions/axis depicted in this plot are PC3 (*yellow*) representing lipophilicity related parameters, PC4 (*pink*) representing aspects of molecular flexibility and rigidity, and PC5 (*blue*) primarily related to electronegativity and number of nitrogen and halogens in the molecules. The compounds from marine lineages have more halogens, a larger molecular flexibility, and a slightly higher lipophilicity, than those from terrestrial lineages

compounds over all eight dimensions of chemical property space. It has been shown that there is a strong correlation between experimentally demonstrated biological activity on one hand, and short Euclidean distances in ChemGPS-NP chemical property space, on the other (Buonfiglio et al. 2015). As a complement, metrics such as various structural fingerprints, or discriminant analyses such as OPLS-DA can also be employed.

What to do, when we know nothing at all? In natural products research, it is fortunately not an uncommon situation that after thorough investigations of a tantalizing and previously unstudied organism, a novel chemical compound is described. In this way unravelling the chemical diversity of Life is as such a fundamentally important task—but if this compound could also be connected to a specific biological activity or function, the winnings would be even larger. So, how could these further steps be taken? One option would be to painstakingly initiate a screening of different biological assays in the hope of finding one where an activity is recorded. This random approach, however often applied, has several important drawbacks. The most obvious of these is probably that the chance of, by coincidence, happening to test a relevant assay that actually is related to the biological function of the compound is at best marginal. Even if an activity in an assay would be identified, there lies a fundamental difference in this as compared to understanding the function for which the compound was honed by evolution over generations. Another very real and common problem in natural product research is the issue of access to the compound. As many of these intriguing natural products are structurally complex, chemical synthesis is often not possible (or very complicated) and the compounds will have to be extracted and isolated from the original source. The subsequent testing, possibly in series of assays, is prone to consume the amount of compound available. A fundamentally different possibility would be to use the predictive approach described above.

The case of barretin. Positioning barretin in ChemGPS-NP chemical property space retrieves a placement at PC1: 0.483931, PC2: 1.200816, PC3: -1.565224, PC4: 1.517407, PC5: 2.459573, PC6: 0.684073, PC7: -0.744329 and PC8: 0.222071 (Fig. 6). Starting from this position, the Euclidean distances to in-house reference databases can be calculated and used as a tool to select the closest neighbours. By interpreting the thus defined chemical property neighbourhood of barretin, several interesting observations can be made. The in-house reference database, at present holding $+8.4 \cdot 10^6$ compounds, contains 87 compounds with a Euclidean distance <1.00 to barretin (Fig. 6a). Submitting these 87 neighbours to 'The Binding Database' (<http://www.bindingdb.org>) returned 134 predicted targets with 'maximum similarity score' ≥ 0.85 . Of these 134 predicted targets, 4 'neighbours' closely related to vitronectin receptor alpha (score 0.99), 8 to protein kinases (scores 0.85–0.94), 12 neighbours related to opioid receptors (0.85–0.93), and 15 compounds to melanocortin receptors MC1R-4R (scores 0.86–0.85). When covisualizing reference sets from compounds experimentally demonstrated to bind to vitronectin receptor alpha (1245 compounds), and melanocortin receptors MC1-4R (8664 compounds), respectively, (Fig. 6) an unexpected pattern emerges. From this it is obvious that barretin and its close neighbours fit better in the context

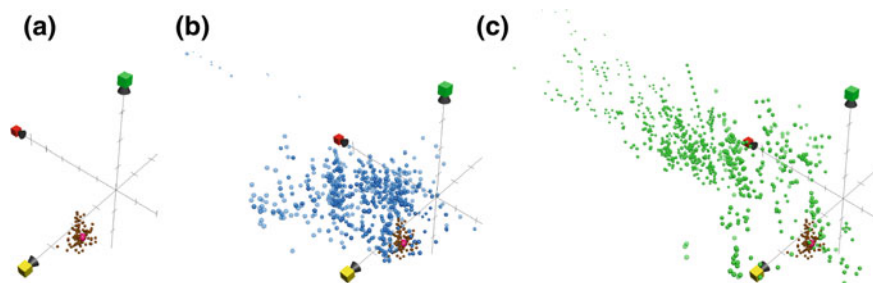


Fig. 6 a–c Plots showing the position of barettin (*red dot*), the 87 compounds with Euclidean distance <1.00 over all eight dimensions (*brown dots*), and the activity volumes of 1245 known ligands to vitronectin alpha (*blue dots*), and 8664 known ligands to melanocortin receptors MC1-4R (*green dots*). The axis marked with *red* is PC1, representing size and weight parameters, the *yellow* axis is PC2 representing aromaticity- and conjugation-related parameters, and the *green* axis is PC3 representing primarily lipophilicity-related parameters

of compounds with activity on vitronectin alpha than melanocortin receptors, but it is also clear that even though some of the 87 neighbours matched with high affinity, they are by no means typical for the compounds with demonstrated binding to those receptors.

10 Conclusion

With more than 6000 species of marine plants and animals, the Kosterfjord area has the richest marine biodiversity in Swedish waters, but it remains understudied. The study of Swedish marine organisms for bioactive molecules initiated in 1981, revived in 2001 and then again with the BlueGenics project, resulted in novel knowledge combining marine biology, chemistry and pharmacology. The extensive research on the deep-sea sponge *Geodia barretti* has given, within the framework of the BlueGenics project, new peptides (the barrettides), further understanding of barettings and antifouling activity, and new tools such as metabolic fingerprinting and ChemGPS-NP to continue investigating secondary metabolites of this fascinating animal.

A new strategy has been developed using bioinformatics methods for prediction and selection of marine organisms for further studies, combined with chemoinformatic approaches that might aid in unravelling the biological activities of novel chemical entities described. The chemical diversity of marine organisms in cold waters may not be so limited compared to temperate/tropical waters. We believe that more detailed studies of cold-water organisms, especially in the deep sea, could lead to the discovery of novel structure–activity relationships important for understanding the role of secondary metabolites. These are all important aspects in developing methods for natural products research aiming for a sustainable environment.

Acknowledgements The authors are very grateful for all the work that graduate students and postdocs have performed during the years, together with scientific colleagues. Especially, the late Director of Tjärnö Marine Biological Laboratory, Lars Afzelius (1936–2001), should be remembered for great help in introducing this research programme. Also Martin Sjögren and Mia Dahlström should be acknowledged for the development of the antifouling research. The Swedish Research Councils, Carl Tryggers Stiftelse and the EU project BlueGenics (grant agreement No. 311848) should be acknowledged for financial support. PC acknowledges funding by the EU Horizon 2020 programme SponGES under grant agreement No. 679849.

References

- Akondi KB, Muttenthaler M, Dutertre S, Kaas Q, Craik DJ, Lewis RJ, Alewood PF (2014) Discovery, synthesis, and structure-activity relationships of conotoxins. *Chem Rev* 114 (11):5815–5847. doi:[10.1021/cr400401e](https://doi.org/10.1021/cr400401e)
- Albert VA, Backlund A, Bremer K (1994a) DNA characters and cladistics: the optimization of functional history. In: Scotland RW, Siebert DJ (eds) *Systematics associations* (vol 52) (Special Volume 52). Clarendon Press, London, pp 249–272
- Albert VA, Backlund A, Bremer K, Chase MW, Manhart JR, Mishler BD, Nixon KC (1994b) Functional constraints and rbcL evidence for land plant phylogeny. *Ann Mo Bot Gard* 81 (3):534–567. doi:[10.2307/2399902](https://doi.org/10.2307/2399902)
- Amade P, Pesando D, Chevolut L (1982) Antimicrobial activities of marine sponges from French Polynesia and Brittany. *Mar Biol* 70(3):223–228
- Anderson CL, Bremer K, Friis EM (2005) Dating phylogenetically basal eudicots using rbcL sequences and multiple fossil reference points. *Am J Bot* 92(10):1737–1748. doi:[10.3732/ajb.92.10.1737](https://doi.org/10.3732/ajb.92.10.1737)
- Andersson L, Bano S, Bohlin L, Riccio R, Minale L (1985) Studies of the Swedish marine organisms. Part 6. A Novel bioactive steroidal glycoside from the starfish *Crossaster papposus*. *J Chem Res* (12):366–367
- Andersson L, Lidgren G, Bohlin L, Magni L, Ogren S, Afzelius L (1983) Studies of Swedish marine organisms. I. Screening of biological activity. *Acta Pharm Suec* 20(6):401–414
- Andersson L, Lidgren G, Bohlin L, Pisa P, Wigzell H, Kiessling R (1986) Studies of Swedish marine organisms. V. Screening of biological activity. *Acta Pharm Suec* 23:91–100
- Beglinger C (2002) Tegaserod: a novel, selective 5-HT₄ receptor partial agonist for irritable bowel syndrome. *Int J Clin Pract* 56(1):47–51
- Blumenberg M, Michaelis W (2007) High occurrences of brominated lipid fatty acids in boreal sponges of the order Halichondrida. *Mar Biol* 150(6):1153–1160. doi:[10.1007/s00227-006-0445-7](https://doi.org/10.1007/s00227-006-0445-7)
- Blunt JW, Copp BR, Keyzers RA, Munro MHG, Prinsep MR (2016) Marine natural products. *Nat Prod Rep* 33(3):382–431. doi:[10.1039/C5NP00156K](https://doi.org/10.1039/C5NP00156K)
- Bohacek RS, McMartin C, Guida WC (1996) The art and practice of structure-based drug design: a molecular modeling perspective. *Med Res Rev* 16(1):3–50. doi:[10.1002/\(SICI\)1098-1128\(199601\)16:1<3:AID-MED1>3.0.CO;2-6](https://doi.org/10.1002/(SICI)1098-1128(199601)16:1<3:AID-MED1>3.0.CO;2-6)
- Buonfiglio R, Engkvist O, Várkonyi P, Henz A, Vikeved E, Backlund A, Kogej T (2015) Investigating pharmacological similarity by charting chemical space. *J Chem Inf Model* 55 (11):2375–2390. doi:[10.1021/acs.jcim.5b00375](https://doi.org/10.1021/acs.jcim.5b00375)
- Burman R, Gunasekera S, Strömstedt AA, Göransson U (2014) Chemistry and biology of cyclotides: circular plant peptides outside the box. *J Nat Prod* 77(3):724–736. doi:[10.1021/np401055j](https://doi.org/10.1021/np401055j)
- Cárdenas P (2010) Phylogeny, taxonomy and evolution of the Astrophorida (Porifera, Demospongiae). PhD thesis, available at <http://hdl.handle.net/1956/4020>, University of Bergen, Bergen

- Cárdenas P (2016) Who produces ianthelline? The arctic sponge *Stryphnus fortis* or its sponge epibiont *Hexadella dedritifera*: a probable case of sponge-sponge contamination. *J Chem Ecol* 42(4):339–347
- Cárdenas P, Pérez T, Boury-Esnault N (2012) Sponge systematics facing new challenges. *Adv Mar Biol* 61:79–209
- Cárdenas P, Rapp HT (2013) Disrupted spiculogenesis in deep-water Geodiidae (Porifera, Demospongiae) growing in shallow waters. *Invertebr Biol* 132(3):173–194
- Cárdenas P, Rapp HT (2015) Demosponges from the Northern Mid-Atlantic Ridge shed more light on the diversity and biogeography of North Atlantic deep-sea sponges. *J Mar Biol Assoc UK* 95(7):1475–1516. doi:[10.1017/S0025315415000983](https://doi.org/10.1017/S0025315415000983)
- Cárdenas P, Rapp HT, Klitgaard AB, Best M, Thollessen M, Tendal OS (2013) Taxonomy, biogeography and DNA barcodes of *Geodia* species (Porifera, Demospongiae, Tetractinellida) in the Atlantic boreo-arctic region. *Zool J Linn Soc* 169:251–311
- Cárdenas P, Rapp HT, Schander C, Tendal OS (2010) Molecular taxonomy and phylogeny of the Geodiidae (Porifera, Demospongiae, Astrophorida)—combining phylogenetic and Linnaean classification. *Zool Scr* 39(1):89–106. doi:[10.1111/j.1463-6409.2009.00402.x](https://doi.org/10.1111/j.1463-6409.2009.00402.x)
- Cárdenas P, Xavier JR, Reveillaud J, Schander C, Rapp HT (2011) Molecular phylogeny of the Astrophorida (Porifera, Demospongiae) reveals an unexpected high level of spicule homoplasy. *PLoS ONE* 6(4):e18318
- Carstens BB, Rosengren KJ, Gunasekera S, Schempp S, Bohlin L, Dahlström M, Clark RJ, Göransson U (2015) Isolation, characterization, and synthesis of the barrettides: disulfide-containing peptides from the marine sponge *Geodia barretti*. *J Nat Prod* 78(8):1886–1893
- Chaudhary C, Saedi H, Costello MJ (2016) Bimodality of latitudinal gradients in marine species richness. *Trends Ecol Evol* (in press) doi:[10.1016/j.tree.2016.06.001](https://doi.org/10.1016/j.tree.2016.06.001)
- Darwin C (1859) *The Origin of Species by means of natural selection or the preservation of favoured races in the struggle for life*, 1st edn. John Murray, London
- Demain AL, Sanchez S (2009) Microbial drug discovery: 80 years of progress. *J Antibiot* 62(1):5–16
- Durek T, Craik DJ (2015) Therapeutic conotoxins: a US patent literature survey. *Expert Opin Ther Pat* 25(10):1159–1173. doi:[10.1517/13543776.2015.1054095](https://doi.org/10.1517/13543776.2015.1054095)
- Ebada S, Proksch P (2012) *The Chemistry of Marine Sponges*. In: Fattorusso E, Gerwick WH, Tagliatalata-Scafati O (eds) *Handbook of marine natural products*. Springer, Netherlands, pp 191–293. doi:[10.1007/978-90-481-3834-0_4](https://doi.org/10.1007/978-90-481-3834-0_4)
- Einarsdóttir E, Liu H-B, Freysdóttir J, Gottfredsen CH, Omarsdóttir S (2016) Immunomodulatory N-acyl Dopamine Glycosides from the Icelandic Marine Sponge *Myxilla incrustans* Collected at a Hydrothermal Vent Site. *Planta Med* 82(09/10):903–909. doi:[10.1055/s-0042-105877](https://doi.org/10.1055/s-0042-105877)
- Erwin DH, Laflamme M, Tweedt SM, Sperling EA, Pisani D, Peterson KJ (2011) The Cambrian conundrum: early divergence and later ecological success in the early history of animals. *Sci* 334(6059):1091–1097. doi:[10.1126/science.1206375](https://doi.org/10.1126/science.1206375)
- Evans SM, Evans PM, Leksono T (1996) Widespread recovery of dogwhelks, *Nucella lapillus* (L.), from tributyltin contamination in the North Sea and Clyde Sea. *Mar Pollut Bull* 32(3):263–269. doi:[10.1016/0025-326X\(95\)00127-9](https://doi.org/10.1016/0025-326X(95)00127-9)
- Friis EM (1990) *Silvianthemum suecicum* gen. et sp. nov., a new saxifragalean flower from the Late Cretaceous of Sweden. *Biologiske skrifter (Kongelige Danske videnskabernes selskab)* 36:1–35
- Gerwick WH, Fenner AM (2013) Drug discovery from marine microbes. *Microb Ecol* 65(4):800–806. doi:[10.1007/s00248-012-0169-9](https://doi.org/10.1007/s00248-012-0169-9)
- Goloboff PA, Catalano SA, Marcos Mirande J, Szumik CA, Salvador Arias J, Källersjö M, Farris JS (2009) Phylogenetic analysis of 73 060 taxa corroborates major eukaryotic groups. *Cladistics* 25(3):211–230. doi:[10.1111/j.1096-0031.2009.00255.x](https://doi.org/10.1111/j.1096-0031.2009.00255.x)
- Haeckel E (1866) *Generelle Morphologie der Organismen. Allgemeine grundzüge der organischen formen-wissenschaft, mechanisch begründet durch die von Charles Darwin reformirte descendenztheorie*. Band 2., vol 2. Geork Reimer, Berlin

- Hanssen KØ, Andersen JH, Stiberg T, Engh RA, Svenson J, Genevière A-M, Hansen E (2012) Antitumoral and mechanistic studies of ianthelline isolated from the Arctic sponge *Stryphnus fortis*. *Anticancer Res* 32(10):4287–4297
- Hanssen KØ, Cervin G, Trepos R, Petitbois J, Haug T, Hansen E, Andersen JH, Pavia H, Hellio C, Svenson J (2014) The bromotyrosine derivative ianthelline isolated from the arctic marine sponge *Stryphnus fortis* inhibits marine micro- and macrobiofouling. *Mar Biotechnol* 16(6):684–694. doi:10.1007/s10126-014-9583-y
- Hedner E, Sjögren M, Fröndberg P-A, Johansson T, Göransson U, Dahlström M, Jonsson P, Nyberg F, Bohlin L (2006) Brominated Cyclodipeptides from the marine sponge *Geodia barretti* as selective 5-HT ligands. *J Nat Prod* 69(10):1421–1424
- Hedner E, Sjögren M, Hodzic S, Andersson R, Göransson U, Jonsson PR, Bohlin L (2008) Antifouling activity of a dibrominated cyclopeptide from the marine sponge *Geodia barretti*. *J Nat Prod* 71(3):330–333
- Heinrich M, Gibbons S (2001) Ethnopharmacology in drug discovery: an analysis of its role and potential contribution. *J Pharm Pharmacol* 53(4):425–432. doi:10.1211/0022357011775712
- Höller U, König GM, Wright AD (1999) Three new metabolites from marine-derived fungi of the genera *Coniothyrium* and *Microsphaeropsis*. *J Nat Prod* 62(1):114–118. doi:10.1021/np980341e
- Holzwarth M, Trendel J-M, Albrecht P, Maier A, Michaelis W (2005) Cyclic peroxides derived from the marine sponge *Plakortis simplex*. *J Nat Prod* 68(5):759–761. doi:10.1021/np049665v
- Hougaard L, Christophersen C, Nielsen PH, Klitgaard A, Tendal O (1991) The chemical composition of species of *Geodia*, *Isops* and *Stryphnus* (Choristida: Demospongia: Porifera): a comparative study with some taxonomical implications. *Biochem Syst Ecol* 19(3):223–235
- Johnson A-L, Bergman J, Sjogren M, Bohlin L (2004) Synthesis of barettin. *Tetrahedron* 60(4):961–965
- Karlsson A, Berggren M, Lundin K, Sundin R (2014) Svenska artprojektets marina inventering—slutrapport. ArtDatabanken, SLU, Uppsala
- Kimura M (1983) The neutral theory of molecular evolution. Cambridge University Press, Cambridge
- Kingston JF, Benson E, Gregory B, Fallis AG (1979) Sterols from the marine sponges *Orina arcoferus* and *Geodia megastrella*. *J Nat Prod* 42(5):528–531
- Klitgaard AB, Tendal OS (2004) Distribution and species composition of mass occurrences of large-sized sponges in the northeast Atlantic. *Prog Oceanogr* 61(1):57–98
- Köck M, Muñoz J, Cychon C, Timm C, Schmidt G (2013) The Arctic sponge *Haliclona viscosa* as a source of a wide array of 3-alkyl pyridine alkaloids. *Phytochem Rev* 12(3):391–406. doi:10.1007/s11101-012-9249-1
- Kong F, Andersen RJ (1993) Polymastiamide A, a novel steroid/amino acid conjugate isolated from the Norwegian marine sponge *Polymastia boletiformis* (Lamarck, 1815). *J Org Chem* 58(24):6924–6927. doi:10.1021/jo00076a073
- Kong F, Andersen RJ (1996) Polymastiamides B–F, novel steroid/amino acid conjugates isolated from the Norwegian marine sponge *Polymastia boletiformis*. *J Nat Prod* 59(4):379–385. doi:10.1021/np960098o
- Larsson J, Gottfries J, Muresan S, Backlund A (2007) ChemGPS-NP: tuned for navigation in biologically relevant chemical space. *J Nat Prod* 70(5):789–794. doi:10.1021/np070002y
- Leal MC, Hilario A, Munro MHG, Blunt JW, Calado R (2016) Natural products discovery needs improved taxonomic and geographic information. *Nat Prod Rep* 33(6):747–750. doi:10.1039/c5np00130g
- Leal MC, Puga J, Serôdio J, Gomes NCM, Calado R (2012) Trends in the discovery of new marine natural products from invertebrates over the last two decades—where and what are we bioprospecting? *PLoS ONE* 7(1):e30580
- Lee S, Kirby J (1963) The X-Men #1. Marvel Comics
- Li H, Bowling JJ, Fronczek FR, Hong J, Jabba SV, Murray TF, Ha N-C, Hamann MT, Jung JH (2013) Asteropsin A: an unusual cystine-crosslinked peptide from porifera enhances neuronal

- Ca²⁺ + influx. *Biochim Biophys Acta (BBA)—General Subjects* 1830(3):2591–2599. doi:[10.1016/j.bbagen.2012.11.015](https://doi.org/10.1016/j.bbagen.2012.11.015)
- Li H, Bowling JJ, Su M, Hong J, Lee B-J, Hamann MT, Jung JH (2014) Asteropsins B-D, sponge-derived knottins with potential utility as a novel scaffold for oral peptide drugs. *Biochim Biophys Acta* 1840(3):977–984. doi:[10.1016/j.bbagen.2013.11.001](https://doi.org/10.1016/j.bbagen.2013.11.001)
- Lidgren G, Andersson L, Bohlin L (1985) Studies of Swedish marine organisms. IV. Screening of biological activity. *Acta Pharm Suec* 22:351–356
- Lidgren G, Bohlin L, Bergman J (1986) Studies of Swedish marine organisms VII. A novel biologically active indole alkaloid from the sponge *Geodia baretti*. *Tetrahedron Lett* 27(28):3283–3284
- Lidgren G, Bohlin L, Christophersen C (1988) Studies of Swedish marine organisms, part X. biologically active compounds from the marine sponge *Geodia baretti*. *J Nat Prod* 51(6):1277–1280
- Lind K, Hansen E, Østerud B, Eilertsen K-E, Bayer A, Engqvist M, Leszczak K, Jørgensen T, Andersen J (2013) Antioxidant and anti-inflammatory activities of barettin. *Mar Drugs* 11(7):2655–2666
- Lind KF, Østerud B, Hansen E, Jørgensen TØ, Andersen JH (2015) The immunomodulatory effects of barettin and involvement of the kinases CAMK1 α and RIPK2. *Immunopharmacol Immunotoxicol* 37(5):458–464. doi:[10.3109/08923973.2015.1082584](https://doi.org/10.3109/08923973.2015.1082584)
- Lipinski C, Hopkins A (2004) Navigating chemical space for biology and medicine. *Nat* 432(7019):855–861. doi:[10.1038/nature03193](https://doi.org/10.1038/nature03193)
- Lippert H, Brinkmeyer R, Mülhaupt T, Iken K (2003) Antimicrobial activity in sub-Arctic marine invertebrates. *Polar Biol* 26(9):591–600. doi:[10.1007/s00300-003-0525-9](https://doi.org/10.1007/s00300-003-0525-9)
- Molinski TF, Dalisay DS, Lievens SL, Saludes JP (2009) Drug development from marine natural products. *Nat Rev Drug Discov* 8(1):69–85
- Montaser R, Luesch H (2011) Marine natural products: a new wave of drugs? *Future Med Chem* 3(12):1475–1489. doi:[10.4155/fmc.11.118](https://doi.org/10.4155/fmc.11.118)
- Morrow C, Cárdenas P (2015) Proposal for a revised classification of the Demospongiae (Porifera). *Frontiers in Zool* 12(7):1–27. doi:[10.1186/s12983-015-0099-8](https://doi.org/10.1186/s12983-015-0099-8)
- Muigg P, Rosén J, Bohlin L, Backlund A (2013) In silico comparison of marine, terrestrial and synthetic compounds using ChemGPS-NP for navigating chemical space. *Phytochem Rev* 12(3):449–457. doi:[10.1007/s11101-012-9256-2](https://doi.org/10.1007/s11101-012-9256-2)
- Murillo FJ, Muñoz PD, Cristobo J, Ríos P, González C, Kenchington E, Serrano A (2012) Deep-sea sponge grounds of the Flemish Cap, Flemish Pass and the Grand Banks of Newfoundland (Northwest Atlantic Ocean): distribution and species composition. *Mar Biol Res* 8(9):842–854
- Newman DJ, Cragg GM (2016) Drugs and drug candidates from marine sources: an assessment of the current “State of Play”. *Planta Med* 82(09/10):775–789. doi:[10.1055/s-0042-101353](https://doi.org/10.1055/s-0042-101353)
- O’Keefe BR (2001) Biologically active proteins from natural product extracts. *J Nat Prod* 64(10):1373–1381. doi:[10.1021/np0103362](https://doi.org/10.1021/np0103362)
- Olsen EK, Hansen E, Moodie LW, Isaksson J, Sepčić K, Cergolj M, Svenson J, Andersen JH (2016a) Marine AChE inhibitors isolated from *Geodia baretti*: natural compounds and their synthetic analogs. *Org Biomol Chem* 14:1629–1640. doi:[10.1039/C5OB02416A](https://doi.org/10.1039/C5OB02416A)
- Olsen EK, Søderholm KL, Isaksson J, Andersen JH, Hansen E (2016b) Metabolomic profiling reveals the N-Acyl-Taurine Geodiataurine in extracts from the marine sponge *Geodia macandrewii* (Bowerbank). *J Nat Prod* 79(5):1285–1291. doi:[10.1021/acs.jnatprod.5b00966](https://doi.org/10.1021/acs.jnatprod.5b00966)
- Oprea TI, Gottfries J (2001) Chemography: the art of navigating in chemical space. *J Comb Chem* 3(2):157–166. doi:[10.1021/cc0000388](https://doi.org/10.1021/cc0000388)
- Pearson K (1901) On lines and planes of closest fit to systems of points in space. *Phil Mag Ser 6* 2(11):559–572. doi:[10.1080/14786440109462720](https://doi.org/10.1080/14786440109462720)
- Radax R, Rattei T, Lanzen A, Bayer C, Rapp HT, Urich T, Schleper C (2012) Metatranscriptomics of the marine sponge *Geodia baretti*: tackling phylogeny and function of its microbial community. *Environ Microbiol* 14(5):1308–1324

- Rasmussen T, Jensen J, Anthoni U, Christophersen C, Nielsen PH (1993) Structure and synthesis of bromoindoles from the marine sponge *Pseudosuberites hyalinus*. *J Nat Prod* 56(9):1553–1558. doi:[10.1021/np50099a014](https://doi.org/10.1021/np50099a014)
- Sjöblom T, Bohlin L, Christophersen C (1983) Studies of Swedish marine organisms. II. Muscle-relaxant alkaloids from the marine bryozoan *Flustra foliacea*. *Acta pharma Suec* 20(6):415–418
- Sjögren M, Dahlström M, Göransson U, Jonsson PR, Bohlin L (2004a) Recruitment in the field of *Balanus improvisus* and *Mytilus edulis* in response to the antifouling cyclopeptides baretin and 8,9-dihydrobaretin from the marine sponge *Geodia barretti*. *Biofouling* 20(6):291–297
- Sjögren M, Göransson U, Johnson AL, Dahlstrom M, Andersson R, Bergman J, Jonsson PR, Bohlin L (2004b) Antifouling activity of brominated cyclopeptides from the marine sponge *Geodia barretti*. *J Nat Prod* 67(3):368–372
- Sjögren M, Johnson A-L, Hedner E, Dahlström M, Göransson U, Shirani H, Bergman J, Jonsson PR, Bohlin L (2006) Antifouling activity of synthesized peptide analogs of the sponge metabolite baretin. *Peptides* 27(9):2058–2064. doi:[10.1016/j.peptides.2006.03.027](https://doi.org/10.1016/j.peptides.2006.03.027)
- Sjögren M, Jonsson PR, Dahlström M, Lundälv T, Burman R, Göransson U, Bohlin L (2011) Two brominated cyclic dipeptides released by the coldwater marine sponge *Geodia barretti* act in synergy as chemical defense. *J Nat Prod* 74(3):449–454
- Skropeta D (2008) Deep-sea natural products. *Nat Prod Rep* 25(6):1131–1166. doi:[10.1039/b808743a](https://doi.org/10.1039/b808743a)
- Skropeta D, Wei L (2014) Recent advances in deep-sea natural products. *Nat Prod Rep* 31(8):999–1025. doi:[10.1039/C3NP70118B](https://doi.org/10.1039/C3NP70118B)
- Sölter S, Dieckmann R, Blumenberg M, Francke W (2002) Baretin, revisited? *Tetrahedron Lett* 43(18):3385–3386
- Strese Å, Backlund A, Alsmark C (2014) A recently transferred cluster of bacterial genes in *Trichomonas vaginalis*—lateral gene transfer and the fate of acquired genes. *BMC Evol Biol* 14(1):1–13. doi:[10.1186/1471-2148-14-119](https://doi.org/10.1186/1471-2148-14-119)
- Su M, Li H, Wang H, Kim EL, Kim HS, Kim E-H, Lee J, Jung JH (2016) Stable and biocompatible cystine knot peptides from the marine sponge *Asteropus* sp. *Bioorg Med Chem* 24(13):2979–2987. doi:[10.1016/j.bmc.2016.05.006](https://doi.org/10.1016/j.bmc.2016.05.006)
- Tadesse M, Gulliksen B, Strøm MB, Styrvold OB, Haug T (2008) Screening for antibacterial and antifungal activities in marine benthic invertebrates from northern Norway. *J Invertebr Pathol* 99(3):286–293. doi:[10.1016/j.jip.2008.06.009](https://doi.org/10.1016/j.jip.2008.06.009)
- Takada K, Hamada T, Hirota H, Nakao Y, Matsunaga S, van Soest RWM, Fusetani N (2006) Asteropine a, a sialidase-inhibiting conotoxin-like peptide from the marine sponge *Asteropus simplex*. *Chem Biol* 13(6):569–574. doi:[10.1016/j.chembiol.2006.05.010](https://doi.org/10.1016/j.chembiol.2006.05.010)
- Théel H (1908) Om utvecklingen af Sveriges zoologiska hafsstation Kristineberg och om djurlifvet i angränsande haf och fjordar. *Arkiv För Zoologi* 4(5):1–136
- Thiel V, Blumenberg M, Hefter J, Pape T, Pomponi S, Reed J, Reitner J, Wörheide G, Michaelis W (2002) A chemical view of the most ancient metazoa—biomarker chemotaxonomy of hexactinellid sponges. *Naturwissenschaften* 89(2):60–66
- Verdes A, Anand P, Gorson J, Jannetti S, Kelly P, Leffler A, Simpson D, Ramrattan G, Holford M (2016) From mollusks to medicine: a venomics approach for the discovery and characterization of therapeutics from Terebridae peptide toxins. *Toxins* 8(4). doi:[10.3390/toxins8040117](https://doi.org/10.3390/toxins8040117)ARTN 117
- Vikeved E, Backlund A, Alsmark C (2016) The dynamics of lateral gene transfer in genus *Leishmania*—a route for adaptation and species diversification. *PLoS Negl Trop Dis* 10(1):e0004326. doi:[10.1371/journal.pntd.0004326](https://doi.org/10.1371/journal.pntd.0004326)
- Wahl M (1989) Marine epibiosis. I. Fouling and antifouling: some basic aspects. *Mar Ecol Prog Ser* 58(1–2):175–189. doi:[10.3354/meps058175](https://doi.org/10.3354/meps058175)

Major Antimicrobial Representatives from Marine Sponges and/or Their Associated Bacteria

Fei He, Linh H. Mai, Johan Gardères, Amjad Hussain, Vesna Erakovic Haber and Marie-Lise Bourguet-Kondracki

Abstract The rapid emergence of resistant bacteria during the last 20 years has stimulated research efforts in order to overcome this thorny problem. Marine sponges and their associated bacteria, which have been proven to be a source of bioactive natural products, have appeared as a promising opportunity to identify new antibiotic compounds. An overview of the major antibacterial compounds isolated from marine sponges and/or their associated bacteria is presented in this chapter, highlighting new potential antibiotics.

1 Introduction

The effectiveness of antimicrobial therapy is frequently mentioned as a great success story of modern medicine. The introduction of antibiotics into the medical practices has drastically changed the survival rates of human beings all around the world and has significantly increased the average life expectancy. Although one can be very happy, when one compares today's situation with that of 100 years ago, one should not forget that human pathogens are living organisms that have extraordinary capability to change and adapt to the new environment, including in the presence of antimicrobials. Therefore, emerging resistance to current antimicrobial therapy is all but surprising and presents serious threat to humans.

Fei He, Linh H. Mai, Johan Gardères, Amjad Hussain, Vesna Erakovic Haber, and Marie-Lise Bourguet-Kondracki are equally contributed.

F. He · L.H. Mai · J. Gardères · A. Hussain · M.-L. Bourguet-Kondracki (✉)
Laboratoire Molécules de Communication et Adaptation des Micro-organismes,
UMR 7245 MNHN-CNRS, Muséum National d'Histoire Naturelle,
57 rue Cuvier (C.P. 54), 75005 Paris, France
e-mail: bourguet@mnhn.fr

V. Erakovic Haber
Fidelta d.o.o., Prilaz baruna Filipovića 29, 10000 Zagreb, Croatia

Antimicrobial resistance is a resistance of microorganisms, such as bacteria, fungi parasites, and viruses, to antimicrobial drugs. Lack of adequate clinical treatment can lead to serious and/or persistent infections of affected individuals, in some cases causing even lethal outcome.

World Health Organization, in its April 2015 Fact sheet, reported that 480,000 cases of multidrug-resistant tuberculosis happened during 2013, an appearance of resistance against artemisinin-based combination therapies for *falciparum* malaria in Great Mekong subregion. High proportions of antibiotic resistance in bacteria that cause common infections (e.g., urinary tract infections, pneumonia, blood-stream infections) are reported in almost all regions of the world, as well as resistance to treatment for gonorrhea in 10 countries (WHO Fact sheet No. 194).

Immuno-compromised patients, either suffering from diseases causing immunological incompetence or being treated with therapies that suppress activity of the immunological system, are particularly prone towards bacterial infections caused by organisms not particularly virulent such as *Pseudomonas aeruginosa*, *Stenotrophomonas maltophilia*, and *Acinetobacter* spp. Acquired drug resistance by such microorganisms presents extremely serious life-threatening medical situation.

The highly methicillin-resistant *Staphylococcus aureus* bacteria (MRSA) represent 18% of the isolated *S. aureus* in Europe, 44% in the United States (CDDEP 2015), 16% in Canada, 47% in India (2014), and 90% in Latin America hospitals (2013 PAHO) (CDDEP, The state of world's antibiotics 2015). In addition, an increased number of infections caused by Gram-negative bacteria, such as *Escherichia coli* and *Klebsiella pneumoniae*, resistant to the current antibiotics, presents growing medical problem. Especially difficult to treat are extended-spectrum beta-lactamase (ESBL) producers which are resistant to third generation cephalosporins, whereas carbapenem-resistant enterobacteriaceae (CRE) are resistant even to the last resort antibiotic carbapenem (Glasner et al. 2013). During the year 2013, in 17 of 22 European countries, 85–100% of *E. coli* isolates were ESBL positive and five European countries reported an increase of carbapenem-resistant bacteria (CDDEP, The state of world's antibiotics 2015). The carbapenem resistance has been reported among 11% of *K. pneumoniae* and 2% of *E. coli* in USA hospitals during 2011. In India, resistance rate to carbapenem has been reported to be 13% among *E. coli* during 2013 and 57% among *K. pneumoniae* during 2014 (CDDEP, The state of world's antibiotics 2015).

Unlike other drug classes, only two new classes of antibiotics have been discovered in the past couple of decades: oxazolidinones and cyclic lipopeptides, former being synthetic molecules and latter natural products. According to the PEW Charitable Trust, there are 39 new antibiotics with the potential to treat serious bacterial infections currently in clinical development for the U.S. market. Two new drugs, approved by FDA last year, are combinations of already existing drug classes: cephalosporins and beta-lactamase inhibitors (Zerbaxa: Ceftolazane/Tazobactam and Avycaz: Ceftazidime/Avibactam) (The PEW Charitable Trust 2015). They are approved for complicated urinary tract and intra-abdominal infections, hospital-acquired pneumonia, and ventilator associated pneumonia. These combinations are active against ESKAPE pathogens but not against carbapenem-resistant *Enterobacteriaceae* and drug-resistant

Neisseria gonorrhoeae. Some of the compounds currently in Phase 3 of the clinical development demonstrate a potential to address carbapenem resistance; however all of them belong to already known antibiotic classes with no new mechanism of action (The PEW Charitable Trust 2015).

To cope with these issues, the search of novel antibiotics remains both urgency and a great challenge. Marine organisms have been found as a potential source of novel bioactive compounds and have been intensively explored, especially marine sponges with over 8600 valid species currently described. These metazoans, which live fixed on a substrate, are active filter feeders, which concentrate bacteria from environment for their nutrition. However, they also host various microbes such as heterotrophic bacteria, cyanobacteria, facultative anaerobes, archaea, unicellular protists, and fungi. They are now described as holobionts (Taylor et al. 2007; Webster and Taylor 2012). Their associated-bacteria have been particularly investigated because they can account up to 35% of the biomass of some demosponge species, reaching a density of bacterial population much greater than that of the surrounding water column. The mechanisms by which these sponge–microbe associations are established and maintained are still poorly understood. A complex process of acquisitions over time, both by vertical transmission through the embryos and/or by horizontal transmission through the filtration activity of environmental seawater by these animals, has been suggested (Schmitt et al. 2008; Bright and Bulgheresi 2010). The reported benefits that these associations may provide to the sponge include photosynthetic carbon fixation from symbiotic cyanobacteria, nitrogen fixation and nitrification, sulfate reduction, dehalogenation, anaerobic metabolism, contribution to sponge structural rigidity, or production of secondary metabolites for chemical defence (Webster and Blackall 2009; Roué et al. 2012). Those secondary metabolites, exactly because of their nature and function, are very likely to be of particular importance for novel antibiotic discovery.

Intensive chemical investigations during the last few decades on marine sponges collected from different geographical locations (The Bahamas, Indonesia, Mexico, Palau, Papua New Guinea, Philippines...) and/or from their associated microbes led to the discovery of thousands of bioactive compounds which revealed significant pharmacological activities such as anticancer, anti-kinase, antibacterial, antifungal, antimalarial, or anti-HIV activities.

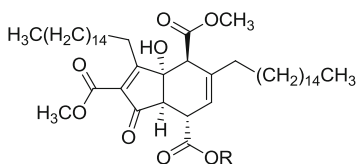
This chapter is an overview of the main antibacterial compounds isolated from marine sponges and/or their associated bacteria. The aim was not to be exhaustive but to present the major diverse antimicrobial representatives. From 2001 to 2010, 145 antibacterial compounds, isolated from marine sponges, have been reported, mainly from the order Dictyoceratida (Mehbub et al. 2014). So far, additional new molecules have enhanced this chemodiversity. The major antibacterial compounds from marine sponges presented in this chapter have been classified into different chemical classes including, lipids, polyketides, steroids, terpenoids, alkaloids, peptides, and miscellaneous brominated derivatives. This selection has been enriched by some representatives obtained from sponge-associated bacteria.

2 Antimicrobial Compounds from Marine Sponges

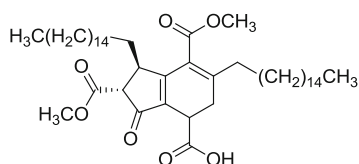
2.1 Lipids

The lipids are a broad and diverse group of naturally occurring organic compounds. Study of sponge lipids has been well documented (Bergé and Barnathan 2005; Barnathan 2009), and some sponge lipids have been reported as antimicrobials as illustrated by these few examples including fatty acid derivatives, glycolipids, and lysophospholipids.

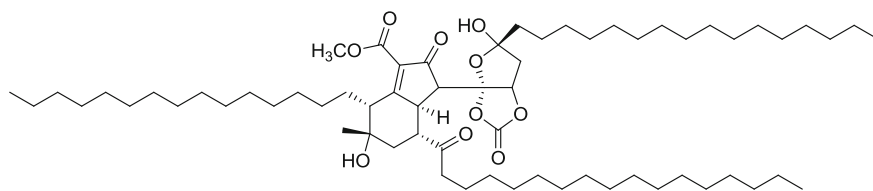
Three fatty acid derivatives, manzamenones L, M, and N were isolated from the Okinawan sponge *Plakortis* sp. These compounds consist of a tetrahydroindenone with three carboxyl groups and two hexadecanyl chains. Manzamenone M displayed moderate antimicrobial activities against the bacteria *E. coli* (MIC = 32 $\mu\text{g mL}^{-1}$) and *S. aureus* (MIC = 16 $\mu\text{g mL}^{-1}$) and against the yeasts *Candida albicans* (IC₅₀ = 32 $\mu\text{g mL}^{-1}$) and *Cryptococcus neoformans* (IC₅₀ = 8 $\mu\text{g mL}^{-1}$). Manzamenone N also exhibited moderate antimicrobial activities against *E. coli* (MIC = 32 $\mu\text{g mL}^{-1}$), *C. albicans* (IC₅₀ = 32 $\mu\text{g mL}^{-1}$), and *C. neoformans* (IC₅₀ = 4 $\mu\text{g mL}^{-1}$). According to the structure of the compounds, since Manzamenone L did not show any antimicrobial activity, the presence of a free carboxylic acid at C-5 position was reported as being important for the antimicrobial activities (Kubota et al. 2013a). The trimeric fatty acid Manzamenone O, with a novel skeleton consisting of C–C bonded octahydroindenone and dioxabicyclo[3.3.0]octane moieties and three long aliphatic chains, exhibited antimicrobial activities against *Micrococcus luteus*, *Aspergillus niger*, and *Trichophyton mentagrophytes* with MIC values of 4, 8, and 8 $\mu\text{g mL}^{-1}$, respectively (Tanaka et al. 2013a).



Manzamenone L: R = OCH₃
Manzamenone M: R = H

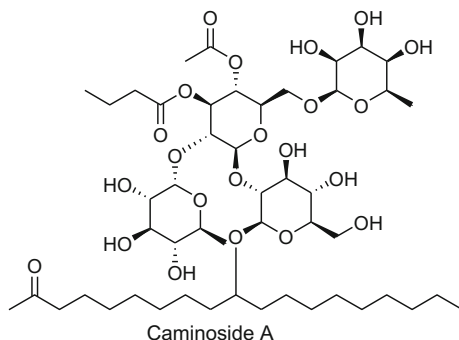


Manzamenone N

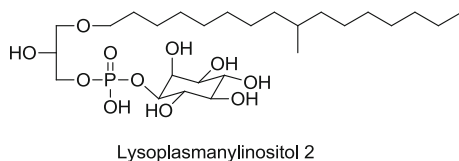
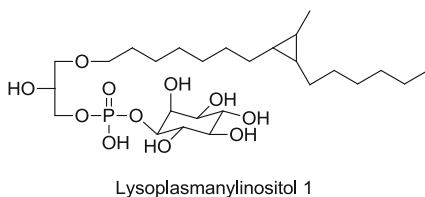


Manzamenone O

Bioassay-guided fractionation of the *Caminus sphaeroconia* extract led to the isolation of the antimicrobial glycolipid caminoside A (Lington et al. 2002). This was the first natural product known to be active ($IC_{50} = 20 \mu M$) in a bioassay designed to screen type III secretion inhibitors that potentially represent novel agents to control pathogenic *E. coli* by thwarting their pathogenicity without killing the bacteria. In addition, caminoside A showed potent in vitro inhibition against methicillin-resistant *S. aureus* ($MIC = 12 \mu g mL^{-1}$) and vancomycin-resistant *Enterococcus* ($MIC = 12 \mu g mL^{-1}$). It did not show any inhibition against the Gram-negative bacteria *E. coli*.

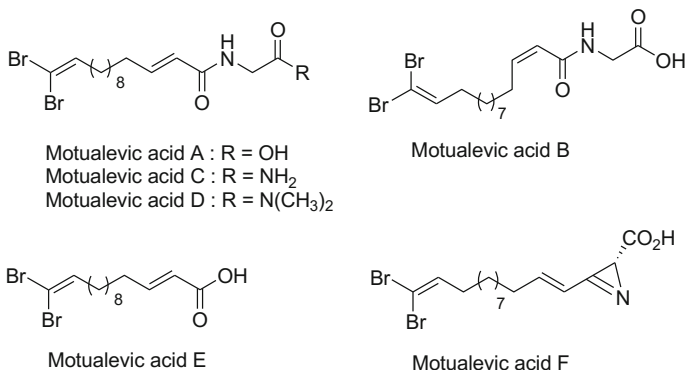


Two antimicrobial lysoplasmanylinositols 1 and 2 were isolated from the marine sponge, *Theonella swinhoei* (Matsunaga et al. 2001). Lysoplasmanylinositol 1 was active against *E. coli*, showing a 12 mm inhibitory zone at $50 \mu g disk^{-1}$, whereas lysoplasmanylinositol 2 was found only active in bioautography, used as a means of target-directed isolation of active molecules on chromatogram. Both compounds were inactive against the fungus *Mortierella rammaniana*.

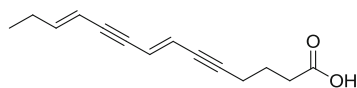


Six brominated antibacterial lipids namely, motualevic acids A–F, were isolated from the Fijian sponge *Siliquariaspongia* sp. (Keffer et al. 2009). Motualevic acid F

was reported as the first example of a long-chain 2*H*-azirine containing a C-2 carboxylic acid. Motualevic acids (A–D) are the first glyceryl conjugates of the ω -brominated lipid (*E*)-14,14-dibromotetradeca-2,13-dienoic acid. Motualevic acids A and F, both containing a carboxylic acid, are the only compounds to inhibit the growth of *S. aureus* and methicillin-resistant *S. aureus* at 10.9–1.2 and 9.3–3.9 $\mu\text{g mL}^{-1}$, respectively. These results provided a starting point for optimization of new MRSA-inhibitors.

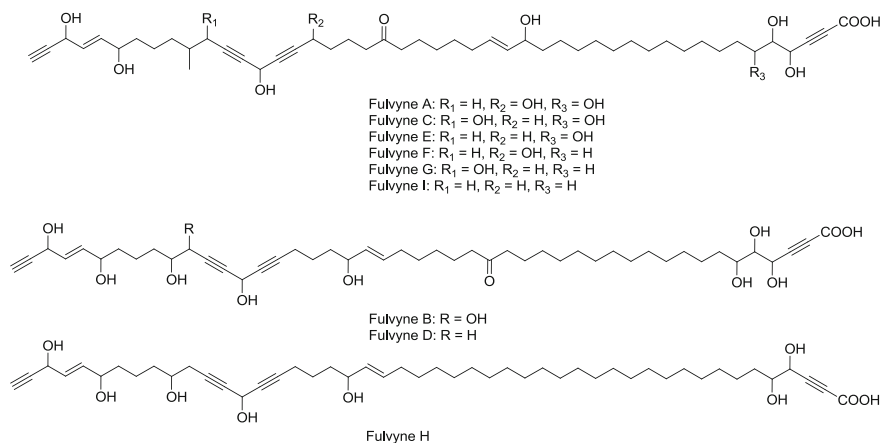


The C₁₄ acetylenic acid, isolated as an antimicrobial compound from a marine sponge *Oceanapia* sp. (Matsunaga et al. 2000), revealed inhibitory activity against both Gram-positive and Gram-negative bacterial strains, as well as various yeasts and fungi. In particular, this C₁₄ unsaturated acetylenic fatty acid was moderately active against four mutants of *Saccharomyces cerevisiae* and *C. albicans*, but was inactive against *Penicillium chrysogenum* and *Mortierella ramanniana*.

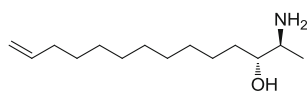


(7*E*,11*E*)-tetradeca-7,11-dien-5,9-diynoic acid

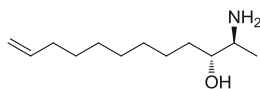
Nine linear polyoxygenated acetylene derivatives, named fulvynes A–I, exhibiting the uncommon propargylic acid terminal functionality, were isolated from the butanolic extract of the Mediterranean sponge *Haliclona fulva* (Nuzzo et al. 2012). All these fulvynes were found to be active against a chloramphenicol-resistant Gram-positive strain of *Bacillus subtilis* Cm (PY79) with IC₅₀ values ranging from 12 to 60 μM ; the fulvynes A, D, E, F, and I were the most active.



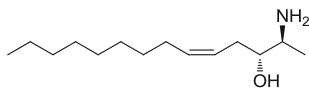
Halaminols A–C are three amino alcohols, reported as presumably derived from *L*-alanine from the tropical marine sponge *Haliclona* n. sp. They revealed antimicrobial activities against the growth of *E. coli*, *B. subtilis*, *C. albicans*, *T. mentagrophytes*, and *Cladosporium resinae*. Halaminols A and B were the most effective, showing antifungal activity against *T. mentagrophytes*, and *C. resinae* with a 10 mm zone of inhibition in a standard paper disk assay (0.12 mg disk⁻¹) (Clark et al. 2001). It is suggested that the antimicrobial activity of these linear amino alcohols may result from their detergent-like nature, which is likely to disrupt cell membranes. Authors reported that acetylation of these halaminols revealed a decrease of the antimicrobial activity, probably by altering the surfactant properties of the metabolites. Furthermore, they are presented as potential antifouling agents due to their capacity to disrupt the developmental processes of induced larval settlement of the ascidian *Herdmania curvata*.



Halaminol A



Halaminol B

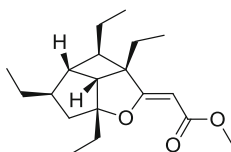


Halaminol C

2.2 Polyketides

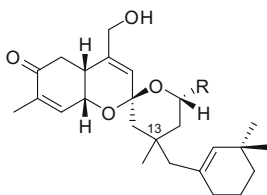
The polyketides are a structurally very diverse family of natural products. A wide range of biological activities have been reported for this class of metabolites, including antimicrobial activities.

Hippolachnin A, isolated from the sponge *Hippospongia lachne*, is an antifungal polyketide with an unusual carbon skeleton containing a four-membered ring. This compound was found active against *C. neoformans*, *Trichophyton rubrum*, and *Microsporium gypseum* with MIC values of 0.41 μM for each fungal strain. No significant cytotoxic activity was observed against the human colon carcinoma HCT116, the lung carcinoma A549, and the cervical cancer cell lines HeLa (Piao et al. 2013).



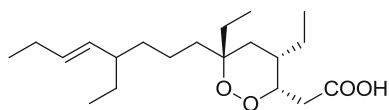
Hippolachnin A

The tetracyclic sesterterpene gombaspiroketal A and its corresponding hemiacetal C, isolated from the sponge *Clathria gombawuiensis*, exhibited activities against *S. aureus* ATCC6538p (MIC = 25.0 $\mu\text{g mL}^{-1}$, for both compounds), *B. subtilis* ATCC6633 (MIC = 6.25 $\mu\text{g mL}^{-1}$, for both compounds), *Kocuria rhizophila* NBRC 12708 (MIC = 12.5 and 25.0 $\mu\text{g mL}^{-1}$, respectively), *Salmonella enterica* ATCC14028 (MIC = 12.5 and 25.0 $\mu\text{g mL}^{-1}$, respectively), and *Proteus hauseri* NBRC3851 (MIC = 6.25 and 12.5 $\mu\text{g mL}^{-1}$, respectively). They also displayed cytotoxic activities against the human myelogenous leukemia cell line K562 and the carcinomic human alveolar basal epithelial cell line A549 with LC_{50} values from 0.70 to 4.65 μM (Woo et al. 2014).



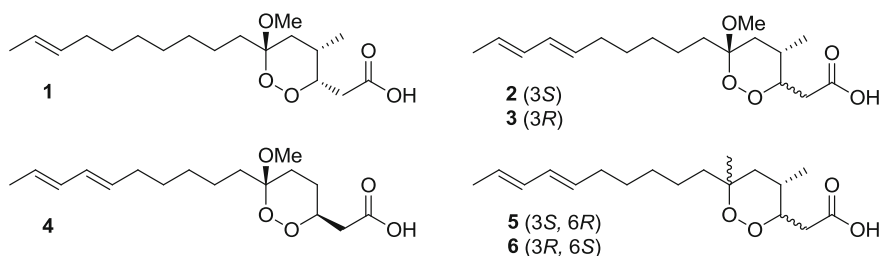
Gombaspiroketal A (R = OMe, 13R)
Gombaspiroketal C (R = OH, 13R)

Manadodioxan E, a polyketide endoperoxide isolated from the marine sponge *Plakortis bergquistae* collected from north Sulawesi, Indonesia, displayed antibacterial activities at the concentration of $10 \mu\text{g disk}^{-1}$ against *E. coli* (zone of inhibition of 16 mm) and *Bacillus cereus* (zone of inhibition of 9 mm), while its oxocongener was found inactive (Gushiken et al. 2015).



Manadodioxan E

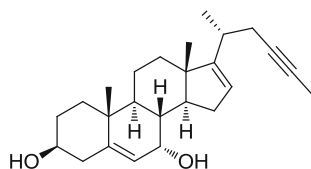
Cyclic peroxides **1–6**, isolated from the Korean sponge *Plakortis simplex*, showed interesting antifungal activities against *C. albicans* at the concentration of $10 \mu\text{g disk}^{-1}$ with growth inhibition zones from 16 to 20 mm, compared to the control amphotericin (15 mm). However, these compounds displayed a high cytotoxicity against the RAW264.7 cell line (murine macrophage cell line) with EC_{50} values from 2 to $4 \mu\text{g mL}^{-1}$ (Oh et al. 2013).



2.3 Steroids

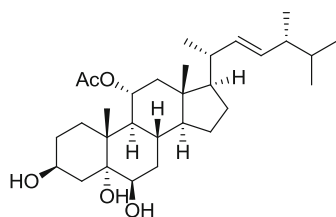
Polyhydroxylated sterols as well as some sulfated derivatives of revealed potential antimicrobial activities.

A sterol, gelliusterol E, was isolated from the Red Sea sponge *Callyspongia* aff. *implexa* (26,27-bisnorcholest-5,16-dien-23-yn-3 β ,7 α -diol), which inhibited the formation and growth of *Chlamydia trachomatis* inclusions in a dose-dependent manner with an IC_{50} value of $2.3 \mu\text{M}$ (Abdelmohsen et al. 2015).

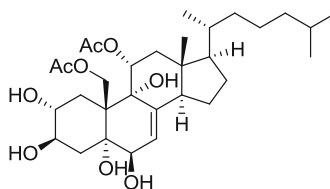


Gelliusterol E

The sponge *Haliclona crassibola* provided polyhydroxylated antimicrobial sterols. Halicrasterol D was efficient against the Gram-positive bacteria *Enterococcus faecalis* ATCC 29212 (MIC = 4.0 $\mu\text{g mL}^{-1}$). The polyhydroxylated sterol H (5 α -cholest-7-ene-2 α ,3 β ,5 α ,6 β ,9 α ,11 α ,19-heptol 11,19-diacetate) revealed the same antibacterial activity (MIC value of 8.0 $\mu\text{g mL}^{-1}$) against both the methicillin-sensitive *S. aureus* strain ATCC 29213, and the methicillin-resistant *S. aureus* strains 43300. This sterol also exhibited a moderate activity against *B. subtilis* ATCC 21332, and *Bacillus licheniformis* ATCC 10716 with MIC values of 16 $\mu\text{g mL}^{-1}$ (Cheng et al. 2013).

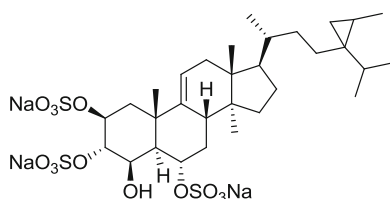
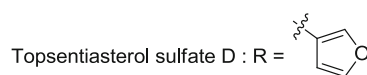
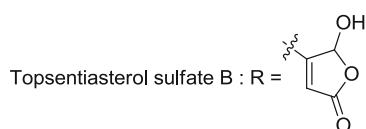
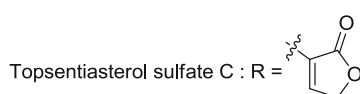
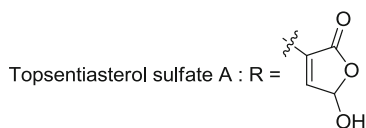
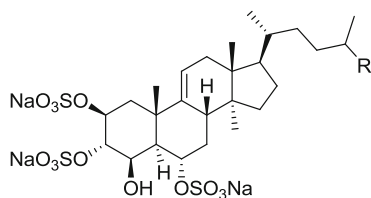


Halicrasterol D



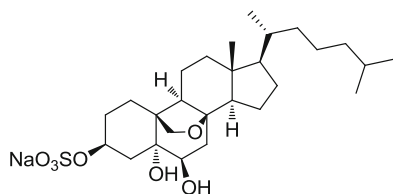
Polyhydroxylated sterol H

Topsentiasterol sulfates A–E were identified from a marine sponge *Topsentia* sp. collected at Ishigaki Island, Okinawa. The polysulfated sterols A–D have the particularity to possess a butenolide or a furan functionality at the end of the side chain. They all showed antibacterial activities against *P. aeruginosa* and *E. coli* at the concentration of 10 $\mu\text{g disk}^{-1}$, but only topsentiasterol sulfates D and E displayed antifungal activities against *M. ramanniana* and *C. albicans* at the same concentration (Fusetani et al. 1994).

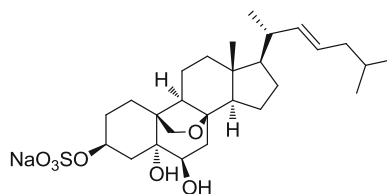


Topsentiasterol sulfate E

Two other steroid sulfates namely, eurysterols A and B, were isolated from an unidentified marine sponge of the genus *Euryspongia* collected in Palau (Boonlarppradab and Faulkner 2007). Both compounds exhibited the same antifungal activity against amphotericin B-resistant and wild-type strains of *C. albicans* with MIC values of 15.6 and 62.5 $\mu\text{g mL}^{-1}$, respectively. But they also displayed cytotoxicity against the human colon carcinoma cell line HCT116 with IC_{50} values of 2.9 and 14.3 $\mu\text{g mL}^{-1}$, respectively. These results predicted the presence of the double bond as a responsible factor for reducing the biological activities.



Eurysterol A

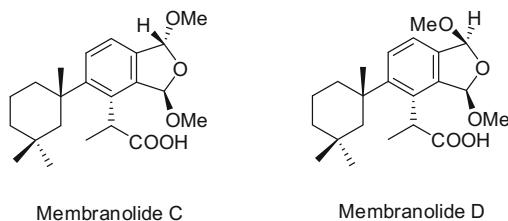


Eurysterol B

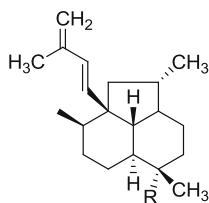
2.4 Terpenoids

Various terpenoids exhibiting the antimicrobial potential have been reported so far. Among the subclasses of terpenoids, sesquiterpenes, diterpenes are the most prominent ones. Some meroterpenes have also been found associated with antimicrobial activities.

Two diterpenes, named membranolides C and D, bearing a carboxylic group, were isolated from the Antarctic sponge *Dendrilla membranosa* (Ankisetty et al. 2004). Both exhibited moderate antibacterial activities against *E. coli*, and *C. albicans* with inhibitory zones ranging from 4 to 9 mm ($200 \mu\text{g disk}^{-1}$). At the same concentration, membranolidide D was the only compound to show a 7 mm zone of inhibition against *S. aureus*.

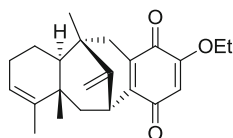


The Caribbean sponge *Svenzea flava* provided three tricyclic marine diterpenes possessing the isoneoamphilectane backbone with antibacterial activities against *Mycobacterium tuberculosis* H₃₇Rv. The three natural compounds identified as 7-isocyanoisoneoamphilecta-1(14),15-diene, 7-methylaminoisoneoamphilecta-1(14),15-diene, and 7-formamidoisoneoamphilecta-1(14),15-diene revealed a MIC value of 8, 15, and 32 $\mu\text{g mL}^{-1}$, respectively. However, the most effective derivative was the semisynthetic compound 7-amidoisoneoamphilecta-1(14),15-diene with a MIC value of 6 $\mu\text{g mL}^{-1}$ and no cytotoxicity has been shown against VERO cells (until 128 $\mu\text{g mL}^{-1}$). This data suggests that the isoneoamphilectane skeleton, and not the isocyanide functionality, that might be the molecular feature responsible for the antituberculosis activity (Avilés et al. 2013).



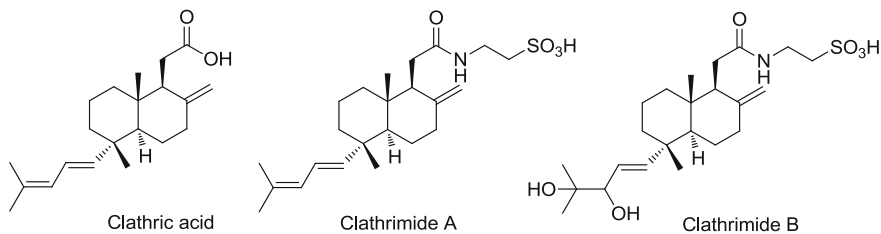
- 7-Isocyanoisoneoamphilecta-1(14),15-diene : R = NC
 7-Methylaminoisoneoamphilecta-1(14),15-diene : R = NHCH₃
 7-Formamidoisoneoamphilecta-1(14),15-diene : R = NHCHO
 7-Amidoisoneoamphilecta-1(14),15-diene : R = NH₂

Dysidarvarone A, a sesquiterpene quinone characterized by an unprecedented tetracyclic core, was initially isolated from the sponge, *Dysidea avara* (Jiao et al. 2012). The total synthesis of this compound was realized by a highly concise strategy in 10 steps (total yield of 11%) involving an advantageous intramolecular R-arylation of an elaborate ketone in order to access sufficient material for further biological evaluation of this important metabolite (Schmalzbauer et al. 2013). Dysidarvarone A, revealed a potent inhibitory effects against Gram-positive bacterial strains, in particular against various *Staphylococci* even at very low concentrations (*S. aureus* DSM346: MIC = 7.1 $\mu\text{g mL}^{-1}$, multidrug resistant *S. aureus* DSM11822: MIC₅₀ = 9.9 $\mu\text{g mL}^{-1}$, methicillin-resistant *S. aureus* N315: MIC₅₀ = 4.0 $\mu\text{g mL}^{-1}$, *S. aureus* Newman MIC₅₀ = 6.5 $\mu\text{g mL}^{-1}$, *Staphylococcus carnosus* DSM20501: MIC₅₀ = 0.2 $\mu\text{g mL}^{-1}$). Furthermore, it also showed inhibitory activity against *M. luteus* (MIC₅₀ = 5.5 $\mu\text{g mL}^{-1}$) but no inhibitory activity against various fungi/yeast and Gram-negative bacterial strains were observed. Dysidarvarone A also showed antiproliferative activities against various human cancer cell lines by changing the morphology of the treated cells as well as inhibitory activities against protein tyrosine phosphatase 1B (PTP1B).



Dysidarvarone A

Three unusual bicyclicditerpene, clathric acid and two *N*-acyl taurine derivatives, clathrimides A and B, were isolated from the marine sponge *Clathria compressa* (Gupta et al. 2012). Clathric acid showed MIC values of 32 $\mu\text{g mL}^{-1}$ against the *S. aureus* strain ATTC 6538P and 64 $\mu\text{g mL}^{-1}$ against both *S. aureus* strains methicillin-resistant ATTC33591 and vancomycin-resistant *S. aureus*. Clathrimides A and B showed no activity at concentrations up to 128 $\mu\text{g mL}^{-1}$, revealing the importance of the acid function. None of the compounds was found active against the Gram-negative bacterial strains *E. coli* KCTC 1923 and *Klebsiella pneumonia* ATCC 10031 when tested at 128 $\mu\text{g mL}^{-1}$.

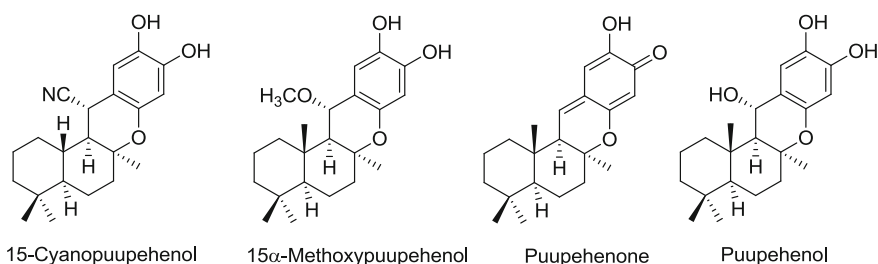


Clathric acid

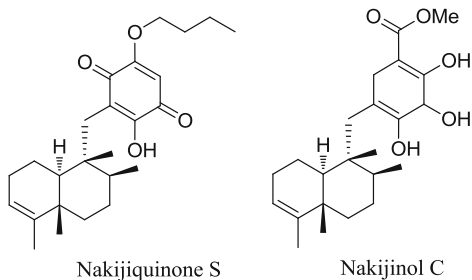
Clathrimide A

Clathrimide B

15-Cyanopuupehenol is an adduct of HCN and a mixed sesquiterpene—shikimate sponge metabolite of the order Dictyoceratida (Hamann and Scheuer 1991). It exhibited antimicrobial activity of 6 mm disk⁻¹ at 5 µg mL⁻¹ against *Penicillium notatum* (10 mm partial inhibition), *T. mentagrophytes* (9 mm), and *S. cerevisiae* (7 mm). The related compounds puupehenone and 15α-methoxypuupehenol were isolated from the newly identified Caledonian marine sponge *Hyrtios* sp. 15α-Methoxypuupehenol displayed similar antimicrobial activities as puupehenone against *S. aureus* (7 mm of growth inhibitory zone at 1 µg disk⁻¹) and *Candida tropicalis* (9 mm of growth inhibitory zone at 50 µg disk⁻¹). In addition, both compounds displayed cytotoxicity towards KB cells, with an IC₅₀ value of 0.5 and 6 µg mL⁻¹, respectively (Bourguet-Kondracki et al. 1999). Recently, puupehenol and puupehenone, isolated from a Hawaiian deepwater sponge of *Dactylospongia* sp., revealed the same antimicrobial activities at the concentration of 10 µg disk⁻¹ against the Gram-positive bacteria *S. aureus* (4 mm) and *B. cereus* (3 mm), respectively. Both were inactive against *E. coli* and *P. aeruginosa* at this concentration (Hagiwara et al. 2015).



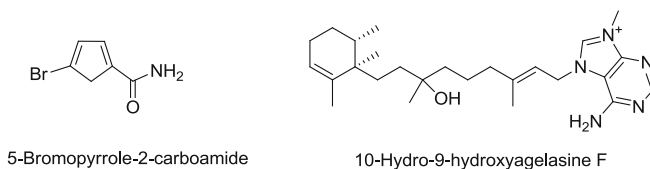
Two meroterpenoids, nakijiquinone S and nakijinol C, isolated from an Okinawan of *Spongiidae* sp., consist of a clerodane-type decalin ring connected to 2-butoxy-5-hydroxy-benzoquinone unit or methyl 2,3,4-trihydroxybenzoate unit through a methylene, respectively. Both displayed antibacterial activities against several bacteria and fungi. Nakijiquinone S appeared to be the most efficient antimicrobial against *S. aureus*, *B. subtilis* and *M. luteus* (MIC values of 1 µg mL⁻¹) and showed a less activity against the Gram-negative bacteria *E. coli* (MIC from 8 µg mL⁻¹) but it also revealed antifungal activities against *A. niger*, *T. mentagrophytes* and *C. albicans* (IC₅₀ from 4 to 16 µg mL⁻¹). Nakijinol C revealed activities against *S. aureus* and *M. luteus* (MIC values of 8 and 4 µg mL⁻¹, respectively) as well as against *A. niger* and *T. mentagrophytes* (IC₅₀ = 8 µg mL⁻¹). Both compounds did not exhibit any cytotoxicity against the murine lymphoma L1210 and human epidermoid carcinoma KB cells (IC₅₀ > 10 µg mL⁻¹) (Suzuki et al. 2014).

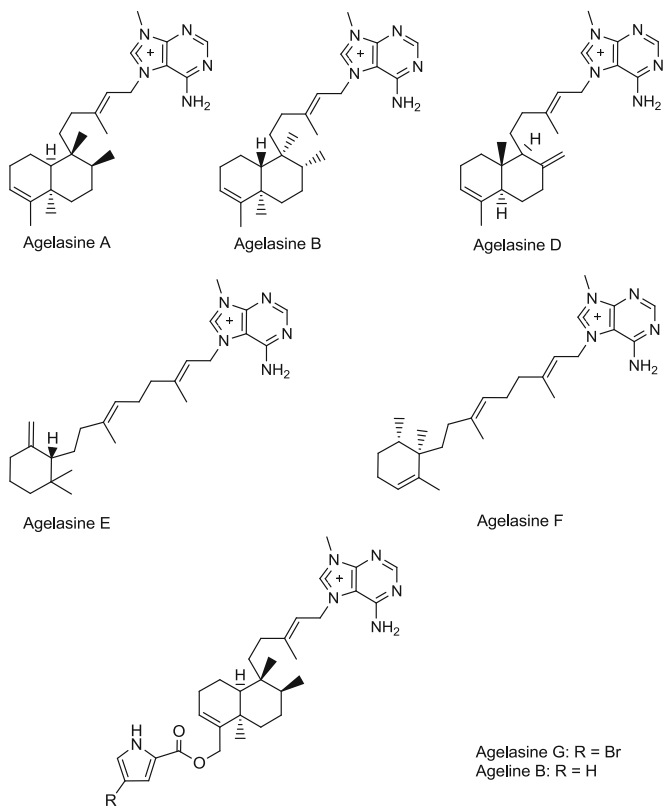


2.5 Alkaloids

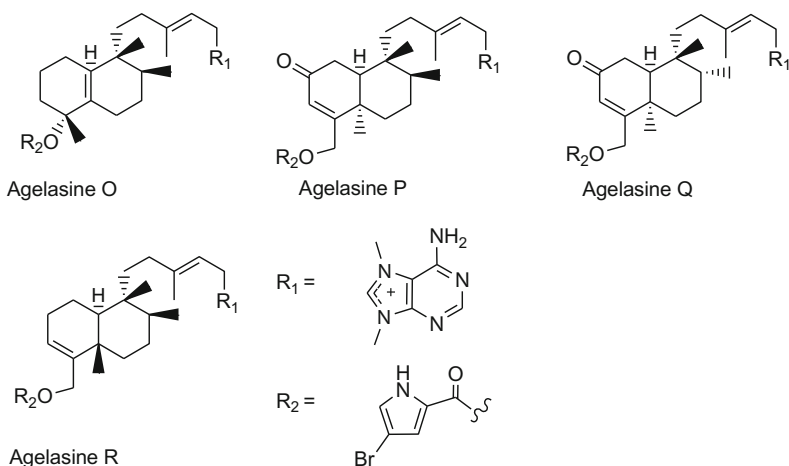
Marine sponges have afforded a wide variety of alkaloids, usually with complex skeletons. Their antimicrobial activities have been frequently reported.

Sponges belonging to the genus *Agelas* have also proved to be a rich source of purinoditerpenes in addition to bromopyrrole derivatives. 5-Bromopyrrole-2-carboamide and agelasine B were initially isolated from the Guinean sponge, *Agelas nakamurai* (Iwagawa et al. 1998). Both compounds showed antimicrobial activity against Gram-positive bacteria and fungi. Therefore, both showed the same IC_{50} values of 6.25, 3.13, 0.78, and 3.13 $\mu\text{g mL}^{-1}$ against *E. faecalis* 12964, *E. faecalis* 12367, *S. aureus* 12732MRSa and *C. neoformans* TIMM0354, respectively. Agelasine B was more active than 5-bromopyrrole-2-carboamide against *S. epidermidis* 13889 ($IC_{50} = 1.56$ vs. 3.13 $\mu\text{g mL}^{-1}$) but less active against *C. albicans* IFO1269 ($IC_{50} > 12.5$ vs. 6.25 $\mu\text{g mL}^{-1}$). Recently, the compounds 10-hydro-9-hydroxyagelasine F, agelasines A, B, D, E, F, and G and the ageline B, isolated from the sponge *A. nakamurai*, were evaluated for their antibacterial activities against the bacterium *Mycobacterium smegmatis* showing antimycobacterial activities at the concentration of 20 $\mu\text{g disk}^{-1}$ with inhibition zones ranging from 10 to 18 mm, compared to 30 mm of the control streptomycin sulfate at the same concentration. None of these compounds exhibited any cytotoxic activity against the human hepatoma Huh7 and bladder EJ1 carcinoma ($IC_{50} > 10 \mu\text{M}$) (Abdul et al. 2015).

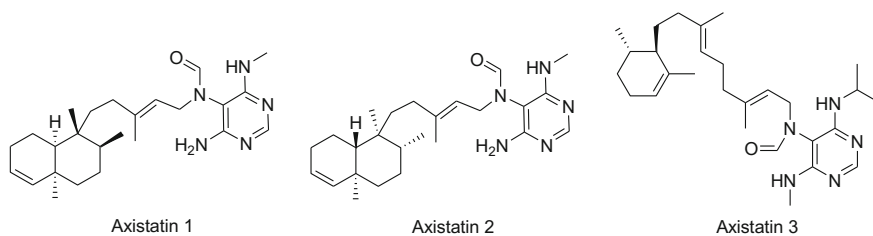




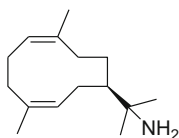
From an unidentified Okinawan marine sponge of *Agelas* sp. some diterpene alkaloids with a 9-*N*-methyladenine and a pyrrole units were isolated, especially agelasines O, P, Q, (Kubota et al. 2012). These latter showed potent growth inhibition activities against the bacteria *S. aureus*, *B. subtilis*, and *M. luteus* with MIC values ranging from 8.0 to 32.0 $\mu\text{g mL}^{-1}$, as well as against the fungi *A. niger*, *T. mentagrophytes*, *C. albicans*, and *C. neoformans* with more or less similar IC_{50} values.



Three pyrimidine diterpenes, identified as axistatins 1, 2, and 3, were isolated from the marine sponge, *Agelas axifera* (Pettit et al. 2013). Axistatins 1, 2, and 3 have identical antimicrobial profiles, inhibiting Gram-positive bacteria, the sensitive Gram-negative pathogen *N. gonorrhoeae*, and the opportunistic fungus *C. neoformans* (ranges from 1 to 64 $\mu\text{g mL}^{-1}$).

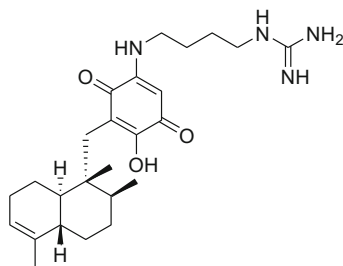


The germacranol sesquiterpene (1*Z*, 4*Z*)-7 α H-11-aminogermacra-1(10),4-diene, isolated from a Thai marine sponge of *Axinyssa* n. sp., exhibited interesting antimicrobial activities at the concentration of 500 $\mu\text{g disk}^{-1}$ against *S. aureus*, *B. subtilis*, and *C. albicans* with inhibition zones of 23, 22, and 27 mm, respectively (Satitpatipan and Suwanborirux 2004).



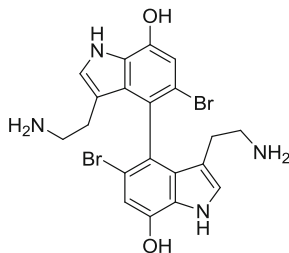
(1*Z*, 4*Z*)-7 α H-11-Aminogermacra-1(10),4-diene

The original sesquiterpenoid quinone nakijiquinone H with an aminogroup derived from amino acids, was isolated from Okinawan marine sponges of the family *Spongiidae*. It showed antibacterial activity against *M. luteus* (MIC = $16.7 \mu\text{g mL}^{-1}$), and antifungal activities against *C. neoformans* and *C. albicans* (same MIC values of $8.35 \mu\text{g mL}^{-1}$), as well as against *A. niger* (MIC = $16.7 \mu\text{g mL}^{-1}$) (Takahashi et al. 2008).



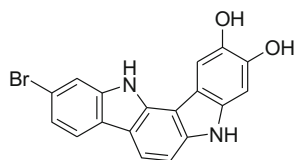
Nakijiquinone H

A unique C_2 -symmetrical 4,4'-bis (7-hydroxy) indole alkaloid, dendridine A, was isolated from an Okinawan marine sponge *Dictyodendrilla* sp. Dendridine A exhibited inhibitory activities against both Gram-positive bacteria *B. subtilis* and *M. luteus* with MIC values of 8.3 and $4.2 \mu\text{g mL}^{-1}$, respectively and the fungus *C. neoformans* with MIC value of $8.3 \mu\text{g mL}^{-1}$ (Tsuda et al. 2005).

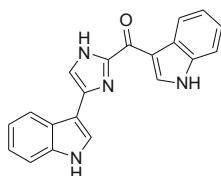


Dendridine A

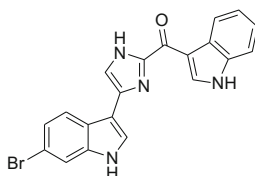
An antimicrobial compound, indolo[3,2-*a*]carbazole, was discovered from a deepwater sponge *Ateropus* sp. It also displayed antimicrobial activities against *C. albicans* with a MIC value of $25 \mu\text{g mL}^{-1}$ and methicillin-resistant *S. aureus* with a MIC value of $50 \mu\text{g mL}^{-1}$. No cytotoxicity was observed against the human PANC1 pancreatic carcinoma and NCI/ADR-Res ovarian adenocarcinoma cell lines at $5 \mu\text{g mL}^{-1}$ (Russell et al. 2013).

Indolo[3,2-*a*]carbazole

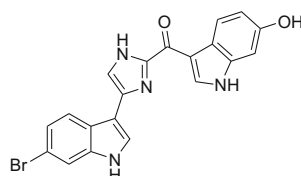
Bis-indole alkaloids, of the topsentin and hamacanthin classes, isolated from the sponge *Spongosorites* sp. were evaluated for their antimicrobial activities against various bacterial and fungi strains (Oh et al. 2006). Compounds of the hamacanthin class exhibited more potent antibacterial activity against medically important pathogenic fungi than those of the topsentin class. Deoxytopsentin and hamacanthin A also exhibited significant antibacterial activity against methicillin-resistant *S. aureus*, with MIC values less than $12.5 \mu\text{g mL}^{-1}$. In addition, hamacanthin A also showed potent antifungal activity against *C. albicans*, *T. rubrum*, *T. mentagrophytes*, and *Aspergillus fumigatus* with MIC values ranging from 6.25 to $50 \mu\text{g mL}^{-1}$.



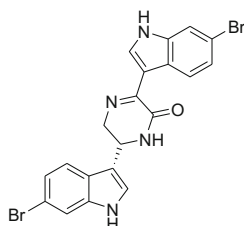
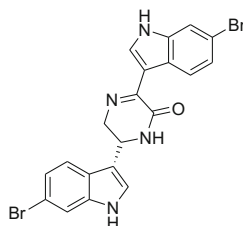
Deoxytopsentin



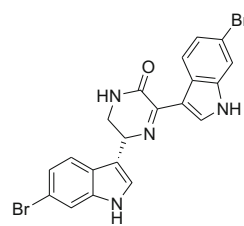
Bromodeoxytopsentin



Bromotopsentin

*trans*-4,5-Dihydro-hamacanthin A

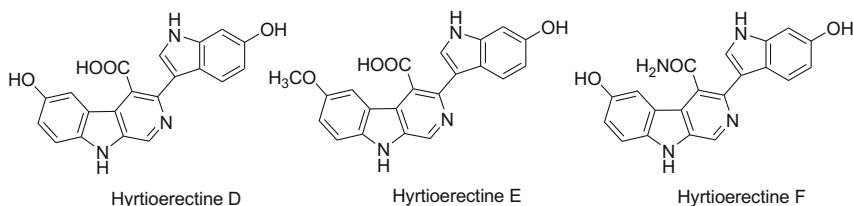
Hamacanthin A



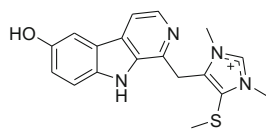
Hamacanthin B

Hyrtioerectines D, E, and F, isolated from a Red Sea sponge belonging to the genus *Hyrtios* are rare alkaloids possessing an indole nucleus and a β -carboline skeleton linked through C-3/C-3' of both fragments. They displayed moderate antifungal activities against *C. albicans* at the concentration of $10 \mu\text{g disk}^{-1}$ with inhibition zones of 17, 9, and 14 mm, respectively, compared to 35 mm at the same concentration for the control clotrimazole. They also showed to inhibit the growth

of *S. aureus* with inhibition zones of 20, 10, and 16 mm, respectively, compared to the control ampicillin (30 mm). But they were inactive against *E. coli*. It was reported that the three compounds exhibited low cytotoxic activity against the lung carcinoma A549, colorectal carcinoma HT29, and breast adenocarcinoma MDAMB231 with GI_{50} (concentration required to achieve 50% growth inhibition of the cells) from 25 to 100 μM ; hyrtioerectines D and F being slightly more cytotoxic than hyrtioerectine E (Youssef et al. 2013).

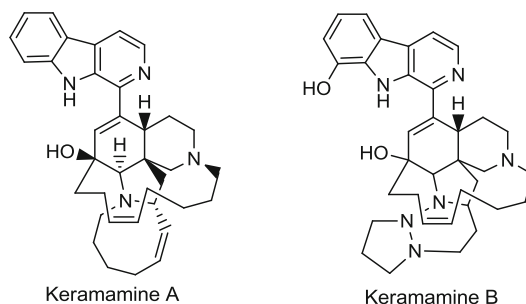


A β -carboline alkaloid with an imidazole ring, gesashidine A (Inuma et al. 2005), was isolated from an Okinawan marine sponge of the family *Thorectidae*. This compound showed antibacterial activity against *M. luteus* ($MIC = 16.6 \mu\text{g mL}^{-1}$).

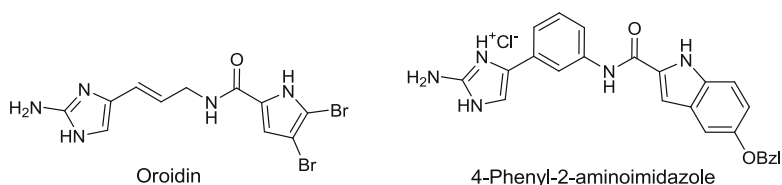


Gesashidine A

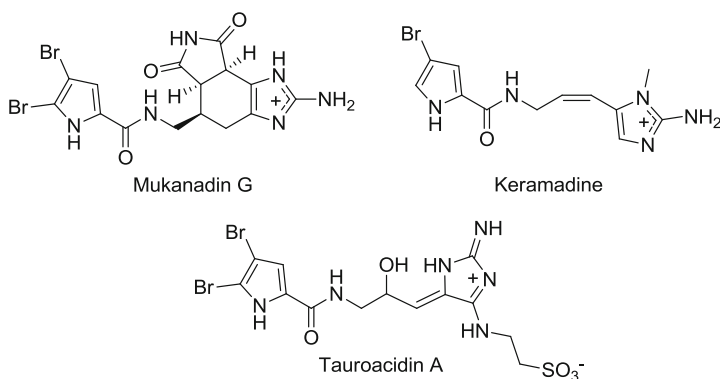
Keramamine A and B are β -carboline alkaloids having a 13-membered ring, which were isolated from the Okinawan marine sponge *Pellina* sp. as antimicrobial substances (Nakamura et al. 1987). Their MIC values against *S. aureus* were established as being 6.3 and 25 $\mu\text{g mL}^{-1}$, respectively.



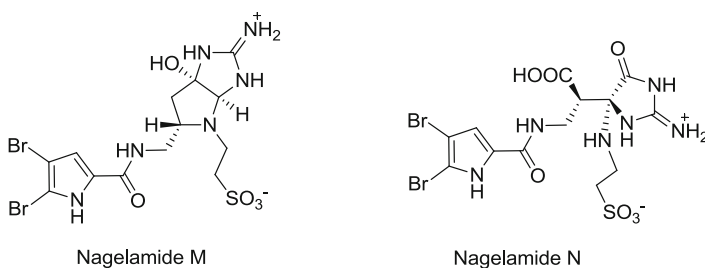
Marine sponges have produced diverse bromopyrrole alkaloids, in particular from the genus *Agelas*. The marine alkaloid oroidin, isolated from an unidentified sponge of the genus *Agelas*, as well as the preparation of an oroidin derivative series, were evaluated for their antimicrobial potencies. Oroidin showed to inhibit the growth of the Gram-positive bacterial strain *S. aureus* with a MIC₉₀ value of 100 μM. Interestingly, the 4-phenyl-2-aminoimidazole was found to have a MIC₉₀ value of 12.5 μM against both *S. aureus* and *E. faecalis* and 50 μM against *E. coli*. This latter alkaloid revealed no cytotoxic activity at the highest tested concentration (IC₅₀ > 100 μM) against the human hepatocellular carcinoma Huh-7 cell line whereas oroidin showed an IC₅₀ value of 21.2 μM (Zidar et al. 2014).



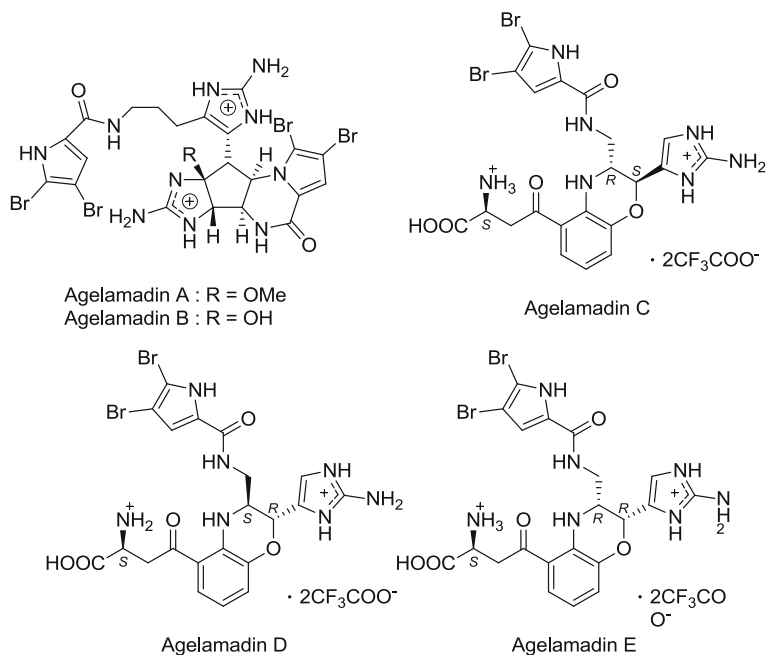
A series of bromopyrrole alkaloids, purified from an Okinawan marine sponge *Agelas* sp., were evaluated for their antimicrobial activities against diverse Gram-positive and Gram-negative bacterial strains as well as yeasts and fungi. The new bromopyrrole alkaloid mukanadin G, which has a tricyclic skeleton consisting of a fused tetrahydrobenzaminoimidazole and 2,5-dioxopyrrolidine functions, was the only one to show moderate antifungal activities against *C. albicans* and *C. neoformans* with IC₅₀ values of 16 and 8.0 μg mL⁻¹, respectively. Both known alkaloids keramadine and tauroacidin A exhibited antibacterial activity against *M. luteus* with MIC values of 4.0 and 8.0 μg mL⁻¹, respectively (Kusama et al. 2014c).



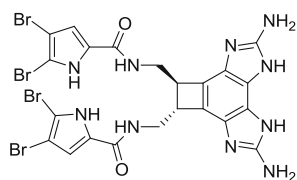
Nagelamides M and N are two additional bromopyrrole alkaloids isolated from an Okinawan marine sponge *Agelas* species (Kubota et al. 2008). Nagelamide M carries a 2-amino-octahydropyrrolo[2,3-*d*] imidazole ring with a taurine unit, while nagelamide N consists of a 2-amino-tetrahydroimidazole-4-one ring with a taurine unit and 3-(dibromopyrrole-2-carboxamido) propanoic acid moiety. Both compounds showed inhibitory activity against *A. niger*, each with a MIC value of $33.3 \mu\text{g mL}^{-1}$.



Bromopyrrole alkaloids derived from oroidin, hymenidin, and clathrocin monomers have also gained sufficient great interest due to their fascinating complex chemical structures with a high N to C ratio ($\sim 1:2$) and promising biological activities, including significant antimicrobial activities. Agelamadins A-B, isolated from an *Agelas* sp. sponge, are bromopyrrole alkaloids consisted of agelastatin-like tetracyclic and oroidin-like linear moieties, while agelamadins C, D, and E present an original structure combining oroidin structure coupled to a 3-hydroxykynurenine through a dihydro-1,4-oxazine moiety. Agelamadins D and E are a C-9/C-10 diastereomer and a 10-epimer of Agelamadin C, respectively. Both agelamadins A and B have exhibited the same antibacterial activity against *B. subtilis* (MIC = $16 \mu\text{g mL}^{-1}$) and a MIC value of 4.0 and $8.0 \mu\text{g mL}^{-1}$ against *M. luteus*, respectively. All compounds showed antifungal activities against *C. neoformans* with IC_{50} values from $4.0\text{--}32 \mu\text{g mL}^{-1}$. No cytotoxic activity was shown by agelamadins A and B ($\text{IC}_{50} > 10 \mu\text{g mL}^{-1}$) against the murine lymphoma L1210 and human epidermoid carcinoma cell lines (Kusama et al. 2014a, b).



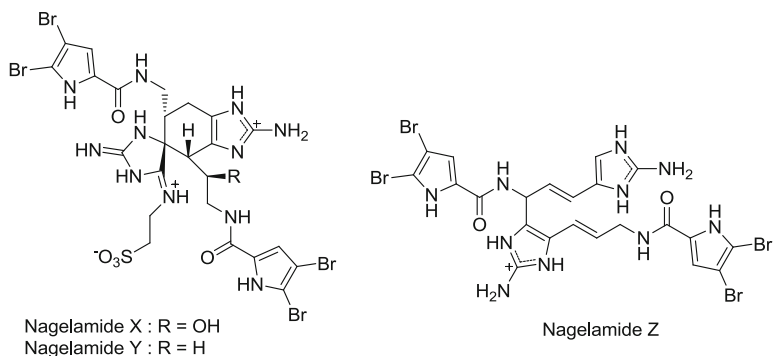
A dimeric bromopyrrole alkaloid, consisting of a benzocyclobutane ring, named bromosceptrin C, was isolated from an Okinawan marine sponge *Agelas* sp. It has shown antimicrobial activities against *B. subtilis*, *E. coli*, *M. luteus*, *S. aureus*, *T. mentagrophytes*, *C. neoformans*, *C. albicans*, and *A. niger* with MIC values ranging from 6.0 to 13.0 $\mu\text{g mL}^{-1}$ (Kubota et al. 2009).



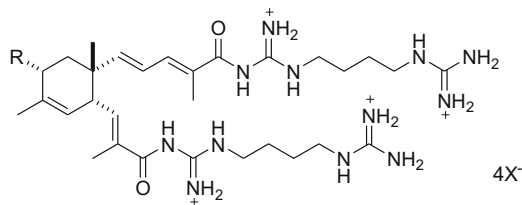
Bromosceptrin C

More recently, three dimeric bromopyrrole alkaloids, namely nagelamides X–Z, consisting of a novel tricyclic skeleton with spiro-bonded tetrahydrobenzaminimidazole and aminoimidazolidine moieties, were isolated from the sponge *Agelas* sp. Nagelamines X and Z exhibited antibacterial activities against *S. aureus* and *M. luteus* with MIC values ranging from 8.0 to 16.0 $\mu\text{g mL}^{-1}$. All the three

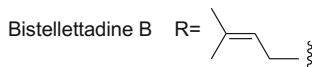
compounds showed significant activities against *C. albicans* with MIC values ranging from 0.25 to 2 $\mu\text{g mL}^{-1}$. Nagelamide Z also displayed broad antifungal activities against *A. niger*, *T. mentagrophytes*, and *C. neoformans* with IC_{50} values of 4.0 and 2.0 $\mu\text{g mL}^{-1}$, respectively (Tanaka et al. 2013b).



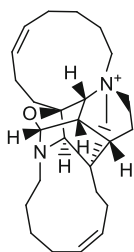
Two other dimeric alkaloids, namely bistellettadines A and B, were isolated from *Stelletta* sp. collected from Shikine-jima island, located at 200 kms from South of Tokyo. These compounds inhibited the growth of the bacterium *E. coli* at 10 $\mu\text{g disk}^{-1}$ (Tsukamoto et al. 1999).



Bistellettadine A R=H

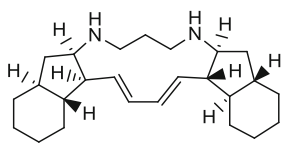


A manzamine-related alkaloid, zamamiphidin A, possessing an original heptacyclic ring system was isolated from an Okinawan marine sponge *Amphimedon* sp. (Kubota et al. 2013b). Zamamiphidin A showed a specific antibacterial activity against *S. aureus* with a MIC value of 32 $\mu\text{g mL}^{-1}$, while no activity was observed neither against *E. coli*, *B. subtilis*, and *M. luteus*, nor against diverse yeasts and fungi.

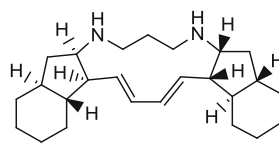


Zamamiphidin A

Marine sponge of *Haliclona* sp. collected from Papua New Guinea showed the existence of an unsymmetrical diastereoisomer of papuamine, namely haliclona-diamine, as the major antimicrobial alkaloid produced by the sponge along with the minor amount of papuamine. The structure of haliclona-diamine was established by X-ray crystallography. Both of the compounds inhibited the growth of *C. albicans*, *B. subtilis*, and *S. aureus* in the standard disk assay at the concentrations of 1.0–5.0 $\mu\text{g disk}^{-1}$ (Fahy et al. 1988).



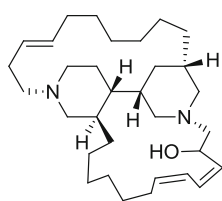
Haliclonadamine



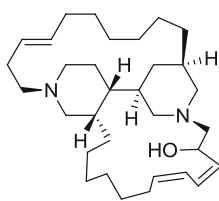
Papuamine

Arenosclerins A–C and haliclona-cyclamine E, tetracyclic alkyl-bis-piperidine alkaloids isolated from the marine sponge, *Arenosclera brasiliensis*, were evaluated for antimicrobial activities against 14 microorganisms including the Gram-positive bacterial strains *S. aureus* ATCC 6538 as well as 9 MRSA strains isolated in hospital environment, the Gram-negative bacterial strain *E. coli* ATCC 25922, the antibiotic-resistant strain *P. aeruginosa*, and the yeast *C. albicans* (Torres et al. 2002). The four compounds displayed antibacterial activity against the bacterial strains methicillin-resistant *S. aureus* and *P. aeruginosa*, showing an inhibition zone between 7 and 13 mm, but did not show any effect against *E. coli* and *C. albicans*. Arenosclerin A and haliclona-cyclamine E, which differ by the presence of one additional hydroxyl group, showing the same MIC value of 10 $\mu\text{g mL}^{-1}$ against one MRSA bacterial strain, indicating that the hydroxyl group does not play any significant role in the antibacterial activity. In contrast, the modification of the stereochemistry of the bis-piperidine ring system seems to have a major influence on the activity. Both arenosclerins B and C exhibited the same MIC value of

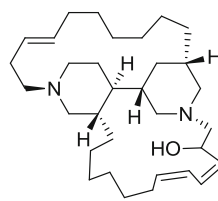
$5 \mu\text{g mL}^{-1}$, a much lower than those of arenosclerin A and haliclonaclamine E. Another closely related bis-piperidine alkaloid, namely halicyclamine A, was isolated from the Australian sponge of the genus *Haliclona*. Halicyclamine A was also reported as a lead antituberculosis agent from a marine sponge of *Haliclona* sp. (Arai et al. 2008). It showed a growth inhibition against *M. smegmatis*, *Mycobacterium bovis* BCG, and *M. tuberculosis* H37Ra with the same MIC values of 2.5, 1.0, and $5.0 \mu\text{g mL}^{-1}$, respectively, under both aerobic and hypoxic conditions namely in growing and dormant states. Another bis-piperidine alkaloid, identified as neopetrosiamine A from the Caribbean marine sponge *Neopetrosia proxima* (Wei et al. 2010), also showed a good MIC value of $7.5 \mu\text{g mL}^{-1}$ when tested in vitro against a pathogenic strain of *M. tuberculosis* H₃₇Rv in a microplate Alamar Blue assay (MABA). It also displayed antiplasmodial activity against *Plasmodium falciparum* with an IC₅₀ value of 2.3 μM as well as cytotoxic activities against a panel of cancer cell lines.



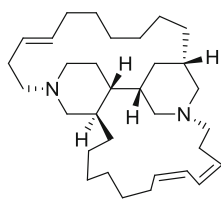
Arenosclerin A



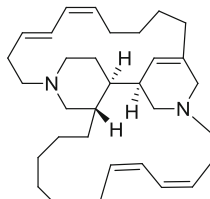
Arenosclerin B



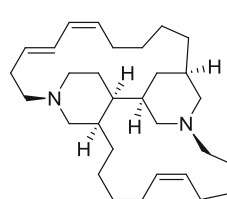
Arenosclerin C



Haliclonaclamine E

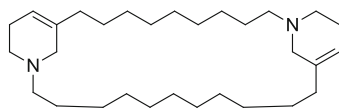


Halicyclamine A

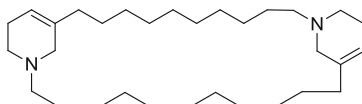


Neopetrosiamine A

Haliclamines C and D are 3-alkyl tetrahydropyridine alkaloids isolated from the Arctic marine sponge, *Haliclona viscosa* (Volk et al. 2004). Such compounds are of special interest as possible precursors in the biosynthesis of the bioactive manzamine alkaloids (Baldwin et al. 1999). When tested at the concentration of 5 mg mL^{-1} , they showed strong inhibition against *Polaribacter* spp. (inhibition zones of the bacterial growth from 3 to 7 mm) or very strong inhibition (inhibition zones of the bacterial growth from 7 to 15 mm) against *Planococcus* spp.

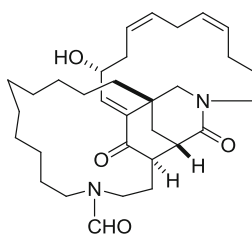


Haliclamine C



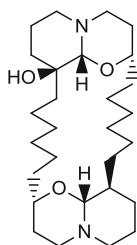
Haliclamine D

Haliclonin A is an original macrocyclic diamide metabolite isolated from the marine sponge, *Haliclona* sp. collected from Korean waters (Jang et al. 2009). When tested against Gram-positive and Gram-negative bacteria, haliclamin A exhibited moderate antibacterial activities with MIC values of 25.0, 6.25, 12.5, and 12.5 $\mu\text{g mL}^{-1}$ against the strains *S. aureus* ATCC 6538p, *B. subtilis* ATCC 6633, *M. luteus* IFO12708 and *Proteus vulgaris* ATCC3851, respectively. It did not show any activity against *E. coli* ATCC25922 up to 100 $\mu\text{g mL}^{-1}$. It also displayed moderate cytotoxicity against the K562 leukemia cell lines with an IC_{50} value of 15.9 $\mu\text{g mL}^{-1}$.



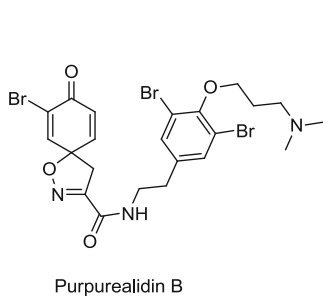
Haliclonin A

In 1996, Pettit's group reported the occurrence of the racemic (\pm)-Xestospongin D from the Singapore marine sponge *Niphates* sp. (Pettit et al. 1996). Previously, the natural macrocyclic 1-oxaquinolizidine (+)-xestospongin D was reported from the Australian marine sponge *Xestospongia exigua* (Nakagawa et al. 1984). Xestospongin D was found to inhibit the growth of the Gram-positive opportunist *M. luteus* with a MIC value ranging from 12.5–25 $\mu\text{g disk}^{-1}$. *M. luteus*, a part of normal human skin flora, has been shown to cause prosthetic valve endocarditis in immuno-compromised patients (Dürst et al. 1991).

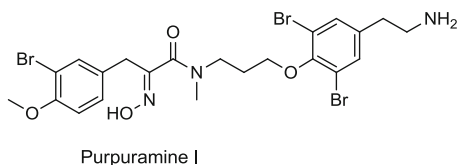


(+)-Xestospongine D

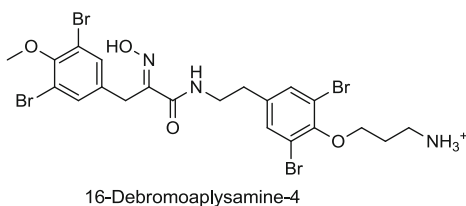
Three bromotyrosine alkaloids purpurealidin B, purpuramine I, and 16-debromoaplysamine-4, isolated from the marine sponge *Psammoplysilla purpurea*, exhibited a moderate or a weak in vitro antimicrobial activity against *E. coli*, *S. aureus*, and *Vibrio cholerae* (Tilvi et al. 2004) with the exception of purpurealidin B, which showed a good activity against *S. aureus* (MIC = 10 $\mu\text{g mL}^{-1}$) and *V. cholerae* (MIC = 25 $\mu\text{g mL}^{-1}$).



Purpurealidin B

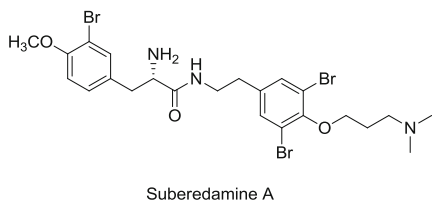


Purpuramine I

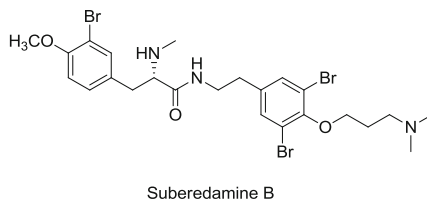


16-Debromoaplysamine-4

Two rare antimicrobial bromotyrosine alkaloids having a primary amino or an *N*-methyl amino group at the α -carbon, namely suberedamines A and B, were isolated from an Okinawan marine sponge *Suberea* sp. Each one of them showed antimicrobial activity against *M. luteus* with MIC values of 12.6 $\mu\text{g mL}^{-1}$ (Tsuda et al. 2001).

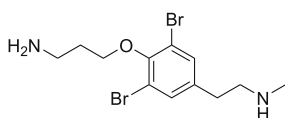
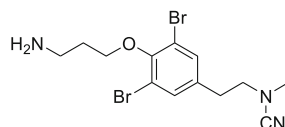
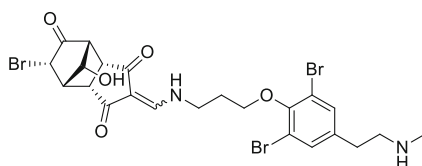


Suberedamine A



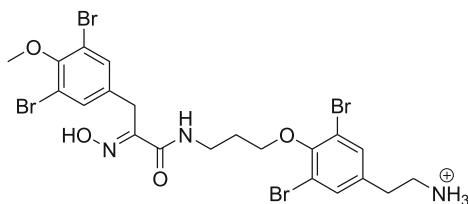
Suberedamine B

Three bromotyrosine derivatives, 11-*N*-methylmoloka'iamine, 11-*N*-cyano-11-*N*-methylmoloka'iamine and kuchinoenamine, were isolated as antibacterial constituents from a marine sponge *Hexadella* sp. (Matsunaga et al. 2005). They showed antibacterial activity in disk agar diffusion assay against the fish pathogenic bacteria *Aeromonas hydrophila* at the concentration of 100 $\mu\text{g disk}^{-1}$ with the zone of inhibition of 7.5, 8.0, and 7.0 mm, respectively.

11-*N*-methylmoloka'iamine11-*N*-cyano-11-*N*-methylmoloka'iamine

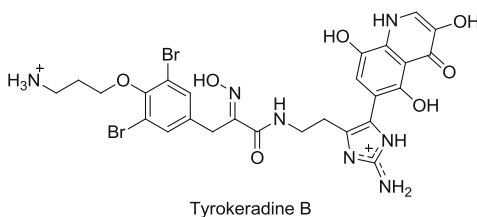
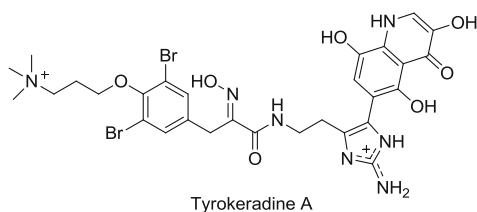
Kuchinoenamine

Another bromotyrosine compound, namely aplysamine 8, was isolated from the marine sponge *Pseudoceratina purpurea*, collected from the Australian coasts. This compound showed a moderate activity against *S. aureus* (MIC = 31 $\mu\text{g mL}^{-1}$) and *E. coli* (MIC = 125 $\mu\text{g mL}^{-1}$) (Gotsbacher and Karuso 2015).

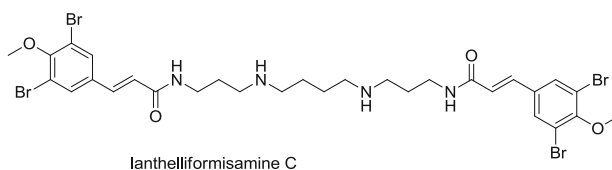
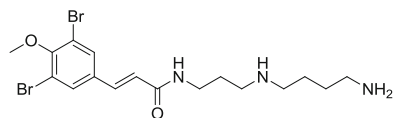
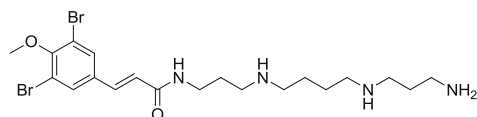


Aplysamine 8

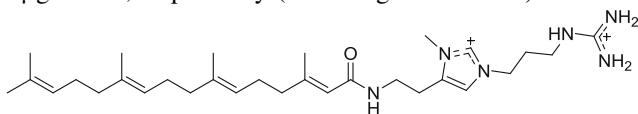
Tyrokeradines A and B are two rare bromotyrosine alkaloids (Mukai et al. 2009) possessing an imidazolyl-quinolinone moiety isolated from an Okinawan marine sponge of the order Verongida. The alkaloid tyrokeradine B showed inhibitory activity against *M. luteus*, *S. aureus*, and *T. mentagrophytes* (MIC value of 25.0 $\mu\text{g mL}^{-1}$, each), and against *C. neoformans*, *C. albicans*, and *A. niger* (MIC value of 12.5 $\mu\text{g mL}^{-1}$, each). In contrast, tyrokeradine A did not show any activity up to 25 $\mu\text{g mL}^{-1}$.



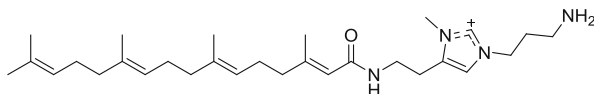
Only few bromotyrosine derivatives contain spermine or spermidine moiety as illustrated with ianthelliformisamines A-C isolated from the marine sponge *Suberea ianthelliformis* (Xu et al. 2012). Ianthelliformisamine A revealed a selective activity against *P. aeruginosa* PAO1 with an IC_{50} value of $6.8 \mu\text{g mL}^{-1}$ ($MIC = 35 \mu\text{g mL}^{-1}$), and 77% inhibition against *S. aureus* O1A1095 at $175 \mu\text{g mL}^{-1}$. Ianthelliformisamine B showed only a minor inhibition (80% at $87.5 \mu\text{g mL}^{-1}$) against *P. aeruginosa*, while ianthelliformisamine C showed IC_{50} values of 8.9 ($MIC = 17.5 \mu\text{g mL}^{-1}$) and $4.1 \mu\text{g mL}^{-1}$ ($MIC = 8.75 \mu\text{g mL}^{-1}$) against both *P. aeruginosa* and *S. aureus*, respectively.



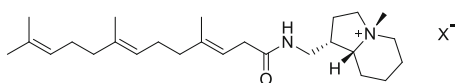
From a marine sponge of the genus *Stelletta*, three highly polar alkaloids, namely stelletazole B, stelletazole C, and stelletamide C, were isolated as antibacterial compounds against *E. coli*, showing inhibitory zones of 6.1, 6.2, and 10.5 mm at 20 $\mu\text{g disk}^{-1}$, respectively (Matsunaga et al. 1999).



Stelletazole B

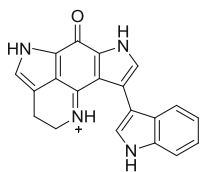


Stelletazole C

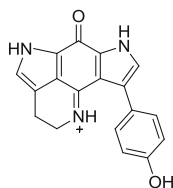


Stelletamide C

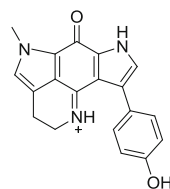
Two bis-pyrroloiminoquinone alkaloids, namely tsitsikammamines A and B along with both brominated discorhabdin C derivatives named 14-bromodiscorhabdin C and 14-bromodihydrodiscorhabdin C, isolated from an undescribed South African Latrunculid sponge, exhibited antimicrobial activity against *B. subtilis* comparable with that of wakayin ($\text{MIC} = 0.3 \mu\text{g mL}^{-1}$), previously isolated from the ascidian *Clavelina* sp. While tsitsikammamines A and B and related derivatives showed murine cell line cytotoxicity, they did not reveal, in contrast to wakayin, any topoisomerase II inhibition (Copp et al. 1991; Hooper et al. 1996).



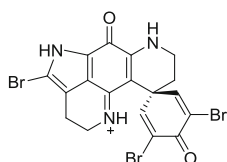
Wakayin



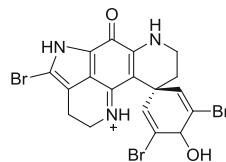
Thetsitsikammamine A



Thetsitsikammamine B

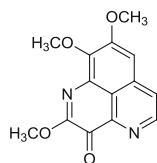


14-Bromodiscorhabdin C

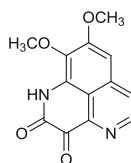


14-Bromodihydrodiscorhabdin C

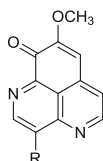
From the sponge *Aaptos* sp. collected at Kupang, Indonesia, the aaptamine alkaloid 2-methoxy-3-oxoaaptamine was isolated along with other known aaptamines, including 2,3-dihydro-2,3-dioxoaaptamine, demethyl(oxy)aaptamine, 3-aminodemethyl-aaptamine and 3-(methylamino)demethyl(oxy)aaptamine, as antimicrobials. Under active growing aerobic condition, 2-methoxy-3-oxoaaptamine and both amino derivatives showed antimicrobial activity against dormancy-induced *M. smegmatis* with a MIC value of $6.25 \mu\text{g mL}^{-1}$, while both 2,3-dihydro-2,3-dioxoaaptamine and demethyl(oxy)aaptamine exhibited a moderate activity with a MIC value of $25 \mu\text{g mL}^{-1}$, revealing the positive effect of the presence of the carbonyl in C-3 position. Under hypoxic condition, both amino derivatives appeared as the most promising with a MIC value of $1.5 \mu\text{g mL}^{-1}$, in contrast to the others derivatives, for which a MIC value of $6.25 \mu\text{g mL}^{-1}$ was observed (Arai et al. 2014).



2-Methoxy-3-oxoaaptamine



2,3-Dihydro-2,3-dioxoaaptamine

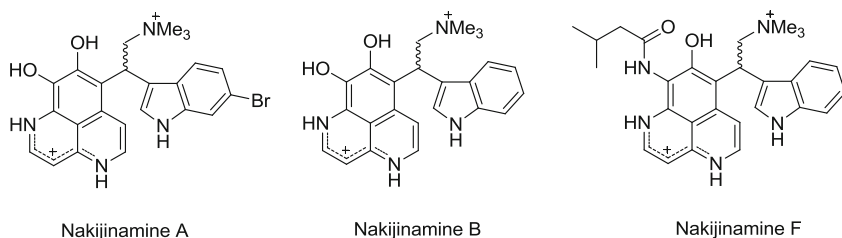


Demethyl(oxy)aaptamine : R = H

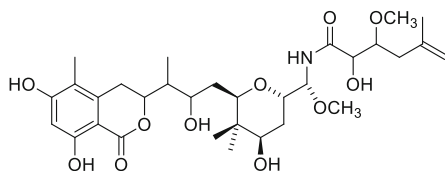
3-Aminodemethyl(oxy)aaptamine : R = NH₂

3-(Methylamino)demethyl(oxy)aaptamine : R = NHCH₃

Out of seven secondary metabolites isolated from the Okinawan marine sponge, *Suberites* sp., the three bromodiscorhabdin derivatives, nakijinamines A, B, and F showed antimicrobial activities (Takahashi et al. 2012). Nakijinamine A exhibited activities against *C. albicans* ($IC_{50} = 0.25 \mu\text{g mL}^{-1}$), *C. neoformans* ($IC_{50} = 0.5 \mu\text{g mL}^{-1}$), *T. mentagrophytes* ($IC_{50} = 0.25 \mu\text{g mL}^{-1}$), *S. aureus* (MIC = $16 \mu\text{g mL}^{-1}$), *B. subtilis*, (MIC = $16 \mu\text{g mL}^{-1}$), and *M. luteus* (MIC = $2 \mu\text{g mL}^{-1}$), while both nakijinamines B and F showed activity against *C. albicans* ($IC_{50} = 8 \mu\text{g mL}^{-1}$). The three alkaloids did not show any cytotoxic activity against the murine lymphoma L1210 and human epidermoid carcinoma KB ($IC_{50} > 10 \mu\text{g mL}^{-1}$).

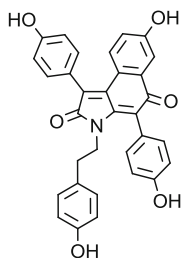


Irciniastatin A, isolated from the Indo-Pacific marine sponge *Ircinia ramosa*, revealed antifungal and antibacterial activities, with MIC values of 16 and $64 \mu\text{g mL}^{-1}$ against *C. neoformans* and *N. gonorrhoeae*, respectively (Pettit et al. 2004). It also exhibited strong activities against the murine P388 leukemia cell line and diverse human cancer cell lines with GI_{50} values of 10^{-3} – $10^{-4} \mu\text{g mL}^{-1}$.



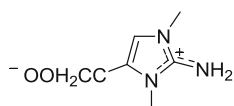
Irciniastatin A

Out of the three 3,4-diaryl pyrrole alkaloids isolated from the marine sponge *Dendrilla nigra*, denigrin C, isolated as an antimycobacterial compound against *M. tuberculosis* H37Rv (MIC = $4.0 \mu\text{g mL}^{-1}$), is the only compound found active against both *B. subtilis* ATCC6633 and *S. aureus* ATCC25923 bacterial strains with the same MIC value of $6.25 \mu\text{g mL}^{-1}$ (Kumar et al. 2014).

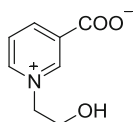


Denigrin C

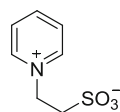
Three betaine alkaloids, aminozooanemonin, pyridinebetaine A, and pyridinebetaine B, were isolated from the Caribbean sponge *Agelas dispar* (Caferi et al. 1998). Evaluation of their antibacterial activities against Gram-positive bacterial strains, *B. subtilis* ATCC6633 and *S. aureus* ATCC 6538 as well as the Gram-negative bacterial strain *Salmonella typhi* ATCC 19430 showed activities against Gram-positive bacteria for aminozooanemonin and pyridinebetaine with MIC values ranging from 2.5 to 8 $\mu\text{g mL}^{-1}$.



Aminozooanemonin

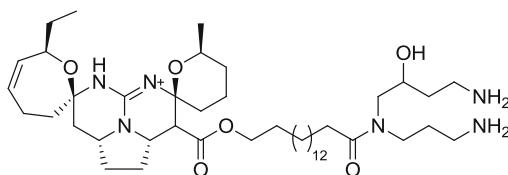


Pyridinebetaine A



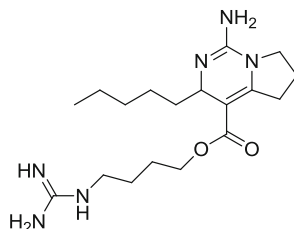
Pyridinebetaine B

Crambescidin 800 was isolated from the marine sponge *Clathria cervicornis*. This pentacyclic guanidine compound showed significant activities against *Acinetobacter baumannii*, *Klebsiella pneumonia* and *P. aeruginosa* with MIC values of 2.0, 1.0, and 1.0 $\mu\text{g mL}^{-1}$, respectively (Sun et al. 2015b).



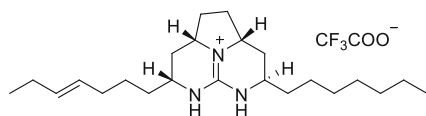
Crambescidin 800

The antibacterial bicyclic bis-guanidine type of alkaloid, namely sch 575948, isolated from the marine sponge *Ptilocaulis spiculifer*, exhibited antibacterial activity against a super sensitive strain of *S. aureus*, with inhibition zones of 13, 15, and 18 mm at the concentrations of 25, 50, and 100 $\mu\text{g disk}^{-1}$, respectively (Yang et al. 2003).

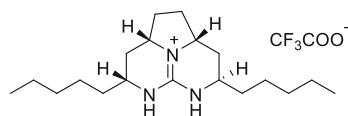


Sch 575948

Merobatzelladines A and B are tricyclic guanidine derivatives isolated from a marine sponge *Monanchora* sp. as antibacterial constituents (Takishima et al. 2009). They exhibited of a moderate antimicrobial activity against *Vibrio anguillarum* with inhibitory zones of 9–10 mm at 50 $\mu\text{g disk}^{-1}$ (6 mm diameter).



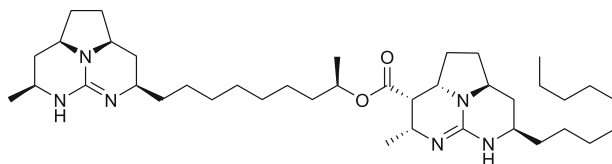
Merobatzelladine A



Merobatzelladine B

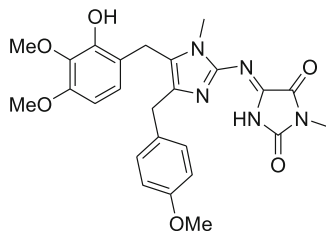
Interestingly is also the promising activity of the polycyclic guanidine alkaloid batzelladine L. This latter, isolated from the sponge *Monanchora arbuscula*, exhibited antifungal activities with MIC values ranging from 1.9 to 7.8 $\mu\text{g mL}^{-1}$ against different strains of *Aspergillus flavus*, isolated from stored peanuts. Furthermore, batzelladine L showed significant antifungal activities against two resistant strains (MIC value of 3.9 $\mu\text{g mL}^{-1}$ against both), in comparison with cercobin (MIC values of 15 and >250 $\mu\text{g mL}^{-1}$, respectively), an antifungal agent used in agriculture for a wide range of fungal diseases. As the world production of shelled peanuts (*Arachis hypogaea*) is around 38.6 and 5.8 million tons of peanut oil, we can

evaluate the impact of such result! Indeed, contamination of peanuts by aflatoxigenic fungi is an important economic problem in many tropical and subtropical areas of the world. Batzelladine L and derivatives could be useful constituents to overcome the thorny problem of aflatoxigenic strains (Arevabini et al. 2014).



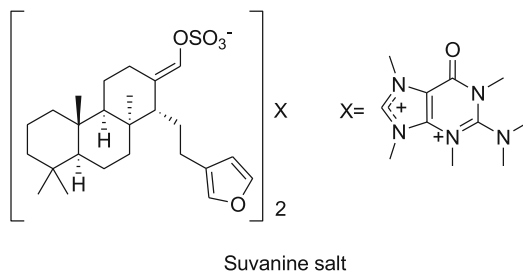
Batzelladine L

The imidazole alkaloid pyronaamidine (Plubrukarn et al. 1997), isolated from the Northern Mariana island sponge *Leucetta* sp. cf. *chagosensis* exhibited antimicrobial activities against *B. subtilis* and *C. albicans* at a concentration of $100 \mu\text{g disk}^{-1}$ (zones of inhibition of 10 and 7 mm, respectively).



Pyronaamidine

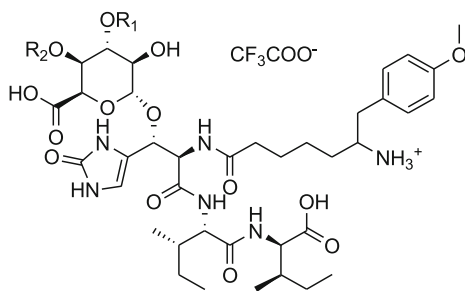
The suvanine *N,N*-dimethyl-1,3-dimethylherbipoline salt was isolated from a sponge of *Coscinoderma* sp. collected from Chuuk Island, Micronesia. This sulfated sesterterpene derived suvanine displayed antibacterial activities against the Gram-positive bacterial strains *S. aureus* ATCC6538, *B. subtilis* ATCC 6633, *K. rhizophila* NBRC12708 with MIC values of 6.25, 0.78, 6.25 $\mu\text{g mL}^{-1}$ and against the Gram-negative strains *S. enterica* ATCC14028 and *P. hauseri* NBRC3851 with MIC values of 0.78 and 6.25 $\mu\text{g mL}^{-1}$, respectively. It was also reported having a moderate cytotoxicity against the human erythroleukemic cell line K562 and the adenocarcinomic human alveolar basal epithelial cell line A549 with LC_{50} values of 2.2 and 1.9 μM , respectively (Kim et al. 2014).



2.6 Peptides

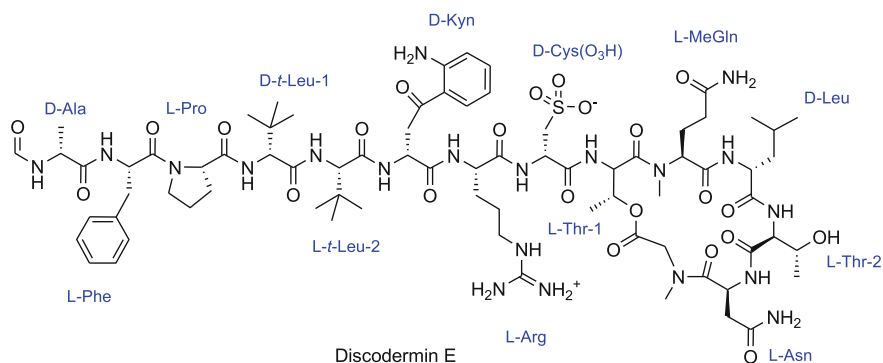
Marine peptides are structurally diverse and display a broad spectrum of bioactivities (Cheung et al. 2015). Recently, they have been reported as an alternative for innovative medicines (Da Costa et al. 2015). Cyclic peptides have been particularly studied because they provide potential anti-infective drug candidates (Kang et al. 2015), in particular as novel antifungal agents.

Two linear tetrapeptides, citronamides A and B, were isolated from the Australian sponge *Citronia astra* (Carroll et al. 2009). The peptides contained two previously unreported amino acids, 3-(2-oxo-2,3-dihydro-1*H*-imidazol-4-yl) serine and 6-amino-7-(4-methoxyphenyl) heptanoic acid, and α -iduronic acid modified at either C-3 or C-4 with a carbamate. Citronamide A showed moderate antifungal activity against *S. cerevisiae*.

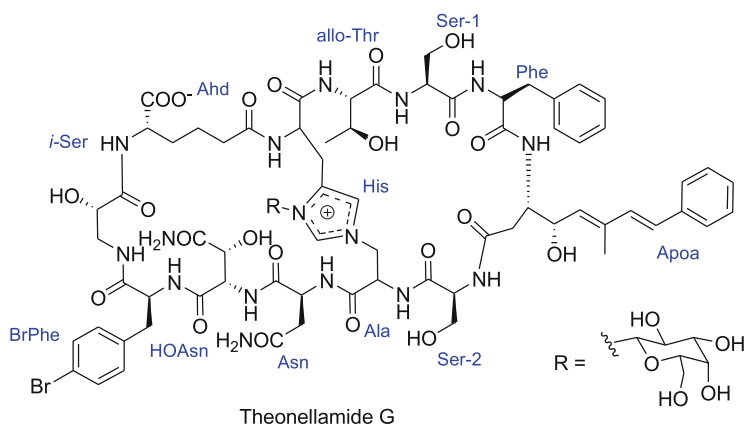


Citronamide A $R_1 = \text{CONH}_2$, $R_2 = \text{H}$
 Citronamide B $R_1 = \text{H}$, $R_2 = \text{CONH}_2$

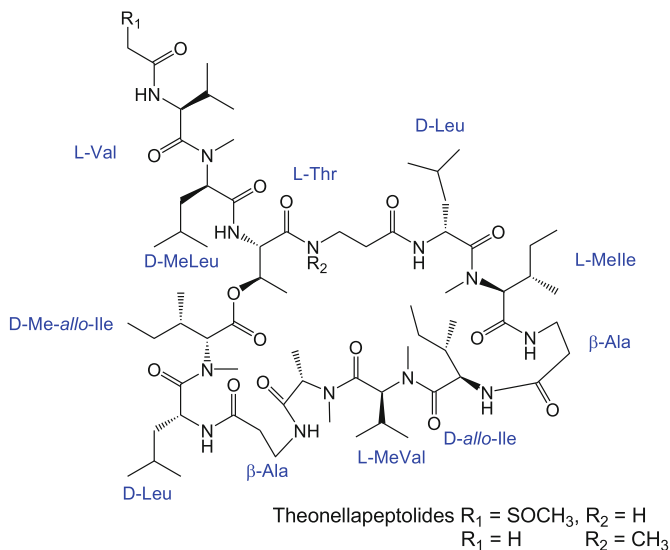
Discodermin E, was initially isolated from the marine sponge, *Discodermia kiiensis* as a cytotoxic compound against P388 leukemia cells ($IC_{50} = 0.02 \mu\text{g mL}^{-1}$). It also showed inhibition of the growth of *B. subtilis*, *S. aureus*, *E. coli*, and *P. aeruginosa* at $2.5 \mu\text{g disk}^{-1}$, and *Mortierella ramannianus*, *C. albicans*, and *P. chrysogenum* at $25 \mu\text{g disk}^{-1}$. This tetradecapeptide also inhibited the development of *Asterinu pectiniferu* starfish embryo at $5 \mu\text{g mL}^{-1}$.



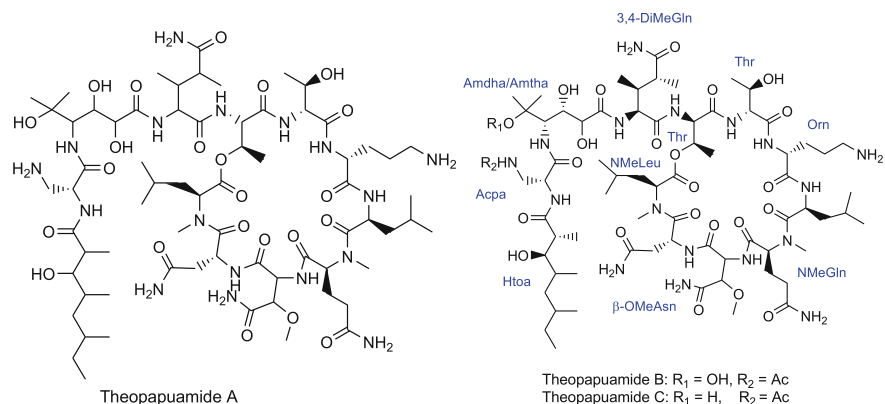
A bicyclic glycopeptide, theonellamide G, purified from the Red Sea sponge *T. swinhoei*, showed antifungal activities against wild (ATCC 32354) and amphotericin B-resistant (ATCC 90873) *C. albicans* strains with IC_{50} values of 4.5 and 2.0 μM , respectively. It also displayed a cytotoxic activity against the human colon adenocarcinoma cell line HCT-16 with an IC_{50} of 6.0 μM (Youssef et al. 2014).



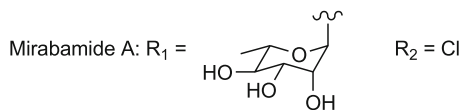
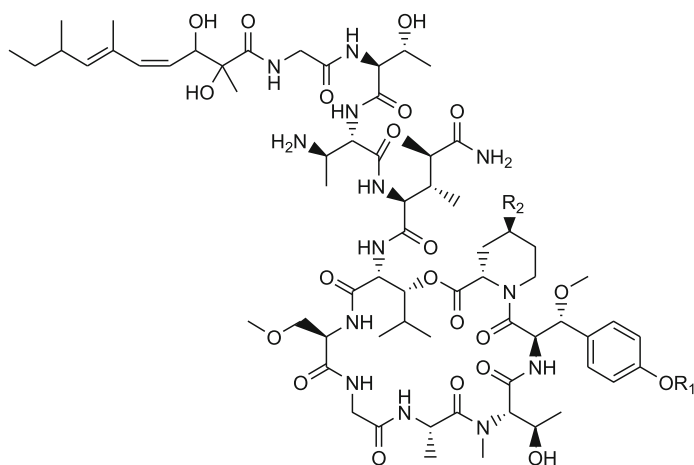
The following two theonellapeptolide-related cyclic depsipeptides have been isolated from an Okinawan marine sponge *Theonella* sp. (Tsuda et al. 1999). These depsipeptides showed moderate antimicrobial activities against some Gram-positive bacteria such as *S. aureus* (MIC = 8.0, and $> 16 \mu\text{g mL}^{-1}$, respectively), *M. luteus* (MIC = $8.0 \mu\text{g mL}^{-1}$ for both compounds), *B. subtilis* (MIC = 8.0 and $16.0 \mu\text{g mL}^{-1}$, respectively), *M. smegmatis* (MIC = 16 and $66 \mu\text{g mL}^{-1}$, respectively), and against fungi such as *T. mentagrophytes* (MIC = 4.0 and $8.0 \mu\text{g mL}^{-1}$, respectively), and *A. niger* (MIC > 66 and $8.0 \mu\text{g mL}^{-1}$, respectively).

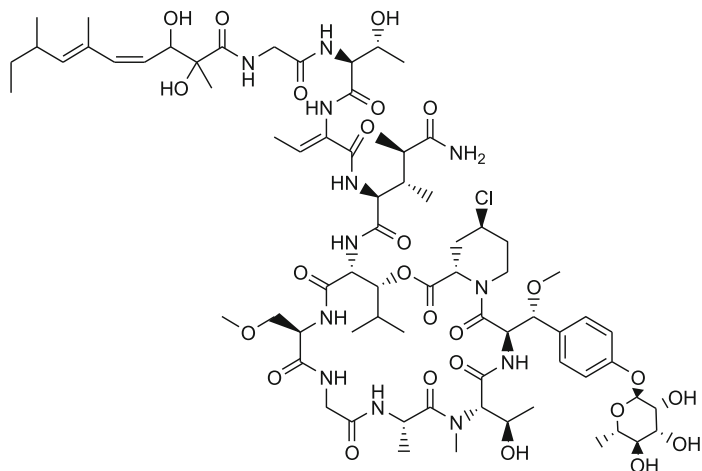


Theopapuamides A–C are depsipeptides isolated from the Indonesian marine sponge *Siliquariaspongia mirabilis*. The undecapeptides theopapuamides B–C revealing an *N*-terminal fatty acid moiety containing two original amino acids, 3-acetamido-2-aminopropanoic acid and 4-amino-2,3-dihydroxy-5-methylhexanoic acid. Theopapuamides A–C exhibited strong antifungal activities against wild-type and amphotericin B-resistant strains of *C. albicans* at the concentration of $1\text{--}5 \mu\text{g disk}^{-1}$. They also showed cytotoxicity against human colon carcinoma HCT-116 cells with IC_{50} values ranging from 2.1 to $4.0 \mu\text{g mL}^{-1}$ (Ratnayake et al. 2006; Plaza et al. 2008).



Mirabamides A–C, are other depsipeptides previously isolated from the same sponge, that inhibited the growth of *B. subtilis* and *C. albicans* at 1–5 $\mu\text{g disk}^{-1}$ in disk diffusion assays (Plaza et al. 2007). They are also reported as inhibitors of the envelope-mediated membrane fusion (HIV-fusion).



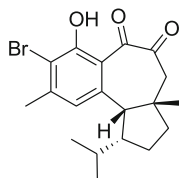


Mirabamide B

2.7 Miscellaneous Brominated Derivatives

Marine sponges have also provided various brominated organic compounds, especially diverse polybrominated ethers.

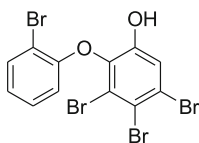
Hamigerans constitute a diverse structural family of brominated derivatives isolated from the sponge *Hamigera tarangaensis* (collected off New Zealand). Out of them, Hamigeran G was reported as an antifungal agent against the budding yeast *S. cerevisiae* (Singh et al. 2013).



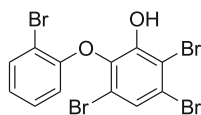
Hamigeran G

The marine sponge *Dysidea herbacea* collected from Indonesia yielded four tri-brominated diphenyl ether congeners as well as known tetrabromo and dibromoderivatives (Handayani et al. 1997). All of the compounds were active against the Gram-positive bacteria *B. subtilis* and the phytopathogenic fungus *Cladosporium cucumerinum*. The isolated polybrominated compounds were also active in the brine shrimp lethality assay. Both 3,4,5,6- and 2,3,4,5-tetrabromo

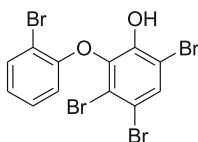
derivatives were found as the most active with IC_{50} values of 0.96 and 0.94 $\mu\text{g mL}^{-1}$, respectively.



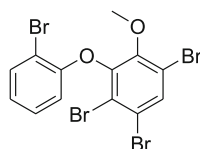
3,4,5-Tribromo-2-(2'-bromophenoxy)phenol



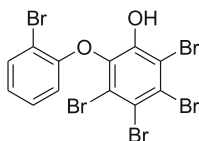
3,5,6-Tribromo-2-(2'-bromophenoxy)phenol



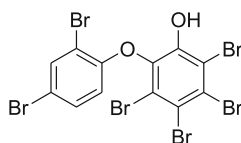
3,4,6-Tribromo-2-(2'-bromophenoxy)phenol



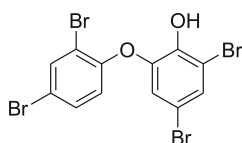
3,5,6-Tribromo-1-(2'-bromophenoxy)-2-benzene methyl ether



3,4,5,6-Tetrabromo-2-(2'-bromophenoxy)phenol

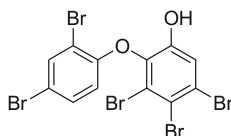


2,3,4,5-Tetrabromo-6-(2',4'-dibromophenoxy)phenol

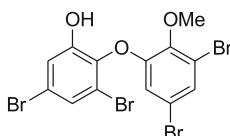


4,6-Dibromo-2-(2',4'-dibromophenoxy)phenol

The 2,3,4,5-tetrabromo-6-(2',4'-dibromophenoxy)phenol, previously mentioned, as well as the polybrominated compounds 3,4,5-tribromo-2-(2',4'-dibromophenoxy)phenol and 3,5-dibromo-2-(3',5'-dibromo-2'-methoxyphenoxy)phenol, isolated from unidentified marine sponges, exhibited a high activity against *S. aureus* ($MIC_{100} = 0.36, 0.36, 0.15 \mu\text{g mL}^{-1}$, respectively) and *T. mentagrophytes* ($MIC_{100} = 3.12, 3.12, 1.56 \mu\text{g mL}^{-1}$, respectively). They were found inactive towards *E. coli* and *Saccharomyces carlsbergensis* strains (Popov et al. 1999).

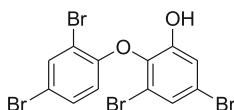


3,4,5-Tribromo-2-(2',4'-dibromophenoxy)phenol



3,5-Dibromo-2-(3',5'-dibromo-2'-methoxyphenoxy)phenol

More recently, the new 3,5-dibromo-2-(2',4'-dibromophenoxy)phenol as well as the 3,4,5-tribromo-2-(2',4'-dibromophenoxy)phenol were isolated as powerful antimicrobial compounds from the marine sponge *Dysidea granulosa*. These polybrominated diphenyl ethers revealed a broad spectral antimicrobial activity with MIC values in the range of 0.1–4.0 and 0.1–16.0 mg mL⁻¹ against Gram-positive and -negative bacteria, respectively. In particular, they showed a MIC value of 0.1 mg L⁻¹ against MRSA bacteria. Furthermore, the dibromophenol revealed a MIC value of 0.1 µg mL⁻¹ against the Gram-negative bacterial strain *K. pneumoniae*. This result is particularly exciting since this activity is comparable and even stronger than the available antibiotics such as ciprofloxacin (MIC = 0.125 µg mL⁻¹), cefoxitin (MIC = 0.25 µg mL⁻¹), and imipenem (MIC = 0.25 µg mL⁻¹), used as positive controls in the assays. As *K. pneumoniae* can cause different types of healthcare-associated infections and have developed resistance to multiple antimicrobial drugs, especially to the class of carbapenems, 3,5-dibromo-2-(2',4'-dibromophenoxy)phenol appeared as a lead compound for clinical applications. In addition, both compounds also inhibited a wide variety of Gram-negative pathogens, which the treatment options are greatly limited (Sun et al. 2015a).



3,5-Dibromo-2-(2',4'-dibromophenoxy)phenol

3 Antimicrobial Compounds from Sponge-Associated Bacteria

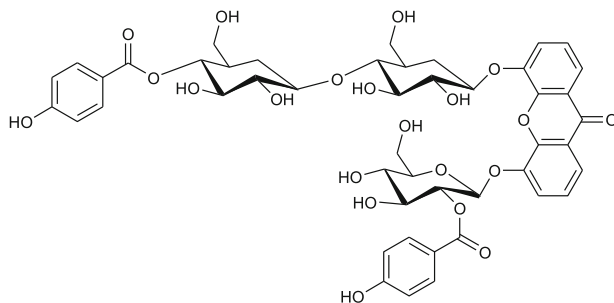
Intriguingly, close inspection of the structures of pharmacologically active natural products isolated from sponges and other marine invertebrates have revealed striking chemical similarities to known microbial metabolites. These observations, combined with those of the pioneer microscopic studies of sponge tissues from Vacelet and Wilkinson in the early 70s of the twentieth century, have attracted the attention of scientists towards sponge-associated bacteria in view of their potential involvement in the production of molecules of interest, in particular of antimicrobial molecules. So far, more than 30 bacterial phyla have been identified in Demospongiae such as Actinobacteria, Acidobacteria, Chloroflexi, Planctomycetes, Proteobacteria, Nitrospira, Cyanobacteria, Bacteroidetes, Verrucomicrobia, and Poribacteria (Taylor et al. 2007); some of them appearing specific to the Porifera, as illustrated with the bacterial phylum Poribacteria.

Although it is difficult to state with full surety about the biosynthetic marine natural products due to the complexity of the associations, the research of their localization within sponge-microorganisms associations has been conducted. Genome sequencings and heterologous expression of biosynthetic pathways can provide the ultimate proof for the production of secondary metabolites by associated microbes.

Using differential centrifugation experiment followed by chemical analysis of the different fractions, Faulkner and coworkers brought the first experimental evidence of the production of natural products by sponge-associated microbiome. Therefore, they demonstrated that the cytotoxic macrolide swinholide A was localized in unicellular heterotrophic bacteria and that the antifungal cyclic peptide theopalauamide was found within filamentous heterotrophic bacteria (Bewley et al. 1998).

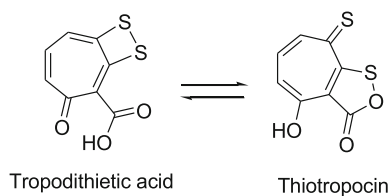
A cultivation of sponge-associated bacteria has been emerged as a novel source for obtaining novel chemical skeletons in large quantity and to overcome the thorny problem of supply of molecules of interest. However, it has been estimated that less than 1% of bacteria can be cultivated in laboratory conditions (Bernard et al. 2000). Therefore, novel strategies will have to be developed in order to cultivate so far uncultivable organisms. Several attempts have been made to improve the situation by changes in culture media and introduction of up-to-date technologies within cultivation procedures (Vartoukian et al. 2010; Stewart 2012; Rocha-Martin et al. 2014).

Microluside A, a *O*-glycosylated substituted xanthone, was obtained from the actinobacterium *Micrococcus* sp. EG45 isolated from the Red Sea marine sponge *Spheciospongia vagabunda*. This compound displayed antibacterial activities against *S. aureus* NCTC 8325 (MIC = 13 μ M) and *E. faecalis* JH 212 (MIC = 10 μ M), enterococci being common causes of nosocomial infections. No cytotoxicity against J774.1 macrophages was detected (IC₅₀ > 200 μ M) (Eltamany et al. 2014).

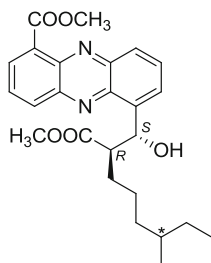


Microluside A

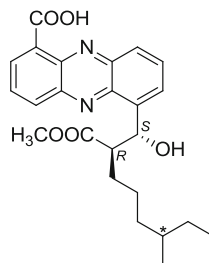
Pseudovibrio species are ubiquitous bacteria in the marine environment, especially within marine sponges. *Pseudovibrio* isolates from the sponges *Axinella dissimilis*, *Polymastia boletiformis* and *Haliclona simulans* showed to produce the antibacterial sulfur containing compound tropodithietic acid (TDA). This latter is formed by a dithiet moiety fused to tropone-2-carboxylic acid, which can coexist with its tautomer thiotropocin. A bacterial extract containing 95% TDA was effective against a range of human-pathogenic bacteria, including both Gram-negative and -positive bacteria. TDA has shown to have a strong inhibitory activity against a wide range of marine bacteria, such as *S. enterica* serovar Typhimurium SL 1344, *E. coli*, NCTC 10538, *P. aeruginosa* NCTC 10662, *S. aureus* NCTC 8532, and *V. anguillarum* 90-11-287 (MIC from 3 to 25 $\mu\text{g mL}^{-1}$) (Porsby et al. 2011; Harrington et al. 2014).



A *Streptomyces* bacterium, *Streptomyces* sp. HB202, was isolated from the sponge *Halichondria panicea* collected from the Baltic Sea. Eight streptophenazines were purified from in vitro cultures of this bacterium using a dereplication strategy. Among these compounds, streptophenazine G and K displayed moderate antibacterial activities against *Staphylococcus epidermidis* (MIC = 8.4 and 14.5 μM , respectively) and *B. subtilis* (MIC = 8.2 μM and 21.6 μM , respectively) (Kunz et al. 2014).



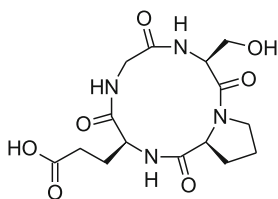
Streptopenazine G



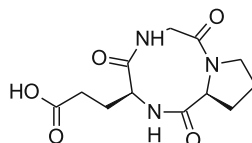
Streptopenazine K

The lantibiotic (e.g., a ribosomally synthesized and posttranslationally modified peptide with potent antimicrobial activities), namely subtilomycin, was isolated from the *B. subtilis* strain MMA7 isolated from the marine sponge *H. simulans*. This peptide, confirmed as T-W-A-T-I-G-K-T-I-V-Q-S-V-K-K, displayed antibacterial activities against Gram-positive and Gram-negative pathogens (*B. cereus*, *Bacillus megaterium*, *Listeria monocytogenes* and *Listeria innocua*) and against the fungus *Candida sporogenes* (Phelan et al. 2013).

Two cyclic peptides, identified as cyclo-(glycyl-L-seryl-L-prolyl-L-glutamyl) and cyclo-(glycyl-L-prolyl-L-glutamyl), were isolated from the *Ruegeria*, SDC-1 strain associated with cell cultures of *Suberites domuncula* (Mitova et al. 2004). Both peptides showed moderate effects against *B. subtilis* (MIC = 25 and 50 $\mu\text{g mL}^{-1}$, respectively) and no activity against *E. coli* and *S. cerevisiae*.

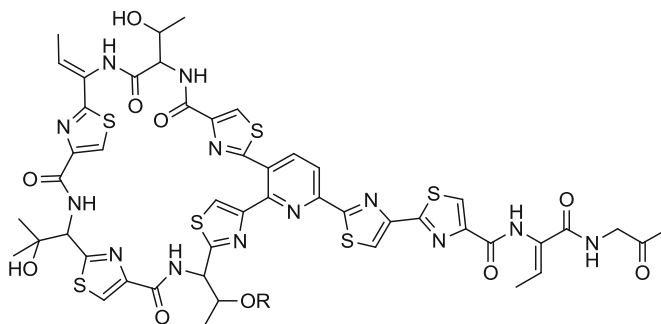


Cyclo-(glycyl-L-seryl-L-prolyl-L-glutamyl)



Cyclo-(glycyl-L-prolyl-L-glutamyl)

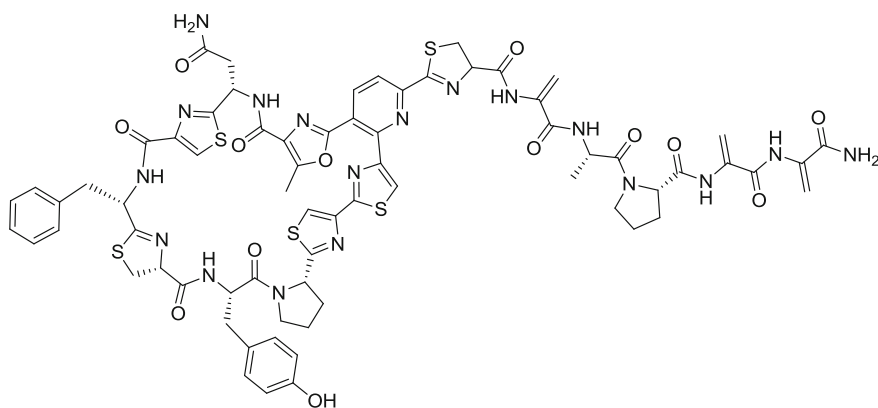
Novel antibiotics, YM-266183 and YM-266184, were found in the culture broth of *B. cereus* QN03323 which was isolated from the marine sponge *Halichondria japonica*. These thiopeptides exhibited potent antibacterial activities against the Gram-negative staphylococci and enterococci including multiple drug-resistant strains, whereas they were inactive against Gram-negative bacteria (Suzumura et al. 2003).



YM-266183: R= H

YM-266184: R= CH₃

Fourty four *Micrococcus* and *Kocuria* bacterial strains were collected from Florida Keys, Fort Lauderdale and Maryland sponges. Three isolates showed to produce in vitro a thiazolyl peptide, kocurin, of which the antimicrobial activity profile has shown to have extremely potent activities against Gram-positive bacteria with MIC values of 0.25–0.5 $\mu\text{g mL}^{-1}$ against MRSA and no activity against the Gram-negative bacterial pathogens, *A. baumannii*, *P. aeruginosa*, and *E. coli*. None of these compounds exhibited cytotoxicity against human promyelocytic leukemia HL-60, human lung carcinoma A549, cervical carcinoma HeLa, and chronic leukemia K562 cell lines (Palomo et al. 2013).



Kocurin

4 Conclusions and Future Challenges

In the light of current medical need, activity against methicillin-resistant *S. aureus* (MRSA), extended-spectrum beta-lactamase producers (ESBL), carbapenem-resistant enterobacteriaceae (CRE), and drug-resistant *N. gonorrhoeae*, as well as discovery of novel druggable antimicrobial mechanisms of action, are of the great importance. Even if we are able to tackle the current challenges, some new resistances are likely to develop by the bacteria, which will devalue all the available antimicrobial drugs. Therefore, constant efforts are required for the introduction of new potent antibacterials. The value of natural products in such efforts is well recognized (Payne et al. 2007).

Marine sponge research produces more than 200 new compounds each year (Laport et al. 2009), providing an exceptional source of diverse marine bioactive compounds, especially, antibacterials. Activity against MRSA has been reported for sponges, as illustrated with the glycolipid caminoside A, the brominated lipids motualevic acids, the steroids halicrasterol H, the terpenes dysidavarone A, clathric acid, the tetracyclic alkylpiperidine haliclonyclamine E, arenosclerins A–C, the indolo [3,2-*a*] carbazole, and the bis-indole alkaloid deoxytopsentin. Activities of those marine natural molecules span between 1.2 to 136.6 $\mu\text{g mL}^{-1}$ and there is an obvious need for better understanding their mechanisms of action. Some indication of activity against *E. coli* has been detected with several reviewed molecules, nevertheless, no data is presented in relationship to ESBL producers. Axistatins are the only reviewed molecules that have been tested and demonstrated activity against *N. gonorrhoeae* in the concentration range which also influenced eukaryotic cells. Two polybrominated diphenylethers, namely 3,5-dibromo-2-(2',4'-dibromophenoxy)phenol and 3,4,5-tribromo-2-(2',4'-dibromophenoxy)phenol have shown nice potency against *K. pneumonia* and definitely should be tested against ESBL producers and CRE strains since such activities would be of great medical interest.

Vast majority of the currently used antibiotics came from nature and medicinal chemists working on novel antibiotic projects are painfully aware how hard it is to make better molecules. Therefore, it is most likely that next generation of great antimicrobial molecules will come from nature, too. It is just the extent and duration of optimization that nature did that one cannot adequately compete within the laboratory.

Obvious next step is to look at places in nature which were less accessible before, such as seas and oceans, and use techniques that humans were not able to use in last century when first generations of antibiotics have been discovered.

It is very important to test systematically and promptly all newly discovered natural molecules against resistant pathogens of medical interest and to elucidate their antimicrobial mode of action. Even if not being optimal drugs themselves, because of their relatively poor potency, lack of selectivity against human cells, or our inability to produce such molecules in significant quantities, they could be

excellent starting point for synthesis of analogues, biotechnological chemical investigations, and/or bioengineering. Furthermore, such novel molecules with potential novel modes of action could shed the light on still undiscovered mechanisms that play significant role in bacterial survival and virulence and that could be exploited as potential novel drug targets. Furthermore, quorum sensing, which controls many virulence factors responsible for bacterial infections appears to be a new promising path in the search of alternative antibiotic drugs (Saurav et al. 2016). Addressing quorum sensing has remarkable potential to weaken bacterial virulence and still does not put such pressure on bacteria that pushes them towards further mutations/changes. Therefore, anti-virulence therapy emerges as a new alternative that might be able to unlock the drug resistance threat and extensive research of symbiotic microbes could provide the clue where the right therapeutic interventions should be.

Bibliography

- Abdelmohsen UR, Cheng C, Reimer A, Kozjak-Pavlovic V, Ibrahim AK, Rudel T, Hentschel U, Edrada-Ebel R, Ahmed SA (2015) Antichlamydial sterol from the red sea sponge *Callyspongia* aff. *Implexa*. *Planta Med* 81:382–387
- Abdul DB, Yamazaki H, Kanno S, Takahashi O, Kirikoshi R, Ukai K, Namikoshi M (2015) Structures and biological evaluations of agelasines isolated from the Okinawan marine sponge *Agelas nakamurai*. *J Nat Prod* 78:1428–1433
- Ankisetty S, Amsler CD, McClintock JB, Baker BJ (2004) Further membranolid diterpenes from the antarctic sponge *Dendrilla membranosa*. *J Nat Prod* 67(7):1172–1174
- Arai M, Sobou M, Vilchéze C, Baughn A, Hashizume H, Pruksakorn P, Ishida S, Matsumoto M, Jacobs WR, Kobayashi M (2008) Halicyclamine A, a marine spongean alkaloid as a lead for anti-tuberculosis agent. *Bioorg Med Chem* 16:6732–6736
- Arai M, Han C, Yamano Y, Setiawan A, Kobayashi M (2014) Aaptamines, marine spongean alkaloids, as anti-dormant mycobacterial substances. *J Nat Med* 68(2):372–376
- Arevabini C, Crivelenti YD, de Abreu MH, Bitencourt TA, Santos MFC, Berlinck RGS, Hajdu E, Belebony RO, Fachin AL, Marin M (2014) Antifungal activity of metabolites from the marine sponges *Amphimedon* sp. and *Monanchora arbuscula* against *Aspergillus flavus* strains isolated from peanuts (*Arachis hypogaea*). *Nat Prod Commun* 9(1):33–36
- Avilés E, Rodríguez AD, Vicente J (2013) Two rare-class tricyclic diterpenes with antitubercular activity from the caribbean sponge *Svenzea flava*. application of vibrational circular dichroism spectroscopy for determining absolute configuration. *J Org Chem* 78(22):11294–11301
- Baldwin JE, Claridge TDW, Culshaw AJ, Heupel FA, Lee V, Spring DR, Whitehead RC (1999) Studies on the biomimetic synthesis of the manzamine alkaloids. *Chem Eur J* 5:3154–3161
- Barnathan G (2009) Non-methylene-interrupted fatty acids from marine invertebrates: occurrence, characterization and biological properties. *Biochimie* 91(6):671–678
- Bergé JP, Barnathan G (2005) Fatty acids from lipids of marine organisms: molecular biodiversity, roles as biomarkers, biologically active compounds, and economical aspects. *Adv Biochem Eng Biotechnol* 96:49–125
- Bernard L, Schäfer H, Joux F, Courties C, Muyzer G, Lebaron P (2000) Genetic diversity of total, active and culturable marine bacteria in coastal seawater. *Aquat Microb Ecol* 23:1–11
- Bewley CA, Holland ND, Faulkner DJ (1996) Two classes of metabolites from *Theonella swinhoei* are localized in distinct populations of bacterial symbionts. *Experientia* 52(7):716–722

- Bewley CA, Faulkner DJ (1998) Lithistid sponges: star performers or hosts to the stars. *Angew Chem Int Ed* 37:2162–2178
- Boonlarpadab C, Faulkner DJ (2007) Eurysterols A and B, cytotoxic and antifungal steroidal sulfates from a marine sponge of the genus *Euryspongia*. *J Nat Prod* 70(5):846–848
- Bourguet-Kondracki ML, Lacombe F, Guyot M (1999) Methanol adduct of puupehenone, a biologically active derivative from the marine sponge *Hyrtios* species. *J Nat Prod* 62(9):1304–1305
- Bright M, Bulgheresi S (2010) A complex journey: transmission of microbial symbionts. *Nat Rev Microbiol* 8:218–230
- Cafieri F, Fattorusso E, Tagliatalata-Scafati O (1998) Novel bromopyrrole alkaloids from the sponge *Agelas dispar*. *J Nat Prod* 61(9):122–125, 1171–1173
- Carroll AR, Duffy S, Avery VM (2009) Citronamides A and B, tetrapeptides from the Australian sponge *Citronia astra*. *J Nat Prod* 72(4):764–768
- Cheng Z-B, Xiao H, Fan C-Q, Lu Y-N, Zhang G, Yin S (2013) Bioactive polyhydroxylated sterols from the marine sponge *Haliclona crassiloba*. *Steroids* 78(14):1353–1358
- Cheung RCF, Ng TB, Wong JH (2015) Marine peptides: bioactivities and applications. *Mar Drugs* 13:4006–4043
- Clark RJ, Garson MJ, Hooper JNA (2001) Antifungal alkyl amino alcohols from the tropical marine sponge *Haliclona* n. sp. *J Nat Prod* 64:1568–1571
- Copp BR, Ireland CM, Barrows LR (1991) Wakayin: a novel pyrroloiminoquinone alkaloid from the ascidian *Calvalina* species. *J Org Chem* 56:4596–4597
- Da Costa JP, Cova M, Ferreira R, Vitorino R (2015) Antimicrobial peptides: an alternative for innovative medicines? *Appl Microbiol Biotechnol* 99:2023–2040
- Dürst UN, Bruder E, Egloff L, Wüst J, Schneider J, Hirzel HO (1991) *Micrococcus luteus*: a rare pathogen of valve prosthesis endocarditis. *Z Kardiol* 80(4):294–298
- Eltamany EE, Abdelmohsen UR, Ibrahim AK, Hassanean HA, Hentschel U, Ahmed SA (2014) New antibacterial xanثone from the marine sponge-derived *Micrococcus* sp. EG45. *Bioorg Med Chem Lett* 24(21):4939–4942
- Fahy E, Molinski TF, Harper MK, Sullivan BW, Faulkner DJ, Parkanyi L, Clardy J (1988) Haliclonadiamine, an antimicrobial alkaloid from the sponge *Haliclona* sp. *Tetrahedron Lett* 29:3427–3428
- Fusetani N, Takahashi M, Matsunaga S (1994) Topsentasterol sulfates, antimicrobial sterol sulfates possessing novel side chains, from a marine sponge, *Topsentia* sp. *Tetrahedron* 50(26):7765–7770
- Gelband H, Miller-Petrie M, Pant S, Gandra S, Levinson J, Barter D, White A, Laxminarayan R (2015) The state of world's antibiotics 2015. CDDEP
- Glasner C, Albiger B, Buist G, Tambić Andrašević A, Canton R, Carmeli Y, Friedrich AW, Giske CG, Glupczynski Y, Gniadkowski M, Livermore DM, Nordmann P, Poirel L, Rossolini GM, Seifert H, Vatopoulos A, Walsh T, Woodford N, Donker T, Monnet DL, Grundmann H (2013) European Survey on Carbapenemase-producing Enterobacteriaceae (ESCAPE) Working Group. Carbapenemase-producing Enterobacteriaceae in Europe: a survey among national experts from 39 countries, February 2013. *Euro Surveill* 18(28), pii: 20525
- Gotsbacher M, Karuso P (2015) New antimicrobial bromotyrosine analogues from the sponge *Pseudoceratina purpurea* and its predator *Tylodina corticalis*. *Mar Drugs* 13(3):1389–1409
- Gros E, Al-Mourabit A, Martin MT, Sorres J, Vacelet J, Frederich M, Aknin M, Kashman Y, Gauvin-Bialecki A (2014) Netamines H-N, tricyclic alkaloids from the marine sponge *Biemna laboutei* and their antimalarial activity. *J Nat Prod* 77(4):818–823
- Gupta P, Sharma U, Schulz TC, McLean AB, Robins AJ, West LM (2012) Bicyclic C21 terpenoids from the marine sponge *Clathria compressa*. *J Nat Prod* 75:1223–1227
- Gushiken M, Kagiya I, Kato H, Kuwana T, Losung F, Mangindaan REP, de Voogd NJ, Tsukamoto S (2015) Manadodioxans A–E: polyketide endoperoxides from the marine sponge *Plakortis bergquistae*. *J Nat Med* 6:1–6

- Hagiwara K, Garcia Hernandez JE, Harper MK, Carroll A, Motti CA, Awaya J, Nguyen H-Y (2015) Puupehenol, a potent antioxidant antimicrobial meroterpenoid from a Hawaiian deep-water *Dactylospongia* sp. sponge. *J Nat Prod* 78:325–329
- Hamann MT, Scheuer PJ (1991) Cyanopuupehenol, an antiviral metabolite of a sponge of the order Verongida. *Tetrahedron Lett* 32(41):5671–5672
- Handayani D, Edrada RA, Proksch P, Wray V, Witte L, Van Soest RWM, Kunzmann A, Soedarsono (1997) Four new bioactive polybrominated diphenyl ethers of the sponge *Dysidea herbacea* from West Sumatra, Indonesia. *J Nat Prod* 60(12):1313–1316
- Harrington C, Reen F, Mooij M, Stewart F, Chabot J-B, Guerra A, Glöckner F, Nielsen K, Gram L, Dobson A, Adams C, O’Gara F (2014) Characterisation of non-autoinducing tropodithietic acid (TDA) production from marine sponge *Pseudoivibrio* species. *Mar Drugs* 12(12):5960–5978
- Hooper GJ, Davies-Coleman MT, Kelly-Borges M, Coetzee PS (1996) New alkaloids from a south African *Latrunculiid* sponge. *Tetrahedron Lett* 37(39):7135–7138
- Iinuma Y, Kozawa S, Ishiyama H, Tsuda M, Fukushi E, Kawabata J, Fromont J, Kobayashi J (2005) Gesashidine A, a β -carboline alkaloid with an imidazole ring from a *Thorectidae* sponge. *J Nat Prod* 68(7):1109–1110
- Iwagawa T, Kaneko M, Okamura H, Nakatani M, Van Soest RWM (1998) New alkaloids from the Papua New Guinean sponge *Agelas nakamurai*. *J Nat Prod* 61(10):1310–1312
- Jang KH, Kang GW, Jeon JE, Lim C, Lee HS, Sim CJ, Oh KB, Shin J (2009) Haliclolin A, a new macrocyclic diamide from the sponge *Haliclona* sp. *Org Lett* 11(8):1713–1716
- Jiao WH, Huang XJ, Yang JS, Yang F, Piao SJ, Gao H, Li J, Ye WC, Yao XS, Chen WS, Lin HW (2012) Dysidavarones A-D, new sesquiterpene quinones from the marine sponge *Dysidea avara*. *Org Lett* 14(1):202–205
- Kang HK, Seo CH, Park Y (2015) Marine peptides and their anti-infective activities. *Mar Drugs* 13:618–654
- Keffer JL, Plaza A, Bewley CA (2009) Motualevic acids A-F, antimicrobial acids from the sponge *Siliquariaspongia* sp. *Org Lett* 11(5):1087–1090
- Kim CK, Song IH, Park HY, Lee YJ, Lee HS, Sim CJ, Oh DC, Oh KB, Shin J (2014) Suvanine sesterterpenes and deacyl irciniasulfonic acids from a tropical *Coscinoderma* sp. sponge. *J Nat Prod* 77(6):1396–1403
- Kubota T, Araki A, Ito J, Mikami Y, Fromont J, Kobayashi J (2008) Nagelamides M and N, new bromopyrrole alkaloids from sponge *Agelas* species. *Tetrahedron* 64:10810–10813
- Kubota T, Araki A, Yasuda T, Tsuda M, Fromont J, Aoyama K, Mikami Y, Wälchli MR, Kobayashi J (2009) Benzosceptrin C, a new dimeric bromopyrrole alkaloid from sponge *Agelas* sp. *Tetrahedron Lett* 50:7268–7270
- Kubota T, Iwai T, Takahashi-Nakaguchi A, Fromont J, Gonoï T, Kobayashi J (2012) Agelasines O-U, new diterpene alkaloids with a 9-N-methyladenine unit from a marine sponge *Agelas* sp. *Tetrahedron* 68:9738–9744
- Kubota T, Ishiguro Y, Takahashi-Nakaguchi A, Fromont J, Gonoï T, Kobayashi J (2013a) Manzamenones L-N, new dimeric fatty-acid derivatives from an Okinawan marine sponge *Plakortis* sp. *Bioorg Med Chem Lett* 23(1):244–247
- Kubota T, Kamijyo Y, Takahashi-Nakaguchi A, Fromont J, Gonoï T, Kobayashi J (2013b) Zamamiphidin A, a new manzamine related alkaloid from an Okinawan marine sponge *Amphimedon* sp. *Org Lett* 15(3):610–612
- Kumar MKM, Naik D, Satyavathi J, Ramana K, Varma HR, Nagasree PP, Desaraju KS, Rao VD (2014) Denigrins A-C: new antitubercular 3,4-diarylpyrrole alkaloids from *Dendrilla nigra*. *Nat Prod Res* 28(12):888–894
- Kunz AL, Labes A, Wiese J, Bruhn T, Bringmann G, Imhoff JF (2014) Nature’s lab for derivatization: new and revised structures of a variety of streptophenazines produced by a sponge-derived *Streptomyces* strain. *Mar Drugs* 12(4):1699–1714
- Kusama T, Tanaka N, Sakai K, Gonoï T, Fromont J, Kashiwada Y, Kobayashi J (2014a) Agelamadins A and B, dimeric bromopyrrole alkaloids from a marine sponge *Agelas* sp. *Org Lett* 16(15):3916–3918

- Kusama T, Tanaka N, Sakai K, Gonoï T, Fromont J, Kashiwada Y, Kobayashi J (2014b) Agelamadins C-E, bromopyrrole alkaloids comprising oroidin and 3-hydroxykynurenine from a marine sponge *Agelas* sp. *Org Lett* 16(19):5176–5179
- Kusama T, Tanaka N, Takahashi-nakaguchi A, Gonoï T, Fromont J, Kobayashi J (2014c) Bromopyrrole alkaloids from a marine sponge *Agelas* sp. *Chem Pharm Bull* 62(5):499–503
- Laport MS, Santos OC, Muricy G (2009) Marine sponges: potential sources of new antimicrobial drugs. *Curr Pharm Biotechnol* 10(1):86–105
- Linington RG, Robertson M, Gauthier A, Finlay BB, MacMillan JB, Molinski TF, Van Soest R, Andersen RJ (2002) Caminoside A, an antimicrobial glycolipid isolated from the marine sponge *Caminus sphaeroconia*. *Org Lett* 4(23):4089–4092
- Majik MS, Shirodkar D, Rodrigues C, D'Souza L, Tilvi S (2014) Evaluation of single and joint effect of metabolites isolated from marine sponges, *Fasciospongia cavernosa* and *Axinella donnani* on antimicrobial properties. *Bioorg Med Chem Lett* 24(13):2863–2866
- Matsunaga S, Yamashita T, Tsukamoto S, Fusetani N (1999) Three new antibacterial alkaloids from a marine sponge *Stelletta* species. *J Nat Prod* 62(8):1202–1204
- Matsunaga S, Okada Y, Fusetani N, Van Soest RWM (2000) An antimicrobial c14 acetylenic acid from a marine sponge *Oceanapia* species. *J Nat Prod* 63(5):690–691
- Matsunaga S, Nishimura S, Fusetani N (2001) Two new antimicrobial lysoplasmaynositols from the marine sponge *Theonella swinhoei*. *J Nat Prod* 64(6):816–818
- Matsunaga S, Kobayashi H, Van Soest RWM, Fusetani N (2005) Novel bromotyrosine derivatives that inhibit growth of the fish pathogenic bacterium *Aeromonas hydrophila*, from a marine sponge *Hexadella* sp. *J Org Chem* 70:1893–1896
- Mehub M, Lei J, Franco C, Zhang W (2014) Marine sponge derived natural products between 2001 and 2010: trends and opportunities for discovery of bioactivities. *Mar Drugs* 12(8):4539–4577
- Mitova M, Popov S, Rosa S De (2004) Cyclic peptides from a ruegeria strain of bacteria associated with the sponge *Suberites domuncula*. *J Nat Prod* 67(7):1178–1181
- Mukai H, Kubota T, Aoyama K, Mikami Y, Fromont J, Kobayashi J (2009) Tyrokeradines A and B, new bromotyrosine alkaloids with an imidazolyl-quinolinone moiety from a *Verongid* sponge. *Bioorg Med Chem Lett* 19:1337–1339
- Nakagawa M, Endo M, Tanaka N, Lee GP (1984) Structures of xestospongins A, B, C, D; novel vasodilative compounds from marine sponge *Xestospongia exigua*. *Tetrahedron Lett* 25:3227–3230
- Nakamura H, Deng S, Kobayashi J, Ohizumi Y (1987) Keramamine A and B, novel anti-microbial alkaloids from the Okinawan marine sponge *Pellina* sp. *Tetrahedron Lett* 28(6):621–624
- Nuzzo G, Ciavatta ML, Villani G, Manzo E, Zanfardino A, Varcamonti M, Gavagnin M (2012) Fulvynes, antimicrobial polyoxygenated acetylenes from the mediterranean sponge *Haliclona fulva*. *Tetrahedron* 68:754–760
- Oh K-B, Mar W, Kim S, Kim J-Y, Lee T-H, Kim J-G, Shin D, Sim CJ, Shin J (2006) Antimicrobial activity and cytotoxicity of bis(indole) alkaloids from the sponge *Spongosorites* sp. *Biol Pharm Bull* 29(3):570–573
- Oh J, Hwang B, Kang O-H, Kwon D-Y, Rho J-R (2013) New constituents from the Korean sponge *Plakortis simplex*. *Mar Drugs* 11(11):4407–4418
- Palomo S, González I, De La Cruz M, Martín J, Tormo JR, Anderson M, Hill RT, Vicente F, Reyes F, Genilloud O (2013) Sponge-derived *Kocuria* and *Micrococcus* spp. as sources of the new thiazolyl peptide antibiotic kocurin. *Mar Drugs* 11(4):1071–1086
- Payne DJ, Gwynn MN, Holmes DJ, Pompliano DL (2007) Drugs for bad bugs: confronting the challenges of antibacterial discovery. *Nat Rev Drug Discov* 6:29–40
- Pettit GR, Orr B, Herald DL, Doubek DL, Tackett L, Schmidt JM, Boyd MR, Pettit RK, Hooper JNA (1996) Isolation and X-ray crystal structure of racemic xestospongins D from the Singapore marine sponge *Niphates* sp. *Bioorg Med Chem Lett* 6:1313–1318
- Pettit GR, Xu JP, Chapuis JC, Pettit RK, Tackett LP, Doubek DL, Hooper JNA, Schmidt JM (2004) Antineoplastic agents. 520. Isolation and structure of irciniastatins A and B from the Indo-Pacific marine sponge *Ircinia ramosa*. *J Med Chem* 47(5):1149–1152

- Pettit GR, Tang Y, Zhang Q, Bourne GT, Arm CA, Leet JE, Knight JC, Pettit RK, Chapuis J-C, Doubek DL, Ward FJ, Weber C, Hooper JNA (2013) Isolation and structures of axistatins 1–3 from the republic of palau marine sponge *Agelas axifera* hentschel. *J Nat Prod* 76(3):420–424
- Phelan RW, Barret M, Cotter PD, O'Connor PM, Chen R, Morrissey JP, Dobson ADW, O'Gara F, Barbosa TM (2013) Subtilomycin: a new lantibiotic from *Bacillus subtilis* strain MMA7 isolated from the marine sponge *Haliclona simulans*. *Mar Drugs* 11(6):1878–1898
- Piao S-J, Song Y-L, Jiao W-H, Yang F, Liu X-F, Chen W-S, Han B-N, Lin H-W (2013) Hippolachnin A, a new antifungal polyketide from the South China sea sponge *Hippospongia lachne*. *Org Lett* 15(14):3526–3529
- Plaza A, Gustchina E, Baker HL, Kelly M, Bewley CA (2007) Mirabamides A–D, depsipeptides from the sponge *Siliquariaspongia mirabilis* that inhibit HIV-1 fusion. *J Nat Prod* 70(11):1753–1760
- Plaza A, Bifulco G, Keffler JL, Lloyd JR, Baker HL, Bewley CA (2008) Celebesides A–C and theopapuamides B–D, depsipeptides from an Indonesian sponge that inhibit HIV-1 entry. *J Org Chem* 74(2):504–512
- Plubrukarn A, Smith DW, Cramer RE, Davidson BS (1997) (2*E*,9*E*)-Pyronaamidine 9-(*N*-methylimine), a new imidazole alkaloid from the northern Mariana islands sponge *Leucetta* sp. cf. *chagosensis*. *J Nat Prod* 60(7):712–715
- Popov AM, Stekhova SI, Utkina NK, Rebachuk NM (1999) Antimicrobial and cytotoxic activity of sesquiterpenoquinones and brominated diphenyl esters. *Pharm Chem J* 33(2):71–73
- Porsby CH, Webber MA, Nielsen KF, Piddock LJ, Gram L (2011) Resistance and tolerance to tropodithietic acid, an antimicrobial in aquaculture, is hard to select. *Antimicrob Agents Chemother* 55:1332–1337
- Ratnayake AS, Bugni TS, Feng X, Harper MK, Skalicky JJ, Mohammed KA, Andjelic CD, Barrows LR, Ireland CM (2006) Theopapuamide, a cyclic depsipeptide from a Papua New Guinea Lithistid sponge *Theonella swinhoei*. *J Nat Prod* 69(11):1582–1586
- Rocha-Martin J, Harrington C, Dobson ADW, O'Gara F (2014) Emerging strategies and integrated systems microbiology technologies for biodiscovery of marine bioactive compounds. *Mar Drugs* 12(6):3516–3559
- Roué M, Quévrain E, Domart-Coulon I, Bourguet-Kondracki M-L (2012) Assessing calcareous sponges and their associated bacteria for the discovery of new bioactive natural products. *J Nat Prod* 29:739–751
- Russell F, Harmody D, McCarthy PJ, Pomponi SA, Wright AE (2013) Indolo[3,2-*a*]carbazoles from a deep-water sponge of the genus *Asteropus*. *J Nat Prod* 76(10):1989–1992
- Ryu G, Matsunaga S, Fusetani N (1994) Discodermin E, a cytotoxic and antimicrobial tetradecapeptide from the marine sponge *Discodermia kiiensis*. *Tetrahedron Lett* 35(44):8251–8254
- Santos OCS, Soares AR, Machado FLS, Romanos MTV, Muricy G, Giambiagi-deMarval M, Laport MS (2014) Investigation of biotechnological potential of sponge-associated bacteria collected in Brazilian coast. *Lett Appl Microbiol* 60(2):140–147
- Satitpatipan V, Suwanborirux K (2004) New nitrogenous germacrane from a Thai marine sponge, *Axinyssa* N. sp. *J Nat Prod* 67(3):503–505
- Saurav K, Bar-Shalom R, Haber M, Burgsdorf I, Oliviero G, Costantino V, Morgenstern D, Steindler L (2016) In search of alternative antibiotic drugs: quorum-quenching activity in sponges and their bacterial isolates. *Front Microbiol* 7(1130). doi:10.3389/fmicb.2016.00416
- Schmalzbauer B, Herrmann J, Müller R, Menche D (2013) Total synthesis and antibacterial activity of dysidavarone A. *Org Lett* 15(4):964–967
- Schmitt S, Angermeier H, Schiller R, Lindquist N, Hentschel U (2008) Molecular microbial diversity survey of sponge reproductive stages and mechanistic insights into vertical transmission of microbial symbionts. *Appl Environ Microbiol* 74:7694–7708
- Singh AJ, Dattelbaum JD, Field JJ, Smart Z, Woolly EF, Barber JM, Heathcott R, Miller JH, Northcote PT (2013) Structurally diverse hamigerans from the New Zealand marine sponge *Hamigera tarangaensis*: NMR-directed isolation, structure elucidation and antifungal activity. *Org Biomol Chem* 11(46):8041–8051

- Stewart EJ (2012) Growing unculturable bacteria. *J Bacteriol* 194:4151–4160
- Sun S, Canning CB, Bhargava K, Sun X, Zhu W, Zhou N, Zhang Y, Zhou K (2015a) Polybrominated diphenyl ethers with potent and broad spectrum antimicrobial activity from the marine sponge *Dysidea*. *Bioorg Med Chem Lett* 25(10):2181–2183
- Sun X, Sun S, Ference C, Zhu W, Zhou N, Zhang Y, Zhou K (2015b) A potent antimicrobial compound isolated from *Clathria cervicornis*. *Bioorg Med Chem Lett* 25(1):67–69
- Suzuki H, Kubota T, Takahashi-nakaguchi A, Fromont J, Gonoï T, Kobayashi J (2014) Nakijiquinone S and nakijinol C, new meroterpenoids from a marine sponge of the family *Spongiidae*. *Chem Pharm Bull* 62:209–212
- Suzumura K, Yokoi T, Funatsu M, Nagai K, Tanaka K, Zhang H, Suzuki K (2003) YM-266183 and YM-266184, novel thiopeptide antibiotics produced by *Bacillus cereus* isolated from a marine sponge. *J Antibiot* 56:129–134
- Takahashi Y, Kubota T, Ito J, Mikami Y, Fromont J, Kobayashi J (2008) Nakijiquinones G-I, new sesquiterpenoid quinones from marine sponge. *Bioorg Med Chem* 16(16):7561–7564
- Takahashi Y, Tanaka N, Kubota T, Ishiyama H, Shibazaki A, Gonoï T, Fromont J, Kobayashi J (2012) Heteroaromatic alkaloids, nakijinamines, from a sponge *Suberites* sp. *Tetrahedron* 68(41):8545–8550
- Takishima S, Ishiyama A, Iwatsuki M, Otoguro K, Yamada H, Ômura S, Kobayashi H, Van Soest RWM, Matsunaga S (2009) Merobatzelladines A and B, anti-infective tricyclic guanidines from a marine sponge *Monanchora* sp. *Org Lett* 11(12):2655–2658
- Tanaka N, Asai M, Takahashi-Nakaguchi A, Gonoï T, Fromont J, Kobayashi J (2013a) Manzamenone O, new trimeric fatty acid derivative from a marine sponge *Plakortis* sp. *Org Lett* 15(10):2518–2521
- Tanaka N, Kusama T, Takahashi-Nakaguchi A, Gonoï T, Fromont J, Kobayashi J (2013b) Nagelamides X-Z, dimeric bromopyrrole alkaloids from a marine sponge *Agelas* sp. *Org Lett* 15:3262–3265
- Taylor MW, Radax R, Steger D, Wagner M (2007) Sponge-associated microorganisms: evolution, ecology, and biotechnological potential. *Microbiol Mol Biol Rev* 71:295–347
- The PEW charitable trusts (2015) www.pewtrusts.org/antibiotics
- Tilvi S, Rodrigues C, Naik CG, Parameswaran PS, Wahidhulla S (2004) New bromotyrosine alkaloids from the marine sponge *Psammaphysilla purpurea*. *Tetrahedron* 60(45):10207–10215
- Torres YR, Berlinck RGS, Nascimento GGF, Fortier SC, Pessoa C, de Moraes MO (2002) Antibacterial activity against resistant bacteria and cytotoxicity of four alkaloids isolated from the marine sponge *Arenosclera brasiliensis*. *Toxicon* 40:885–891
- Tsuda M, Shimbo K, Kubota T, Mikami Y, Kobayashi J (1999) Two theonellapeptolide congeners from marine sponge *Theonella* sp. *Tetrahedron* 55(34):10305–10314
- Tsuda M, Sakuma Y, Kobayashi J (2001) Suberedamines A and B, new bromotyrosine alkaloids from a sponge *Suberea* species. *J Nat Prod* 64(7):980–982
- Tsuda M, Yohei T, Fromont J, Kobayashi J (2005) Hyrtinadine A, a bis-indole alkaloid from a marine sponge. *J Nat Prod* 68(8):1277–1278
- Tsukamoto S, Yamashita T, Matsunaga S, Fusetani N (1999) Bistellettadines A and B: two bioactive dimeric stelletadines from a marine sponge *Stelletta* sp. *J Org Chem* 64:3794–3795
- Vartoukian SR, Palmer RM, Wade WG (2010) Strategies for culture of unculturable bacteria. *FEMS Microbiol Lett* 309:1–7
- Viegelmann C, Parker J, Ooi T, Clements C, Abbott G, Young L, Kennedy J, Dobson ADW, Edrada-Ebel R (2014) Isolation and identification of antitrypanosomal and antimycobacterial active steroids from the sponge *Haliclona simulans*. *Mar Drugs* 12(5):2937–2952
- Volk CA, Lippert H, Lichte E, Köck M (2004) Two new haliclamines from the arctic sponge *Haliclona viscosa*. *Eur J Org Chem* 14:3154–3158
- Webster NS, Blackall LL (2009) What do we really know about sponge-microbial symbioses? *ISME J* 3:1–3
- Webster NS, Taylor MW (2012) Marine sponges and their microbial symbionts: love and other relationships. *Environ Microbiol* 2012(14):335–346
- Webster NS, Thomas T (2016) The sponge hologenome. *Mbio.asm.org*. 7(2):e00135–16

- Wei X, Nieves K, Rodríguez AD (2010) Neopetrosiamine A, biologically active bis-piperidine alkaloid from the Caribbean sea sponge *Neopetrosia proxima*. *Bioorg Med Chem Lett* 20:5905–5908
- Woo JK, Kim CK, Kim SH, Kim H, Oh DC, Oh KB, Shin J (2014) Gombaspiroketal A-C, sesterterpenes from the sponge *Clathria gombawuiensis*. *Org Lett* 16(11):2826–2829
- Xu M, Davis RA, Feng Y, Sykes ML, Shelper T, Avery VM, Camp D, Quinn RJ (2012) Ianthelliformisamines A-C, antibacterial bromotyrosine-derived metabolites from the marine sponge *Suberea ianthelliformis*. *J Nat Prod* 75:1001–1005
- Yang S-W, Chan T-M, Pomponi S, Chen G, Wright AE, Patel M, Gullo V, Pramanik B, Chu M (2003) A new bicyclic guanidine alkaloid, sch 575948, from a marine sponge, *Ptilocaulis spiculifer*. *J Antibiot (Tokyo)* 56(11):970–972
- Yang F, Gan J, Liu X, Lin H (2014) Scalarane sesterterpenes from the paracel islands marine sponge *Hyrtilos*. *Nat Prod Commun* 9(6):763–764
- Youssef DT, Shaala L, Asfour HZ (2013) Bioactive compounds from the red sea marine sponge *Hyrtilos* species. *Mar Drugs* 11(4):1061–1070
- Youssef DT, Shaala L, Mohamed G, Badr JM, Bamanie FH, Ibrahim SRM (2014) Theonellamide G, a potent antifungal and cytotoxic bicyclic glycopeptide from the Red Sea marine sponge *Theonella swinhoei*. *Mar Drugs* 12(4):1911–1923
- Zidar N, Montalvão S, Hodnik Ž, Nawrot DA, Žula A, Ilaš J, Kikelj D, Tammela P, Mašič LP (2014) Antimicrobial activity of the marine alkaloids, clathrodin and oroidin, and their synthetic analogues. *Mar Drugs* 12(2):940–963

Discovery and Development of Novel Drugs

Vesna Erakovic Haber and Radan Spaventi

Abstract Drug discovery and development process is nowadays conducted in relatively standardised sequence of phases, starting with Discovery and being followed by Preclinical, Clinical and Non-Clinical Development. Discovery phase is divided in Hit Finding, Lead generation, Lead Optimisation and Candidate Identification Phase. Main drivers of the whole process are regulatory requirements and the aim to eliminate the unnecessary spending by early elimination of unlikely drug candidates. Marine products, once purified, isolated and produced in required quantities, follow the same route as any other synthetic drug.

1 Introduction

Human life expectantly has increased significantly during the course of the last century, at least partially due to the discovery of large number of drugs and therefore, the 20th century can be rightfully called true pharmaceutical century. Although number of diseases that were incurable hundred years ago can be easily cured today, modern medicine is still facing significant changes in its aim to ensure good quality of life and extended life-span. New and better drugs are needed to address diseases of the ageing population, such as degenerative diseases and cancer, as well as to overcome continuous threat of novel infections caused by micro-organisms resistant to current therapies.

Throughout the human history, nature was the obvious place to search for medicines. Based on a “trial and error” approach, traditional medicine has collected a body of knowledge that was passed from generation to generation. In the last century, supported by the modern science, people have continued that quest in even

V. Erakovic Haber (✉)

Fidelta d.o.o., Prilaz baruna Filipovića 29, Zagreb, Croatia
e-mail: Vesna.ErakovicHaber@glpg.com

R. Spaventi (✉)

Triadelta Partners d.o.o., Međimurska 19/2, Zagreb, Croatia
e-mail: radan.spaventi@gmail.com

more methodical and controlled manner. This resulted in 1453 drugs that have obtained FDA approval till the end of 2013 (Kinch et al. 2014).

First modern drugs, such as hormones or antibiotics, have provided a basis for the next generations of semisynthetic and synthetic drugs. Initially, compounds were synthesized and tested individually to be followed by chemical libraries produced by combinatorial chemistry (Seneci et al. 2014) and, most recently, DNA-encoded libraries (Mullard 2016). Initial generations of modern drugs are not very selective and numerous serendipitous observations related to their add-on activates inspired 1988 Nobel Laureate in Physiology and Medicine, Sir James Black, to say: “The most fruitful basis for the discovery of a new drug is to start with an old drug”. Furthermore, novel informed insights and technological platforms have provided basis for repositioning of some relatively old drugs, as well as for optimising current drug discovery and development paradigm.

Beforehand, compounds were tested for their activity on animals and sometimes humans, whereas compound screening in vitro systems was subsequently introduced once scientific and technological progress made it possible. Extensive exploration of pathophysiology of human diseases led into several decades of focused TARGET BASED DRUG DISCOVERY. In vitro-centric target based approach resulted with lower than expected number of new drugs due to the very high attrition rate of drug development process. Relatively recently, hope of better predictability has been raised by introduction of PHENOTYPIC ASSAYS that are not focused on specific targets but reconstruct the elements of human disease as accurately as possible.

Evolution of drug discovery and development in modern times has been catalysed by progress and/or limitations in the several areas: our understanding of disease ethiology, knowledge about potential druggable targets, advancement of technologies related to drug pharmaceutical R&D, as well as diversity and number of scaffolds that can be utilised for derivatisation of new drugs. Whereas majority of these areas have been advancing significantly, availability of new natural scaffolds/compounds has been mostly limited by availability of natural sources. Although humans have been attempting to understand and utilise marine resources for therapeutic purposes since ancient times, modern drugs are predominantly based on terrestrial natural origins. Nowadays, pharmaceutical R&D is increasingly turning towards the sea as a source of new therapeutics with the aim to expand innovation potential and maximise utilisation of great advancements in science and technologies. Marine environment represents almost unlimited source of biodiversity and novel bioactive natural products, with structural and chemical features generally not found in terrestrial natural products. To date, a rather limited number of drugs with marine origin have been put to the market or are currently in late phases of development (Table 1). However, relatively rich early-phase pipeline suggests that we are going to see many more of them in the near future (Mayer et al. 2016; <http://marinepharmacology.midwestern.edu/clinPipeline.htm>).

Although every disease and every scientific approach have their particularities, drug discovery and development process itself is nowadays conducted in relatively standardised sequence of discovery and development phases. They are driven by regulatory requirements and the aim to avoid the unnecessary cost by early elimination of unlikely drug candidates. Marine products, once purified, isolated and produced in required quantities, follow the same route as any other synthetic drug (Martins et al. 2014).

Table 1 Marine-derived marketed pharmaceuticals and late stage pipeline (6)

Compound	Trademark (first registration)	Marine organism	Chemical class	Molecular target	Disease area
<i>FDA approved</i>					
Trabectedin (E7-743)	Yondelis (2015)	Tunicate	Alkaloid	Minor groove of DNA	Cancer: Soft Tissue Sarcoma, Ovarian Cancer
Brentuximab vedotin (SGN-35)	Adcetris (2011)	Mollusk/cyanobacterium	ADC (MMAE)	CD30 and microtubules	Cancer: Anaplastic Large T-cell malignant Lymphoma, Hodgkin's Disease
Eribulin Mesylate (E7389)	Halavri (2011)	Sponge	Macrolide	Microtubules	Cancer: Metastatic Breast Cancer
Omega-3-acid ethyl esters	Lovaza (2004)	Fish	Obega-3 fatty acids	Triglyceride synthesising enzymes	Hypertriglyceridemia
Ziconotide	Prialt (2004)	Cone snail	Peptide	DNA polymerase	Pain: Severe Chronic Pain
Vidarabine (Ara-A)	Vira-A (1976)	Sponge	Nucleoside	Viral DNA polymerase	Antiviral: Herpes Simplex Virus
Cytarabine (Ara-C)	Cytosar-U (1969)	Sponge	Nucleoside	DNA polymerase	Cancer: Leukaemia
<i>Late stage pipeline (Phase III)</i>					
Pinabulin (NPI-2358)	N.A.	Fungus	Diketopiperazine	Microtubules	Cancer: Non-Small Cell Lung Cancer, Brain Tumours
Pitipepsin	Aplidin	Tunicate	Dipeptide	Racl and JNK activation	Cancer: Multiple Myeloma, Leukaemia, Lymphoma
Tetrodotoxin	Tectin	Pufferfish	Guanidin alkaloid	Sodium channel	Pain: Chronic pain

2 Project Planning Phase

Basis for every successful drug discovery project is clear understanding of the problem that is intended to be solved and what would successful outcome look like. This type of clarity is usually achieved by precise description of the medical and market needs, target product profile (Table 2) and understanding of the competitive environment. These elements should provide exact answers to the below listed questions.

- **Medical need**

Which medical problem is intended to be solve?
 How relevant would the intervention be for the human health?
 Are there already treatment options available?

- **Market need**

Are there other drugs which already address the problem?
 Would anybody be ready to pay for the new drug with the expected superiority in comparison with exiting treatment options?

Table 2 Example of target product profile (TPP)

Current value proposition	Profile
Indications at launch	Minimal
	Desired
Indications post launch	Minimal
	Desired
Target label	Minimal
	Desired
Pharmacological profile	Minimal
	Desired
Clinical efficacy	Minimal
	Desired
Safety and tolerability	Minimal
	Desired
Health outcomes	Minimal
	Desired
API stability	Minimal
	Desired
Route of administration/Final form	Minimal
	Desired
Dosing regimen	Minimal
	Desired
Contra-indications/Warnings/Precautions/Food and drug interactions	Minimal
	Desired

- **Competition/Comparators**

Are there other drugs in the market or in the drug discovery and development pipeline that address that particular need? Which feature(s) of those drugs should be improved?

- **Target product profile (desired versus. minimal)**

What should new drug be like and which criteria should it fulfil? (Table 2)

3 Where to Start?

One should always start with the disease and disease related knowledge. The better understanding of medical problem, the better will be a selection of relevant drug targets and phenotypic testing systems. Nowadays, a wealth of patient and disease relevant information is present in a public domain collected by clinical and basic researchers, such as human genome project data, genome wide association studies, numerous population studies, etc. Many diseased and healthy human tissues have been compared so far by using number of different technologies, either directly upon removal from donor's body or after cultivation in ex vivo culture systems.

If drug discovery programme is focused around a particular target, the process starts with TARGET VALIDATION. The goal of these efforts is to confirm that particular target is relevant for the pathophysiological process of interest and that its modulation would not present unnecessary health hazard. This is typically done, in addition to extensive literature search, via genetic interventions (e.g. gene knock in/out, siRNA, CRISPER, etc.) and/or using tool compounds within particular biological systems (Bunnage et al. 2013). Both approaches have their limitations. Genetic intervention takes whole protein out of equation and not only its particular function that drug substance actually targets, possibly resulting with an overestimation of potential drug activity, no matter positive or negative. On the other hand, usefulness of tool compounds in target validation process depends highly on their selectivity and potency. Ultimate target validation can be done only in clinical disease setting when selective drug, with appropriate PK/PD properties, is administered to carefully selected patient population.

Even if drug discovery process starts with PHENOTYPIC APPROACH, there is always a clear notion to seek for drug-target(s) interaction that can explain activity in such phenotypic system. Current paradigm of the modern drug discovery stipulates understanding of drug target(s) and affected pathways in order to decrease likelihood of negative surprises later in the drug development process as well as to enable a rational drug design. In contrast to a single target approach, phenotypic-based approach can result with identification of several targets that are

hit by the some compound and combination of which is optimal for achievement of the desired effect.

Once biological strategy is defined and decision has been made weather to use the target-based assays or phenotypic assays, one needs to select which molecules to test in such tests.

4 Drug Discovery

Typical discovery process (Fig. 1) is stepwise approach which starts with hit finding phase. HITS are molecules that show activity in primary screening/test system in dose response manner and demonstrate certain structure-activity relationship (SAR).

Next phase is frequently called Lead generation phase. During this phase hit molecules are optimised for various properties such as potency, selectivity, drug-like physical and chemical properties, etc. A LEAD is a molecule that shows activity and selectivity *in vitro* and first evidence of *in vivo* activity. During the Lead optimisation phase lead is further optimised until it reaches desired pharmacodynamic (PD) and pharmacokinetic (PK) properties, both *in vitro* and *in vivo*, and becomes a CANDIDATE molecule. Toxicity of that molecule is evaluated in non-GLP toxicological tests and PK/PD relationship is explored in animal efficacy models. In addition to biological profiling, assessment of chemical and pharmaceutical developability is performed in order to estimate the likelihood that final drug product containing such active principle can eventually reach the market. If the molecule criteria, it becomes a PRECLINICAL CANDIDATE. Such molecule is

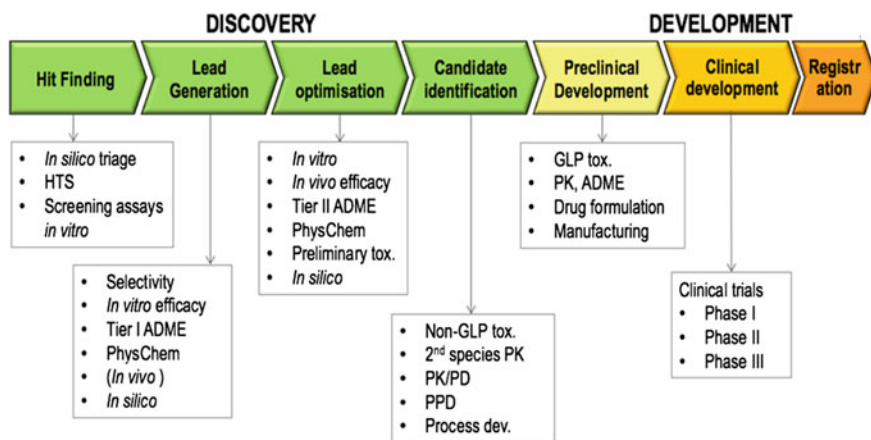


Fig. 1 Drug discovery process. *HITS* High Throughput Screening, *ADME* Absorption Distribution Metabolism Elimination, *GLP* Good Laboratory Practice, *PK* Pharmacokinetics, *PK/PD* Pharmacokinetic vs. Pharmacodynamics, *PPD* Pharmaceutical Product Development

made in larger quantities in order to Preclinical development program, performed in line with Good Laboratory Practice (GLP), which include GLP toxicology, ADME (Absorption, Distribution, Metabolism and Elimination) and PK. A molecule that successfully completes preclinical development phase is ready to enter clinical phase of the drug development and therefore is called a CLINICAL CANDIDATE.

The clinical candidate is then progressed through comprehensive clinical development programme, and, in if it meets required criteria, it is submitted to regulatory bodies for approval.

4.1 Chemical Tactics—Where to Get First Hits?

Several past decades have been characterised by high throughput screening of large chemical libraries composed of hundreds of thousands of random compounds or relatively smaller focused libraries, likely to hit particular type of biological targets, such as kinases, GPCRs, etc. Large compound libraries are mainly made by combinatorial chemistry and their significant portion might not have drug-like physical–chemical properties. On the other hand, when drug target is well explored, rational drug design can lead chemists in the process of making specific compounds with higher likelihood to interact with the target and its active site. Relatively recently, screening of fragment-based libraries has proven to be good strategy in revealing small fragments that interact with a target active site. In the next step, those hit fragments are combined in larger, more potent and selective molecules. Finally, number of chemical structures linked to DNA, combined in DNA-encoded libraries, are currently being used for screening in various biological systems, DNA being unique coding tag and chaperon (Mullard 2016).

In addition to testing pure compounds, some researchers test extracts obtained from various natural sources, including marine organisms (Martins et al. 2014). Such extracts most likely contain molecules that have never been synthesized by researchers and therefore bare potential to hit the targets that have not been conquered so far and reveal novel chemical space. Furthermore, such extracts present mixture of molecules which can have additive or synergistic effects in particular biological assays. Complexity is further added when testing natural extracts in phenotypic assay and observed activity could be result of multiple molecules and multiple targets. Next step, isolation of active structure(s), is very labour intensive process which is frequently unsuccessful or results with structures which cannot be made by chemical synthesis. Sometimes, decent quantities of active molecules can be produced by using biotechnological approaches. Although there is a whole universe of microbes out there, that produce secondary metabolites, we do not have optimal knowledge and/or technology to cultivate them. Please find more details in an excellent review by Martins et al. (2014).

4.2 *Biological Tactics—Screening Cascade*

Drug discovery and development attrition rate is extremely high with only one out of 100,000 synthesized molecules reaching the market in approximately 15 years. Sequences of biological tests that are meant to select the best molecules, most likely to be successful at the end, are called screening or testing cascades (9). If properly designed, testing cascade should reflect target product profile and eliminate inadequate molecules as early as possible, reducing unnecessary spending in the following, always more expensive, stages. Complexity and predictive potential of the testing cascades varies among various therapeutic areas and various diseases. For example, potent antibiotics can be spotted already in *in vitro* systems, whereas efficacy of drugs addressing various psychiatric diseases can only truly be tested within clinical trials and therefore, later therapeutic area is known to be associated with significantly high number of failures during Clinical development.

Testing starts in *in vitro* systems which address all three biological aspects of every drug: PD, PK and toxicology. Cascade starts with more simple and high throughput screening (HTS) assays and gradually moves to more complex systems (Jelic et al. 2013). Typically, first answer one looks for is which compound interacts with the target and that answer can be very frequently obtained in biochemical cell free assay (Fig. 2). Furthermore, it is important to recognise if there is functional consequence of that interaction, as well as, how potent and how selective is the compound.

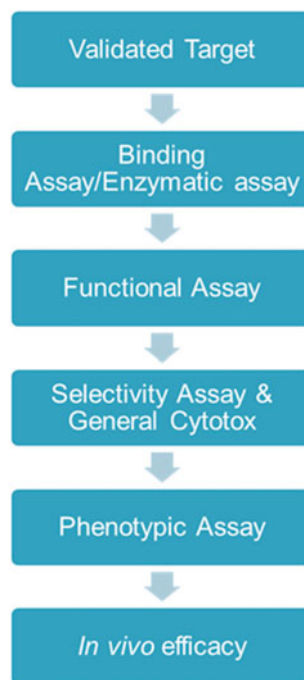
Cellular system adds complexity and only the compounds that are able to reach their biological target and exhibit activity in such living system are selected for further progression. Observed activity is a combined result of several properties of the molecule, next to its target interaction, such as, ability to cross the cell membrane or accumulate in particular subcellular compartment, if necessary for the action. Furthermore, cells are used to evaluate cytotoxicity potential.

Next level of complexity is addressed in whole blood assays, which, in addition to mix cell population, obviously contain various extracellular components that compound will be exposed to during clinical trials. For many years, *in vitro* testing has been done on immortalised cell lines, which provides excellent platform for particular target or pathway related testing, but seriously lack similarity with the disease conditions. Lately, significant efforts have been put into setting up disease-relevant phenotypic assays on primary cells and/or human tissues, with the aim of early evidence of disease-relevant effects.

In parallel with *in vitro* efficacy and toxicity testing, compounds are screened for their plasma protein binding potential, CYP inhibition, solubility, permeability, microsomal and hepatocyte stability in order to identify potential PK liabilities very early in the process.

After successful completion of *in vitro* testing, an evidence of activity in complex living organism is required in order to manage the risk for further progression

Fig. 2 Target-based testing cascade



of the compound and to increase probability of positive clinical outcome. For proper *in vivo* evaluation of the drug candidate molecules, it is essential to fully understand the limitations of the animal efficacy models and recognise that animal models reflect particular pathophysiological elements/pathways and do not represent equivalent of human disease.

In vivo compound testing on laboratory animals provides information on effective dose and route of administration and generates toxicology, safety pharmacology and PK data. That information allows a ranking of potential drug candidates in “head to head” comparison and generates proof of concept for regulatory authorities, as a preparation for “first in human” studies. Establishment of PK/PD relationship and PK/PD modelling provides basis for the clinical dose prediction.

5 Drug Development

Drug development (Fig. 3) is a complex set of activities with a goal to transform a promising drug candidate into new drug. In comparison to drug discovery phase, it is highly regulated and closely monitored by regulatory authorities. Since drug

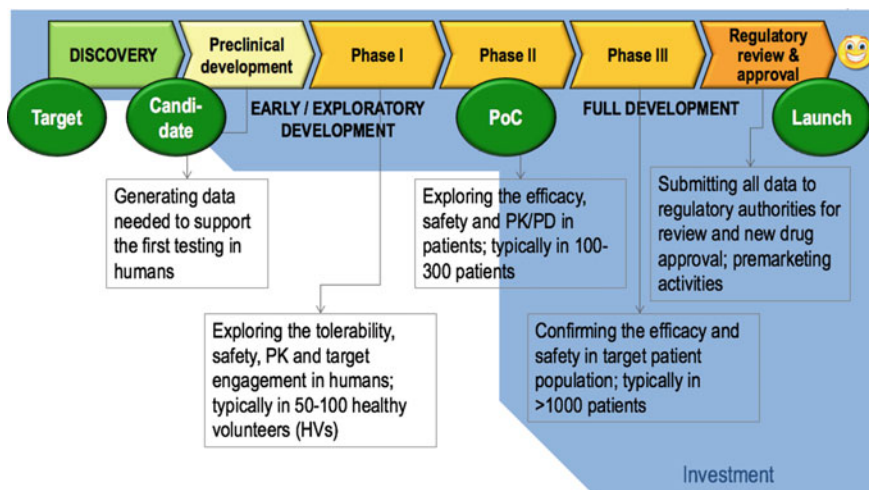


Fig. 3 Drug development process. *PoC* Proof of Concept, *PK* Pharmacokinetics, *PK/PD* Pharmacokinetic vs. Pharmacodynamics

development represents substantial investment, with no guarantee of success, it is crucial that risks are identified and eliminated at the earliest possible stage, or understood and managed while caring forward, in order to build confidence for subsequent investments. In parallel, the progress of the project is continuously assessed via a number of milestones at which obtained results are confronted with the target product profile, potential competition and the market developments.

Drug development can be divided into preclinical development, Clinical development and Non-Clinical development.

6 Preclinical Development

The main goal of Preclinical development is to determine ultimate safety profile of experimental drug candidate with purpose of, as much as possible, limiting risks of its use in humans during clinical trials. This critical phase includes a number of activities required to progress a new drug candidate through toxicology, pharmacology and pharmacokinetic testing. All these activities must be performed in a regulatory compliant manner to ensure that quality of data and the safety of human subjects involved in future clinical trials.

During preclinical studies (Table 3), it is especially important to:

- Define initial safe dose and dose escalation schemes for application in humans
- Identify target organs that are at risk for potential toxicity

Table 3 Preclinical Development

Preclinical development	
Safety, drug metabolism and pharmacokinetics	Chemistry/formulation, manufacturing and controls, regulatory support
GLP Toxicology <ul style="list-style-type: none"> • Single dose tox in two species • Repeated dose tox studies in two species (2 weeks up to 3 months, depending on proposed duration of use in clinical trials) • Carcinogenicity • Genotoxicity • Safety pharmacology • Reproductive tox (if fertile women will be in trials) Comprehensive ADME <ul style="list-style-type: none"> • Bioanalytical method development and validation (for each matrix and species of interest) • Comprehensive PK • GLP Toxicokinetic (TK) assessment • Metabolite identification in tox species • Mass-balance studies 	<ul style="list-style-type: none"> • Form and version screening • Scale-up—Drug substance production for Pharm Dev, Tox and Phase I • Analytical method development and validation <ul style="list-style-type: none"> – Purity, impurities, residual solvents • Drug substance stability testing; Preliminary specification • Prototype formulation development <ul style="list-style-type: none"> – Compatibility w. excipients and closure systems, compressibility, content uniformity, dissolution, stability • Analytical method development and validation • Preliminary specification and QC procedure • Clinical trial material production for Phase I • ICH Stability and release testing • IND preparation and submission

GLP Good Laboratory Practice, *ADME* Absorption Distribution Metabolism Elimination, *PK* Pharmacokinetics, *QC* Quality control

- Explore if observed toxicity is reversible
- Identify safety parameters for clinical monitoring

The other important aspects of Preclinical development are related to the formulation development, manufacturing and procurement of clinical samples of experimental drug.

7 Clinical Development

Clinical programme is a set of studies designed to investigate the benefits and risks of a specific drug in human subjects and patients. While preclinical testing provides basic evidences about drug's safety and efficacy, it cannot replace studies focused on drug interaction with human body. Therefore, the results of clinical trials represent the crucial set of data to support registration and eventual use of future drug in clinical practice.

Human testing of experimental drugs, before drug is approved for consumer sale, is typically conducted in three phases. Each phase is regarded as separate trial,

and after completion of each of them, investigators are required to submit results and obtain approval from the regulatory body to progress into next phase.

Phase I of clinical trials is a first point at which an experimental therapy is administered to people and represents initial testing in a small number (usually 100 or less) of healthy volunteers. These trials are primarily focused on assessing if drug is safe for use in human subjects. In addition to monitoring of side effects, the scope also includes evaluation of how the drug is absorbed, metabolised and excreted, as well as to determine the safe dose range for use in the next phases.

Studies on healthy volunteers can also provide very valuable information linked to “proof of mechanism (PoM) in humans”, confirming that drug, once administered to humans, at particular dose and dosing schedule, triggers drug mechanism-related cascade of events.

Phase II studies evaluate safety and efficacy in a small number of patients (typically 100–300). The most Phase II studies are designed in the way in which the study group of patients who receives the experimental drug is compared with patients receiving either inactive substance (placebo), or a drug that is considered as the standard of therapy. Many of these studies are “double-blinded”, meaning that neither the patients nor investigators have information on who has received the investigated drug. Besides information about drug behaviour, safety of therapy, side effects and potential risks, the scope of trials is to determine the most effective dosing scheme for the experimental therapy as well as optimal method of delivery.

Phase II clinical trials are usually divided in Phase IIA studies, exploratory (non-pivotal) studies that have clinical efficacy, pharmacodynamics or biological activity as primary endpoint, and Phase IIB studies, that are definite dose ranging studies in patients with efficacy as primary endpoint. These days, results of Phase IIA are considered as “proof-of-concept (PoC) in humans”, and represent a major go-non-go milestone in drug development process.

Phase III studies are to demonstrate safety and efficacy of experimental therapy in a large group of patients. The goal of these pivotal studies is to generate statistically significant evidence of safety and efficacy, as required for approval. The goal is also to establish overall risk–benefit relationship of investigational medicine. Finally, the scope of Phase III studies also includes studies that will serve as a basis for labelling instructions and post marketing commitments.

Phase III studies usually enrol thousands of patients across multiple clinical sites around the world, and represent the largest investment in the whole drug discovery and development process.

8 Non-clinical Development

In parallel to the clinical development programme a number of non-clinical activities are performed with aim to support clinical trials and to generate data for approval. Some of these activities represent continuation of activities that have been initiated during preclinical development, and other follow the project evolution.

Table 4 Non-clinical development activities

Non-clinical development	Phase I	Phase II	Phase III
Safety	<ul style="list-style-type: none"> • Repeat dose (1–3 months) tox studies to support Phase II dosing • Reproductive tox (embryo-fetal dev) 	<ul style="list-style-type: none"> • Repeat dose (6/9 months) tox studies • Reproductive tox (fertility) • Juvenile tox (if needed) 	<ul style="list-style-type: none"> • Reproductive tox (pre- and post-natal development) • Carcinogenicity (if needed) • “Bridging” studies
DMPK	<ul style="list-style-type: none"> • Met Id in clinical samples • TK studies (1–3 months, RepTox) 	<ul style="list-style-type: none"> • Met Id from human radiolabel study • Whole body autoradiography • TK studies (6/9 months, Rep Tox) 	<ul style="list-style-type: none"> • ADME for carcinogenicity species, TK • TK studies (Rep Tox)
Chemical (substance) development	<ul style="list-style-type: none"> • Scale-up, DS production for Pharm Dev, Tox and Ph II • Analytical methods refinement, technology documentation 	<ul style="list-style-type: none"> • Scale-up—Final synthetic route • Manufacturing process validation (critical process parameters and critical quality attributes defined) • Final analytical method validation, final specification 	<ul style="list-style-type: none"> • 3 commercial batches for NDA submission • ICH stability for 3 batches • Process documentation for NDA
Pharmaceutical development	<ul style="list-style-type: none"> • Clinical trial material production for Ph II • Further formulation development 	<ul style="list-style-type: none"> • Final formulation and closure system • Scale-up and process validation, Phase III supplies • Final analytical method validation • Final specification 	<ul style="list-style-type: none"> • 3 commercial batches for NDA submission • ICH stability for 3 batches • Process documentation for NDA

Met Id Metabolite Identification, *DS* Drug Substance, *TK* Toxicokinetics, *Rep Tox* Reproductive Toxicology, *ADME* Absorption Distribution Metabolism Elimination, *NDA* New Drug Application, *ICH* International Conference of Harmonisation

Non-clinical activities can be divided in four major categories: safety, DMPK, chemical/substance development and pharmaceutical development (Table 4).

Drug development is exceptionally complex; lengthy and costly process in which project planning and project management play the role of utmost importance. Although clinical part of the project progresses mostly in consecutive manner, supporting extensive and complex set of non-clinical activities has to be carefully planned and executed in order to ensure fast progression, informed decision-making at milestone points, and stringent cost control.

References

- Bunnage ME, Piatnitski Chekler EL, Jones LH (2013) Target validation using chemical probes. *Nat Chem Biol* 9:195–199
- Jelic D, Brajsa K, Banjanac M, Spaventi R, Erakovic Haber V (2013) In vitro biology screening in discovery of hits and leads. 9th chapter in the book medicinal chemistry in drug discovery. In: Jelić D (ed) Design, synthesis and screening, research signpost—Transworld Research Network. ISBN 978-81-7895-560-5
- Kinch MS, Haynesworth A, Kinch SL, Hoyer D (2014) An overview of FDA-approved new molecular entities: 1827–2013. *Drug Discovery Today* 8:1034–1039
- Martins A, Vieira H, Gaspar H, Santos S (2014) Marketed marine natural products in the pharmaceutical and cosmeceutical industries: tips for success. *Mar Drugs* 12:1066–1101
- Mayer AM, Nguyen M, Newman DJ, Glaser KB (2016) The marine pharmacology and pharmaceuticals pipeline in 2015. *FASEB J* 30(Supplement):932.7
- Mullard A (2016) DNA tugs help the hunt for drugs. *Nature* 530:367–369
- Seneci P, Fassina G, Frecer V, Miertus S (2014) The effects of combinatorial chemistry and technologies on drug discovery and biotechnology—a mini review. *Nova Biotechnol Chim* 2:87–108

Computer-Aided Drug Discovery from Marine Compounds: Identification of the Three-Dimensional Structural Features Responsible for Antimalarial Activity

Caterina Fattorusso, Francesca Rondinelli, Marco Persico, Nausicaa Orteca and Antonio Di Dato

Abstract An integrated computational approach, based on molecular dynamics/mechanics, semi-empirical, and DFT calculations as well as dynamic docking studies, has been employed to gain insight into the mechanism of action of new antimalarial agents characterized by the scaffold of the marine compounds plakortin and aplidinone. The results of this approach show that these molecules, after interaction with Fe(II), likely coming from the heme molecule, give rise to the formation of radical species, that should represent the toxic intermediates responsible for subsequent reactions leading to plasmodium death. The three-dimensional structural requirements necessary for the activity of these new classes of anti-malarial agents have been identified and discussed throughout the chapter.

1 Introduction

The studies herein reported concerned the following groups of marine compounds: antimalarial endoperoxides and quinones.

The therapeutic choices to treat malaria cases are still too limited and the prospect of resistance is high (Arav-Boger and Shapiro 2005). For these reasons, there is an urgent need for the rapid development of effective, safe, and synthetically affordable antimalarial agents. In this regard, nature remains an ever evolving resource; bioactive natural compounds form a rich source of unique chemical scaffolds suited for optimization to obtain new improved therapeutics (Jung et al. 2003). A number of well-known antimalarial natural drugs, such as endoperoxides

C. Fattorusso (✉) · F. Rondinelli · M. Persico · N. Orteca · A. Di Dato
Department of Pharmacy, University of Napoli “Federico II”,
Via D. Montesano 49, 80131 Naples, Italy
e-mail: caterina.fattorusso@unina.it

and quinones, have shown potent antimalarial activities impairing the parasite antioxidant defences. Despite the large use of natural endoperoxides as antimalarials and their proved clinical efficacy, the exact molecular mechanism of their biological activity is still a matter of debate (Haynes et al. 2010; Mercer et al. 2011). Nevertheless, the ability of these molecules to interact with Fe(II)-heme and to increase Plasmodium oxidative stress has been proved (Wang et al. 2015). On the other hand, redox-active quinones are reported to act as “subversive substrates” in biological systems (Ehrhardt et al. 2013). Subversive substrates are compounds that are reduced by enzymes in a single-electron step to the respective radical, which then spontaneously react to yield superoxide anion radicals, thus leading to cell death. On these bases, the two series of synthetic analogs of marine natural compounds, such as plakortin (endoperoxides) and aplidinone A and B (thiazinoquinone), and a new series of marine natural endoperoxides, showing varying antimalarial activity, were subjected to molecular modeling studies in order to identify the three-dimensional structural features responsible for the observed activity (Persico et al. 2013; Chianese et al. 2014; Lombardo et al. 2014; Sonawane et al. 2015; Imperatore et al. 2015).

2 Materials and Methods: Molecular Modeling Studies

Computational studies were performed on SGI Origin 200 8XR12000 and E4 Server Twin 2 × Dual Xeon 5520, equipped with two nodes. Each node consisted of 2 × Intel Xeon QuadCore E5520, 2.26 GHz, 36 GB RAM. The molecular modeling graphics were carried out on SGI Octane 2 workstations. The apparent pK_a and Log D values were calculated by using the ACD/ pK_a DB and ACD/Solubility DB, version 12.00, software (ACD/Labs, Advanced Chemistry Development Inc., Toronto, Canada). Accordingly, percentage of neutral/ionized forms were computed at pH 7.2 (cytoplasm) and pH 5.5 [Food vacuole (FV) of *Plasmodium falciparum* (Pf)] using the Handerson–Hasselbalch equation.

The new natural polyketide endoperoxides (**Pik1–7**) and the synthetic analogs of plakortin (**7–10**) and Aplidinone A and B (**11–22**) were built using the Insight 2005 Builder module (Accelrys Software Inc., San Diego, CA) taking into account the prevalent ionic forms of each tautomer at the considered pH values (i.e., 7.2 and 5.5). Atomic potentials and charges were assigned using the CFF91 force field (Maple et al. 1994). The conformational space of compounds was sampled through 200 cycles of simulated annealing ($\epsilon = 80^*r$). In simulated annealing, the temperature is altered in time increments from an initial temperature to a final temperature by adjusting the kinetic energy of the structure (by rescaling the velocities of the atoms). The following protocol was applied: the system was heated up to 1000 K over 2000 fs (time step of 3.0 fs). A temperature of 1000 K was applied to the system for 2000 fs (time step of 1.0 fs) with the aim of surmounting torsional barriers. Successively, the temperature was linearly reduced to 300 K in 1000 fs (time step of 1.0 fs). Resulting conformations were then subjected to molecular

mechanics (MM) energy minimization within the Insight 2005 Discover module ($\epsilon = 80^*r$) until the maximum rms derivative was less than 0.001 kcal/Å, using conjugate gradient as minimization algorithm. All MM conformers were then subjected to a full geometry optimization by semiempirical calculations, using the quantum-mechanical methods PM6 (Stewart 2007) or PM7 (Stewart 2013) in the MOPAC2012 package and EF (eigenvector following routine) as geometry optimization algorithm (Baker 1986). The GNORM value was set to 0.01. To reach a full geometry optimization, the criterion for terminating all optimizations was increased by a factor of 100, using the keyword PRECISE.

As reported below, the resulting quantum-mechanical conformers were analyzed using for each new series of antimalarial derivatives a different procedure.

First series of synthetic analogs of plakortin. Resulting conformers of the first series of synthetic analogs of plakortin (7–9) were ranked by their potential energy values (i.e., ΔE from the global energy minimum) and grouped into families on the basis of their 1,2-dioxane ring conformation (i.e., chair A, chair B; skew boat A and skew boat B). All PM6 conformers within 5 kcal/mol from the GM characterized by chair A 1,2-dioxane ring conformation were further classified on the basis of (i) distance between endoperoxide oxygens (O1 and O2) and possible partners for a ‘through space’ (1,4 and 1,5) intramolecular radical shift (≤ 3 Å) and (ii) steric accessibility of endoperoxide oxygen lone pairs. The accessible surface area of endoperoxide oxygens lone pairs has been evaluated by calculating Connolly surfaces (Insight 2005, Accelrys Software Inc., San Diego). The occurrence rates of putative bioactive conformers for all new designed endoperoxides were calculated. The low energy conformers meeting the assumed pharmacophoric requirements, in complex with Fe(II), were subjected to DFT calculations. All possible Fe(II) coordination geometries (i.e., O1, O1/O2, O2/O7, and O1/O2/O7) were used as starting structures for the DFT study. All DFT calculations have been performed with the Gaussian 09 program suite (Frisch et al. 2009) by using the B3LYP/6-311++G** level of theory (Frisch et al. 1984). Particular attention was devoted to the metal orbitals treatment through DZVP (opt), an all-electron orbital basis set specific for B3LYP (Chiodo et al. 2004). It is in fact well known that the combination of a hybrid exchange-correlation functional and a pseudopotential fails in the representation of spin density distribution (Liu 2001). All structures were optimized without imposing geometric constraints and the vibrational analysis was performed at the same level of theory. APT charges were evaluated for every system. Furthermore, a complete insight of spin density distribution was ensured by evaluating both Mulliken and NBO approaches (Ruiz et al. 2005). Gabedit 2.3.5 software graphical interface was used to plot spin density isosurfaces (Allouche 2011).

Second series of new synthetic analogs of plakortin. PM7 resulting conformers of the second series of synthetic analogs of plakortin (10) were ranked by their potential energy values (i.e., ΔE from the global energy minimum). All PM7 conformers within 5 kcal/mol from the GM were classified on the basis of: (i) 1,2-dioxane ring conformation; (ii) intramolecular hydrogen bonds and (iii) distance between endoperoxide oxygens (O1 or O2) and possible partners for a

'through space' intramolecular radical shift (≤ 3 Å). Then, the occurrence rates were calculated. In order to further investigate the role of the conformational behavior on antimalarial activity, docking studies were carried out on **10c** di-protonated form in complex with heme, using a docking methodology (Affinity, SA_Docking; Insight 2005, Accelrys, San Diego, CA) which considers all the systems flexible (i.e., ligand and heme). Atomic potentials of heme were assigned using the Heme29.frc (Holtje and Fattorusso 1998), a force field including heme parameters and atomic partial charges were assigned using the quantum mechanical method PM7. Heme apparent pK_a values were calculated by using ACD/Percepta software. Accordingly, one propionic chain was considered protonated and the heme net total charge was set at +1. Although during the subsequent dynamic docking protocol all the systems were perturbed by means of Monte Carlo and simulated annealing procedures, a reasonable starting structure is anyway required. Thus, the PM7 lowest energy conformer of **10c** meeting the hypothesized pharmacophoric requirements for antimalarial activity was selected as the ligand starting conformation. The ligand was then placed above the heme, taking as template the crystal structure of a peroxo-bridged heme-copper dinuclear complex (CSD code UKACIS) and considering the O2/O7 iron coordination complex. During the docking calculations, all atoms in the complex were left free to move during the entire docking calculations with the exception of heme pyrrolic carbons, which were kept fixed and, in order to avoid unrealistic results, the distance between the iron and the interacting oxygens (i.e. O2 and O7) was restrained within 2.0 Å (100–1000 kcal/mol/Å²). The Cell_Multipole method has been used to calculate nonbond interactions (Ding et al. 1992). A Monte Carlo/minimization approach for the random generation of a maximum of 20 acceptable ligand/heme complexes was used. During the first step, starting from the previously obtained roughly docked structures, the ligand was moved by a random combination of translation, rotation, and torsional changes (Flexible_Ligand option, considering all rotatable bonds) to sample both the conformational space of the ligand and its orientation with respect to the heme (MxRChange = 3 Å; MxAngChange = 180°). During this step, van der Waals (vdW) and Coulombic terms were scaled to a factor of 0.1 to avoid very severe divergences in the Coulombic and vdW energies. If the energy of a complex structure resulting from random moves of the ligand was higher by the energy tolerance parameter than the energy of the last accepted structure, it was not accepted for minimization. To ensure a wide variance of the input structures to be successively minimized, an energy tolerance value of 10⁶ kcal mol⁻¹ from the previous structure has been used. After the energy minimization step (conjugate gradient, 2500 iterations, $\epsilon = 1$), the Metropolis test, at a temperature of 310 K, and a structure similarity check (rms tolerance of 0.3 kcal Å⁻¹) were applied to select the 20 acceptable structures. Each subsequent structure was generated from the last accepted structure. All the accepted complexes resulting from the Monte Carlo/minimization approach were subjected to a molecular dynamics simulated annealing protocol, including 5 ps of a dynamic run divided in 50 stages (100 fs each) during which the temperature of the system was linearly decreased from 500 to 300 K (Verlet velocity integrator; time step of 1.0 fs). Molecular dynamics

calculations were performed using a constant temperature and constant volume (NVT) statistical ensemble, and the direct velocity scaling as temperature control method (temp window, 10 K). In the first stage, initial velocities were randomly generated from the Boltzmann distribution according to the desired temperature, while during the subsequent stages initial velocities were generated from dynamics restart data. A temperature of 500 K was applied to surmount torsional barriers, thus allowing an unconstrained rearrangement of the ligand and the heme (initial vdW and Coulombic scale factors of 0.1). Successively temperature was linearly reduced to 300 K in 5 ps, and concurrently the scale factors have been similarly decreased from their initial values (0.1) to their final values (1.0). A final round of 10^5 minimization steps (conjugate gradient, $\epsilon = 1$) followed the last dynamics steps, and the minimized structures were saved in a trajectory file. After this procedure, the resulting docked structures were ranked by their conformational energy. The complex with the best conformational energy was selected as structure representing the most probable binding mode.

New natural polyketide endoperoxides. PM7 resulting conformers of new natural polyketide endoperoxides were ranked by their potential energy values (i.e., ΔE from the global energy minimum) and grouped into families on the basis of their 3,6-dihydro-1,2-dioxine ring (**Plk1–3**) or 1,2-dioxane ring (**Plk5–7**) conformation. All PM7 conformers within 5 kcal/mol from the GM were further classified on the basis of (i) distance between endoperoxide oxygen O1 and possible partners for a ‘through space’ (1,4 and 1,5) and (ii) steric accessibility of endoperoxide oxygen lone pairs. The accessible surface area of endoperoxide oxygens lone pairs has been evaluated by calculating Connolly surfaces (Insight 2005, Accelrys Software Inc., San Diego). Conformers owning interatomic distances suitable for a radical shift from O1 (≤ 3 Å) and the steric accessibility of the endoperoxide oxygens were selected as the putative bioactive conformers.

Synthetic analogs of Aplidinone A and B. PM7 resulting conformers of the synthetic analogues of Aplidinone A and B (**11–22**) within 5 kcal/mol from the GM ($\Delta E_{GM} \leq 5$ kcal/mol) were analyzed and grouped into conformational families according to the amide conformation. The occurrence rates and ΔE_{GM} range for each conformational family were calculated. The GM conformers of the synthetic analogues of Aplidinone A and B were subjected to further quantum mechanical calculations. In particular, starting from the structure of the GM conformers, the redox states Q^- , QH_i and QH_{ii} were generated and used as starting structures for further semi-empirical (PM7) calculations. In view of the fact that the Q^- , QH_i and QH_{ii} are radical species characterized by just one unpaired electron, the unrestricted Hartree–Fock method (UHF, PM7 method, Mopac2012) was used and the multiplicity was set to doublet. Moreover, EF (Eigenvector Following routine) as geometry optimization algorithm was used and GNORM value was set to 0.01. To reach a full geometry optimization the criteria for terminating all optimizations was increased by a factor of 100, using the keyword PRECISE. Finally, to analyze the charge distribution and the spin density, the keywords BONDS and LARGE were used. For each considered redox state, were calculated: (i) the heat of formation

(Hf) and (ii) the energy of the frontier molecular orbitals (HOMO, LUMO, and SOMO). Then, using these values, the redox capacities were assessed calculating: (i) the reaction enthalpies (kcal/mol) for electron/proton transfer [i.e., $\Delta H_f(Q \rightarrow Q^-)$: $H_f(Q^-) - H_f(Q)$; $\Delta H_f(Q^- \rightarrow QH)$: $H_f(QH) - H_f(Q^-)$ and $\Delta H_f(Q \rightarrow QH)$: $H_f(QH) - H_f(Q)$]; (ii) the electrophilicity index (ω) and (iii) the vertical ionization potential (IP) and electron affinity (EA). In particular, gas phase reaction enthalpy calculations for electron attachment were accomplished by determining ΔH of the reaction $Y + e^- \rightarrow Y^-$ that is, $\Delta H = H_f(Y^-) - H_f(Y)$, where Y is Q or QH and Hf is the calculated heat of formation. Reaction enthalpies for proton attachment were calculated by determining ΔH of the reaction $Y + H^+ \rightarrow YH$ that is $\Delta H = H_f(YH) - H_f(Y)$, where Y is Q^- or QH (Sawyer et al. 1996). The electrophilicity index (ω) was calculated following the expression $\omega = (\mu^2/2\eta)$, where μ is the chemical potential given by $\mu = -(IP + EA)/2$ and η is the chemical hardness given by $\eta = (IP - EA)$ (Parr et al. 1999). Finally, the vertical ionization potential (IP) and the vertical electron affinity (EA) were calculated from the energy of the LUMO of the non-radical cations and from the energy of HOMO of the non-radical anions in the geometry of the radicals, respectively. At this purpose, a single-point PM7 calculation (ISCF) was performed on the non-radical cations and anions of the obtained species Q^- and QH (Colson and Sevilla 1995).

3 Identification of the Three-Dimensional Structural Features Responsible for the Antimalarial Activity

3.1 First Series of New Synthetic Analogues of Plakortin

According to our hypothesized antimalarial mechanism of action for plakortins (Fig. 1) the “bioactive” reaction (i.e., the reaction responsible for antimalarial activity) is thought to proceed through a concerted mechanism, where the following events occur in a single step: (i) one electron uptake from iron(II), (ii) O1–O2 bond breaking with consequent O1 radical formation, (iii) O1–C9 bond formation with the consequent radical shift on C10 (Taglialatela-Scafati et al. 2010).

This latter species represents the key toxic intermediate responsible for plakortin antimalarial activity being involved in subsequent intermolecular reactions. Thus, the structure must simultaneously orientate all intramolecular reaction partners in order to trigger production of the toxic carbon radical. The results of this investigation also evidenced that the ester side-chain is not directly involved in the formation of carbon radical intermediates; nevertheless, our computational results demonstrated that the presence of the ester group may play a role in the interaction with iron, affecting the approach of the endoperoxide to heme (Taglialatela-Scafati et al. 2010).

This guided us in the design of series of simple differently substituted endoperoxides characterized by a 3-methoxy-1,2-dioxane scaffold (**2**, Fig. 2), a

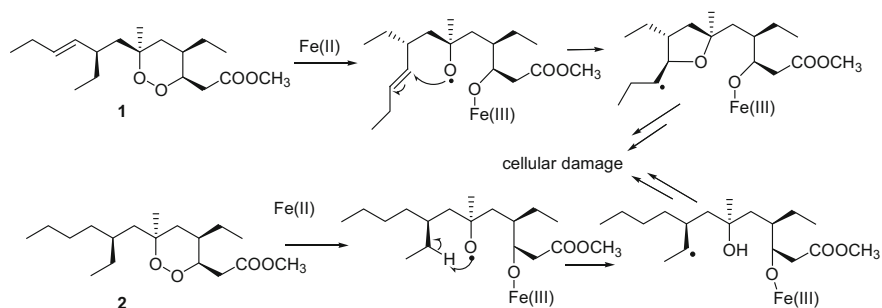
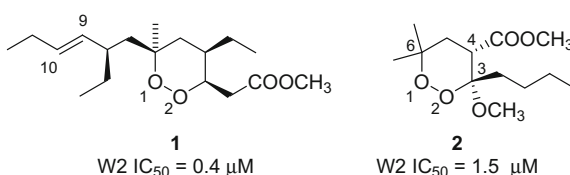


Fig. 1 Proposed antimalarial mechanism of action of plakortin (**1**) and dihydroplakortin (**2**). Figure reproduced from reference Chianese et al. (2014) with permission from Elsevier (<http://dx.doi.org/10.1016/j.bmc.2014.07.034>)

Fig. 2 Plakortin **1** and synthetic analogue **2**. Figure reproduced from reference Persico et al. (2013) with permission from Elsevier (<http://dx.doi.org/10.1016/j.ejmech.2013.10.050>)



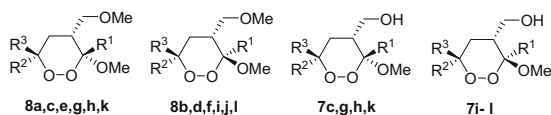
cheap two-pot Mn(III)-mediated synthesis, and an antimalarial activity against CQ-R *Pf* strains in the low micromolar-high nanomolar range (Persico et al. 2011).

To gain a better insight into the structure-activity relationships (SARs), we developed three new families of differently substituted 3-methoxy-1,2-dioxanes (Persico et al. 2013; Lombardo et al. 2014). The structures and the antimalarial activity of the new series of synthetic plakortin analogs (**7–9**), modified at C4 side chain with respect to the previous ester series represented by **2** (Fig. 2), are reported in Tables 1 and 2.

The results reported in Table 1 indicate that most of new 4-methoxymethyl derivatives (i.e., **8e**, **8g**, **8h**, **8i**, and **8k**) show an improved antimalarial activity compared to the corresponding ester analogs (Persico et al. 2011). In particular, compound **8g** reached the activity of the natural lead **1** (Table 1), while the activity of its ester precursor was three times lower (IC₅₀ = 1.5 μM) (Persico et al. 2011).

On the other hand, compounds bearing a hydroxymethyl group at C4 resulted generally less active than their ether analogs and, in some cases, also than their ester analogs (i.e., **7c**, **7h**, and **7i**; Table 1). These results are in agreement with our pharmacophore model for plakortin analogues (Fig. 3) (Tagliatalata-Scafati et al. 2010).

The antimalarial activity is affected by the presence of a novel iron-interacting function, in addition to the endoperoxide, able to interfere with iron coordination and/or endoperoxide bridge reduction. Importantly, the inactivity of the two diastereoisomers **8a** and **8b** (Table 1) confirmed also for this series of compounds the hypothesized antimalarial mechanism of action (Persico et al. 2011).

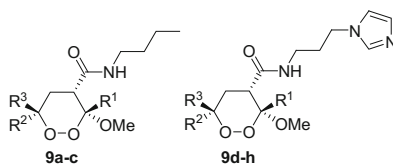
Table 1 Structures and antimalarial activity of the new synthetic analogs of plakortins (**7** and **8**) against Chloroquine-sensitive (D10) and Chloroquine-resistant (W2) *Pf* strains

Cmp	R ¹	R ²	R ³	D10 IC ₅₀ (μM) ^a	W2 IC ₅₀ (μM) ^a
8a	Me	Me	Me	>30	>30
8b	Me	Me	Me	>30	>30
7c	<i>n</i> -Bu	Me	Me	17.2 ± 4.2	7.3 ± 3.6
8c	<i>n</i> -Bu	Me	Me	8.6 ± 2.8	2.8 ± 0.9
8d	<i>n</i> -Bu	Me	Me	>30	>30
8e	Me	<i>n</i> -Bu	<i>n</i> -Bu	nd ^b	1.7 ± 0.7
8f	Me	<i>n</i> -Bu	<i>n</i> -Bu	nd	1.5 ± 0.6
7g	<i>n</i> -Bu	<i>n</i> -Bu	Me	5.4 ± 1.0	1.9 ± 0.5
7h	<i>n</i> -Bu	Me	<i>n</i> -Bu	6.0 ± 2.2	2.3 ± 1.2
7i	<i>n</i> -Bu	<i>n</i> -Bu	Me	>30	11.2 ± 2.5
8g	<i>n</i> -Bu	<i>n</i> -Bu	Me	0.8 ± 0.2	0.5 ± 0.1
8h	<i>n</i> -Bu	Me	<i>n</i> -Bu	0.9 ± 0.1	0.7 ± 0.2
8i	<i>n</i> -Bu	<i>n</i> -Bu	Me	4.3 ± 0.8	2.0 ± 0.2
8j	<i>n</i> -Bu	Me	<i>n</i> -Bu	2.3 ± 0.4	1.2 ± 0.2
7k	<i>n</i> -Bu	<i>n</i> -Bu	<i>n</i> -Bu	4.0 ± 1.4	1.6 ± 0.4
7l	<i>n</i> -Bu	<i>n</i> -Bu	<i>n</i> -Bu	2.4 ± 0.5	1.0 ± 0.2
8k	<i>n</i> -Bu	<i>n</i> -Bu	<i>n</i> -Bu	nd	0.7 ± 0.3
8l	<i>n</i> -Bu	<i>n</i> -Bu	<i>n</i> -Bu	nd	1.0 ± 0.3
Plakortin, 1	–	–	–	0.9 ± 0.4	0.4 ± 0.1

Table adapted from reference Persico et al. (2013) with permission from Elsevier (<http://dx.doi.org/10.1016/j.ejmech.2013.10.050>)

^aData are the mean ± SD of three different experiments in duplicate

^bnd not determined

Table 2 Structures and antimalarial activity of the new synthetic analogs of plakortins (**9**) against Chloroquine-sensitive (D10) and Chloroquine-resistant (W2) *Pf* strains

Cmp	R ¹	R ²	R ³	D10 IC ₅₀ (μM) ^a	W2 IC ₅₀ (μM) ^a
9a	Me	Me	Me	>30	>30
9b	<i>n</i> -Bu	Me	Me	5.1 ± 0.2	2.2 ± 0.8
9c	Me	<i>n</i> -Bu	<i>n</i> -Bu	3.8 ± 0.8	1.95 ± 0.05

(continued)

Table 2 (continued)

Cmp	R ¹	R ²	R ³	D10 IC ₅₀ (μM) ^a	W2 IC ₅₀ (μM) ^a
9d	<i>n</i> -Bu	Me	Me	>30	11 ± 2
9e	Me	<i>n</i> -Bu	<i>n</i> -Bu	0.7 ± 0.1	0.5 ± 0.2
9f	<i>n</i> -Bu	<i>n</i> -Bu	Me	2.6 ± 0.7	1.7 ± 0.3
9g	<i>n</i> -Bu	Me	<i>n</i> -Bu	3.1 ± 0.8	1.5 ± 0.3
9h	<i>n</i> -Bu	<i>n</i> -Bu	<i>n</i> -Bu	1.8 ± 0.4	0.84 ± 0.05
Plakortin, 1	–	–	–	0.9 ± 0.4	0.4 ± 0.1

Table adapted from reference Lombardo et al. (2014) with permission from Wiley-VCH Verlag GmbH & Co. KGaA (<http://dx.doi.org/10.1002/ejoc.201301394>)

^aData are the mean ± SD of three different experiments in duplicate

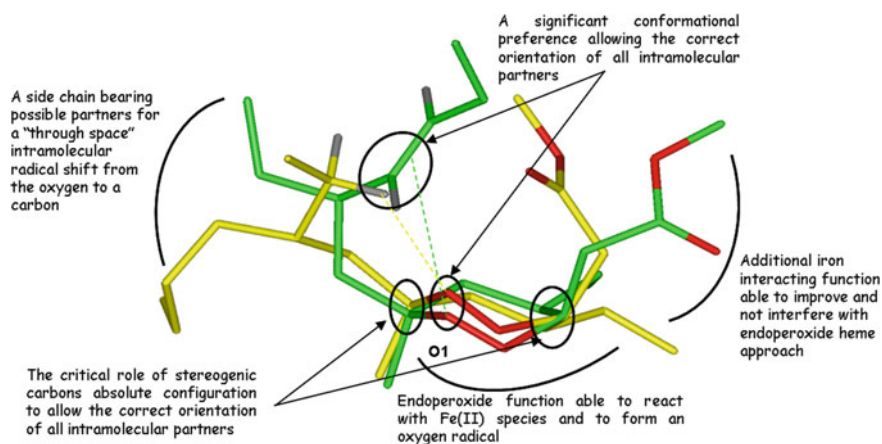


Fig. 3 Three-dimensional pharmacophore model of plakortin analogs. Figure adapted from reference Tagliatalata-Scafati et al. (2010) with permission from the Royal Society of Chemistry (<http://dx.doi.org/10.1039/b918600j>)

Indeed these compounds, presenting only methyl substituents, are not able to form the putative carbon-centered radical on the alkyl chains installed at C3 and/or C6.

Moreover, since the steric repulsion between C3, C4, and C6 substituents drives the conformational preference of the 1,2-dioxane ring, then the most populated ring conformer is the chair characterized by the equatorial position of substituent at C4, named chair A (Table 3).

The only exceptions are represented by compounds **8a** and **8b**, which, indeed, possess only methyl substituents at C3 and C6. These results indicated that the replacement of the ester function at C4 with different groups, such as, methoxymethyl and hydroxymethyl, did not affect the overall conformational preference of the 1,2-dioxane ring, which was proved to be crucial for antimalarial activity. Then, we selected low energy conformers (within 5 kcal/mol from the global energy minimum) owning the required structural features for antimalarial activity

Table 3 Occurrence rate (%) of 1,2-dioxane ring conformations of biologically tested **7** and **8** considering conformers within 5 kcal/mol from the global minimum

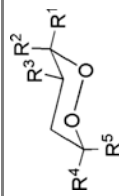
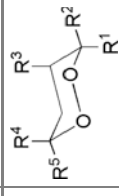
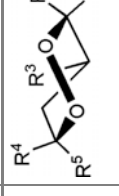
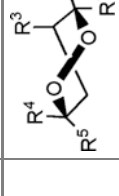
Cmp	Chair A	Chair B	Skew boat A	Skew boat B
				
8a	35	13	39	13
8b	32	18	36	14
7c	48	7	35	10
8c	60	9	24	7
8d	50	9	36	5
8e	62	9	23	6
8f	49	8	38	5
7g	70	4	17	9
7i	66	6	25	3
7h	71	4	20	5
8g	70	5	21	4
8i	77	2	17	4
8h	60	7	21	12
8j	67	6	19	8
7k	69	3	21	7
7l	62	7	28	3
8k	64	3	28	5
8l	70	4	19	7

Table reproduced from reference Persico et al. (2013) with permission from Elsevier (<http://dx.doi.org/10.1016/j.ejmech.2013.10.050>)

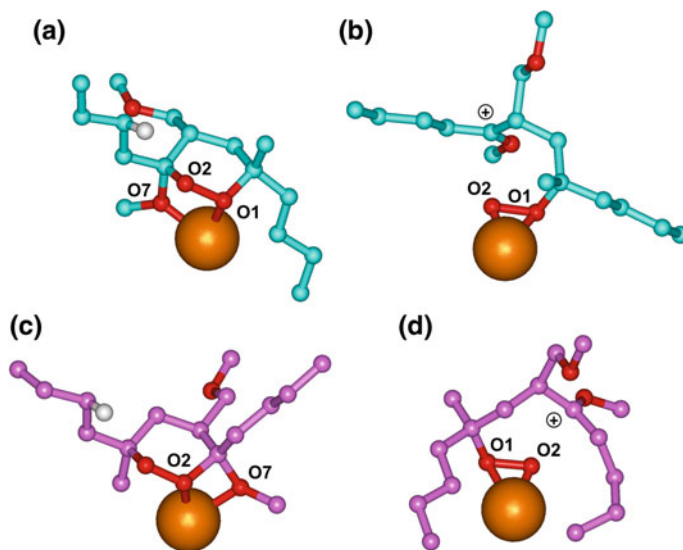


Fig. 4 DFT structures of **8g** and **8i** bioactive conformers in complex with Fe(II): **a** **8g** O1/O2/O7 complex; **b** **8g** heterolytic scission product of the O1/O2 complex; **c** **8i** O2/O7 complex; **d** **8i** heterolytic scission product of the O1/O2 complex. van der Waals volume of iron is shown (scaled by 50% for clarity of presentation). The oxygens interacting with iron are labelled. Atoms are colored as follows: C = cyan (**8g**); pink (**8i**); O = red; H = white; Fe(II) = orange. Hydrogens are omitted for the sake of clarity with the exception of that involved in the 1,4-H shift. Figure adapted from reference Persico et al. (2013) with permission from Elsevier (<http://dx.doi.org/10.1016/j.ejmech.2013.10.050>)

according to our pharmacophore model (Fig. 3), that is: (i) chair A conformation of the 1,2-dioxane ring, (ii) distance of the endoperoxide oxygens from the putative partner for a 1,5- or 1,4-intramolecular radical shift ≤ 3 Å, and (iii) steric accessibility of endoperoxide oxygen lone pairs.

According to previous results (Persico et al. 2011), iron coordination mode is supposed to be determinant for the formation of the radical on O1 rather than on O2, and, by consequence, for its possible evolution on C6 instead of C3 butyl chain. To investigate this issue, previously selected PM6 conformers were subjected to DFT calculations, using as starting structures all possible Fe(II) coordination complexes. First, the results obtained confirmed that the Fe(II)–O1/O2 starting complex led to the inactive O2–C3 heterolytic scission product either in 3,4-*cis* and in 3,4-*trans* diastereoisomers (Fig. 4b, d).

Consequently, similarly to the ester series, iron coordination mode depends on the stereochemistry of the C3 substituted carbon. In particular, results obtained for 3,4-*cis* diastereoisomers indicated that the methoxy group in the axial position is able to induce the formation of the energetically favored pre-reactive complex showing O1/O2/O7 coordinating Fe(II) (Fig. 4a). This pre-reactive iron complex is potentially able to form the oxygen radical on both O1 and O2, and to evolve either

on C3 or C6 butyl chain (Persico et al. 2011). On the other hand, DFT calculations on 3,4-*trans* stereoisomers presenting the C3 methoxy substituent in the equatorial position, confirmed that they coordinate Fe(II) only by O2 and O7 (Fig. 4c), with the consequent radical formation on the endoperoxide oxygen O1, and a possible evolution only on C6 butyl chain (Persico et al. 2011).

In agreement with these results, the SARs indicated that: (i) 3,4-*cis* stereoisomers are generally more active than 3,4-*trans* stereoisomers (Table 1); (ii) the presence of the butyl chain at C3 improves antimalarial activity particularly in 3,4-*cis* (Table 1). Moreover, considering **8c** and **8d**, which bear a butyl chain at C3 and two methyl groups at C6, only the first shows some antimalarial activity.

The rates of putative bioactive conformers of 3,4-*cis* and 3,4-*trans* diastereoisomers were calculated. All analyzed compounds presented a significant rate of low energy conformers potentially able to undergo an intramolecular H shift from the butyl chain to the oxygen radical.

In agreement with the observed antimalarial activity (Table 1), stereoisomers bearing *cis* C3 and C6 butyl chains presented a decreased rate of putative bioactive conformers with respect to stereoisomers with *trans* C3 and C6 butyl chains (**8g** vs. **8h**, **7g** vs. **7h**, and **8j** vs. **8i**).

Although our results on C4-methoxymethyl and C4-hydroxymethyl derivatives evidenced some similarities with the previous series of endoperoxides characterized by the ester function at C4, they revealed also some peculiarities. In particular, in 3,4-*cis* stereoisomers the replacement of the carbonyl group with the methylene group at C4 favors the evolution of the oxygen radical preferentially on C6 rather than C3 butyl chain [opposite to what previously observed for the ester series (Persico et al. 2011)].

DFT calculations evidenced that, regardless of the orientation used as starting structure, Fe(II) always induced the same orientation of the C3 methoxy group. In putative bioactive conformers this caused a rearrangement of the substituent at C4, still maintaining C3 and C6 alkyl chains in a conformation suitable for a radical shift from the endoperoxide oxygens. Therefore, the introduction of a methylene at C4 did not prevent the formation of the Fe(II)–O1/O2/O7 pre-reactive complex. Nevertheless, only one of the three possible methylene conformations (named Conf1, Conf2, and Conf3) was compatible with the evolution of the putative radical from O2 to C3 butyl chain (Fig. 5a).

Indeed, the H-shift from C3 alkyl chain to O2 radical implies the motion of the reacting carbon to achieve the sp^2 transition state, which is impaired by the presence of the bulky methoxymethyl group at C4 (Fig. 5b, c).

In the ether series, it resulted that, assuming Conf1, more than 50% of 3,4-*cis* stereoisomers is still potentially able to undergo a H shift from C3 butyl chain to O2 (**8c**, **8g**, **8h**, and **8k**). Thus, there is still a contribution of C3 butyl chain to antimalarial activity, as demonstrated by the decreased activity of **8e** with respect to **8k**.

In agreement with the results of our computational analysis, the methyl ether analog **8c**, bearing only a butyl chain on C3, is less potent than its ester equivalent (W2 IC_{50} = 1.5 μ M) (Persico et al. 2011) and the analogues presenting a butyl chain on, both, C3 and C6 (**8g** and **8h**; Table 1). In particular, **8g** resulted the most

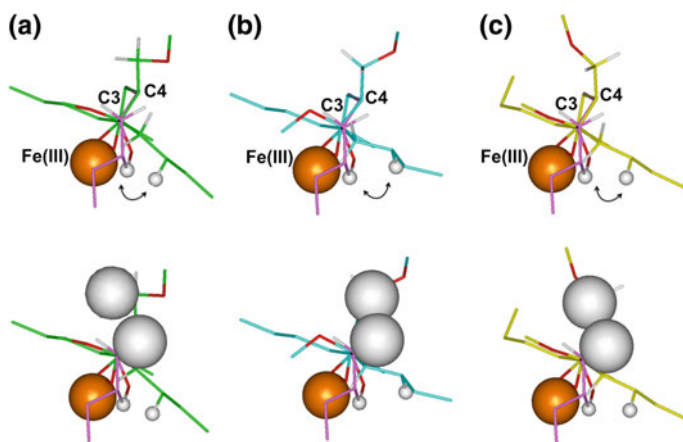


Fig. 5 Superimposition of the calculated transition state on the pre-reactive complex of **8g** assuming the C4 methylene conformation Conf1 (light green; **a**), Conf2 (cyan; **b**) and Conf3 (yellow; **c**). *Top* C3, C4 and, Fe(III) are labelled. The movement of C3 butyl chain from the pre-reactive complex to the transition state is highlighted with an arrow. *Bottom* van der Waals volumes of hydrogens responsible for steric hindrance between C3 and C4 are shown. van der Waals volume of iron is shown (scaled by 50% for clarity of presentation). Atoms are colored as follows: O = red; H = white; Fe(III) = orange. Hydrogens are omitted for the sake of clarity with the exception of those involved in the 1,4-H shift (evidenced as balls) or responsible for steric hindrance between C3 and C4 substituents. Figure adapted from reference Persico et al. (2013) with permission from Elsevier (<http://dx.doi.org/10.1016/j.ejmech.2013.10.050>)

active compound of this series and of the previous one, reaching the antimalarial activity of the natural lead **1** (Table 1). Indeed, likely due to unfavorable steric effects, the presence of two butyl chains at C6 did not increase the occurrence of putative bioactive conformations, and, consequently, the antimalarial activity of **8k** with respect to **8g** or **8h** (Table 1).

When the methoxy group at C4 of **8c**, **8g**, **8h**, and **8k** is replaced by a hydroxyl function, the resulting analogs showed decreased antimalarial activity (**7c**, **7g**, **7h**, and **7k**; Table 1). Besides being able to interfere with the iron coordination, the hydroxyl function at C4 also determined the formation of an intra-molecular hydrogen bond with O7, stabilizing the positioning of the methoxy substituent at C3 in a conformation not compatible with the formation of the Fe(II)–O1/O2/O7 pre-reactive complex (Fig. 6a).

The hydrogen bond is formed when the methylene at C4 assumes Conf3, further disfavoring the evolution of the putative toxic radical on C3 butyl chain (which can only occur assuming Conf1), in agreement with the low activity of **7c** (Table 1). On the other hand, 3,4-*trans* stereoisomers **8d**, **8i**, **8j**, **7i**, **8f**, **8l**, and **7l** present the butyl chain at C3 and the C4 substituent in *cis* orientation (Table 1).

By consequence, when also the butyl chains at C3 and C6 are *cis* (**8i** and **7i**; Table 1), the steric crowding among C4, C3, and C6 substituents reduce the rate of low energy conformers presenting intramolecular distances suitable for the putative

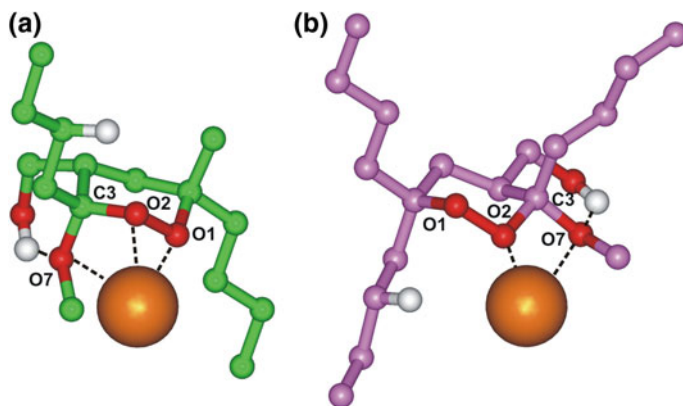


Fig. 6 Putative pre-reactive complex of 3,4-*cis* diastereoisomer **7g** (green; **a**) and 3,4-*trans* diastereoisomer **7l** (pink; **b**). van der Waals volume of iron is shown (scaled by 50% for clarity of presentation). The endoperoxide oxygens, the methoxy oxygen and the carbon C3 are labelled. Atoms are colored as follows: O = red; H = white; Fe(II) = orange. Hydrogens are omitted for the sake of clarity with the exception of those involved in the 1,4-H shift or in the hydrogen bonds. The hydrogen and coordination bonds are highlighted by a black dashed line. Figure adapted from reference Persico et al. (2013) with permission from Elsevier (<http://dx.doi.org/10.1016/j.ejmech.2013.10.050>)

H shift from C6 butyl chain. In line with these results, due to the configuration of the alkyl chains at C3 and C6: (i) **8j** showed higher antimalarial activity with respect to **8i**; (ii) the introduction of an additional butyl chain at C6 produced a compound (**8l**) more active than **8i** but equally active to **8j** (Table 1). This SAR is accentuated in the case of hydroxymethyl derivatives **7i** and **7l**. Indeed, these compounds present a high rate of putative bioactive conformers which, assuming Conf1, are potentially able to form Fe(II)–O2/O7 pre-reactive complex (Fig. 6b). Nevertheless, all Conf1 conformers present an intra-molecular hydrogen bond between OH and O7 (Fig. 6b).

Thus, the dramatic loss of antimalarial activity of **7i** is due to the formation of the rigid *trans*-decalin like structure which further improved the steric hindrance between *cis* butyl chains at C3 and C6, thus impairing any H transfer to O2. On the other hand, the introduction of an additional butyl chain at C6, on the other face of the dioxane ring, completely restored antimalarial activity, thus, although presenting an additional iron coordinating group potentially able to interfere with endoperoxide reduction, the hydroxyl derivative **7l** is equally active to its ether analog **8l** (Table 1).

Regarding the nine derivatives (Table 2), in agreement with our pharmacophore model (Fig. 3), compound **9a**, presenting only methyl substituents on the endoperoxide ring, is not able to form the carbon centered radical on the alkyl side-chains, thus resulting completely inactive (Table 2). The introduction of a butyl side-chain at C3 or of two butyl side-chains on C6 restores some activity, with a potency comparable to those of their parent methyl esters (W2 IC₅₀ 2.2 ± 0.8 μM

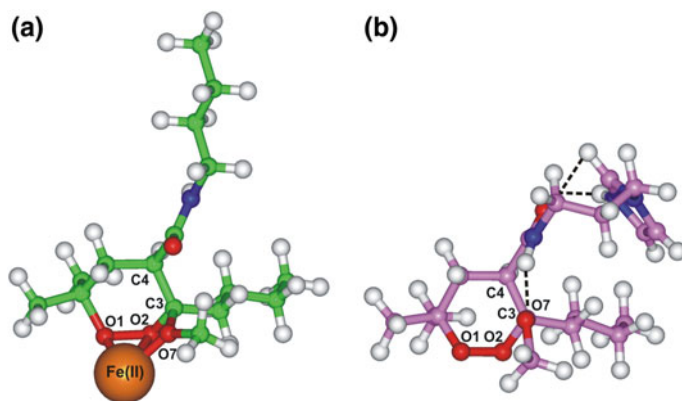


Fig. 7 DFT structure of **9b** pre-reactive complex. van der Waals volume of iron is shown (scaled by 50% for clarity of presentation) (a). PM7 conformer of **9d** presenting an intra-molecular distance suitable for the 1,4-H shift (b). Hydrogen bonds are highlighted by a *black dashed line*. O1, O2, O7, C3, C4, and Fe(II) atoms are labelled. Atoms are colored by atom type (O = red; N = blue; H = white; Fe(II) = orange). Figure adapted from reference Lombardo et al. (2014) with permission from Wiley-VCH Verlag GmbH & Co. KGaA (<http://dx.doi.org/10.1002/ejoc.201301394>)

for **9b** vs. 1.5 ± 0.5 for the corresponding methyl ester, 1.95 ± 0.05 μM for **9c** vs. 2.5 ± 0.7 for the corresponding methyl ester) (Persico et al. 2011).

Our DFT studies (Persico et al. 2011) indicate that in the absence of iron there is no definite preference between O1 and O2 for the acquisition of the radical after the O–O reductive scission. Thus, iron coordination is determinant for the formation of the radical on one oxygen rather than the other and on its possible evolution. In agreement with their observed antimalarial activities, the optimization of a low energy conformer of **9b** in complex with Fe(II) at density functional level of theory (DFT) showed that: (i) the methoxy group in the axial position led to the formation of the Fe(II)–O1/O2/O7 pre-reactive complex, able to form the oxygen radical on both O1 and O2, and to evolve either on C3 or C6 butyl chain (Fig. 7a), (ii) the Fe(II)–O1/O2 starting complex led to the inactive O2–C3 heterolytic scission product, as reported for the previous series (Fig. 4d).

The results of our 3D-SAR studies, performed on the members of a library of about 50 compounds (Persico et al. 2011, 2013; Lombardo et al. 2014), are consistent with the so-called C-radical hypothesis (i.e., antimalarial mechanism of action proposed for plakortin (see Fig. 1), with the endoperoxide group of these compounds undergoing one electron reductive bioactivation to generate first O-radicals which then collapse to C-radicals that are held to be the cytotoxic agents (Posner et al. 1995; Wu et al. 1999; Wang and Wu 2000; Kapetanaki and Varotsis 2001; Laurent et al. 2005; Meunier and Robert 2010). Indeed, the C-radical hypothesis fits very well the SARs found in these compounds, in particular with the need of *n*-butyl groups on C3 and/or C6, which are necessary for the C-radical generation *via* H-transfer to the initially formed short-lived O-radical. In this regard,

the observations that replacing all the *n*-butyl groups by methyl (Persico et al. 2011, 2013; Lombardo et al. 2014) or propyl chains¹ led to virtually inactive molecules, were especially meaningful. Moreover, the 3D-SAR study proved the active role of the C4 substituent in determining the antimalarial activity, allowing us to obtain IC₅₀ on the chloroquine-resistant (CQ-R) strains in the low micromolar range and, at the same time, very low toxicity against human cells.

3.2 Second Series of New Synthetic Analogues of Plakortin

Malaria parasites catabolise haemoglobin in an acidic (pH \approx 5.5) FV, producing toxic free heme, which is detoxified by conversion into insoluble hemozoin (O'Neill and Posner 2004). This process is crucial for the activity of many anti-malarial drugs; indeed, chloroquine, and related drugs are believed to interfere with this detoxification process (Beckera et al. 2004; Müller 2004; Ginsburg et al. 1999), while artemisinin and, generally, endoperoxides are probably bioactivated by interaction with heme-Fe(II), yielding to the homolytic cleavage of the endoperoxide bond and the production of toxic radical species (O'Neill and Posner 2004; Beckera et al. 2004; Müller 2004; Ginsburg et al. 1999; Krishna et al. 2004). To exploit its antimalarial activity, the endoperoxide must be able to reach the parasite cytoplasm and enter the ferrous-rich acidic FV. On these bases, we reasoned that the presence in the endoperoxide structure of a basic side chain containing an imidazole ring may both enhance iron interaction and cause drug accumulation in the acidic FV. Thus, we prepared a series of amides (**9d–h**) using the commercially available 1-(3-aminopropyl)-imidazole. Calculated log *D* and prevalent ionic forms of the designed compounds at cytoplasmic and parasite FV pH for compounds **9a–h** are reported in Table 4.

Some interesting and unexpected results were obtained for amides **9d–h**. Indeed, the introduction of an imidazole ring at C4 chain abolished any contribution of the C3 butyl chain to antimalarial activity (**9d** vs. **9b**, Table 2). In this new series, antimalarial activity seems to be solely dependent on the number of butyl chains at C6 (**9e** and **9h** vs. **9f** and **9g**, Table 2). It is noteworthy that **9e** is fourfold more active than the analog **9c** and fivefold more active than methyl ester analog (W2 IC₅₀ 2.5 \pm 0.7 μ M) (Persico et al. 2011), thus, in this case, the introduction of the imidazole ring produced the expected increase in antimalarial activity.

Indeed, the presence of the imidazole side-chain at C4 (**9d** and **9e**), both, in neutral and protonated form (Table 4), determined the formation of intramolecular hydrogen bonds with O7 and/or amide group. Consequently, C4 chain folds toward itself and/or C3. Considering the rotation of the methoxy group upon iron binding

¹Both 3,4-*cis* and 3,4-*trans* esters **4** possessing one methyl substituent on C3 (R¹ = Me) and two propyl substituents on C6 (R² and R³ = *n*-propyl), resulted completely inactive (IC₅₀ > 10 mM) against D10 and W2 *Pf* strains.

Table 4 Occurrence rate of ionic forms and log *D* of 1,2-dioxane-4-carboxamides (**9**)

Cmp	Ionic form (%) ^{a,b}		log <i>D</i> ^b	
	pH 7.2	pH 5.5	pH 7.2	pH 5.5
9a	N (100)	N(100)	1.98	1.98
9b	N (100)	N (100)	3.36	3.36
9c	N (100)	N (100)	4.66	4.66
9d	P (38), N (62)	P (97), N (3)	2.06	0.8
9e	P (38), N (62)	P (97), N (3)	3.35	2.09
9f	P (38), N (62)	P (97), N (3)	3.35	2.09
9g	P (38), N (62)	P (97), N (3)	3.35	2.09
9h	P (38), N (62)	P (97), N (3)	4.85	3.59

Table adapted from reference Lombardo et al. (2014) with permission from Wiley-VCH Verlag GmbH & Co. KGaA (<http://dx.doi.org/10.1002/ejoc.201301394>)

^aPercentage of ionic form in brackets; *P* protonated form; *N* neutral form

^bCalculated using ACD/Percepta software, version 14.0.0 (Advanced Chemistry Development, Inc., Toronto, ON, Canada)

(Fig. 7a), it is likely that the steric crowding between C3 and C4 substituents (Fig. 7b) prevents the correct orientation of all reaction partners for the radical shift on C3 butyl chain.

On the contrary, low energy PM7 conformers of **9b** presented an extended conformation of C4 chain, pointing away from C3 butyl chain, thus allowing the hypothesized radical shift, in agreement with the observed antimalarial activity (**9b** vs. **9d**, Table 2). The positioning of C4 imidazole side-chain does not interfere with the putative radical shift on C6 butyl chains. Accordingly, **9e** showed the expected improvement in antimalarial activity compared to **9c** (Table 2). Further study, including the rational synthesis of new analogs, will be performed to investigate a possible role of the imidazole moiety in iron coordination and/or radical evolution, to be exploited for the development of new potential antimalarial drugs.

Starting from these results and since the amine chains are known to play a crucial role both on cellular pharmacokinetic and pharmacodynamic properties of several antimalarials (Coleman et al. 1994; Charman et al. 2011; O'Neill et al. 2012), we designed new plakortin analogs introducing a substituted amine chain at C4 of 3-methoxy-1,2-dioxane scaffold (Sonawane et al. 2015). In particular, we introduced a methylamino group, which, through a flexible spacer, binds a second amino-containing scaffold or a N-heterocyclic moiety. Among the polyamine chains introduced at C4, the aromatic substructure of chloroquine or primaquine was included, thus leading to the generation of new endoperoxide-quinoline hybrids. The structures and the antimalarial activity of the new series of synthetic plakortin analogs, modified at C4 side chain with respect to the previous series, are reported in Tables 5 and 6.

The results reported in Tables 5 and 6 evidence that the imidazol-1-yl derivatives **10a–c** displayed IC₅₀ values in the high nanomolar range (200–400 nM) against both parasite strains, an activity higher than the whole library of

Table 5 Structure, antimalarial activity against CQ-S (D10) and CQ-R (W2) *Pf* strains, and cytotoxicity against the human endothelial cell line (HMEC-1) of 3,4-*cis*-3-methoxy-4-aminomethyl-1,2-dioxanes **10a-j**

Cmp	10a-g, 10j			10i			10h		
	R ¹	R ²	R ³	D10 IC ₅₀ ^a (μM)	W2 IC ₅₀ ^a (μM)	R1 ^b	D10 SI ^c	W2 SI ^c	HMEC-1 IC ₅₀ ^d (μM)
10a	<i>n</i> -Bu	Me		0.42 ± 0.09	0.21 ± 0.04	0.5	>140	>280	>59
10b	Me	<i>n</i> -Bu		0.37 ± 0.05	0.4 ± 0.1	1.1	–	–	–
10c	<i>n</i> -Bu	<i>n</i> -Bu		0.24 ± 0.06	0.2 ± 0.1	0.8	21.4	25.7	5.14 ± 0.08
10d	<i>n</i> -Bu	Me	NMe ₂	0.6 ± 0.1	0.39 ± 0.02	0.7	–	–	–
10e	Me	<i>n</i> -Bu	NMe ₂	0.54 ± 0.09	0.33 ± 0.05	0.6	6.7	11.0	3.624 ± 0.001
10f	<i>n</i> -Bu	<i>n</i> -Bu	NMe ₂	0.8 ± 0.1	0.6 ± 0.3	0.8	–	–	–
10g	<i>n</i> -Bu	Me		1.4 ± 0.4	0.55 ± 0.06	0.4	–	–	–
10h	Me	<i>n</i> -Bu	–	0.6 ± 0.1	0.4 ± 0.2	0.7	–	–	–
10i	Me	–		2.1 ± 0.8	0.7 ± 0.1	0.3	–	–	–
10j	Me	Me		>10	>10	–	–	–	–
CQ ^d	–	–	–	0.05 ± 0.02	0.7 ± 0.2	14	>760	>54	>38

Table adapted from reference Sonawane et al. (2015) with permission from the Royal Society of Chemistry (<http://dx.doi.org/10.1039/c5ra10785g>)

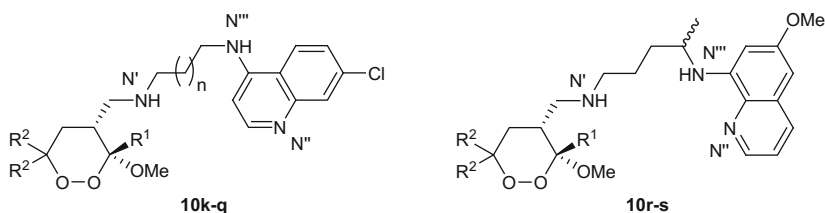
^aData are the mean ± SD of three different experiments in duplicate

^bR1 Resistance Index: IC₅₀ ratio for CQ-R/CQ-S strains of *Pf*

^cSI Selectivity Index: IC₅₀ ratio for HMEC-1/CQ-R or CQ-S strains of *Pf*

^dCQ chloroquine

Table 6 Structure, antimalarial activity against CQ-S (D10) and CQ-R (W2) *Pf* strains, and human endothelial cell line (HMEC-1) cytotoxicity of 3,4-*cis*-3-methoxy-4-aminomethyl-1,2-dioxanes **10k-s**



Cmp	R ¹	R ²	n	D10 IC ₅₀ ^a (μM)	W2 IC ₅₀ ^a (μM)	RI ^b	D10 SI ^c	W2 SI ^c	HMEC-1 IC ₅₀ (μM)
10k	<i>n</i> -Bu	Me	1	0.050 ± 0.002	0.11 ± 0.04	2.2	110	50	5.5 ± 0.7
10l	Me	<i>n</i> -Bu	1	0.072 ± 0.004	0.11 ± 0.03	1.5	46	30	3.31 ± 0.08
10m	<i>n</i> -Bu	<i>n</i> -Bu	1	0.09 ± 0.01	0.13 ± 0.02	1.4	61	42	5.49 ± 0.05
10n	<i>n</i> -Bu	Me	2	0.05 ± 0.01	0.13 ± 0.02	2.6	50	19	2.51 ± 0.2
10o	Me	<i>n</i> -Bu	2	0.074 ± 0.003	0.13 ± 0.01	1.8	30	17	2.24 ± 0.01
10p	<i>n</i> -Bu	<i>n</i> -Bu	2	0.09 ± 0.01	0.11 ± 0.03	1.2	–	–	–
10q	Me	Me	2	0.048 ± 0.006	0.34 ± 0.09	7.1	521	74	25 ± 2
10r	<i>n</i> -Bu	Me	–	0.5 ± 0.1	0.31 ± 0.07	0.6	–	–	–
10s	Me	<i>n</i> -Bu	–	0.94 ± 0.04	0.5 ± 0.1	0.5	–	–	–
CQ ^d	–	–	–	0.05 ± 0.02	0.7 ± 0.2	14	>760	>54	>38

Table adapted from reference Sonawane et al. (2015) with permission from the Royal Society of Chemistry (<http://dx.doi.org/10.1039/c5ra10785g>)

^aData are the mean ± SD of three different experiments in duplicate

^bRI Resistance Index: IC₅₀ ratio for CQ-R/CQ-S strains of *Pf*

^cSI Selectivity Index: IC₅₀ ratio for HMEC-1/CQ-R or CQ-S strains of *Pf*

^dCQ chloroquine

endoperoxides previously reported by us. The need of butyl chain(s) either at position C3 or C6 of the 1,2-dioxane ring is confirmed by the lack of activity displayed by **10j**. Moreover, the replacement of the butyl chains at C6 with a spiro cycloheptane ring (**10i**) decreased the antimalarial activity (Table 5). Indeed, the corresponding spiro-derivatives prepared in the course of our work on the previous series, owning a methyl ester and a methyl amide substituent at C4, respectively, are were both completely inactive.

A partial small but significant loss of antimalarial activity is associated to the replacement of the imidazole ring with simple aliphatic tertiary amines (**10d-h**), particularly when the tertiary amine is included into a morpholine ring (**10g**). In

general all the compounds reported in Table 5 are more active against CQ-R (W2) than on CQ-S (D10) *Pf* strains ($RI \leq 1$; Table 5) and show variable cytotoxicity against human cells HMEC-1. In particular, compound **10a**, as CQ, was very safe when tested for cytotoxicity against the human cell line.

The hybridization of the 1,2-dioxane scaffold with 4-amino-7-chloroquinoline (**10k–q**) produced a set of compounds with significantly higher activity against both *Pf* strains (Table 6).

It is noteworthy that, as in the case of the derivatives reported in Table 5, the compound that does not show any significant toxicity against HMEC-1 cells (**10q**, Table 6) is the one characterized by the lowest *c* Log *D* value at physiological pH.

Regarding the antimalarial activity, although it is difficult to differentiate the role of the two pharmacophoric moieties (1,2-dioxane and CQ), the low CQ-S (D10) IC_{50} values of this latest series against the CQ-S (D10) strain seem to be due to the quinoline moiety. This hypothesis is firstly corroborated by compound **10q**. Indeed, possessing only methyl substituents at C3 and C6, the 1,2-dioxane moiety of **10q** cannot contribute to the antimalarial activity; nevertheless, this compound is as active as CQ on D10 (CQ-S) strain (Table 6). At the same time, **10q**, due to its lower activity against W2 (CQ-R) strain, presents an increased resistance index (RI) compared to **10k–p** (Table 6). Compounds **10k–p** are indeed significantly more active than CQ against the W2 (CQ-R) strain with a leveling effect of IC_{50} at the 100 nM level, which could reflect the contribution of the endoperoxide pharmacophore to the observed antimalarial activity. Thus, a synergic and/or a resistance reverting effect of the two pharmacophores seem to occur in the case of the CQ-R (W2) *Pf* strain. The 8-Aminoquinoline containing hybrids **10r,s** are interesting, too, for the known potential activity against the *Pf* hepatic stage and as transmission blocking agents. The primaquine containing hybrids **10r,s** showed increased IC_{50} with respect to **10k–p** (Table 6) against both CQ-R and CQ-S *Pf* strains.

All the structures reported in Tables 5 and 6 (compounds **10a–j** and **10k–s**, respectively) were subjected to computational studies in order to investigate their SARs and to identify their three-dimensional structural features responsible for the antimalarial activity (for details see paragraph 2). The investigation studies started with the estimation of the ionic forms present at pH 7.4 (blood), 7.2 (cytoplasm), and 5.5 (*Pf* FV) (Table 7).

Then, in order to explore the role on antimalarial activity of a possible accumulation in the FV, the distribution coefficient (Log *D*) values at blood, cytoplasm, and FV pH, were calculated using the ACD/Percepta software (version 14.0.0, Advanced Chemistry Development, Inc., Toronto, ON, Canada). Results are reported in Tables 8 and 9.

Log *D* is an expression of the lipophilicity of the compounds which reflects the equilibria of ionic forms at a given pH. It is generally accepted (Kerns and Di 2008; Han et al. 2010) that compounds with moderate lipophilicity (Log *D* 0–3) have a good balance between solubility and permeability and are optimal for cell membrane permeation. When the Log *D* lies in the 3–5 range, the compounds still display a good membrane permeability, but absorption is lower owing to their lower solubility.

Table 7 Calculated ionic forms of 3-methoxy-4-aminomethyl-1,2-dioxanes **9a–s**

Cmp	Ionic form (%) ^a		
	pH 7.4	pH 7.2	pH 5.5
10a	DP(15) P(85)	DP(22) P(78)	DP(93) P(7)
10b	DP(15) P(85)	DP(22) P(78)	DP(93) P(7)
10c	DP(15) P(85)	DP(22) P(78)	DP(93) P(7)
10d	DP(80) P(20)	DP(86) P(14)	DP(100)
10e	DP(80) P(20)	DP(86) P(14)	DP(100)
9f	DP(80) P(20)	DP(86) P(14)	DP(100)
10g	DP(2) P(98)	DP(3) P(97)	DP(56) P(44)
10h	P(68) N(32)	P(77) N(23)	P(99) N(1)
10i	DP(15) P(85)	DP(22) P(78)	DP(93) P(7)
10j	DP(15) P(85)	DP(22) P(78)	DP(93) P(7)
10k	DP(14) P(86)	DP(21) P(79)	DP(100)
10l	DP(14) P(86)	DP(21) P(79)	DP(100)
10m	DP(14) P(86)	DP(21) P(79)	DP(100)
10n	DP(11) P(89)	DP(16) P(84)	DP(100)
10o	DP(11) P(89)	DP(16) P(84)	DP(100)
10p	DP(11) P(89)	DP(16) P(84)	DP(100)
10q	DP(11) P(89)	DP(16) P(84)	DP(100)
10r	P(100)	P(100)	P(100)
10s	P(100)	P(100)	P(100)

Table reproduced from reference Sonawane et al. (2015) with permission from the Royal Society of Chemistry (<http://dx.doi.org/10.1039/c5ra10785g>)

^aPercentage of ionic form in brackets. *P* protonated form; *DP* di-protonated form (ACD/Percepta software, version 14.0.0, Advanced Chemistry Development, Inc., Toronto, ON, Canada)

Table 8 *c* Log *D* values of 3-methoxy-4-aminomethyl-1,2-dioxanes **10a–j**

Cmp	<i>c</i> Log <i>D</i>		
	pH 7.4	pH 7.2	pH 5.5
10a	0.5	0.3	−1.3
10b	1.9	1.7	0.1
10c	3.2	3.0	1.4
10d	−0.3	−0.6	−1.9
10e	1	0.8	−0.3
10f	2.4	2.1	0.8
10g	0.2	0.0	−0.6
10h	5.4	5.3	4.0
10i	0.4	0.2	−1.3
10j	−0.9	−1.1	−2.6

Table adapted from reference Sonawane et al. (2015) with permission from the Royal Society of Chemistry (<http://dx.doi.org/10.1039/c5ra10785g>)

Table 9 *c* Log *D* values of 3,4-*cis*-3-methoxy-4-aminomethyl-1,2-dioxanes **10k–s**

Cmp	<i>c</i> Log <i>D</i>		
	pH 7.4	pH 7.2	pH 5.5
10k	1.9	1.6	0.4
10l	3.1	2.9	1.7
10m	4.6	4.4	3.1
10n	2.1	1.9	0.7
10o	3.3	3.1	2.0
10p	4.8	4.5	3.4
10q	0.8	0.5	−0.6
10r	2.8	2.7	2.5
10s	4.1	4.0	3.7

Table adapted from reference Sonawane et al. (2015) with permission from the Royal Society of Chemistry (<http://dx.doi.org/10.1039/c5ra10785g>)

On the contrary, hydrophilic compounds ($\text{Log } D < 0$) have good solubility but poor membrane permeability (Kerns and Di 2008; Han et al. 2010). Thus, according to the data reported in Tables 8 and 9, although a certain degree of accumulation in the FV of the parasite is expected for all compounds, there is no clear correlation between the calculated Log *D* (*c* Log *D*) values and the antimalarial activity. A similar observation has been reported for 1,2,4-trioxaquinines, molecular hybrids containing both a quinoline and 1,2,4-trioxane pharmacophore moieties. In our case, this is true also if we exclude the quinoline-hybrids **10k–s** and we only consider the new endoperoxide derivatives **10a–j** reported in Table 5. The *c* Log *D* values do not account for the activity trend observed with the introduction of the amino chain at C4, such as, 3-(1H-imidazol-1-yl)-N-methylpropan-1-amine (**10a–c**) > N1,N1,

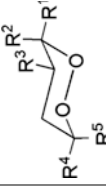
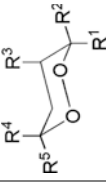

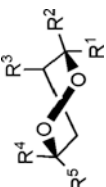
N3-trimethylpropane-1,3-diamine (**10d–f**) \approx octahydro-1-methyl-1H-pyrido[1,2-a]pyrimidine (**10h**) > N-methyl-3-morpholinopropan-1-amine (**10g**). Moreover, compound **10c**, differently from **10a** and **10b**, should be able to diffuse back to the parasite cytoplasm across the FV membrane. This property did not interfere with the antimalarial activity of **10a–c**, which is almost identical (Table 5). To investigate the role of the C4 amino-imidazole chain in determining the antimalarial activity of compounds **10a–c** (the amido-imidazole analog of **10a** was inactive) (Lombardo et al. 2014), compound **10j** was synthesized. Its complete loss of activity demonstrated that the presence of at least one butyl chain at C3 is necessary for antimalarial activity (**10j** vs. **10a**, Table 5). However, due to the unfavorable $c \text{ Log } D$ value at physiological pH (i.e., -0.9 , Table 8), the observed inactivity of **10j** could in principle be ascribed to cellular pharmacokinetics. To obtain an amino-imidazole analog with increased $c \text{ Log } D$ without affecting the pharmacodynamic properties, we used the 3-methoxy-1,2-dioxaspiro[5.6]dodecane moiety. Indeed, in the ester series, the spiro derivative resulted inactive despite its favorable $c \text{ Log } D$, demonstrating that the spiro-cycloheptane substituent at C6 do not possess the pharmacodynamic requirements for antimalarial activity. Thus, we replaced the C4 substituent of the inactive analogs, with the amino-imidazole chain, through the synthesis of the analog **10i** (Tables 5 and 8). The amino-imidazole derivative **10i** demonstrated that, when combined with a sufficient lipophilicity, just the installation of the amino-imidazole chain at C4 is sufficient to restore some antimalarial activity (Table 5). Finally, according to the data reported in Tables 8 and 9, the minimum $c \text{ Log } D_{7.4}$ value for activity against human HMEC-1 cell line appears to be $+1$. Compounds **10a** and **10q**, characterized by a $c \text{ Log } D_{7.4}$ value <1 , are indeed devoid of any significant activity.

Starting from these results we investigated also their conformational and the electronic properties. Our computational studies evidenced that the series of derivatives **10** present peculiar conformational parameters compared to the previous analogs. Indeed, the presence of the amino chain at C4 stabilizes the Skew Boat B conformation of the 1,2-dioxane ring, which becomes by far the most populated conformer at the FV pH (Table 10).

This boat-like conformation of the 1,2-dioxane ring favors endoperoxide oxygens accessibility and reproduces the endoperoxide ring conformation of artemisinin (Fig. 8).

The structural analysis of the low energy conformers [i.e., within 5 kcal/mol from the global energy minimum (GM)], highlighted that the amino-imidazole derivatives **10a–c**, **10j** and the di-amino derivatives **10d–f** (Table 5), present GM conformers showing similar conformational features, both in the protonated (N') and di-protonated (N' and N'') forms. These GM conformers are characterized by the Skew Boat B conformation of the 1,2-dioxane ring and by a network of intramolecular hydrogen bonds involving O1 and the secondary amine N' (Fig. 9). Moreover, they also present (with the obvious exception of **10j**) the intramolecular distances required for a H-shift from a butyl chain to the putative oxygen radical,

Table 10 Occurrence rate (%) of 1,2-dioxane ring conformations considering PM7 conformers within 5 kcal/mol from the global minimum

Cmp	Ionic form ^a	Chair A 	Chair B 	Skew boat A 	Skew boat B 
10a	P	68	0	0	32
	DP	17	0	0	83
10b	P	17	0	0	83
	DP	0	0	0	100
10c	P	0	0	0	100
	DP	0	0	0	100
10d	P	65	0	0	35
	DP	0	0	0	100
10e	P	71	0	0	29
	DP	0	0	0	100
10f	P	78	0	0	22
	DP	0	0	0	100
10g	P	48	0	7	45
	DP	0	0	0	100
10h^b	P	9	0	9	82
10h^c	P	23	6	0	71
10i	P	63	5	0	32
	DP	0	0	0	100
10j	P	41	0	0	59
	DP	0	0	0	100

(continued)

Table 10 (continued)

Cmp	Ionic form ^a	Chair A	Chair B	Skew boat A	Skew boat B
10k	P	36	15	12	36
	DP	50	0	0	50
10l	P	50	0	20	30
	DP	0	0	0	100
10m	P	29	13	29	29
	DP	0	0	0	100
10n	P	50	6	19	25
	DP	33	17	0	50
10o	P	25	0	12.5	62.5
	DP	0	50	0	50
10p	P	25	0	0	75
	DP	0	0	0	100
10q	P	45	7	13	35
	DP	20	0	0	80
10r^b	P	64	12	3	21
10r^c	P	55	17	0	28
10s^b	P	50	0	0	50
10s^c	P	56	0	0	44

Table adapted from reference Sonawane et al. (2015) with permission from the Royal Society of Chemistry (<http://dx.doi.org/10.1039/c5ra10785g>)

^aDP di-protonated form, P protonated form

^bDiastereomer with (R)-configured stereocenter in the side-chain

^cDiastereomer with (S)-configured stereocenter in the side-chain

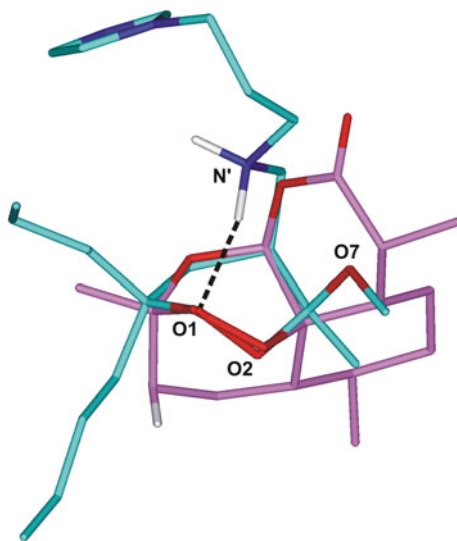


Fig. 8 Superimposition of PM7 global minimum of **10b** (cyan) in protonated form on artemisinin X-ray structure (pink; CSDS code: QNGHSU). The molecules are colored by atom type (O = red, N = blue, and H = white). Hydrogens are omitted for sake of clarity, with the exception of those involved in the hydrogen bonds (highlighted by a black dashed line). Figure adapted from reference Sonawane et al. (2015) with permission from the Royal Society of Chemistry (<http://dx.doi.org/10.1039/c5ra10785g>)

according to the pharmacophoric model resulting from our previous computational studies (Figs. 9 and 10).

In order to further investigate the impact of this conformational behavior on antimalarial activity, we performed a dynamic docking simulation of **10c** in complex with heme. The protonation state of **10c** and heme has been calculated considering the pH of the FV, where heme digestion mainly occurs (Egan et al. 2000). Heme parameters and atomic partial charges were assigned using the QM method PM7. During the dynamic docking procedure, which combines Monte Carlo and SA calculations, all rotatable bonds of **10c** and heme are left fully free to move. Docking studies indicated only one possible complex structure (Fig. 11).

The docked conformation of **9c** reproduces the key features (i.e., Skew Boat B and O1–N' interaction) of the GM conformer identified by the conformational search (Fig. 9b). Moreover, in the docked complex the two protonated nitrogens N' and N'' establish charge-assisted hydrogen bonds with the ionized and neutral propionic groups of heme, respectively, similarly to what reported for the protonated amine chain of chloroquine (Dodd and Bohle 2014). As already mentioned, at *Pf* FV pH, when both the basic centers are protonated, compounds **10a–f** show a higher propensity for the conformation characterized by the Skew Boat B and the hydrogen bond between N' and O1 (Table 8 and Fig. 9). In the case of compounds **10a–c**, this is due to the lack of an additional electron donating group (i.e.,

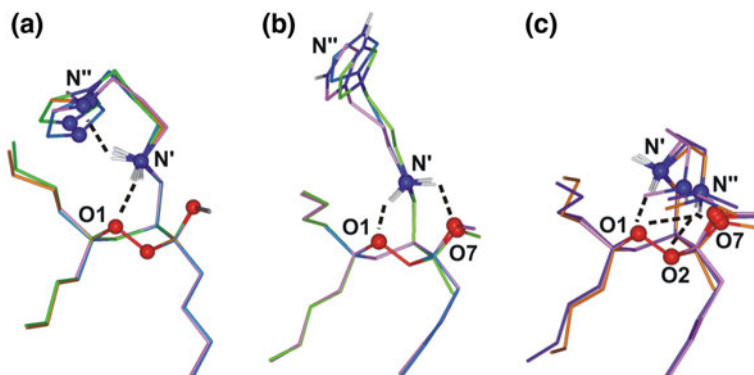


Fig. 9 Superimposition of GM conformers of: **a** **10a** (light blue), **10b** (light green), **10c** (yellow), **10d** (pink), **10e** (orange), and **10f** (violet); all protonated on N'; **b** **10a** (light blue), **10b** (light green), and **10c** (pink) in di-protonated form; **c** **10d** (pink), **10e** (orange), and **10f** (violet); protonated on N' and N''. The molecules are colored by atom type (O = red, N = blue, and H = white). The heteroatoms involved in hydrogen bonds (highlighted by a black dashed line) are displayed in ball. Hydrogens are omitted for sake of clarity, with the exception of those involved in hydrogen bonds. Figure adapted from reference Sonawane et al. (2015) with permission from the Royal Society of Chemistry (<http://dx.doi.org/10.1039/c5ra10785g>)

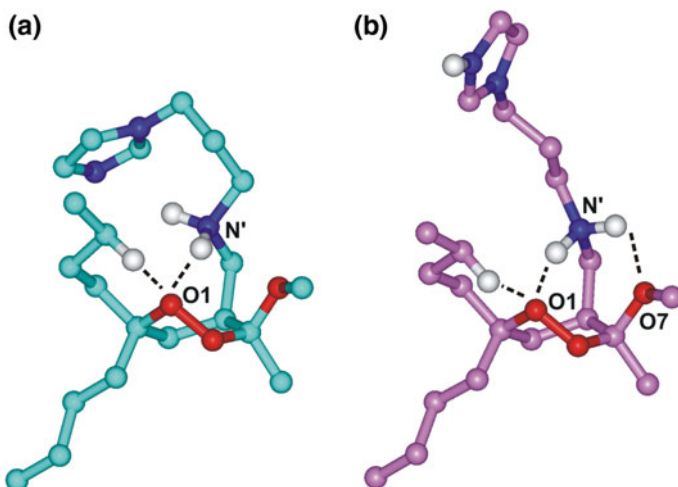


Fig. 10 PM7 global minimum of **10c** presenting intra-molecular distances suitable for the 1,5-H shift in protonated (cyan; **a**) and di-protonated (pink; **b**) form. Atoms are colored by atom type (O = red, N = blue, and H = white). Hydrogens are omitted for sake of clarity, with the exception of those involved as possible partners in a “through-space” intra-molecular radical shift and in the hydrogen bonds (highlighted by a black dashed line). Figure adapted from reference Sonawane et al. (2015) with permission from the Royal Society of Chemistry (<http://dx.doi.org/10.1039/c5ra10785g>)

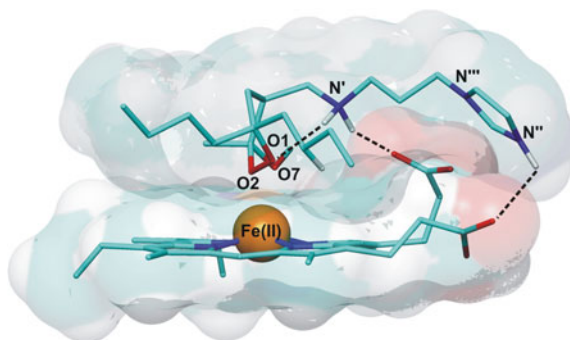


Fig. 11 Docking results of **10c** (protonated on N' and N'') in complex with heme. The molecules are colored by atom type (C = cyan; O = red; N = blue; Fe = orange and H = white). Iron atom vdW volume is shown (scaled by 50% for clarity of presentation). Hydrogens are omitted for sake of clarity, with the exception of those involved in hydrogen bonds (highlighted by a black dashed line). Figure adapted from reference Sonawane et al. (2015) with permission from the Royal Society of Chemistry (<http://dx.doi.org/10.1039/c5ra10785g>)

unprotonated imidazole) competing with the endoperoxide oxygen O1 in establishing favorable interactions (i.e., cation- π) with the protonated secondary amine N' (Fig. 9a vs. 9b). In the case of compounds **10d–f**, this is due to the further stabilization of the Skew Boat B conformation, caused by the interaction of the distal, protonated, tertiary amine group (N'') with O1, O2, and O7 (Fig. 9a vs. 9c). By consequence, the only difference between the amino-imidazole (**10a–c**) and the di-amino (**10d–f**) derivatives is that, in the di-protonated form, the GM conformers of the former adopt an extended conformation of the substituent at C4, with the protonated imidazole ring pointing away from the rest of the molecule. Thus, the GM conformers of **10a–c** correspond to the heme interacting conformation resulting from docking calculations (Fig. 5a vs. Fig. 11). On the contrary, in the GM conformers of **10d–f** the protonated tertiary amine N'' is hydrogen bonded to O1, O2, and O7 (Fig. 9a vs. 9b). Accordingly, when the di-amino derivatives **10d–f** approach heme, the distal protonated amine N'' should firstly release the intramolecular hydrogen bonds to then establish ionic interactions with the propionate groups. This could account for the overall higher antimalarial activity of **10a–c** with respect to **10d–f** (Table 5). According to the calculated apparent pK_a values (Table 7), unlike compounds **10a–f**, the significantly less active morpholine analog **10g** is still (44%) mono-protonated at the acidic FV pH. In this form, the GM conformer of **10g** does not present the Skew Boat B conformation and the O1- N' interaction, and the first conformer with these features is at ≈ 1 kcal/mol from the GM. On the other hand, in the di-protonated form, **10g** behaves similarly to **10d–f** (Fig. 9c), i.e., with the protonated tertiary amine (N'') establishing hydrogen bonds with O7. Thus, also in the case of di-protonated **10g**, the morpholine nitrogen could establish an extra-interaction with heme propionate only after losing its intramolecular h-bond. A peculiar case is represented by compound

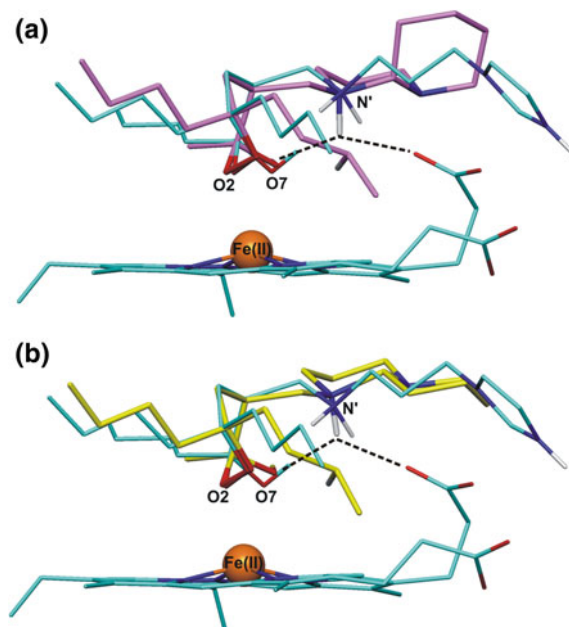


Fig. 12 Superimposition of the putative bioactive conformer of **10h** (a (pink): (*R*)-configured stereocenter in the side-chain; b (yellow): (*S*)-configured stereocenter in the side-chain) on the docking results of **10c** in complex with heme (cyan). The molecules are colored by atom type (O = red; N = blue; Fe = orange; H = white). Iron atom vdW volume is shown (scaled by 50% for clarity of presentation). Hydrogens are omitted for sake of clarity, with the exception of those involved in hydrogen bonds (highlighted by a black dashed line). Figure adapted from reference Sonawane et al. (2015) with permission from the Royal Society of Chemistry (<http://dx.doi.org/10.1039/c5ra10785g>)

10h (W2 $IC_{50} = 400$ nM, Table 5), evaluated as a mixture of two diastereomers differing for the configuration at the stereogenic carbon of the bicyclic ring.

In this analog, the two equally basic nitrogens (single pK_{a1} : 7.56 ± 0.20 and single pK_{a2} : 7.24 ± 0.20) are constrained into a bicyclic structure and, according to the calculated apparent pK_a value, only the mono-protonated form is present at both cytoplasm and FV pHs (Table 7). Although not showing the hydrogen bond between N' and O1, the GM conformer of one of the two diastereomers still presented the Skew Boat B conformation of the 1,2-dioxane ring with the two conformationally constrained amine nitrogens correctly positioned to interact with the negatively charged heme propionate group (Fig. 12).

Finally, the amino-imidazole spiro derivative **10i** (Table 5), is again present in the di-protonated form at FV pH (Table 7). The GM conformer of this form presents either the Skew Boat B and the O1- N' interaction, but, according to experimental peroxide oxygen-heme iron distances taken from the Cambridge Crystallographic Structural Data Bank (Chishiro et al. 2003), the presence of the

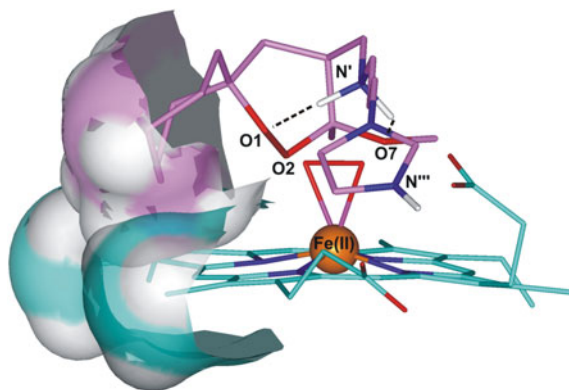


Fig. 13 Di-protonated form of **10i** in complex with heme superimposed (coordination O2/O7) on the X-ray structure of peroxo-bridged heme complex (CSD code: UKACIS). The molecules are colored by atom type (C = pink and cyan for PM7 conformer and heme, respectively; O = red; N = blue; Fe = orange; H = white). The solvent accessible surface of atoms responsible for steric hindrance between **10i** and heme is shown (transparency = 50%). Iron atom vdW volume is shown (scaled by 50% for clarity of presentation). Hydrogens are omitted for sake of clarity, with the exception of those involved in the intra-molecular hydrogen bonds (highlighted by a black dashed line). Figure adapted from reference Sonawane et al. (2015) with permission from the Royal Society of Chemistry (<http://dx.doi.org/10.1039/c5ra10785g>)

rigid spirocycloheptane at C6 impairs the endoperoxide approach to heme iron (Fig. 13).

The conformational behavior of the endoperoxide-aminoquinoline hybrids **10k–s** (Table 6) was evaluated by applying the same computational protocol used for **10a–j**. The presence of the bulky quinoline moiety determined a less homogeneous conformational behavior of the low energy conformers of **10k–s**. Indeed, due to the hydrophobic interaction between the quinoline system and the butyl chain(s), the conformational preference is also affected by the substitution at C6 (Table 10). Nevertheless, the GM conformers of compounds **10k–s** are still characterized by the Skew Boat B, both, in the mono- and di-protonated forms.

The endoperoxide-7-chloroquinoline hybrids **10k–q** (Table 6) are entirely present in the di-protonated form at FV pH, while they are mostly ($\approx 80\%$) mono-protonated at cytoplasm pH (Table 7). Considering the mono-protonated form, N' is hydrogen bonded to O1 and O7 in **10k**, **10n**, and **10q** (Fig. 14a), and only to O1 in **10l**, **10m**, **10o**, and **10p** (Fig. 14b). On the other hand, in the di-protonated form N' is hydrogen bonded to O1 (**10k–m**) or to O7 (**10n–q**), while N''' always interact with O1, O2, and O7 (Fig. 14c). Thus, the exact pattern of intramolecular hydrogen bonds is determined by the presence of the butyl chains at C6 in the protonated forms (Fig. 14a, b), and by the length of the alkyl chain connecting the two protonated amino groups in the di-protonated forms (Fig. 14c). It has to be underlined that, anyway, the GM conformers of **10k–q** show the

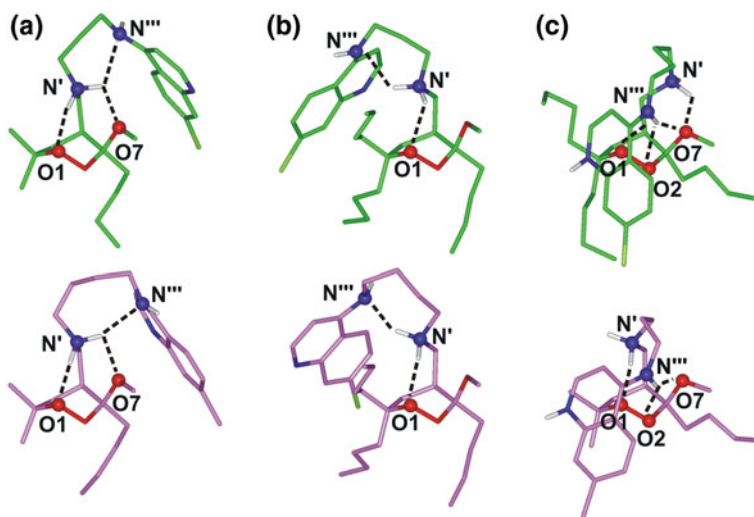


Fig. 14 GM conformers of: **a** **10k** (green) and **10n** (pink) (protonated on N'); **b** **10m** (green) and **10p** (pink) (protonated on N'); **c** **10m** (green) and **10q** (pink) (protonated on N' and N''). The molecules are colored by atom type (O = red, N = blue, and H = white). The heteroatoms involved in hydrogen bonds (highlighted by a black dashed line) are displayed in ball. Hydrogens are omitted for sake of clarity, with the exception of those involved in hydrogen bonds. Figure adapted from reference Sonawane et al. (2015) with permission from the Royal Society of Chemistry (<http://dx.doi.org/10.1039/c5ra10785g>)

quinoline nitrogen (N'') accessible to heme iron interaction, while the endoperoxide function is sterically hindered by the quinoline ring (Fig. 14).

The primaquine-type hybrids **10r** and **10s** are only present in the mono-protonated form at, both, FV and cytoplasm pH (Table 7), and, as observed for the mono-protonated GM conformers of **10k–q**, N' is hydrogen bonded to O1, or to O1 and O7, depending on the presence of the butyl chains at C6 (Fig. 15). Contrarily to **10k–q**, in hybrids **10r–s** the quinoline ring does not hinder the endoperoxide group (Fig. 14a, b vs. Fig. 15a, b).

We analyzed the SARs of our new compounds considering the possible roles of the amine chain at C4 on the antimalarial activity. Several amines are known either to be active themselves as antimalarials (McCann et al. 1981; Whaun and Brown 1985) or to be present as additional, favorable, pharmacophoric features (i.e., bioactive substructure) in a variety of molecular scaffolds already exhibiting antimalarial activity (Coleman et al. 1994; Charman et al. 2011; O'Neill et al. 2012). This is the case of the new series of endoperoxides **10a–s**, which show an enhanced antimalarial activity compared to the previous compounds, thanks to the amine substituent at C4. This improvement in the activity can be ascribed to cellular pharmacokinetics and/or pharmacodynamics. Polyamines are known to play a crucial role as radical scavengers in biological environments (Ha et al. 1998) and their ability to shuttle a free-radical from oxygen to carbon atoms has been broadly

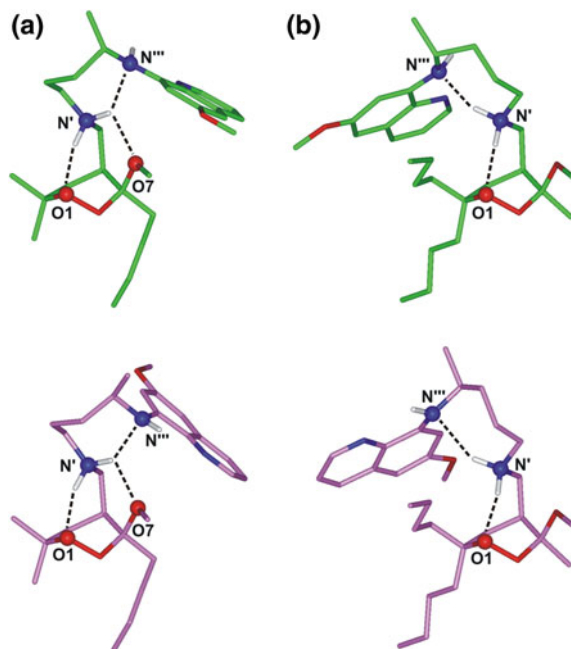


Fig. 15 GM conformers of: **a** **10r** diastereomer with (*S*)-configured stereocenter in the side-chain (*green*) and diastereomer with (*R*)-configured stereocenter in the side-chain (*pink*); **b** **10s** diastereomer with (*R*)-configured stereocenter in the side-chain (*green*) and diastereomer with (*S*)-configured stereocenter in the side-chain (*pink*). The molecules are colored by atom type (O = *red*, N = *blue*, and H = *white*). The heteroatoms involved in hydrogen bonds (highlighted by a *black dashed line*) are displayed in ball. Hydrogens are omitted for sake of clarity, with the exception of those involved in hydrogen bonds. Figure adapted from reference Sonawane et al. (2015) with permission from the Royal Society of Chemistry (<http://dx.doi.org/10.1039/c5ra10785g>)

investigated (Maeda and Ingold 1980; Griller et al. 1981; Tanko et al. 2001; Pischel and Nau 2001; Das and Misra 2004). Accordingly, the polyamine substituent could increase the activity of molecular scaffolds whose activity is strictly related to their redox potential by playing an active role in the formation/propagation of toxic radical species. In addition, for compounds supposed to interact with free heme, a basic chain could be involved in favorable interactions with heme propionate groups. At this regard, the conformational analysis performed on members of the series **10** revealed a strong tendency of the protonated secondary amine to hydrogen bond to O1, stabilizing a 1,2-dioxane ring conformation which favors peroxide oxygen accessibility. This was confirmed by docking calculation of **10c** in complex with heme, which also highlighted favorable interactions between the polyamine chain and the heme propionate groups. Given the formation of this pre-reactive complex, a possible scenario is that, after the Fe(II) catalyzed generation of the distonic radical anion, the secondary amine could simultaneously protonate the oxygen anion and shuttle the oxygen radical to an adjacent carbon via a hydrogen

radical shift (Maeda and Ingold 1980; Griller et al. 1981; Tanko et al. 2001; Pischel and Nau 2001; Das and Misra 2004).

In addition, the presence of multiple basic functionalities may favor the accumulation of compounds **10a–s** in the infected erythrocyte and, in particular, in the acidic FV of the parasites. More than be achieved through a polyamine transporter (Reguera et al. 2005; Niemand et al. 2013), most likely this could be due to an impairment of the back diffusion across the membrane of a single, or better double protonated derivative. Calculated pK_a and $\text{Log } D$ values at cytoplasm and FV pH pointed out that compounds **10a–s** can accumulate in the parasite FV but no linear relation was observed between the antimalarial activity and the $c \text{Log } D$ values, indicating that other parameters also affect the antimalarial activity. It is noteworthy that most of the low energy conformers (i.e., within 5 kcal/mol from the GM) of compounds **10a–s** present an intramolecular hydrogen bond between the two amine functions. The formation of intramolecular hydrogen bonds involving ionized groups, can “mask” the charge of the molecule and affect its passage through cellular membranes.

The subgroup of 1,2-dioxanes **10k–s** hybridizes two biologically active entities, the 1,2-dioxane scaffold and a quinoline-based pharmacophore. Over the last 10 years examples of artemisinin-quinolines hybrids have been reported (Grellepois et al. 2005; Walsh et al. 2007; Capela et al. 2011). A recent survey shows the most interesting results obtained with hybrid molecules containing fully synthetic 1,2,4-trioxanes or 1,2,4-trioxolane and an aminoquinoline derivative (Muregi and Ishih 2010; Flannery et al. 2013). These hybrid molecules display a dual mode of action, a concept referred to as “covalent bitherapy,” thus they promote heme alkylation with the peroxy entity, and heme stacking with the aminoquinoline moiety resulting in a reinforced inhibition of haemozoin formation (Loup et al. 2007; Cosledan et al. 2008). Targeting the parasite by two distinct mechanisms has also the advantage of delaying or circumventing the development of resistance (Araujo et al. 2009).

In the case of the hybrids **10k–p**, the higher activity of chloroquine with respect to the peroxide moiety is likely to play a major role in the antimalarial activity against *Pf* CQ-S strains. On the contrary, **10k–p** are more active than chloroquine against *Pf* CQ-R strains and resulting SARs suggest that the peroxide pharmacophore is responsible for the observed antimalarial activity. It cannot be excluded that the increased activity against CQ-R strains is attributable to the modification of the basic side chain of chloroquine, which would not be recognized by the mutated CQ-transporter. Contrarily to chloroquine, primaquine is known to be poorly active in vitro against *Pf* infected erythrocytes, both on CQ-S and CQ-R strains ($W2 \text{IC}_{50} = 3.3 \mu\text{M}$) (Capela et al. 2011). By consequence, the significant antimalarial activity displayed by the hybrids **10r** and **10s** has to be attributed to the mechanism of action of the peroxide moiety, while the primaquine moiety behaves, in this case, just as an amine-containing C4 substituent.

In summary, optimization of the cellular pharmacokinetics of our antimalarial peroxides through the introduction of a substituted amino side-chain at C4, seems not to be the only factor responsible for their increased antimalarial activity. As

previously observed (Persico et al. 2011, 2013; Lombardo et al. 2014), the substituent at C4 could also play a pharmacodynamic role by affecting the ability of the peroxide bridge to undergo reductive cleavage and to generate/propagate the putative toxic radical chain. Molecular modeling studies suggest that the increased antimalarial activity is related to the stabilization of a conformation which favors the hypothesized reductive cleavage of the endoperoxide bridge with a possible involvement of the introduced amine functions in putative toxic radical formation/propagation. This is supported by the fact that replacing the amide group with an amino group not only increased the antimalarial activity of the whole series but also determined different SARs. Indeed, the amido-imidazole analog of **10a** (one butyl chain at C3; W2 (CQ-R) $IC_{50} = 0.21 \mu M$) was inactive as antimalarial, while the amido-imidazole analog of **10b** (two butyl chain at C6, W2 (CQ-R) $IC_{50} = 0.4 \mu M$) was one of our most active derivatives (W2 (CQ-R) $IC_{50} = 0.5 \mu M$) (Lombardo et al. 2014). Thus, replacing the amide group with an amino group increased the antimalarial activity independently from the position of the butyl chain(s). Although the inactivity of **10j** demonstrated the need of at least one butyl chain at C3 (**10j** vs. **10c**), the activity of **10i** compared to its previous analogs indicated that the secondary amine function at C4 is sufficient to restore some antimalarial activity and that the inactivity of **10j** is likely due to its unfavorable $\text{Log } D$. At this regard, it is worth of note, that, according to our $c \text{ Log } D_{7.4}$ values, the minimum lipophilicity threshold to be active against infected erythrocytes and normal human cells is ~ -1 and $\sim +1$, respectively. By consequence, compound **10a**, with $c \text{ Log } D_{7.4} = 0.5$, shows a 210 nM IC_{50} on *Pf* W2 strain and no activity on human HMEC-1 cells, presenting an optimal SI.

3.3 New Natural Polyketide Endoperoxides

New polyketide endoperoxides have been isolated from the sponge *Plakortia simplex* (**Plk1-7** derivatives). The isolated endoperoxide derivatives have been tested for their in vitro antimalarial activity against D10 [chloroquine-sensitive (CQ-S)] and W2 [chloroquine-resistant (CQ-R)] *Pf* strains, showing IC_{50} values in the low micromolar range (Chianese et al. 2014).

The structures and the antimalarial activity of these new natural endoperoxides are reported in Table 11.

The isolation of these new endoperoxide metabolites represented a convenient opportunity to extend the SARs previously established for the antimalarial activity of the plakortin family. Since our pharmacophoric model (Fig. 3) for antimalarial 1,2-dioxanes had been designed utilizing compounds embedding a saturated heterocyclic ring, the isolation of 1,2-diox-4-enes (**Plk1-3**) offered us an interesting opportunity to further extend the SARs and refine our knowledge on the mechanism of action of this class of simple antimalarials.

The obtained SARs evidenced that, with respect to plakortin and dihydroplakortin, (i) the presence of the double bond in the 1,2-dioxane ring (**Plk1-3**) or

Table 11 In vitro antimalarial activity of plakortin, dihydroplakortin and compounds **Plk1–7** against D10 (CQ-S) and W2 (CQ-R) strains of *Pf*

Cmp	Structure	D10 IC ₅₀ (μM) ^a	W2 IC ₅₀ (μM) ^a
Plk1		3.89 ± 0.15	2.91 ± 0.94
Plk2		4.05 ± 0.53	2.70 ± 0.68
Plk3		1.77 ± 0.15	1.56 ± 0.47
Plk5		6.18 ± 1.11	4.98 ± 1.83
Plk6		NA ^b	11.4 ± 2.74
Plk7		5.12 ± 1.09	4.10 ± 0.57
Plakortin		0.87 ± 0.35	0.39 ± 0.13
Dihydroplakortin		0.90 ± 0.56	0.43 ± 0.16

Table adapted from reference Chianese et al. (2014) with permission from Elsevier (<http://dx.doi.org/10.1016/j.bmc.2014.07.034>)

^aData are the mean ± SD of three different experiments in duplicate

^bNA not active

(ii) the inversion of the chirality at C6 (**Plk5**), or (iii) at C3 and C6 (**Plk6–7**), reduced the antimalarial activity (Table 11). Overall, the derivatives characterized by the 3,6-dihydro-1,2-dioxine ring (**Plk1–3**) resulted more active than the derivatives characterized by the 1,2-dioxane ring (**Plk5–7**), but still less active than plakortin and dihydroplakortin (Table 11). The SARs of the new natural compounds were rationalized taking into account our hypothesized mechanism of actions of plakortins (Fig. 1) (Tagliatela-Scafati et al. 2010). As reported above, plakortin and dihydroplakortin, upon reaction with Fe(II), generate a radical at O1, which is simultaneously transferred by means of a “through-space” mechanism to the double bond of plakortin or to a C13 hydrogen of dihydroplakortin (Fig. 1). The resulting carbon radicals should then represent the toxic species responsible for the antimalarial activity. The hypothesized concerted dissociative electron transfer (DET) mechanism was confirmed by the reported SARs of plakortins, being the

Table 12 Occurrence rate (%) of endoperoxide ring conformations considering PM7 conformers within 5 kcal/mol from the global minimum of plakortin, dihydroplakortin, and **Plk1-7**

Cmp	Chair A ^a	Chair B ^a	Skew boat A	Skew boat B
Plk1	11	89	–	–
Plk2	23	77	–	–
Plk3	14	86	–	–
Plk5	82	7	11	0
Plk6	50	13	34	4
Plk7^b	41	20	38	1
Plk7^c	49	15	34	1
Plakortin	82	6	11	1
Dihydroplakortin	85	8	7	–

Table adapted from reference Chianese et al. (2014) with permission from Elsevier (<http://dx.doi.org/10.1016/j.bmc.2014.07.034>)

^aHalf-chair A and half-chair B in the case of compounds **Plk1-3**

^bDiastereomer with (R)-C10

^cDiastereomer with (S)-C10

antimalarial activity related to the reactivity of the C6 alkyl chain and its ability to correctly orientate with respect to O1 without affecting endoperoxide oxygens accessibility to iron interaction. Thus, a pivotal role was played by conformational parameters in the antimalarial activities of plakortins.

On these bases, a comprehensive conformational analysis has been performed on the novel series of plakortin analogs and the obtained results were compared with those achieved for plakortin and dihydroplakortin (for details see paragraph 2). All the generated conformers were ranked by their potential energy values and grouped on the basis of their ring conformation (Table 12).

Then, we calculated the rate of low energy conformers (i.e., within 5 kcal/mol from the global minimum) owning the required structural features for antimalarial activity (Tagliatalata-Scafati et al. 2010) that is: (i) the steric accessibility of the endoperoxide oxygens and (ii) the distance between the endoperoxide oxygen O1 and possible partners for a ‘through space’ (1,4 or 1,5) intramolecular radical shift (Table 13).

Our previous results (Fattorusso et al. 2011) indicated that, due to the steric repulsion of the 1,3-diaxial substituents, the 1,2-dioxane ring of plakortin and dihydroplakortin shows a definite conformational preference for a chair conformation named Chair A (Table 12 and Fig. 16), where the equatorial position of the reacting alkyl chain at C6 allows its approach to O1 in a significant number of conformations (Table 13 and Fig. 17a).

In the case of the 1,2-dioxine derivatives **Plk1-3**, it also resulted a definite conformational preference for one ring chair conformation, but this time it was the half-chair B (Table 12 and Fig. 18), presenting the pseudo-axial position of the

Table 13 Occurrence rates and endoperoxide ring conformations of putative bioactive PM7 conformers of plakortin, dihydroplakortin, and **Plk1-7**

Cmp	CNF ^a (%)	Chair A ^{b, c} (%)	Chair B ^{b, c} (%)	Skew boat A ^b (%)	Skew boat B ^b (%)
Plk1	14	2	12	–	–
Plk2	16	2	14	–	–
Plk3	22	1	21	–	–
Plk5	10	6	2	2	–
Plk6	6	3	1	2	–
Plk7^d	15	8	1	6	–
Plk7^e	9	4	1	3	1
Plakortin	23	22	–	1	–
Dihydroplakortin	32	29	2.5	0.5	–

Table adapted from reference Chianese et al. (2014) with permission from Elsevier (<http://dx.doi.org/10.1016/j.bmc.2014.07.034>)

^aRate of bioactive conformers within 5 kcal mol⁻¹ from the global minimum

^bRate of bioactive conformers belonging to this family

^cHalf-chair in the case of compounds **Plk1-3**

^dDiastereomer with (R)-C10

^eDiastereomer with (S)-C10

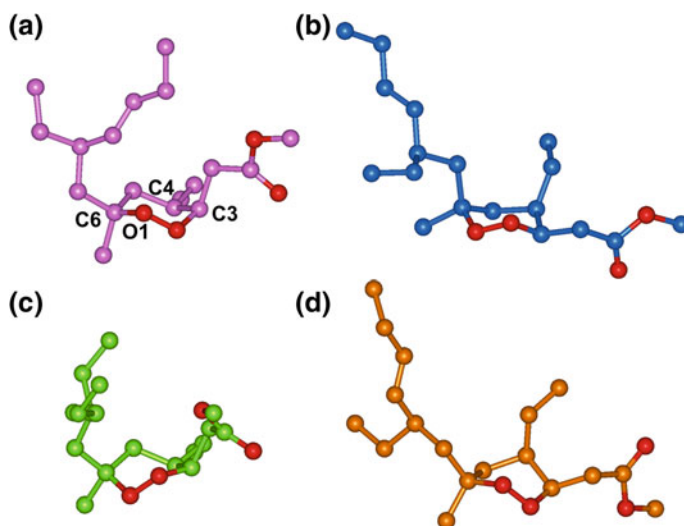


Fig. 16 Lowest energy minima of each 1,2-dioxane ring conformation family of plakortin. Carbons are in pink (chair **a**), blue (chair **b**), light green (skew boat **c**), and orange (skew boat **d**); oxygens are in red. All hydrogens are omitted for clarity. Figure adapted from reference Chianese et al. (2014) with permission from Elsevier (<http://dx.doi.org/10.1016/j.bmc.2014.07.034>)

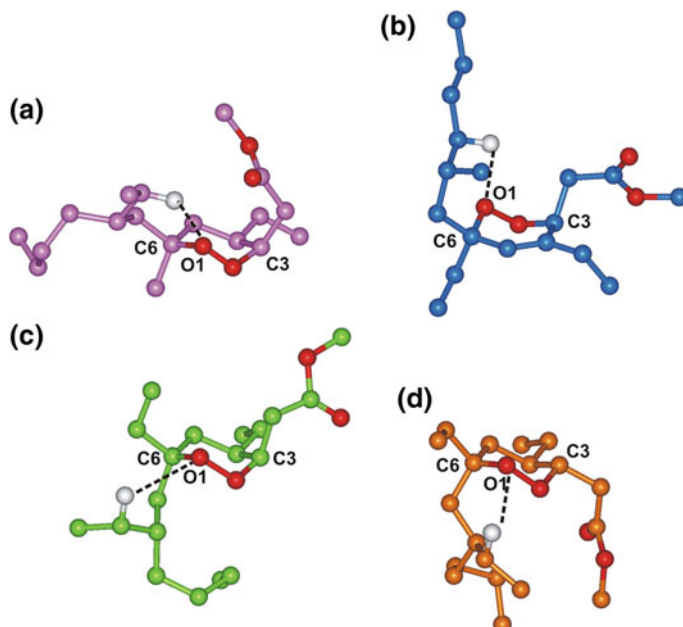


Fig. 17 Bioactive conformations of dihydroplakortin (**a**, *pink*), **Plk3** (**b**, *blue*), **Plk5** (**c**, *light green*) and **Plk6** (**d**, *orange*). The molecules are colored by atom type (O = *red* and H = *white*). Hydrogens are omitted for sake of clarity with the exception of those involved in the intra-molecular radical shift (highlighted by a *black dashed line*). Figure adapted from reference Chianese et al. (2014) with permission from Elsevier (<http://dx.doi.org/10.1016/j.bmc.2014.07.034>)

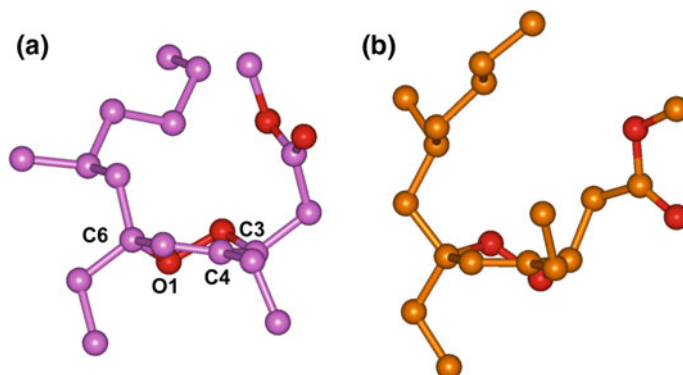


Fig. 18 Lowest energy minima of each 1,2-dioxane ring conformation family of **Plk3**. Carbons are in *pink* (half-chair **a**) and *orange* (half-chair **b**); oxygens are in *red*. All hydrogens are omitted for clarity. Figure adapted from reference Chianese et al. (2014) with permission from Elsevier (<http://dx.doi.org/10.1016/j.bmc.2014.07.034>)

ester group at C3 and the pseudo-equatorial position of the alkyl chain at C6. Thus, although the introduction of the double bond changed the conformational behavior of the endoperoxide ring of **Plk1–3** (Table 12), the simultaneous inversion of chirality at C3 and at C6 resulted in a similar orientation of the putative reactive chain at C6 with respect to O1, when compared to plakortin and dihydroplakortin (Fig. 17a vs. 17b).

However, in the case of **Plk1** and **Plk2**, we also observed a reduction of the rate of putative bioactive conformers with respect to plakortin and dihydroplakortin (Table 13), in agreement with their decreased antimalarial activity (Table 11). This is due to the presence of the double bond which constrains the ring geometry, causing a steric crowding around the putative reaction partners and impairing oxygen lone pairs accessibility. Accordingly, when the steric bulk of the C6 alkyl chain is reduced, as in **Plk3**, the number of bioactive conformers (Table 13) and the antimalarial activity (Table 11) are partially restored. Although **Plk3** showed the same amount of bioactive conformers of plakortin (Table 13), this latter presents 15% of bioactive conformers where the double bond is the partner for the reaction with the putative O1 radical. As already reported (Fattorusso et al. 2011), the higher reactivity of the C6 side chain of plakortin in a radical transfer reaction counterbalances its lower rate of putative bioactive conformers with respect to **2** (23% vs. 32%; Table 13). Accordingly, **Plk3**, presenting the same reactivity of dihydroplakortin and the same rate of bioactive conformers of plakortin (22% vs. 32%; Table 13), resulted to be less active than both reference compounds (Table 11).

In the 1,2-dioxane derivatives **Plk5–7**, similarly to what observed for plakortin and dihydroplakortin, the conformational preference is driven by the 1,3-diaxial steric effect between C4 and C6. Thus, the low energy conformers of **Plk5–7** tend not to assume “B type” conformations, which present the ethyl group at C4 in axial position (Table 12, Figs. 19 and 20). In particular, while **Plk5** showed a strong conformational preference for the Chair A, the inversion of chirality at C3, as in **Plk6** and **Plk7**, reduced the percentage of conformations characterized by the Chair A, which presented a gauche interaction between the equatorial substituents at C3 and C4, in favor of the Skew Boat A, with the C3 substituent in axial position (Table 13 and Fig. 20).

In any case, compound **Plk5–7**, due to the inversion of chirality at C6 with respect to plakortin and dihydroplakortin, showed most of the low energy conformers with C6 in axial position and this largely reduced the rate of low energy putative bioactive conformers (Table 13; Fig. 17) and, accordingly, the antimalarial activity (Table 11). The reduction of the rate of putative bioactive conformers (and of antimalarial activity) is accentuated in **Plk6** where the chirality is inverted also at C3 and, by consequence, the C3 and C6 substituents are in *cis* configuration (Fig. 17d), thus confirming the unfavorable effect on antimalarial activity played by the steric crowding around C6 alkyl chain. Interestingly, the (R)-C10 diastereomer of **Plk7** presented a slightly increased number of putative bioactive conformers with respect to **Plk5** and **Plk6** (Table 13), in agreement with the restoration of some antimalarial activity observed for **Plk7** (Table 11).

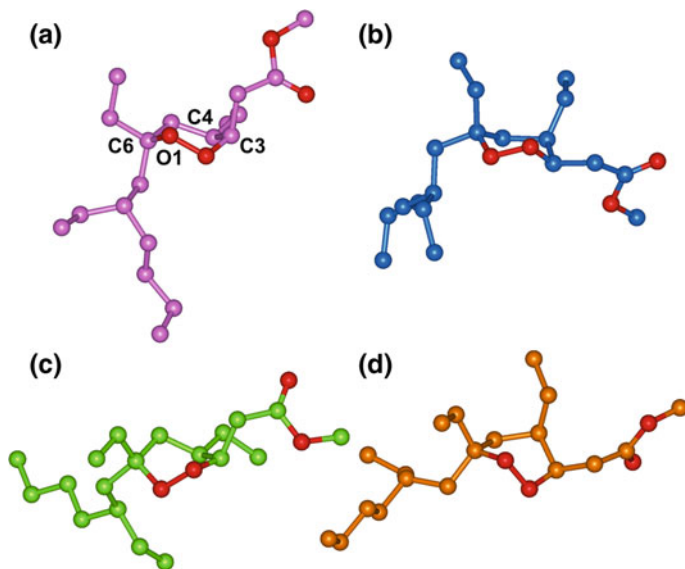


Fig. 19 Lowest energy minima of each 1,2-dioxane ring conformation family of **Plk5**. Carbons are in *pink* (chair **a**), *blue* (chair **b**), *light green* (skew boat **c**), and *orange* (skew boat **d**); oxygens are in *red*. All hydrogens are omitted for clarity. Figure adapted from reference Chianese et al. (2014) with permission from Elsevier (<http://dx.doi.org/10.1016/j.bmc.2014.07.034>)

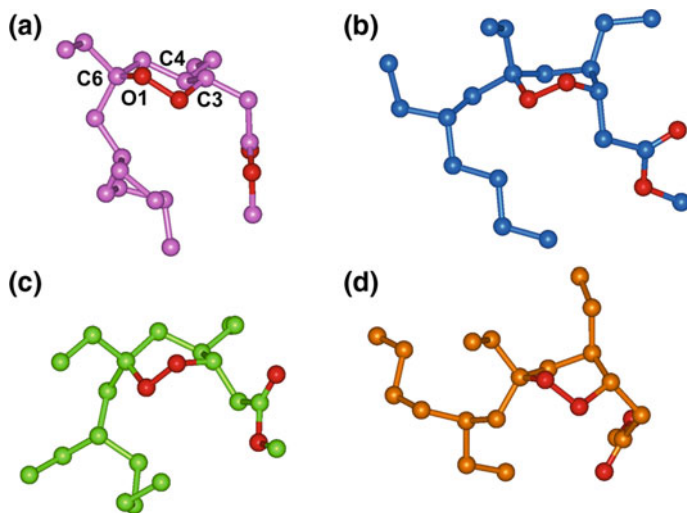


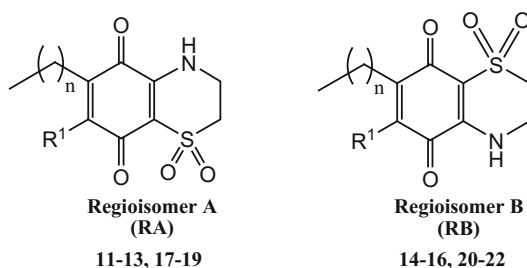
Fig. 20 Lowest energy minima of each 1,2-dioxane ring conformation family of **Plk6**. Carbons are in *pink* (chair **a**), *blue* (chair **b**), *light green* (skew boat **c**), and *orange* (skew boat **d**); oxygens are in *red*. All hydrogens are omitted for clarity. Figure adapted from reference Chianese et al. (2014) with permission from Elsevier (<http://dx.doi.org/10.1016/j.bmc.2014.07.034>)

3.4 Synthetic Analogs of Aplidinone A and B

A new series of synthetic quinones were produced starting from the natural compounds aplidinone A and B and the resulting compounds showed an interesting antimalarial activity against both CQ-sensitive (D10) and CQ-resistant (W2) *Pf* strains (Imperatore et al. 2015). The structures and the antimalarial activity of the new synthetic aplidinone analogs are reported in Table 14.

The IC₅₀ values obtained, reported in Table 14, show that the most active compounds have antimalarial activity in the low micromolar range with the regiochemistry of the dioxothiazine ring playing a role on the observed activity. In particular, when R₁ is OMe group, only the regioisomers B (RB, **14–16**) resulted active, whereas, when R¹ is an amide substituent (PivNH), the regioisomers

Table 14 Effect of compounds **11–22** on the growth of CQ-sensitive (D10) and CQ-resistant (W2) *Pf* strains^a. Cytotoxicity against human microvascular endothelial (HMEC-1) cells



Cmp	R ¹	n	D10 IC ₅₀ (μM) ^b	W2 IC ₅₀ (μM) ^b	HMEC-1 IC ₅₀ (μM) ^b
11	OMe	1	NA ^c	NA ^c	NA ^c
12	OMe	7	NA ^c	NA ^c	NA ^c
13	OMe	13	NA ^c	NA ^c	NA ^c
17	NHCOC(CH ₃) ₃	1	0.39 ± 0.15	0.58 ± 0.12	1.60 ± 0.34
18	NHCOC(CH ₃) ₃	4	1.56 ± 0.12	2.70 ± 0.72	0.90 ± 0.11
19	NHCOC(CH ₃) ₃	10	0.56 ± 0.02	1.06 ± 0.58	0.44 ± 0.15
14	OMe	1	2.45 ± 0.42	2.37 ± 0.42	NA ^c
15	OMe	7	0.82 ± 0.23	0.80 ± 0.36	5.52 ± 1.20
16	OMe	13	1.73 ± 0.93	1.32 ± 0.26	4.41 ± 1.25
20	NHCOC(CH ₃) ₃	1	6.15 ± 1.10	6.31 ± 2.33	NA ^c
21	NHCOC(CH ₃) ₃	4	6.93 ± 0.24	7.87 ± 0.25	NA ^c
22	NHCOC(CH ₃) ₃	10	NA ^b	NA ^b	6.87 ± 3.23

Table adapted from reference Imperatore et al. (2015) with permission from the Royal Society of Chemistry (<http://dx.doi.org/10.1039/c5ra09302c>)

^aCloroquine (CQ) has been considered as positive control (D10 IC₅₀ = 0.04 ± 0.01; W2 IC₅₀ = 0.54 ± 0.28; not cytotoxic)

^bData are the mean ± SD of three different experiments in duplicate

^cNA not active (IC₅₀ > 10 μM against D10 and W2 strains of *Pf* and IC₅₀ > 100 μM against HMEC-1)

A (RA, **17–19**) resulted significantly more active than regioisomers B (RB, **20–22**). The same regiochemistry depending trend is observed for the cytotoxicity against human cells (HMEC-1), see Table 14. Nevertheless, in the active regioisomers, the length of alkyl side chain distinguishes the antimalarial from the cytotoxic activity. Indeed, while toxicity against HMEC-1 cells increase with the length of the alkyl side chain, becoming determinant in the methoxy-derivatives, the antimalarial activity did not show any linear correlation with the length of the alkyl chain in both series, being anyway not dramatically affected (see Table 14). According to the above SARs, the active RA amide-derivative **17** (ethyl side chain) is the most potent antimalarial agent of the series, with IC_{50} 0.39 μ M (D10) and 0.58 μ M (W2), but it also resulted significantly cytotoxic (IC_{50} 1.60 μ M); on the other hand, its RB regioisomer **14** is still active as antimalarial at low micromolar concentration, with IC_{50} 2.45 μ M (D10) and 2.37 μ M (W2), but it was not cytotoxic. In summary, some of the new synthetic derivatives showed a significant pharmacological activity and, mainly, some structural requirements critical for both the antiplasmodial effect and cytotoxicity, have been evidenced.

The preliminary computational studies evidenced a possible relation between antimalarial activity and the propensity to undergo a one electron reduction. In order to fully rationalize the SARs and to investigate the putative antimalarial mechanism of action of these new thiazinoquinones, the two couples of regioisomers with the highest difference in the antimalarial activity and the smallest structural variation (i.e., **12, 15** and **19, 22**; Table 14), were subjected to an in-depth computational analysis (for details see paragraph 2). Firstly, we calculated the prevalent ionic forms at pH 7.2 (cytoplasm) and pH 5.5 (*Pf* FV) (Table 15).

Then, in order to sample the conformational space of the compounds under investigation, a calculation protocol including a simulated annealing procedure followed by molecular mechanics (MM) energy minimization and semi-empirical PM7 full geometry optimization, was applied. Obtained conformers were ranked by their potential energy values and the GM conformer of each compound was selected as starting structure for subsequent calculations.

The mechanism of action of antimalarial quinones has been related to their redox properties, and, in particular, to the capacity to form toxic semiquinone radical species (QH \cdot) through a one-electron reduction reaction (Ehrhardt et al. 2013).

Table 15 Prevalent ionic forms of new thiazinoquinones

Cmp	Prevalent ionic form (%) ^a	
	pH 7.2	pH 5.5
12	N(100)	N(100)
15	N(100)	N(100)
19	N(100)	N(100)
22	N(100)	N(100)

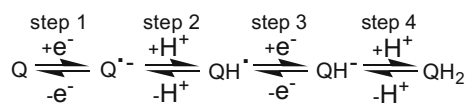
Table reproduced from reference Imperatore et al. (2015) with permission from the Royal Society of Chemistry (<http://dx.doi.org/10.1039/c5ra09302c>)

^aPercentage of ionic form in brackets; N neutral form

Indeed, the two-electron, two-proton, reduction pathway of quinones (Q) to hydroquinones (QH₂) involves a sequence of steps in which reversible one-electron reduction reactions are followed by proton uptake reactions producing the semiquinone species (QH), as illustrated in Scheme 1 (Guin et al. 2011).

On these bases, we investigated the redox properties of **12**, **15**, **19**, and **22**, focusing on the ability to form the toxic semiquinone radical species. The putative reduction pathway of our new thiazinoquinones involves the formation of two possible semiquinone species (QH_i and QH_{ii}, Fig. 21).

Thus, starting from the structure of the GM conformers of **12**, **15**, **19**, and **22**, the respective Q⁻, QH_i•, and QH_{ii}• radicals were generated and subjected to further semi-empirical (PM7) calculations to obtain a full geometry and energy optimization. The reaction enthalpies (kcal/mol) for the formation of the two possible semiquinone radical species QH_i• and QH_{ii}• (i.e., steps 1 and 2, Scheme 1) were then calculated (Table 16).



Scheme 1 Sequence of steps in quinone reduction pathway. Scheme reproduced from reference Imperatore et al. (2015) with permission from the Royal Society of Chemistry (<http://dx.doi.org/10.1039/c5ra09302c>)

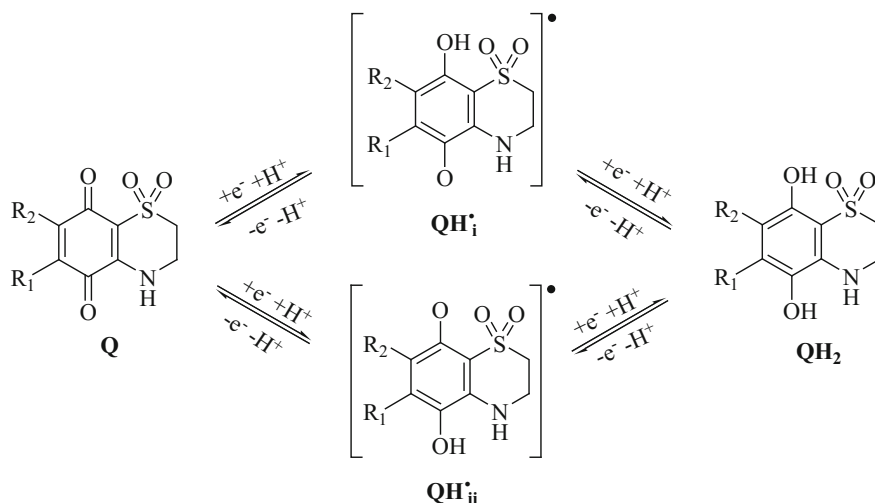


Fig. 21 Schematic representation of the putative thiazinoquinone reduction pathway. Figure reproduced from reference Imperatore et al. (2015) with permission from the Royal Society of Chemistry (<http://dx.doi.org/10.1039/c5ra09302c>)

Table 16 Reaction Enthalpies (ΔH_f ; kcal/mol) of **12**, **15**, **19**, and **22** for the formation of the two possible semiquinone species reported in Fig. 21

Cmp	$\Delta H_f(Q \rightarrow Q^-)$	$\Delta H_f(Q^- \rightarrow QH_i)$	$\Delta H_f(Q \rightarrow QH_i)$	$\Delta H_f(Q^- \rightarrow QH_{ii})$	$\Delta H_f(Q \rightarrow QH_{ii})$
12	-60.38	53.00	-7.38	53.91	-6.47
15	-66.05	45.82	-20.23	59.45	-6.60
19	-62.76	50.01	-12.75	56.33	-6.43
22	-50.68	38.20	-12.48	46.99	-3.69

Table reproduced from reference Imperatore et al. (2015) with permission from the Royal Society of Chemistry (<http://dx.doi.org/10.1039/c5ra09302c>)

The obtained results highlighted that all compounds present a definite preference for the formation of the semiquinone species named QH_i in Fig. 21 ($\Delta H_f(Q \rightarrow QH_i)$ vs. $\Delta H_f(Q \rightarrow QH_{ii})$; Table 16).

The higher stability of QH_i with respect to QH_{ii} is likely due to the presence of a hydrogen bond between the reduced oxygen and the SO_2 group (Figs. 22 and 23).

According to these results, for the Q , Q^- , and QH_i species of each compound, the energy of the frontier molecular orbitals [highest occupied molecular orbital

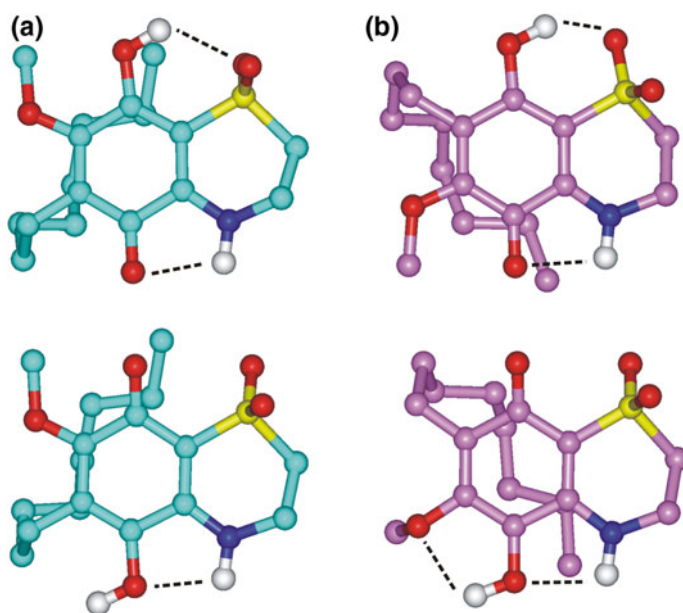


Fig. 22 QH_i (top) and QH_{ii} (bottom) species of **12** GM (cyan; a) and **15** GM (pink; b). The ligands are colored by atom type (O = red, N = blue, S = yellow and H = white). Hydrogen bonds are highlighted by black dashed lines. Hydrogens are omitted for the sake of clarity with the exception of those involved in hydrogen bonds. Figure adapted from reference Imperatore et al. (2015) with permission from the Royal Society of Chemistry (<http://dx.doi.org/10.1039/c5ra09302c>)

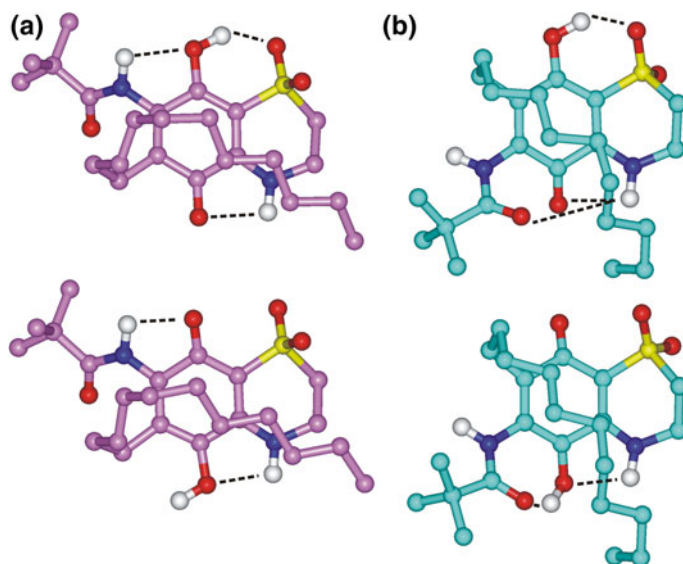


Fig. 23 QH_i (top) and QH_{ii} (bottom) species of **19** GM (pink; **a**) and **22** GM (cyan; **b**). The ligands are colored by atom type (O = red, N = blue, S = yellow and H = white). Hydrogen bonds are highlighted by black dashed lines. Hydrogens are omitted for the sake of clarity with the exception of those involved in hydrogen bonds. Figure adapted from reference Imperatore et al. (2015) with permission from the Royal Society of Chemistry (<http://dx.doi.org/10.1039/c5ra09302c>)

(HOMO), lowest unoccupied molecular orbital (LUMO), and singly occupied molecular orbital (SOMO)] was calculated. Then, using these values, the redox capacities were assessed by calculating: (i) vertical ionization potential (IP), (ii) electron affinity (EA), (iii) electrophilicity index (ω) (Chattaraj et al. 2006). All the above data are reported in Table 17. The whole of the data reported in Tables 16 and 17 evidenced a relationship between the ability of thiazinoquinones

Table 17 PM7 calculated orbital energies (LUMO and SOMO), electrophilicity index (ω), vertical ionization potential (IP) and vertical electron affinity (EA) for Q, Q^- , QH_i species of **12**, **15**, **19**, and **22**

Cmp	Q		Q^-		QH_i			ω
	E_{LUMO} (Ev)	ω	E_{SOMO} (Ev)	Vertical IP (Ev)	E_{SOMO} (Ev)	Vertical IP (Ev)	Vertical EA (Ev)	
12	-1.614	1.968	-3.768	2.341	-8.194	6.681	2.897	3.030
15	-1.791	2.080	-3.928	2.465	-7.969	6.607	2.694	2.763
19	-1.598	1.931	-3.859	2.361	-7.968	6.391	2.863	3.034
22	-1.189	1.711	-3.215	1.749	-7.685	6.084	2.655	2.784

Table reproduced from reference Imperatore et al. (2015) with permission from the Royal Society of Chemistry (<http://dx.doi.org/10.1039/c5ra09302c>)

to form the QH_i radical species and their antimalarial activity. In particular, the regioisomers **15** and **19**, active as antimalarials, showed lower reaction enthalpies for the first step of the reduction process (Scheme 1) with respect to the corresponding inactive regioisomers **12** and **22** ($\Delta H_{f(Q \rightarrow Q^-)}$; Table 16). In addition, the Q species of **15** and **19** showed lower LUMO energy and higher ω values than those of **12** and **22**, respectively (Table 17). Interestingly, the vertical IP and SOMO energy values indicate that the Q^- species of the inactive regioisomer **22** tend to be reoxidized to the parent quinone Q more than that of the active **19**. The same is valid comparing **12** (inactive) and **15** (active) (Table 17). Although, in the case of **12** and **15**, the difference is minimal, there is a larger difference in the sum of the reaction enthalpies of step 1 and 2 (Scheme 1) leading to the formation of QH_i ($\Delta H_{f(Q \rightarrow \text{QH}_i)}$; Table 16).

Last but not least, we investigated if conformational parameters play a role in the redox properties of the inactive regioisomer **22** with respect to the active **19**. Indeed, contrarily to **12** and **15**, the GM conformers of **19** and **22** differed significantly (Fig. 24a vs. 24b) and, in particular, presented a different conformation of the amide function and different intramolecular H-bond interactions.

As evidenced in Fig. 24a, the intra-molecular H-bond between the amide nitrogen and the quinone oxygen favors the planarity of thiazoquinone ring of **19**. On the contrary, as evidenced in Fig. 24b, due to the intramolecular H-bond between the amide oxygen and the ring amine function, the thiazoquinone ring

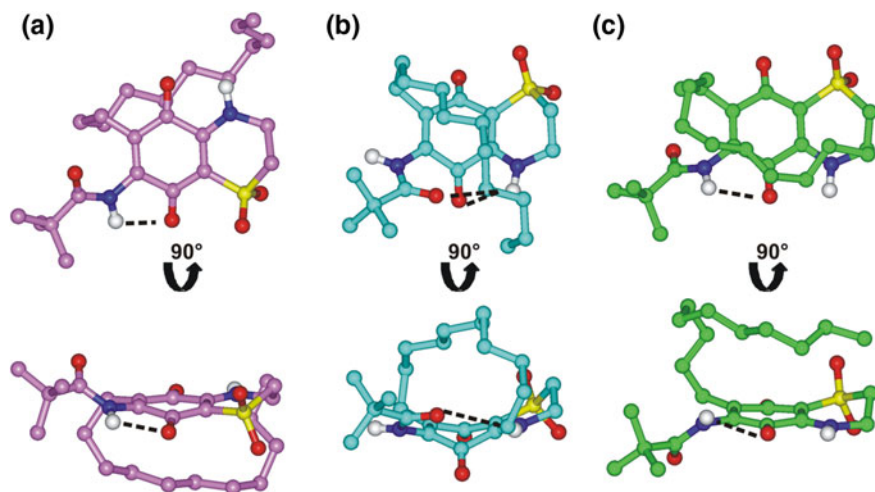


Fig. 24 PM7 GM conformer of **19** (pink; a); PM7 GM conformer of **22** (cyan; b) and PM7 conformer **22B** (green; c). Front view (top) and longitudinal view (bottom). The ligands are colored by atom type (O = red, N = blue, S = yellow and H = white). H-bonds between the amide function and the thiazoquinone ring are highlighted by green dashed lines. Hydrogens are omitted for the sake of clarity with the exception of those involved in H-bonds. Figure adapted from reference Imperatore et al. (2015) with permission from the Royal Society of Chemistry (<http://dx.doi.org/10.1039/c5ra09302c>)

system of **22** significantly deviate from planarity. In order to investigate if this is related to the lower propensity of **22** to undergo a one electron reduction with respect to **19** ($\Delta H_{f(Q \rightarrow Q^-)}$, Table 16; ω of Q, Table 17), we selected the conformer of **22** having the same conformation of the amide substituent of the GM conformer of **19** (named **22B**; Fig. 24c).

It has to be underlined that conformer **22B** is not a low energy conformer of **22**, showing a ΔE from the GM conformer of 5.24 kcal/mol, hence it was not included in our previous analysis. The redox properties of conformer **22B** were calculated applying the same approach previously described.

It resulted that, compared to the GM conformer of **22**, conformer **22B** presents: (i) lower reaction enthalpies for both the first step of the reduction process ($\Delta H_{f(Q \rightarrow Q^-)}$) and the formation of QH_i ($\Delta H_{f(Q \rightarrow QH_i)}$) (Tables 18 vs. 16), (ii) lower LUMO energy and higher ω values of the Q species (Tables 19 vs. 17). Moreover, the SOMO energy and vertical IP values indicate that the Q^- species of conformer **22B** tend to be reoxidized to the parent quinone Q less than that of the GM conformer (Tables 19 vs. 17). These results indicate that the thiazinoquinone ring system planarity (Fig. 24c vs. 24b) plays a crucial role in the reductive activation leading to the formation of QH_i radical.

Finally, the Log *D* values of all compounds were calculated (*c* Log *D*; Table 20) to investigate a possible role of pharmacokinetic parameters in the observed activities of thiazinoquinones.

Results evidenced that there is no correlation between the *c* Log *D* values (Table 20) and the antimalarial activity (Table 14).

In summary, the results of our computational analysis strongly suggest that the higher antimalarial activity of thiazinoquinones **15** and **19** with respect to **12** and **22**, is related to their greater ability to form a stable semiquinone species. In this

Table 18 Reaction enthalpies (ΔH_f ; kcal/mol) of conformer **22B** for the formation of the two possible semiquinone species reported in Fig. 21

Cmp	$\Delta H_{f(Q \rightarrow Q^-)}$	$\Delta H_{f(Q^- \rightarrow QH_i)}$	$\Delta H_{f(Q \rightarrow QH_i)}$	$\Delta H_{f(Q^- \rightarrow QH_i)}$	$\Delta H_{f(Q \rightarrow QH_i)}$
22B	-67.56	48.01	-19.55	54.60	-12.96

Table reproduced from reference Imperatore et al. (2015) with permission from the Royal Society of Chemistry (<http://dx.doi.org/10.1039/c5ra09302c>)

Table 19 PM7-calculated orbital energies (LUMO and SOMO), electrophilicity index (ω), vertical ionization potential (IP) and vertical electron affinity (EA) for Q, Q^- , QH_i species of conformer **22B**

Cmp	Q		Q^-		QH_i			ω
	E_{LUMO} (Ev)	ω	E_{SOMO} (Ev)	Vertical IP (Ev)	E_{SOMO} (Ev)	Vertical IP (Ev)	Vertical EA (Ev)	
22B	-1.843	2.098	-4.056	2.486	-7.955	6.431	2.911	3.099

Table reproduced from reference Imperatore et al. (2015) with permission from the Royal Society of Chemistry (<http://dx.doi.org/10.1039/c5ra09302c>)

Table 20 $c \log D$ values of new thiazinoquinones

Cmp	$c \log D$
11	-0.25
12	2.87
13	5.71
14	-0.25
15	2.87
16	5.71
17	-0.19
18	1.40
19	4.70
20	-0.19
21	1.40
22	4.70

Table adapted from reference Imperatore et al. (2015) with permission from the Royal Society of Chemistry (<http://dx.doi.org/10.1039/c5ra09302c>)

way they could act, like other antimalarial quinones, as “subversive substrates” by shuttling single electrons from reduced systems to key oxidants such as hemoglobin-associated or free Fe(III)-protoporphyrin IX (Muller et al. 2011; Davioud-Charvet and Lanfranchi 2011; Blank et al. 2012). This could not only contribute to the production of reactive oxygen species through Fenton chemistry but also prevent both the digestion of hemoglobin and the formation of hemozoin. In this way, the redox equilibrium is affected leading to the death of the parasite. Finally, the results of our computational studies were confirmed by electrochemical studies performed on these compounds evidencing that an intense interaction with Fe(III)-Heme, through the formation of the $QH \cdots Fe(III)$ -Heme surface adduct, is a necessary prerequisite for antimalarial activity (Imperatore et al. 2015).

4 Conclusion

The molecular modeling studies described in this chapter concurred to clarify the mechanism of action of antimalarial agents characterized by the scaffold of the marine compounds plakortin and aplidinone. This mechanism is based on the interaction with Fe(II)-heme and it involves the formation of radical toxic intermediate able to directly react with *Plasmodium* biomolecules increasing its oxidative stress. In particular, as reported below, these studies allowed to identify, for each of the new classes of potential therapeutic agents, the three-dimensional structural requirements essential for their antimalarial activity. These results could guide the development of further optimized antimalarials.

First series of new synthetic analogs of plakortins. The new synthetic plakortin analogs (**7–9**) showed that the modification at position 4 resulted in an improved antimalarial activity, especially in compound **8g**, which reached the activity of the natural lead plakortin. On the other hand, results obtained for the new series of 1,2-dioxane-4-carboxamides **9** showed that alkyl substituents at C6 largely dominate in determining the antimalarial activity and the introduction of a side-chain at C4 containing an imidazole ring improves antimalarial activity. In particular, compound **9e** resulted fivefold more active than its methyl ester analog, showing an antimalarial activity comparable to the natural lead plakortin.

Second series of new synthetic analogs of plakortins. The new synthetic plakortin analogs **10** evidenced that the inclusion of a substituted amine moiety at C4 on our easily accessible 1,2-dioxane-3-methoxy scaffold improved significantly the antimalarial activity (more active than the natural lead plakortin); this is due both to pharmacokinetic and pharmacodynamic effects. Indeed, the amine function at C4 favors the ability of the peroxide bridge to undergo reductive cleavage and to generate/propagate the putative toxic radical.

The acquired information suggested that the essential pharmacophoric requirements for antimalarial activity should include:

- (i) a 1,2 dioxane ring able to react with Fe(II) species through its endoperoxide group, forming an oxygen radical,
- (ii) additional iron interacting with functionalities, favoring the approach to iron without interfering with the redox reaction,
- (iii) the *cis* configuration of the methoxy group at C3 and the substituent at C4 to allow accessibility of iron to 1,2-dioxane oxygens and O7,
- (iv) C6 and/or C3 chains bearing possible partners for a “through-space” intramolecular radical shift to a carbon atom,
- (v) a significant number of low energy conformers allowing the correct orientation of all the intramolecular reaction partners,
- (vi) the ability of the generated carbon radical to propagate via intermolecular reactions,
- (vii) the presence of protonatable function at *Pf* FV pH (i.e., 5.5).

New natural polyketide endoperoxides. These new series of natural endoperoxides evidenced the crucial role on the antimalarial activity of plakortins played by the stereochemical parameters affecting the relative orientation of the atoms involved in the putative radical generation and transfer reaction.

Synthetic analogs of aplidinones. The thiazinoquinone compounds evidenced that both the regiochemistry of the dioxothiazine ring and the nature of the substituent on the quinone ring play a crucial role in the antimalarial effect whereas, in the active regioisomers, the length of the alkyl side chain distinguishes the antimalarial from the cytotoxic activity. Moreover, these studies support the hypothesis that the antiplasmodial activity of thiazinoquinones is related to their redox properties and, in particular, to the capacity to form toxic semiquinone species that can affect the parasite redox equilibrium leading to its death. Also in this case iron is

involved in the reductive activation of the compounds, as well as, in the propagation of the resulting radical anion. Accordingly, the thiazinoquinone ring system planarity plays a crucial role in the reductive activation leading to the intermediate semiquinone formation.

Acknowledgments The content of this chapter was reproduced from references: Persico et al. (2013) with permission from Elsevier (<http://dx.doi.org/10.1016/j.ejmech.2013.10.050>); Chianese et al. (2014) with permission from Elsevier (<http://dx.doi.org/10.1016/j.bmc.2014.07.034>); Lombardo et al. (2014) with permission from Wiley-VCH Verlag GmbH & Co. KGaA (<http://dx.doi.org/10.1002/ejoc.201301394>); Sonawane et al. (2015) with permission from the Royal Society of Chemistry (<http://dx.doi.org/10.1039/c5ra10785g>); Imperatore et al. (2015) with permission from the Royal Society of Chemistry (<http://dx.doi.org/10.1039/c5ra09302c>). This work was supported by the following grants: POR Campania FESR 2007–2013 FARMABIONET (B25C1300023007), MIUR—FIRB 2012 RBFR12WB3W, and EU Project Bluegenics (Grant 311848).

References

- Allouche AR (2011) A graphical user interface for computational chemistry softwares. *J Comput Chem* 32:174–182
- Araujo NC, Barton V, Jones M, Stocks PA, Ward SA, Davies J, Bray PG, Shone AE, Cristiano ML, O'Neill PM (2009) Semi-synthetic and synthetic 1,2,4-trioxoquinones and 1,2,4-trioxolaquinones: synthesis, preliminary SAR and comparison with acridine endoperoxide conjugates. *Bioorg Med Chem Lett* 19:2038–2043
- Arav-Boger R, Shapiro TA (2005) Molecular mechanisms of resistance in antimalarial chemotherapy: the unmet challenge. *Annu Rev Pharmacol Toxicol* 45:565–585
- Baker J (1986) An algorithm for the location of transition states. *J Comput Chem* 7:385–395
- Beckera K, Tilley L, Vennerstrom JL, Roberts D, Rogerson S, Ginsburg H (2004) Oxidative stress in malaria parasite-infected erythrocytes: host-parasite interactions. *Int J Parasitol* 34:163–189
- Blank O, Davioud-Charvet E, Elhabiri M (2012) Interactions of the antimalarial drug methylene blue with methemoglobin and heme targets in *Plasmodium falciparum*: a physico-biochemical study. *Antioxid Redox Signaling* 17:544–554
- Capela R, Cabal GG, Rosenthal PJ, Gut J, Mota MM, Moreira R, Lopes F, Prudencio M (2011) Design and evaluation of primaquine-artemisinin hybrids as a multistage antimalarial strategy. *Antimicrob Agents Chemother* 55:4698–4706
- Charman SA, Arbe-Barnes S, Bathurst IC, Brun R, Campbell M, Charman WN, Chiu FC, Chollet J, Craft JC, Creek DJ, Dong Y, Matile H, Maurer M, Morizzi J, Nguyen T, Papastogiannidis P, Scheurer C, Shackelford DM, Sriraghavan K, Stingelin L, Tang Y, Urwyler H, Wang X, White KL, Wittlin S, Zhou L, Vennerstrom JL (2011) Synthetic ozonide drug candidate OZ439 offers new hope for a single-dose cure of uncomplicated malaria. *Proc Natl Acad Sci USA* 108:4400–4405
- Chattaraj PK, Sarkar U, Roy DR (2006) Electrophilicity index. *Chem Rev* 106(2006):91
- Chianese G, Persico M, Yang F, Lin HW, Guo YW, Basilio N, Parapini S, Taramelli D, Tagliatela-Scafati O, Fattorusso C (2014) Endoperoxide polyketides from a Chinese *Plakortis* simplex: further evidence of the impact of stereochemistry on antimalarial activity of simple 1,2-dioxanes. *Bioorg Med Chem* 22:4572–4580
- Chiodo S, Russo N, Sicilia E (2004) Newly developed basis sets for density functional calculations. *J Comput Chem* 26:175–183

- Chishiro T, Shimazaki Y, Tani F, Tachi Y, Naruta Y, Karasawa S, Hayami S, Maeda Y (2003) Isolation and crystal structure of a peroxo-bridged heme-copper complex. *Angew Chem Int Ed* 42:2788–2791
- Coleman RE, Nath AK, Schneider I, Song GH, Klein TA, Milhous WK (1994) Prevention of sporogony of *Plasmodium falciparum* and *P. Berghei* in *Anopheles stephensi* mosquitoes by transmission-blocking antimalarials. *Am J Trop Med Hyg* 50:646–653
- Colson AO, Sevilla MD (1995) Ab initio molecular orbital calculations of radicals formed by H and *OH addition to the DNA bases: electron affinities and ionization potentials. *J Phys Chem* 99:13033–13037
- Cosledan F, Fraisse L, Pellet A, Guillou F, Mordmuller B, Kreamsner PG, Moreno A, Mazier D, Maffrand JP, Meunier B (2008) Selection of a trioxaquine as an antimalarial drug candidate. *Proc Natl Acad Sci U S A* 105:17579–17584
- Das KC, Misra HP (2004) Hydroxyl radical scavenging and singlet oxygen quenching properties of polyamines. *Mol Cell Biochem* 262:127–133
- Davioud-Charvet E, Lanfranchi DA (2011) Subversive substrates of glutathione reductases from *Plasmodium falciparum*-infected red blood cells as antimalarial agents. In: Selzer P (ed) *Drug discovery in infectious diseases*, vol 2. Wiley-VCH, Weinheim, Germany, pp 375–396
- Ding HQ, Karasawa N, Goddard WA III (1992) Atomic level simulations on a million particles: the cell multipole method for Coulomb and London non-bond interactions. *J Chem Phys* 97:4309–4315
- Dodd EL, Bohle DS (2014) Orienting the heterocyclic periphery: a structural model for chloroquine's antimalarial activity. *Chem Commun* 50:13765–13768
- Egan TJ, Combrinck JM, Egan J, Hearne GR, Marques HM, Ntenti S, Sewell BT, Smith PJ, Taylor D, Van Schalkwyk DA, Walden JC (2000) Fate of haem iron in the malaria parasite *Plasmodium falciparum*. *Biochem J* 365:343–347
- Ehrhardt K, Davioud-Charvet E, Ke H, Vaidya AB, Lanzer M, Deponte M (2013) The antimalarial activities of methylene blue and the 1,4-naphthoquinone 3-[4-(trifluoromethyl)benzyl]-menadione are not due to inhibition of the mitochondrial electron transport chain. *Antimicrob Agents Chemother* 57:2114–2120
- Fattorusso C, Persico M, Basilico N, Taramelli D, Fattorusso E, Scala F, Tagliatalata-Scafati O (2011) Antimalarials based on the dioxane scaffold of plakortin. A concise synthesis and SAR studies. *Bioorg Med Chem* 19:312–320
- Flannery EL, Chatterjee AK, Winzeler EA (2013) Antimalarial drug discovery—approaches and progress towards new medicines. *Nat Rev Microbiol* 11:849–862
- Frisch MJ, Pople JA, Binkley JS (1984) Self-consistent molecular orbital methods. 25. Supplementary functions for Gaussian basis sets. *J Chem Phys* 80:3265–3269
- Frisch, M. J.; Trucks, G. W.; Schlegel, H. B.; Scuseria, G. E.; Robb, M. A.; Cheeseman, J. R.; Scalmani G, Barone V, Mennucci B, Petersson GA, Nakatsuji H, Caricato M, Li X, Hratchian HP, Izmaylov AF, Bloino J, Zheng G, Sonnenberg JL, Hada M, Ehara M, Toyota K, Fukuda R, Hasegawa J, Ishida M, Nakajima T, Honda Y, Kitao O, Nakai H, Vreven T, Montgomery JAJr, Peralta JE, Ogliaro F, Bearpark M, Heyd JJ, Brothers E, Kudin KN, Staroverov VN, Kobayashi R, Normand J, Raghavachari K, Rendell A, Burant JC, Iyengar SS, Tomasi J, Cossi M, Rega N, Millam NJ, Klene M, Knox JE, Cross JB, Bakken V, Adamo C, Jaramillo J, Gomperts R, Stratmann RE, Yazyev O, Austin AJ, Cammi R, Pomelli C, Ochterski JW, Martin RL, Morokuma K, Zakrzewski VG, Voth GA, Salvador P, Dannenberg JJ, Dapprich S, Daniels AD, Farkas Ö, Foresman JB, Ortiz JV, Cioslowski J, Fox DJ (2009) *Gaussian 09*, revision A.1; Gaussian, Inc. Wallingford, CT
- Ginsburg H, Ward SA, Bray PG (1999) An integrated model of chloroquine action. *Parasitol Today* 15:357–360
- Grellepois F, Grellier P, Bonnet-Delpon D, Begue JP (2005) Design, synthesis and antimalarial activity of trifluoromethylartemisinin-mefloquine dual molecules. *ChemBioChem* 6:648–652
- Griller D, Howard JA, Marriott PR, Scaiano JC (1981) Absolute rate constants for the reactions of tert-butoxyl, tert-butylperoxyl, and benzophenone triplet with amines: the importance of a stereoelectronic effect. *J Am Chem Soc* 103:619–623

- Guin PS, Das S, Mandal PC (2011) Electrochemical reduction of quinones in different media: a review. *Int J Electrochem* 2011:816202–816222
- Ha HC, Sirisoma NS, Kuppusamy P, Zweier JL, Woster PM, Casero RA (1998) The natural polyamine spermine functions directly as a free radical scavenger. *Proc Natl Acad Sci USA* 95:11140–11145
- Han C, Davis CB, Wang B (2010) Evaluation of drug candidates for preclinical development: pharmacokinetics, metabolism, pharmaceuticals, and toxicology. Wiley, New Jersey, pp 1–289
- Haynes RK, Chan WC, Wong HN, Li KY, Wu WK, Fan KM, Sung HHY, Williams ID, Prospero D, Melato S, Coghi P, Monti D (2010) Facile oxidation of leucomethylene blue and dihydroflavins by artemisinin: relationship with flavoenzyme function and antimalarial mechanism of action. *ChemMedChem* 5:1282–1299
- Holtje HD, Fattorusso C (1998) Construction of a model of the *Candida albicans* lanosterol 14- α -demethylase active site using the homology modelling technique. *Pharm Acta Helv* 72:271–277
- Imperatore C, Persico M, Aiello A, Luciano P, Guiso M, Sanasi MF, Taramelli D, Parapini S, Cebrián-Torrejón G, Doménech-Carbó A, Fattorusso C, Menna M (2015) Marine inspired antiplasmodial thiazinoquinones: synthesis, computational studies and electrochemical assays. *RSC Advances* 5:70689–70702
- Jung M, Kim H, Lee K, Park M (2003) Naturally occurring peroxides with biological activities. *Mini Rev Med Chem* 3:159–165
- Kapetanaki S, Varotsis C (2001) Fourier transform infrared investigation of non-heme Fe(III) and Fe(II) decomposition of artemisinin and of a simplified trioxane alcohol. *J Med Chem* 44:3150–3156
- Kerns EH, Di L (2008) Drug-Like properties: concepts, structure design and methods: from ADME to toxicity optimization. Academic Press, Amsterdam, pp 1–526
- Krishna S, Uhlemanna AC, Haynes RK (2004) Artemisinins: mechanisms of action and potential for resistance. *Drug Resist Updates* 7:233–244
- Laurent SA, Loup C, Mourgues S, Robert A, Meunier B (2005) Heme alkylation by artesunic acid and trioxaquine DU1301, two antimalarial trioxanes. *ChemBioChem* 6:653–658
- Liu YP (2001) Applications of effective core potentials and density functional theory to the spin states of iron porphyrin. *J Chem Inf Comput Sci* 41:22–29
- Lombardo M, Sonawane DP, Quintavalla A, Trombini C, Dhavale DD, Taramelli D, Corbett Y, Rondinelli F, Fattorusso C, Persico M, Tagliatalata-Scafati O (2014) Optimized synthesis and antimalarial activity of 1,2-dioxane-4-carboxamides. *Eur J Org Chem* 2014:1607–1614
- Loup C, Lelievre J, Benoit-Vical F, Meunier B (2007) Trioxaquinones and heme-artemisinin adducts inhibit the in vitro formation of hemozoin better than chloroquine. *Antimicrob Agents Chemother* 51:3768–3770
- Maeda Y, Ingold KU (1980) Kinetic applications of electron paramagnetic resonance spectroscopy. 35. The search for a dialkyl-aminyl rearrangement. Ring opening of N-cyclobutyl-N-n-propyl-aminyl. *J Am Chem Soc* 102:328–331
- Maple JR, Hwang MJ, Stockfisch TP, Dinur U, Waldman M, Ewig CS, Hagler AT (1994) Derivation of class II force fields. I. Methodology and quantum force field for the alkyl function group and alkane molecules. *J Comput Chem* 15:162–182
- McCann PP, Bacchi CJ, Hanson WL, Cain GD, Nathan HC, Hutner SH, Sjoerdsma A (1981) Effect on parasitic protozoa of α -difluoromethylornithine an inhibitor of ornithine carboxylase. *Adv Polyamine Res* 3:97–110
- Mercer AE, Copple IM, Maggs JL, O'Neill PM, Park BK (2011) The role of heme and the mitochondrion in the chemical and molecular mechanisms of mammalian cell death induced by the artemisinin antimalarials. *J Biol Chem* 286:987–996
- Meunier B, Robert A (2010) Heme as trigger and target for trioxane-containing antimalarial drugs. *Acc Chem Res* 43:1444–1451
- Müller S (2004) Redox and antioxidant systems of the malaria parasite *Plasmodium falciparum*. *Mol Microbiol* 53:1291–1305

- Muller T, Johann L, Jannack B, Bruckner M, Lanfranchi DA, Bauer H, Sanchez C, Yardley V, Deregnacourt C, Schrevel J, Lanzer M, Schirmer RH, Davioud-Charvet E (2011) Glutathione reductase-catalyzed cascade of redox reactions to bioactivate potent antimalarial 1,4-naphthoquinones a new strategy to combat malarial parasites. *J Am Chem Soc* 133:11557–11571
- Muregi FW, Ishih A (2010) Next-generation antimalarial drugs: hybrid molecules as a new strategy in drug design. *Drug Dev Res* 71:20–32
- Niemand J, Burger P, Verlinden BK, Reader J, Joubert AM, Kaiser A, Louw AI, Kirk K, Phanstiel O, Birkholtz LM (2013) Anthracene-polyamine conjugates inhibit in vitro proliferation of intraerythrocytic *Plasmodium falciparum* parasites. *Antimicrob Agents Chemother* 57:2874–2877
- O'Neill OM, Posner GH (2004) A medicinal chemistry perspective on artemisinin and related endoperoxides. *J Med Chem* 47:2945–2964
- O'Neill PM, Barton VE, Ward SA, Chadwick J (2012) 4-Aminoquinolines: chloroquine, amodiaquine and next-generation analogues. In: *Treatment and prevention of malaria*, Springer, pp 19–44
- Parr RG, Szentpaly L, Lui S (1999) Electrophilicity index. *J Am Chem Soc* 121:1922–1924
- Persico M, Parapini S, Chianese G, Fattorusso C, Lombardo M, Petrizza L, Quintavalla A, Rondinelli F, Basilico N, Taramelli D, Trombini C, Fattorusso E, Tagliatalata-Scafati O (2013) Further optimization of plakortin pharmacophore: structurally simple 4-oxymethyl-1,2-dioxanes with promising antimalarial activity. *Eur J Med Chem* 70:875–886
- Persico M, Quintavalla A, Rondinelli F, Trombini C, Lombardo M, Fattorusso C, Azzarito V, Taramelli D, Parapini S, Corbett Y, Chianese G, Fattorusso E, Tagliatalata-Scafati O (2011) A new class of antimalarial dioxanes obtained through a simple two-step synthetic approach: rational design and structure-activity relationship studies. *J Med Chem* 54:8526–8540
- Pischel U, Nau WM (2001) Switch-over in photochemical reaction mechanism from hydrogen abstraction to exciplex-induced quenching: interaction of triplet-excited versus singlet-excited acetone versus cumyloxy radicals with amines. *J Am Chem Soc* 123:9727–9737
- Posner GH, Cumming JN, Ploypradith P, Oh CH (1995) Evidence for Fe(IV): O in the molecular mechanism of action of the trioxane antimalarial artemisinin. *J Am Chem Soc* 117:5885–5886
- Reguera RM, Tekwani BL, Balana-Fouce R (2005) Polyamine transport in parasites: a potential target for new antiparasitic drug development. *Comp Biochem Physiol Part C Toxicol Pharmacol* 140:151–164
- Ruiz E, Cirera J, Alvarez S (2005) Spin density distribution in transition metal complexes. *Coord Chem Rev* 249:2469–2660
- Sawyer A, Sullivan E, Mariam YH (1996) A semiempirical computational study of electron transfer reactivity of one- vs. two-ring model systems for anthracycline pharmacophores. I. A rationale for mode of action. *J Comput Chem* 17:204–225
- Sonawane DP, Persico M, Corbett Y, Chianese G, Di Dato A, Fattorusso C, Tagliatalata-Scafati O, Taramelli D, Trombini C, Dhavale DD, Quintavalla A, Lombardo M (2015) New antimalarial 3-methoxy-1,2-dioxanes: optimization of cellular pharmacokinetics and pharmacodynamics properties by incorporation of amino and N-heterocyclic moieties at C4. *RSC Adv* 5:72995–73010
- Stewart JJP (2007) Optimization of parameters for semiempirical methods V: modification of NDDO approximations and application to 70 elements. *J Mol Model* 13:1173–1213
- Stewart JJP (2013) Optimization of parameters for semiempirical methods VI: more modifications to the NDDO approximations and re-optimization of parameters. *J Mol Model* 19:1–32
- Tagliatalata-Scafati O, Fattorusso E, Romano A, Scala F, Barone V, Cimino P, Stendardo E, Catalanotti B, Persico M, Fattorusso C (2010) Insight into the mechanism of action of plakortins, simple 1,2-dioxane antimalarials. *Org Biomol Chem* 8:846–856
- Tanko JM, Friedline R, Suleman NK, Castagnoli N (2001) Tert-Butoxyl as a model for radicals in biological systems: caveat emptor. *J Am Chem Soc* 123:5808–5809
- Walsh JJ, Coughlan D, Heneghan N, Gaynor C, Bell A (2007) A novel artemisinin-quinine hybrid with potent antimalarial activity. *Bioorg Med Chem Lett* 17:3599–3602

- Wang DY, Wu YL (2000) A possible antimalarial action mode of qinghaosu (artemisinin) series compounds. Alkylation of reduced glutathione by C-centered primary radicals produced from antimalarial compound qinghaosu and 12-(2,4-dimethoxyphenyl)-12-deoxoqinghaosu. *Chem Commun* 22:2193–2194
- Wang J, Zhang CJ, Chia WN, Loh CC, Li Z, Lee YM, He Y, Yuan LX, Lim TK, Liu M, Liew CX, Lee YQ, Zhang J, Lu N, Lim CT, Hua ZC, Liu B, Shen HM, Tan KS, Lin Q (2015) Haem-activated promiscuous targeting of artemisinin in *Plasmodium falciparum*. *Nat Commun* 6:10111–10121
- Whaun JM, Brown ND (1985) Ornithine decarboxylase inhibition and the malaria-infected red cell: a model for polyamine metabolism and growth. *J Pharmacol Exp Ther* 233:507–511
- Wu YK, Wu ZY, Wu YL (1999) Interaction of qinghaosu (artemisinin) with cysteine sulfhydryl mediated by traces of non-heme iron. *Angew Chem Int Ed Engl* 38:2580–2582

Bluegenics: Bioactive Natural Products of Medicinal Relevance and Approaches to Their Diversification

Joseph S. Zarins-Tutt, Emily R. Abraham, Christopher S. Bailey
and Rebecca J.M. Goss

Abstract Nature provides a valuable resource of medicinally relevant compounds, with many antimicrobial and antitumor agents entering clinical trials being derived from natural products. The generation of analogues of these bioactive natural products is important in order to gain a greater understanding of structure activity relationships; probing the mechanism of action, as well as to optimise the natural product's bioactivity and bioavailability. This chapter critically examines different approaches to generating natural products and their analogues, exploring the way in which synthetic and biosynthetic approaches may be blended together to enable expeditious access to new designer natural products.

1 History of Natural Products in Medicine

For millennia, natural products have been utilised by humans for medicinal purposes, with some of the earliest examples documented being that of the ancient Egyptians, who would use honey to aid wound healing and opium-soaked cloths during surgical procedures (Simon et al. 2009; Brownstein 1993). Today, we are far more aware of the chemistry and biology that surround their use. For example, the antimicrobial activity of honey has been shown to be the result of peroxide activity (Irish et al. 2011) and the natural product morphine **1** has been isolated and characterised from the opium poppy *Papaver somniferum*. To this day, medicinal grade honey is utilised as a surgical dressing, whilst morphine and codeine are used extensively to control pain. It was not until the first half of the twentieth century that natural products from microbes came to the forefront of modern medicine, with the seminal discovery by Sir Alexander Fleming that the mould *Penicillium notatum* was able to produce compounds with antibiotic properties (Fleming 1945). In 1945 the structure of the bioactive compound was determined by Dorothy Hodgkin revealing a central beta-lactam motif, the warhead of the penicillins **2** (Robinson 1949).

J.S. Zarins-Tutt · E.R. Abraham · C.S. Bailey · R.J.M. Goss (✉)
School of Chemistry, University of St Andrews, St Andrews, Scotland, UK
e-mail: rjmg@st-andrews.ac.uk

Such early discoveries inspired the search for further medicinally useful natural products from both plants and microbes and resulted in the discovery of numerous compounds with a diverse array of chemical architectures and biological activities. Examples include antimicrobial compounds such as erythromycin **3**, daptomycin **4** and vancomycin **5**, the cholesterol lowering lovastatin **6**, the antiparasitic avermectin **8** and from plants the anticancer drug taxol **7** and the antimalarial artemisinin **9** (Fig. 1). The current and historical medicinal importance of natural products to society was acknowledged through the 2015 Nobel Prize in Physiology or Medicine being awarded for the discovery of avermectin **8** and artemisinin **9** (Egerton et al. 1979; Tu et al. 1981).

2 The Role of Natural Products in Nature

For many secondary metabolites it is unclear as to what function they have evolved for. For some compounds, it is clear that they have a role in defence. For instance, plants and bacteria may produce antimicrobial agents for protection against pathogens or as means of killing off their competition. Other molecules are used for signalling, for example in quorum sensing or as siderophores, chelating and uptaking metals, that are in limited abundance. However, the function for many natural products, if they indeed have one, remains unknown; whilst investment in the synthesis of natural products is energetically and resource costly for an organism, it provides an evolutionary advantage to have the ability to access diverse series of compounds and to rapidly modify the portfolio of compounds that are generated. It is also questionable as to whether the effects that we observe under an artificial laboratory environment are akin to those in nature. For example many compounds classified as antimicrobials in a laboratory environment may function purely as warning signals and not as the agents of death that their artificially high laboratory titres result in (Ratcliff and Denison 2011). Regardless of “evolution’s original intentions”, modern science has shown many of these molecules to function medicinally by binding specific protein targets and it has been suggested that ‘during evolution, there has existed a natural product ligand that could bind to all protein folds’ (Dixon et al. 2007). Despite being evolutionarily separated from many of the natural product producers, conserved protein folds may have therefore led to unintentional secondary function of natural products which we can exploit.

3 The Antibiotic Crisis and the Need for New Medicine

Antibiotics are chemical agents that are capable of inhibiting or perturbing bacterial growth. In order to exert a toxic effect, the chemical agent must prevent or interfere with cellular processes that are essential to the survival and proliferation of the bacterium. For this to be of medicinal use, there must be a high level of selectivity,

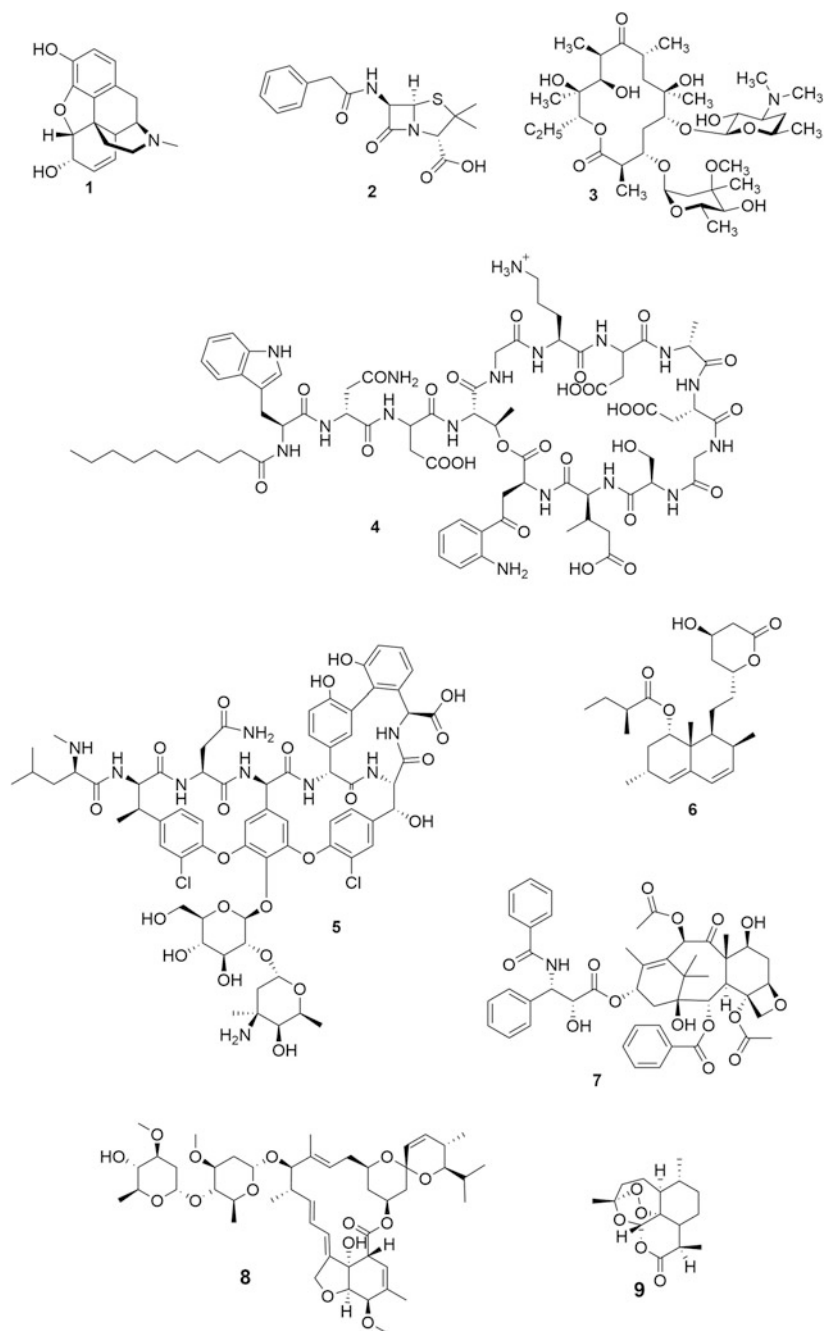


Fig. 1 Clinically relevant natural products: morphine **1**, penicillin G **2**, erythromycin **3**, daptomycin **4**, vancomycin **5**, lovastatin **6**, taxol **7**, Avermectin A1b **8** and artemisinin **9**

exploiting differences between the biochemistry of the bacterium and the host such that the bacterium is targeted but the animal host is not. There are six main targets: cell wall biosynthesis, protein synthesis, cell membrane integrity, RNA synthesis, folate synthesis and DNA synthesis and integrity; these are summarised in Fig. 2a. Antibiotic resistance is however a serious threat, resistance to antibiotics is observed alarmingly soon after a new antibiotic is introduced (Fig. 2b).

4 Antibiotic Resistance

Antibiotic resistance is by no means a new phenomenon, indeed, Fleming in his 1945 lecture (Fleming 1945) warned of the danger of resistance resulting from the inappropriate usage of antibiotics, by exposing bacteria to concentrations not sufficient to kill them to train them to be resistant. Antibiotic resistance has now been observed for all clinically used classes of antibiotics (Fig. 2b) and multidrug resistant (MDR) strains exist including strains that are resistant to all clinically available drugs—extreme drug resistance (EDR). The problem is exacerbated by the lack of new antibiotics with novel structures and new modes of action being introduced into the clinic. This means that there exist few alternatives for the treatment of resistant strains. The rise in antibiotic resistance has many causes, however, poor antibiotic stewardship has no doubt exacerbated the problem (Goossens et al. 2005).

Bacteria acquire resistance to antibiotics through a number of different pathways; these include proactive responses such as mutations in pre-existing genes to render antibiotic targets resistant (for example resistance to rifampicin through mutations in the RNA polymerase) (Srivastava et al. 2011; Ho et al. 2009; Floss and Yu 2005; Mariani and Maffioli 2009), horizontal gene transfer (HGT), where resistance genes are transferred between environmental species through transfection, conjugation or transformation, and physiological and behavioural changes such as biofilm formation in which the bacterial cells are protected by an extracellular polysaccharide matrix and metabolic dormancy enables persister cells to escape inhibition (Cantón 2009).

The majority of antibiotics in use are natural products, or derivatives of natural products, where the organisms generating them have an endemic resistance system built in so that their own survival is not compromised through the production of the antibiotic compound. As such, these resistance genes are already present in nature and can be transmitted between bacterial species. These genes include detoxifying enzymes, such as the beta lactamases which break down beta-lactam antibiotics through the hydrolysis of the beta-lactam ring, genes that encode the modification of the target so that the antibiotic can no longer bind effectively and genes responsible for the rapid export or efflux of the bioactive compound. Due to this widespread resistance, there is an urgent need for new antibiotics with novel structures that are not recognised by or susceptible to the most common and prevalent mechanisms of resistance and preferably compounds that inhibit clinically unexploited targets.

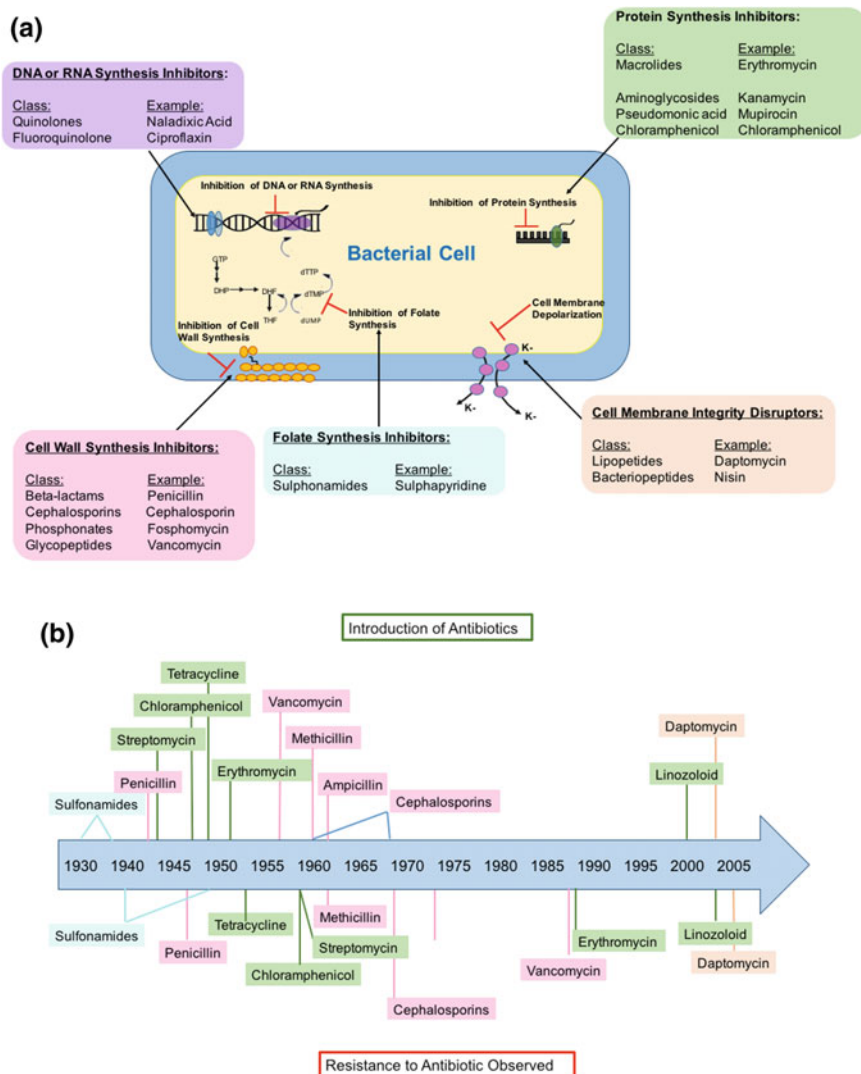


Fig. 2 Main antibiotic targets with clinical examples alongside a timeline highlighting when resistance to the clinical example was first observed. **a** The cartoon illustrates the main antibiotic targets and highlights classes of drugs which affect each bacterial target and clinical examples which belong to each class. Cartoon adapted from Clatworthy et al. (2007). **b** Timeline illustrating the introduction of antibiotics, (top) compared with when resistance to the antibiotic was first observed. The colours of the antibiotic correspond to the antibiotic’s target shown in Fig. 2a. Figure adapted from Clatworthy et al. (2007)

5 Natural Products and the Clinic. Towards New Antibiotics in the Battle Against Resistance

In the past three decades over 70% of antibiotics entering clinical trials have been based on natural products, compounds generated by organisms, in particular microbes (Van Lanen and Shen 2006). Strikingly, investment into exploration of streptomycetes, perhaps the most chemically characterised microbial genus to date, has resulted in the discovery of over two-thirds of all known antibiotics.

Whilst the direct use of a natural product only currently accounts for 6% of all currently clinically used medicines, a further 27 and 17% result from derivatisation of a natural product or the inclusion of a pharmacophore from a natural product respectively. This means a staggering 50% of medicines are based on natural products (Fig. 3), with further synthetic compounds designed to inhibit targets that have been revealed through the use of natural products (Newman and Cragg 2012).

Figure 4 displays an overview of the number of new antibiotics that have reached the clinic between 2000 and 2012 and highlights examples of synthetic and natural product derived molecules in phase III clinical trials, illustrating the importance of natural product research in this therapeutic arena. However, only a small proportion (0.5%) of antibiotic-producing microbes are currently cultivable in the lab, although innovative culturing methods have enabled success in antibiotic discovery with the recent identification of teixobatin from a previously uncultured microbe (Ling et al. 2015). The marine environment represents a rich source of biologically active compounds, with marine organisms accounting for approximately half of the earth's biodiversity. Though the marine microbiome has been

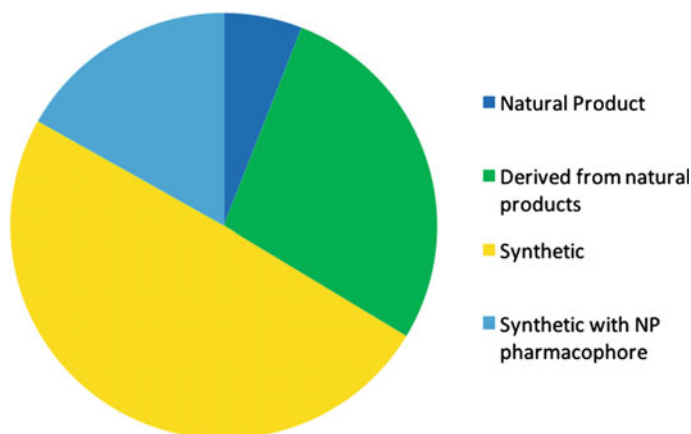


Fig. 3 Percentage and origin of all clinically used drugs. Adapted from Newman and Cragg (2012)

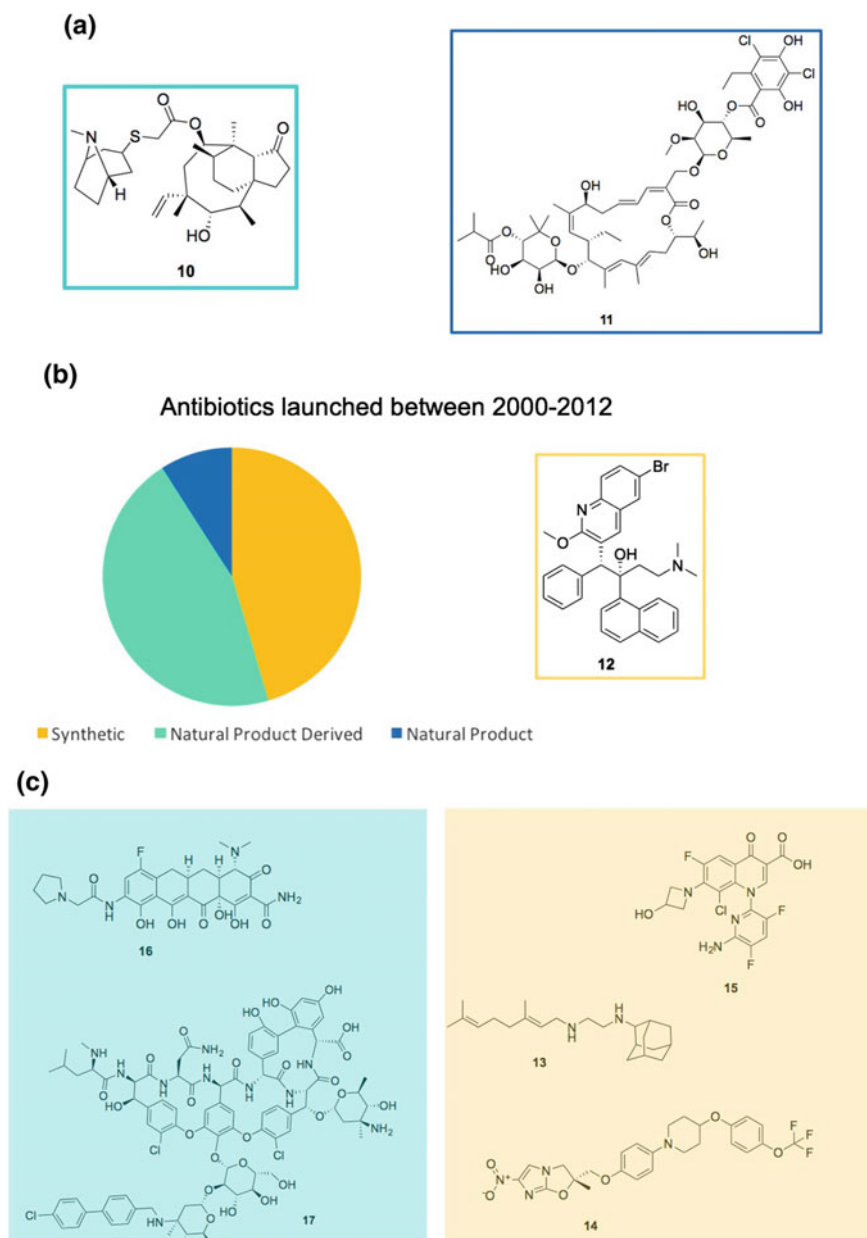


Fig. 4 An overview of the number of new antibiotics that have reached the clinic between 2000 and 2012 as well as an example of both synthetic and natural product derived molecules in phase III clinical trials, displaying the continued importance of natural products in this therapeutic arena. Included within these 22 new drugs, are three novel structural classes spanning both synthetic and natural product origins. **a** examples of new antibiotic classes launched for human use since 2000 including natural product derived retapamulin **10**, the natural product fidaxomicin **11**, and the synthetic bedaquiline **12**. **b** chart displaying the number of new antibiotics launched in the clinic between 2000 and 2012. **c** Example of synthetic compounds in phase III clinical trials SQ109 **13**, delamanid **14** and delafloxacin **15** and of natural product derived compounds in phase III trials eravacycline **16** and oritavancin **17**. Data obtained from Butler et al. (2013)

little explored for compound discovery, evidence indicates searches will be fruitful. In July 2014 a total of 7 marine-derived compounds had already received EU/FDA approval, with a further 25 in phase i–iii clinical trials. Studies thus far, have focussed predominantly on collection and examination of marine invertebrates, (such as sponges, and tunicates) rather than microbes, leaving this a largely unexplored resource. Marine microbes therefore represent an important discovery opportunity; in many of these systems the mutualistic microbes are suspected, and in some cases shown, to be the originators of the isolated bioactive compounds.

6 A Growing Focus on Marine Natural Products

There is a growing focus on natural products from the marine environment. New drug leads, with rich and novel chemical architectures, have been identified and include the novel antibacterial polyene marinomycin A **18**, the proteasome inhibitor salinosporamide A **19**, (Gulder and Moore 2010) and the cyclic peptide patellamide A **20** (Schmidt et al. 2005). A number of novel marine scaffolds, such as analogues of plinabulin **21**, plitidepsin **22** and bryostatin **23** (Mayer et al. 2010) have been progressed into clinical trials as anticancer agents (Fig. 5).

The oceans cover two-thirds of the earth's surface and provide a plethora of distinct environmental niches giving rise to huge diversity of species. In order to survive in these unique environments, many of the organisms have developed unique adaptations and relationships, which are reflected in the chemical diversity found in the oceans. Many marine tunicates have symbiotic relationships with a number of bacteria that are capable of producing highly toxic compounds (Donia et al. 2011). Furthermore, many marine-derived compounds are halogenated, due in part to the natural concentrations of bromine and chlorine (Gerwick and Moore 2012). With such chemical diversity, many of the clinically approved marine natural products can be deemed 'first in class' (Gerwick and Moore 2012). Currently, a total of seven marine or marine-derived natural products have been approved clinically, two of which are unmodified natural products (Gerwick and Moore 2012). These seven drugs span four therapeutic areas; anticancer; Yondelis[®] **24**, Cytosar-U[®] **25** and Halaven[®] **26**, antiviral, pain; Prialit[®] **27** and hypertriglyceridemia (Fig. 6) (Mayer et al. 2010; Gerwick and Moore 2012).

As described above, natural products have evolved for utility within their producing organisms, therefore it is essential to access analogues of natural products not only to determine the target of interaction and the way in which the natural

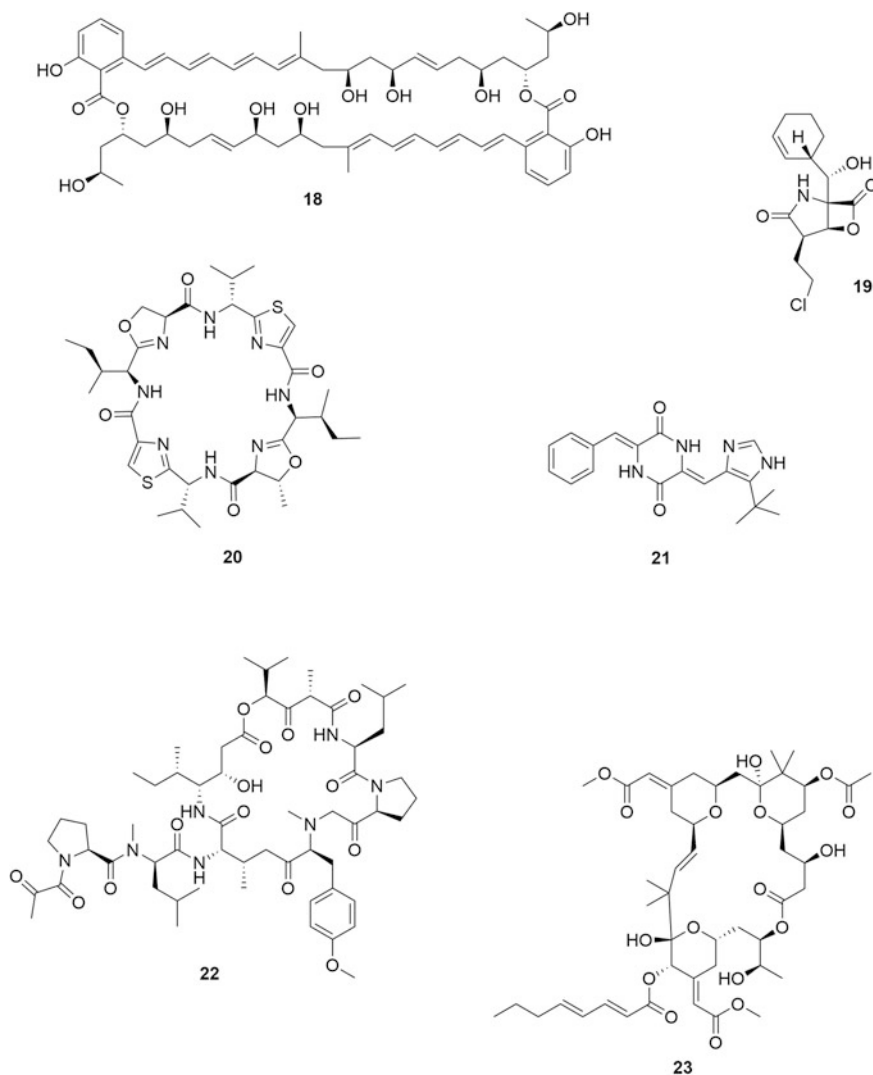


Fig. 5 Marine natural products. Marinomycin **18**, salinosporamide A **19**, patellamide A **20**, plinabulin **21**, plitidepsin **22**, bryostatin **23**

product interrelates with it at the molecular level, but also to generate materials with improved activities and oral bioavailability. *The remainder of this chapter looks particularly at approaches that may be utilised to enable access to series of analogues of natural products, with a particular focus on natural products with antibiotic activities.*

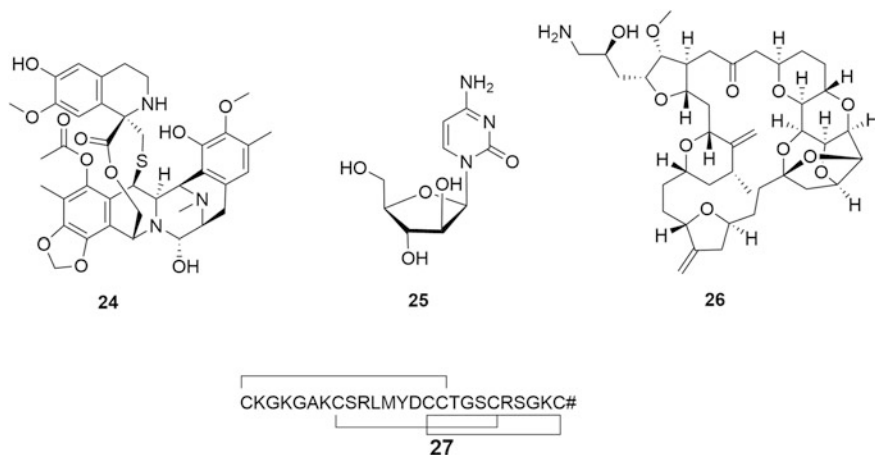


Fig. 6 Example of marine natural products in clinical use. trabectedin (Yondelis[®]) **24**, cytarabine (Cytosar-U[®]) **25**, eribulin (Halaven[®]) **26**, ziconotide (Prialt[®]) **27**

7 Generating Natural Product Analogues

Natural products are made by biomolecules and therefore naturally predisposed to interact with biomolecules, thus as discussed above, they make an excellent starting point for drug discovery. The ability to access series of natural product analogues is crucial in order to gain understanding as to the structure activity relationship of a natural product, investigate its precise interactions with its target at the molecular level and develop compounds with improved bioactivity as well as other desirable qualities such as good solubility, low toxicity, appropriate stability, and oral bioavailability. Due to the structural and chemical complexity of natural products they have in been perceived to be “unmedchemable”, and challenging to make analogues of. This viewpoint comes from focussing on the more traditional approaches to analogue generation, including semisynthesis and total synthesis (Fig. 7), however opportunities are being developed that utilise synthetic biology and synthetic chemistry combining the best of both worlds in order to more readily generate designer analogues of natural products.

Today, approaches to natural product analogue generation include semisynthesis (in which a natural product is directly chemically modified), total synthesis (chemically generating the compound de novo from simple readily abundant starting materials) and a variety of ways in which biosynthesis is harnessed.



Fig. 7 Image demonstrating drugs which are available for use, which have been derived from natural products. For example, simvastatin 6b is a semi synthetic derivate of the natural statin lovastatin 6, and is used to treat patients suffering from high cholesterol levels

7.1 Total Synthesis

Total synthesis and semisynthesis are the most traditional methods of accessing natural product analogues. Total synthesis is particularly useful in cases where the natural product is small and chemically simplistic, where the natural product is available in extremely limited quantities or not at all, or where the producing organism is not readily manipulated. Total synthesis also is regularly proven essential in the determination of the absolute structure of recently isolated natural products. With total synthesis, the approach is simply to synthesise the entire compound from inexpensive and readily available starting materials. Derivatives can be prepared by modifying either the reactants or the reactions used in each step of the synthesis. Whilst this approach still affords the greatest potential for accessing diverse analogues, the syntheses are often long, complex, inefficient, and give low yields. Furthermore, for particularly complex natural products, the initial synthetic route may be difficult to establish.

It is rare to be able to access more than a few milligrams of any one bioactive compound from certain marine organisms. Tunicates and sponges are far from simple to culture in laboratories making sustainable access to bioactive compounds isolated from such organisms challenging. For such systems total synthesis of the

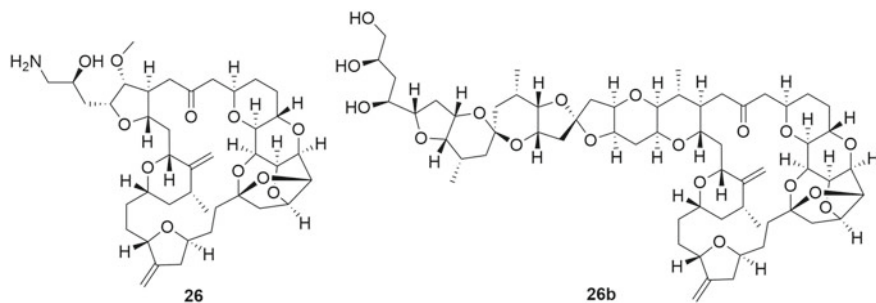
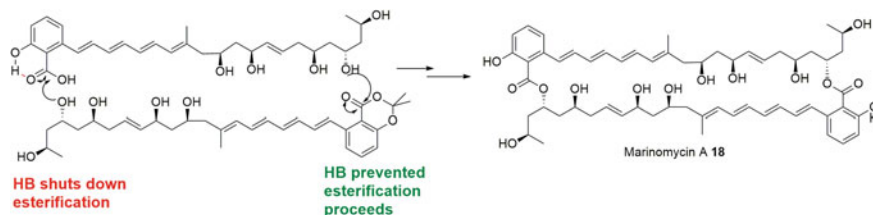


Fig. 8 Eribulin mesylate **26**, a derivative of halichondrin B **26b**, has stereogenic centres and is the most synthetically challenging drug to be generated by the pharmaceutical industry to date

parent compound and any analogues is often the only option. Eribulin mesylate **26** (Fig. 8), marketed by Esai Ltd. as Halaven is a polyketide macrocycle that has potent anticancer activity and is used in the treatment of breast cancer. Eribulin mesylate **26** is an analogue of the natural product halichondrin B **26b**, produced by the *Halichondria* genus of sponge. Total synthesis however, in 1998, revealed the active portion of the molecule, this allowed for simpler structural analogues be developed. This ultimately resulted in the delivery of eribulin **26** to the clinic (Yu et al. 2011). This structurally elaborate natural product analogue is accessed through an impressive total synthesis. Halaven **26** is considerably more structurally complex than other marketed pharmaceutical that has been accessed through total synthesis and represents a step change demonstrating the enhanced skill and determination of the pharmaceutical industry in order to access this important anticancer agent in scale. It is noteworthy that investment in the industrial total synthesis of a drug that attracts significant revenue, such as anticancer agents, due to the need of the patient to take it for long periods is viable. However, the revenue from the sales of antibiotics, which are typically administered as short, one to two week courses are currently considerably less. Complex syntheses of antibiotics are not currently a viable option for industry.

Marinomycin **18**, a polyene of polyketide origin, was isolated from the marine actinomycete *Marinospora* CNQ-140 by Fenical (Kwon et al. 2006) and showed excellent antibiotic activity (0.1–0.6 μM) against methicillin-resistant *Staphylococcus aureus* (MRSA) and vancomycin-resistant *Enterococcus faecium* (VREF) as well as promising and selective activity against a variety of cell lines associated with skin cancer. A key drawback of this potentially promising, new structural class of antibiotic is its high propensity to photoisomerise (Kwon et al. 2006). Nevertheless, the compound produced in low titre by the microbe (0.5–2 mg/L) (Kwon et al. 2006) has attracted significant attention as a target for total synthesis with the compound initially being synthesized by Nicolaou et al. (2007). Evans and his team were elegantly able to assemble the challenging dimeric compound demonstrating the selective deactivation and activation of a salicylate



Scheme 1 Marinomycin **18** and its curious salicylate switching mechanism

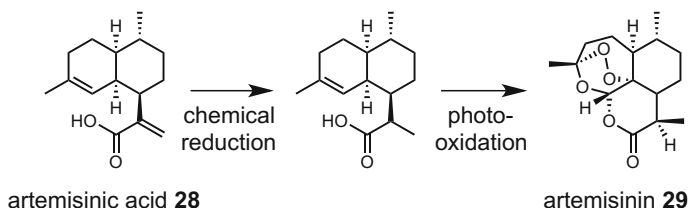
moiety, through the formation of a short strong hydrogen bond, to esterification—a switching mechanism that perhaps operates naturally in controlling the macrolactonisation of the two dimers (Scheme 1) (Evans et al. 2012). Semisynthetic studies around marinomycin **18** to generate the diacetonide and hexa-acetate derivatives both resulted in slightly reduced antibiotic activity (Kwon et al. 2006).

7.2 Semisynthesis

Semisynthesis is the direct chemical derivitisation of an extracted and isolated natural product. The nature of chemical derivitisation possible and the regio-chemistry of the diversification is dictated by the chemical reactivity of the natural product and in particular the presence of reactive and chemically orthogonal functional groups. It also can be utilised to convert an abundant natural product into a desired compound that is naturally in short supply. Trabectedin **24**, for example was originally isolated from the marine tunicate *Ecteinascidia turbinata* at a yield of 0.0001% (Cuevas and Francesch 2009). As such it required a semisynthetic routes from the structurally similar cyanosfracin B (Cuevas and Francesch 2009).

A further example of the application of semisynthesis, relating to the supply of the desired natural product, is the generation of the antimalarial drug artemisinin **9** from artemisinic acid **28** (Ro et al. 2006). Artemisinin **9** is generated by the plant *Artemisia annua* (sweet wormwood) which takes eight months to reach maturity. Though much of the artemisinin **9** used clinically is extracted directly from plants alternative and sustainable approaches to access the compound are sought. The total synthesis for this compound has been established, but using this approach it is not possible to produce sufficient quantities for the clinic (Kennedy 2008). Instead, artemisinic acid **28** is extracted from an extensively engineered strain of *Saccharomyces cerevisiae*, and modified in two steps to artemisinin **9** (Scheme 2) (Kennedy 2008). Using this method, artemisinin **9** can be produced in sufficient quantities to meet the demand for this drug, and cheaply enough to be accessible to the developing world (Kennedy 2008).

There are a number of considerations when using this approach. First, there must be sufficient amounts of the natural product to use as a reactant. Second, there are often many similar functional groups in natural products and so selectively reacting



Scheme 2 Artemisinic acid **28**, available from the fermentative culture of *S. cerevisiae*, then chemically modified to artemisinin **9** (Kennedy 2008)

only certain ones requires either highly specific reactions or the extensive use of protecting groups. Third, the possible modifications are limited by the molecule itself; the stability of the molecule towards certain reagents and the presence or absence of certain groups may prevent or hinder certain modifications.

Extension and modification of the pharmaceutical scaffold is a common strategy employed to combat drug resistance. By changing the drug scaffold, it may no longer be recognised as a substrate by the enzyme involved in drug resistance. This is also for true for resistance mechanisms which modify the drug target as opposed to the drug itself. This is because extension of drug scaffolds can change physical as well as chemical properties such as lipophylicity, electronegativity and sterics, all of which control binding and recognition.

Penicillin **2**, whose serendipitous discovery is attributed to Fleming, a β -lactam antibiotic produced by the fungus *Penicillium notatum*, acts by inhibiting bacterial cell wall biosynthesis. Specifically, it prevents the natural cell wall rigidification that is enabled by the cross-linking of the constituent peptidoglycan chains. Peptidoglycan is a key component in bacterial cell walls, providing much of the strength and rigidity. It is composed of a β -1,4-linked glycan backbone of alternating *N*-acetylglucosamine (GlcNAc) and *N*-acetylmuramic acid (MurNAc) units. Pendant pentapeptide chains are attached to the 3-position of each muramic acid with the terminal residues being D-Ala-D-Ala; neighbouring this motif are either L-lysine or *meso*-diaminopimelic acid (DAP) residues. Cross-linking of these residues by amide bond formation serves to rigidify the polymer. The introduction of penicillin **2** into the clinic in 1943 was soon followed by the rapid emergence of wide spread resistance due to the spread of β -lactamase activity. To overcome this resistance, semisynthetic analogues were developed.

The macrolides are a series of antibiotics that include erythromycin **3**, from the actinomycete *Saccharopolyspora erythraea* and inhibit protein synthesis. Drug resistance mechanisms against erythromycin include *ermB*, a *N*-6-methyltransferase that modifies the adenine base of adenosine 2058 in 23S rRNA thereby enabling translation and protein synthesis to occur in the presence of erythromycin **3** and *mefA*, an efflux pump (Roberts et al. 1999). These resistance mechanisms are found to be inducible rather than constitutive.

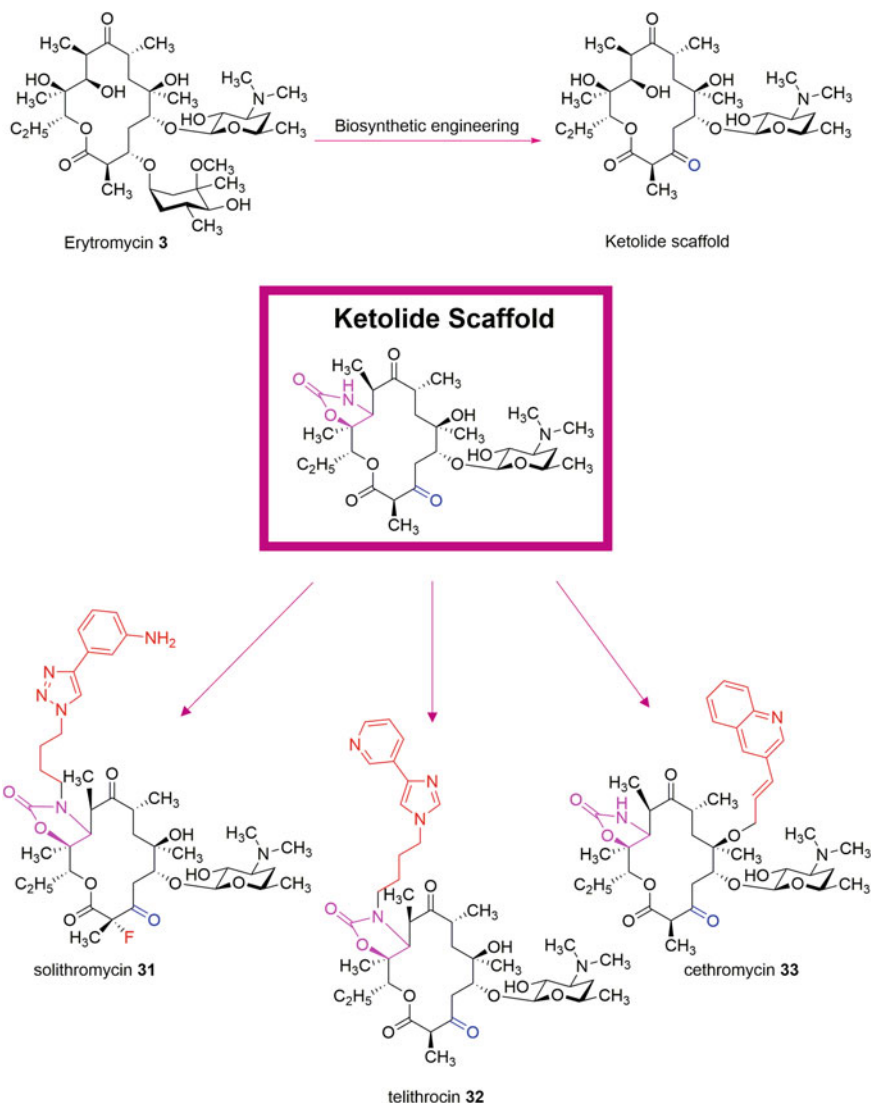
The ketolides are an important example of clinically successful extended scaffolds accessed by semisynthesis (as well as biosynthetic engineering). Whilst the

polyketide core of erythromycin **3** is elaborated by post PKS glycosylation with both a D-desosamine and L-cladinose sugar, in the ketolides the L-cladinose sugar moiety is absent and replaced by a ketone (as found naturally in the antibiotic pikromycin **29**). A semisynthetic preparation of the ketolide scaffold is achieved through selective cleavage of the L-cladinose followed by oxidation (Zhan et al. 2002). Access to 5-*O*-desosaminyl erythronolide A **30** through biosynthetic engineering provides a precursor that may simply be oxidized to the ketolide (Zhan et al. 2002). The ketolide analogues lacking the L-cladinose do not induce resistance (Zhan et al. 2002). Whilst the lack of the L-cladinose results in poorer binding to the ribosome, this can be more than compensated for by the semisynthetic addition of an 11,12 carbamate extension. Further semisynthetic extension of the scaffold results in the drugs solithromycin **31**, telithromycin **32** and cethromycin **33** (Scheme 3). The ketolides remain biologically active in strains expressing efflux pumps, perhaps due to their higher binding affinity to their target, and an ability to bind to methylated ribosomes (Capobianco et al. 2000).

Vancomycin **5**, generated by the bacterium *Amycolatopsis orientalis*, is often referred to as the antibiotic of last resort. It has been used in the treatment of Gram-positive bacterial infections including methicillin-resistant *S. aureus* for 6 decades, however in recent times its potency has been observed to have reduced and vancomycin-resistant *Enterococci* and *S. aureus* strains have emerged (Courvalin 2006). The generation synthetic and semisynthetic analogues of vancomycin **5** are sought to combat resistant strains (Nakama et al. 2010; Xie et al. 2011). Vancomycin **5** prevents cross-linking by forming 5 hydrogen bonds to D-Ala-D-Ala to overcome this resistant strains have evolved in which replacement of D-Ala-D-Ala with D-Ala-D-Lac reduces hydrogen bonding to vancomycin **5** (Pinchman and Boger 2013). Analogues capable of killing vancomycin-resistant strains are being sought. Recent work in this area includes the Boger lab's work on vancomycin aglycone converting the chloride to a boronic acid giving rise to a variety of function groups via cross-coupling modification (Fig. 9) (Pinchman and Boger 2013).

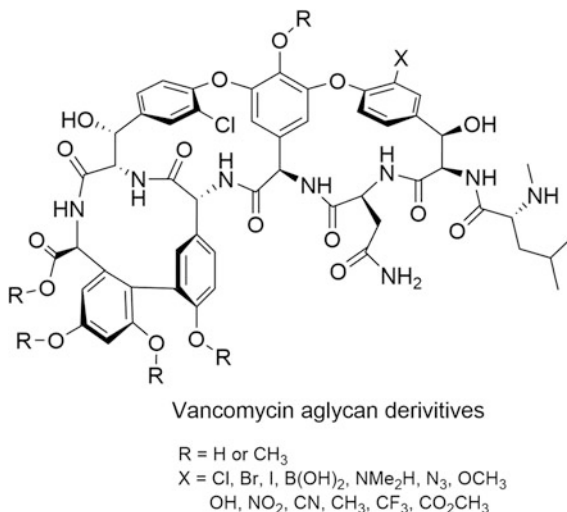
Complementary to this research, Miller has recently been taking semisynthesis in an exciting new direction utilising peptides, as catalysts, to control the site selective halogenation of the vancomycin **5** and the related glycopeptide antibiotic teicoplanin (Pathak and Miller 2012, 2013). Basing the design of the peptide agent on the vancomycin-binding site, regioselective halogenation has been achieved (Pathak and Miller 2012). Using screened peptide libraries, new semisynthetic routes utilising regiocontrolled halogenation of benzamides (Barrett and Miller 2013) and epoxidation of various isoprenols have been explored (Lichter and Miller 2012). Recently, the groups have developed this approach to enable selective late stage epoxidation of series of compounds (Abascal et al. 2014).

Semisynthesis may also be used to modify potency and reduce toxicity, for example dolastatin, a peptide from the mollusc *Dolabella auricularia*, though likely to be of cyanobacterial origin, proved too potent to be used as a single agent. As such a synthetic analogue was developed called monomethyl auristatin E and is linked to a monoclonal antibody to be only the second antibody drug conjugate in clinical use (Schrama et al. 2006).



Scheme 3 Scaffold Extension. Semisynthetic ketolides can be accessed from the through the removal of the cladinose sugar of erythromycin **3** and oxidation to the ketode (*blue*). A cyclic carbonate is also added synthetically (*magenta*). Further synthetic elaboration of the scaffold (*red*) produces series of active compounds

Fig. 9 Derivatives of the vancomycin aglycon E-ring aryl chloride to determine its effect on D-Ala-D-Ala binding and antimicrobial activity (Kwon et al. 2006)



7.3 Precursor-Directed Biosynthesis

Precursor-directed biosynthesis provides perhaps the least technologically demanding approach for harnessing a biosynthetic pathway to the natural product of interest, and takes advantage of the inherently flexible nature of many biosynthetic enzymes. If the biogenic assembly of the natural product is understood, analogues of the precursors may be designed, synthesised and administered to the producing organism. In other words, alternative biosynthetic building blocks may be supplied for the organism to utilise in the construction of a new to nature natural product. For multifunctional enzymes such as polyketide synthases and nonribosomal peptide synthetases the loading module at the beginning of the assembly process, which uploads and processes the first biosynthetic precursor, named the “starter unit” tends to be particularly flexible and able to tolerate a range of substrates. Scoping studies to explore the key components that are required within the precursor and investigate the extent of flexibility of the pathway are often useful. One example of a natural product with a strikingly flexible pathway is the uridyl peptide antibiotic pacidamycins **34** which is able to incorporate methylated and halogenated amino acids at high level into both the N and C termini (Grüschow et al. 2009; Ragab et al. 2010). Through scoping studies the flexibility for tolerance of bulky groups present at the 2 or 7 position of the indole ring is particularly apparent (Fig. 10).

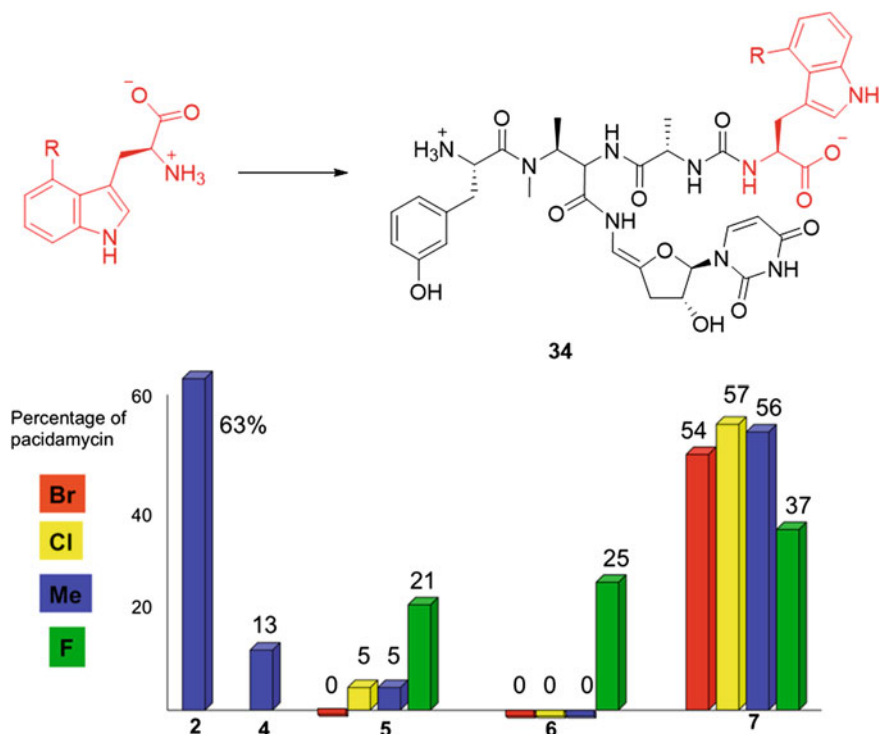


Fig. 10 Precursor-directed biosynthesis to yield analogues of pacidamycins **34**. Tolerance for tryptophans substituted at the 2 and 7 positions of the indole ring is particularly apparent (Grüschow et al. 2009)

7.4 Mutasynthesis

Mutasynthesis is a variation on precursor biosynthesis in which the organism is first engineered to either:

- (i) Have extended substrate flexibility, as for example in the generation of the fluorinated erythromycin analogue (Goss and Hong 2005).

Or

- (ii) Not be able to generate the natural starting material and so only be able to produce the compound of interest or its analogues if its media is supplemented with a suitable biosynthetic precursor.

Using the former approach, utilised to explore the generation of modified analogues of erythromycin **3** by *Saccharopolyspora erythraea*, a series of fluorinated precursor analogues were administered to the wild type strain and a strain engineered to incorporate the more flexible loading module from avermectin biosynthesis. Whilst the pathway in the wild type organism was unable to process extended fatty



Fig. 11 Exploration of utilisation of alternative biosynthetic precursors/building blocks by both wild type and engineered microorganisms

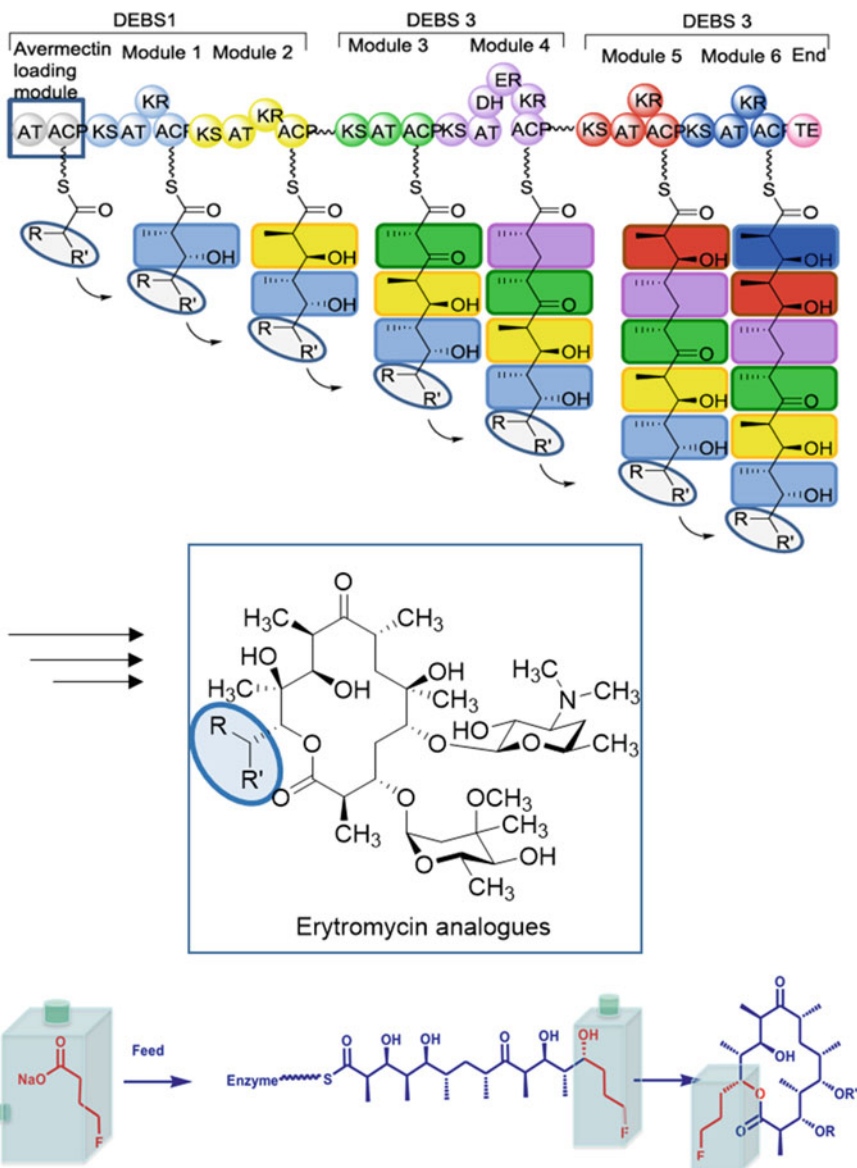
acids, the engineered strain enabled their incorporation into fully functionalised erythromycin analogues (Fig. 11) (Goss and Hong 2005; Marden et al. 1998).

The second approach has been applied to many systems including the generation of epothilone analogues and access to analogues of rapamycin **35** (Grüschow et al. 2009; Gregory et al. 2005; Goss et al. 2006) (Fig. 11 and Schemes 4 and 5).

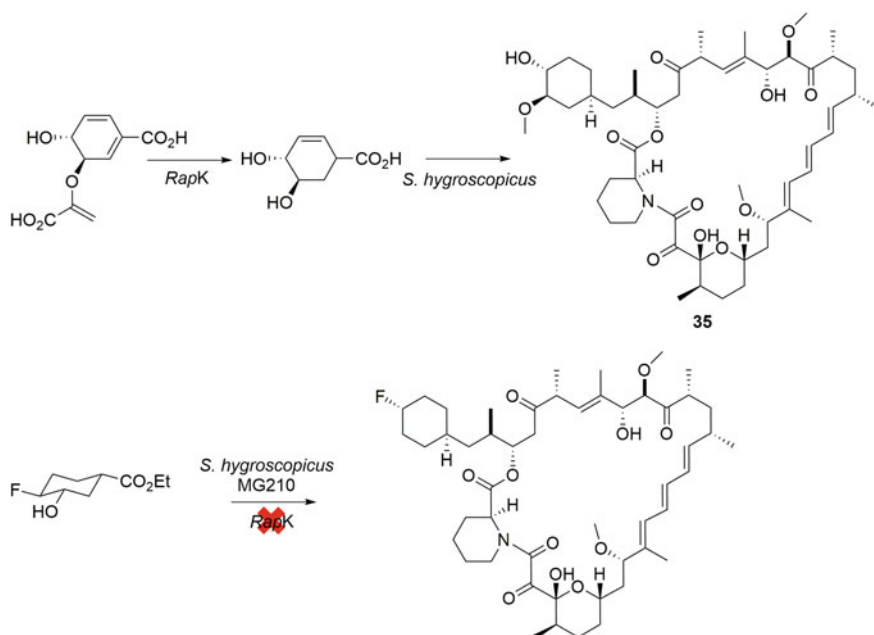
The fact that the organism is rendered incapable of suitable biosynthetic precursor analogue is particularly attractive. In precursor-directed biosynthesis the analogue is produced alongside the parent molecule and purification of the novel and desired compound that is generated can prove challenging. In this second approach to mutasynthesis, conveniently only the analogue and not the parent molecule may be fermentatively accessed, and purification of the desired new to nature compound is simplified. In the case of rapamycin **35** the generation of the dihydroxylated cyclohexenoic acid starter unit is catalysed by RapK which mediates the loss of pyruvate from chorismate. Mutants deficient in RapK can be utilised to enable selective access to series of analogues with modified starter units (Gregory et al. 2005). Initial scoping experiments reveal that only precursor analogues in which there is a hydrogen bond acceptor within the cyclohexane ring are tolerated (Goss et al. 2006). This information enabled the design of fluorohydrins which could be synthesised, fed and incorporated into the natural product (Ragab et al. 2010).

7.5 Combinatorial Biosynthesis

Combinatorial biosynthesis describes the ambition to be able to utilise enzymatic components from various different biosynthetic pathways in a combinatorial fashion, mixing and matching genetic elements encoding enzymes and creating designer biosynthetic pathways at will. Before the dream of combinatorial biosynthesis in its fullest sense can be realised, there is a long way to go in terms of understanding multifunctional enzyme structures, how these enzymes interact and passage intermediates, and how their substrate specificity of individual domains as well as entire systems may be reprogrammed. So far combinatorial biosynthesis has been used to achieve ring contraction (Thomas et al. 2002; Wu et al. 2000, 2002) or



Scheme 4 a Mutasynthetic access to analogues of erythromycin **3**. The flexibility of the multifunctional enzyme is extended through the incorporation of the loading module from avermectin biosynthesis. *AT* acyltransferase, *ACP* acyl carrier protein, *KS* ketosynthase, *KR* ketoreductase, *DH* dehydratase, *ER* enoyl reductase, *TE* thioesterase. **b** This system may be used to access fluorinated analogues of erythromycin **3** (Goss and Hong 2005)



Scheme 5 Utilising mutasynthesis to generate analogues of rapamycin **35**

ring expansion (Kao et al. 1997), modification of the stereochemistry of moieties within polyketide synthases (Caffrey 2005) to alter glycosylation patterns (Shepherd et al. 2011; Pérez et al. 2008) and to generate new to nature halogenated metabolites (Heide et al. 2008; O'Connor 2012; Roy et al. 2010). The Goss group have been developing such studies during the Bluegenics programme. Recent example in this area being the impressive engineering of the fluorinase into the DEBS1-TE system (Walker et al. 2013).

One of the earliest examples of the combining of gene clusters or the introduction of a gene with a desired function into another cluster in order to transform a natural product in a desired way was the engineering of a bacterial strain by Omura et al. (Omura et al. 1986). This engineered strain produced the novel polyketide antibiotic mederrhodin **36**, a hybrid antibiotic produced by introducing the actinorhodin gene cluster heterologously into the medermycin producer (Omura et al. 1986). As part of this work, a plasmid containing part of or the entire actinorhodin gene cluster were introduced into the medermycin producing *Streptomyces* sp. strain *AM7161* and ex-conjugants were screened for the production of novel secondary metabolites. Two new secondary metabolites were isolated, mederrhodin A **36a** and mederrhodin B **36b** (Fig. 12). Mederrhodin A **36a** showed similar gram negative antibacterial activity to medermycin **37** but mederrhodin B **36b** showed no activity against all Gram-positive and Gram-negative bacteria tested.

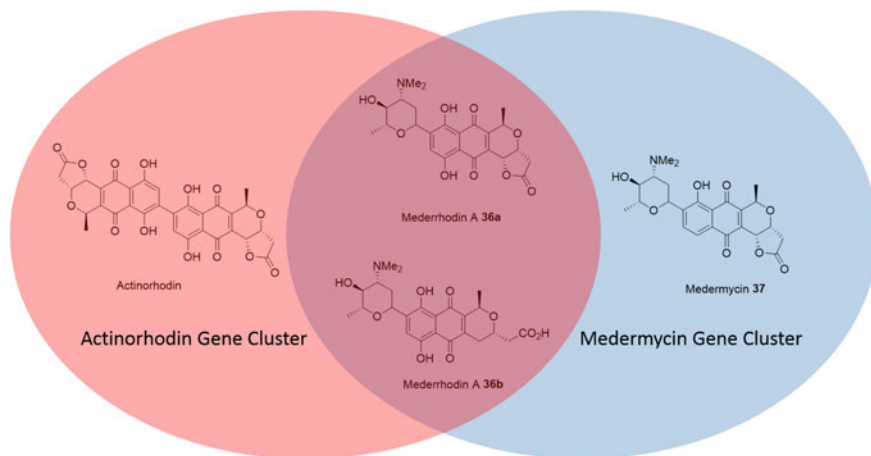


Fig. 12 Introduction of the actinorhodin gene cluster into the medermycin producer in a combinatorial biosynthesis approach yields the new antibiotics mederrhodin A **36a** and mederrhodin B **36b** (Omura et al. 1986)

Daptomycin **4** is a cyclolipopeptide used clinically for the treatment of skin infections caused by Gram-positive pathogens, bacteremia and endocarditis. Baltz and co-workers have generated analogues of daptomycin **4** by the exchange of single or multiple modules of the DptBC subunit of the NRPS and inactivation of a tailoring enzyme glutamic acid 3-methyltransferase from the producing organism *Streptomyces roseosporus*. Using this approach Baltz and co-workers were able to generate analogues with similar or better activities (Nguyen et al. 2006).

7.6 Genochemetics: gene expression enabling synthetic diversification

Genochemetics is a novel approach to the diversification of natural products. Described as ‘gene expression enabling synthetic diversification (Roy et al. 2010), genochemetics uses molecular biological pathway engineering to add in a chemically orthogonal handle into a natural product that may be selectively modified using synthetic organic chemistry.

Genochemetics can be considered blending together complementary tools from combinatorial biosynthesis and semisynthesis. In genochemetics, an enzyme from an unrelated biosynthetic pathway that is capable of introducing a reactive, chemically orthogonal, and selectively functionalisable handle into a natural product of interest is genetically introduced into the producing organism. The system is designed such that the gene encoding the enzyme is expressed to enable the enzyme to be produced such that it acts in concert with the native biosynthetic machinery to

generate a modified, un-natural product—sometimes alongside the unmodified natural product. The presence of the reactive and chemically orthogonal handle enables subsequent chemical derivatisation to be performed selectively on the unnatural product, ideally as a component of the crude extracts and without need for prior purification or the use of protecting group chemistry.

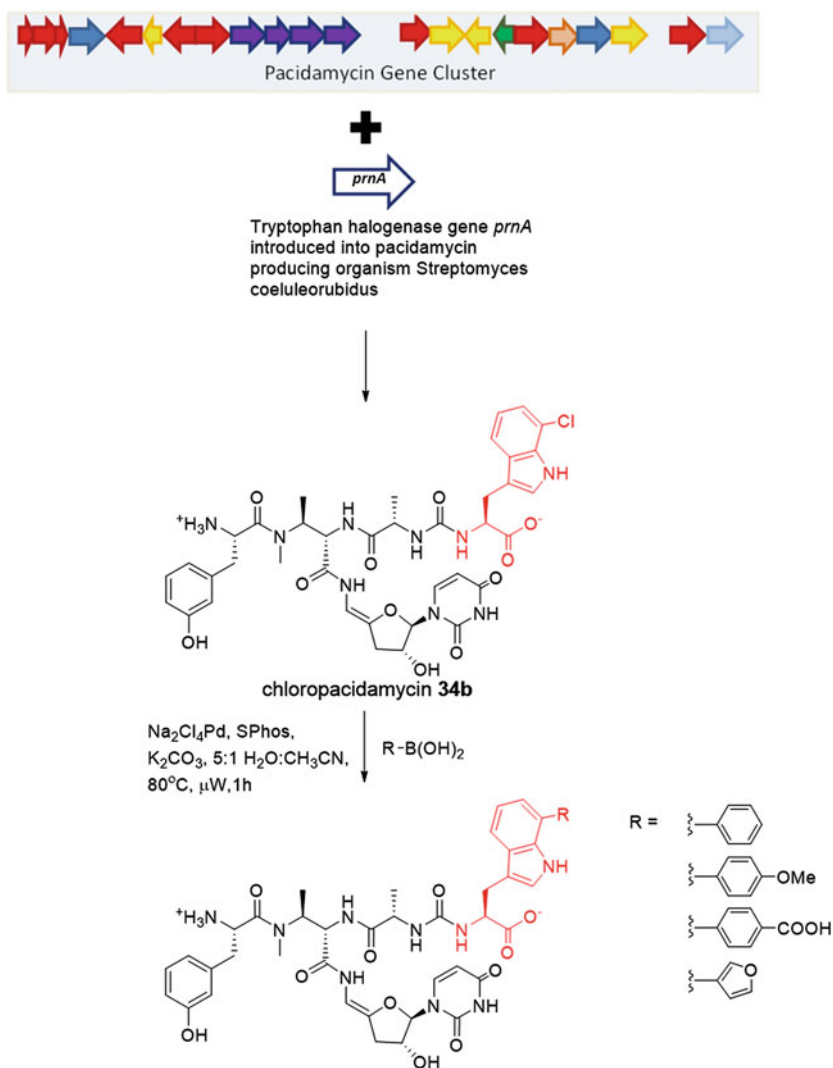
To facilitate the genochemetic approach to natural product diversification, handles must be enzymatically installable and should enable facile and selective chemistry (such as cross-coupling or click chemistries). Series of genetically installable handles are required and new mild chemistries that enable the selective modification of the new functionalised natural products. During the course of the Bluegenics programme, the Goss group have been particularly looking at new halogenases that might be developed and utilised within the genochemetic portfolio, investigating the stability of these natural and engineered compounds and developing new chemistries for the selective modification of halogenated natural and unnatural products.

The first example of genochemetic access to natural product analogues was demonstrated by the Goss group in 2010 (Scheme 6) using the uridyl peptide antibiotic pacidamycin **34** as the test bed (Roy et al. 2010). The aim was to biosynthetically introduce a carbon–halide bond, which could subsequently be modified using cross-coupling chemistries. The halotryptophan motif is found in several natural products, such as rebeccamycin **38** and pyrrolnitrin **39** (Fig. 13), and tryptophan halogenases have been widely studied (Smith et al. 2013). PrnA is responsible for the chlorination of tryptophan at the 7-position, which is the first step in pyrrolnitrin biosynthesis (Dong et al. 2005). The *prnA* gene was incorporated into the genome of the Pacidamycin producer *Streptomyces coeruleorubidus* under the control of the constitutive promoter *ermE**. This allowed production of the halogenase alongside the pacidamycin biosynthetic machinery, and resulted in *in vivo* generation of chlorinated pacidamycin **34b** (Scheme 6) (Roy et al. 2010).

The group developed this example of combinatorial biosynthesis into a full genochemetic system by exploiting the selective reactivity of the newly introduced halogen through aqueous, palladium-catalysed Suzuki-Miyaura cross-coupling chemistry under microwave irradiation, utilising a sulfonated form of the SPhos ligand developed by Buchwald et al. (Barder et al. 2005).

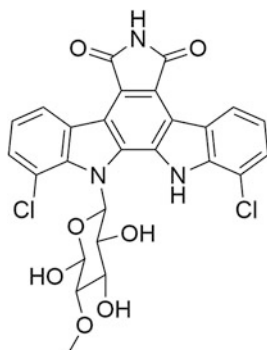
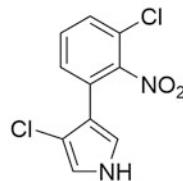
The conversion could be performed on the crude extracts of fermentation cultures without need for purification beforehand. Using a series of 5 boronic acids, pacidamycin analogues were produced and identified by LCMS/MS fragmentation patterns, in yields ranging from 33% to in excess of 95%. Two of these analogues, the phenyl and the *p*-methoxyphenyl substituted derivatives, were isolated in 52% and 67% respectively (Fig. 13) (Roy et al. 2010).

Recent work from the O'Connor group has presented the second example of genochemetic natural product analogue generation, this time in *Catharanthus roseus* as a development of their previous studies of the indole alkaloid metabolites of this plant (*vide supra*). The group employed cross-coupling chemistry similar to that previously used by the Goss group in order to functionalise halogenated metabolites generated both by precursor-directed biosynthesis and by combinatorial



Scheme 6 Integration of the tryptophan halogenase gene *prnA* into the pacidamycin **34** producer *Streptomyces coeluleorubidus* gave access to halogenated pacidamycin analogues which could be further functionalized as part of a genochematic approach using Suzuki-Miyaura cross-coupling chemistries, in aqueous solvents and under mild conditions (Roy et al. 2010)

Fig. 13 Antibiotics such as rebeccamycin **38** and pyrrolnitrin **39** contain halogens derived from the flavin-dependent tryptophan halogenases RebH and PrnA. These enzymes can be introduced into other biosynthetic systems to generate halotryptophans *in vivo*

Rebeccamycin **38**Pyrrolnitrin **39**

biosynthesis, with the latter giving the first eukaryotic genochemetic system (Roy et al. 2010; Runguphan and O'Connor 2013).

8 Concluding Remarks and Future Perspective

The marine environment holds much potential as a largely underexplored source of new compounds for human medicine. There is an urgent need to discover and develop new antibiotics with new scaffolds and modes of action, by carefully trawling the oceans new compounds to combat this crisis may be found. To fully exploit this potential new tools for the discovery of bioactive compounds are required as well as new approaches to finding, culturing and manipulating marine organisms and their biosynthetic pathways. By dovetailing biosynthetic and synthetic approaches analogues with designer properties may be accessed.

References

- Abascal NC, Lichtor PA, Giuliano M, Miller SJ (2014) Function-oriented investigations of a peptide-based catalyst that mediates enantioselective allylic alcohol epoxidation. *Chem Sci* 5:4504–4511
- Barder TE, Walker SD, Martinelli JF, Buchwald SL (2005) Catalysts for Suzuki–Miyaura coupling processes: scope and studies of the effect of ligand structure. *J Am Chem Soc* 127:4685–4696
- Barrett KT, Miller SJ (2013) Enantioselective synthesis of atropisomeric benzamides through peptide-catalyzed bromination. *J Am Chem Soc* 135:2963–2966
- Brownstein MJ (1993) A brief history of opiates, opioid peptides, and opioid receptors. *Proc Natl Acad Sci USA* 90:5391–5393
- Butler MS, Blaskovich MA, Cooper MA (2013) Antibiotics in the clinical pipeline in 2013. *J Antibiot (Tokyo)* 66:571–591

- Caffrey P (2005) The stereochemistry of ketoreduction. *Chem Biol* 12:1060–1062
- Cantón R (2009) Antibiotic resistance genes from the environment: a perspective through newly identified antibiotic resistance mechanisms in the clinical setting. *Clin Microbiol Infect* 15 (Suppl 1):20–25
- Capobianco JO, Cao Z, Shortridge VD, Ma Z, Flamm RK, Zhong P (2000) Studies of the novel ketolide abt-773: transport, binding to ribosomes, and inhibition of protein synthesis in *Streptococcus pneumoniae*. *Antimicrob Agents Chemother* 44:1562–1567
- Clatworthy AE, Pierson E, Hung DT (2007) Targeting virulence: a new paradigm for antimicrobial therapy. *Nat Chem Biol* 3:541–548
- Courvalin P (2006) Vancomycin resistance in gram-positive cocci. *Clin Infect Dis* 42:S25–S34
- Cuevas C, Francesch A (2009) Development of Yondelis® (Trabectedin, ET-743). a semisynthetic process solves the supply problem. *Nat Prod Rep* 26:322–337
- Dixon N, Wong LS, Geerlings TH, Micklefield J (2007) Cellular targets of natural products. *Nat Prod Rep* 24:1288–1310
- Dong C, Flecks S, Unversucht S, Haupt C, van Pee KH, Naismith JH (2005) Tryptophan 7-Halogenase (PmA) structure suggests a mechanism for regioselective chlorination. *Science* 309:2216–2219
- Donia MS, Fricke WF, Partensky F, Cox J, Elshahawi SI, White JR, Phillippy AM, Schatz MC, Piel J, Haygood MG, Ravel J, Schmidt EW (2011) Complex microbiome underlying secondary and primary metabolism in the tunicate-prochloron symbiosis. *Proc Natl Acad Sci USA* 108: E1423–E1432
- Egerton JR, Ostlind DA, Blair LS, Eary CH, Suhayda D, Cifelli S, Riek RF, Campbell WC (1979) Avermectins, new family of potent anthelmintic agents: efficacy of the b1a component. *Antimicrob Agents Chemother* 15:372–378
- Evans PA, Huang M-H, Lawler MJ, Maroto S (2012) Total synthesis of Marinomycin A using salicylate as a molecular switch to mediate dimerization. *Nat Chem* 4:680–684
1. Fleming S (1945) A nobel lecture. *Nobel Lect Physiol Med 1942–1962*(1945):83–93
- Fleming A (1980) Classics in infectious diseases: on the antibacterial action of cultures of a *Penicillium*, with special reference to their use in the isolation of *B. influenzae* by Alexander Fleming. Reprinted from the *British Journal of Experimental Pathology* 10:226–236. *Rev Infect Dis* 2 (1):129–139
- Floss HG, Yu TW (2005) Rifamycin-mode of action, resistance, and biosynthesis. *Chem Rev* 105:621–632
- Gerwick WH, Moore BS (2012) Lessons from the past and charting the future of marine natural products drug discovery and chemical biology. *Chem Biol* 19:85–98
- Goossens H, Ferech M, Vander Stichele R, Elseviers M (2005) Outpatient antibiotic use in Europe and association with resistance: a cross-national database study. *Lancet* 365:579–587
- Goss RJM, Hong H (2005) A novel fluorinated erythromycin antibiotic. *Chem. Commun. (Camb)* 3983–3985
- Goss RJM, Lanceron SE, Wise NJ, Moss SJ (2006) Rapamycin: requirement for hydroxylation of the cyclohexane ring of starter acids prior to incorporation. *Org Biomol Chem* 22:4071–4073
- Gregory MA, Petkovik H, Lill RE, Moss SJ, Wilkinson B, Gaisser S, Leadlay PF, Sheridan RM (2005) Mutasynthesis of rapamycin analogues through the manipulation of a gene governing starter unit biosynthesis. *Angew Chem Int Ed Engl* 44:4757–4760
- Grüschow S, Rackham EJ, Elkins B, Newill PLA, Hill LM, Goss RJM (2009) New pacidamycin antibiotics through precursor-directed biosynthesis. *Chem Bio Chem* 10:355–360
- Gulder TAM, Moore BS (2010) Salinosporamide natural products: potent 20 s proteasome inhibitors as promising cancer chemotherapeutics. *Angew Chem Int Ed Engl* 49:9346–9367
- Heide L, Westrich L, Anderle C, Gust B, Kammerer B, Piel J (2008) Use of a halogenase of hormaomycin biosynthesis for formation of new clorobiocin analogues with 5-chloropyrrole moieties. *ChemBioChem* 9:1992–1999
- Ho MX, Hudson BP, Das K, Arnold E, Ebright RH (2009) Structures of RNA polymerase-antibiotic complexes. *Curr Opin Struct Biol* 19:715–723

- Irish J, Blair S, Carter DA (2011) The antibacterial activity of honey derived from Australian flora. *PLoS ONE* 6:e18229
- Kao CM, McPherson M, McDaniel RN, Fu H, Cane DE, Khosla CJ (1997) Gain of function mutagenesis of the erythromycin polyketide synthase. 2. engineered biosynthesis of an eight-membered ring tetraketide lactone. *J Am Chem Soc* 119:11339–11340
- Kennedy J (2008) Mutasynthesis, chemobiosynthesis, and back to semi-synthesis: combining synthetic chemistry and biosynthetic engineering for diversifying natural products. *Nat Prod Rep* 25:25–34
- Kwon HC, Kauffman CA, Jensen PR, Fenical W (2006) Marinomycins A–D, antitumor-antibiotics of a new structure class from a marine actinomycete of the recently discovered genus “*Marinispora*”. *J Am Chem Soc* 128: 1622–1632
- Lichter PA, Miller SJ (2012) Combinatorial evolution of site- and enantioselective catalysts for polyene epoxidation. *Nat Chem* 4:990–995
- Ling LL, Schneider T, Peoples AJ, Spoering AL, Engels I, Conlon BP, Mueller A, Schäberle TF, Hughes DE, Epstein S, Jones M, Lazarides L, Steadman VA, Cohen DR, Felix CR, Fetterman KA, Millett WP, Nitti AG, Zullo AM, Chen C, Lewis K (2015) A new antibiotic kills pathogens without detectable resistance. *Nature* 517: 455–459
- Marden AFA, Wilkinson B, Corte’s J, Dunster NJ, Staunton J, Leadlay PF (1998) Engineering broader specificity into an antibiotic-producing polyketide synthase. *Science* 279:199–202
- Mariani R, Maffioli SI (2009) Bacterial RNA polymerase inhibitors: an organized overview of their structure, derivatives, biological activity and current clinical development status. *Curr Med Chem* 16:430–454
- Mayer AM, Glaser KB, Cuevas C, Jacobs RS, Kem W, Little RD, McIntosh JM, Newman DJ, Potts BC, Shuster DE (2010) The odyssey of marine pharmaceuticals: a current pipeline perspective. *Trends Pharmacol Sci* 31:255–265
- Nakama Y, Yoshida O, Yoda M, Araki K, Sawada Y, Nakamura J, Xu S, Miura K, Maki H, Arimoto H (2010) Discovery of a novel series of semisynthetic vancomycin derivatives effective against vancomycin-resistant bacteria. *J Med Chem* 53:2528–2533
- Newman DJ, Cragg GM (2012) Natural products as sources of new drugs over the 30 years from 1981 to 2010. *J Nat Prod* 75:311–335
- Nguyen KT, Ritz D, Gu JQ, Alexander D, Chu M, Miao V, Brian P, Baltz RH (2006) Combinatorial biosynthesis of novel antibiotics related to daptomycin. *Proc Natl Acad Sci USA* 103:17462–17467
- Nicolaou KC, Nold AL, Milburn RR, Schindler CS, Cole KP, Yamaguchi J (2007) Total synthesis of Marinomycins A–C and of their monomeric counterparts Monomarinomycin A and iso-Monomarinomycin A. *J Am Chem Soc* 129:1760–1768
- O’Connor SE (2012) Strategies for engineering plant natural products: the iridoid-derived monoterpene indole alkaloids of *Catharanthus roseus*. *Methods Enzymol* 515:189–206
- Omura S, Ikeda H, Malpartida F, Kieser HM, Hopwood DA (1986) Production of new hybrid antibiotics, Mederrhodins A and B, by a genetically engineered strain. *Antimicrob Agents Chemother* 29:13–19
- Pathak TP, Miller SJ (2012) Site-selective bromination of vancomycin. *J Am Chem Soc* 134:6120–6123
- Pathak TP, Miller SJ (2013) Chemical tailoring of teicoplanin with site-selective reactions. *J Am Chem Soc* 135:8415–8422
- Pérez M, Baig I, Braña AF, Salas JA, Rohr J, Méndez C (2008) Generation of new derivatives of the antitumor antibiotic mithramycin by altering the glycosylation pattern through combinatorial biosynthesis. *Chem Bio Chem* 9:2295–2304
- Pinchman JR, Boger DL (2013) Probing the Role of the Vancomycin E-Ring Aryl Chloride: selective divergent synthesis and evaluation of alternatively substituted E-ring analogues. *J Med Chem* 56:4116–4124
- Ragab AE, Grünschow S, Rackham EJ, Goss RJM (2010) New pacidamycins biosynthetically: probing N and C terminal substrate. *Org Biomol Chem* 8:3128–3129
- Ratcliff WC, Denison RF (2011) Alternative actions for antibiotics. *Science* 332:547–548

- Ro D-K, Paradise EM, Ouellet M, Fisher K, Newman KL, Ndungu JM, Ho KA, Eachus RA, Ham TS, Kirby J, Chang M, Withers ST, Shiba Y, Sarpong R, Keasling JD (2006) Production of the antimalarial drug precursor artemisinic acid in engineered yeast. *Nature* 440:940–943
- Roberts MC, Sutcliffe J, Courvalin P, Jensen LB, Rood J, Seppala H (1999) Nomenclature for Macrolide and Macrolide-Lincosamide-Streptogramin B resistance determinants. *Antimicrob Agents Chemother* 43:2823–2830
- Robinson FA (1949) The chemistry of Penicillin. *J Pharm Pharmacol* 1:634–635
- Roy AD, Grüşchow S, Cairns N, Goss RJM (2010) Gene expression enabling synthetic diversification of natural products: chemogenetic generation of pacidamycin analogs. *J Am Chem Soc* 132:12243–12245
- Runguphan W, O'Connor SE (2013) Diversification of monoterpene indole alkaloid analogs through cross-coupling. *Org Lett* 15:2850–2853
- Schmidt EW, Nelson JT, Rasko DA, Sudek S, Eisen JA, Haygood MG, Ravel J (2005) Patellamide A and C biosynthesis by a microcin-like pathway in prochloron didemni, the cyanobacterial symbiont of lissoclinum patella. *Proc Natl Acad Sci USA* 102:7315–7520
- Schrama D, Reisfeld RA, Becker JC (2006) Antibody targeted drugs as cancer therapeutics. *Nat Rev Drug Discov* 5:147–159
- Shepherd MD, Liu T, Mendez C, Salas JA (2011) Engineered biosynthesis of gilvocarcin analogues with altered deoxyhexopyranose moieties. *Appl Environ Microbiol* 77:435–441
- Simon A, Traynor K, Santos K, Blaser G, Bode U, Molan P (2009) Medical honey for wound care —still the 'latest resort'? *Evid Based Complement Alternat Med* 6:165–173
- Smith DR, Grüşchow S, Goss RJ (2013) Scope and potential of halogenases in biosynthetic applications. *Curr Opin Chem Biol* 17:276–283
- Srivastava A, Talawa M, Liu S, Degen D, Ebright RY, Sineva E, Chakraborty A, Druzhinin SY, Chatterjee S, Mukhopadhyay J, Ebright YW, Zozula A, Shen J, Sengupta S, Niedfeldt RR, Xin C, Kaneko T, Irschik H, Jansen R, Donadio S, Connell N, Ebright RH (2011) New target for inhibition of bacterial RNA Polymerase: 'switch region'. *Curr Opin Microbiol* 14:532–543
- Thomas I, Martin CJ, Wilkinson CJ, Staunton J, Leadlay PF (2002) Skipping in a Hybrid Polyketide Synthase. Evidence for ACP-to-ACP chain transfer. *Chem Biol* 9:781–787
- Tu Y, Ni M, Zhong Y, Li L, Cui S, Zhang M, Wang X, Liang X (1981) Studies on the constituents of *Artemisia annua* L. *Yao Xue Xue Bao* 16:366–370
- Van Lanen SG, Shen B (2006) Microbial genomics for the improvement of natural product discovery. *Curr Opin Microbiol* 9:252–260
- Walker MC, Thuronyi BW, Charkoudian LK, Lowry B, Khosla C, Chang MY (2013) Expanding the fluorine chemistry of living systems using engineered polyketide synthase pathways. *Science* 341:1089–1094
- Wu N, Kudo F, Cane DE, Khosla CJ (2000) Analysis of the molecular recognition features of individual modules derived from the Erythromycin Polyketide synthase. *J Am Chem Soc* 122:4847–4852
- Wu N, Cane DE, Khosla C (2002) Quantitative Analysis of the relative contributions of donor Acyl Carrier Proteins, Acceptor Ketosynthases, and linker regions to intermodular transfer of Intermediates in Hybrid Polyketide synthases. *Biochemistry* 41:5056–5066
- Xie J, Pierce JG, James RC, Okano A, Boger DL (2011) A redesigned vancomycin engineered for dual D-Ala-D-Ala and D-Ala-D-Lac binding exhibits Potent Antimicrobial Activity against Vancomycin-Resistant Bacteria. *J Am Chem Soc* 133:13946–13949
- Yu M, Zheng W, Seletsky B, Littlefield B, Kishi Y (2011) Case history: discovery of Eribulin (Halaven) a Halichondrin B analogue that prolongs overall survival in patients with metastatic breast cancer. *Annu Rep Med Chem* 46:227–241
- Zhanel GG, Walters M, Noreddin A, Vercaigne LM, Wierzbowski A, Embil JM, Gin AS, Douthwaite S, Hoban DJ (2002) The ketolides: a critical review. *Drugs* 62:1771–1804

New Target Sites for Treatment of Osteoporosis

Werner E.G. Müller, Xiaohong Wang and Heinz C. Schröder

Abstract In the last few years, much progress has been achieved in the discovery of new drug target sites for treatment of osteoporotic disorders, one of the main challenging diseases with a large burden for the public health systems. Among these new agents promoting bone formation, shifting the impaired equilibrium between bone anabolism and bone catabolism in the direction of bone synthesis are inorganic polymers, in particular inorganic polyphosphates that show strong stimulatory effects on the expression of bone anabolic marker proteins and hydroxyapatite formation. The bone-forming activity of these polymers can even be enhanced by combination with certain small molecules like quercetin, or if given as functionally active particles with certain divalent cations like strontium ions even showing by itself biological activity. This chapter summarizes recent developments in the search and development of novel anti-osteoporotic agents, with a particular focus on therapeutic approaches based on the potential application of inorganic polymers and combinations.

1 Introduction

Osteoporosis is a widespread bone disease with high socioeconomic impact. The main reason for the increasing prevalence of the disease is the increased life expectancy not only in the Western countries but even worldwide. Osteoporosis is characterized by a low bone mineral density, associated with an increased risk of bone fractures (Kanis 1994; Mosley 2000; Cummings and Melton 2002). The

W.E.G. Müller (✉) · X.H. Wang · H.C. Schröder
ERC Advanced Investigator Group, Institute for Physiological Chemistry,
University Medical Center of the Johannes Gutenberg University, Duesbergweg 6,
55128 Mainz, Germany
e-mail: wmueller@uni-mainz.de

W.E.G. Müller · X.H. Wang · H.C. Schröder
NanotecMARIN GmbH, Duesbergweg 6, 55128 Mainz, Germany

© Springer International Publishing AG 2017
W.E.G. Müller et al. (eds.), *Blue Biotechnology*, Progress in Molecular
and Subcellular Biology 55, DOI 10.1007/978-3-319-51284-6_6

decrease in bone strength, bone mass, and consequently bone quality is caused by an imbalance between mineral formation and mineral resorption during bone remodeling process, as a consequence of hormonal changes with age, like in postmenopausal osteoporosis, but also age-related changes in calcium and vitamin D metabolism (Raisz 2005; Sambrook and Cooper 2006; Tang et al. 2007).

The development of efficient therapies for treatment of osteoporosis is one of most important biomedical challenges today. In view of the limitations of current medications of the disease, research efforts are focused not only on the development of drugs with improved tolerability, efficacy, and safety, based on conventional approaches, but also on the search for new target sites for drug candidates, like hormones, enzymes, receptors, or molecules involved in signaling pathways, which influence the bone remodeling process. The increased knowledge about the molecular and cellular mechanisms involved in bone formation is giving hope that new therapeutic regimens, in particular for an individualized treatment of patients, can be found. Intensive research efforts in the last few years already resulted in the development of a series of new drug candidates, including antibodies, many of them acting on the level of signaling mechanisms, like the Wnt signaling pathway (Hoepfner et al. 2009) that plays an important role in regulation of osteoblast function. Our studies of the basic mechanisms involved in biomineralization processes led to the discovery of two new potential target sites for therapeutic intervention of osteoporosis and other bone diseases. The first one is on the level of the carbonic-anhydrase-mediated formation of amorphous calcium carbonate bio-seeds during early bone formation (see chapter “[Biocalcite and Carbonic Acid Activators](#)” by X.H. Wang, M. Neufurth, E. Tolba, S.F. Wang, H.C. Schröder, and W.E.G. Müller of this volume). The second target, investigated in the European Union FP7 BlueGenics project and included/discussed in this chapter is based on the discovery of morphogenetically active inorganic bio-polymers, in particular inorganic polyphosphates (polyP) that are crucially involved in the bone mineralization process, opening the possibility for the development of novel therapeutic approaches, in combination with other (natural) biomolecules. As an example for a new compound/compound combination with a novel two-fold potential target site for antiosteoporotic therapy, polyP and isoquercitrin are presented, which show a co-enhancing effect on bone mineral formation. In addition, combinations of polyP with certain cations, such as strontium, revealed promising results. These new compounds/compound combinations and target sites might be of potential value for the development of future strategies for prevention/treatment of the disease.

2 Osteoporosis

Osteoporosis is a systemic skeletal disorder that can affect both men and women. This progressive bone disorder is characterized by a decrease in bone mineral density and bone quality (micro-architectural deterioration and decreased bone

strength) with an increased predisposition to bone fractures (for a review, see Lane 2006; Bullamore et al. 1970; Gardner et al. 2006; Garnero 2008). According to the clinical definition of WHO (World Health Organization), a (female) patient has osteoporosis, if the bone mineral density determined by dual-energy X-ray absorptiometry is 2.5 standard deviations below the typical peak bone mass of young healthy women (Blake and Fogelman 2007). The progression of the disease can be accelerated by several factors, e.g., sedentary lifestyle and obesity.

Three main classes of osteoporosis can be distinguished: (i) primary osteoporosis, including osteoporosis in postmenopausal women and in the elderly in both genders; (ii) secondary osteoporosis, caused by other disorders, e.g., hyperparathyroidism, hypophosphatasia, and diabetes mellitus, or treatments with glucocorticosteroids; (iii) juvenile osteoporosis, as well as pregnancy-related osteoporosis or postpartum osteoporosis (Lindsay 1996; Adachi 1997; Taxel and Kenny 2000; Schnatz et al. 2010; Cook et al. 2014). The costs associated with osteoporotic fractures in the elderly (typical are fractures of the femoral neck and the vertebra) for the health systems are enormous (Hopkins et al. 2013).

The aim of any therapy of osteoporosis is to prevent such fractures to occur (Sun et al. 2013). Possible strategies in therapy of osteoporosis can be roughly subdivided into strategies aiming to suppress bone resorption (use of antiresorptive drugs; Lewiecki 2013) and strategies to enhance bone formation (use of drugs that stimulate osteoblastic activity; Khan and Khan 2006).

3 Bone Remodeling

On the cellular level, osteoporosis is characterized by an imbalance between the bone resorbing cells, the osteoclasts, and the bone-forming cells, the osteoblasts. The human skeleton underlies a continuous remodeling throughout life. This process is impaired with age, and the unbalanced bone formation, due to age-dependent disturbances of the tuned equilibrium between bone-forming osteoblasts and bone resorbing osteoclasts is the main mechanism involved in the pathogenesis of osteoporosis. The interplay between these cells is controlled by a number of cytokines or growth factors, among them the receptor activator of the nuclear factor κ -B ligand [RANKL] (Leibbrandt and Penninger 2008); Fig. 1. RANKL that is produced by osteoblasts activates osteoclasts by binding to its receptor RANK (Pacifci 1996; Riggs et al. 1998). The activity of RANKL is under the control of osteoprotegerin [OPG], the RANKL antagonist that is released by osteoblasts (Simonet et al. 1997; Hofbauer et al. 2000). The secretion of OPG, in turn, is stimulated by estrogen (Hofbauer et al. 2000). In addition, estrogens decrease the production of RANK (Shevde et al. 2000) and M-CSF (Pacifci 1996). In case of estrogen deficiency, e.g., in postmenopausal women, OPG secretion by osteoblasts becomes down-regulated (Bucay et al. 1998).

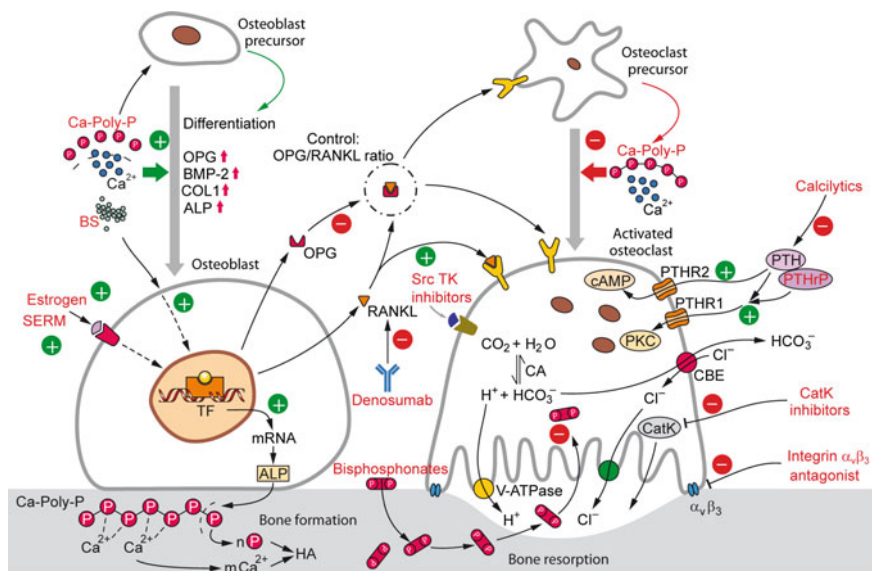


Fig. 1 Target sites of anabolic antiosteoporotic agents that stimulate bone synthesis and of antiresorptive agents that inhibit bone resorption. The mode of action of biosilica [BS] has been described in a previous volume of this series (Schröder et al. 2011). The importance of the carbonic anhydrase [CA] as a novel target for potential antiosteoporotic drugs (carbonic anhydrase activators) has been highlighted in chapter “[Biocalcine and Carbonic Acid Activators](#)” of this volume (by X.H. Wang, M. Neufurth, E. Tolba, S.F. Wang, H.C. Schröder, and W.E.G. Müller). For modulators of the canonical Wnt signaling pathway, see Fig. 2

In addition, the cytokine network that regulates the differentiation and activity of osteoblasts and osteoclasts comprises a number of further factors, including interleukin 1 [IL-1] and tumor necrosis factor α [TNF- α] that stimulate preosteoblasts to release IL-6, IL-11, transforming growth factor [TGF], macrophage colony-stimulating factor [M-CSF], and granulocyte macrophage colony-stimulating factor [GM-CSF] (Gallagher and Tella 2014).

4 Drug Therapy/Treatment of Osteoporosis

Anti-osteoporotic drugs can be subdivided into anabolic agents that stimulate bone synthesis anti-resorptive agents that inhibit bone resorption (Reid 2008; Minisola et al. 2014). The target sites for these drugs comprise both soluble extracellular molecules, like cytokines, and (cell) surface-bound molecules, like receptors, as well as intracellular molecules, like enzymes or proteins involved in intracellular signaling pathways (Fig. 1).

4.1 *Hormone-Replacement Therapies*

Estrogen treatment has been widely used in therapy or for prevention of osteoporosis until it has been repeatedly reported to be associated with an increased number in heart attacks and breast cancer (Maclean et al. 2008). Later developed hormone-replacement therapies of postmenopausal women that turned out to be beneficial in improving bone mineral density use agents that mimic estrogen but with less side-effects, e.g., raloxifene, a selective estrogen receptor modulator (see Sect. 4.3.2).

Further bone anabolic treatments mimicking the effects of natural hormones involved in bone formation are based on recombinant human parathyroid hormone (PTH) analogs, e.g., teriparatide [hPTH(1-34)] (Neer et al. 2001; Blick et al. 2009).

4.2 *Bisphosphonates*

The group of bisphosphonates comprises potent drugs that inhibit bone resorption and have become the leading drugs for many years in the treatment of osteoporosis (Russell et al. 1999; Devogelaer 2000; Gallagher and Tella 2014). These compounds, e.g., alendronate, ibandronate, risedronate, and zoledronic acid, are non-hydrolysable analogs of pyrophosphate [PP_i] (Fleisch 2002) that tightly bind to the bone surface and thereby prevent bone resorption (Fig. 1). In addition, bisphosphonates inhibit the farnesyl pyrophosphate synthase, an enzyme involved in the cytoskeleton formation of the osteoclasts. With time, a series of adverse side-effects of bisphosphonates have been reported, the most severe is osteonecrosis of the jaw (Aspenberg 2006; Khosla et al. 2007; Rizzoli et al. 2008).

4.3 *New Therapies for Osteoporosis*

New drug targets for treatment of osteoporosis comprise, among others, the canonical wntless-int [Wnt] signaling and sclerostin (Bringham 2002; Deal 2009; Lim and Clarke 2012), as well as the RANKL/RANK/OPG system. One successful development targeting the latter system is a monoclonal antibody, Denosumab, that binds to and thereby blocks the function of the RANKL.

4.3.1 **Denosumab**

Denosumab is a human monoclonal antibody that inhibits the maturation and functional activity of osteoclasts (bone resorption) via binding to RANKL (Fig. 1). As a consequence, RANKL cannot bind to RANK; a reduced bone resorption and

an enhanced bone density is observed (Cummings et al. 2009; Bone et al. 2013). Denosumab has already been successfully introduced into clinics (Singer and Grauer 2010).

4.3.2 SERMs

Raloxifene is a second generation selective estrogen receptor modulator (SERM; Fig. 1) that has been approved and introduced into clinics. This estrogen agonist has been shown to strengthen bone mineral density (Taranta et al. 2002). In addition, it decreases the concentrations of low-density lipoprotein [LDL] and cholesterol. Meanwhile, in the European Union, third-generation SERMs, such as Bazedoxifene (Miller et al. 2008) and Lasofoxifene (Cummings et al. 2010) have been approved for therapy of osteoporosis in postmenopausal women with an increased risk of bone fractures.

4.3.3 PTH-Related Protein

New analogs and formulations of the parathyroid hormone [PTH] that stimulates bone formation have been developed. PTH has been shown to increase the number of osteoblasts (Wang et al. 2007). The effects of PTH are mediated by a G-protein-coupled receptor, the PTH receptor 1 [PTHr1] (Whitfield 2006; Maeda et al. 2013; Van der Lee et al. 2013); Fig. 1. The PTH-related protein [PTH-rP] protein is a PTH analogue that binds to PTHr1 and modulates the Wnt signaling pathway (Villardaga et al. 2011). In addition to PTH(1-34) and PTH(1-84), new PTH formulations are under development (Baron and Hesse 2012). Moreover, a series of recombinant peptides that mimic the PTHr1 are available (Fraher et al. 1999; Henriksen et al. 2013).

4.3.4 Calcilytics

The release of PTH is under the control of the calcium-sensing receptor [CaSR], a G-protein-coupled, seven-pass transmembrane protein that is found in the cell membrane of the cells in the parathyroid gland, as well as in osteoblasts and osteocytes and in the kidney (Brown 2007; Fromigue et al. 2009; Xue et al. 2012). PTH is released if the calcium level in the blood is low. The resulting increase in calcium level then activates the CaSR and inhibits PTH secretion. This regulatory system can be influenced by allosteric modulators of the CaSR (Trivedi et al. 2008; Riccardi 2012). Calcilytics are negative modulators, CaSR antagonists, that inhibit the function of the receptor and cause a release of PTH (Cabal et al. 2013); Fig. 1. They have enabled new approaches for treatment of osteoporosis (Fraser et al. 2004; Nemeth 2004; John et al. 2011). Ronacaleret is a calcilytic agent that has been shown to cause a strong PTH response and an increased formation of both

trabecular and cortical bone in rodents (Balan et al. 2009; Atchison et al. 2011). A number of further calcilytic compounds is available that have been described to promote the release of PTH in animals and humans (Gowen et al. 2000; Nemeth 2002; Kumar et al. 2010; John et al. 2011).

4.3.5 Activin A Antagonists

Activins are proteins expressed in the extracellular matrix of bone that belong to the TGF- β /BMP [bone morphogenetic protein] group of signaling molecules. Activin A [Act A], the most prominent member of this group of proteins, influences the Smad pathway (Barruet et al. 2016). This protein binds to two receptors on the cell membrane. Binding of activin to the type II receptor [Act RIIA] has a significant function in osteoclast development. The inhibition of Smad signaling by Act A has an agonistic effect on differentiation of osteoblasts. After application of a fusion protein of the extracellular domain of Act RIIA and the Fc portion of murine IgG2a, an increased bone strength and improved bone microarchitecture have been found (Fajardo et al. 2010).

4.3.6 Peroxisome Proliferator-Activated Receptors

Peroxisome proliferator-activated receptors, PPAR γ and PPAR β/δ , are transcription factors that play an important role in osteogenesis and regulation of bone metabolism (Davidge Pitts and Kearns 2011; Ahmadian et al. 2013). PPAR γ has been shown to direct the differentiation of mesenchymal precursor cells to the adipogenic lineage rather than to the osteogenic lineage (Akune 2004). Therefore, inhibition of the function of PPAR γ provides a promising therapeutic approach for treatment of osteoporosis (Wan et al. 2007; Wei et al. 2010). On the other hand, activation of PPAR β/δ has been found to result in an amplification of canonical Wnt signaling in osteoblasts, as well as increased OPG expression and thereby a suppression of differentiation and activation of osteoclasts (Scholtyssek et al. 2013).

4.3.7 Cathepsin-K Inhibitors

Cathepsin K (CatK) is a lysosomal protease involved in bone resorption by osteoclasts (Fig. 1). This cysteine protease mediates the proteolysis of type I collagen in the resorption lacunae and plays an important role in degradation of the organic bone matrix during bone remodeling. The expression of Cathepsin K is up-regulated by PTH, RANKL, vitamin D and tumor necrosis factor [TNF], while estrogens suppress the expression of the enzyme. Specific inhibitors of Cathepsin K include Odanacatib [ODA], an inhibitor that decreases bone resorption and hence enhances bone mineral density in postmenopausal women (Gauthier et al. 2008; Bone et al. 2010); Fig. 1. Other inhibitors, e.g., Balicatib and Relacatib proved less

effective. ODA turned out to be safe and well-tolerated in phase I and phase II studies in postmenopausal women (Rodan and Duong 2008; Stoch et al. 2009; Bone et al. 2010; Costa et al. 2011; Eisman et al. 2011; Langdahl et al. 2012). Besides Cathepsin K mediated bone resorption, the drug does not affect other specific cell functions of the osteoblasts (Kong 2012; Zerbinì and McClung 2013).

4.3.8 Src Tyrosine Kinase Inhibitors

Src tyrosine kinase (Src TK) is essential for the function of osteoclasts, in particular their bone resorbing activity (Miyazaki et al. 2004). Deletion of the *src* gene causes osteopetrosis in mice (Miyazaki et al. 2004). Saracatinib is an inhibitor of the Src tyrosine kinase (Fig. 1) that has been evaluated in phase I clinical trials (Hannon et al. 2010).

4.3.9 Glucagon-like Peptide 2

The glucagon-like peptide 2 [GLP-2] is a gut hormone (Austin et al. 2016) that influences the rate of bone resorption. This rate has been shown to be higher under fasting conditions at night (Henriksen et al. 2004). In a phase II study, GLP-2 has been demonstrated to uncouple bone resorption phase from bone formation phase (Henriksen et al. 2009). In ovariectomised mice, chronic administration of GLP-2 receptor agonists has been reported to improve trabecular bone mass and architecture (Pereira et al. 2015).

4.3.10 Integrin $\alpha_v\beta_3$ Antagonists

The integrin $\alpha_v\beta_3$ [vitronectin] is present in osteoclasts and allows the attachment of the cells at the bone surface (Fig. 1). The interaction of the osteoclasts with bone matrix proteins is required for the formation of the resorption lacunae. In one study, an $\alpha_v\beta_3$ integrin antagonist (L-000845704) has been described that inhibited bone resorption and caused a significant increase in bone mineral density (Murphy et al. 2005).

4.3.11 Wnt Signaling, Sclerostin, and Dickkopf-1

The proteins involved in the Wnt signaling pathway comprise a series of extracellular cysteine-rich glycoproteins. This pathway plays an important function in bone development and remodeling (Kim et al. 2007; Choi et al. 2009). Two Wnt signaling pathways are distinguished: the canonical (or β -catenin) pathway and β -catenin-independent noncanonical pathway. In bone, the canonical Wnt signaling pathway is mostly important (Fig. 2). This pathway involves the extracellular Wnt

ligands that bind to the frizzled proteins or the lipoprotein receptor-related protein [LRP] 5/6 co-receptors at the cell surface. The intracellular transduction of the signal then results in the activation of the transcription factor β -catenin that is inhibited by phosphorylation, ubiquitination, and degradation. In the absence of the Wnt ligands, the β -catenin concentration is low because the protein becomes phosphorylated, mainly by the glycogen synthase kinase-3 β [GSK-3 β], and available for ubiquitination and subsequent degradation by the proteasomal complex (Boudin et al. 2013). After binding of the Wnt ligands and activation of the Wnt signaling pathway, the phosphorylation of β -catenin is inhibited as a result of a process that involves the phosphorylation of the intracellular Dishevelled [Dsh] proteins and degradation of GSK-3 β . Consequently, β -catenin is not degraded and accumulates in the cytoplasm. The protein is then translocated into the nucleus where it interacts with specific transcription factors, resulting in the transcription of target genes involved to bone formation (Lee et al. 2010; Baron and Kneissel 2013; Boudin et al. 2013).

The noncanonical Wnt pathway or frizzled-initiated signaling is independent of β -catenin (Lee et al. 2010; Baron and Kneissel 2013) and includes, among others, the Wnt-mTOR [mammalian target of rapamycin] signaling (Lee et al. 2010; Sassi et al. 2013).

The canonical Wnt signaling pathway is regulated by a series of intra- and extracellular antagonists, including sclerostin and the Dickkopf-1 [DKK-1] protein (Fig. 2). Based on its involvement in differentiation, proliferation, and activation of osteoblasts, the development of agents that modulate this pathway is of particular interest in the development of novel strategies for treatment of osteoporosis (Canalis 2013; Kim et al. 2013). For example, it can be expected that signaling inhibitor antagonists, such as anti-sclerostin antibodies, promote bone formation.

The DKK-1 protein binds to two proteins, Kremen-1 and Kremen-2, resulting in the dissociation of LRP5/6 from the cell surface (Mao et al. 2002). The inhibitor targets of the Wnt signaling pathway include LRP5/6 (binding of sclerostin and DKK1), frizzled (binding of serum frizzled-related proteins), and Wnt (binding of Wnt inhibitory factors) (Rybchyn et al. 2011). Binding of these agonists results in a decreased Wnt signaling and, therefore, a decreased bone formation, while the absence of these inhibitors or the presence of antibodies against these inhibitors induce Wnt signaling and, in turn, enhance bone formation (Glantschnig et al. 2010, 2011).

It should be noted that molecules involved in the Wnt signaling pathway are well conserved in evolution. They are already present in early invertebrates, such as sponges (Adell et al. 2007; Wiens et al. 2008) and cnidarians (Lengfeld et al. 2009). Several Wnt pathway-related genes, encoding for the soluble frizzled molecule, TCF/LEF, GSK-3, and the Wnt regulator LZIC have been isolated from the demosponges *Suberites domuncula* and *Lubomirskia baicalensis* (Adell et al. 2003, 2007; Wiens et al. 2008). The Wnt antagonist DKK1 has been reported to be expressed in *Hydra* (Guder et al. 2006). On the other hand, expression of sclerostin has only been found in vertebrates.

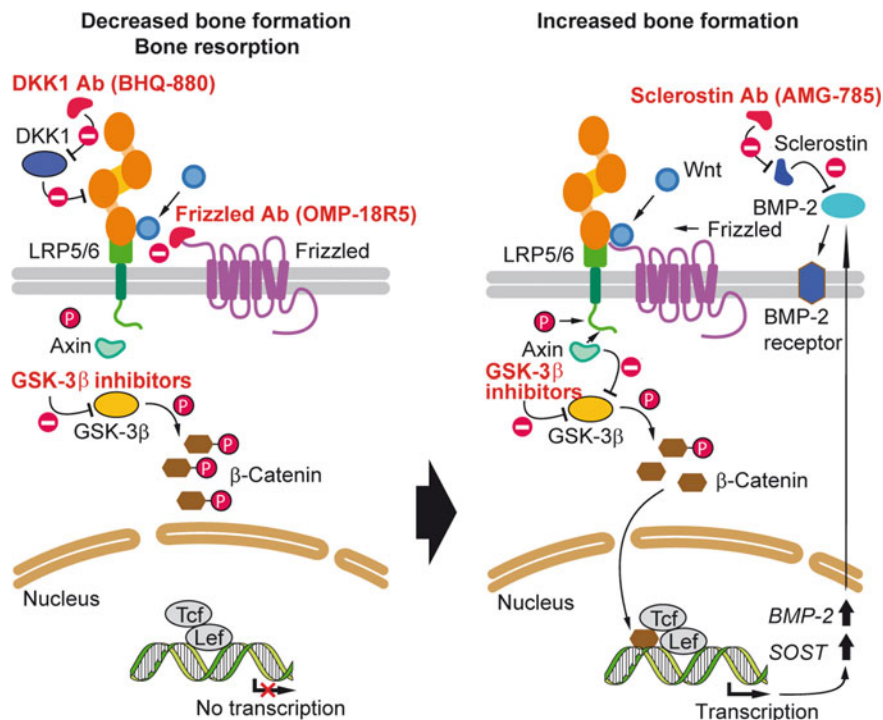


Fig. 2 Modulators of the canonical Wnt signaling pathway. This pathway plays a crucial role in regulation of cell proliferation and differentiation. In the absence of Wnt, β -catenin is phosphorylated by glycogen synthase kinase 3 β (GSK-3 β), which is a component of a destruction complex, resulting in ubiquitylation and degradation of β -catenin by the proteasomal complex. After binding of Wnt to the Frizzled receptors and the co-receptors LRP5 and LRP6 [low-density lipoprotein receptor-related proteins 5 and 6], the destruction complex is inhibited, resulting in the transport of β -catenin into the nucleus, where it induces, in combination with transcription factors, including the Tcf [T cell factor family of transcription factors] and co-activators, the expression of specific genes

4.3.12 Sclerostin Inhibitors and Anti-sclerostin Antibodies

Sclerostin is a protein that is expressed almost exclusively by osteocytes and encoded by the *SOST* gene (Winkler et al. 2003; Robling et al. 2008; Cohen-Kfir et al. 2011; Rochefort 2014; Compton and Lee 2014). Sclerostin is an antagonist of the anabolic Wnt signaling pathway and down-regulates osteoblast activity (Malinauskas and Jones 2014). This protein presents an optimal target for osteoporosis therapy because this protein specifically acts on osteoblasts and osteocytes (Shah et al. 2015); therefore, it can be expected that it has no effects on extraskeletal tissues/cells. Monoclonal antibodies against sclerostin have been shown to enhance the Wnt signaling pathway and to show potent bone anabolic activity (Winkler et al. 2003; Van Bezooijen et al. 2005; Robling et al. 2008); Fig. 2. In animal models,

using ovariectomized rats (Li et al. 2009, 2010), dexamethasone-treated mice (Marenzana et al. 2011) and models of fracture healing (closed femoral fracture model in rats and a fibular osteotomy model in cynomolgus monkeys; Ominsky et al. 2011), administration of anti-sclerostin antibodies has been shown to prevent bone loss, resulting in an increased bone mass. Similar results have been obtained with type 2 diabetes patients (Gaudio et al. 2012). Results from phase I, phase II, and phase III trials on postmenopausal women with low bone mineral density using a humanized anti-sclerostin monoclonal antibody (romosozumab or AMG 785) revealed a substantial increase in bone mineral density and the expression of markers of bone formation, as well as a decrease in the expression of markers for bone resorption (Padhi et al. 2011; www.amgen.com). A significant dose-related increase in spine and hip bone mineral density has also been found in phase I and phase II studies on postmenopausal women with Blososumab (LY2541546), another monoclonal anti-sclerostin antibody (McColm et al. 2014; Recker et al. 2015).

4.3.13 Dickkopf-1 Antagonists

The Dickkopf-1 [DKK-1] protein is another endogenous inhibitor of Wnt signaling that, besides sclerostin, is crucially involved in regulation of bone mineral formation (Fig. 2). High levels of DKK-1 have been found in postmenopausal women with osteoporosis (Anastasilakis et al. 2010; Butler et al. 2011). Neutralization of DKK-1 has been reported to protect ovariectomized rats or rats overexpressing TNF from bone loss (Heiland et al. 2010). Inhibition of DKK-1 has also been reported to attenuate glucocorticoid induction of apoptosis of osteoblasts, as well as rheumatoid arthritis associated bone damage (Wang et al. 2005; Diarra et al. 2007). Different human monoclonal antibodies (RH2-18, PF-04840082, RN564, and BHQ880) have been developed and evaluated with respect to safety and efficacy in animal models, as well as in clinical trials (Li et al. 2006, 2011; Yaccoby et al. 2007; Betts et al. 2010; Agholme et al. 2011). The antibodies were found to induce an increase of bone mass. Therefore, besides antisclerostin antibodies, targeting Wnt signaling by antibodies inhibiting Dickkopf binding to LRP5/6 (Fig. 2; Ahn et al. 2011) has been proposed to be a further useful strategy for the treatment of patients with low bone mass.

4.3.14 Glycogen Synthase Kinase-3 Inhibitors

Glycogen synthase kinase-3 [GSK-3 β] is a serine/threonine protein kinase involved in a number of signal transduction pathway, among them Wnt signaling (Fig. 2). Inhibition of GSK-3 β in ovariectomized rats has been shown to increase bone mineral density and bone strength, as well as the expression of markers of bone formation (Kulkarni et al. 2006). Inhibition of GSK-3 β by 6-bromoindirubin-3'-oxime revealed promising results in animal model of steroid-induced osteoporosis (Wang et al. 2009).

4.4 *PolyP-based Combinations*

Combinations of inorganic polyP with other molecules or certain cations turned out to be efficient stimulators of bone formation *in vitro*, potentially capable to antagonize bone loss (decrease in bone mineral density) during osteoporotic disorders. One example is the combination of polyP (Ca²⁺ salt; Müller et al. 2011) and the dietary phytoestrogen isoquercitrin (Woo et al. 2004), two components, each of them already showing by itself mineralization-promoting activity, that supports the mineralization process of osteoblasts in a strongly synergistic way (Wang et al. 2014c). The other example is strontium-polyP microparticles that were found to be much more effective than their Ca-polyP counterparts, acting on the level of the Wnt signaling pathway (Müller et al. 2016b).

4.4.1 Polyphosphates

Our group was the first to demonstrate that inorganic polyP, a naturally occurring inorganic polymer, potently induces bone formation both *in vitro* and *in vivo* (Müller et al. 2011; Wang et al. 2012). In addition, polyP plays a central role in extracellular energy metabolism as a transportable metabolic fuel and energy storage (Müller et al. 2015a, b; Wang et al. 2016b). In mammalian cells, polyP is most likely synthesized in the mitochondria (Pavlov et al. 2010) and accumulates especially in platelets (Morrissey et al. 2012), but also in bone-forming osteoblasts (Leyhausen et al. 1998; Lorenz et al. 1997). Besides of silica/biosilica (Wiens et al. 2010a, b; Müller et al. 2013b; Wang et al. 2014a, b) and of carbonic anhydrase activators (Wang et al. 2014d), this inorganic bioproduct/biopolymer has turned out to be a potential potent material for therapy or prevention of osteoporotic bone disorders, including osteoporosis-associated bone fractures, as corroborated by promising results of first animal studies. All these three inorganic components have been shown to strengthen bone mineral (hydroxyapatite, HA) formation and to accelerate healing of bone defects/fractures, and hence to have the potential to ameliorate the consequences of reduced mineral density in osteoporotic patients (Wang et al. 2014a, b). These stimulatory effects have been found to be caused by an induction of the expression of genes, associated with the development of osteoporosis and other bone disorders, encoding for OPG [osteoclastogenesis inhibitory factor], bone morphogenetic protein 2 [BMP2; stimulator of bone formation], and alkaline phosphatase [ALP; hydrolysis of the mineralization inhibitor pyrophosphate, PP_i, and delivery of orthophosphate, P_i, for bone mineral formation by degradation of polyP] (for a review, see Wang et al. 2012; Müller et al. 2013a). Here we focus on polyP. The potential usefulness of amorphous calcium carbonate (formed by carbonic anhydrase and promoted by carbonic anhydrase activators) has been summarized in chapter “*Bioalcite and Carbonic Acid Activators*” of this volume (by X.H. Wang, M. Neufurth, E. Tolba, S.F. Wang, H.C. Schröder, and W.E.G. Müller), and the effects of silica/biosilica, in a previous volume of this series (Schröder et al. 2011).

Already 15 years ago, we demonstrated that the ALP is able to hydrolyze polyP under formation of monomeric P_i (Lorenz and Schröder 2001). PolyP is an efficient chelator of calcium ions. Therefore, this polymer has been proposed to exist in vivo mainly as a 1:2 complex between Ca^{2+} and polyP (based on phosphate) that can serve, after enzymatic, ALP-mediated hydrolysis, both as a calcium source and as a phosphate source for bone HA deposition (Omelon and Grynepas 2008; Omelon et al. 2009; Müller et al. 2011). In addition, the ALP hydrolyzes the mineralization inhibitor PP_i produced by the ecto-enzyme ectonucleotide pyrophosphatase/phosphodiesterase-1 [ENPP1]. ENPP1 is expressed in plasma membranes and matrix vesicles of osteoblasts (Johnson et al. 2000) and regulates the extracellular PP_i levels by cleavage of ATP. Both PP_i and P_i are involved in regulation of bone mineral deposition, but with different target sites. PP_i is an inhibitor of HA mineralization process (Fleisch et al. 1966; Hessle et al. 2002), while P_i inhibits the carbonic anhydrase, which is involved in the synthesis of amorphous calcium carbonate bio-seeds, preceding calcium phosphate/HA deposition (Müller et al. 2013a). As a consequence, compounds that are able to modulate the activity of the two enzymes which regulate the extracellular level of P_i (and PP_i), the ALP and ENPP1, are of potential interest for pharmacological intervention of bone diseases, like osteoporosis. One of such compounds is quercetin, an inducer of ALP (Prouillet et al. 2004).

PolyP, on the other side, acts both as an inducer of expression and as an activator of the bone ALP (Müller et al. 2011). This polymer is morphogenetically/biologically active only if present as a Ca^{2+} complex (Müller et al. 2011). Besides of ALP gene expression, the Ca^{2+} -polyP complex upregulates in osteoblast-like SaOS-2 cells the expression of further genes implicated in bone formation, in particular the transcript levels of BMP2. Moreover, the Ca^{2+} -polyP complex down-regulates of the gene encoding for the tartrate-resistant acid phosphatase [TRAP], as well as cell proliferation in osteoclast-like RAW 264.7 cells, presumably via inhibition of phosphorylation of $I\kappa B\alpha$, an inhibitor of the transcription factor NF- κ B (Wang et al. 2013). PolyP exhibits no toxicity on mammalian cells in vitro up to concentrations of 100 μ M.

4.4.2 Quercetin—Flavonoids

Flavonoids are a widespread distributed group of naturally occurring compounds. These compounds are ubiquitous in plants. They are found, in particular, in medicinal plants. Flavonoids show various pharmacological activities, including anti-inflammatory, antiallergic, antihepatotoxic, antitumor, antidiabetic, and antiosteoporotic activities (Di Carlo et al. 1999). They can be subdivided into different groups and subgroups: Flavones (2-phenylchromen-4-ones), e.g., apigenin, flavonols (3-hydroxyflavones or 3-hydroxy-2-phenylchromen-4-ones), e.g., quercetin, kaempferol, and myricetin, and flavanones (2,3-dihydro-2-phenylchromen-4-ones), e.g., naringenin, flavanonols (3-hydroxyflavanones or 2,3-dihydroflavonols or 3-hydroxy-2,3-dihydro-2-phenylchromen-4-ones), e.g.,

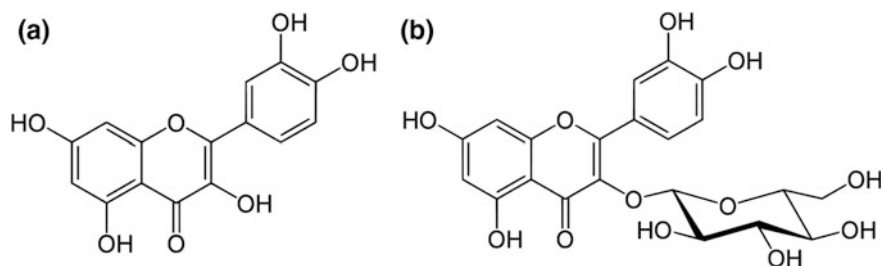


Fig. 3 Structural formula of quercetin (*left*) and isoquercitrin (*right*)

taxifolin, and isoflavonoids, e.g., genistein. Both aglycons (without sugar) and glycosides with one or more sugar residues are found, e.g., quercetin (aglycon) and its glycoside, isoquercitrin (quercetin 3- β -D-glucoside); Fig. 3.

Some flavonols have been reported to strengthen bone mineral formation. They are used by postmenopausal women to prevent bone loss (Branca 2003). Among these flavonols is quercetin; this compound is able to penetrate through the plasma cell membrane/lipid bilayer (Košinová et al. 2012) and has been shown to potently inhibit osteoclastic bone resorption *in vitro*, at a concentration of 1–10 μ M (Wattel et al. 2003), but also proliferation, differentiation, and mineralization of osteoblasts, at about 10 μ M (Notoya et al. 2004). On the other hand, at a concentration of 50 μ M, quercetin has been found to act as a strong stimulator of mineralization of MG-63 human osteoblasts (Prouillet et al. 2004). The latter effect, controversial to Notoya et al. (2004), has been explained by an interaction of quercetin with the estrogen receptor [ER], resulting in an activation of the mitogen activated protein kinase [MAPK]/ERK pathway and the ALP. In addition, quercetin has been described to accelerate the TNF- α -induced growth inhibition and apoptosis in MC3T3-E1 osteoblastic cells (Son et al. 2006). Moreover, quercetin has been reported to interact with Na⁺/K⁺-ATPase (Mezesova et al. 2010) and to inhibit phosphoinositide-3-kinase [PI3K], MAPK phosphorylations and collagen-induced ATP release from platelets (Oh et al. 2012).

The quercetin content of edible plants ranges from 10 to 100 mg per 100 g of edible portion (Bhagwat et al. 2011), while the concentration of isoquercitrin is about 30-fold higher (Kalinova and Vrchotova 2009). Administration of quercetin at doses of 40–1900 mg/kg/day to rats revealed no effects on survival and no toxicity (Dunnick and Hailey 1992); however, the compound shows only a poor absorption. Isoquercitrin has a likewise low toxicity; the acute toxicity, LD₅₀ [lethal dose] in mice (intraperitoneal) is >5.000 mg/kg (Drozen and Foley 2007).

4.4.3 Synergistic Action of PolyP and Isoquercitrin

In our studies, we could demonstrate that both natural products, Ca²⁺-polyP and isoquercitrin, if given in combination, show a strong synergistic effect on the

biomineralization of bone-forming cells. These studies revealed that polyP and isoquercitrin, if given in combination, increase bone mineral formation in SaOS-2 cells via two different modes of action/signal transduction pathways, involving the Runt-related transcription factor 2 [RUNX2] and the cofactors ATF6 [activating transcription factor 6] and Ets1 [E26 transformation-specific-1] (Wang et al. 2014c).

The combined effects of isoquercitrin, the cell membrane permeable 3-*O*-glucoside of quercetin, and polyP, in form of the Ca²⁺ salt/complex, on mineralization have been studied in vitro, using human osteoblast-like SaOS-2 cells. Isoquercitrin has been applied instead of the non-glucosylated aglycon quercetin because of its better bioavailability (Paulke et al. 2012). This secondary metabolite is produced by many medicinal plants, e.g., the Mongolian plant *Dracocephalum ruyschiana* (Selenge et al. 2013).

Both compounds, isoquercitrin and polyP (applied as a Ca²⁺ salt with an average chain length of 40 phosphate units), if given individually, showed negligible, or low, toxicity in the XTT cell proliferation assay with SaOS-2 cells and did not impair the growth of the cells at concentrations ≤3 μM (isoquercitrin) and within the concentration range of 3–100 μM polyP (Ca²⁺ salt), respectively (Fig. 4). Only at the high concentration of 10 μM, isoquercitrin showed a low toxicity. Ca²⁺-polyP even had a significant stimulatory effect on cell growth within the concentration range of 0.3–1 μM polyP (Fig. 4).

At non-toxic concentrations the individual compounds significantly enhance biomineral formation onto SaOS-2 cells at concentrations ≥1 μM (isoquercitrin) and ≥3 μM (Ca²⁺-polyP) in the presence of mineralization activation cocktail (MAC; containing β-glycerophosphate, ascorbic acid, and dexamethasone). The stimulatory activity of Ca²⁺-polyP was more than two-fold higher compared to isoquercitrin (Wang et al. 2014c).

Fig. 4 Effect of increasing concentrations of isoquercitrin [IQC] and polyP (Ca²⁺ salt); XTT assay. SaOS-2 cells remained either untreated or were exposed to isoquercitrin or polyP (Ca²⁺ salt) for 3 days. Means ± SD (*n* = 10); **P* < 0.01 (modified from Wang et al. 2014c)

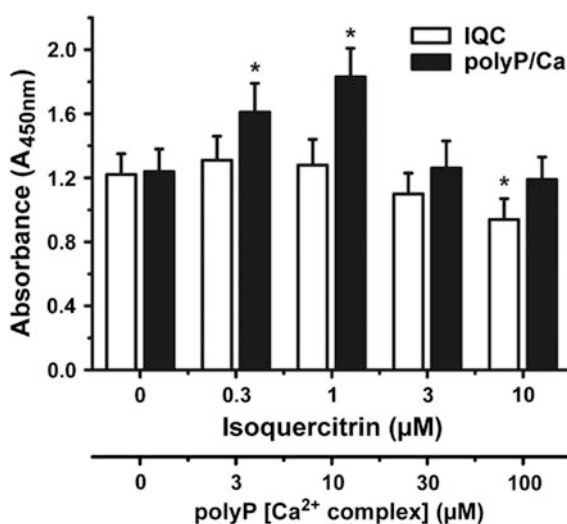
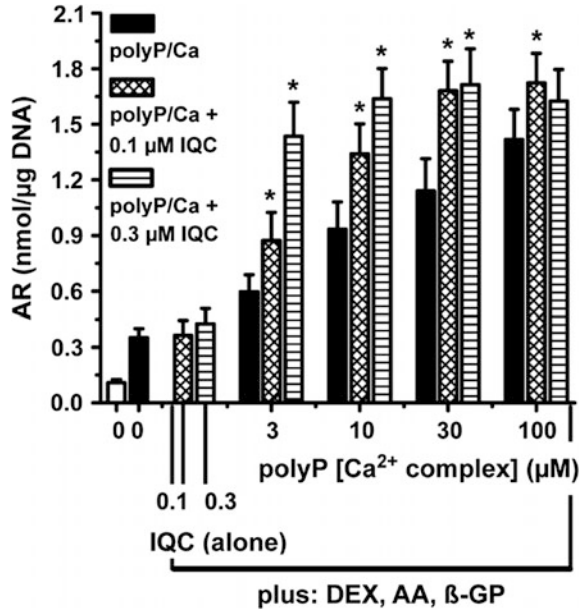


Fig. 5 Synergistic effect of isoquercitrin and polyP (Ca^{2+} salt) on mineralization of SaOS-2 cells. The cells were incubated for 7 days without MAC or with MAC (mineralization activation cocktail). polyP (Ca^{2+} salt) was added either alone or together with isoquercitrin, as indicated; * $P < 0.01$ (modified from Wang et al. 2014c)



Co-incubation experiments revealed that if applied simultaneously, isoquercitrin significantly potentiates the mineralization-enhancing effect of Ca^{2+} -polyP in a synergistic manner, even if the flavonoid is given at concentrations (0.1 and 0.3 μM) that cause no significant effect on biomineralization, as reflected by the Alizarin Red S staining assay (Wang et al. 2014c); Fig. 5. If 0.3 μM isoquercitrin is co-administered with 3 μM Ca^{2+} -polyP the mineralization effect is amplified by 2.4-fold compared to assays with the Ca^{2+} -polyP alone. These results already suggested, as shown in the following, that the two compounds, Ca^{2+} -polyP and isoquercitrin, act via two different pathways on the mineralization process.

4.4.4 Mode of Action of PolyP and Isoquercitrin Underlying the Synergistic Effect

The expression of genes involved in bone mineralization has been studied in order to elucidate the mechanism underlying the synergistic effect of polyP and isoquercitrin. Determinations of the expression level of the gene encoding for RUNX2, after incubation of the cells with isoquercitrin or Ca^{2+} -polyP revealed that both compounds cause a significant upregulation of the expression of this transcription factor to almost the same extent (Wang et al. 2014c). RUNX2 is an essential transcription factor that controls the differentiation of osteoblasts from multipotent mesenchymal precursor cells (Zhang et al. 2009; Dalle Carbonare et al. 2012) and responds to growth factor signaling, e.g., BMP2, Ets1, MAPK, or fibroblast growth factor (Jang et al. 2012; Itoh et al. 2010, 2012).

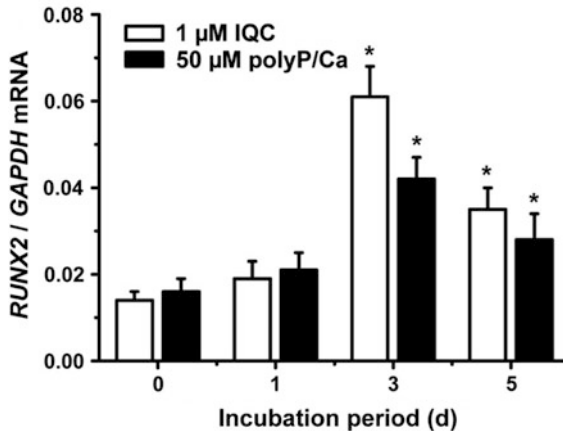


Fig. 6 Effect of polyP (Ca^{2+} salt) and isoquercitrin [IQC] on the expression of RUNX2 in SaOS-2 cells; RT-qPCR experiment. The expression of GAPDH was used as a reference gene for normalization. The cells were kept first for 5 days in medium/serum and then transferred to the MAC and continued to be incubated for 5 days. Means \pm SD ($n = 5$); * $P < 0.01$ (modified from Wang et al. 2014c)

We were able to demonstrate that the expression of RUNX2 is under the control of isoquercitrin and Ca^{2+} -polyP (Wang et al. 2014c). Our experiments revealed that isoquercitrin and Ca^{2+} -polyP at a concentration that induces a significant increase in mineral deposition (1 and 50 μM , respectively) cause significant increase in the steady-state expression of RUNX2 (Fig. 6).

Determinations of the effects of the two compounds on the expression of the two co-activators of RUNX2, ATF6 and Ets1, subsequently revealed that isoquercitrin causes an activating effect on a signal transduction pathway that is independent from the mechanism induced by Ca^{2+} -polyP (Wang et al. 2014c).

ATF6 is a basic leucine zipper domain transcription factor bound to the endoplasmic reticulum [ER] membrane that acts as a transducer of ER stress response during bone formation (Murakami et al. 2009). This transcription factor is expressed in osteoblasts and is processed by intramembrane proteolysis in response to ER stress (for a review, see Jang et al. 2012). The expression of ATF6 is under the control of RUNX2 that is induced by BMP2. Even more, cleavage of ATF6 precursor protein at the ER is elicited again through BMP2. After binding to its corresponding DNA-binding response element, the mature ATF6 induces osteocalcin [OCAL], a major non-collagenous protein in bone (Barille et al. 1996). It has already been reported that the expression of BMP2 is induced by quercetin/isoquercitrin (Kim et al. 2006).

The results revealed that isoquercitrin but not Ca^{2+} -polyP causes a strong increase in the expression of ATF6 and OCAL (Wang et al. 2014c); Fig. 7a, b. Consequently, isoquercitrin causes an increased synthesis of OCAL via induction of RUNX2 and ATF6 and subsequent BMP2-initiated maturation of ATF6p to ATF6 (see Fig. 8).

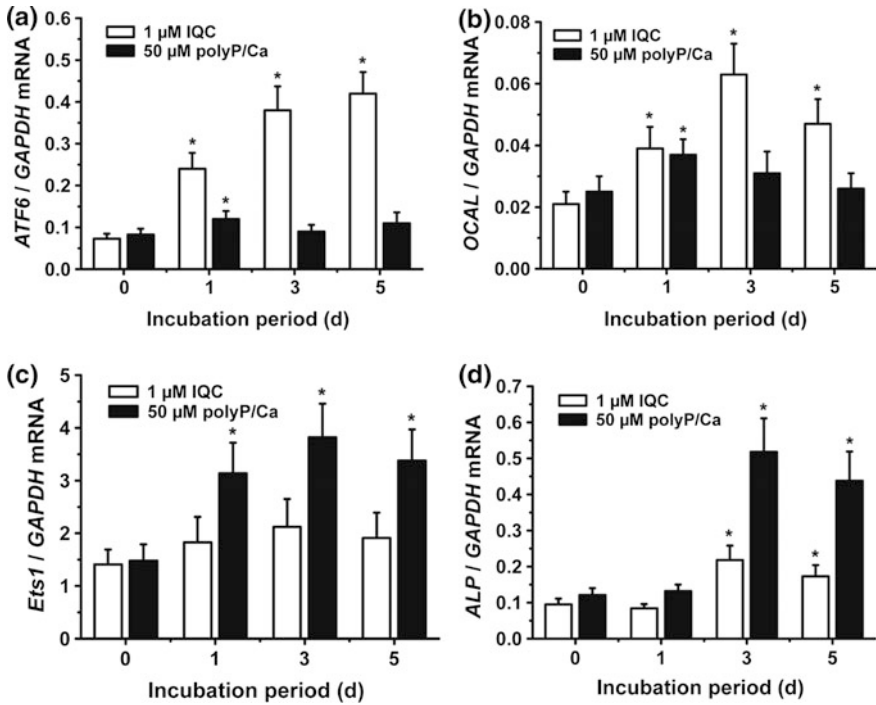


Fig. 7 Differential effect of polyP (Ca²⁺ salt) and isoquercitrin on the steady-state expression levels of *ATF6* (a), *OCAL* (b), *Ets1* (c) and *ALP* (d). Incubation in the presence of MAC was performed for up to 5 days. Means ± SD (n = 5); *P < 0.01 (modified from Wang et al. 2014c)

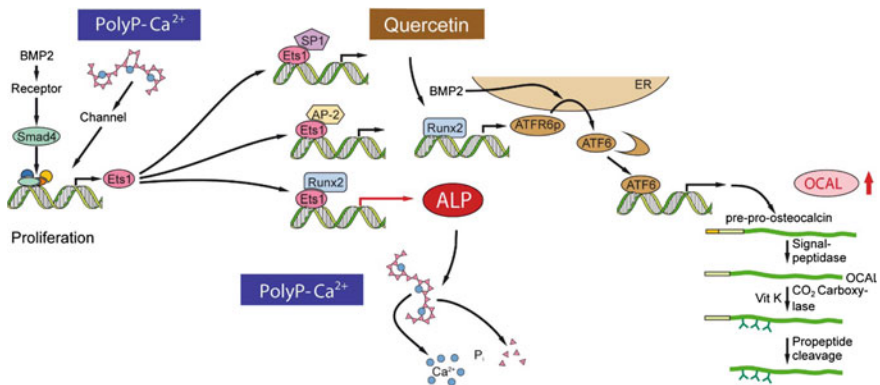


Fig. 8 Schematic presentation showing the differential modes of action of isoquercitrin and of Ca²⁺-polyP (modified from Wang et al. 2014c)

On the other hand, Ca^{2+} -polyP (salt) but not isoquercitrin strongly upregulates the transcript levels of the genes encoding for the transcription factor Ets1 (Fig. 7c) and the ALP (Fig. 7d). The expression of Ets1 as well as BMP2 is assumed to be regulated by a microRNA resulting in an attenuation of BMP2-induced osteoblast differentiation (Itoh et al. 2012). Ets1 is involved in transcriptional regulation of matrix metalloproteinases (Okuducu et al. 2006). Ets1 itself is regulated by the Smads. These transcription factors which form hetero-oligomeric complexes and are BMP signaling activator receptor-regulated, interact with RUNX2, AP-1 and SP-1, leading to a target gene-specific gene expression (Itoh et al. 2010). The expression of *RUNX2* initiated by Smad leads to the association of RUNX2 with Ets1, resulting in the induction of ALP (Itoh et al. 2010; Kim and Kim 2010); see Fig. 8.

Based on these results, the modes of action through which isoquercitrin and Ca^{2+} -polyP upregulate osteoblast mineralization are different. Both biomolecules increase the expression of *RUNX2*. Isoquercitrin is a potent stimulator of the expression of the two co-activators of RUNX2, ATF6, and Ets1, in contrast to Ca^{2+} -polyP, and causes an upregulation of the expression of *OCAL*, while polyP strongly increases the expression of the *Ets1* gene and the gene encoding for the ALP.

The signaling pathway through which polyP modulates gene expression most likely involves mTOR (Kornberg et al. 1999; Zakharian et al. 2009). mTOR is involved in the regulation of cell proliferation and mitochondrial activity (Abramov et al. 2007). In the proposed signal transduction pathway, polyP, in the form of its Ca^{2+} complex, regulates the expression of the effector gene *ALP* most likely through induction of Ets1, along with RUNX2 (Fig. 8).

As result of these two different but complementary mechanisms, a synergistically enhanced effect of Ca^{2+} -polyP and isoquercitrin on bone mineral formation occurs. The results suggest that the two natural compounds, polyP and quercetin and their derivatives, which are already used in food preservation (polyP) and diet (quercetin) might be of beneficial value in therapy and prophylaxis of osteoporosis and related bone diseases.

4.4.5 Strontium and Strontium-PolyP Microparticles

The BMP2—RUNX2 pathway that is activated by polyP (see above) is most likely also induced by strontium (Römer et al. 2011). Strontium (Sr^{2+}) has been shown to exhibit a dual activity (Marie 2006; Bonnelye et al. 2008): it promotes bone formation (Nielsen 2004) and inhibits bone resorption (Canalis et al. 1996). As a result, an increase in bone density and strength occurs. Therefore, strontium has been reported to be potentially useful in the therapy of osteoporosis (Qin et al. 2013). Strontium is usually administered in the form of ranelate (Neuprez et al. 2008; Reginster et al. 2015). Strontium salts have also been shown to interact with the cell surface calcium-sensing receptor [CaSR], followed by a decrease in

intracellular cAMP level and an increase of inositol 1,4,5-trisphosphate, via stimulation of phospholipase C β , resulting in the release of intracellular Ca $^{2+}$ (Brown and MacLeod 2001). This signal transduction pathway finally leads to an activation of the MAP kinases and an upregulation of *OPG* expression and a down-regulation of *RANKL* expression in osteoblasts (Peng et al. 2011). It has been shown that strontium-doped Ca-polyP enhances the growth of osteoblasts (Gu et al. 2013). The mechanism by which (crystalline) Sr-doped Ca-polyP promotes bone formation is not yet clear, but it might be caused by Sr $^{2+}$ ions which are released besides Ca $^{2+}$ ions during degradation of this material. Moreover, Sr-doped Ca-polyP has the ability to stimulate the expression VEGF and bFGF in osteoblasts, and therefore accelerates bone regeneration and vascularization (Gu et al. 2013).

Recently, we presented evidence that the effect of strontium is partially mediated by a reduction of *sclerostin* (*SOST* gene) expression (Müller et al. 2016b). Sclerostin, the *SOST* gene product, acts as an inhibitor of bone formation via the canonical Wnt/ β -catenin signaling pathway, which has a decisive function in the control of bone remodeling (Niedźwiedzki and Filipowska 2015; see Sect. 4.3.11); Fig. 9. This Wnt antagonist has gained increasing attention in the development of therapeutic strategies for skeletal diseases associated with impaired bone remodeling and decreased mineral density, such as osteoporosis.

In order to investigate the combined effects of polyP and strontium, we prepared amorphous Sr-polyP microparticles (Sr-a-polyP-MP; Müller et al. 2016b) from Na-polyP and SrCl $_2$ applying a similar procedure like used for the formation of amorphous Ca-polyP microparticles (Ca-a-polyP-MP; Müller et al. 2015c); Fig. 10.

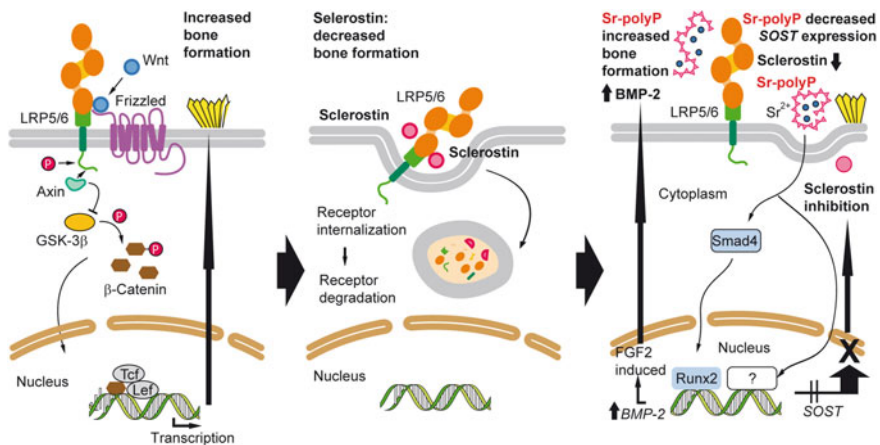


Fig. 9 Scheme of the effect of sclerostin on the differentiation and mineralization in bone cells via the Wnt/LRP5/6 pathway (*left*). Sclerostin acts as inhibitor of the Wnt pathway through interfering with the LRP5/6 co-receptor. After internalization, sclerostin is degraded together with the co-receptor (*middle*). Preliminary results show that Sr-polyP particles upregulate the expression of BMP2 and ALP, while the expression of the *SOST* gene, encoding for sclerostin, is not affected (modified from Müller et al. 2016b)

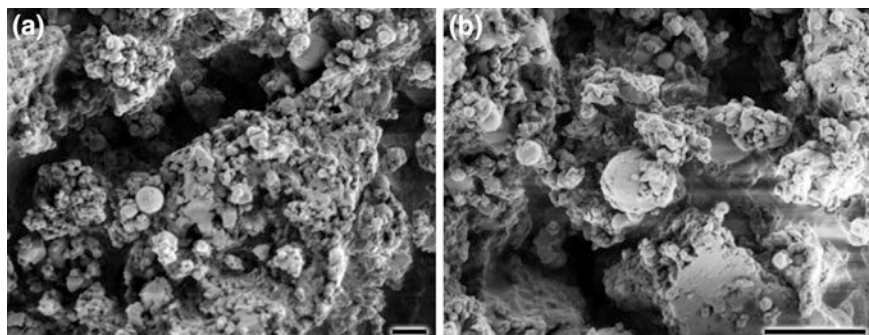


Fig. 10 Morphology of the amorphous strontium-polyP microparticles “Sr-a-polyP-MP” (a); SEM. **b** Higher magnification. Bar 1 μm (modified from Müller et al. 2016b)

Only the amorphous materials show biological activity. These particles are biodegradable (hydrolysis by ALP) (Müller et al. 2016b). We demonstrated that Sr-a-polyP-MP exhibit a markedly higher stimulatory effect on growth and mineralization of human mesenchymal stem cells [MSC] and SaOS-2 cells than calcium-polyP microparticles and cause a strong upregulation of the expression of the genes encoding for ALP and BMP-2 in SaOS-2 cells (Müller et al. 2016b). On the other hand, the expression of osteocyte-specific *sclerostin* gene (*SOST* gene) that acts as a negative regulator of the Wnt signaling pathway and inhibitor of bone cell differentiation and mineralization was only slightly changed by Sr-a-polyP-MP, in contrast to Ca-a-polyP-MP that strongly enhances the expression of this gene. Sclerostin is expressed in osteocytes but also in SaOS-2 cells. These effects on *sclerostin* expression, found in in vitro experiments (SaOS-2 cells) under ambient conditions (21% O_2 tension) (Müller et al. 2016b), might be of disadvantage to Sr-a-polyP-MP, in particular to Ca-a-polyP-MP, and are not in line with the very positive results obtained in vivo animal experiments (Müller et al. 2016b). The reason might be that under hypoxic/normoxic conditions, Ca-a-polyP-MP strongly upregulates the expression of HIF-1/2, as revealed in SaOS-2 cells (Müller et al. 2016a). It has been proposed that HIF-1 becomes stabilized under hypoxia and induces the expression of *gremlin* and *noggin* that inhibit BMP2, resulting in a decreased phosphorylation of Smad and a decrease in *SOST* expression (Fujiwara et al. 2016). A reduced *SOST* expression under hypoxia has also been reported by other authors (Genetos et al. 2010).

Besides Sr-a-polyP-MP, polyP complexed with trivalent cations, such as Gd^{3+} (polyP-Gd) have been shown to exhibit a strong morphogenetic activity (Wang et al. 2016a). The polyP-Gd displays a strong potency to induce bone HA formation in vitro (SaOS-2 cells), as well as ALP activity, in a synergistic manner, if compared with polyP (as calcium salt) and GdCl_3 alone, paving the way for a further class of polyP-based potential anti-osteoporotic agents.

Acknowledgements W.E.G. Müller is a holder of an ERC Advanced Investigator Grant (no. 268476 “BIOSILICA”) as well as of the two ERC Proof-of-Concept grants “Si-Bone-PoC” (no. 324564) and “MorphoVES-PoC” (No. 662486). This work was supported by grants from the European Commission (large-scale integrating project “BlueGenics” No. 266033 and project “Bio-Scaffolds” No. 604036), as well as the BiomaTiCS research initiative of the University Medical Center Mainz.

References

- Abramov AY, Fraley C, Diao CT, Winkfein R, Colicos MA, Duchon MR, French RJ, Pavlov E (2007) Targeted polyphosphatase expression alters mitochondrial metabolism and inhibits calcium-dependent cell death. *Proc Natl Acad Sci USA* 104:18091–18096
- Adachi JD (1997) Corticosteroid-induced osteoporosis. *Am J Med Sci* 313:41–49
- Adell T, Nefkens I, Müller WEG (2003) Polarity factor ‘Frizzled’ in the demosponge *Suberites domuncula*: identification, expression and localization of the receptor in the epithelium/pinacoderm. *FEBS Lett* 554:363–368
- Adell T, Thakur AN, Müller WEG (2007) Isolation and characterization of Wnt pathway-related genes from Porifera. *Cell Biol Int* 31:939–949
- Agholme F, Isaksson H, Kuhstoss S, Aspenberg P (2011) The effects of Dickkopf-1 antibody on metaphyseal bone and implant fixation under different loading conditions. *Bone* 48:988–996
- Ahmadian M, Suh JM, Hah N, Liddle C, Atkins AR, Downes M, Evans RM (2013) PPAR γ signaling and metabolism: the good, the bad and the future. *Nat Med* 19:557–566
- Ahn V, Chu M, Choi H, Tran D, Abo A, Weis W (2011) Structural basis of Wnt signaling inhibition by Dickkopf binding to LRP5/6. *Dev Cell* 21:862–873
- Akune T (2004) The role of insuline receptor substrates in bone metabolism. *Clin Calcium* 14:289–292
- Anastasilakis AD, Polyzos SA, Avramidis A, Toulis KA, Papatheodorou A, Terpos E (2010) The effect of teriparatide on serum Dickkopf-1 levels in postmenopausal women with established osteoporosis. *Clin Endocrinol* 72:752–757
- Aspenberg P (2006) Osteonecrosis of the jaw: what do bisphosphonates do? *Expert Opin Drug Saf* 5:743–745
- Atchison D, Harding P, Beierwaltes W (2011) Hypercalcemia reduces plasma renin via parathyroid hormone, renal interstitial calcium, and the calcium-sensing receptor. *Hypertension* 58:604–610
- Austin K, Markovic MA, Brubaker PL (2016) Current and potential therapeutic targets of glucagon-like peptide-2. *Curr Opin Pharmacol* 31:13–18
- Balan G, Bauman J, Bhattacharya S, Castrodad M, Healy DR, Herr M, Humphries P, Jennings S, Kalgutkar AS, Kapinos B, Khot V, Lazarra K, Li M, Li Y, Neagu C, Oliver R, Piotrowski DW, Price D, Qi H, Simmons HA, Southers J, Wei L, Zhang Y, Paralkar VM (2009) The discovery of novel calcium sensing receptor negative allosteric modulators. *Bioorg Med Chem Lett* 19:3328–3332
- Barille S, Pellat-Deceunynck C, Bataille R, Amiot M (1996) Ectopic secretion of osteocalcin, the major non-collagenous bone protein, by the myeloma cell line NCI-H929. *J Bone Miner Res* 11:466–471
- Baron R, Hesse E (2012) Update on bone anabolics in osteoporosis treatment: rationale, current status and perspectives. *J Clin Endocrinol Metab* 97:311–325
- Baron R, Kneissel M (2013) WNT signaling in bone homeostasis and disease: from human mutations to treatments. *Nat Med* 19:179–192
- Barruet E, Morales BM, Lwin W, White MP, Theodoris CV, Kim H, Urrutia A, Wong SA, Srivastava D, Hsiao EC (2016) The ACVR1 R206H mutation found in fibrodysplasia ossificans progressiva increases human induced pluripotent stem cell-derived endothelial cell

- formation and collagen production through BMP-mediated SMAD1/5/8 signaling. *Stem Cell Res Ther* 7:15. doi:[10.1186/s13287-016-0372-6](https://doi.org/10.1186/s13287-016-0372-6)
- Betts AM, Clark TH, Yang J, Treadway JL, Li M, Giovanelli MA, Abdiche Y, Stone DM, Paralkar VM (2010) The application of target information and preclinical pharmacokinetic/pharmacodynamic modeling in predicting clinical doses of a Dickkopf-1 antibody for osteoporosis. *J Pharmacol Exp Ther* 1:2–13
- Bhagwat S, Haytowitz DB, Holden JM (2011) USDA database for the flavonoid content of selected foods; release 3. US Department of Agriculture, Beltsville
- Blake G, Fogelman I (2007) Role of dual-energy X-ray absorptiometry in the diagnosis and treatment of osteoporosis. *J Clin Densitom* 10:102–110
- Blick SK, Dhillon S, Keam SJ (2009) Spotlight on teriparatide in osteoporosis. *BioDrugs* 23: 197–199
- Bone HG, McClung MR, Roux C, Recker RR, Eisman JA, Verbruggen N (2010) Odanacatib, a cathepsin-K inhibitor for osteoporosis: a two year study in postmenopausal women with low bone density. *J Bone Miner Res* 25:937–947
- Bone HG, Chapurlat R, Brandi ML, Brown JP, Czerwinski E, Krieg MA, Mellström D, Radominski SC, Reginster JY, Resch H, Ivorra JA, Roux C, Vittinghoff E, Daizadeh NS, Wang A, Bradley MN, Franchimont N, Geller ML, Wagman RB, Cummings SR, Papapoulos S (2013) The effect of three or six years of denosumab exposure in women with postmenopausal osteoporosis: results from the FREEDOM extension. *J Clin Endocrinol Metab* 98:4483–4489
- Bonnelye EA, Saltel F, Jurdic P (2008) Dual effect of strontium ranelate: stimulation of osteoblast differentiation and inhibition of osteoclast formation and resorption in vitro. *Bone* 42:129–138
- Boudin E, Fijalkowski I, PETERS E, Van Hul W (2013) The role of extracellular modulators of canonical Wnt signaling in bone metabolism and diseases. *Semin Arthritis Rheum* 43:220–240
- Branca F (2003) Dietary phyto-oestrogens and bone health. *Proc Nutr Soc* 62:877–887
- Bringhurst F (2002) PTH receptors and apoptosis in osteocytes. *J Musculoskelet Neuronal Interact* 2:245–251
- Brown E (2007) The calcium-sensing receptor: physiology, pathophysiology and CaR-based therapeutics. *Subcell Biochem* 45:139–167
- Brown EM, MacLeod RJ (2001) Extracellular calcium sensing and extracellular calcium signaling. *Physiol Rev* 81:239–297
- Bucay N, Sarosi I, Dunstan CR, Morony S, Tarpley J, Capparelli C, Scully S, Tan HL, Xu W, Lacey DL, Boyle WJ, Simonet WS (1998) Osteoprotegerin-deficient mice develop early onset osteoporosis and arterial calcification. *Genes Dev* 12:1260–1268
- Bullamore JR, Wilkinson R, Gallagher JC, Nordin BE, Marshall DH (1970) Effect of age on calcium absorption. *Lancet* 2(7672):535–537
- Butler JS, Murray DW, Hurson CJ, O'Brien J, Doran PP, O'Bryne JM (2011) The role of Dkk1 in bone mass regulation: correlating serum Dkk1 expression with bone mineral density. *J Orthop Res* 29:414–418
- Cabal A, Mehta K, Ross DS, Shrestha RP, Comisar W, Denker A, Pai SM, Ishikawa T (2013) A semimechanistic model of the time-course of release of PTH into plasma following administration of the calcilytic JTT-305/MK-5442 in humans. *Bone Miner Res* 28:1830–1836
- Canalis E (2013) Wnt signaling in osteoporosis: mechanisms and novel therapeutic approaches. *Nat Rev Endocrinol* 9:575–583
- Canalis E, Hott M, Deloffre P, Tsouderos Y, Marie PJ (1996) The divalent strontium salt S12911 enhances bone cell replication and bone formation in vitro. *Bone* 18:517–523
- Choi H, Dieckmann M, Herz J, Niemeier A (2009) Lrp4, a novel receptor for Dickkopf 1 and sclerostin, is expressed by osteoblasts and regulates bone growth and turnover in vivo. *PLoS ONE* 4:e7930
- Cohen-Kfir E, Artsi H, Levin A, Abramowitz E, Bajayo A, Gurt I, Zhong L, D'Urso A, Toiber D, Mostoslavsky R, Dresner-Pollak R (2011) Sirt1 is a regulator of bone mass and a repressor of SOST encoding for sclerostin, a bone formation inhibitor. *Endocrinology* 152:4514–4524
- Compton JT, Lee FY (2014) A review of osteocyte function and the emerging importance of sclerostin. *J Bone Joint Surg Am* 96:1659–1668

- Cook F, Mumm S, Whyte M, Wenkert D (2014) Pregnancy-associated osteoporosis with a heterozygous deactivating LDL receptor-related protein 5 (LRP5) mutation and a homozygous methylenetetrahydrofolate reductase (MTHFR) polymorphism. *J Bone Miner Res* 29:922–928
- Costa AG, Cusano NE, Silva BC, Cremers S, Bilezikian JP (2011) Cathepsin K: its skeletal actions and role as a therapeutic target in osteoporosis. *Nat Rev Rheumatol* 7:447–456
- Cummings SR, Melton LJ (2002) Epidemiology and outcomes of osteoporotic fractures. *Lancet* 359:1761–1767
- Cummings SR, San Martin J, McClung MR, Siris ES, Eastell R, Reid IR, Delmas P, Zoog HB, Austin M, Wang A, Kutilek S, Adams S, Zanchetta J, Libanati C, Siddhanti S, Christiansen C, Trial FREEDOM (2009) Denosumab for prevention of fractures in postmenopausal women with osteoporosis. *N Engl J Med* 361:756–765
- Cummings SR, Ensrud K, Delmas PD, LaCroix AZ, Vukicevic S, Reid DM, Goldstein S, Sriram U, Lee A, Thompson J, Armstrong RA, Thompson DD, Powles T, Zanchetta J, Kendler D, Neven P, Eastell R; PEARL Study Investigators (2010) Lasofoxifene in postmenopausal women with osteoporosis. *N Engl J Med* 362:686–696
- Dalle Carbonare L, Innamorati G, Valenti MT (2012) Transcription factor Runx2 and its application to bone tissue engineering. *Stem Cell Rev* 8:891–897
- Davidge Pitts CJ, Kearns A (2011) Update on Medications with adverse skeletal effects. *Mayo Clin Proc* 86:338–343
- Deal C (2009) Potential new drug targets for osteoporosis. *Nat Clin Pract Rheumatol* 5:20–27
- Devogelaer J (2000) Treatment of bone diseases with bisphosphonates, excluding osteoporosis. *Curr Opin Rheumatol* 12:331–335
- Di Carlo G, Mascolo N, Izzo AA, Capasso F (1999) Flavonoids: old and new aspects of a class of natural therapeutic drugs. *Life Sci* 65:337–353
- Diarra D, Stolina M, Polzer K, Zwerina J, Ominsky MS, Dwyer D (2007) Dickkopf-1 is a master regulator of joint remodeling. *Nat Med* 13:156–163
- Drozen MS, Foley JF (2007) Gras notification: alpha-glycosyl isoquercitrin. <http://www.fda.gov/ucm/groups/fdagov-public/@fdagov-foods-gen/docu-ments/document/ucm269110.pdf>
- Dunnick JK, Hailey JR (1992) Toxicity and carcinogenicity studies of quercetin, a natural component of foods. *Fundam Appl Toxicol* 19:423–431
- Eisman JA, Bone HG, Hosking DJ, McClung MR, Reid IR, Rizzoli R (2011) Odanacatib in the treatment of postmenopausal women with low bone mineral density: three year continued therapy and resolution effect. *J Bone Miner Res* 26:242–251
- Fajardo RJ, Manoharan RK, Pearsall RS, Davies MV, Marvell T, Monnell TE, Ucran JA, Pearsall AE, Khanzode D, Kumar R, Underwood KW, Roberts B, Seehra J, Boussein ML (2010) Treatment with a soluble receptor for activin improves bone mass and structure in the axial and appendicular skeleton of female cynomolgus macaques (*Macaca fascicularis*). *Bone* 46:64–71
- Fleisch H (2002) Development of bisphosphonates. *Breast Cancer Res* 4:30–34
- Fleisch H, Straumann F, Schenk R, Bisaz S, Allgöwer M (1966) Effect of condensed phosphates on calcification of chick embryo femurs in tissue culture. *Am J Physiol* 211:821–825
- Fraher LJ, Avram R, Watson PH, Hendy GN, Henderson JE, Chong KL, Goltzman D, Morley P, Willick GE, Whitfield JF, Hodsman AB (1999) Comparison of the biochemical responses to human parathyroid hormone-(1–31)NH₂ and hPTH-(1–34) in healthy humans. *J Clin Endocrinol Metab* 84:2739–2743
- Fraser W, Ahmad A, Vora J (2004) The physiology of the circadian rhythm of parathyroid hormone and its potential as a treatment for osteoporosis. *Curr Opin Nephrol Hypertens* 13:437–444
- Fromigie O, Hay E, Barbara A, Petrel C, Traiffort E, Ruat M, Marie PJ (2009) Calcium sensing receptor-dependent and receptor-independent activation of osteoblast replication and survival by strontium ranelate. *J Cell Mol Med* 13:2189–2199
- Fujiwara M, Kubota T, Wang W, Ohata Y, Miura K, Kitaoka T, Okuzaki D, Namba N, Michigami T, Kitabatake Y, Ozono K (2016) Successful induction of sclerostin in

- human-derived fibroblasts by 4 transcription factors and its regulation by parathyroid hormone, hypoxia, and prostaglandin E2. *Bone* 85:91–98
- Gallagher JC, Tella SH (2014) Prevention and treatment of postmenopausal osteoporosis. *J Steroid Biochem Mol Biol* 142:155–170
- Gardner MJ, Demetrakopoulos D, Shindle MK, Griffith MH, Lane JM (2006) Osteoporosis and skeletal fractures. *HSS J* 2:62–69
- Garnero P (2008) Biomarkers for osteoporosis management: utility in diagnosis, fracture risk prediction and therapy monitoring. *Mol Diagn Ther* 12:157–170
- Gaudio A, Privitera F, Battaglia K, Torrisi V, Sidoti M, Pulvirenti I, Canzonieri E, Tringali G, Fiore CE (2012) Sclerostin levels associated with inhibition of the Wnt/ β -catenin signaling and reduced bone turnover in type 2 diabetes mellitus. *J Clin Endocrinol Metab* 97:3744–3750
- Gauthier JY, Chauret N, Cromlish W, Desmarais S, Duong LT, Falguyet JP, Kimmel DB, Lamontagne S, Léger S, LeRiche T, Li CS, Massé F, McKay DJ, Nicoll-Griffith DA, Oballa RM, Palmer JT, Percival MD, Riendeau D, Robichaud J, Rodan GA, Rodan SB, Seto C, Thérien M, Truong VL, Venuti MC, Wesolowski G, Young RN, Zamboni R, Black WC (2008) The discovery of odanacatib (MK-0822), a selective inhibitor of cathepsin K. *Bioorg Med Chem Lett* 18:923–928
- Genetos DC, Toupadakis CA, Raheja LF, Wong A, Papanicolaou SE, Fyhrie DP, Loots GG, Yellowley CE (2010) Hypoxia decreases sclerostin expression and increases Wnt signaling in osteoblasts. *J Cell Biochem* 110:457–467
- Glantschnig H, Hampton R, Lu P, Zhao J, Vitelli S, Huang L, Haytko P, Cusick T, Ireland C, Jarantow SW, Ernst R, Wei N, Nantermet P, Scott KR, Fisher JE, Talamo F, Orsatti L, Reszka AA, Sandhu P, Kimmel D, Flores O, Strohl W, An Z, Wang F (2010) Generation and selection of novel fully human monoclonal antibodies that neutralize Dickkopf-1 (DKK1) inhibitory function in vitro and increase bone mass in vivo. *J Biol Chem* 285:40135–40147
- Glantschnig H, Scott K, Hampton R, Wei N, Mccracken P, Nantermet P, Zhao JZ, Vitelli S, Huang L, Haytko P, Lu P, Fisher JE, Sandhu P, Cook J, Williams D, Strohl W, Flores O, Kimmel D, Wang F, An Z (2011) A rate-limiting role for Dickkopf-1 in bone formation and the remediation of bone loss in mouse and primate models of postmenopausal osteoporosis by an experimental therapeutic antibody. *J Pharmacol Exp Ther* 338:568–578
- Gowen M, Stroup GB, Dodds RA, James IE, Votta BJ, Smith BR, Bhatnagar PK, Lago AM, Callahan JF, DelMar EG, Miller MA, Nemeth EF, Fox J (2000) Antagonizing the parathyroid calcium receptor stimulates parathyroid hormone secretion and bone formation in osteopenic rats. *J Clin Invest* 105:1595–1604
- Gu Z, Zhang X, Li L, Wang Q, Yu X, Feng T (2013) Acceleration of segmental bone regeneration in a rabbit model by strontium-doped calcium polyphosphate scaffold through stimulating VEGF and bFGF secretion from osteoblasts. *Mater Sci Eng C* 33:274–281
- Guder C, Pinho S, Nacak TG, Schmidt HA, Hobmayer B, Niehrs C, Holstein TW (2006) An ancient Wnt-Dickkopf antagonism in Hydra. *Development* 133:901–911
- Hannon RA, Clack G, Rimmer M, Swaisland A, Lockton JA, Finkelman RD, Eastell R (2010) Effects of the Src kinase inhibitor saracatinib (AZD0530) on bone turnover in healthy men: a randomized, double-blind, placebo-controlled, multiple-ascending-dose phase I trial. *J Bone Miner Res* 25:463–471
- Heiland GR, Zwerina K, Baum W, Kireva T, Distler JH, Grisanti M, Asuncion F, Li X, Ominsky M, Richards W, Schett G, Zwerina J (2010) Neutralisation of Dkk-1 protects from systemic bone loss during inflammation and reduces sclerostin expression. *Ann Rheum Dis* 69:2152–2159
- Henriksen DB, Alexandersen P, Byrjalsen I, Hartmann B, Bone HG, Christiansen C, Holst JJ (2004) Reduction of nocturnal rise in bone resorption by subcutaneous GLP-2. *Bone* 34:140–147
- Henriksen DB, Alexandersen P, Hartmann B, Adrian CL, Byrjalsen I, Bone HG, Holst JJ, Christiansen C (2009) Four-month treatment with GLP-2 significantly increases hip BMD: a randomized, placebo-controlled, dose-ranging study in postmenopausal women with low BMD. *Bone* 45:833–842

- Henriksen K, Andersen JR, Riis BJ, Mehta N, Tavakkol R, Alexandersen P, Byrjalsen I, Valter I, Nedergaard BS, Teglbaerg CS, Stern W, Sturmer A, Mitta S, Nino AJ, Fitzpatrick LA, Christiansen C, Karsdal MA (2013) Evaluation of the efficacy, safety and pharmacokinetic profile of oral recombinant human parathyroid hormone [rhPTH(1–31)NH₂] in postmenopausal women with osteoporosis. *Bone* 53:160–166
- Hessle L, Johnson KA, Anderson HC, Narisawa S, Sali A, Goding JW, Terkeltaub R, Millan JL (2002) Tissue-nonspecific alkaline phosphatase and plasma cell membrane glycoprotein-1 are central antagonistic regulators of bone mineralization. *Proc Natl Acad Sci USA* 99:9445–9449
- Hoepfner L, Secreto F, Westendorf J (2009) Wnt signaling as a therapeutic target for bone diseases. *Expert Opin Ther Targets* 13:485–496
- Hofbauer LC, Khosla S, Dunstan CR, Lacey DL, Boyle WJ, Riggs BL (2000) The roles of osteoprotegerin and osteoprotegerin ligand in the paracrine regulation of bone resorption. *J Bone Miner Res* 15:2–12
- Hopkins RB, Tarride JE, Leslie WD, Metge C, Lix LM, Morin S, Finlayson G, Azimaee M, Pullenayegum E, Goeree R, Adachi JD, Papaioannou A, Thabane L (2013) Estimating the excess costs for patients with incident fractures, prevalent fractures, and nonfracture osteoporosis. *Osteoporos Int* 24:581–593
- Itoh T, Takeda S, Akao Y (2010) MicroRNA-208 modulates BMP-2-stimulated mouse preosteoblast differentiation by directly targeting V-ets erythroblastosis virus E26 oncogene homolog 1. *J Biol Chem* 285:27745–27752
- Itoh T, Ando M, Tsukamasa Y, Akao Y (2012) Expression of BMP-2 and Ets1 in BMP-2-stimulated mouse pre-osteoblast differentiation is regulated by microRNA-370. *FEBS Lett* 586:1693–1701
- Jang WG, Kim EJ, Kim DK, Ryoo HM, Lee KB, Kim SH, Choi HS, Koh JT (2012) BMP2 protein regulates osteocalcin expression via Runx2-mediated Atf6 gene transcription. *J Biol Chem* 287:905–915
- John MR, Widler L, Gamse R, Buhl T, Seuwen K, Breitenstein W, Bruin GJ, Belleli R, Klickstein LB, Kneissel M (2011) ATF936, a novel oral calcilytic, increases bone mineral density in rats and transiently releases parathyroid hormone in humans. *Bone* 49:233–241
- Johnson KA, Hessle L, Vaingankar S, Wennberg C, Mauro S, Narisawa S, Goding JW, Sano K, Millan JL, Terkeltaub R (2000) Osteoblast tissue-nonspecific alkaline phosphatase antagonizes and regulates PC-1. *Am J Physiol Regul Integr Comp Physiol* 279:R1365–R1377
- Kalinova J, Vrchotova N (2009) Level of catechin, myricetin, quercetin and isoquercitrin in buckwheat (*Fagopyrum esculentum* Moench), changes of their levels during vegetation and their effect on the growth of selected weeds. *J Agric Food Chem* 57:2719–2725
- Kanis JA (1994) WHO Study Group. Assessment of fracture risk and its application to screening for postmenopausal osteoporosis: synopsis of a WHO report. *Osteoporos Int* 4:368–381
- Khan A, Khan A (2006) Anabolic agents: a new chapter in the management of osteoporosis. *J Obstet Gynaecol Can* 28:136–141
- Khosla S, Burr D, Cauley J, Dempster DW, Ebeling PR, Felsenberg D, Gagel RF, Gilsanz V, Guise T, Koka S, McCauley LK, McGowan J, McKee MD, Mohla S, Pendrys DG, Raisz LG, Ruggiero SL, Shafer DM, Shum L, Silverman SL, Van Poznak CH, Watts N, Woo SB, Shane E; American Society for Bone and Mineral Research (2007) Bisphosphonate-associated osteonecrosis of the jaw: report of a task force of the American Society for Bone and Mineral Research. *J Bone Miner Res* 22:1479–1491
- Kim HJ, Kim SH (2010) Tanshinone IIA enhances BMP-2-stimulated commitment of C2C12 cells into osteoblasts via p38 activation. *Amino Acids* 39:1217–1226
- Kim YJ, Bae YC, Suh KT, Jung JS (2006) Quercetin, a flavonoid, inhibits proliferation and increases osteogenic differentiation in human adipose stromal cells. *Biochem Pharmacol* 72:1268–1278
- Kim JB, Leucht P, Lam K, Luppen C, Ten Berge D, Nusse R, Helms JA (2007) Bone regeneration is regulated by wnt signaling. *J Bone Miner Res* 22:1913–1923
- Kim JH, Liu X, Wang J, Chen X, Zhang H, Kim SH, Cui J, Li R, Zhang W, Kong Y, Zhang J, Shui W, Lamplot J, Rogers MR, Zhao C, Wang N, Rajan P, Tomal J, Statz J, Wu N, Luu HH,

- Haydon RC, He TC (2013) Wnt signaling in bone formation and its therapeutic potential for bone diseases. *Ther Adv Musculoskelet Dis* 5:13–31
- Kong WN (2012) Potential role of odanacatib in the treatment of osteoporosis. *Clin Interv Aging* 12:235–247
- Kornberg A, Rao NN, Ault-Riche D (1999) Inorganic polyphosphate: a molecule of many functions. *Annu Rev Biochem* 68:89–125
- Košínová P, Berka K, Wykes M, Otyepka M, Trouillas P (2012) Positioning of antioxidant quercetin and its metabolites in lipid bilayer membranes: implication for their lipid-peroxidation inhibition. *J Phys Chem B* 116:1309–1318
- Kulkarni NH, Onyia JE, Zeng Q, Tian X, Liu M, Halladay DL, Frolik CA, Engler T, Wei T, Kriauciunas A, Martin TJ, Sato M, Bryant HU, Ma YL (2006) Orally bioavailable GSK-3 α /beta dual inhibitor increases markers of cellular differentiation in vitro and bone mass in vivo. *J Bone Miner Res* 21:910–920
- Kumar S, Matheny CJ, Hoffman SJ, Marquis RW, Schultz M, Liang X, Vasko JA, Stroup GB, Vaden VR, Haley H, Fox J, DelMar EG, Nemeth EF, Lago AM, Callahan JF, Bhatnagar P, Huffman WF, Gowen M, Yi B, Danoff TM, Fitzpatrick LA (2010) An orally active calcium-sensing receptor antagonist that transiently increases plasma concentrations of PTH and stimulates bone formation. *Bone* 46:534–542
- Lane NE (2006) Epidemiology, etiology, and diagnosis of osteoporosis. *Am J Obstet Gynecol* 194 (Suppl):S3–S11
- Langdahl B, Binkley N, Bone H, Gilchrist N, Resch H, Rodriguez Portales J, Denker A, Lombardi A, Le Bailly De Tillegem C, Dasilva C, Rosenberg E, Leung A (2012) Danacatib in the treatment of postmenopausal women with low bone mineral density: five years of continued therapy in a phase 2 study. *J Bone Miner Res* 27:2251–2258
- Lee D, Kim H, Ku S, Kim S, Choi Y, Kim J (2010) Association between polymorphisms in Wnt signaling pathway genes and bone mineral density in postmenopausal Korean women. *Menopause* 17:1064–1070
- Leibbrandt A, Penninger JM (2008) RANK/RANKL: regulators of immune responses and bone physiology. *Ann NY Acad Sci* 1143:123–150
- Lengfeld T, Watanabe H, Simakov O, Lindgens D, Gee L, Law L, Schmidt HA, Ozbek S, Bode H, Holstein TW (2009) Multiple Wnts are involved in *Hydra* organizer formation and regeneration. *Dev Biol* 330:186–199
- Lewiecki E (2013) Monoclonal antibodies for the treatment of osteoporosis. *Expert Opin Biol Ther* 13:183–196
- Leyhausen G, Lorenz B, Zhu H, Geurtsen W, Bohnensack R, Müller WEG, Schröder HC (1998) Inorganic polyphosphate in human osteoblast-like cells. *J Bone Miner Res* 13:803–812
- Li J, Sarosi I, Cattlely RC, Pretorius J, Asuncion F, Grisanti M, Morony S, Adamu S, Geng Z, Qiu W, Kostenuik P, Lacey DL, Simonet WS, Bolon B, Qian X, Shalhoub V, Ominsky MS, Zhu Ke H, Li X, Richards WG (2006) Dkk1-mediated inhibition of Wnt signaling in bone results in osteopenia. *Bone* 39:754–766
- Li X, Ominsky MS, Warmington KS, Morony S, Gong J, Cao J, Gao Y, Shalhoub V, Tipton B, Haldankar R, Chen Q, Winters A, Boone T, Geng Z, Niu QT, Ke HZ, Kostenuik PJ, Simonet WS, Lacey DL, Paszty C (2009) Sclerostin antibody treatment increases bone formation, bone mass, and bone strength in a rat model of postmenopausal osteoporosis. *J Bone Miner Res* 24:578–588
- Li X, Warmington KS, Niu QT, Asuncion FJ, Barrero M, Grisanti M, Dwyer D, Stouch B, Thway TM, Stolina M, Ominsky MS, Kostenuik PJ, Simonet WS, Paszty C, Ke HZ (2010) Inhibition of sclerostin by monoclonal antibody increases bone formation, bone mass, and bone strength in aged male rats. *J Bone Miner Res* 25:2647–2656
- Li X, Grisanti M, Fan W, Asuncion FJ, Tan HL, Dwyer D, Han CY, Yu L, Lee J, Lee E, Barrero M, Kurimoto P, Niu QT, Geng Z, Winters A, Horan T, Stevenson S, Jacobsen F, Chen Q, Haldankar R, Lavallee J, Tipton B, Daris M, Sheng J, Lu HS, Daris K, Deshpande R, Valente EG, Salimi-Moosavi H, Kostenuik PJ, Li J, Liu M, Li C, Lacey DL, Simonet WS, Ke HZ, Babij P, Stolina M, Ominsky MS, Richards WG (2011) Dickkopf-1 regulates bone

- formation in young growing rodents and upon traumatic injury. *J Bone Miner Res* 26: 2610–2621
- Lim V, Clarke B (2012) New therapeutic targets for osteoporosis: beyond denosumab. *Maturitas* 73:269–272
- Lindsay R (1996) The menopause and osteoporosis. *Obstet Gynecol* 87:16S–19S
- Lorenz B, Schröder HC (2001) Mammalian intestinal alkaline phosphatase acts as highly active exopolyphosphatase. *Biochim Biophys Acta* 1547:254–261
- Lorenz B, Münkner J, Oliveira MP, Kuusksalu A, Leitão JM, Müller WEG, Schröder HC (1997) Changes in metabolism of inorganic polyphosphate in rat tissues and human cells during development and apoptosis. *Biochim Biophys Acta* 1335:51–60
- MacLean C, Newberry S, Maglione M, McMahon M, Ranganath V, Suttrop M, Mojica W, Timmer M, Alexander A, McNamara M, Desai SB, Zhou A, Chen S, Carter J, Tringale C, Valentine D, Johnsen B, Grossman J (2008) Systematic review: comparative effectiveness of treatments to prevent fractures in men and women with low bone density or osteoporosis. *Ann Intern Med* 148:197–213
- Maeda A, Okazaki M, Baron DM, Dean T, Khatri A, Mahon M, Segawa H, Abou-Samra AB, Jüppner H, Bloch KD, Potts JT Jr, Gardella TJ (2013) Critical role of parathyroid hormone (PTH) receptor-1 phosphorylation in regulating acute responses to PTH. *Proc Natl Acad Sci USA* 110:5864–5869
- Malinauskas T, Jones EY (2014) Extracellular modulators of Wnt signalling. *Curr Opin Struct Biol* 29:77–84
- Mao B, Wu W, Davidson G, Marhold J, Li M, Mechler BM, Delius H, Hoppe D, Stanek P, Walter C, Glinka A, Niehrs C (2002) Kremen proteins are Dickkopf receptors that regulate Wnt/ β -catenin signalling. *Nature* 417:664–667
- Marenzana M, Greenslade K, Eddleston A, Okoye R, Marshall D, Moore A, Robinson MK (2011) Sclerostin antibody treatment enhances bone strength but does not prevent growth retardation in young mice treated with dexamethasone. *Arthritis Rheum* 63:2385–2395
- Marie PJ (2006) Strontium ranelate: a dual mode of action rebalancing bone turnover in favour of bone formation. *Curr Opin Rheumatol* 18(Suppl1):S11–S15
- McColm J, Hu L, Womack T, Tang CC, Chiang AY (2014) Single- and multiple-dose randomized studies of blosozumab, a monoclonal antibody against sclerostin, in healthy postmenopausal women. *J Bone Miner Res* 29:935–943
- Mezesova L, Bartekova M, Javorkova V, Vlkovicova J, Breier A, Vrbjar N (2010) Effect of quercetin on kinetic properties of renal Na, K-ATPase in normotensive and hypertensive rats. *J Physiol Pharmacol* 61:593–598
- Miller PD, Chines AA, Christiansen C (2008) Effects of bazedoxifene on BMD and bone turnover in postmenopausal women: 2-yr results of a randomized, double-blind, placebo-, and active-controlled study. *J Bone Miner Res* 23:525–535
- Minisola G, Iuliano A, Prevete I (2014) Emerging therapies for osteoporosis. *Reumatismo* 66:112–124
- Miyazaki T, Sanjay A, Neff L, Tanaka S, Home WC, Baron R (2004) Src kinase activity is essential for osteoclast function. *J Biol Chem* 279:17660–17666
- Morrissey JH, Choi SH, Smith SA (2012) Polyphosphate: an ancient molecule that links platelets, coagulation, and inflammation. *Blood* 119:5972–5979
- Mosley J (2000) Osteoporosis and bone functional adaptation: mechanobiological regulation of bone architecture in growing and adult bone, a review. *J Rehabil Res Dev* 37:189–199
- Müller WEG, Wang XH, Diehl-Seifert B, Kropf K, Schloßmacher U, Lieberwirth I, Glasser G, Wiens M, Schröder HC (2011) Inorganic polymeric phosphate/polyphosphate as an inducer of alkaline phosphatase and a modulator of intracellular Ca^{2+} level in osteoblasts (SaOS-2 cells) in vitro. *Acta Biomater* 7:2661–2671

- Müller WEG, Schröder HC, Schlossmacher U, Grebenjuk VA, Ushijima H, Wang XH (2013a) Induction of carbonic anhydrase in SaOS-2 cells, exposed to bicarbonate and consequences for calcium phosphate crystal formation. *Biomaterials* 34:8671–8680
- Müller WEG, Wang XH, Grebenjuk V, Diehl-Seifert B, Steffen R, Schloßmacher U, Trautwein A, Neumann S, Schröder HC (2013b) Silica as a morphogenetically active inorganic polymer: effect on the BMP-2-dependent and RUNX2-independent pathway in osteoblast-like SaOS-2 cells. *Biomater Sci* 1:669–678
- Müller WEG, Tolba E, Feng QL, Schröder HC, Markl JS, Kokkinopoulou M, Wang XH (2015a) Amorphous Ca²⁺ polyphosphate nanoparticles regulate the ATP level in bone-like SaOS-2 cells. *J Cell Sci* 128:2202–2207
- Müller WEG, Tolba E, Schröder HC, Wang XH (2015b) Polyphosphate: a morphogenetically active implant material serving as metabolic fuel for bone regeneration. *Macromol Biosci* 15:1182–1197
- Müller WEG, Tolba E, Schröder HC, Wang SF, Glaßer G, Muñoz-Espí R, Link T, Wang XH (2015c) A new polyphosphate calcium material with morphogenetic activity. *Mater Lett* 148:163–166
- Müller WEG, Schröder HC, Tolba E, Neufurth M, Diehl-Seifert B, Wang XH (2016a) Mineralization of bone-related SaOS-2 cells under physiological hypoxic conditions. *FEBS J* 283:74–87
- Müller WEG, Tolba E, Neufurth M, Wang SF, Ackermann M, Feng QL, Schröder HC, Wang XH (2016b) Fabrication of amorphous strontium polyphosphate microparticles that induce mineralization of bone cells in vitro and in vivo. Submitted
- Murakami T, Saito A, Hino S, Kondo S, Kanemoto S, Chihara K, Sekiya H, Tsumagari K, Ochiai K, Yoshinaga K, Saitoh M, Nishimura R, Yoneda T, Kou I, Furuichi T, Ikegawa S, Ikawa M, Okabe M, Wanaka A, Imaizumi K (2009) Signalling mediated by the endoplasmic reticulum stress transducer OASIS is involved in bone formation. *Nat Cell Biol* 11:1205–1211
- Murphy MG, Cerchio S, Stoch A, Gottesdiener K, Wu M, Recker R (2005) Effect of L000845704, an $\alpha\beta 3$ integrin antagonist, on markers of bone turnover and bone mineral density in postmenopausal osteoporotic women. *J Clin Endocrinol Metab* 90:2022–2028
- Neer RM, Arnaud CD, Zanchetta JR, Prince R, Gaich GA, Reginster JY, Hodsman AB, Eriksen EF, Ish-Shalom S, Genant HK, Wang O, Mitlak BH (2001) Effect of parathyroid hormone (1-34) on fractures and bone mineral density in postmenopausal women with osteoporosis. *N Engl J Med* 344:1434–1441
- Nemeth EF (2002) The search for calcium receptor antagonists (calcilytics). *J Mol Endocrinol* 29:15–21
- Nemeth E (2004) Calcimimetic and calcilytic drugs: just for parathyroid cells? *Cell Calcium* 35:283–289
- Neuprez A, Hiligsmann M, Scholtissen S, Bruyere O, Reginster JY (2008) Strontium ranelate: the first agent of a new therapeutic class in osteoporosis. *Adv Ther* 25:1235–1256
- Niedzwiedzki T, Filipowska J (2015) Bone remodeling in the context of cellular and systemic regulation: the role of osteocytes and the nervous system. *J Mol Endocrinol* 55:R23–R36
- Nielsen SP (2004) The biological role of strontium. *Bone* 35:583–588
- Notoya M, Tsukamoto Y, Nishimura H, Woo JT, Nagai K, Lee IS, Hagiwara H (2004) Quercetin, a flavonoid, inhibits the proliferation, differentiation, and mineralization of osteoblasts in vitro. *Eur J Pharmacol* 485:89–96
- Oh WJ, Endale M, Park SC, Cho JY, Rhee MH (2012) Dual roles of quercetin in platelets: phosphoinositide-3-kinase and MAP kinases inhibition, and cAMP-dependent vasodilator-stimulated phosphoprotein stimulation. *Evid Based Complement Alternat Med* 2012:485262. doi:10.1155/2012/485262
- Okuducu AF, Zils U, Michaelis SA, Mawrin C, von Deimling A (2006) Increased expression of avian erythroblastosis virus E26 oncogene homolog 1 in World Health Organization grade I meningiomas is associated with an elevated risk of recurrence and is correlated with the expression of its target genes matrix metalloproteinase-2 and MMP-9. *Cancer* 107:1365–1372

- Omelson SJ, Grynepas MD (2008) Relationships between polyphosphate chemistry, biochemistry and apatite biomineralization. *Chem Rev* 108:4694–4715
- Omelson S, Georgiou J, Henneman ZJ, Wise LM, Sukhu B, Hunt T, Wynnyckyj C, Holmyard D, Bielecki R, Grynepas MD (2009) Control of vertebrate skeletal mineralization by polyphosphates. *PLoS ONE* 4:e5634. doi:[10.1371/journal.pone.0005634](https://doi.org/10.1371/journal.pone.0005634)
- Ominsky MS, Li C, Li X, Tan HL, Lee E, Barrero M, Asuncion FJ, Dwyer D, Han CY, Vlasseros F, Samadfar R, Jolette J, Smith SY, Stolina M, Lacey DL, Simonet WS, Paszty C, Li G, Ke HZ (2011) Inhibition of sclerostin by monoclonal antibody enhances bone healing and improves bone density and strength of nonfractured bones. *J Bone Miner Res* 26:1012–1021
- Pacifici R (1996) Estrogen, cytokines, and pathogenesis of postmenopausal osteoporosis. *J Bone Miner Res* 11:1043–1051
- Padhi D, Jang G, Stouch B, Fang L, Posvar E (2011) Single-dose, placebo-controlled, randomized study of AMG 785, a sclerostin monoclonal antibody. *J Bone Miner Res* 26:19–26
- Paulke A, Eckert GP, Schubert-Zsilavecz M, Wurglics M (2012) Isoquercitrin provides better bioavailability than quercetin: comparison of quercetin metabolites in body tissue and brain sections after six days administration of isoquercitrin and quercetin. *Pharmazie* 67:991–996
- Pavlov E, Aschar-Sobbi R, Campanella M, Turner RJ, Gómez-García MR, Abramov AY (2010) Inorganic polyphosphate and energy metabolism in mammalian cells. *J Biol Chem* 285:9420–9428
- Peng S, Liu XS, Huang S, Li Z, Pan H, Zhen W, Luk KD, Guo XE, Lu WW (2011) The cross-talk between osteoclasts and osteoblasts in response to strontium treatment: involvement of osteoprotegerin. *Bone* 49:1290–1298
- Pereira M, Jeyabalan J, Jørgensen CS, Hopkinson M, Al-Jazzar A, Roux JP, Chavassieux P, Orriss IR, Cleasby ME, Chenu C (2015) Chronic administration of Glucagon-like peptide-1 receptor agonists improves trabecular bone mass and architecture in ovariectomised mice. *Bone* 81:459–467
- Prouillet C, Mazière JC, Mazière C, Wattel A, Brazier M, Kamel S (2004) Stimulatory effect of naturally occurring flavonols quercetin and kaempferol on alkaline phosphatase activity in MG-63 human osteoblasts through ERK and estrogen receptor pathway. *Biochem Pharmacol* 67:1307–1313
- Qin DW, Gu Z, Dai L, Ji C (2013) Protective effects of gallium, germanium, and strontium against ovariectomized osteoporosis in rats. *Biol Trace Elem Res* 153:350–354
- Raisz LG (2005) Pathogenesis of osteoporosis: concepts, conflicts, and prospects. *J Clin Invest* 115:3318–3325
- Recker RR, Benson CT, Matsumoto T, Bolognese MA, Robins DA, Alam J, Chiang AY, Hu L, Kregg JH, Sowa H, Mitlak BH, Myers SL (2015) A randomized, double-blind phase 2 clinical trial of bloszumab, a sclerostin antibody, in postmenopausal women with low bone mineral density. *J Bone Miner Res* 30:216–224
- Reginster JY, Brandi ML, Cannata-Andía J, Cooper C, Cortet B, Feron JM, Genant H, Palacios S, Ringe JD, Rizzoli R (2015) The position of strontium ranelate in today's management of osteoporosis. *Osteoporos Int* 26:1667–1671
- Reid IR (2008) Anti-resorptive therapies for osteoporosis. *Semin Cell Dev Biol* 19:473–478
- Riccardi D (2012) Antagonizing the calcium-sensing receptor: towards new bone anabolics? *Curr Mol Pharmacol* 5:182–188
- Riggs BL, Khosla S, Melton LJ (1998) A unitary model for involutional osteoporosis: estrogen deficiency causes both type I and type II osteoporosis in postmenopausal women and contributes to bone loss in aging men. *J Bone Miner Res* 13:763–773
- Rizzoli R, Burret N, Cahall N, Delmas PD, Eriksen EF, Felsenberg D, Grbic J, Jontell M, Landesberg R, Laslop A, Wollenhaupt M, Papapoulos S, Sezer O, Sprafka M, Reginster JY (2008) Osteonecrosis of the jaw and bisphosphonate treatment for osteoporosis. *Bone* 42:841–847

- Robling AG, Niziolek PJ, Baldrige LA, Condon KW, Allen MR, Alam I, Mantila SM, Gluhak-Heinrich J, Bellido TM, Harris SE, Turner CH (2008) Mechanical stimulation of bone in vivo reduces osteocyte expression of Sost/sclerostin. *J Biol Chem* 283:5866–5875
- Rocheffort GY (2014) The osteocyte as a therapeutic target in the treatment of osteoporosis. *Ther Adv Musculoskel Dis* 6:79–91
- Rodan SB, Duong LT (2008) Cathepsin K—a new molecular target for osteoporosis. *Bonekey Osteovision* 5:16–24
- Römer P, Behr M, Proff P, Faltermeier A, Reicheneder C (2011) Effect of strontium on human Runx²/⁺ osteoblasts from a patient with cleidocranial dysplasia. *Eur J Pharmacol* 654:195–199
- Russell RG, Croucher PI, Rogers MJ (1999) Bisphosphonates: pharmacology, mechanisms of action and clinical uses. *Osteoporos Int* 9(Suppl 2):S66–S80
- Rybchyn MS, Slater M, Conigrave AD, Mason RS (2011) An Akt-dependent increase in canonical Wnt signaling and a decrease in sclerostin protein levels are involved in strontium ranelate-induced osteogenic effects in human osteoblasts. *J Biol Chem* 286:23771–23779
- Sambrook P, Cooper C (2006) Osteoporosis. *Lancet* 367:2010–2018
- Sassi N, Laadhar L, Allouche M, Zandieh-Doulabi B, Hamdoun M, Klein-Nulend J, Makni S, Sellami S (2013) The roles of canonical and non-canonical Wnt signaling in human de-differentiated articular chondrocytes. *Biotech Histochem* 13:384–392
- Schnatz P, Marakovits K, O'Sullivan D (2010) Assessment of postmenopausal women and significant risk factors for osteoporosis. *Obstet Gynecol Surv* 65:591–596
- Scholtyssek C, Katzenbeisser J, Fu H, Uderhardt S, Ipseiz N, Stoll C, Zaiss MM, Stock M, Donhauser L, Böhm C, Kleyer A, Hess A, Engelke K, David JP, Djouad F, Tuckermann JP, Desvergne B, Schett G, Krönke G (2013) PPAR β/δ governs Wnt signaling and bone turnover. *Nat Med* 19:608–613
- Schröder HC, Wiens M, Wang XH, Schloßmacher U, Müller WEG (2011) Biosilica-based strategies for treatment of osteoporosis and other bone diseases. *Prog Mol Subcell Biol* 52:283–312
- Selenge E, Murata T, Kobayashi K, Batkhuu J, Yoshizaki F (2013) Flavone tetraglycosides and benzyl alcohol glycosides from the Mongolian medicinal plant *Dracocephalum ruyschiana*. *J Nat Prod* 76:186–193
- Shah AD, Shoback D, Lewiecki EM (2015) Sclerostin inhibition: a novel therapeutic approach in the treatment of osteoporosis. *Int J Womens Health* 7:565–580
- Shevde NK, Bendixen AC, Dienger KM, Pike JW (2000) Estrogens suppress RANK ligand-induced osteoclast differentiation via a stromal cell independent mechanism involving c-Jun repression. *Proc Natl Acad Sci USA* 97:7829–7834
- Simonet WS, Lacey DL, Dunstan CR, Kelley M, Chang MS, Lüthy R, Nguyen HQ, Wooden S, Bennett L, Boone T, Shimamoto G, DeRose M, Elliott R, Colombero A, Tan HL, Trail G, Sullivan J, Davy E, Bucay N, Renshaw-Gegg L, Hughes TM, Hill D, Pattison W, Campbell P, Sander S, Van G, Tarpley J, Derby P, Lee R, Boyle WJ (1997) Osteoprotegerin: a novel secreted protein involved in the regulation of bone density. *Cell* 89:309–319
- Singer A, Grauer A (2010) Denosumab for the management of postmenopausal osteoporosis. *Postgrad Med* 122:176–187
- Son YO, Kook SH, Choi KC, Jang YS, Jeon YM, Kim JG, Lee KY, Kim J, Chung MS, Chung GH, Lee JC (2006) Quercetin, a bioflavonoid, accelerates TNF-alpha-induced growth inhibition and apoptosis in MC3T3-E1 osteoblastic cells. *Eur J Pharmacol* 529:24–32
- Stoch SA, Zajic S, Stone J, Miller DL, Van Dick K, Gutierrez MJ (2009) Effect of the cathepsin K inhibitor odanacatib on bone resorption biomarkers in healthy postmenopausal women: two double blind, randomized, placebo-controlled phase I studies. *Clin Pharmacol Ther* 86:175–182
- Sun G, Guo T, Chen Y, Xu B, Guo JH, Zhao J (2013) Significant pathways detection in osteoporosis based on the bibliometric network. *Eur Rev Med Pharmacol Sci* 17:1–7
- Tang BM, Eslick GD, Nowson C, Smith C, Bensoussan A (2007) Use of calcium or calcium in combination with vitamin D supplementation to prevent fractures and bone loss in people aged 50 years and older: a meta-analysis. *Lancet* 370:657–666

- Taranta A, Brama M, Teti A, De luca V, Scandurra R, Spera G, Agnusdei D, Termine JD, Migliaccio S (2002) The selective estrogen receptor modulator raloxifene regulates osteoclast and osteoblast activity in vitro. *Bone* 30:368–376
- Taxel P, Kenny A (2000) Differential diagnosis and secondary causes of osteoporosis. *Clin Cornerstone* 2:11–21
- Trivedi R, Mithal A, Chattopadhyay N (2008) Recent updates on the calcium-sensing receptor as a drug target. *Curr Med Chem* 15:178–186
- Van Bezooijen R, Ten Dijke P, Papapoulos S, Lowik C (2005) SOST/sclerostin, an osteocyt-derived negative regulator of bone formation. *Cytokine Growth Factor Rev* 16:319–327
- Van der Lee MM, Verkaar F, Wat JW, van Offenbeek J, Timmerman M, Voorneveld L, van Lith LH, Zaman GJ (2013) Beta-arrestin-biased signaling of PTH analogs of the type 1 parathyroid hormone receptor. *Cell Signal* 25:527–538
- Vilardaga JP, Romero G, Friedman PA, Gardella TJ (2011) Molecular basis of parathyroid receptor signaling and trafficking: a family B GPCR paradigm. *Cell Mol Life Sci* 68:1–13
- Wan Y, Chong LW, Evans RM (2007) PPAR-gamma regulates osteoclastogenesis in mice. *Nat Med* 13:1496–1503
- Wang FS, Lin CL, Chen YJ, Wang CJ, Yang KD, Huang YT, Sun YC, Huang HC (2005) Secreted frizzled-related protein 1 modulates glucocorticoid attenuation of osteogenic activities and bone mass. *Endocrinology* 146:2415–2423
- Wang Y, Liu Y, Rowe D (2007) Effects of transient PTH on early proliferation, apoptosis, and subsequent differentiation of osteoblast in primary osteoblast cultures. *Am J Physiol Endocrinol Metab* 292:E594–E603
- Wang FS, Ko JY, Weng LH, Yeh DW, Ke HJ, Wu SL (2009) Inhibition of glycogen synthase kinase 3 β attenuates glucocorticoid induced bone loss. *Life Sci* 85:685–692
- Wang XH, Schröder HC, Wiens M, Ushijima H, Müller WEG (2012) Bio-silica and bio-polyphosphate: applications in biomedicine (bone formation). *Curr Opin Biotechnol* 23:570–578
- Wang XH, Schröder HC, Diehl-Seifert B, Kropf K, Schlossmacher U, Wiens M, Müller WEG (2013) Dual effect of inorganic polymeric phosphate/polyphosphate on osteoblasts and osteoclasts in vitro. *J Tissue Eng Regen Med* 7:767–776
- Wang XH, Schröder HC, Grebenjuk V, Diehl-Seifert B, Mailänder V, Steffen R, Schloßmacher U, Müller WEG (2014a) The marine sponge-derived inorganic polymers, biosilica and polyphosphate, as morphogenetically active matrices/scaffolds for differentiation of human multipotent stromal cells: potential application in 3D printing and distraction osteogenesis. *Mar Drugs* 12:1131–1147
- Wang XH, Schröder HC, Müller WEG (2014b) Enzymatically synthesized inorganic polymers as morphogenetically active bone scaffolds: application in regenerative medicine. *Int Rev Cell Mol Biol* 313:27–77
- Wang XH, Schröder HC, Feng Q, Diehl-Seifert B, Grebenjuk VA, Müller WEG (2014c) Isoquercitrin and polyphosphate co-enhance mineralization of human osteoblast-like SaOS-2 cells via separate activation of two RUNX2 cofactors AFT6 and Ets1. *Biochem Pharmacol* 89:413–421
- Wang XH, Schröder HC, Schlossmacher U, Neufurth M, Feng Q, Diehl-Seifert B, Müller WEG (2014d) Modulation of the initial mineralization process of SaOS-2 cells by carbonic anhydrase activators and polyphosphate. *Calcif Tissue Int* 94:495–509
- Wang XH, Huang J, Wang K, Neufurth M, Schröder HC, Wang SF, Müller WEG (2016a) The morphogenetically active polymer, inorganic polyphosphate complexed with GdCl₃, as an inducer of hydroxyapatite formation in vitro. *Biochem Pharmacol* 102:97–106
- Wang XH, Schröder HC, Müller WEG (2016b) Polyphosphate as a metabolic fuel in Metazoa: a foundational breakthrough invention for biomedical applications. *Biotechnol J* 11:11–30
- Wattel A, Kamel S, Mentaverri R, Lorget F, Prouillet C, Petit JP, Fardelonne P, Brazier M (2003) Potent inhibitory effect of naturally occurring flavonoids quercetin and kaempferol on in vitro osteoclastic bone resorption. *Biochem Pharmacol* 65:35–42

- Wei W, Wang X, Yang M, Smith LC, Dechow PC, Sonoda J, Evans RM, Wan Y (2010) PGC1 β mediates PPAR γ activation of osteoclastogenesis and rosiglitazone-induced bone loss. *Cell Metab* 11:503–516
- Whitfield J (2006) Osteoporosis-treating parathyroid hormone peptides: What are they? What do they do? How might they do it? *Curr Opin Investig Drugs* 7:349–359
- Wiens M, Belikov SI, Kaluzhnaya OV, Adell T, Schröder HC, Perovic-Ottstadt S, Kaandorp JA, Müller WEG (2008) Regional and modular expression of morphogenetic factors in the demosponge *Lubomirskia baicalensis*. *Micron* 39:447–460
- Wiens M, Wang XH, Schloßmacher U, Lieberwirth I, Glasser G, Ushijima H, Schröder HC, Müller WEG (2010a) Osteogenic potential of bio-silica on human osteoblast-like (SaOS-2) cells. *Calcif Tissue Intern* 87:513–524
- Wiens M, Wang XH, Schröder HC, Kolb U, Schloßmacher U, Ushijima H, Müller WEG (2010b) The role of biosilica in the osteoprotegerin/RANKL ratio in human osteoblast-like cells. *Biomaterials* 31:7716–7725
- Winkler DG, Sutherland MK, Geoghegan JC, Yu C, Hayes T, Skonier JE, Shpektor D, Jonas M, Kovacevich BR, Staehling-Hampton K, Appleby M, Brunkow ME, Latham JA (2003) Osteocyte control of bone formation via sclerostin, a novel BMP antagonist. *EMBO J* 22:6267–6276
- Woo JT, Nakagawa H, Notoya M, Yonezawa T, Udagawa N, Lee IS, Ohnishi M, Hagiwara H, Nagai K (2004) Quercetin suppresses bone resorption by inhibiting the differentiation and activation of osteoclasts. *Biol Pharm Bull* 27:504–509
- Xue Y, Xiao Y, Liu J, Karaplis AC, Pollak MR, Brown EM, Miao D, Goltzman D (2012) The calcium-sensing receptor complements parathyroid hormone-induced bone turnover in discrete skeletal compartments in mice. *Am J Physiol Endocrinol Metab* 302:E841–E851
- Yaccoby S, Ling W, Zhan F, Walker R, Barlogie B, Shaughnessy JD (2007) Antibody-based inhibition of DKK1 suppresses tumor-induced bone resorption and multiple myeloma growth in vivo. *Blood* 109:2106–2111
- Zakharian E, Thyagarajan B, French RJ, Pavlov E, Rohacs T (2009) Inorganic polyphosphate modulates TRPM8 channels. *PLoS ONE* 4:e5404. doi:[10.1371/journal.pone.0005404](https://doi.org/10.1371/journal.pone.0005404)
- Zerbini CA, McClung MR (2013) Odanacatib in postmenopausal women with low bone mineral density: a review of current clinical evidence. *Ther Adv Musculoskelet Dis* 5:199–209
- Zhang S, Xiao Z, Luo J, He N, Mahlios J, Quarles LD (2009) Dose-dependent effects of Runx2 on bone development. *J Bone Miner Res* 24:1889–1904

Biocalcite and Carbonic Acid Activators

Xiaohong Wang, Meik Neufurth, Emad Tolba, Shunfeng Wang,
Heinz C. Schröder and Werner E.G. Müller

Abstract Based on evolution of biomineralizing systems and energetic considerations, there is now compelling evidence that enzymes play a driving role in the formation of the inorganic skeletons from the simplest animals, the sponges, up to humans. Focusing on skeletons based on calcium minerals, the principle enzymes involved are the carbonic anhydrase (formation of the calcium carbonate-based skeletons of many invertebrates like the calcareous sponges, as well as deposition of the calcium carbonate bioseeds during human bone formation) and the alkaline phosphatase (providing the phosphate for bone calcium phosphate-hydroxyapatite formation). These two enzymes, both being involved in human bone formation, open novel not yet exploited targets for pharmacological intervention of human bone diseases like osteoporosis, using compounds that act as activators of these enzymes. This chapter focuses on carbonic anhydrases of biomedical interest and the search for potential activators of these enzymes, as well as the interplay between carbonic anhydrase-mediated calcium carbonate bioseed synthesis and metabolism of energy-rich inorganic polyphosphates. Beyond that, the combination of the two metabolic products, calcium carbonate and calcium-polyphosphate, if applied in an amorphous form, turned out to provide the basis for a new generation of scaffold materials for bone tissue engineering and repair that are, for the first time, morphogenetically active.

X.H. Wang (✉) · M. Neufurth · E. Tolba · S.F. Wang · H.C. Schröder · W.E.G. Müller (✉)
ERC Advanced Investigator Group, Institute for Physiological Chemistry,
University Medical Center of the Johannes Gutenberg University,
Duesbergweg 6, 55128 Mainz, Germany
e-mail: wang013@uni-mainz.de

W.E.G. Müller
e-mail: wmueller@uni-mainz.de

X.H. Wang · H.C. Schröder · W.E.G. Müller
NanotecMARIN GmbH, Duesbergweg 6, 55128 Mainz, Germany

1 Calcium Carbonate Skeletons

Calcitic skeletons are widely distributed in nature, mainly in invertebrates like corals, mollusks, and echinoderms, as well as calcareous sponges. Even in humans, and other higher vertebrates, calcium carbonate (CaCO_3) exists, not only as the dominant mineral of the otoliths in the inner ear, but also in bone hydroxyapatite (HA) that has a small but basically important carbonate content. The crucial role of CaCO_3 in human bone formation has been underestimated for a long time and only very recently, it has been demonstrated that the deposition of CaCO_3 bioseeds, mediated by carbonic anhydrase(s) [CA(s)], is a fundamental step in bone mineralization not yet considered in any present-day therapeutical concepts of bone diseases, nor in surgery and orthopedics. The discovery of biocalcite as a bioseed essential in human bone formation has started to lend importance to this “invention” of the early invertebrates to new approaches in pharmacology and material development in regenerative medicine.

1.1 Evolutionary Aspects

Going back in evolution, the oldest multicellular organisms forming CaCO_3 skeletons are the calcareous sponges (Class Calcarea). These animals emerged on Earth approximately 540 MYA (Schütze et al. 1999). It should be noted, however, that CaCO_3 is not the first inventive biomineral of the metazoans; the earliest metazoans, the hexactinellid sponges, and the demosponges that evolved from the common metazoan ancestor the Urmetazoa (Müller et al. 2004) between the Sturtian glaciation (710–680 MYA) and the Varanger-Marinoan glaciation (605–585 MYA) have a siliceous (biosilica) skeleton. The processes that contributed to the change of the skeletal system, from biosilica (Hexactinellida and Demospongia) to biocalcite (Calcarea) (Knoll 2003), are not known but may be caused by the increase in calcium carbonate in the ancient oceans (Walker 2003; Müller et al. 2007).

1.2 Energetic Aspects

The formation of CaCO_3 (Li et al. 2013a, b), as well as the formation of calcium phosphate (Posner et al. 1978), is an exergonic process. The reactions leading to the formation of both minerals, although thermodynamically favored, are, however, controlled due to the activation-energy barriers that must be surpassed to enable them to occur. Similar like to other biochemical reactions, prevented or slowed down by energy barriers, even these inorganic reactions can be speeded up by enzymes, providing the organism the capability to control, in a fine-tuned manner, the extent and time-dependent variations of biomineral deposits (Meldrum and Cölfen 2008). The CAs, as well as the alkaline phosphatase (ALP), besides of

further exo/endopolyphosphatases, as well as silicatein (biosilica synthesis) represent a novel class of enzymes that catalyze/regulate the formation/metabolism of inorganic constituents of living beings.

1.3 Calcium Carbonate Polymorphs

CaCO_3 is a mineral that exists in several amorphous polymorphs and crystalline polymorphs (Cartwright et al. 2012). Besides of amorphous calcium carbonate (ACC) five crystalline polymorphs (crystalline calcium carbonate, CCC) are found: calcite, aragonite, and vaterite, as well as the hydrated phases monohydrocalcite (calcium carbonate monohydrate) and ikaite (calcium carbonate hexahydrate). The transformation of ACC into the crystalline polymorphs (CCC), along the energetical downhill sequence (negative free energy, ΔG) vaterite, aragonite, and calcite (Towe and Lowenstam 1967; Addadi et al. 2003; Gower 2008; Weiner et al. 2009; Fig. 1, Left), involves a series of dehydration and crystallization processes

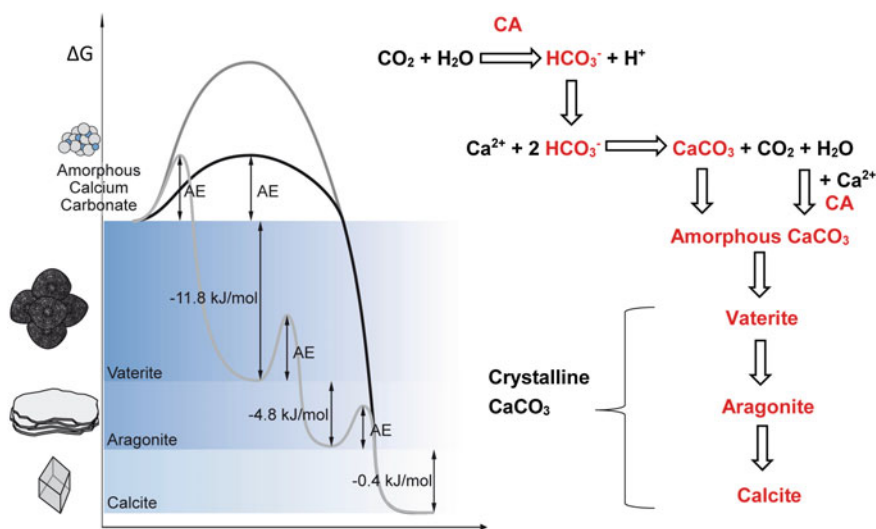


Fig. 1 Enzymatic calcium carbonate formation. *Left* Deposition of calcium carbonate, starting with precipitation of amorphous calcium carbonate (ACC) that is transformed into the three more stable phases vaterite, aragonite, and calcite, following the downhill sequence according to the decrease/release of Gibbs free energy (ΔG negative values, given in kJ/mol). The transformations into the next lower energy phases are impeded by activation-energy (AE; E_A) barriers that must be overcome to allow the reactions to occur. These energy barriers can be lowered by enzymes, like the CA. *Right* Reaction scheme of CA-mediated calcium carbonate formation, leading to amorphous CaCO_3 deposits (ACC) and finally calcite crystals. Under physiological conditions, ACC and defined crystalline phases (e.g., vaterite) can be stabilized by ions, peptides, proteins or certain polymers/polyanions (Müller et al. 2014b; Tolba et al. 2015) (modified from Müller et al. 2013c)

(Cölfen and Mann 2003). These polymorphs are separated from each other by activation-energy barriers (E_A) that can be potentially lowered by enzymes that accelerate the transformation reactions under physiological, ambient conditions. The principal enzyme in CaCO_3 metabolism is the CA (Müller et al. 2013b). Figure 1, Right, shows a schematic presentation of the reactions occurring during CA-mediated formation of amorphous CaCO_3 and its transformation into the crystalline phases. Certain CaCO_3 polymorphs can be “frozen,” i.e., the transformation into a polymorph with a lower energy level can be prevented/retarded by addition of organic macromolecules; e.g., addition of aspartic acid/glutamic acid (D/E)-rich peptides/proteins such as silintaphin-2, a sponge protein (Wiens et al. 2011), has been shown to freeze CaCO_3 deposition at the vaterite stage in *in vitro* experiments (Müller et al. 2014b).

2 Enzymes Involved in Calcium Carbonate Formation: The Carbonic Anhydrase (CA)

In sponges (Porifera), it has been reported for the first time that in animals the formation of CaCO_3 skeletons is driven enzymatically. This paradigm shift in understanding biomineral formation originated from the discovery of a unique enzyme, silicatein, which catalyzes the synthesis of the biogenic inorganic silica (“biosilica”) of the siliceous sponge spicular elements (Müller et al. 2004; Morse 1999; Müller 2003, 2013a). Later it has been recognized that also the biocalcite skeleton of the calcareous sponges is formed enzymatically, mediated by CAs that catalyze the rate-determining step of CaCO_3 deposition (Wang et al. 2014a).

The CAs (EC 4.2.1.1) are a large family of enzymes found across all living taxa. These enzymes catalyze the reversible hydration of carbon dioxide (CO_2) to bicarbonate (HCO_3^- ; Lindskog 1997; Supuran 2008a) and in turn, in the presence of calcium ions the precipitation of CaCO_3 (Ramanan et al. 2009; Sanyal and Maren 1981). The initial reaction, the formation of HCO_3^- from CO_2 and H_2O , is the rate-limiting step in CaCO_3 deposition (Wilbur and Jodrey 1955; Reddy 1981).

The CAs are zinc-containing enzymes (Simkiss and Wilbur 1989). The zinc ion binds an OH^- from the water (see Fig. 8, Sect. 6.1.3) and is involved in the catalytic mechanism of the enzymes, which proceeds via a nucleophilic attack of a Zn-bound OH^- to a CO_2 molecule, resulting in the formation of the HCO_3^- ion (Lindskog 1997). The CAs have an extremely high turnover number; they belong to the fastest enzymes known. It should be noted that these enzymes can act both as anabolic enzymes, accelerating the formation of bicarbonate ions for CaCO_3 synthesis, and as catabolic enzymes, causing CaCO_3 dissolution, e.g., in corals (Müller et al. 1984).

The deposition of CaCO_3 is an exergonic and hence thermodynamically favored reaction (Li et al. 2013a, b). The CA-mediated HCO_3^- formation facilitates overcoming the activation-energy barrier of this process (Wang et al. 2014a, b). In bone

formation, the CA provides the HCO_3^- anions that are required for CaCO_3 formation in the presence of Ca^{2+} cations. The CO_2 and water released during reaction of Ca^{2+} and two HCO_3^- anions under formation/deposition of CaCO_3 can again serve as a substrate for the CA, resulting in a further round of biocatalytic CaCO_3 deposition (Fig. 1, Right). In addition, the CA provides HCO_3^- to transporters in the osteoblast membrane, and removes the HCO_3^- ions after translocation into the intracellular compartment (see Fig. 5, Sect. 4.6). The HCO_3^- ions can also be taken up by cells via special co-transporters of HCO_3^- and silicate, the second inorganic biomaterial precursor, as discovered in the demosponge *Suberites domuncula* (Schröder et al. 2004).

2.1 CA Isoforms

Various isoforms of CA are found in living organisms (for a review, see: Badger and Price 1994). These enzymes are grouped into the α -CAs (animals), the β -CAs (plant chloroplasts and most prokaryotes), γ -CAs (methane-producing bacteria), δ -CAs (diatoms), and ε -CAs (bacteria). In humans, 15 α -CA isoforms have been described (for a review, see: Frost 2014; Supuran 2008a; Aggarwal et al. 2013; Aspatwar et al. 2014). These enzymes differ in their oligomeric structure: the CAs VI, IX, and XII are dimeric, while all other CAs are monomeric. The CA isoforms I, II, III, VII, and XIII are cytosolic enzymes, while the CA IV, IX, XII, and XIV are cell membrane-associated (Purkerson and Schwartz 2005). The latter enzymes either contain a transmembrane domain (CAs IX, XII, and XIV) or are attached at the cell membrane via a GPI anchor (e.g., CA IV). The CA VI is the only isoform that is secreted by cells. The CAs VA and VB are localized in the matrix compartment of the mitochondria. Three isoforms, the CAs VIII, X, and XI, do not show biocatalytic activity. The most studied CA isoform is the CA II. This widespread enzyme is involved in the regulation of the intracellular pH (Sly and Hu 1995).

First evidence that the CAs are involved bone formation have been presented by Chang et al. (2012). It was found that the cytosolic CA II can be targeted to the cell membrane (Alvarez et al. 2001; Mahieu et al. 1994; Chang et al. 2012). This enzyme was found to be upregulated after exposure of cells (SaOS-2) to bicarbonate, resulting in the deposition of CaCO_3 (Müller et al. 2013b). The CA II, as well as the deposition of CaCO_3 , is inhibited by acetazolamide, a specific inhibitor of this enzyme (Shinohara et al. 2007). Later results from our group revealed that it is primarily the CA IX that is involved CaCO_3 deposition during bone mineralization (Müller et al. 2016). This membrane-bound enzyme exists as a dimer and contains a twisted β -sheet surrounded by α -helices; in addition, the CA IX comprises, besides of an intracellular tail, a unique proteoglycan-like domain (Innocenti et al. 2009).

3 *Sycon raphanus* CA

The biomineral of the calcitic spicules of the calcareous sponges is almost pure CaCO_3 (Jones 1970; Simpson 1984; Uriz 2006). These spicules, e.g., of the calcareous sponge *Sycon raphanus* (Fig. 2a; Müller et al. 2012, 2014c) are characterized by an almost single crystalline morphology (Fig. 2b; Aizenberg et al. 1995; Sethmann and Wörheide 2008). The synthesis of this mineral occurs extracellularly

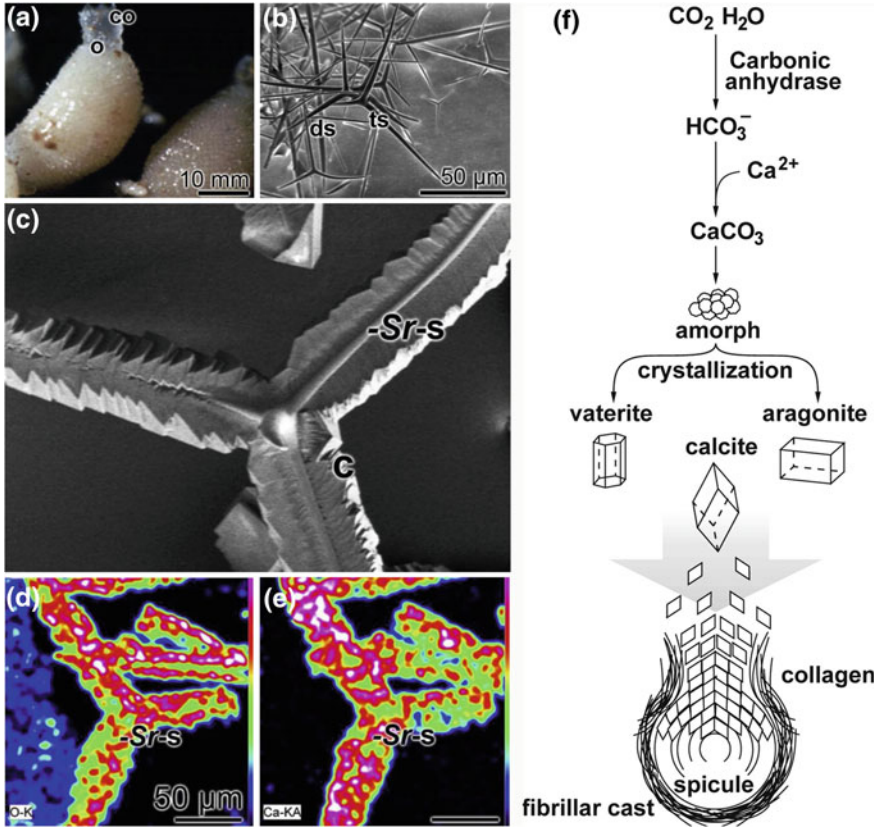


Fig. 2 Enzymatic synthesis of the calcium carbonate skeleton of a calcareous sponge. **a** The *Calcareia Sycon raphanus* with osculum (o) and surrounding corona (co). **b** Calcareous spicule of *S. raphanus*. Both diactines (ds) and triactines (ts) are shown. **c** Electron microscopic image (SEM) of a spicule from *S. raphanus* (Sr-s) after incubation with the CA. The enzymatically formed rhomboid/rhomboedric CaCO_3 crystals (c) are deposited in a highly regular manner along the spicule. **d, e** Detection of the elements oxygen (**d**) and calcium (**e**) within the crystals on the surface of the spicule applying the method of element mapping (pseudocolor image; the concentrations of the elements increase from blue to red). **f** Sketch of CA-mediated formation of amorphous CaCO_3 deposits, their transformation into crystalline polymorphs and the potential role of the collagen fibrillar network in cast molding of the formed material (modified from Müller et al. 2014c)

by special cells, the sclerocytes (Jones 1967; Ledger and Jones 1977). We succeeded to obtain a first insight in the mechanism of formation of the calcareous sponge spicules through the isolation, cloning, expression and investigation of function of the CA from *S. raphanus* in in vitro CaCO_3 precipitation experiments (Müller et al. 2012, 2013c, 2014c).

3.1 Properties of the Enzyme

The *S. raphanus* CA with a deduced polypeptide size of 33 kDa (Müller et al. 2014c) belongs to the α -CA class, like all metazoan CAs (Müller et al. 2012; Breton 2001). The Zn-binding sites involved in the enzymatic mechanism of the sponge CA are present in the CA- α group stretch of the protein. The Zn ion is bound through three His residues in the catalytic site of the enzyme, in addition to one water molecule (Tripp et al. 2001; see Fig. 8, Sect. 6.1.3). The zinc-bound hydroxide ion from the water is capable of performing a nucleophilic attack at the carbon atom of the CO_2 . The active site becomes regenerated via ionization of the zinc-bound water and removal of the proton from the active site (Henry 1996). The sponge enzyme is further characterized by a signal peptide cleavage site, supporting the assumption that this protein is either secreted by the cells or bound to the cell membrane.

We demonstrated that the recombinant *S. raphanus* CA, as well as the human CA, significantly accelerates the reaction velocity of CaCO_3 deposition in in vitro experiments (Müller et al. 2013c); Fig. 3a. The CA-mediated CaCO_3 deposition shows a typical substrate saturation kinetics, as found for other enzyme reactions. Determinations of the Michaelis–Menten constant (K_m) for the sponge recombinant CA revealed an apparent K_m value of 6.2 mM for the esterase [with the substrate 4-nitrophenylacetate (McIntosh 1970)] and a maximal reaction velocity of 0.32 mmol $\text{ml}^{-1} \text{min}^{-1}$ (Müller et al. 2013c). The apparent K_m constant in the hydratase/ CO_2 diffusion assay (using CO_2 as substrate (Wstrand et al. 1975); see Fig. 3b) was 9.9 mM (with respect to CaCl_2) at a corresponding V_{\max} of 24.9 mM CaCO_3 . From these values, a turnover rate of the *S. raphanus* CA of 50–230 $\text{CO}_2 \cdot \text{s}^{-1} \times \text{molecule CA}^{-1}$ has been calculated.

Even more impressive, the in vitro experiments using the diffusion assay revealed that two morphologically different CaCO_3 deposits are successively formed in the presence of the CA: initially (i) round-shaped deposits (average size of 80–120 μm) which are subsequently transformed into (ii) rhombohedral prisms with an average size of around 50 μm (Müller et al. 2013c, 2014c; Wang et al. 2014a); Fig. 3c. FT-IR spectra revealed that the round-shaped deposits consist of the metastable vaterite with the characteristic peaks at 875 and 744 cm^{-1} , while the prisms consist of calcite with peaks at 873 and 711 cm^{-1} (Müller et al. 2013b; Wang et al. 2014d).

In nanoindentation experiments it turned out that the hardness of the CaCO_3 particles is similar like the hardness of calcareous spicules (Merkel et al. 2009).

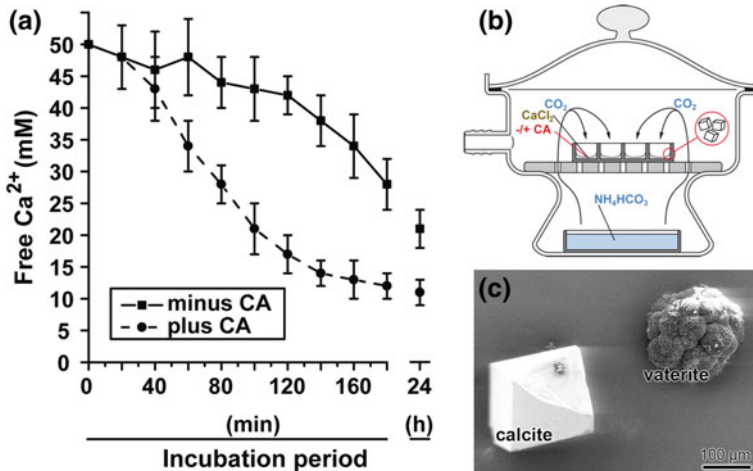


Fig. 3 Acceleration of the reaction velocity of CaCO_3 deposition by the recombinant *S. raphanus* CA in the diffusion assay. **a** The concentration of soluble Ca^{2+} was determined by EDTA titration as a measure for the formation of insoluble CaCO_3 . **b** Principle of the ammonium carbonate diffusion assay (“desiccator assay”). **c** The two different CaCO_3 deposits formed in the presence of the CA, the round-shaped vaterite deposits and rhombohedral prisms of calcite (modified from Müller et al. 2013c and Wang et al. 2014a)

A hardness for the round-shaped vaterite deposits of 1.38 GPa was determined, while the rhombohedral calcite had a hardness of 1.98 GPa. The elastic modulus for the vaterite deposits was 39.13 GPa, and the rhombohedral calcite prisms had a modulus of 72.83 GPa (Müller et al. 2014c).

3.2 Association of the CA and Calcitic Crystals with the Spicule Surface

Using antibodies raised against the recombinant affinity purified *S. raphanus* CA revealed that the sponge CA is located on the surface of spicules (Müller et al. 2014c).

Spectacular results were obtained when CA-mediated CaCO_3 formation was performed in the presence of the homologous calcareous spicules. Both light microscopical and scanning electron microscopical images demonstrated that the newly formed calcitic crystals are arranged along the two opposing planes of the *S. raphanus* spicules with almost perfect orientation (Müller et al. 2014c); Fig. 2c. The elements calcium and oxygen within the newly formed crystals on the spicule

surface could be identified using the method of element mapping (Fig. 2d, e). In addition, a model has been proposed in which the collagen fibrillar network may assist the formation of the 3D skeletal structure via a cast molding process (Fig. 2f).

3.3 CA-Mediated Calcium Carbonate Precipitation

The recombinant enzyme was used to determine the CaCO_3 formation using the in vitro ammonium carbonate diffusion assay (“desiccator assay”; Fig. 3b) (Müller et al. 2013b). It was calculated that the reaction velocity of CaCO_3 formation in the absence of CA is not sufficient to explain the rates of CaCO_3 deposition determined in vivo for spicule formation, e.g., in *Sycon* sp. (Ilan et al. 1996). It could be demonstrated that the recombinant sponge CA causes a marked acceleration of calcium carbonate formation in the in vitro diffusion assay (Müller et al. 2014c; Wang et al. 2014d). The enzymatic reaction was allowed to occur by passing a CO_2 vapor, generated from NH_4HCO_3 solution, over a solution of 50 mM CaCl_2 at pH 7.5 (Müller et al. 2013b); Fig. 3b. Addition of the recombinant CA significantly increased the reaction velocity of the mineralization, as determined by measuring the decrease of free Ca^{2+} concentration (Fig. 3a). The enzymatic, CA-mediated CaCO_3 deposition is pH and temperature dependent and abolished almost completely after addition of the CA inhibitor acetazolamide (3 μM ; Müller et al. 2013b).

4 CA: Involvement in Bone Hydroxyapatite Formation

4.1 Bone and Calcium Carbonate

Bone is an inorganic–organic composite material that is composed both of a mineral phase and an organic matrix (for a review, see: Xie and Nancollas 2010; Weiner and Wagner 1998; Beniash 2011). The inorganic phase predominantly consists of HA [$\text{Ca}_5(\text{PO}_4)_3(\text{OH})$; 60–70 wt%], while the organic matrix mainly formed by collagen (20–30 wt%); the content of water in bone is around 10% (v/w). Early studies already revealed that bone also contains a significant amount of carbonate (3–8 wt%) (Posner and Duyckaerts 1954; Pellegrino and Biltz 1970; Termine et al. 1973; Biltz and Pellegrino 1977). Within the crystal lattice of apatite, carbonate [CO_3^{2-}] ions substitute either for hydroxide [OH^-] (type A apatite) ions or, mainly, for phosphate [PO_4^{3-}] (reviewed in: Posner 1969; Murugan et al. 2006). In the mineralic apatite phase of bone, only the concentrations of phosphate and calcium are higher than those of carbonate (Rey et al. 1989). It has been proposed that bone formation around collagen fibrils starts with the deposition of poorly crystalline carbonated apatite aggregates (Rey et al. 1996; Matsuura et al. 2009;

Boonrungsiman et al. 2012). In the carbonated HA, the CO₂ component consists of 30% bicarbonate [HCO₃⁻] and 70% carbonate [CO₃²⁻] (Poyart et al. 1975).

4.2 *Cells Involved in Bone Formation*

The mineralization of bone is a process tightly controlled by both bone-forming cells that synthesize new bone mineral (osteoblasts) and bone-resorbing cells (osteoclasts). This process occurs in close association with a three-dimensional extracellular organic network of collagen fibrils around which first poorly crystalline carbonated apatite crystals/aggregates are deposited (Rey et al. 1996; Boonrungsiman et al. 2012). The balance between bone anabolism and catabolism depends on the tuned interaction and cross talk between the osteoblasts and the osteoclasts, allowing a continual remodeling of bone tissue during growth and aging of the organism (Matsuo and Irie 2008; Parra-Torres et al. 2013).

The bone anabolic cells, the osteoblasts, derive from mesenchymal stem cells (MSC). The mature cells are characterized by the expression of high levels of type I collagen and proteoglycans/glycosaminoglycans forming the osteoid/bone matrix. In addition, these cells synthesize a variety of cytokines/growth factors, including bone morphogenic proteins (BMPs), transforming growth factor- β (TGF- β), platelet derived growth factors (PDGFs), insulin-like growth factors (IGFs), interleukin-6 (IL-6), interleukin-11 (IL-11), granulocyte-macrophage colony stimulating factor (GM-CSF), and macrophage colony stimulating factor (M-CSF). Terminally differentiated osteoblasts also express the receptors for the major hormones that regulate bone formation, the parathyroid hormone (PTH) and 1,25-dihydroxyvitamin D [1,25(OH)₂D₃]. The osteoblasts can align under formation of lining cells via adherens-type junctions (desmosomes and tight junctions) (Safadi et al. 2009). The mineralization of the osteoid very likely involves the release of matrix vesicles from the osteoblasts (Hohling et al. 1978; Landis et al. 1993; Müller et al. 2013b).

The bone catabolic cells, the osteoclasts, are multinucleated cells that arise from hematopoietic stem cells (Boyle et al. 2003). Their differentiation and maturation is induced in the presence of M-CSF and the receptor activator of NF- κ B ligand (RANKL). Typical markers for mature osteoclasts are the tartrate-resistant acid phosphatase (TRAP), the calcitonin receptor (CTR), and integrin $\alpha_v\beta_3$.

4.3 *Otoliths: Almost Pure Calcium Carbonate Deposits in the Human Inner Ear*

In humans and other mammalian organisms, one biomineral deposit even exists that is predominantly formed of CaCO₃, the otoliths in the vestibular labyrinth of the ear

(Mann et al. 1983; Pizam et al. 2002). These mineral deposits are composed of 90–95% of CaCO_3 which is present as aragonite, in addition to a small amount of organic matrix proteins (Mann et al. 1983; Pizam et al. 2002). Among the major protein components of the otoliths are otolin, a structural glycoprotein that plays a role in otolith formation (Murayama et al. 2002; Deans et al. 2010) and the otoconins, calcium-binding proteins, onto which CaCO_3 deposition is initiated (Andrade et al. 2012).

4.4 Formation of Amorphous Calcium Carbonate (ACC) Bioseeds

Applying in-depth scanning electron microscopical (SEM)/energy-dispersive X-ray (EDX) and element mapping analyses, we succeeded to demonstrate that the mineralic deposits newly formed in vitro onto SaOS-2 cells contain not only calcium and phosphorus, but also significant amounts of carbon (Müller et al. 2013b). Investigations using SaOS-2 cells revealed that, after exposure of the cells to bicarbonate significant amounts of Ca-deposits are formed on the cells surface (Müller et al. 2013b). The experiments were performed in the presence of a mineralization activation cocktail (MAC), containing β -glycerophosphate (as a phosphate source), ascorbic acid (required for collagen synthesis), and dexamethasone (for cell differentiation of osteoblast precursor cells; Park 2012). The increase in Ca-deposit formation was paralleled by an enhanced expression of the *CA II* gene. Further studies using inhibitors of the CA revealed a strong reduction of Ca-P/HA formation in the presence of these compounds (see Sect. 4.5). From these results, we concluded that the deposition of calcium phosphate/HA in bone tissue is preceded by the synthesis of calcium carbonate, mediated by the increased CA activity (Müller et al. 2013b). We proposed that the CaCO_3 deposits (consisting of ACC) formed during the initial phase of bone mineral synthesis act as bioseeds for HA formation. Accordingly, the deposition of calcium carbonate and calcium phosphate consecutively occurs; first CaCO_3 is synthesized that is subsequently replaced by calcium phosphate. The studies suggested that the CA is involved in the Ca-deposit formation. This enzyme also plays an important role in bone resorption (Margolis et al. 2008).

Our results agree with previous observations that during the initial phase of bone mineralization a deposition of poorly crystalline carbonated apatite occurs (see Sect. 4.1). The presence of carbon in the mineral nodules, originating from the CaCO_3 deposits, formed in the presence of inorganic polyphosphate (polyP; see Sect. 4.8) as a phosphate source under physiological, low oxygen conditions, could also be detected by applying a highly sensitive Bruker XFlash Flat QUAD 5060F EDS mapping device (Müller et al. 2016); Fig. 4.

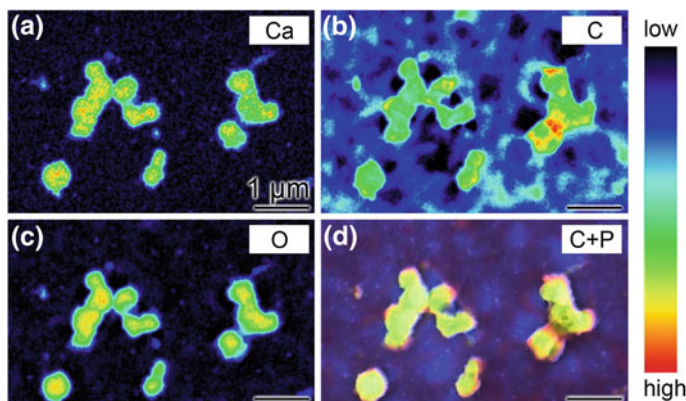


Fig. 4 Element mapping of the surface of SaOS-2 cells; SEM analysis, coupled with EDS (pseudocolor imaging). The cells were incubated at low oxygen (8%; normoxic) conditions in the presence of a mineralization activation cocktail (MAC; containing β -glycerophosphate, ascorbic acid and dexamethasone) and Ca-polyP microparticles. **a–d** Element mappings of the surfaces of the Ca-deposits for the elements (a) calcium [Ca], (b) carbon [C], (c) oxygen [O], and (d) phosphorus, together with carbon [C + P], are shown (modified from Müller et al. 2016)

4.5 Inhibition of Calcium Carbonate Deposit Formation

The formation of Ca-deposits onto SaOS-2 cells can be prevented, as we have shown (Müller et al. 2013b), by the CA II inhibitor acetazolamide (Barrese et al. 2008). Based on the finding that acetazolamide abolishes the biomineral formation onto SaOS-2 cells, we concluded that the CA II is responsible for the CaCO_3 deposition onto the SaOS-2 cell membranes (Müller et al. 2013b). The involvement of this enzyme in bone formation has also been proposed by Sly and Hu (1995). It is known that the CA II, which is primarily a cytosolic enzyme, can also be localized at the plasma membrane; in the membrane-associated state, this enzyme has been assumed to be involved in pH regulation and the secretion of bicarbonate ions via the $\text{Cl}^-/\text{HCO}_3^-$ exchanger or another HCO_3^- channel (Alvarez et al. 2001). Later results from our group revealed that it is the CA IX, a membrane-associated CA, which is primarily responsible for the initial rise in CaCO_3 formation during bone mineralization (Müller et al. 2016; see below).

Moreover, an inhibitory effect of orthophosphate, formed by hydrolysis of polyP, on CA II was observed already in the concentration range of 10 μM (based on phosphate; Müller et al. 2013b). This concentration is found at the sites of calcium phosphate deposition within bone tissue (Collin et al. 1992).

4.6 Bicarbonate Transport

It is assumed that the bicarbonate (HCO_3^-) used as the substrate for the enzymatic CaCO_3 formation is at least partially provided by the Na^+ -independent $\text{Cl}^-/\text{HCO}_3^-$ exchanger [AE] in the neighborhood of the sites of CaCO_3 deposition, at the surface, in the extracellular space of the osteoblasts, or intracellularly, in the plasma membrane by the Na^+ -driven $\text{Na}^+:\text{HCO}_3^-$ cotransporter [NBC] (Müller et al. 2013b).

A scheme summarizing the initial steps in biomineral formation of bone tissue with the CA-driven CaCO_3 precipitation preceding the subsequent transformation of this (amorphous) mineral into amorphous calcium phosphate and finally crystalline HA is shown in Fig. 5. As shown in the scheme, HCO_3^- accumulates on the cell membrane surface in the proximity of the AE (Lindsey et al. 1990) and the NBC (Roos and Boron 1981; Haddad and Boron 2000). These channels are involved in the regulation of the intracellular pH and some of them are linked with the CA, e.g., the AE3 $\text{Cl}^-/\text{HCO}_3^-$ exchanger that is linked with the CA XIV (Casey et al. 2009).

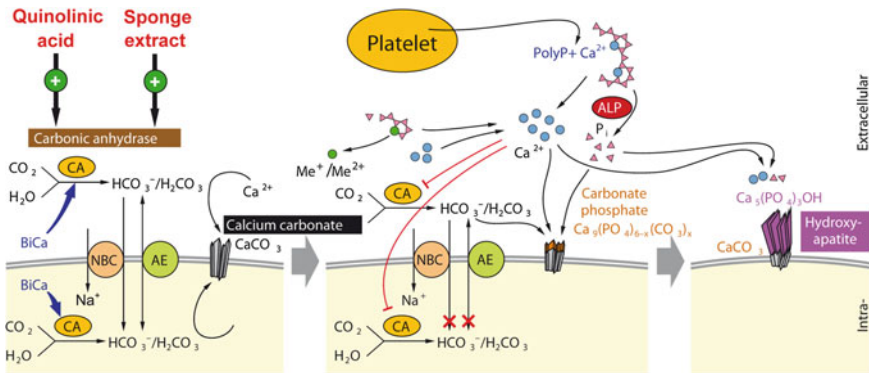


Fig. 5 Schematic representation of target sites of CA activators during early stages of bone HA formation: CA-mediated CaCO_3 bioseed formation and transformation into Ca-phosphate. At the surface of the osteoblasts, CaCO_3 bioseeds are formed in close association with the cell membrane. The CaCO_3 synthesis is controlled both extracellularly and intracellularly by the CA that catalyzes the rate-limiting step of HCO_3^- formation. The exchange of the enzymatically formed HCO_3^- ions between the extracellular and intracellular compartments is facilitated by bicarbonate transporters or exchangers, e.g., NBC or AE. PolyP is stored as a Ca^{2+} salt in vesicles within platelets secreted into the extracellular space. The ALP, which is induced by polyP accelerates the hydrolysis of polyP (Ca^{2+} salt), resulting in a local increase of the concentration of PO_4^{3-} and Ca^{2+} ions, the substrates for HA formation. The amorphous CaCO_3 bioseeds are transformed into Ca-P/HA by $\text{HCO}_3^-/\text{PO}_4^{3-}$ exchange via the intermediate formation of amorphous calcium-carbonated phosphate. The activity of the two regulator enzymes, the ALP and the CA, is controlled by positive/negative feedback mechanisms. The CaCO_3 bioseed formation is down-regulated as soon as the local concentration of PO_4^{3-} increases, as a result of ALP-mediated degradation of polyP (Ca^{2+} salt), via PO_4^{3-} -caused inhibition of the activity of the CA. The ALP is activated by polymeric phosphate (polyP). In addition, it is shown that the enzyme-mediated mineralization process can be accelerated by CA activators, e.g., quinolinic acid (modified from Wang et al. 2014d)

4.7 *Calcium Carbonate Dissolution*

Our results show that in bone formation/remodeling the CA can act both as an anabolic enzyme that accelerates bicarbonate formation and CaCO_3 deposition (osteoblasts), and as a catabolic enzyme that facilitates CaCO_3 dissolution (osteoclasts). The role of CA II in bone resorption, mediated by bone-resorbing osteoclasts, is well known (Margolis et al. 2008; Zhu et al. 2010). The resorption/dissolution of bone tissue in osteoclasts occurs through an increased proton production (acidification of the resorption lacuna) by CA II via modulating of the V-ATPase (Laitala and Väänänen 1994). CA II deficiency, a rare autosomal recessive disorder, is characterized by osteopetrosis, renal tubular acidosis, and cerebral calcifications (Sly et al. 1983). The function of CA in CaCO_3 dissolution has also been demonstrated in corals (Müller et al. 1984).

4.8 *Transformation into Calcium Phosphate*

The next step is the transformation of ACC to amorphous calcium phosphate (ACP). The detailed mechanism of this second step, the exchange of the carbonate ion of the calcium carbonate by the phosphate ion under formation of calcium phosphate is not yet understood. While the first step, the deposition of calcium carbonate, is enzyme (CA)-mediated, the second step is a nonenzymatic process (Müller et al. 2015a). Our studies revealed that this step only depends on the presence of orthophosphate (P_i). Hitherto it has been assumed, and current *in vitro* assays are based on this assumption, that the phosphate used for HA formation is delivered by an organic compound, β -glycerophosphate. We could present evidence that the source of the monomeric phosphate is inorganic polyP that is enzymatically hydrolyzed by the ALP (Müller et al. 2011; Wang et al. 2014c). This polymer (polyP) is synthesized and stored both in osteoblasts and in blood platelets coming into contact with osteoblasts during bone fracture/repair (Müller et al. 2011). In the scheme in Fig. 5, it is shown that the ALP which is induced by polyP (Müller et al. 2011) is localized at the extracellular surface where it hydrolyzes Ca^{2+} -polyP under formation of Ca^{2+} and PO_4^{3-} . As a result, the amorphous CaCO_3 bioseeds are transformed to amorphous carbonated phosphate and finally calcium phosphate/HA (Wang et al. 2014d). In a negatively feedback control mechanism, the PO_4^{3-} liberated from the polyP by ALP hydrolysis down-regulates CaCO_3 formation by inhibiting the CA, allowing a control of the extent of new bone mineral formation (Müller et al. 2013b).

It should be noted that both the deposition of calcium phosphate (Posner et al. 1978) and the deposition of calcium carbonate are exergonic processes (Li et al. 2013a, b). Therefore, from the thermodynamic point of view, the formation of both minerals is a favored chemical reaction, but the velocity of both chemical reactions is controlled by the activation-energy barriers that must be overcome (Wang et al. 2014b).

In living system, such reactions can be accelerated by enzymes, and indeed it is an enzyme, the CA, very like the cell membrane-associated CA IX (Müller et al. 2016), which catalyzes the formation/deposition of amorphous CaCO_3 (Müller et al. 2013b).

4.9 Inorganic Polyphosphates

PolyP is a biopolymer found in almost all living organisms (see: Rao et al. 2009). In mammals, high contents of polyP are accumulated in the blood platelets (Morrissey et al. 2012), but also in the osteoblasts (Leyhausen et al. 1998). The natural bio-polyP is a linear molecule consisting of up to hundreds of phosphate units that are linked together via high-energy phosphoanhydride linkages. Due to the relatively high activation energies for hydrolysis of these phosphoanhydride bonds (similar to the activation energies needed for hydrolysis of the α - β and β - γ phosphoanhydride bonds of ATP), the polymer is stable and hydrolyzes only slowly under ambient conditions (Kulaev et al. 2004). The sodium salt of polyP with chain lengths <100 phosphate units is soluble in water (Van Wazer 1958; Rao et al. 2009) but the solubility of the polymer markedly decreases in the presence of calcium as counterions; the biogenic polyP (most likely existing as a calcium salt) has an amorphous state (Kulaev et al. 2004; Omelon and Grynepas 2008; Rao et al. 2009). The mechanism of formation of polyP in animal cells is not fully understood, in contrast to polyP in prokaryotic organisms which is synthesized via polyP kinases (Rao et al. 2009).

PolyP has been attributed multiple functions, both in microorganisms and in animals (Kulaev 1979; Wood and Clark 1988; Schröder and Müller 1999). The most important function in animals may be its role in bone mineralization, which has been proposed already more than 15 years ago (Schröder et al. 2000). Later results revealed that it is the calcium salt of polyP that is biologically active and able to promote the maturation and functional activity of osteoblasts. In osteoblast-like cell lines, e.g., MC3T3-E1, polyP causes an increased expression of the genes encoding for proteins crucial for bone formation, like ALP, bone sialoprotein (BSP), OCN, and osterix (Sinha et al. 2010). In contrast to polyP anabolism, the enzymatic basis of polyP catabolism in animal cells is better understood. PolyP is enzymatically degraded via exopolyphosphatases. One prominent enzyme showing exopolyphosphatase activity is the ALP that has been identified to hydrolyze the polymer under formation of orthophosphate (Lorenz et al. 1994a, b, 1997; Lorenz and Schröder 2001). As a consequence of the enzymatic, ALP-mediated degradation of polyP, both PO_4^{3-} and Ca^{2+} ions are formed that can be utilized during HA formation (Omelon and Grynepas 2008; Omelon et al. 2009).

We demonstrated that polyP exhibits morphogenetic activity (Müller et al. 2014a); if present as polyP- Ca^{2+} complex it promotes the functional activity of bone-forming osteoblasts and inhibits the activity of bone-degrading osteoclasts (Wiens et al. 2010a, b; Müller et al. 2011; Wang et al. 2013). The most important function of polyP may be the induction of expression of the ALP, the enzyme that

provides inorganic phosphate for HA synthesis (Müller et al. 2011). PolyP released from the storage vesicles within bone or platelets into the extracellular space undergoes degradation to orthophosphate via the ALP. The orthophosphate, P_i , formed during hydrolysis of polyP and serving as a substrate for bone HA formation, on the other side, inhibits the CA in a feedback manner and thereby down-regulates the enzymatic synthesis of the bioseeds required for HA formation (Müller et al. 2013b); see above and Fig. 5.

4.10 Source of Calcium Ions

The scheme depicted in Fig. 5, however, does not sufficiently explain the source of the calcium ions, required as the cationic component of both the carbonate and phosphate minerals formed onto the bone cell surface. One source for the Ca^{2+} ions is surely the polyP that exists as a calcium salt and, after degradation via ALP, not only provides phosphate for Ca-P/HA formation, but also serves as a calcium source due to the liberation of the Ca^{2+} counterions during hydrolysis of the inorganic polymer. Another possibility is that at the sites of bioseed formation at the osteoblast cell membrane the Ca^{2+} ions are provided via osteocalcin (OCAL), a Ca^{2+} -binding protein. OCAL binds calcium after carboxylation via the γ -glutamyl carboxylase (GGCX), a process that depends on vitamin K (Wood and Suttie 1988; Lian and Gundberg 1988; Thraikill et al. 2012).

5 CA: Potential Drug Target

The discovery of the CA-mediated bioseed formation as an initial step in bone HA formation has opened a new target for potential drugs that are beneficial for therapy and prophylaxis of bone diseases. It is conceivable and can be expected that compounds that enhance CA activity will have a stimulatory effect on new bone formation and can shift the balance, or repair the disbalance, between bone anabolic and bone catabolic processes in the direction of bone anabolism. The screening for such compounds that affect this new target enzyme in bone metabolism is a promising task in pharmaceutical research, in particular because bone diseases, like osteoporosis, are besides neurodegenerative diseases, e.g., Alzheimer disease, and cardiovascular diseases the predominant disorders in the aging societies of the developed countries.

However, only a relatively few CA activators have been identified until today (Pastorekova et al. 2004; Supuran 2008a, b, 2011). In addition, there is only very little knowledge on the potential therapeutic effect of such CA activators, in particular on bone metabolism (Supuran and Scozzafava 2000a). This situation is different from that in the area of CA inhibitors; a systematic search had revealed a high number of CA inhibitors, mainly of the mammalian α -class enzymes that

inhibit the enzyme in an isoform-specific manner (for a review, see: Supuran and Scozzafava 2000a).

In contrast to CA inhibitors that have been developed or are used for a number of clinical applications (e.g., as diuretics, for treatment of glaucoma or intracranial hypertension, as anticonvulsant to treat epilepsy, for prevention of migraine headaches, or treatment of altitude sickness; see: Supuran et al. 2004b, 2008b, 2016; Winum et al. 2009) CA activators have not yet been introduced in human therapy or even not been evaluated for their potential beneficial effects in therapy of human bone disorders.

5.1 CA Activators

It has been demonstrated that a series of natural compounds which can be protonated, such as biogenic amines (e.g., histamine, serotonin, and catecholamines), amino acids, and peptides can act as CA activators (Briganti et al. 1997; Supuran and Scozzafava 2000c; Ilies et al. 2004; Temperini et al. 2006b). The group of Supuran has investigated all 16 isoforms (CA I–CA XV) of the mammalian α -CAs with respect to their activation by amino acids and amines (Ilies et al. 2002; Scozzafava and Supuran 2002; Temperini et al. 2006c; Pastorekova et al. 2008; Supuran 2008b). In addition to kinetic studies, this group has performed and reported the data from X-ray crystallographic analyses of the interaction of all human CA isoforms hCA I–hCA XV with the amino acid and amine activators. These studies allowed a detailed insight into the mechanism of activation of this class of CA modulators at the molecular level (Briganti et al. 1997; Supuran and Scozzafava 2000c; Ilies et al. 2004; Temperini et al. 2005, 2006a, b, c, 2007; Pastorekova et al. 2008).

5.2 Mode of Action

Most CA isozymes contain within the active site a zinc ion. This Zn^{2+} ions plays an essential role in the catalytic mechanism of the enzyme: it decreases the pK_a of a coordinated water molecule and facilitates, in the rate-limiting step of the catalytic reaction, the ionization of the water molecule under formation of the Zn -bound hydroxide group that then performs a nucleophilic attack at the CO_2 molecule. The proton is then transferred from the catalytic site to the environment via a proton shuttle, which involves the His64 residue (in the CA isoforms II, IV, VI, VII, IX, and XII) (Supuran 2004, 2008b, 2009; Supuran et al. 2004a; Alterio et al. 2009).

Detailed kinetic and X-ray crystallographic studies revealed that the activators bind at the entrance of the catalytic pocket of the enzyme at a site different of the substrate or inhibitor binding sites. Thereby the rate-determining step of the catalytic cycle, the shuttling of a proton from the Zn^{2+} -bound water molecule to the

external medium is facilitated (Supuran and Scozzafava 2000c; Scozzafava and Supuran 2002; Ilies et al. 2002, 2004; Supuran 2008b). In most CA isoforms, this process is promoted by a histidine residue (His64) in the middle of the catalytic pocket of the enzyme molecule.

5.3 *Activation of Different Human CA Isozymes and Mechanisms of Specific CA Activators*

The first X-ray crystallographic data have been obtained for the adduct of hCA II with histamine. These data showed that histamine, after binding at the entrance of the catalytic pocket, actively participates in the proton shuttling via its imidazole moiety (Briganti et al. 1997). It forms a second proton shuttle, in addition to His64 of the enzyme (Briganti et al. 1997). The amino group of the histamine molecule does not contribute to this mechanism.

Subsequent X-ray crystallographic studies on the adducts formed between hCA I or hCA II and further activators, including, among others, L- and D-His (Temperini et al. 2005, 2006a, b), L- and D-Phe (Temperini et al. 2006c) and D-Trp (Temperini et al. 2008) revealed that all of them, with the exception of D-Trp, bind in the same region, at the entrance, of the CA catalytic pocket. It was found that D-Trp binds at a more external site of the CA II catalytic pocket.

L-His turned out to be a potent activator of the hCA isozymes I, VA, VII, and XIV, and a less potent activator of hCA II and IV, while D-His was a better activator of hCA I, VA, and VII than of hCA XIV; hCA II, and IV are only weakly activated (Temperini et al. 2006b). L-Phe potently activates hCA I, II, and XIV and weakly activated hCA VA and VII, and is a quite inefficient hCA IV activator, while D-Phe was a good activator of hCA II, but only moderately active towards hCA VA, VII, and XIV; it had only a small effect on hCA I and IV (Temperini et al. 2006c).

Interestingly, the activity of D- and L-Trp tryptophan on the mammalian isozyme CA II turned out to be time-dependent (Temperini et al. 2008). Analysis of the high-resolution X-ray crystal structure of the hCA II—D-Trp adduct revealed that this amino acid unexpectedly binds to a different site at the catalytic pocket of the enzyme as compared to L-His, D-His L-Phe, D-Phe, histamine, or L-adrenaline. D-Trp binds at a second activator binding site located at the edge of the entrance of the CA II catalytic site, interacting with several amino acid residues of the protein via hydrogen bonds and van der Waals interactions (Temperini et al. 2008).

The first activation study of hCA IX, as well as hCA XII has been performed by Pastorekova et al. (2008). This cell membrane-associated CA isoform, which is involved in CaCO₃ bioseed formation, was found to be efficiently activated, with K_{AS} of 9 nM–1.07 μM, by dopamine, adrenaline, and heterocyclic amines possessing aminoethyl- or aminomethyl-moieties. The most potent hCA XII activators were D-Phe, L-adrenaline, serotonin, and 4-(2-aminoethyl)-morpholine (K_A of 0.24–0.41 μM) (Pastorekova et al. 2008).

On the other hand, the cytosolic CA isoform III has been reported to be efficiently activated by D-His, serotonin, pyridyl-alkylamines, and aminoethyl-piperazine/morpholine, while the best activators of the membrane-associated CA IV are 4-aminophenylalanine, serotonin, and 4-(2-aminoethyl)-morpholine (Vullo et al. 2008).

A potent activator of the CA I isozyme is L-adrenaline (K_A of 90 nM) which is only a weak activator of CA II (K_A of 96 μ M). The corresponding activation constants for the CA isoforms IV, VA, VII, and XIV are in the range of 36–63 μ M. In the X-ray crystal structure of the CA II—L-adrenaline adduct, the binding of this activator almost totally blocks the entrance of the catalytic pocket, a possible explanation for the lower activity (Temperini et al. 2007).

Based on the finding that the amino group of histamine is not involved in the interaction with amino acid residues of the CA (Briganti et al. 1997), a series of histamine derivatives have been prepared and tested for potentially higher affinity to the CA (Supuran and Scozzafava 2000b; Ilies et al. 2002).

Among them, a group of phenylsulfonylhydrazido L-histidine derivatives only weakly activated hCA I and more efficiently activated hCA II and hCA IX (Abdo et al. 2009). However, the 4-iodophenyl-substituted derivative turned out as a strong and selective activator of the cytosolic hCA II (K_A of 0.21 μ M). This potent compound is the first CA isoform-selective activator that has been identified (Abdo et al. 2009).

Even more interesting might be the 2,4,6-trimethylpyridinium derivative of histamine (Dave et al. 2011). Analysis of the X-ray crystal structure of the complex of hCA II with the 1-[2-(1H-imidazol-4-yl)-ethyl]-2,4,6-trimethylpyridinium salt revealed that this CA activator, unlike other CA activators, binds at the entrance of the catalytic pocket in a way, whereby the 2,4,6-trimethylpyridinium ring is directed towards the Zn^{2+} ion in the center of the catalytic site; in addition, the adduct is stabilized by strong hydrophobic interactions. As a result, this initially effective CA activator becomes, after a longer contact with the enzyme, a potent inhibitor of this enzyme (Dave et al. 2011).

In addition, the clinically used phosphodiesterase-5 inhibitor sildenafil, which is characterized by a piperazine moiety, like some other CA activators, has been reported to act as a potent activator of several CA isozymes, including CA I, VA and VI, and less efficiently, CA III, IV, and VII (Abdülkadir Coban et al. 2009).

5.4 Activators of CA Isozymes from Fungi, Yeast, and Invertebrates

CAs are also found in many pathogenic organisms, such as bacteria or fungi. They have been implicated in the mechanisms of microbial virulence (Smith and Ferry 2000; Supuran 2008b, 2016). Investigation of the β -CA from the pathogenic fungi *Candida albicans* and *Cryptococcus neoformans* revealed that the *C. albicans* CA

was activated by amino acids such as L-His, D-His, L-Tyr, L-Trp, and D-Trp, and more effectively, by amines such as histamine, dopamine, 2-aminoethyl-piperazine, and L-adrenaline. The best activators were L-DOPA and D-DOPA (K_{AS} of 0.96–2.5 μM) (Innocenti et al. 2010). The efficiency of these activators on the *C. neoformans* CA was lower (Innocenti et al. 2010). The β -CA from the pathogenic fungus *Malassezia globosa* was activated by D-Phe, L-Trp, L-DOPA, dopamine, histamine, pyridyl-alkylamines, and 4-(2-aminoethyl)-morpholine, but only weakly by L-His, D-His, L-Phe, D-Trp, L-Tyr, D-Tyr, D-DOPA, and serotonin. The strongest activation was observed for L-adrenaline and 1-(2-aminoethyl)piperazine (K_{AS} of 0.72–0.81 μM) (Vullo et al. 2016).

The best activator of the β -CA from the yeast *Saccharomyces cerevisiae* was L-adrenaline (K_A of 0.95 μM); the enzyme was also activated by histamine, dopamine, serotonin, pyridyl-alkylamines, and aminoethyl-piperazine/morpholine, but only weakly by amino acids (L-His, D-His, Phe, DOPA, and Trp) (Isik et al. 2009).

Among the marine invertebrate organisms, D-DOPA was found to be an efficient activator of the secretory CA of the coral *Stylophora pystillata* (Bertucci et al. 2010).

6 CA: Potential Drug Target to Stimulate Bone Mineral Formation

We succeeded to identify a first CA activator that is capable of stimulating the CA-driven calcium carbonate deposition. The identification of this compound, quinolinic acid, as described in the following, is hoped to encourage further research in an area of medical pharmacology that is characterized mainly by symptomatic but not by causative therapeutic approaches, like pharmacology of bone diseases.

6.1 Quinolinic Acid (QA)

During screening of organic extracts from marine sponges, we discovered that ethyl-acetate extracts from the demosponge *S. domuncula* exhibit a strong stimulatory effect on the CA-driven CaCO_3 deposition onto SaOS-2 cells (Wang et al. 2014d). Further studies revealed that one compound present in these extracts, quinolinic acid [QA] (Fig. 6a; Schröder et al. 2002), strongly stimulates mineralization of SaOS-2 cells in the presence of a phosphate source. The identified compound, QA, was found to act as CA activator both in vitro and in intact cell system (Wang et al. 2014d). Already at a low concentration of 10 μM , QA causes a strong activation of the CA. At this concentration, QA does not cause any apoptotic effect on neuronal cells (Sei et al. 1998).

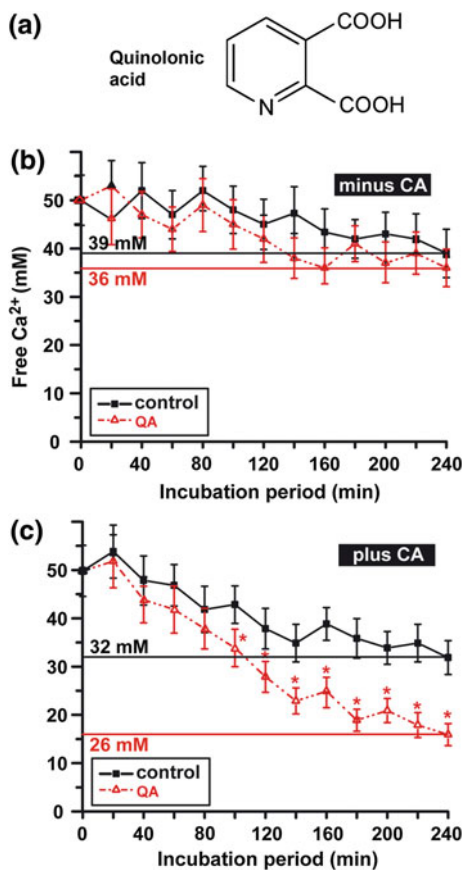


Fig. 6 CA-mediated acceleration of CaCO_3 deposition in the ammonium carbonate diffusion assay and effect of the CA activator quinolinic acid. The structural formula of quinolinic acid is shown in (a). CaCO_3 was allowed to precipitate after reaction of diffusion of CO_2 to a 50 mM CaCl_2 solution in the absence (b) and in the presence of the recombinant human CA II enzyme (70 W-A units/mL) (c). The formation of Ca-carbonate was determined quantitatively on the basis of the consumption of free Ca^{2+} ions using the EDTA titration procedure (Müller et al. 2013c). The assays either remained free of additional compound(s) (black solid line and filled squares) or were supplemented with 10 μM quinolinic acid (QA; red broken line and triangles). The means \pm S.D. from six parallel determinations are given. * $p < 0.05$ (modified from Wang et al. 2014d)

In the experiments shown in Fig. 6b, c, both the *S. domuncula* extract and QA strongly enhance the CA-driven CaCO_3 formation, which amounted to 28% in the absence of the activator or extract during a 4 h incubation period, while in the presence of 10 μM QA, under otherwise identical conditions, 48% of CaCO_3 is formed (Wang et al. 2014d). Interestingly, this effect was further increased in the presence of polyP (Wang et al. 2014d). The latter result suggests that the polyP-degrading enzyme, the ALP, might provide a second, not yet approached

target for pharmacological intervention of bone diseases, besides of the CA. It might also be of interest that the ALP is activated by polymeric phosphate (polyP), while the CA is inhibited by the phosphate monomer (PO_4^{3-}).

6.1.1 Rate of CA-Mediated CaCO_3 Crystal Formation in Dependence on QA

A study of the kinetics of crystal formation in the diffusion/desiccator assays revealed that in the absence of CA only a very few crystals with a size of 40 μm are present after an incubation period of 30 min (Fig. 7, Left c), while in the presence of CA significantly more and larger, about 100 μm sized crystals are formed, compared to the control without the CA (Fig. 7, Left d) (Wang et al. 2014d). The crystals (both

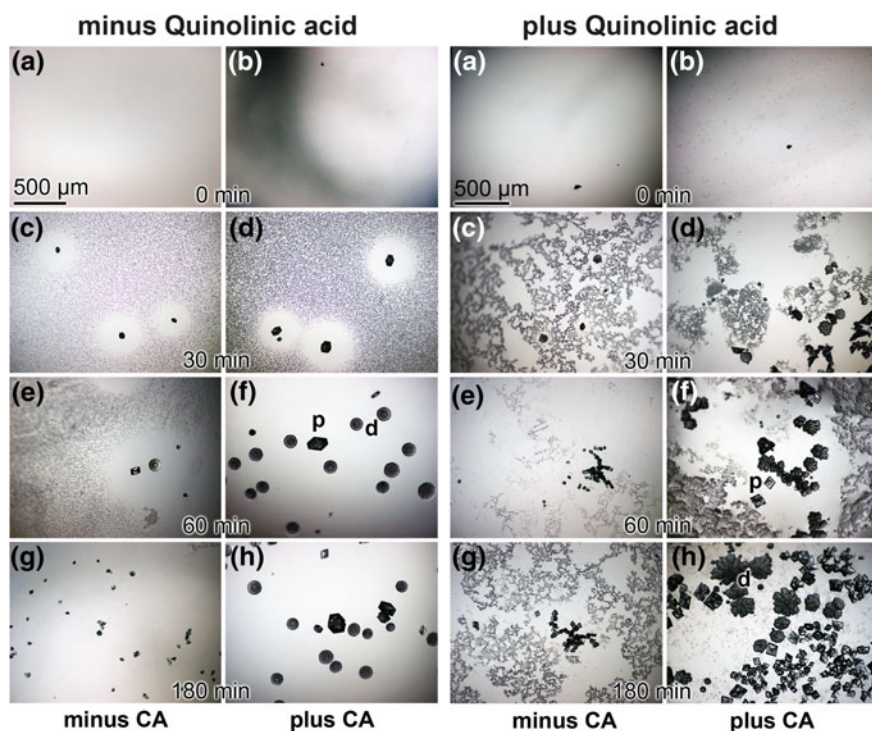


Fig. 7 Enhanced CA-mediated formation of CaCO_3 deposits in the carbonate diffusion assay in the presence of the CA activator QA. *Left side* In vitro crystallization assay without QA. The calcitic crystals formed after incubation for different time periods in the presence of CA (70 W-A units/mL) (b, d, f and h) compared with assays in the absence of the enzyme (a, c, e and g) are shown. *Right side* In vitro crystallization assay with QA. The assays were supplemented with 10 μM QA and performed in the absence (a, c, e and g) or presence of CA (b, d, f and h). Both round-shaped vaterite deposits (d) and rhombohedral prisms of calcite (p) can be seen. Light microscopic images (modified from Wang et al. 2014d)

round-shaped vaterite deposits and rhombohedral prisms of calcite) further grow in size after an extended incubation period of 60 min to about 120 μm both in the absence and in the presence of CA (Fig. 7, Left e and f), but the crystals formed in the presence of the CA are much more abundant. After 180 min (Fig. 7, Left g and h), a further increase in size of the crystals, especially in the assays containing CA, is visible. At the beginning of the reaction, no crystals are observed (Fig. 7, Left a, b). Addition of 10 μM QA in the diffusion/desiccator assays revealed an increase in number of the two different crystals during the 180 min incubation period, which was much more pronounced in the CA containing assays (Fig. 7, Right d, f and h), compared to the assays without CA (Fig. 7, Right c, e, and g). In addition to the crystals, small-sized deposits can be observed (Wang et al. 2014d).

6.1.2 Effect of QA on Biomineralization of SaOS-2 Cells

QA was found to cause a significant upregulation of the biomineralization process by SaOS-2 cells *in vitro*, especially in the presence of polyP (administered as a Ca^{2+} salt) (Wang et al. 2014d). In the absence of the mineralization activation cocktail (MAC; see Sect. 4.4) or in medium with MAC but lacking HCO_3^- , the extent of mineralization was low and not significantly changed by QA. In the presence of HCO_3^- and polyP, as a physiological phosphate source, QA significantly increased the extent of mineralization, compared to controls (Wang et al. 2014d).

The accelerating effect of QA on the biomineralization process by SaOS-2 cells was found to be strongest during the initial phase of mineralization. At day 3, the QA-induced upregulation of the mineralization process amounted to 210%, if the controls were set at 100% (Wang et al. 2014d). The biomineral deposits formed during the initial time period had a high content of carbon, as revealed by SEM coupled with energy-dispersive X-ray (EDX) analysis, both in the presence of pure QA and of *S. domuncula* extracts (Wang et al. 2014d).

6.1.3 Interaction of QA with the Catalytic Site of the CA

A molecular model for the interaction of QA with the catalytic site of the CA has been proposed by Wang et al. (2014d). The QA comprises two groups which could potentially interact with the Zn^{2+} -containing CA: the N-atom in the pyridine ring of the molecule and the two carboxy functional groups in ortho position to one another (dicarboxylic acid structure) (Fig. 8). The zinc prosthetic group of the CA is coordinated in three positions by the histidine side chains His₉₄, His₉₆, and His₁₁₉ of the protein (Lindskog 1997). The fourth coordination position at the Zn ion is occupied by one molecule of water. The Zn ion causes a polarization of the hydrogen–oxygen bond of the water molecule, resulting in an increased negativity of the oxygen and a weakening of the O–H bond. The hydroxide is bound to the zinc and the proton is accepted by a fourth histidine residue, His₆₄. We propose (Wang et al. 2014d) that the mechanism of QA can be formulated analogous to the

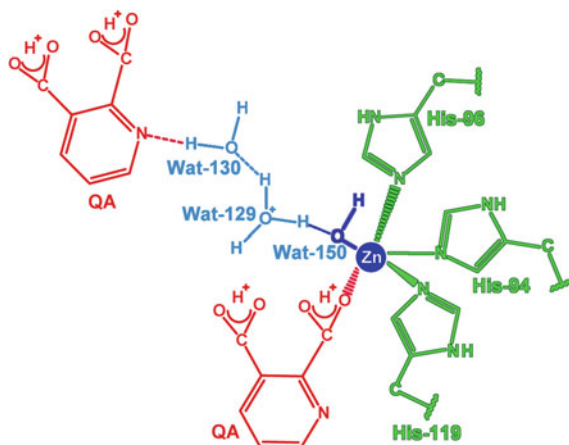


Fig. 8 Proposed interaction of QA (in red) with the catalytic site of the human CA. The three His residues that interact with the Zn^{2+} ion and the hydrogen bond network, formed by the water molecules Wat-150, Wat-129 and Wat-130, are shown (according to Ilies et al. 2004). QA is proposed to interact with its N-heteroatom to Wat-130 and one of its carboxylic acid groups to Zn^{2+} (modified from Wang et al. 2014d)

mechanism proposed for amino acid derivatives (Ilies et al. 2002). It is postulated that a hydrogen bridge bond formed between the N-atom of the pyridine ring of QA and the water₁₃₀ facilitates the rate-limiting proton transfer step of the CA reaction. The QA with its dicarboxylic acid side chains is assumed to interact with the enzyme-bound Zn ion similar like the bipyridyl Zn chelators (An 2009); Fig. 8.

7 Induction of CA IX Under Hypoxia

Under physiological conditions, within human tissues, the oxygen pressure is low, ranging from 1% (bone marrow and cartilage) to 10–13% (arteries, lungs, and liver) (Grant and Smith 1963; Richter et al. 1972; Cipolleschi et al. 1993). We showed that under such normoxic culture conditions (at an oxygen tension of 8% instead of 21% usually used in cell culture), simulating the situation in bone in vivo, the growth of osteoblast-like cells (SaOS-2) is not impaired (Müller et al. 2016). Addition of polyP, in the form of amorphous calcium polyP nanoparticles (Müller et al. 2015b) to those cells grown under normoxic conditions, at low oxygen tension, strongly increased the proliferation of the cells (Müller et al. 2016). Under these conditions, in the presence of polyP, the gene encoding for CA IX (Ziello et al. 2007) was found to become induced (Müller et al. 2016). In addition, the gene encoding for the inducible α -subunit of the hypoxia-inducible factor 1 (HIF-1/2) is upregulated (Wang and Semenza 1995). The latter protein, HIF-1/2, is known to control the expression of CA IX (Potter and Harris 2004).

It is known that mineralization is decreased at low oxygen tension, compared to the “normal” oxygen content of 21% (D’Ippolito et al. 2006; Arnett 2008). We demonstrated that in the presence of polyP, added as nanoparticles, the same extent of mineralization is reached in SaOS-2 cells grown under normoxic conditions (oxygen tension of 8%) like in cells kept under aerobic conditions (Müller et al. 2016). From these results we concluded that polyP acts as a supply of metabolic energy (“metabolic fuel”) during bone mineral formation under normoxic, physiological conditions for the cells to grow (Müller et al. 2016).

It has been reported that polyP, administered in the form of nanoparticles (Müller et al. 2015b) that are taken up by endocytosis (Müller et al. 2015c), increases the number of mitochondria in SaOS-2 cells and the production of ATP of the cells (Müller et al. 2015b). In the absence of polyP, at low oxygen tension, the production and release of lactate, the end product of anaerobic glycolysis, markedly increases, resulting in a drop of the pH value, in particular in the extracellular space (Vezzoli et al. 2003). The decrease in pH can be balanced by the CAs, primarily by the membrane-associated CA IX (Chiche et al. 2009; Sedlakova et al. 2014), that catalyzes the interconversion of bicarbonate and CO₂.

8 Calcium Carbonate in Bone Graft Substitution Materials

The discovery that amorphous CaCO₃ deposits act as bioseeds during human bone formation may allow not only the development of novel strategies for pharmacological intervention of osteoporosis and other bone diseases but also the development of novel biomimetic scaffolds for bone tissue engineering and repair (for a review, see Wang et al. 2014a).

Biomaterials for bone restoration are required to be biocompatible, biore-sorbable, and bioinductive (Wang et al. 2012). These requirements are optimally fulfilled for CaCO₃ in the form of ACC. This natural material has been selected in the course of evolution as a suitable scaffold not only for animals with a calcareous skeleton but also as component involved in vertebrate bone formation (this review). In addition, this material is amorphous and therefore superior as a scaffold material compared to its (more stable) crystalline transformation products (Tolba et al. 2015). Moreover, the synthesis of the natural mineral is controlled by enzymes and therefore regulatable in dependence of the actual metabolic situation of the organism (Wang et al. 2014b).

8.1 *Biocalcite from Corals*

In a number of reports, it has been shown that calcareous scaffolds, derived from corals, exhibit advantageous properties in bone reconstruction (for a review, see:

Cooper et al. 2014). Coral scaffolds have been reported to induce osteogenic differentiation of human MSC and an increased expression of osteogenic differentiation markers like ALP, osteocalcin, and osteonectin (for a review, see: Puvaneswary et al. 2013). Anabolic effects promoting bone restoration have been found both for calcareous scaffolds with CaCO_3 deposits present in the form calcite (soft octocorals) and aragonite (scleractinian hard corals). Such coral grafts have been demonstrated to cause a higher degree of mineralization compared to bone grafts.

8.2 Novel Biomaterial: ACC-Ca-PolyP

In order to prevent the transformation of ACC into its crystalline end product, calcite, ACC must be stabilized. We succeeded to develop a method for stabilization of ACC based on the addition of polyP (Tolba et al. 2015). The amorphous material was prepared by precipitation of CaCO_3 at pH 9.5 from aqueous solutions of $\text{CaCl}_2 \cdot 2\text{H}_2\text{O}$ and Na_2CO_3 at an equimolar $\text{Ca}^{2+}:\text{CO}_3^{2-}$ concentration ratio. The transition of ACC to a crystalline phase was suppressed by precipitation of the material in the presence of 0.1 g Na-polyP per 1 g of CaCO_3 . The ACC-P₁₀ microparticles thereby formed have a size of around 500 nm and mainly consist of ACC, containing a small amount of vaterite (Tolba et al. 2015).

8.2.1 Effect on Mesenchymal Stem Cells

In vitro studies with MSC revealed that the stabilized ACC (ACC-P₁₀) microparticles, as well as amorphous Ca-polyP microparticles significantly enhance the growth of the cells under physiologic normoxic conditions (Wang et al. 2016). Both the ACC-P₁₀ microparticles and the Ca-polyP microparticles exhibit opposite but complementary activities on gene expression: The ACC-P₁₀ microparticles strongly upregulate the expression of the cell membrane-associated *CA IX*, but have only a small effect on the transcript levels of *ALP* (Wang et al. 2016), while the amorphous Ca-polyP microparticles primarily induce *ALP* expression. The simultaneous administration of both microparticles results in a strong expression of both marker genes (Wang et al. 2016). An acceleration of cell growth by ACC and an induction of the steady-state-expression of the *CA IX* and, to a smaller extent, of *ALP* have also been reported for bone-related SaOS-2 cells (Müller et al. 2011; Tolba et al. 2015).

8.2.2 Animal Experiments

The critical size calvarial defect model in rat was applied to investigate the effect of the stabilized ACC microparticles, as well as of the amorphous Ca-polyP microparticles on bone regeneration in vivo (Wang et al. 2016). The particles were encapsulated into PLGA [poly(D,L-lactide-co-glycolide)] microspheres with a

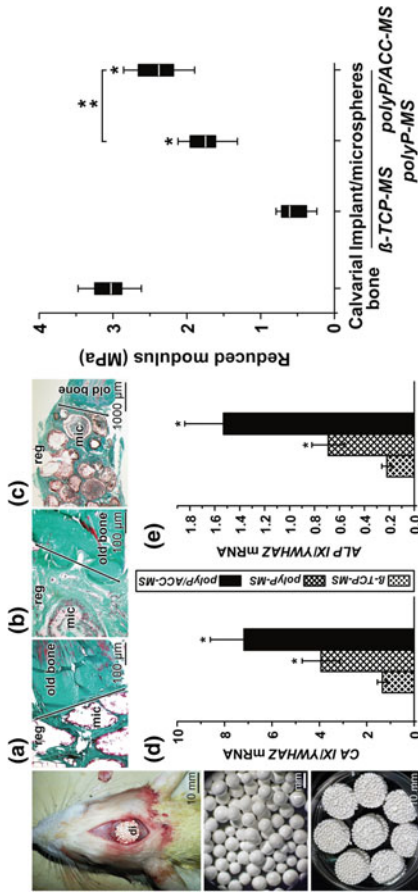


Fig. 9 Animal test using polyP/ACC microspheres disk (critical size calvarial defect of rat). *Right panel. Top* Insertion of implant into critical size calvarial defect. *di, disk. Middle panel. Top* Tissue slices of the defect region stained with Masson's trichrome 4 wk after implantation. **a** Transition zone between old bone and control implant (β-tricalcium phosphate); **b** Region around an implanted polyP/ACC microspheres disk; and **c** Regenerated implant region with polyP/ACC microspheres. *Bottom* Steady-state-expression of the genes encoding *CA IX* and *ALP* in these three areas; qRT-PCR (normalized to the expression of the *YWHAZ* house-keeping gene). *Right panel* Stiffness (reduced Young's modulus) of the regenerating/mineralizing tissue around the implanted microspheres; box plot (modified from Wang et al. 2016)

diameter $\sim 800 \mu\text{m}$ (Tolba et al. 2015; Wang et al. 2016) and 8 mm disks prepared from these microspheres were inserted into holes drilled into rat calvarial bone with a diameter of 10 mm (Fig. 9, Left panel). PLGA microspheres containing β -tricalcium phosphate (β -TCP) were used as control; β -TCP is a ceramic material widely used for bone implants (Trisi et al. 2003; Podaropoulos et al. 2009). The animals were sacrificed after an implantation period of 4, 8, or 12 weeks and subjected to histological analysis. The experiments revealed that the β -TCP microspheres are by far less active in bone regeneration (Wang et al. 2016); the histological sections through the regenerating defect area implanted with β -TCP microspheres are almost empty (Fig. 9 Middle panel a). The amorphous Ca-polyP microparticles were found to considerably accelerate the regeneration of bone tissue; after 12 weeks, both osteocytes and primary ossification centers in the implant regions were observed (Fig. 9 Middle panel b). The activity of the microspheres was markedly enhanced and the effect on bone regeneration was much faster if they were loaded with both the amorphous Ca-polyP microparticles and the ACC-P₁₀ microparticles. At a 1:1 weight ratio between these particles, an almost complete restoration of the defect area was found already after an implantation period of 12 weeks (Fig. 9 Middle panel c) (Wang et al. 2016).

The quantitative analysis of the micromechanical properties of the regeneration zone with the disk implants applying a special nanoindentation technology (Wang et al. 2014e) revealed a Young's modulus for the amorphous Ca-polyP microspheres of 1.74 MPa and for the microspheres containing both ACC-P₁₀ microparticles and amorphous Ca-polyP microparticles of 2.38 MPa, respectively (Fig. 9 Right panel). These values were significantly higher than the β -TCP-controls (0.63 mPa) and close to the value of the surrounding trabecular bone tissue with 3.05 MPa (Wang et al. 2016).

Moreover, in qRT-PCR analyses performed in parallel, we demonstrated that tissue sections through the regeneration zone with microspheres containing both ACC-P₁₀ microparticles and Ca-polyP microparticles show a markedly higher upregulation of expression of the marker genes, *CA IX* and *ALP*, compared to sections with microspheres containing only Ca-polyP or β -TCP (Wang et al. 2016); Fig. 9 Middle panel d and e. In addition, we demonstrated that ACC encapsulated into microspheres is biocompatible, if implanted into rat muscle (Tolba et al. 2015).

Based on their superior properties compared to β -TCP, the combination of both amorphous materials, ACC and Ca-polyP, opens new horizons for the development of regenerative implants for bone reconstruction (Wang et al. 2016).

Acknowledgements W.E.G.M. is a holder of an ERC Advanced Investigator Grant (no 268476 "BIOSILICA") as well as of the two ERC Proof-of-Concept grants "Si-Bone-PoC" (no. 324564) and "MorphoVES-PoC" (No. 662486). This work was supported by grants from the European Commission (large-scale integrating project "BlueGenics" No. 266033 and project "Bio-Scaffolds" No. 604036), as well as the BiomaTiCS research initiative of the University Medical Center Mainz.

References

- Abdo MR, Vullo D, Saada MC, Montero JL, Scozzafava A, Winum JY, Supuran CT (2009) Carbonic anhydrase activators: activation of human isozymes I, II and IX with phenylsulfonylethylhydrazido l-histidine derivatives. *Bioorg Med Chem Lett* 19:2440–2443
- Abdülkadir Coban T, Beydemir S, Gülcin I, Ekinci D, Innocenti A, Vullo D, Supuran CT (2009) Sildenafil is a strong activator of mammalian carbonic anhydrase isoforms I–XIV. *Bioorg Med Chem* 17:5791–5795
- Addadi L, Raz S, Weiner S (2003) Taking advantage of disorder: amorphous calcium carbonate and its roles in biomineralization. *Adv Mater* 15:959–970
- Aggarwal M, Boone CD, Kondeti B, McKenna R (2013) Structural annotation of human carbonic anhydrases. *J Enzyme Inhib Med Chem* 28:267–277
- Aizenberg J, Hanson J, Koetzle TF, Leiserowitz L, Weiner S, Addadi L (1995) Biologically induced reduction in symmetry: a study of crystal texture of calcitic sponge spicules. *Chem Eur J* 1:414–422
- Alterio V, Di Fiore A, D'Ambrosio K, Supuran CT, De Simone G (2009) X-Ray crystallography of CA inhibitors and its importance in drug design. In: Supuran CT, Winum JY (eds) *Drug Design of Zinc-Enzyme Inhibitors: functional Structural and Disease Applications*. Wiley, Hoboken, pp 73–138
- Alvarez L, Fanjul M, Carter N, Hollande E (2001) Carbonic anhydrase II associated with plasma membrane in a human pancreatic duct cell line (CAPAN-1). *J Histochem Cytochem* 49:1045–1053
- An Z (2009) Bis(μ -2'-carboxylatobiphenyl-2-carboxylic acid- κ O2:O2')bis[(2,2'-bipyridine- κ 2 N, N')(2'-carboxylatobiphenyl-2-carboxylic acid- κ O2')zinc(II)]. *Acta Crystallogr Sect E - Struct Rep* E65:m1501
- Andrade LR, Lins U, Farina M, Kachar B, Thalmann R (2012) Immunogold TEM of otoconin 90 and otolin—relevance to mineralization of otoconia, and pathogenesis of benign positional vertigo. *Hear Res* 292:14–25
- Arnett TR (2008) Extracellular pH regulates bone cell function. *J Nutr* 138:415S–418S
- Aspatwar A, Tolvanen MEE, Ortutay C, Parkkila S (2014) Carbonic anhydrase related proteins: molecular biology and evolution. *Subcell Biochem* 75:135–156
- Badger MR, Price GD (1994) The role of carbonic anhydrase in photosynthesis. *Ann Rev Plant Physiol/Plant Molec Biol* 45:369–392
- Barrese AA 3rd, Genis C, Fisher SZ, Orwenyo JN, Kumara MT, Dutta SK, Phillips E, Kiddle JJ, Tu C, Silverman DN, Govindasamy L, Agbandje-McKenna M, McKenna R, Tripp BC (2008) Inhibition of carbonic anhydrase II by thioxolone: a mechanistic and structural study. *Biochemistry* 47:3174–3184
- Beniash E (2011) Biomaterials—hierarchical nanocomposites: the example of bone. *Wiley Interdiscip Rev Nanomed Nanobiotechnol* 3:47–69
- Bertucci A, Zoccola D, Tambuttè S, Vullo D, Supuran CT (2010) Carbonic anhydrase activators. The first activation study of a coral secretory isoform with amino acids and amines. *Bioorg Med Chem* 18:2300–2303
- Biltz RM, Pellegrino ED (1977) The nature of bone carbonate. *Clin Orthop* 129:279–292
- Boonrungsiman S, Gentleman E, Carzaniga R, Evans ND, McComb DW, Porter AE, Stevens MM (2012) The role of intracellular calcium phosphate in osteoblast-mediated bone apatite formation. *Proc Natl Acad Sci USA* 109:14170–14175
- Boyle WJ, Simonet WS, Lacey DL (2003) Osteoclast differentiation and activation. *Nature* 423:337–342
- Breton S (2001) The cellular physiology of carbonic anhydrases. *J Pancreas* 2(Suppl):159–164
- Briganti F, Mangani S, Orioli P, Scozzafava A, Vernaglion G, Supuran CT (1997) Carbonic anhydrase activators: X-ray crystallographic and spectroscopic investigations for the interaction of isozymes I and II with histamine. *Biochemistry* 36:10384–10392

- Cartwright JH, Checa AG, Gale JD, Gebauer D, Sainz-Díaz CI (2012) Calcium carbonate polymorphism and its role in biomineralization: how many amorphous calcium carbonates are there? *Angew Chem Int Ed Engl* 51:11960–11970
- Casey JR, Sly WS, Shah GN, Alvarez BV (2009) Bicarbonate homeostasis in excitable tissues: role of AE3 Cl/HCO³⁻ exchanger and carbonic anhydrase XIV interaction. *Am J Physiol Cell Physiol* 297C:1091–1102
- Chang X, Zheng Y, Yang Q, Wang L, Pan J, Xia Y, Yan X, Han J (2012) Carbonic anhydrase I (CA1) is involved in the process of bone formation and is susceptible to ankylosing spondylitis. *Arthritis Res Ther* 14:R176
- Chiche J, Ilc K, Laferrier J, Trottier E, Dayan F, Mazure N, Brahim-Horn MC, Pouysségur J (2009) Hypoxia-inducible carbonic anhydrase IX and XII promote tumor cell growth by counteracting acidosis through the regulation of the intracellular pH. *Cancer Res* 69:358–363
- Cipolleschi MG, Dello Sbarba P, Olivetto M (1993) The role of hypoxia in the maintenance of hematopoietic stem cells. *Blood* 82:2031–2037
- Cölfen H, Mann S (2003) Higher-order organization by mesoscale self-assembly and transformation of hybrid nanostructures. *Angew Chem Int Ed* 42:2350–2365
- Collin P, Nefussi JR, Wetterwald A, Nicolas V, Boy-Lefevre ML, Fleisch H, Forest N (1992) Expression of collagen, osteocalcin, and bone alkaline phosphatase in a mineralizing rat osteoblastic cell culture. *Calcif Tissue Int* 50:175–183
- Cooper EL, Hirabayashi K, Strychar KB, Sammarco PW (2014) Corals and their potential applications to integrative medicine. *Based Complement Alternat Med* 2014:184959
- Dave K, Ilies MA, Scozzafava A, Temperini C, Vullo D, Supuran CT (2011) An inhibitor-like binding mode of a carbonic anhydrase activator within the active site of isoform II. *Bioorg Med Chem Lett* 21:2764–2766
- Deans MR, Peterson JM, Wong GW (2010) Mammalian otolin: A multimeric glycoprotein specific to the inner ear that interacts with otoconial matrix protein otoconin-90 and cerebellin-1. *PLoS ONE* 5:e12765
- D’Ippolito G, Diabira S, Howard GA, Roos BA, Schiller PC (2006) Low oxygen tension inhibits osteogenic differentiation and enhances stemness of human MIAMI cells. *Bone* 39:513–522
- Frost SC (2014) Physiological functions of the alpha class of carbonic anhydrases. *Subcell Biochem* 75:9–30
- Gower LB (2008) Biomimetic model systems for investigating the amorphous precursor pathway and its role in biomineralization. *Chem Rev* 108:4551–4627
- Grant J, Smith B (1963) Bone marrow gas tensions, bone marrow blood flow, and erythropoiesis in man. *Ann Int Med* 58:801–809
- Haddad GG, Boron WF (2000) Na⁺/HCO₃⁻ cotransporters in rat brain: expression in glia, neurons, and choroid plexus. *J Neurosci* 20:6839–6848
- Henry RP (1996) Multiple roles of carbonic anhydrase in cellular transport and metabolism. *Annu Rev Physiol* 58:523–538
- Hohling HJ, Barchhaus RH, Drefting ER, Quint P, Athoff J (1978) Quantitative electron microscopy of the early stages of cartilage mineralization. *Metab Bone Dis Res* 1:109–114
- Ilan M, Aizenberg J, Gilor O (1996) Dynamics and growth patterns of calcareous sponge spicules. *Proc R Soc Lond B* 263:133–139
- Ilies M, Banciu MD, Ilies MA, Scozzafava A, Caproiu MT, Supuran CT (2002) Carbonic anhydrase activators: design of high affinity isozymes I, II and IV activators, incorporating tri-/tetrasubstituted-pyridinium-azole moieties. *J Med Chem* 45:504–510
- Ilies M, Scozzafava A, Supuran CT (2004) Carbonic anhydrase activators. In: Supuran CT, Scozzafava A, Conway J (eds) *Carbonic anhydrase—its inhibitors and activators*. CRC Press, Boca Raton, pp 317–352
- Innocenti A, Pastorekova S, Pastorek J, Scozzafava A, De Simone G, Supuran CT (2009) The proteoglycan region of the tumor-associated carbonic anhydrase isoform IX acts as an intrinsic buffer optimizing CO₂ hydration at acidic pH values characteristic of solid tumors. *Bioorg Med Chem Lett* 19:5825–5828

- Innocenti A, Hall RA, Scozzafava A, Mühlischlegel FA, Supuran CT (2010) Carbonic anhydrase activators: activation of the β -carbonic anhydrases from the pathogenic fungi *Candida albicans* and *Cryptococcus neoformans* with amines and amino acids. *Bioorg Med Chem* 18:1034–1937
- Isik S, Kockar F, Aydin M, Arslan O, Guler OO, Innocenti A, Scozzafava A, Supuran CT (2009) Carbonic anhydrase activators: activation of the beta-carbonic anhydrase Nce103 from the yeast *Saccharomyces cerevisiae* with amines and amino acids. *Bioorg Med Chem Lett* 19:1662–1665
- Jones WC (1967) Sheath and axial filament of calcareous sponge spicules. *Nature* 214:365–368
- Jones WC (1970) The composition, development, form and orientation of calcareous sponge spicules. *Symp Zool Soc Lond* 25:91–123
- Knoll AH (2003) Biomineralization and evolutionary history. *Rev Mineral Geochem* 54:329–356
- Kulaev IS (1979) The biochemistry of inorganic polyphosphates. Wiley, New York
- Kulaev IS, Vagabov VM, Kulakovskaya TV (2004) The biochemistry of inorganic polyphosphates. Wiley, Chichester, pp 1–277
- Laitala T, Väänänen HK (1994) Inhibition of bone resorption in vitro by antisense RNA and DNA molecules targeted against carbonic anhydrase II or two subunits of vacuolar H⁽⁺⁾-ATPase. *J Clin Invest* 93:2311–2318
- Landis WJ, Song MJ, Leith A, McEwen L, McEwen BF (1993) Mineral and organic matrix interaction in normally calcifying tendon visualized in three dimensions by high-voltage electron microscopic tomography and graphic image reconstruction. *J Struct Biol* 110:39–54
- Ledger PW, Jones WC (1977) Spicule formation in the calcareous sponge *Sycon ciliatum*. *Cell Tiss Res* 181:553–567
- Leyhausen G, Lorenz B, Zhu H, Geurtsen W, Bohnensack R, Müller WEG, Schröder HC (1998) Inorganic polyphosphate in human osteoblast-like cells. *J Bone Mineral Res* 13:803–812
- Li W, Chen WS, Zhou PP, Cao L, Yu LJ (2013a) Influence of initial pH on the precipitation and crystal morphology of calcium carbonate induced by microbial carbonic anhydrase. *Colloids Surf B Biointerfaces* 102:281–287
- Li W, Chen WS, Zhou PP, Zhu SL, Yu LJ (2013b) Influence of initial calcium ion concentration on the precipitation and crystal morphology of calcium carbonate induced by bacterial carbonic anhydrase. *Chemical Engineering J* 218:65–72
- Lian JB, Gundberg CM (1988) Osteocalcin. Biochemical considerations and clinical applications. *Clin Orthop Relat Res* 226:267–291
- Lindsey AE, Schneider K, Simmons DM, Baron R, Lee BS, Kopito RR (1990) Functional expression and subcellular localization of an anion exchanger from choroid plexus. *Proc Natl Acad Sci USA* 87:5278–5282
- Lindskog S (1997) Structure and mechanism of carbonic anhydrase. *Pharmacol Ther* 74:1–20
- Lorenz B, Schröder HC (2001) Mammalian intestinal alkaline phosphatase acts as highly active exopolyphosphatase. *Biochim Biophys Acta* 1547:254–261
- Lorenz B, Marmé S, Müller WEG, Unger K, Schröder HC (1994a) Preparation and use of polyphosphate-modified zirconia for purification of nucleic acids and proteins. *Anal Biochem* 216:118–126
- Lorenz B, Müller WEG, Kulaev IS, Schröder HC (1994b) Purification and characterization of an exopolyphosphatase activity from *Saccharomyces cerevisiae*. *J Biol Chem* 269:22198–22204
- Lorenz B, Münkner J, Oliveira MP, Kuusksalu A, Leitão JM, Müller WEG, Schröder HC (1997) Changes in metabolism of inorganic polyphosphate in rat tissues and human cells during development and apoptosis. *Biochim Biophys Acta* 1335:51–60
- Mahieu I, Hollande E, Carter N (1994) Membrane targeting of carbonic anhydrase II (CAII) in human pancreatic ductal Capan 1 cells in culture. *Biochem Soc Trans* 22:438S
- Mann S, Parker SB, Ross MD, Skarnulis AJ, Williams RJ (1983) The ultrastructure of the calcium carbonate balance organs of the inner ear: an ultra-high resolution electron microscopy study. *Proc R Soc Lond B Biol Sci* 218:415–424
- Margolis DS, Szivek JA, Lai LW, Lien YH (2008) Phenotypic characteristics of bone in carbonic anhydrase II-deficient mice. *Calcif Tissue Int* 82:66–76

- Matsuo K, Irie N (2008) Osteoclast-osteoblast communication. *Arch Biochem Biophys* 473:201–209
- Matsuura A, Kubo T, Doi K, Hayashi K, Morita K, Yokota R, Hayashi H, Hirata I, Okazaki M, Akagawa Y (2009) Bone formation ability of carbonate apatite-collagen scaffolds with different carbonate contents. *Dent Mater J* 28:234–242
- McIntosh JE (1970) Carbonic anhydrase isoenzymes in the erythrocytes and uterus of the rabbit. *Biochem J* 120:299–310
- Meldrum FC, Cölfen H (2008) Controlling mineral morphologies and structures in biological and synthetic systems. *Chem Rev* 108:4332–4432
- Merkel C, Deuschle J, Griesshaber E, Enders S, Steinhäuser E, Hochleitner R, Brand U, Schmahl WW (2009) Mechanical properties of modern calcite- (*Mergerlia truncata*) and phosphate-shelled brachiopods (*Discradisca stella* and *Lingula anatina*) determined by nanoindentation. *J Struct Biol* 168:396–408
- Morrissey JH, Choi SH, Smith SA (2012) Polyphosphate: an ancient molecule that links platelets, coagulation, and inflammation. *Blood* 119:5972–5979
- Morse DE (1999) Silicon biotechnology: harnessing biological silica production to construct new materials. *Trends Biotechnol* 17:230–232
- Müller WEG (2003) [ed] Silicon biomineralization: biology-biochemistry-molecular biology-biotechnology. Berlin: Springer Press; Progress Molec Subcell Biol, vol 33
- Müller WEG, Müller I, Zahn RK, Maidhof A (1984) Intraspecific recognition system in scleractinian corals: morphological and cytochemical description of the autolysis mechanism. *J Histochem Cytochem* 32:285–288
- Müller WEG, Wiens M, Adell T, Gamulin V, Schröder HC, Müller IM (2004) Bauplan of urmetazoa: basis for genetic complexity of Metazoa. *Int Rev Cytol* 235:53–92
- Müller WEG, Li J, Schröder HC, Qiao L, Wang XH (2007) The unique skeleton of siliceous sponges (Porifera; Hexactinellida and Demospongiae) that evolved first from the Urmetazoa during the Proterozoic: a review. *Biogeosciences* 4:219–232
- Müller WEG, Wang XH, Diehl-Seifert B, Kropf K, Schloßmacher U, Lieberwirth I, Glasser G, Wiens M, Schröder HC (2011) Inorganic polymeric phosphate/polyphosphate as an inducer of alkaline phosphatase and a modulator of intracellular Ca^{2+} level in osteoblasts (SaOS-2 cells) in vitro. *Acta Biomater* 7:2661–2671
- Müller WEG, Wang XH, Grebenjuk VA, Korzhev M, Wiens M, Schloßmacher U, Schröder HC (2012) Common genetic denominators for Ca^{++} -based skeleton in metazoa: Role of osteoclast-stimulating factor and of carbonic anhydrase in a calcareous sponge. *PLoS ONE* 7:e34617
- Müller WEG, Schröder HC, Burghard Z, Pisignano D, Wang XH (2013a) Silicateins—a novel paradigm in bioinorganic chemistry: enzymatic synthesis of inorganic polymeric silica. *Chemistry Eur J* 19:5790–5804
- Müller WEG, Schröder HC, Schlossmacher U, Grebenjuk VA, Ushijima H, Wang XH (2013b) Induction of carbonic anhydrase in SaOS-2 cells, exposed to bicarbonate and consequences for calcium phosphate crystal formation. *Biomaterials* 34:8671–8680
- Müller WEG, Schröder HC, Schlossmacher U, Neufurth M, Geurtsen W, Korzhev M, Wang XH (2013c) The enzyme carbonic anhydrase as an integral component of biogenic Ca-carbonate formation in sponge spicules. *FEBS Open Bio* 3:357–362
- Müller WEG, Albert O, Schröder HC, Wang XH (2014a) Bio-inorganic nanomaterials for biomedical applications (Bio-silica and polyphosphate). In: Bhushan B, Luo D, Schrick S, Sigmund W, Zauscher S (eds) *Handbook of nanomaterials properties*. Springer Press, Berlin, pp 389–408
- Müller WEG, Neufurth M, Schlossmacher U, Schröder HC, Pisignano D, Wang XH (2014b) The sponge silicatein-interacting protein silintaphin-2 blocks calcite formation of calcareous sponge spicules at the vaterite stage. *RSC Adv* 4:2577–2585
- Müller WEG, Schlossmacher U, Schröder HC, Lieberwirth I, Glasser G, Korzhev M, Neufurth M, Wang XH (2014c) Enzyme-accelerated and structure-guided crystallization of Ca-carbonate: role of the carbonic anhydrase in the homologous system. *Acta Biomater* 10:450–462

- Müller WEG, Neufurth M, Huang J, Wang K, Feng Q, Schröder HC, Diehl-Seifert B, Muñoz-Espí R, Wang XH (2015a) Non-enzymatic transformation of amorphous CaCO_3 into calcium phosphate mineral after exposure to sodium phosphate in vitro: Implications for in vivo hydroxyapatite bone formation. *ChemBioChem* 16:1323–1332
- Müller WEG, Tolba E, Feng Q, Schröder HC, Markl JS, Kokkinopoulou M, Wang XH (2015b) Amorphous Ca^{2+} polyphosphate nanoparticles regulate ATP level in bone-like SaOS-2 cells. *J Cell Sci* 128:2202–2207
- Müller WEG, Tolba E, Schröder HC, Wang S, Glaßer G, Muñoz-Espí R, Link T, Wang XH (2015c) A new polyphosphate calcium material with morphogenetic activity. *Mater Lett* 148:163–166
- Müller WEG, Schröder HC, Tolba E, Diehl-Seifert B, Wang XH (2016) Mineralization of bone-related SaOS-2 cells under physiological hypoxic conditions. *FEBS J* 283:74–87
- Murayama E, Takagi Y, Ohira T, Davis JG, Greene MI, Nagasawa H (2002) Fish otolith contains a unique structural protein, otolin-1. *Eur J Biochem* 269:688–696
- Murugan R, Ramakrishna S, Rao KP (2006) Nanoporous hydroxy-carbonate apatite scaffold made of natural bone. *Materials Lett* 60:2844–2847
- Omelson SJ, Grynpas MD (2008) Relationships between polyphosphate chemistry, biochemistry and apatite biomineralization. *Chem Rev* 108:4694–4715
- Omelson S, Georgiou J, Henneman ZJ, Wise LM, Sukhu B, Hunt T, Wynnyckyj C, Holmyard D, Ryszard B, Grynpas MD (2009) Control of vertebrate skeletal mineralization by polyphosphates. *PLoS ONE* 4:e5634
- Park JB (2012) The effects of dexamethasone, ascorbic acid, and β -glycerophosphate on osteoblastic differentiation by regulating estrogen receptor and osteopontin expression. *J Surg Res* 173:99–104
- Parra-Torres AY, Valdés-Flores M, Orozco L, Velázquez-Cruz R (2013) Molecular aspects of bone remodeling. InTech: creative commons attribution license; <http://dx.doi.org/10.5772/54905>, pp 1–27
- Pastorekova S, Parkkila S, Pastorek J, Supuran CT (2004) Carbonic anhydrases: current state of the art, therapeutic applications and future prospects. *J Enzyme Inhib Med Chem* 19(19): 199–229
- Pastorekova S, Vullo D, Nishimori I, Scozzafava A, Pastorek J, Supuran CT (2008) Carbonic anhydrase activators: activation of the human tumor-associated isozymes IX and XII with amino acids and amines. *Bioorg Med Chem* 16:3530–3536
- Pellegrino ED, Biltz RM (1970) Calcium carbonate in medullary bone. *Calcif Tissue Res* 6:168–171
- Pisam M, Jammet C, Laurent D (2002) First steps of otolith formation of the zebrafish: role of glycogen? *Cell Tissue Res* 310:163–168
- Podaropoulos L, Veis AA, Papadimitriou S, Alexandridis C, Kalyvas D (2009) Bone regeneration using beta-tricalcium phosphate in a calcium sulfate matrix. *J Oral Implantol* 35:28–36
- Posner AS (1969) Crystal chemistry of bone mineral. *Physiol Rev* 49:760–792
- Posner AS, Duyckaerts G (1954) Infrared study of the carbonate in bone, teeth and francolite. *Experientia* 10:424–425
- Posner AS, Betts F, Blumenthal NC (1978) Properties of nucleating systems. *Metab Bone Dis Rel Res* 1:179–183
- Potter C, Harris AL (2004) Hypoxia inducible carbonic anhydrase IX, marker of tumour hypoxia, survival pathway and therapy target. *Cell Cycle* 3:164–167
- Poyart CF, Bursaux E, Fréminet A (1975) The bone CO_2 compartment: evidence for a bicarbonate pool. *Respir Physiol* 25:89–99
- Purkerson JM, Schwartz GJ (2005) Expression of membrane-associated carbonic anhydrase isoforms IV, IX, XII, and XIV in the rabbit: induction of CA IV and IX during maturation. *Am J Physiol Regul Integr Comp Physiol* 288:R1256–R1263
- Puvanewary S, Balaji Raghavendran HR, Ibrahim NS, Murali MR, Merican AM, Kamarul T (2013) A comparative study on morphochemical properties and osteogenic cell differentiation within bone graft and coral graft culture systems. *Int J Med Sci* 10:1608–1614

- Ramanan R, Kannan K, Sivanesan SD, Ramanan R, Kannan K, Sivanesan SD, Mudliar S, Kaur S, Tripathi AK, Chakrabarti T (2009) Bio-sequestration of carbon dioxide using carbonic anhydrase enzyme purified from *Citrobacter freundii*. *World J Microbiol Biotechnol* 25:981–987
- Rao NN, Gómez-García MR, Kornberg A (2009) Inorganic polyphosphate: essential for growth and survival. *Annu Rev Biochem* 78:605–647
- Reddy MM (1981) Crystal growth of calcite from calcium bicarbonate solutions at constant PCO₂ and 25 C: a test of a calcite dissolution model. *Geochim Cosmochim Acta* 45:1281–1289
- Rey C, Collins B, Goehl T, Dickson IR, Glimcher MJ (1989) The carbonate environment in bone mineral: a resolution-enhanced Fourier transform infrared spectroscopy study. *Calcif Tissue Int* 45:57–164
- Rey C, Kim HM, Gerstenfeld L, Glimcher MJ (1996) Characterization of the apatite crystals of bone and their maturation in osteoblast cell culture: comparison with native bone crystals. *Connect Tissue Res* 35:343–349
- Richter A, Sanford KK, Evans VJ (1972) Influence of oxygen and culture media on plating efficiency of some mammalian tissue cells. *J Natl Cancer Inst* 49:1705–1712
- Roos A, Boron WF (1981) Intracellular pH. *Physiol Rev* 61:296–434
- Safadi FF, Barbe MF, Abdelmagid SM, Rico MC, Aswad RA, Litvin J, Popoff SN (2009) Bone structure, development and bone biology. In: Khurana JS (ed) *Bone pathology*. Springer Science + Business Media, Berlin, pp 1–50
- Sanyal G, Maren TH (1981) Thermodynamics of carbonic anhydrase catalysis. A comparison between human isoenzymes B and C. *J Biol Chem* 256:608–612
- Schröder HC, Müller WEG (1999) Inorganic polyphosphates. *Biochemistry, biology, biotechnology*. Springer, Berlin, vol 23
- Schröder HC, Kurz L, Müller WEG, Lorenz B (2000) Polyphosphate in bone. *Biochemistry (Moscow)* 65:296–303
- Schröder HC, Sudek S, De Caro S, De Rosa S, Perović S, Steffen R, Müller IM, Müller WEG (2002) Synthesis of the neurotoxin quinolinic acid in apoptotic tissue from *Suberites domuncula*: cell biological, molecular biological and chemical analyses. *Mar Biotechnol* 4:546–558
- Schröder H-C, Perović-Ottstadt S, Rothenberger M, Wiens M, Schwertner H, Batel R, Korzhev M, Müller IM, Müller WEG (2004) Silica transport in the demosponge *Suberites domuncula*: fluorescence emission analysis using the PDMPO probe and cloning of a potential transporter. *Biochem J* 381:665–673
- Schütze J, Custodio MR, Efremova SM, Müller IM, Müller WEG (1999) Evolutionary relationship of metazoa within the eukaryotes based on molecular data from Porifera. *Proc Royal Society Lond B* 266:63–73
- Scozzafava A, Supuran CT (2002) Carbonic anhydrase activators: human isozyme II is strongly activated by oligopeptides incorporating the carboxyterminal sequence of the bicarbonate anion exchanger AE1. *Bioorg Med Chem Lett* 12:1177–1180
- Sedlakova O, Svastova E, Takacova M, Kopacek J, Pastorek J, Pastorekova S (2014) Carbonic anhydrase IX, a hypoxia-induced catalytic component of the pH regulating machinery in tumors. *Front Physiol* 4:400; doi:[10.3389/fphys.2013.00400](https://doi.org/10.3389/fphys.2013.00400)
- Sei Y, Fossom L, Goping G, Skolnick P, Basile AS (1998) Quinolinic acid protects rat cerebellar granule cells from glutamate-induced apoptosis. *Neurosci Lett* 241:180–184
- Sethmann I, Wörheide G (2008) Structure and composition of calcareous sponge spicules: a review and comparison to structurally related biominerals. *Micron* 39:209–228
- Shinohara C, Yamashita K, Matsuo T, Kitamura S, Kawano F (2007) Effects of carbonic anhydrase inhibitor acetazolamide (AZ) on osteoclasts and bone structure. *J Hard Tissue Biol* 16:115–123
- Simkiss K, Wilbur K (1989) *Biomineralization. Cell Biology and Mineral Deposition*. Academic Press Inc., San Diego
- Simpson TL (1984) *The cell biology of sponges*. Springer, New York

- Sinha KM, Yasuda H, Coombes MM, Dent SYR, de Crombrugge B (2010) Regulation of the osteoblast-specific transcription factor Osterix by NO66, a Jumonji family histone demethylase. *EMBO J* 29:68–79
- Sly WS, Hu PY (1995) Human carbonic anhydrases and carbonic anhydrase deficiencies. *Annu Rev Biochem* 64:375–401
- Sly WS, Hewett-Emmett D, Whyte MP, Yu YS, Tashian RE (1983) Carbonic anhydrase II deficiency identified as the primary defect in the autosomal recessive syndrome of osteopetrosis with renal tubular acidosis and cerebral calcification. *Proc Natl Acad Sci USA* 80:2752–2756
- Smith KS, Ferry JG (2000) Prokaryotic carbonic anhydrases. *FEMS Microbiol Rev* 24:335–366
- Supuran CT (2004) Carbonic anhydrases: catalytic inhibition mechanisms distribution and physiological roles. In: Carbonic anhydrase: its inhibitors and activators. In: Supuran CT, Scozzafava A, Conway J (eds) CRC Press, Boca Raton, pp 1–23
- Supuran CT (2008a) Carbonic anhydrases—an overview. *Curr Pharm Des* 14:603–614
- Supuran CT (2008b) Carbonic anhydrases: novel therapeutic applications for inhibitors and activators. *Nat Rev Drug Discov* 7:168–181
- Supuran CT (2009) Carbonic anhydrases as drug targets: General presentation. In: Supuran CT, Winum JY (eds) Drug design of zinc-enzyme inhibitors: functional, structural, and disease applications. Wiley, Hoboken, pp 13–38
- Supuran CT (2011) Carbonic anhydrase inhibitors and activators for novel therapeutic applications. *Future Med Chem* 3:1165–1180
- Supuran CT (2016) How many carbonic anhydrase inhibition mechanisms exist? *J Enzyme Inhib Med Chem* 31:345–360
- Supuran CT, Scozzafava A (2000a) Carbonic anhydrase inhibitors and their therapeutic potential. *Expert Opin Ther Patents* 10:575–600
- Supuran CT, Scozzafava A (2000b) Carbonic anhydrase activators: synthesis of high affinity isozymes I, II and IV activators, derivatives of 4-(arylsulfonylureido-amino acyl) ethyl-1H-imidazole. *J Enzyme Inhib* 15:471–486
- Supuran CT, Scozzafava A (2000c) Activation of carbonic anhydrase isozymes. In: Chegwidan WR, Carter N, Edwards Y (eds) The carbonic anhydrases—new horizons. Birkhauser, Basel, pp 197–219
- Supuran CT, Casini A, Scozzafava A (2004a) Development of sulfonamide carbonic anhydrase inhibitors. In: Supuran CT, Scozzafava A, Conway J (eds) Carbonic anhydrase: its inhibitors and activators. CRC Press, Boca Raton, pp 67–147
- Supuran CT, Vullo D, Manole G, Casini A, Scozzafava A (2004b) Designing of novel carbonic anhydrase inhibitors and activators. *Curr Med Chem Cardiovasc Hematol Agents* 2:49–68
- Temperini C, Scozzafava A, Puccetti L, Supuran CT (2005) Carbonic anhydrase activators: X-ray crystal structure of the adduct of human isozyme II with L-histidine as a platform for the design of stronger activators. *Bioorg Med Chem Lett* 15:5136–5141
- Temperini C, Scozzafava A, Supuran CT (2006a) Carbonic anhydrase activators: the first X-ray crystallographic study of an adduct of isoform I. *Bioorg Med Chem Lett* 16:5152–5156
- Temperini C, Scozzafava A, Vullo D, Supuran CT (2006b) Carbonic anhydrase activators. Activation of isozymes I, II, IV, VA, VII, and XIV with L- and D-histidine and crystallographic analysis of their adducts with isoform II: engineering proton-transfer processes within the active site of an enzyme. *Chemistry* 12:7057–7066
- Temperini C, Scozzafava A, Vullo D, Supuran CT (2006c) Carbonic anhydrase activators. Activation of isoforms I, II, IV, VA, VII, and XIV with L- and D-phenylalanine and crystallographic analysis of their adducts with isozyme II: stereospecific recognition within the active site of an enzyme and its consequences for the drug design. *J Med Chem* 49:3019–3027
- Temperini C, Innocenti A, Scozzafava A, Mastrolorenzo A, Supuran CT (2007) Carbonic anhydrase activators: L-Adrenaline plugs the active site entrance of isozyme II, activating better isoforms I, IV, VA, VII, and XIV. *Bioorg Med Chem Lett* 17:628–635
- Temperini C, Innocenti A, Scozzafava A, Supuran CT (2008) Carbonic anhydrase activators: kinetic and X-ray crystallographic study for the interaction of D- and L-tryptophan with the mammalian isoforms I–XIV. *Bioorg Med Chem* 16:8373–8378

- Termine JD, Eanes ED, Greenfield DJ, Nylen MU, Harper RA (1973) Hydrazine-deproteinated bone mineral. Physical and chemical properties. *Calcif Tissue Res* 12:73–90
- Thrailkill KM, Jo CH, Cockrell GE, Moreau CS, Lumpkin CK Jr, Fowlkes JL (2012) Determinants of undercarboxylated and carboxylated osteocalcin concentrations in type 1 diabetes. *Osteoporos Int* 23:1799–1806
- Tolba E, Müller WEG, El-Hady BMA, Neufurth M, Wurm F, Wang S, Schröder HC, Wang XH (2015) High biocompatibility and improved osteogenic potential of amorphous calcium carbonate/vaterite. *J Mat Chem B* 4:376–386
- Towe KM, Lowenstam HA (1967) Ultrastructure and development of iron mineralization in the radular teeth of *Cryptochiton stelleri* (mollusca). *J Ultrastruct Res* 17:1–13
- Tripp BC, Smith K, Ferry JG (2001) Carbonic anhydrase: new insights for an ancient enzyme. *J Biol Chem* 276:48615–48618
- Trisi P, Rao W, Rebaudi A, Fiore P (2003) Histologic effect of pure-phase beta-tricalcium phosphate on bone regeneration in human artificial jawbone defects. *Int J Periodontics Restorative Dent* 23:69–77
- Uriz MJ (2006) Mineral skeletogenesis in sponges. *Can J Zool* 84:322–356
- Van Wazer JR (1958) Phosphorus and its compounds: chemistry, vol 1. Interscience Publishers, New York
- Vezzoli A, Gussoni M, Greco F, Zetta L (2003) Effects of temperature and extracellular pH on metabolites: kinetics of anaerobic metabolism in resting muscle by ^{31}P - and ^1H -NMR spectroscopy. *J Exp Biol* 206:3043–3052
- Vullo D, Nishimori I, Scozzafava A, Supuran CT (2008) Carbonic anhydrase activators: activation of the human cytosolic isozyme III and membrane-associated isoform IV with amino acids and amines. *Bioorg Med Chem Lett* 18:4303–4307
- Vullo D, Del Prete S, Capasso C, Supuran CT (2016) Carbonic anhydrase activators: activation of the β -carbonic anhydrase from *Malassezia globosa* with amines and amino acids. *Bioorg Med Chem Lett* 26:1381–1385
- Walker G (2003) Snowball earth: the story of the great global catastrophe that spawned life as we know it. Crown Publishers, New York
- Wang GL, Semenza GL (1995) Purification and characterization of hypoxia-inducible factor-1. *J Biol Chem* 270:1230–1237
- Wang XH, Schröder HC, Wiens M, Ushijima H, Müller WEG (2012) Bio-silica and bio-polyphosphate: applications in biomedicine (bone formation). *Curr Opin Biotechnol* 23:570–578
- Wang XH, Schröder HC, Diehl-Seifert B, Kropf K, Schlossmacher U, Wiens M, Müller WEG (2013) Dual effect of inorganic polymeric phosphate/polyphosphate on osteoblasts and osteoclasts in vitro. *J Tissue Engin Regen Med* 7:767–776
- Wang XH, Schröder HC, Müller WEG (2014a) Biocalcite, a multifunctional inorganic polymer: building block for calcareous sponge spicules and bioseed for the synthesis of calcium phosphate-based bone. *Beilstein J Nanotechnol* 5:610–621
- Wang XH, Schröder HC, Müller WEG (2014b) Enzyme-based biosilica and biocalcite: biomaterials for the future in regenerative medicine. *Trends Biotechnol* 32:441–447
- Wang XH, Schröder HC, Müller WEG (2014c) Enzymatically synthesized inorganic polymers as morphogenetically active bone scaffolds: application in regenerative medicine. *Int Rev Cell Mol Biol* 313:27–77
- Wang XH, Schröder HC, Schloßmacher U, Neufurth M, Feng Q, Diehl-Seifert B, Müller WEG (2014d) Modulation of the initial mineralization process of SaOS-2 cells by carbonic anhydrase activators and polyphosphate. *Calcif Tissue Int* 94:495–509
- Wang SF, Wang XH, Draenert FG, Albert O, Schröder HC, Mailänder V, Mitov G, Müller WEG (2014e) Bioactive and biodegradable silica biomaterial for bone regeneration. *Bone* 67:292–304
- Wang XH, Ackermann M, Wang SF, Tolba E, Neufurth M, Feng QL, Schröder HC, Müller WEG (2016) Amorphous polyphosphate/amorphous calcium carbonate implant material with enhanced bone healing efficacy in a critical-size defect in rats. *Biomed Mater* 11:035005. doi:10.1088/1748-6041/11/3/035005

- Weiner S, Wagner HD (1998) The material bone: structure-mechanical function relations. *Ann Rev Mat Sci* 28:271–298
- Weiner S, Mahamid J, Politi Y, Ma Y, Addadi L (2009) Overview of the amorphous precursor phase strategy in biomineralization. *Front Mater Sci Chin* 3:104–108
- Wiens M, Wang XH, Schloßmacher U, Lieberwirth I, Glasser G, Ushijima H, Schröder HC, Müller WEG (2010a) Osteogenic potential of bio-silica on human osteoblast-like (SaOS-2) cells. *Calcif Tissue Int* 87:513–524
- Wiens M, Wang XH, Schröder HC, Kolb U, Schloßmacher U, Ushijima H, Müller WEG (2010b) The role of biosilica in the osteoprotegerin/RANKL ratio in human osteoblastlike cells. *Biomaterials* 31:7716–7725
- Wiens M, Schröder HC, Wang XH, Link T, Steindorf D, Müller WEG (2011) Isolation of the silicatein- α interactor silintaphin-2 by a novel solid-phase pull-down assay. *Biochemistry* 50:1981–1990
- Wilbur KM, Jodrey LH (1955) Studies on shell formation. V. The inhibition of shell formation by carbonic anhydrase inhibitors. *Biol Bull* 108:359–365
- Winum JY, Montero JL, Scozzafava A, Supuran CT (2009) Zinc binding functions in the design of carbonic anhydrase inhibitors. In: Supuran CT, Winum JY (eds) *Drug design of zinc-enzyme inhibitors: functional, structural, and disease applications*. Wiley, Hoboken, pp 39–72
- Wistrand J, Lindahl S, Wählstrand T (1975) Human renal carbonic anhydrase. Purification and properties. *Eur J Biochem* 57:189–195
- Wood HG, Clark JE (1988) Biological aspects of inorganic polyphosphates. *Annu Rev Biochem* 57:235–260
- Wood GM, Suttie JW (1988) Vitamin K-dependent carboxylase. *J Biol Chem* 263:3234–3239
- Xie B, Nancollas GH (2010) How to control the size and morphology of apatite nanocrystals in bone. *Proc Natl Acad Sci USA* 107:22369–22370
- Zhu Z, Xue LM, Han T, Jiao L, Qin LP, Li YS, Zheng HC, Zhang QY (2010) Antiosteoporotic effects and proteomic characterization of the target and mechanism of an Er-Xian Decoction on osteoblastic UMR-106 and osteoclasts induced from RAW264.7. *Molecules* 15:4695–4710
- Ziello JE, Jovin IS, Huang Y (2007) Hypoxia-Inducible Factor (HIF)-1 regulatory pathway and its potential for therapeutic intervention in malignancy and ischemia. *Yale J Biol Med* 80:51–60

Electrospinning of Bioactive Wound-Healing Nets

Heinz C. Schröder, Emad Tolba, Bärbel Diehl-Seifert,
Xiaohong Wang and Werner E.G. Müller

Abstract The availability of appropriate dressings for treatment of wounds, in particular chronic wounds, is a task that still awaits better solutions than provided by currently applied materials. The method of electrospinning enables the fabrication of novel materials for wound dressings due to the high surface area and porosity of the electrospun meshes and the possibility to include bioactive ingredients. Recent results show that the incorporation of biologically active inorganic polyphosphate microparticles and microspheres and synergistically acting retinoids into electrospun polymer fibers yields biocompatible and antibacterial mats for potential dressings with improved wound-healing properties. The underlying principles and the mechanism of these new approaches in the therapy wounds, in particular wounds showing impaired healing, as well as for further applications in skin regeneration/repair, are summarized.

1 Introduction

Wound healing can be seriously affected by various factors and pathological conditions. A prominent example is diabetes mellitus and many diabetic patients are suffering from open wounds. Currently, such wounds are treated by surgical debridement, as well as administration of growth factors. However, the prospects of success of such therapies are often not satisfactory. There is still an unmet medical need for novel and more effective strategies in wound therapy, in particular for treatment of chronic wounds (Bjarnsholt et al. 2008).

H.C. Schröder (✉) · E. Tolba · B. Diehl-Seifert · X.H. Wang · W.E.G. Müller (✉)
ERC Advanced Investigator Group, Institute for Physiological Chemistry, University Medical
Center of the Johannes Gutenberg University, Duesbergweg 6, 55128 Mainz, Germany
e-mail: hschroed@uni-mainz.de

W.E.G. Müller
e-mail: wmueller@uni-mainz.de

H.C. Schröder · B. Diehl-Seifert · X.H. Wang · W.E.G. Müller
NanotecMARIN GmbH, Duesbergweg 6, 55128 Mainz, Germany

2 Phases of Wound Healing

The wound-healing process can be divided into at least four phases (for a review, see Guo and Dipietro 2010; Bjarnsholt et al. 2008): (i) Coagulation (hemostasis); (ii) inflammation; (iii) cell proliferation and epithelialisation (matrix repair; “granulation phase”), and (iv) remodeling (Fig. 1). This multistep process with partially overlapping phases can be delayed, in particular as a consequence of bacterial infection.

The coagulation phase immediately starts after wounding and involves vascular constriction and fibrin clot formation. Subsequently, in the inflammation phase, a series of pro-inflammatory cytokines and growth factors, including platelet-derived growth factor [PDGF], fibroblast growth factor [FGF], and epidermal growth factor [EGF], are released. This process is paralleled by an infiltration of neutrophils, macrophages and lymphocytes, which eliminate invading microorganisms, as well as platelets, which release polyphosphate [polyP] (Faxälv et al. 2013) and contribute to prevent blood loss (Nurden et al. 2008). Within the damaged tissue area, these cells contribute to the removal of cellular debris by the production and release of proteases and reactive oxygen species.

Inflammation during wound healing, in principle, is a physiological process, resulting in the elimination of contaminating microorganisms. Prolonged inflammation, however, accompanied by the release of bacterial endotoxins and pro-inflammatory cytokines, such as tumor necrosis factor- α [TNF- α] and interleukin-1 [IL-1], may result in delayed wound healing.

In the next step, the proliferation and epithelialisation phase, granulation tissue is formed and an ingrowth of new capillaries occurs. The newly formed stroma is characterized by a granular appearance (“granulation phase”), as well as the presence of fibroblasts, macrophages, and blood vessels (Clark 1989). In the final phase, the remodeling phase, the functional reconstruction of the tissue occurs, requiring a tuned interaction of the cells, in particular fibroblasts, in the synthesis of the extracellular matrix [ECM]; this step may result in scar formation (McDougall et al. 2006).

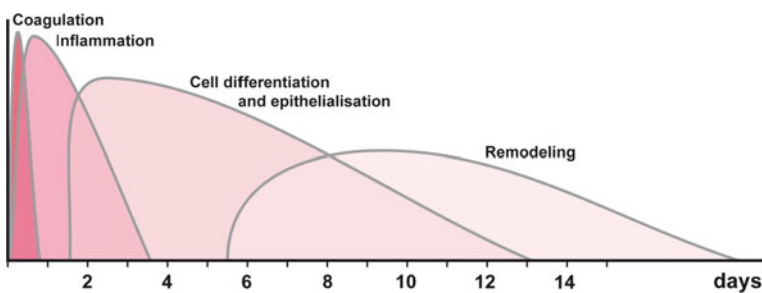


Fig. 1 Phases of wound healing

3 Delayed Wound Healing

Several factors can cause delayed wound healing, e.g., the age of the patient (Keylock et al. 2008). Age-dependent factors that influence wound healing include an altered estrogen:androgen ratio (Gilliver et al. 2007), besides of an age-dependent decrease of collagen synthesis and phagocytic activity of macrophages, and a decreased re-epithelialization and T-cell migration into the wound area. Wound healing may also be impaired in patients with diabetes. Possible reasons include cell dysfunctions and impaired angiogenesis/neo-vascularization resulting in hypoxic cell damage and finally gangrene development (for a review, see Guo and Dipietro 2010).

Local factors that influence wound healing include the formation of superoxide radicals which are involved in oxidative killing of pathogens, as well as infections by microorganisms which are normally restricted to the skin surface and invade the wounded area after damage of the skin barrier. Bacteria leading to wound infection, resulting in delayed wound healing and the development of chronic wounds, comprise both aerobic bacteria, e.g., *Staphylococcus aureus*, in particular methicillin-resistant *S. aureus* [MRSA], *Pseudomonas aeruginosa*, and *Streptococci*, and anaerobic bacteria, e.g., *Bacteroides*, *Porphyromonas*, and *Peptostreptococcus* (Landis 2008).

4 Wound Dressings

Suitable wound dressings should fulfil a number of requirements, such as mechanical protection, shielding against penetration of bacteria, absorption of wound exudate, permeability to oxygen and water vapor, as well as thermal insulation. In addition, they should be nontoxic and not induce allergic reactions, and removable without injury of the wounded tissue area (Lionelli and Lawrence 2003).

Wound dressings can be divided into four classes: (i) passive; (ii) interactive; (iii) advanced; and (iv) bioactive. Among them, passive wound dressings only provide mechanical protection and protection against bacterial infiltration. Interactive wound dressings additionally allow a better exchange of gases and fluids, and efficiently prevent bacterial infiltration (Skórkowska-Telichowska et al. 2013). Advanced dressings, e.g., alginates and hydrocolloids, are capable of preserving a moist environment (Skórkowska-Telichowska et al. 2013). And, finally, bioactive dressings are able to deliver drugs integrated into the wound dressing (Boateng et al. 2008; MacNeil 2007).

It has been proposed that an ideal wound dressing should be able to enhance cell proliferation and accelerate wound healing, and to release antimicrobial substances only after infection of the wound. Currently, only a few dressings combine both properties. Such an ideal wound dressing could be realized by boosting the natural process of wound healing, as well as by the incorporation of markers that help to monitor the progress and possible delays of the healing process (e.g., markers for

temperature, pH, and bacterial infection) and by the incorporation of drug delivery systems that allow a controlled release of bioactive agents (e.g., antibacterial drugs) to support wound healing (MacNeil 2007; Boateng et al. 2008).

Such an ideal wound dressing should suppress the following two processes that impair wound healing: First, the attraction of macrophages and neutrophils by persistent inflammatory stimuli, resulting in an enhanced production and secretion of inflammatory cytokines and metalloproteinases [MMPs], and a reduced production of tissue inhibitors of metalloproteinase [TIMPs]; the degradation of the ECM and of growth factors disrupts the healing process. Second, the biofilm formation, insulating the bacteria from attack by the immune system and protecting them against antibacterial drugs.

5 Electrospun Meshes for Wound Healing

The technique of electrospinning has turned out to be a promising method for the fabrication of innovative dresses for wound healing. The principle of this method is illustrated in Fig. 2a. In electrospinning, polymer fibers are produced from a polymer solution by application of electrical forces (for a review, see: Baji et al. 2010); Fig. 2b–d. Both natural and synthetic polymers can be used to generate fibers with diameters from a few nanometers up to several micrometers. Electrospun meshes are characterized by properties that make them particularly suitable for wound dressings: They have a high surface area and show a high micro-porosity, facilitating gas exchange and preventing desiccation (Zhang et al. 2005). Because of these properties, these meshes have an increased capacity for drug binding or binding of bioactive molecules (for drug delivery) and absorption of body fluids/exudates. Moreover, the high surface area, micro-porosity and structure of the electrospun meshes resemble the ECM and support cell migration and cell proliferation, especially of epithelial cells, as well as hemostasis.

Like wound dressings in general, electrospun meshes can be either passive, interactive, advanced, or bioactive (Abrigo et al. 2014).

Passive electrospun meshes are able to protect the wound tissue from mechanical damage and to maintain sufficient moisture, are permeable for oxygen and water, and show suitable porosity. Examples are electrospun fibers consisting of poly(urethane) (Khil et al. 2003), hyaluronic acid (Uppal et al. 2011) and poly(vinyl alcohol) [PVA] (Supaphol and Chuangchote 2008).

Interactive electrospun meshes are characterized by optimal cell responses, enhanced wound healing and a decreased proliferation of bacteria. They consist of various polymers, e.g., synthetic polymers coated with natural polymers. Examples are electrospun fibers consisting of polyurethane and gelatine (Kim et al. 2009), keratin and poly(hydroxybutyrate-*co*-hydroxyvalerate) [PHBV] (Yuan et al. 2015), or collagen type I, chitosan and poly(ethylene oxide) (Chen et al. 2008).

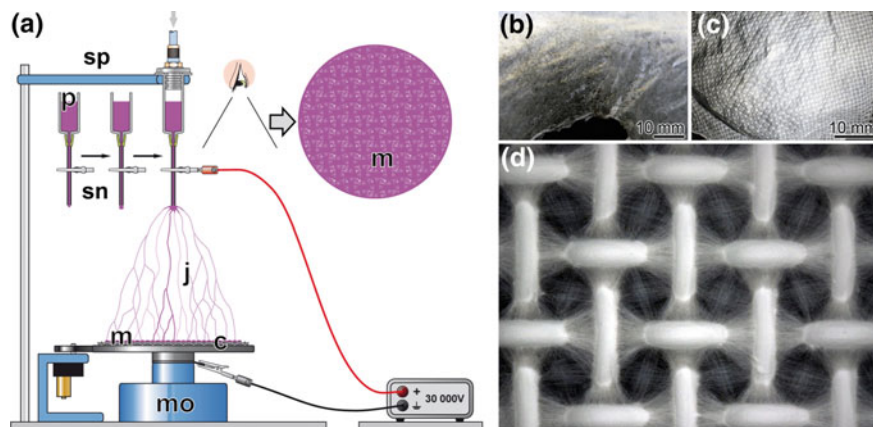


Fig. 2 Electrospinning procedure for fabrication of electrospun wound-healing nets. **a** The solutions with the spinnable materials are poured into the plastic syringe, equipped with a blunt-ended stainless steel needle connected to a high-voltage supply. Electrospinning is performed at a suitable feed rate, voltage, and distance between the nozzle and the collector. A metallic net is used as the collector. The fiber mats are removed from the collector and dried overnight. *sp* syringe pump; *p* polymer solution; *sn* syringe needle with a drop of the polymer solution held at the tip of the needle by the surface tension; *j* jet initiated after application of an electric field using a high-voltage source; *c* collector; *m* motor for driving the collector; *m*, electrospun polymer mat. **b** Electrospun mat after removal from the metal grid onto which the nano/microfibers have been deposited. **c** Dented texture of the electrospun mat caused by the metal grid. **d** Electrospun fibrous mat on metal grid

Advanced interactive electrospun meshes are loaded with antibacterial drugs. They can be produced by the technique of “coaxial electrospinning”; the drugs are incorporated into the network fibers (Lu et al. 2016).

Bioactive electrospun meshes are able to actively stimulate wound healing and control the bacterial load. In addition, they are able to monitor bacterial load and the progress of the healing process (wound status).

According to Abrigo et al. (2014) an ideal wound dressing should be able to monitor the conditions of the wound tissues, to trigger the optimal drug delivery, to promote cell migration and proliferation, but preventing ingrowth into the fibrous mesh structure thereby damage of the wound tissue during removal of the wound dressing. The status of the healing process and the occurrence of wound infection/available antibacterial activity can be monitored by smart wound dressings by the inclusion of pH sensitive dyes or the use of hydrogels that swell in dependence on pH or temperature (Pasche et al. 2013). Biomarker candidates for the assessment of the wound status and phase-dependent triggers present in smart wound dressings may also include alkaline phosphatase [ALP] activity associated with the end of the inflammatory phase (Mamedov et al. 1987; Gallo et al. 1997) and progression of the granulation phase (Alpaslan et al. 1997). The ALP activity increases with the progress of wound healing (Minematsu et al. 2013).

The functionalization of bioactive wound dressings consisting of electrospun fiber mats with expensive growth factors would be commercially not acceptable. In our approach, summarized in this review (see Sect. 6), bioactive silica or polyP, an essential component of our bioactive electrospun meshes, is able to induce (stem) cell recruitment and differentiation, as well as the expression of growth factors by the body's own cells (Müller et al. 2011, 2014a, b, 2015a, d; Wang et al. 2013a, b, 2014a, b, c, d). A schematic presentation of the mode of action of such wound-healing mats is shown in Fig. 3.

A further component of electrospun wound dressing might be chitosan. This natural polymer shows antibacterial activity and is able to encourage wound healing. In addition, chitosan promotes platelet aggregation (Ong et al. 2008). The latter effect is caused by the positively charged (protonated) amine groups of chitosan that attract erythrocytes via binding to negatively charged molecules on their cell membranes, as well as by adsorption of fibrinogen and plasma proteins. Thus, chitosan might be a suitable spinnable polymer to act in combination with polyP which accelerates the generation of thrombin.

Besides of bioactive wound dressings, morphogenetically active amorphous silica or amorphous Ca-polyP microparticles, into which additional bioactive molecules can be packed, are also suitable components to be incorporated into ointments and gels or other topical formulations with, e.g., UV-protective and anti-aging properties (Müller et al. 2015c).

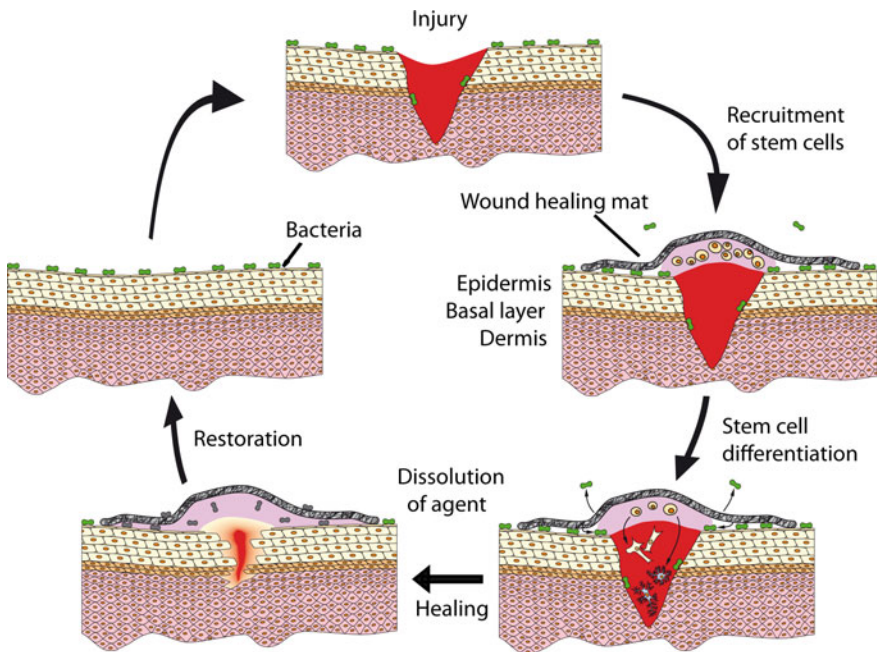


Fig. 3 Schematic presentation of the mode of action of the wound healing mats

6 Microparticles and Microspheres

Microparticles in the low diameter range, with a diameter below 100 nm, can be easily taken up by cells. Such particles are of great interest in the field of biomedicine, in particular for drug delivery, imaging, and diagnosis. Besides the biomedical applications, nano/microparticles are increasingly used in cosmetics, as food supplements or catalysts, in textiles, microelectronics, and antimicrobial or antifungal preparations. They can be divided into (i) soluble and/or biodegradable nano/microparticles and (ii) insoluble and/or nonbiodegradable nano/microparticles. One of the main applications of insoluble nanoparticles is sunscreens containing titanium dioxide [TiO₂] and zinc oxide [ZnO] nanoparticles. Recent results revealed that biodegradable nano/microparticles can be prepared, among others, from inorganic polyP and diverse cations (e.g., calcium ions), a novel class of materials with a variety of applications, including skin regeneration/repair, as summarized in this chapter.

6.1 Amorphous Calcium-Polyphosphate

We developed a preparation method for a novel polyP-based material that is bioactive (Müller et al. 2015e). This material is amorphous and consists of nano- and microparticles of calcium and inorganic polyP. This nontoxic linear polymer of tens to hundreds of phosphate units linked together via high-energy phosphoanhydride bonds (Kulaev et al. 2004) is found in many organisms including bacteria, fungi, algae, plants and animals (Schröder et al. 1999). The amorphous calcium-polyP nano- and microparticles that form the novel material (usually polyP molecules with a chain length of 30 phosphate units are used) are biodegradable and retain the morphogenetic activity of the inorganic polymer (Müller et al. 2015b, d, e).

Naturally occurring polyP is found in particular in platelets (Smith et al. 2006), bone tissue (Leyhausen et al. 1998; Schröder et al. 2000), as well as skin (Simbulan-Rosenthal et al. 2015). We were the first to demonstrate that this inorganic polymer becomes bioactive after complex formation with Ca²⁺ ions; the polyP-Ca²⁺-complex was found to increase, among others, the mineralization of bone-forming osteoblasts (Wang et al. 2013a, b).

The biological activity of polyP has been demonstrated in a series of studies. PolyP induces the expression of ALP, an enzyme that is, among others, essential for bone mineralization (Müller et al. 2011). In addition, polyP enhances the expression of certain cytokines, e.g., bone morphogenetic protein-2 [BMP-2] (inducer of bone formation; Wang et al. 2013a, b), increases intracellular Ca²⁺ levels (Müller et al. 2011), inhibits osteoclast differentiation (Wang et al. 2013a), induces collagen expression (Hacchou et al. 2007; Müller et al. 2015c), shows antibacterial activity (Moon et al. 2011), enhances the cellular ATP level (important under hypoxic conditions; Müller et al. 2015b, c, 2016b; Wang et al. 2016), acts as food preservative (Ohtake et al. 1996), and stimulates differentiation and mineralization

of bone cells. Based on the latter biological activity of polyP, first described by us, new ways for bone tissue engineering and repair have been developed in the past few years (for recent reviews, see Wang et al. 2012, 2014b, c, d). Moreover, polyP inhibits the activity of matrix metalloproteinases (MMPs), as well as bacterial proteases that are relevant in delayed wound healing and prevents, through binding of cations like zinc ions, biofilm formation (McCarty et al. 2015), accelerates clotting (Smith et al. 2006), acts as an activator of fibroblasts (Shiba et al. 2003), is able to chelate alginate produced by biofilm-forming bacteria (Lavery et al. 2014; Müller et al. 2016a), and stimulates the PI3K/AKT/mTOR pathway, one of the main pathways involved in aging (Wang et al. 2003). PolyP can be synthesized either chemically (at high temperature) or enzymatically (at ambient temperature), e.g., via bacterial polyP kinases (Schröder et al. 1999). Several exo- and endopolyphosphatases have been isolated that catalyze the hydrolysis of polyP in bacteria, yeast, and lower eukaryotes (Lorenz et al. 1994, 1995; Schröder et al. 1999). In human tissue, polyP is degraded by the ALP (Lorenz and Schröder 2001).

In addition to the amorphous Ca-polyP microparticles, amorphous Ca-polyP microspheres, containing incorporated bioactive molecules, have been developed. One of the bioactive molecules that can be included in the Ca-polyP microspheres is retinol that acts synergistically with polyP (see Sect. 9). These microspheres can be disintegrated by enzymatic hydrolysis of the polyP component that undergoes degradation by ALP.

6.2 Amorphous Silica

Another natural biologically active inorganic polymer that can be synthesized enzymatically (via the sponge enzyme silicatein; Müller et al. 2013), is silica (biosilica). Biosilica is biodegradable, biocompatible, and exhibits various properties of potential biomedical interest for application in wound dressings:

Biosilica has been shown to act anti-inflammatory (Grotheer et al. 2013) and to up-regulate the expression of pro-inflammatory cytokines that are relevant for wound healing, including IL-1 β , IL-6, and IL-8 (Menke et al. 2007; Barrientos et al. 2008). IL-1 β is a cytokine released by keratinocytes (Feldmeyer et al. 2010) that has been reported to induce the expression of chemokines and the invasion of immune competent cells in the wound region (Dinarello 2011). The secretion of IL-6 by lymphocytes and macrophages has been shown to cause local inflammation (Sawamura et al. 1998). IL-8 is produced by fibroblasts, keratinocytes, and endothelial cells and acts as activator of phagocytes and leukocytes. In addition, this cytokine acts as modulator of the expression of the transcription factor NF- κ B and its inhibitor I κ B (Grotheer et al. 2013). Degradation of I κ B abolishes the inhibition of NF- κ B resulting in the activation the IL-1 β , IL-6, and IL-8 gene expression by the transcription factor (Simmonds and Foxwell 2008).

Both polymers, biosilica and Ca-polyP, can be produced in an amorphous form. They can be used either alone or in combination with other bioactive molecules,

parts of them are acting in a synergistic way; example: activation of collagen/ECM synthesis by polyP and retinol (see Sect. 14).

Based on their properties, we propose that silica and especially polyP are excellent materials for novel types of bioactive wound dressings. These dressings have a modular composition consisting of an electrospun synthetic (e.g., polyP- β -caprolactone) or natural (e.g., chitosan-based) fibers/meshes, into which biologically active amorphous biosilica or amorphous Ca-polyP microparticles/spheres containing entrapped bioactive molecules are incorporated that are released phase-dependently during wound healing.

7 PolyP and Wound Healing

In wound healing, polyP cannot be applied as a sodium salt because of its comparably high solubility. PolyP can also not be applied after calcination which results either in disintegration of the polymer or its transformation into an inactive crystalline form (Pilliar et al. 2001; Ding et al. 2008). The amorphous Ca-polyP microparticles developed by us retain the bioactivity/morphogenetic activity of the polymer, allowing its use for biomedical applications. These microparticles can be applied for the fabrication of wound-healing mats, together with other biocompatible polymers, using electrospinning procedures.

Based on these amorphous Ca-polyP microparticles, we also succeeded to develop amorphous Ca-polyP microspheres, containing incorporated bioactive molecules. One of the bioactive molecules that has been included in the microspheres is retinol. A variety of spinnable polymers, e.g., polylactic acid or its derivatives/copolymers can be loaded with the functionally active microparticles/microspheres.

8 Retinoids and Wound Healing

Retinoids are structurally characterized by a β -ionone ring with a polyunsaturated side chain that consists of four isoprenoid moieties with a terminal alcohol, aldehyde, carboxylic acid, or ester group. The regeneration-promoting properties of retinoic acid and its precursor molecule, retinol, are well known (Mukherjee et al. 2006). It has been demonstrated that retinoids are beneficial for skin regeneration and reconstitution of the collagen network (Abrigo et al. 2014).

The retinol metabolite retinoic acid has been reported to play an essential role in regulation of growths of epithelial cells. Retinoic acid causes a differential gene expression; it down-regulates the expression of the genes involved in lipid metabolism during keratinocyte differentiation (Lee et al. 2009), as well as collagen production. On the other hand, it increases the proliferation of fibroblasts. Retinol, on the other hand, has been shown to improve wound healing (Keleidari et al. 2014).

Retinol is enzymatically transformed into retinoic acid *in vivo*, via retinal, following a two-step reaction. However, only a small fraction of topically applied retinol is metabolized to retinoic acid. Alternatively, retinol is converted into a series of metabolites, including 14-hydroxy-retro-retinol. This metabolite is involved in regulation of cell growth and death of lymphocytes. Retinol also causes the production of reactive oxygen species, resulting in the activation of signaling pathways involved in control of cell proliferation (Gelain et al. 2012) and is able to modulate cell proliferation and differentiation via a differential gene expression (Wang et al. 2004).

9 Synergistic Effect of PolyP and Retinol

We succeeded to demonstrate that polyP, fabricated as microparticles, if administered together with retinol and packed into fibrous mats causes a synergistic effect on the expression of genes, encoding for leptin and the leptin receptor as well as for the fatty acid binding protein 4 [FABP4] in MC3T3-E1 cells (Müller et al. 2015a).

Both polyP and retinol are involved in the regulation of cell growth and differentiation, as well as control of overall energy metabolism.

9.1 *Preparation of Ca-PolyP Microparticles and Ca-PolyP/Retinol Microspheres*

The amorphous Ca-polyP microparticles were prepared by a method introduced by us (Müller et al. 2015e) by drop-wise addition of a solution of CaCl_2 to Na-polyP, dissolved in distilled water. During the procedure, the pH was adjusted to 10.0 with NaOH. Microparticles with various phosphate: Ca^{2+} ratios can be prepared (ranging from 1 to 2 and higher). PolyP with an average chain length of 30 phosphate units was usually used. After stirring the microparticles were collected by filtration.

The amorphous Ca-polyP microspheres containing entrapped retinol (retinol/Ca-polyP microspheres) were prepared, under avoidance of light, using a newly developed fabrication process (Müller et al. 2015a, c); a retinol solution in ethanol, containing CaCl_2 , was drop-wise added to a Na-polyP solution in water (Fig. 4). In order to avoid a phase separation and to stabilize the emulsion poly(ethylene glycol) [PEG] was added to the Na-polyP solution. The emulsion was stirred and the particles formed were collected by filtration and dried. The retinol-containing microspheres have an average diameter of 200–350 nm, while the size of the microparticles ranges from 70 to 200 nm.

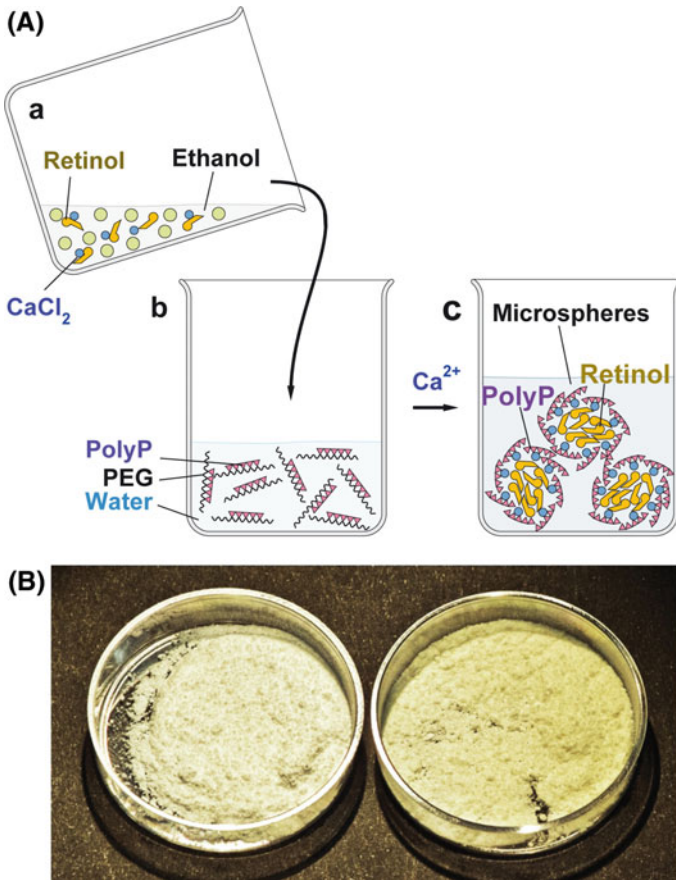


Fig. 4 Preparation of Ca-polyP nano- and microspheres with encapsulated retinol. *A* The retinol solution **a** is added drop-wise to a Na-polyP solution, containing PEG **b**. The emulsion formed contains the Ca-polyP nano- and microspheres with the encapsulated retinol **c**. *B* Photo of the fabricated nano- and microspheres without (*left*) and with retinol (*right*) (Modified from Müller et al. 2015c)

The size of the microparticles and microspheres can be adjusted to a size range that is optimal for endocytotic cellular uptake (Zhang et al. 2009). They are biodegradable and are disintegrated by enzymatic hydrolysis in the extracellular space. The main component, polyP, undergoes degradation by the ALP. In consequence, not only polyP but also other components integrated into the microspheres are released extracellularly. The microparticles and microspheres can be taken up by cells via clathrin-mediated endocytosis.

9.2 *Leptin and Fatty Acid Binding Protein 4 as Biomarkers*

Leptin is a hormone produced by adipose cells. This protein plays an important role in regulation of energy balance via regulating the feeling of hunger. Obesity is associated with a decreased sensitivity to leptin. However, leptin also plays a role in other physiological processes, including wound healing. It has been reported that leptin improves wound re-epithelialization (Frank et al. 2000). Keratinocytes found at the wound margins express the leptin receptor subtype ObRb during wound repair. In addition, ob/ob (leptin null) mice, as well as db/db (leptin receptor null) mice show impaired repair of cutaneous wounds (Friedman and Halaas 1998). Moreover, leptin regulates fat deposition in the body (for a review, see Coppari and Bjørnbæk 2012).

In experimental wounds, the expression of leptin was found to be significantly up-regulated (Murad et al. 2003). In cells of wounds also the leptin receptor is expressed, indicating the existence of an autocrine/paracrine signaling cycle (Murad et al. 2003).

The fatty-acid-binding protein, FABP4, a member of the family of transport proteins for fatty acids, has been shown to bind not only to long-chain fatty acids but also, with a lower affinity, to retinoic acid (Matarese and Bernlohr 1988). FABP4 is found not only in adipocytes but also in other cells, including regenerating endothelial cells and macrophages (Lee et al. 2007). In endothelial cells, the expression of FABP4 is controlled by the vascular endothelial growth factor A/vascular endothelial growth factor 2 [VEGFA/VEGFR2] pathway (Harjes et al. 2014), which is involved in angiogenesis and vasculogenesis; in addition, VEGFA promotes cell migration and elicits mitogenesis of endothelial cells. A reduction of FABP4 expression is associated with a decrease in proliferation, migration, and sprouting of endothelial cells. In wound healing, the FABPs have been reported to be involved in the regulation of cell motility within regenerating epidermis (Kusakari et al. 2006).

Retinoic acid has been reported to suppress the synthesis and secretion of leptin in adipocytes *in vitro*, but a short-time administration of retinoic acid in rats *in vivo* has been found to increase leptin expression (Krskova-Tybitanclova et al. 2008).

In leukemic cells the leptin receptor has been found to be co-expressed with the retinoic acid receptor (Tabe et al. 2004), suggesting that the anabolic effect of retinoic acid on the expression of leptin and the leptin receptor occurs through binding of the retinoid to the retinol–retinal–retinoic acid–retinoid X receptor α [RXR]. Also *in vivo* studies confirmed that retinoids are capable of modulating anabolically leptin signaling and insulin sensitivity in mice (Tsuchiya et al. 2012).

9.3 *Effect of PolyP and PolyP-Retinol Microparticles and Microspheres on Cell Growth*

MC3T3-E1 cells are suitable cells for studying the effect of compounds potentially affecting wound healing (Hatakeyama et al. 2008). Co-incubation of these cells

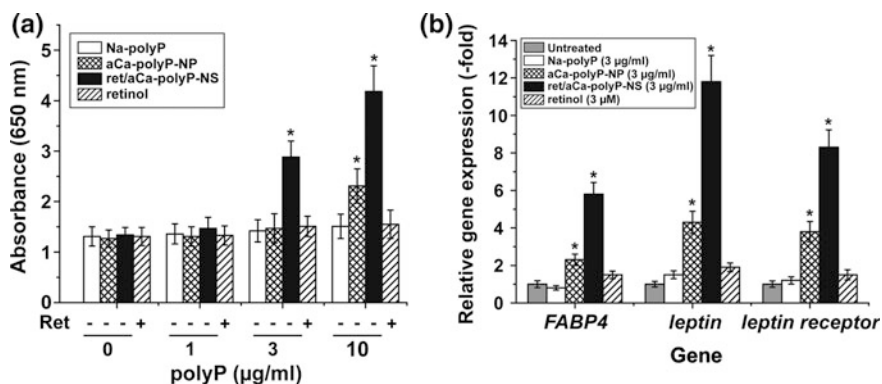


Fig. 5 **a** Effect of amorphous Ca-polyP nano- and microparticles and amorphous retinol-Ca-polyP nano- and microspheres on viability of MC3T3-E1 cells; XTT colorimetric assay. The cells were exposed to different concentrations of Na-polyP (complexed with Ca^{2+}), amorphous Ca-polyP nano- and microparticles (aCa-polyP-NP) and amorphous retinol-Ca-polyP nano- and microspheres (ret-aCa-polyP-NS), or retinol (3 days). Means \pm SEM ($n = 10$); $*p < 0.01$. **b** Steady-state-expression levels of the genes encoding for FABP4, leptin, and leptin receptor in MC3T3-E1 cells which remained untreated or were exposed for 3 d either to soluble Na-polyP (complexed with Ca^{2+}), amorphous Ca-polyP nano- and microparticles (aCa-polyP-NP), amorphous retinol/Ca-polyP nano- and microspheres (ret-aCa-polyP-NS) or to 3 μM retinol; RT-qPCR analysis using *GAPDH* as reference gene. Means \pm SEM ($n = 5$); $*p < 0.01$ (Modified from Müller et al. 2015a)

with Ca-polyP together with retinol, or incubation of the cells with amorphous retinol/Ca-polyP microspheres was found to cause a significant synergistic effect on cell growth compared with particle-free polyP complexed with Ca^{2+} ions or amorphous Ca-polyP microparticles and retinol alone (Müller et al. 2015a). At a concentration below 3 $\mu\text{g/ml}$, both particle-free Ca^{2+} -polyP complexes and amorphous Ca-polyP microparticles have no effect on the number of cells (Fig. 5a). Retinol at a concentration of 3 μM , added as a single component, also does not affect cell growth. If retinol at a concentration of 1 μM that does not affect cell growth is encapsulated into Ca-polyP-based nanoparticles, a strong amplification of cell growth by the resulting retinol/Ca-polyP microspheres is measured, already at the Ca-polyP concentration of 3 $\mu\text{g/ml}$ (Fig. 5a), indicating that the combined application of Ca-polyP and retinol causes in a synergistic effect (Müller et al. 2015a).

9.4 Effect of PolyP and Retinol on Gene Expression

Quantitative reverse transcription polymerase chain reaction [RT-qPCR] experiments revealed that addition of the amorphous Ca-polyP microparticles (3 $\mu\text{g/ml}$)

to MC3T3-E1 cells caused a significant up-regulation of the steady-state-expression of the genes encoding for FABP4, as well as of the genes encoding for leptin and the leptin receptor (Müller et al. 2015a); Fig. 5b. The increased expression of these genes was further enhanced if the retinol/amorphous Ca-polyP microspheres were added to the cells; the rise of the transcript levels amounted to 5.8-fold (FABP4), 11.6-fold (leptin), and 8.3-fold (leptin receptor gene), respectively. No significant changes of the expression levels of the three genes was observed if the cells were incubated with soluble Na-polyP, complexed to Ca^{2+} or with retinol alone (Fig. 5b).

10 Amorphous Retinol-Ca-PolyP Containing Electrospun Wound-Healing Mats

Using the technique of electrospinning, we fabricated three-dimensional porous mats consisting of loosely connected fiber networks with high porosity and high surface area. The principle of the technique has been sketched in Fig. 2a. This procedure has been applied for the fabrication of wound dressings consisting of polyP- β -caprolactone or poly(D,L-lactide) [PLA] mats into which bioactive Ca-polyP microparticles or microspheres, formed from the microparticles and encapsulated retinol (“retinol/aCa-polyP” microspheres), have been incorporated; the method has been described (Müller et al. 2014b, 2015a). The fiber mats were produced using a modified laboratory scale electrospinning unit, Spraybase (Profector Life Sciences). A schematic presentation of the fabrication procedure using PLA as an example is shown in Fig. 6. PLA was mixed with PEG in a ratio of 4:1 (w/w) and dissolved in chloroform (final concentration, 20%; w/v) (Fig. 6a). Retinol was added to the PLA solution to give a final concentration of 20 wt% (with respect to PLA). After addition of the Ca-polyP microparticles to the PLA solution (final concentration, 10 wt%), the suspension containing the formed retinol-Ca-polyP microspheres was sonicated and used for the electrospinning (Fig. 6b, c). The weight ratio between CaCl_2 and polyP was 2:1. Electrospun mats, consisting of 2–4 μm fibers, with an average mesh size of 10–20 μm were fabricated; the retinol-containing mats (Fig. 6e) as well as the mats containing retinol/amorphous Ca-polyP microspheres (Fig. 6f) had a yellow color, while the PLA mats without additions were white (Fig. 6d).

It should be emphasized that the polyP microparticles and microspheres are amorphous; only in the amorphous state, polyP shows morphogenetic activity (Müller et al. 2015a, c, d, e). In addition, the particles can be taken up by endocytosis (Müller et al. 2015b, c). Moreover, polyP has been shown to comprise also antibacterial activity, as well as hemostatic activity (Lorencová et al. 2012).

Wound-healing mats consisting of other spinnable polymers, e.g., *N,O*-carboxymethyl chitosan [*N,O*-CMC], can be produced in a similar way. *N,O*-CMC can be

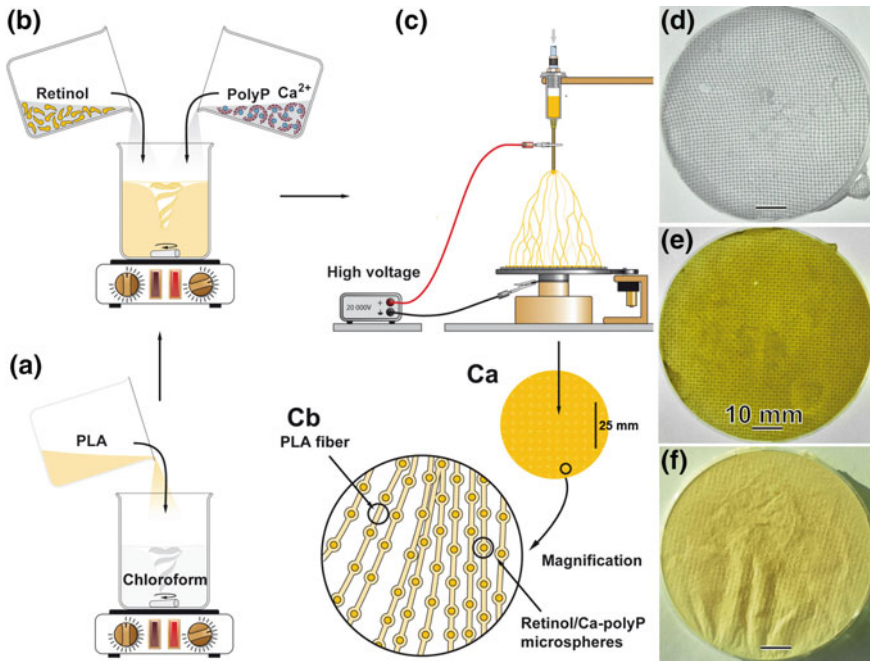


Fig. 6 Schematic presentation of the fabrication procedure of PLA-based electrospun mats. **a** PLA is dissolved in chloroform, followed by the addition of retinol (20 wt%) **b** and of the amorphous Ca-polyP microparticles (10 wt%). After stirring and sonication, the suspension is used for electrospinning **c**. A sketch of the fiber mat with the embedded retinol/Ca-polyP microspheres is shown in **Ca** and **Cb** (magnification). **d** Electrospun mat with **d** PLA alone, **e** PLA and retinol and **f** PLA and retinol/Ca-polyP (Modified from Müller et al. 2015a)

prepared from chitosan as described (Müller et al. 2015d). Electrospun chitosan-based meshes can be loaded with Ca-polyP microparticles or microspheres to produce the respective bioactive wound dressings.

11 Effect of the Electrospun Mats Containing Amorphous Retinol-Ca-PolyP Nanoparticles on Gene Expression

Next we demonstrated that the fabricated electrospun PLA fiber mats, after embedding of amorphous retinol-Ca-polyP microspheres, show morphogenetic activity and increase the expression of FABP4 and of leptin and its receptor (Müller

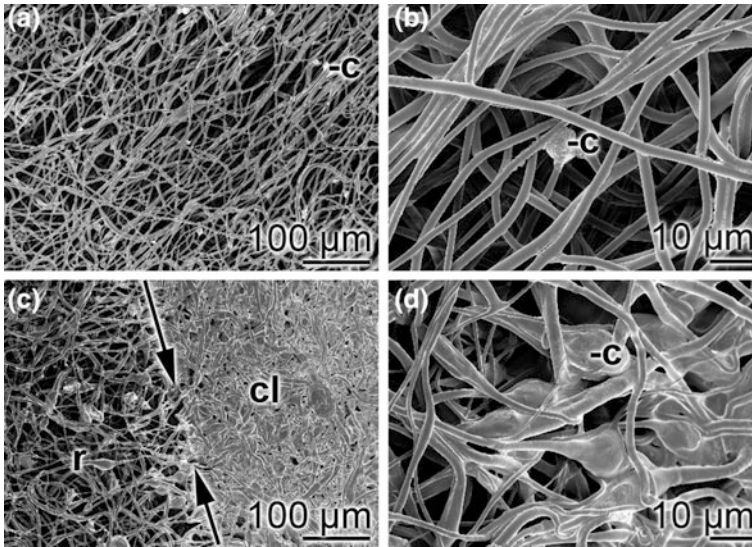


Fig. 7 Effect of the PLA/retinol/aCa-polyP-containing electrospun mats on growth of MC3T3-E1 cells; SEM analysis. **a** and **b** On fibrous mats spun with PLA only, only a few cells are visible (-c), while **c** and **d** dense cell layers *cl* are formed after cultivation of the cells onto fibers formed from PLA/retinol/amorphous Ca-polyP microspheres. Within the rim region *r*, at the left side of the dividing line marked by two single headed arrows the transition from densely packed cells (right side) to mat areas with less cells can be seen (left) (Modified from Müller et al. 2015a)

et al. 2015a). Our results revealed that these mats strongly support the growth of MC3T3-E1 cells. Only a small number of cells was seen on fiber mats fabricated with PLA alone (Fig. 7a, b), while the PLA mats, containing the retinol/amorphous Ca-polyP microparticles, showed a markedly higher cell density (Fig. 7c, d); even densely packed cell layers were visible on the electrospun fiber mats (Fig. 7c). Determinations, using the XTT assay, of viability/growth of MC3T3-E1 cells, cultured onto PLA fiber mats revealed a significant increase in cell number in assays with PLA mats, supplemented with the retinol/amorphous Ca-polyP microspheres, compared to control (Fig. 7a). RT-qPCR analyses revealed a significant up-regulation of the expression levels of the genes, encoding for leptin, leptin receptor and FABP4 in cells grown onto the PLA-amorphous Ca-polyP microparticles (PLA-retinol/amorphous Ca-polyP microspheres) loaded fiber mats by 1.2-fold (3.7-fold), 2.3-fold (5.8-fold) and 2.6-fold (6.1-fold), respectively (Fig. 8). These results demonstrate the morphogenetic properties of PLA fiber mats, supplemented with amorphous Ca-polyP microparticles or, even more, retinol/amorphous Ca-polyP microspheres.

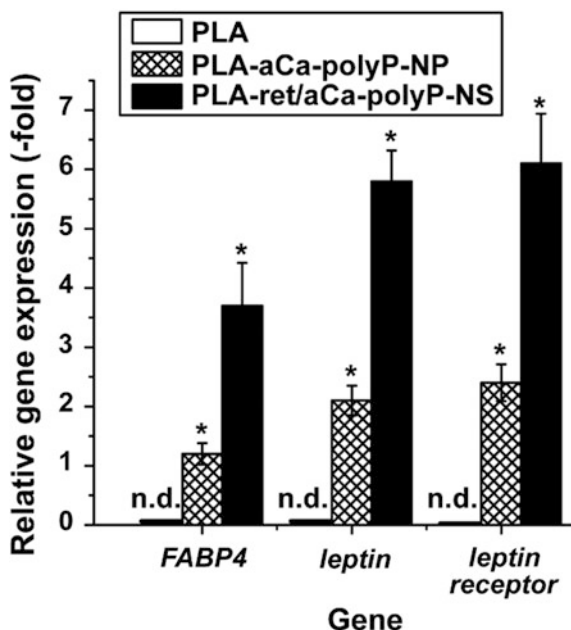


Fig. 8 Effect of the electrospun PLA mats containing amorphous Ca-polyP nano- and microparticles and amorphous retinol/Ca-polyP nanospheres on the transcript levels of the genes encoding for FABP4, leptin, and leptin receptor; RT-qPCR analysis. MC3T3-E1 cells were cultivated for 3 d onto electrospun PLA mats without (cell numbers not determinable; n.d.) or with amorphous Ca-polyP nano- and microparticles (aCa-polyP-NP) or amorphous retinol/Ca-polyP nano- and microspheres (ret/aCa-polyP-NS). Means \pm SEM ($n = 5$); $*p < 0.01$ (Modified from Müller et al. 2015a)

12 Cross-Talk of Retinol-Ca-PolyP Elicited Signaling Pathways

A schematic presentation of cross-talk between different signaling pathways initiated by retinol-Ca-polyP is shown in Fig. 9. In the first pathway, binding of VEGFA to its receptor results in an activation of the Notch ligand DLL4 and the Notch signaling pathway. After translocation to the nucleus, the Notch intracellular domain [NICD] together with the insulin-responsive Foxo1 transcription factor and other transcription factors (e.g., RBPJ κ) causes an increased FABP4 gene expression (Harjes et al. 2014). In the cytoplasm, FABP4 binds, besides to long-chain fatty acids, to retinoic acid. After binding to retinoic acid in the cytoplasm, FABP4 returns to the nucleus, to the nuclear receptor PPAR γ [peroxisome proliferator-activated receptor γ] that forms a heterodimer with the RXRs. The latter receptor is activated by the retinol metabolite 9-

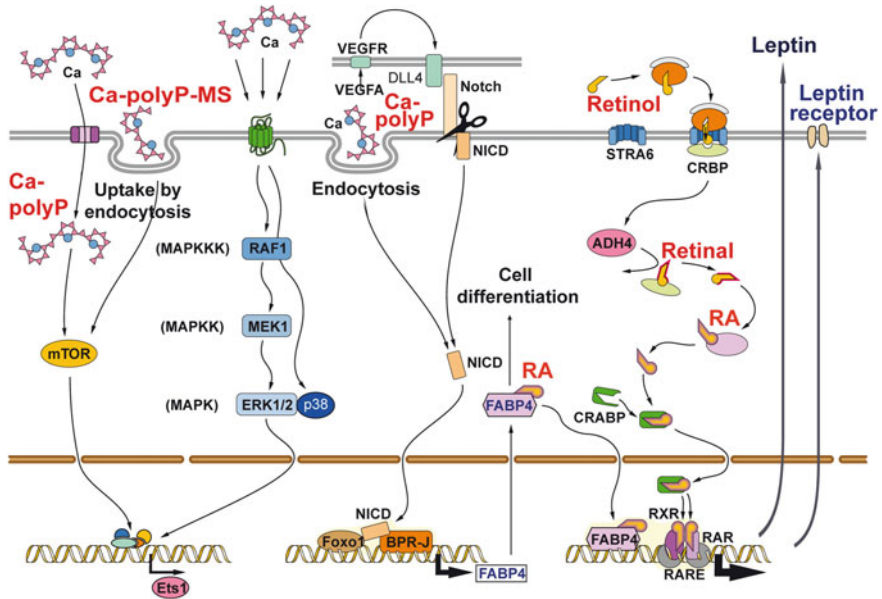


Fig. 9 Schematic outline of the proposed mode of action underlying the synergistic effect of polyP and retinol on the expression of the fatty acid binding protein 4 [FABP4], as well as the expression of leptin and the leptin receptor

cis retinoic acid; this activation is observed not only in adipocytes but also in keratinocytes (Yoshimura et al. 2003). As a result, an induction of the expression of leptin and of the leptin receptor occurs.

In the second pathway, polyP enhances FABP4 expression via the mitogen-activated protein kinase [MAPK] signaling pathway (Girona et al. 2013). This signal transduction pathway is used also by polyP during induction of heat shock protein 27 (Segawa et al. 2011). Based on experimental results available, it is, however, the p38/MAPK pathway and not c-jun that is initiated by polyP.

In addition, polyP has been shown to activate, also in endothelial cells, the mTOR pathway (Mehr et al. 2014) that plays an important role in energy metabolism (Laplante and Sabatini 2009). Finally, the transcription factor Ets1 is expressed (Wang et al. 2014a) that according to this scheme interacts synergistically with the Foxo1/NICD-RBPJ κ complex, resulting in the expression of the *FABP4* gene.

In summary, it is postulated that (i) polyP, if alone (in the form of amorphous Ca-polyP microparticles), acts on the expression of *FABP4* via the MAPK signaling pathway, and (ii) if administered together with retinol (in the form of retinol-amorphous Ca-polyP microspheres), in addition on leptin and the leptin receptor. As a result, an increased differentiation and proliferation, associated with an amplification of the activation of the RXR by retinol and an enhanced expression

of genes controlling inflammation, vascularization, and energy balance occur (Plutzky 2011).

13 Evaluation of PolyP-Containing β -Polycaprolactone Wound-Healing Meshes

Polycaprolactone is a biodegradable polyester that has been approved for uses in human body by the Food and Drug Administration [FDA] as a drug delivery device and scaffold for tissue engineering. The efficiency and wound-healing potential of first electrospun fibrous networks consisting of polycaprolactone containing polyP microparticles have been demonstrated both in vitro and in vivo experiments (to be published).

13.1 Cytotoxicity

The effects of the polyP-containing polyP- β -caprolactone material as well as of the polyP- β -caprolactone on cell viability have been determined on several cell lines, including THP-1 (human monocytic peripheral blood acute monocytic leukemia), HepG2 (human liver hepatocellular carcinoma), U-2 OS (human bone osteosarcoma) and MC3T3-E1 (mouse bone/calvaria preosteoblast). Viability screening to detect potential anti-proliferative effects using the MTS [3-(4,5-dimethylthiazol-2-yl)-5-(3-carboxymethoxyphenyl)-2-(4-sulfophenyl)-2H-tetrazolium] assay did reveal no anti-proliferative effect on THP-1 cells up to 96 h. The preparations affected the viability of U-2 OS and HepG2 cells only at the highest concentrations tested (100 and 50 $\mu\text{g/mL}$); a dose-response anti-proliferative effect on MC3T3-E1 cells, up to the low $\mu\text{g/mL}$ concentration range, was only observed after an incubation period of 48 h or more.

In addition, the number of viable cells has been determined using the cell titer glo assay based on quantitation of ATP (presence of metabolically active cells). The experiments revealed no anti-proliferative effect on U-2 OS and MC3T3-E1 cells after an incubation period of 10 and 60 min, while a dose-dependent effect up to the low $\mu\text{g/mL}$ range was observable after 24 and 72 h.

13.2 Activity in In Vivo Disease Model

The mouse strain T/BKS.CG-M+/+LEPR DB/J (db/db), which is homozygous for the diabetes spontaneous mutation (*Lep^{db}*) has been used as an animal model for impaired wound healing to analyze effects of the polycaprolactone fiber meshes

with the integrated bioactive ingredients on wound healing. The db/db mice develop obesity and insulin-resistant diabetes. A full excisional wound model was used. The electrospun meshes with the integrated bioactive compounds were cut into discs with a diameter of 8 mm, sterilized by γ -irradiation and placed into the wound bed of a full-thickness excisional wound (8 mm in diameter) immediately after wounding.

The extents of re-epithelialization, granulation tissue, and presence of necrosis/inflammation have been evaluated after different time-periods post-treatment. The results revealed that db/db mice treated with polycaprolactone fiber mats with integrated Ca-polyP microparticles show an improved wound healing compared to negative controls or mice with polycaprolactone alone. In comparison to nontreated animals, an accelerated rate of maturation of granulation tissue and collagen deposition was found in wounds of mice treated with polyP-containing polycaprolactone on day 6 and day 9.

Immature granulation tissue, consisting of macrophages, lymphocytes, and plump fibroblasts, was found to cover 0–20% of the whole wound bed on day 3 after wounding. Transformation of immature granulation tissue into mature granulation tissue, characterized by elongation of fibroblasts, deposition of collagen fibers and angiogenesis, was observed on day 6 in mice treated with the fiber mats containing polyP microparticles. On day 9, the wound beds were dominated by mature granulation tissue in animals treated with the polyP-containing fiber mats.

Assessment of re-epithelialization (percentage of the width of the sectioned wound covered with newly formed epithelial layer; Low et al. 2001) revealed that the percentage of wound re-epithelialization in animals treated with the polyP-containing preparations was higher than in nontreated animals on day 6 and day 9. Granulation tissue was assessed using a scoring method (Greenhalgh et al. 1990; Tkalčević et al. 2009). The thickness of the granulation tissue, the amount of acellular matrix, cell infiltration, and the number of newly formed capillaries were assessed. These factors contribute to the time-dependent different architecture of the granulation tissue; e.g., the morphology of fibroblasts that have an important function in wound healing (release of growth factors, collagen formation, and wound contraction) (Lerman et al. 2003; Thorey et al. 2004; Obara et al. 2005) changes with time from a plump shape into an elongated shape. Fibroblasts from db/db mice have been reported to show impaired cell migration, VEGF production, and response to hypoxia compared to wild-type fibroblasts (Lerman et al. 2003). These effects are not caused by absence of the leptin receptor in db/db mice, but might be the result of an impaired function of fibroblasts due to a reduced expression of the genes encoding for the fibroblast growth factors 1 and 2 [FGF1 and FGF2] in genetically diabetic, healing-impaired, mice (Werner and Grose 2003). Both growth factors stimulate angiogenesis (Risau 1990) and exhibit mitogenic activity on fibroblasts and keratinocytes (Abraham and Klagsbrun 1996).

In addition, db/db mice show a reduced expression of collagen type I and the collagen-inducing transcription factor, homeobox D3 [HoxD3] (Hansen et al. 2003).

In a further study, polyP microparticles were topically administered once daily upon directly into the wound bed as 10% physiological solution. On day 7, an increased formation of immature granulation tissue was detected in mice treated with polyP microparticles compared to untreated animals. Prior to day 7, no mature granulation tissue was found in all groups investigated. In addition, it was observed that wound inflammation was significantly reduced in the treated animals on day 7 post wound infliction, compared to untreated controls. This result suggests an anti-inflammatory effect of the tested preparation. At the end of the study (day 13), no significant difference in the composition of granulation tissue was found between treated and untreated animals.

The results of the animal study suggest that the observed acceleration of wound healing by the preparations tested is due to positive effect on the impaired function of fibroblasts in db/db mice.

14 Anti-aging Ointments

There is a strong interest particularly in the field of cosmetics in compounds that can prevent or delay biological aging. There is a huge market for cosmeceuticals, containing biologically active ingredients, in particular for anti-aging/UV protection products. For example, the sales in the anti-aging skin care market are expected to increase up to 50% in the next 5 years.

14.1 Aging of Skin

Aging of skin is characterized by a decrease in collagen content, an accumulation of abnormal elastic fibers and increasing amounts of glycosaminoglycans. The decrease in collagen content during aging of human skin mainly concerns collagen III. The expression of collagen I does practically not change during the lifespan, while the synthesis of collagen III drops by 70%. Due to their long half-life, collagen molecules are susceptible to nonenzymatic glycation. It has been proposed that the formation of advanced glycation end products [AGEs] is at least partially responsible for the observed changes of collagen types I and III gene expression via modulation of signaling pathways (Tang et al. 2008).

The generation of reactive oxygen species in response to UV-radiation (photoaging) is considered to play a major role in the age-dependent changes of the extracellular matrix (Gilchrest and Bohr 1997; Pandel et al. 2013). It is well known

that carotenoids like β -carotene are scavengers of oxygen-free radicals and protective against skin aging (reviewed in: Mukherjee et al. 2006). In addition, evidence has been presented that the PI3K/AKT/mTOR pathway is one of the main pathways involved in aging. This pathway was found to be stimulated by polyP (Wang et al. 2003). Therefore, amorphous Ca-polyP microspheres into which UV-protective compounds or compounds with anti-senescence activity such as retinol have been incorporated provide a suitable material for the development of ointments and gels with UV-protective and anti-senescence properties. Besides of photoaging, such ointments based on UV-protective and anti-senescence Ca-polyP microspheres may also be of potential benefit for application in the prophylaxis or therapy of dermatological conditions such as inflammatory skin disorders and acne, as well as disorders of increased cell turnover like psoriasis.

14.2 Synergistic Effect of the Retinol and Amorphous Ca-PolyP Microspheres

We demonstrated that in MC3T3-E1 cells the retinol/amorphous Ca-polyP microspheres cause an increase in collagen types I, II, and III gene expression at concentrations at which the single components, retinol and amorphous Ca-polyP microspheres, are inactive (Müller et al. 2015c). This synergistic effect was particularly pronounced for the collagen type III gene expression.

Incubation of the cells with the amorphous Ca-polyP microparticles (3 $\mu\text{g/ml}$) in the absence or presence of retinol (1 μM or 3 μM) revealed only a slight change of the expression levels of collagen type I, type II, type III, or type V after a 5-day incubation period if retinol and nano/microparticles were added separately (Fig. 10a). If, however, both components were applied together a significant increase in the expression of the collagen type I to type III levels occurred to 4.8- to 9.4-fold (collagen type I), 31.7- to 55.8-fold (type II), 88.7- to 127.4-fold (type III), and 2.1-fold (type IV), with 1 μM and 3 μM retinol, respectively. Exposure of the cells to the retinol-containing microspheres showed that at concentration higher than ≥ 3 $\mu\text{g/ml}$, the expression levels for *collagen type I*, *collagen type II* and, in particular, of *collagen type III* are significantly higher than the one measured for 0.3 or 1 $\mu\text{g/ml}$ (Fig. 10b).

The dramatic increase in collagen type III expression could be blocked by triflupromazine, an inhibitor of clathrin-mediated endocytosis (Müller et al. 2015e).

From these results, we proposed that the synergistic effect of retinol and amorphous Ca-polyP is based on two different mechanisms of the components (Müller et al. 2015c). The first mechanism is mediated by the retinol/retinoic acid/receptor pathway, while the second mechanism occurs via the polyP/mTOR signaling pathway. It is proposed that polyP acts as a metabolic activator that

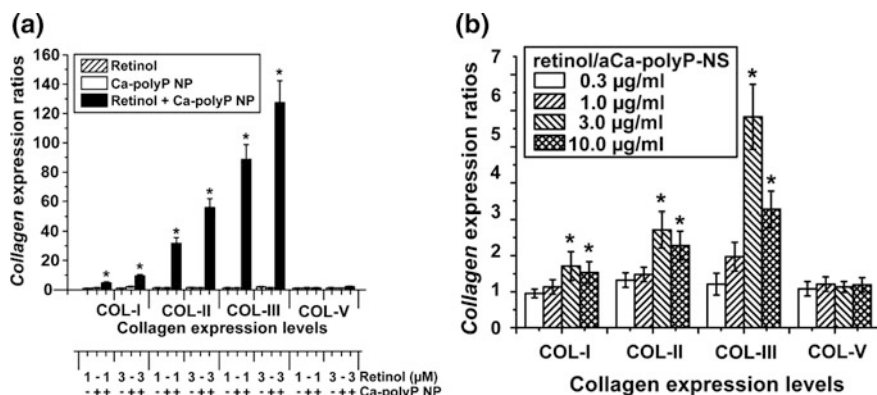


Fig. 10 **a** Steady-state levels of expression of collagens type I (*COL-I*), type II (*COL-II*), type III (*COL-III*), and type V (*COL-V*) in MC3T3-E1 cells after exposure to either retinol or the amorphous Ca-polyP nano-/microparticles (aCa-polyP-NP) alone (3 μg/ml) or in combination with two concentrations of retinol (1 and 3 μM). Collagen expression was determined after a 4 d incubation period by RT-qPCR using the house-keeping gene *GAPDH* as reference. The transcripts levels are given as ratios between treated and untreated cells (no addition of retinol or aCa-polyP-NP). **b** Expression levels of different types of collagen in MC3T3-E1 cells after exposure to retinol-containing amorphous Ca-polyP microspheres (retinol/aCa-polyP-NS). The ratios between treated and untreated cells are shown. Means ± SEM ($n = 5$); * $p < 0.01$ (Modified from Müller et al. 2015c)

stimulates the overall metabolism of the cells while retinol induces the expression of collagen type III (Fig. 11).

15 Phase-Specific Dressings for Wound Healing

The different phase-dependent requirements for wound dressings make certain components particularly suitable for certain phases of wound healing. Based on the results summarized in this chapter and a literature survey, the following components might be suitable to address the specific needs and requirements during different phases of wound healing.

Coagulation phase. The preferred properties for phase-specific dressing for the coagulation phase are mechanical protection, good permeability to oxygen and water vapor, and being removable without damage of the wound tissue. Potential components that fulfil these requirements are: (i) PolyP, added as amorphous Ca-polyP microparticles (acceleration of clotting); (ii) chitosan, applied as electrospun chitosan-based fibers/meshes (promotes platelet aggregation via fibrinogen adsorption; attracts erythrocytes via binding negatively charged residues on their cell surface by the protonated amine groups of chitosan, resulting in hemagglutination); both components, chitosan and polyP, accelerate thrombin generation;

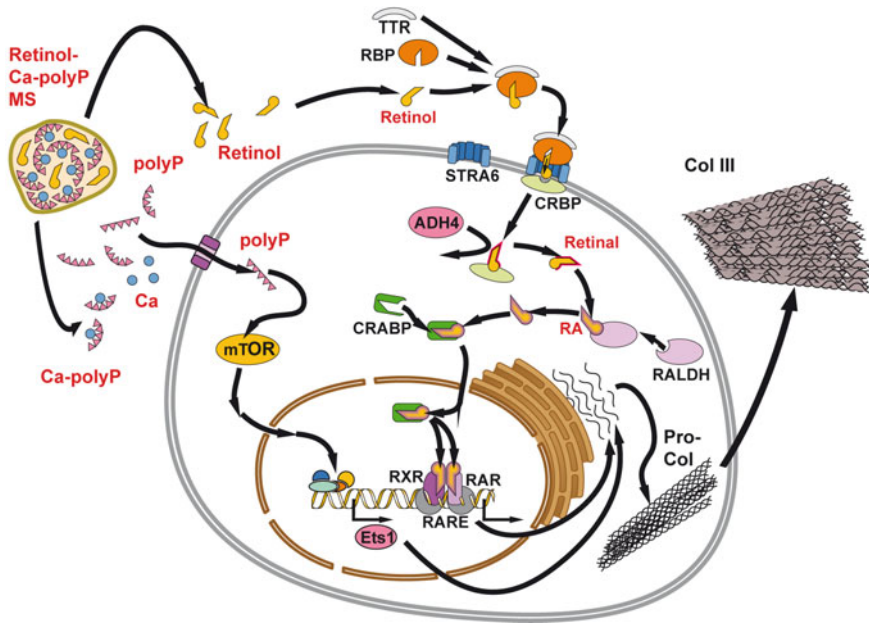


Fig. 11 Schematic sketch showing the proposed mechanism underlying the synergistic effect polyP and retinol, the bioactive constituents of the retinol-Ca-polyP nano- and microspheres, on the expression of the *collagen type III* gene. The retinol-Ca-polyP spheres are either degraded by the ALP in the extracellular space or are taken up *via* clathrin-mediated endocytosis in the intracellular space. There, polyP activates the mTOR pathway. Retinol, released after disintegration of the nano/microspheres in the extracellular space, binds to transthyretin [TTR] and the retinol-binding protein [RBP] *via* the STRA6 receptor. After cellular uptake and binding to the cellular retinol-binding protein [CRBP], retinol is enzymatically oxidized to retinal by alcohol dehydrogenase [ADH4] and to retinoic acid by retinaldehyde dehydrogenases [RALDH]. Retinoic acid then binds to the cellular retinoic acid-binding receptor [CRABP], which is transported into the cell nucleus, where retinoic acid binds to its receptor RAR and/or the retinoid X receptor [RXR]. As a result, the expression of the *collagen type III* gene is up-regulated (Modified from Müller et al. 2015c)

(iii) gelatin or alginate (hemostatic agents; stimulation of macrophage activity and excellent gel/film-forming properties; (iv) calcium ions (inducing self-organization of the polyanionic components).

Inflammation phase. The preferred properties for phase-specific dressing for the inflammation phase are protection against bacterial infiltration, absorption of wound exudate, maintaining a moist environment, as well as mechanical protection, good permeability to oxygen and water vapor, and being removable without damage of the wound tissue. Moreover, release of antibacterial agents (in case of infection). Alginates and hydrocolloids are suitable components to maintain a moist environment. In addition, advantageous properties are shown by the following components: (i) PolyP, added as amorphous Ca-polyP microparticles (antibacterial

activity, inhibition of MMPs and bacterial proteases, chelating alginate produced by biofilm-forming bacteria; (ii) silica (induction of the expression of the pro-inflammatory cytokines, IL-1 β , IL-6 and IL-8); (iii) chitosan, applied in the form of electrospun fibers/meshes (antibacterial activity caused by interaction between the positively charged chitosan molecules and negatively charged residues of the microbial cell wall); alternatively to the natural, chitosan-based fibers, synthetic fibers, e.g., polyP- β -caprolactone, can be used; and (iv) alginate, in the form of polymeric antimicrobial wafers (alternatively, xanthan gum, guar gum, etc., can be used). If required, anti-inflammatory compounds can be added as well as additives that allow monitoring of the healing process (e.g., inclusion of pH sensitive dyes).

Proliferation (epithelialisation) phase. The preferred properties for phase-specific dressing for the proliferation phase are, in particular, encouraging cell proliferation, in addition to mechanical protection, good permeability to oxygen and water vapor, maintaining a moist environment (examples: alginates and hydrocolloids), and being removable without damage of the wound tissue. Suitable components are: (i) PolyP (induction of collagen expression and expression of cytokines, antibacterial activity, inhibition of MMPs and bacterial proteases; (ii) chitosan (induction of proliferation, antibacterial activity); alternatively, use of electrospun fibers consisting of polyP- β -caprolactone, poly(urethane), poly(vinyl alcohol) [PVA], hyaluronic acid, or collagen type I); (iii) retinol, entrapped into the amorphous Ca-polyP microspheres (regulation of epithelial cell growth; activation of collagen/ECM synthesis). The ALP activity which increases during progression of wound healing (during termination of the inflammatory phase and progression of the granulation phase) could be used as a trigger to switch on the release of bioactive compounds incorporated into the amorphous polyP microspheres (via ALP-mediated hydrolysis of polyP, resulting in the disintegration of the amorphous Ca-polyP microspheres). The proposed composition would show several advantages: (i) Activation of the natural mechanisms involved in wound healing and (ii) supplementation of the dressings/functionalization of the electrospun nanofibers with expensive growth factors is not necessary; the proposed polyP component of the electrospun nanofibers would be able to induce the expression of these factors.

Remodeling phase. The preferred properties for phase-specific dressing for the proliferation phase are, besides of good permeability to oxygen and water vapor, induction of collagen expression. These requirements are again fulfilled by polyP, added as amorphous Ca-polyP microparticles (induces collagen expression). In addition, electrospun synthetic (e.g., polyP- β -caprolactone) or natural (e.g., chitosan-based) fibers/meshes can be used.

The proposed wound dressings are of special interest for chronic wounds that show delayed healing and a high risk of infection. These wound dressings would be particularly useful for treatment of diabetic foot ulcers, venous leg ulcers, and pressure ulcers.

16 The Future

We were the first to develop biologically active inorganic polymers that have the potential to induce tissue regeneration and self-repair, and are biodegradable without eliciting adverse immune reactions (Müller et al. 2014a). One of these nature-based polymers is polyP (Müller et al. 2011; Wang et al. 2012, 2013a, b, 2014b, c). Based on these discoveries, novel strategies in tissue engineering have been developed. PolyP as a biologically active polymer can be combined with other biodegradable, but biologically inert, natural polymers, resulting in hybrid materials that can be applied in tissue engineering. For example, the polyanionic polyP can be linked together with alginate, another polyanionic polymer, in the presence of calcium ions under formation of a hydrogel with adjustable hardness (Neufurth et al. 2014). In another approach, instead of alginate, a modified chitosan (*N,O*-CMC) has been used (Müller et al. 2015d). The suitability of the developed methods has already been demonstrated in first animal experiments that revealed that the developed biomaterials are superior to conventional materials at least in the field of bone implants (e.g., Wang et al. 2014d). We even succeeded to bio-print cells entrapped in these hydrogels/matrices without impairing cell proliferation and differentiation (Neufurth et al. 2014). As an alternative approach, the electrospinning technique has been introduced (Müller et al. 2014b). We could demonstrate, even in animal experiments, that this technique can be used for the production of bioactive wound dressings that are promising even in case of delayed wound repair like in diabetes (experiments in db/db mice). In addition, the novel inorganic biopolymer, if present in the form of amorphous Ca-polyP particles and combined with retinol, revealed skin-protective, anti-aging protective activity.

Based on the developed basic technology, a set of narrow-ranged Ca-polyP microparticles and Ca-polyP microspheres into which various anti-inflammatory, UV-protective or anti-senescence compounds that complement the bioactivity of polyP or act synergistically with this polymer can be developed in future. These bioactive compound-loaded Ca-polyP microparticles and microspheres could be used for fabrication of a future generation of bioactive wound dressings based on electrospun fiber networks consisting of polyP- β -caprolactone, chitosan or other natural or synthetic spinnable polymers. In addition, ointments and gels based on the developed wound-repairing, UV-protective, or anti-senescence Ca-polyP microspheres could be prepared and optimized with regard to the intended application, including the release kinetics.

It should be noted that the electrospun mats consisting of our materials combine three properties: (i) antibacterial activity, (ii) efficient gas exchange with the environment, and (iii) morphogenetic activity to the cells involved in wound healing. There are only a few wound dressings that both inhibit microbial infiltration and enhance wound cell regeneration (Abrigo et al. 2014).

The techniques and novel electrospun bioactive polymer-microparticle combinations demonstrated in this article have the potential to provide the basis for the development of smart, phase-sensing dressings which are important in particular for

chronic wounds. A special focus in future will be on impaired wound healing like in diabetic patients (gangrene development). The property of polyP to provide an extracellular source for energy storage and supply, as well as the property of polyP to act as a metabolic regulator that increases mitochondrial ATP production opens radically new prospects in wound healing and therapy of dermatological disorders.

Acknowledgements W.E.G. M. is a holder of an ERC Advanced Investigator Grant (No. 268476 “BIOSILICA”) as well as of the two ERC Proof-of-Concept grants “Si-Bone-PoC” (No. 324564) and “MorphoVES-PoC” (No. 662486). This work was supported by grants from the European Commission (large-scale integrating project “BlueGenics” No. 266033 and project “Bio-Scaffolds” No. 604036), as well as the BiomaTiCS research initiative of the University Medical Center Mainz. In addition, we would like to thank Prof. Dr. Vesna Erakovic Haber, Fidelta d.o.o., Zagreb, Croatia, for the animal experiments in in vivo disease model.

References

- Abraham JA, Klagsbrun M (1996) Modulation of wound repair by members of the fibroblast growth factor family. In: *The molecular and cellular biology of wound repair*. Plenum Press, New York, pp 195–248
- Abriago M, McArthur SL, Kingshott P (2014) Electrospun nanofibers as dressings for chronic wound care: Advances, challenges, and future prospects. *Macromol Biosci* 14:772–792
- Alpaslan G, Nakajima T, Takano Y (1997) Extracellular alkaline phosphatase activity as a possible marker for wound healing: a preliminary report. *J Oral Maxillofac Surg* 55:56–62
- Baji A, Mai YW, Wong SC, Abtahi M, Chen P (2010) Electrospinning of polymer nanofibers: effects on oriented morphology, structures and tensile properties. *Compos Sci Technol* 70:703–718
- Barrientos S, Stojadinovic O, Golinko MS, Brem H, Tomic-Canic M (2008) Perspective article: growth factors and cytokines in wound healing. *Wound Repair Regen* 16:585–601
- Bjarnsholt T, Kirketerp-Møller K, Jensen PØ, Madsen KG, Phipps R, Krogfelt K, Høiby N, Givskov M (2008) Why chronic wounds will not heal: a novel hypothesis. *Wound Repair Regen* 16:2–10
- Boateng JS, Matthews KH, Stevens HN, Eccleston GM (2008) Wound healing dressings and drug delivery systems: a review. *J Pharm Sci* 97:2892–2923
- Chen JP, Chang GY, Chen JK (2008) Electrospun collagen/chitosan nanofibrous membrane as wound dressing. *Colloids Surf A: Physicochem Eng Aspects* 313–314:183–188
- Clark RAF (1989) Wound repair. *Curr Opin Cell Biol* 1:1000–1008
- Coppari R, Bjørnbæk C (2012) Leptin revisited: its mechanism of action and potential for treating diabetes. *Nat Rev Drug Discov* 11:692–708
- Dinarello CA (2011) Blocking interleukin-1b in acute and chronic autoinflammatory diseases. *J Int Med* 269:16–28
- Ding YL, Chen YW, Qin YJ, Shi GQ, Yu XX, Wan CX (2008) Effect of polymerization degree of calcium polyphosphate on its microstructure and in vitro degradation performance. *J Mater Sci Mater Med* 19:1291–1295
- Faxälv L, Boknäs N, Ström JO, Tengvall P, Theodorsson E, Ramström S, Lindahl TL (2013) Putting polyphosphates to the test: evidence against platelet-induced activation of factor XII. *Blood* 122:3818–3824
- Feldmeyer L, Werner S, French LE, Beer H-D (2010) Interleukin-1, inflammasomes and the skin. *Eur J Cell Biol* 89:638–644

- Frank S, Stallmeyer B, Kämpfer H, Kolb N, Pfeilschifter J (2000) Leptin enhances wound re-epithelialization and constitutes a direct function of leptin in skin repair. *J Clin Invest* 106:501–509
- Friedman JM, Halaas JL (1998) Leptin and the regulation of body weight in mammals. *Nature* 395:763–770
- Gallo RL, Dorschner RA, Takashima S, Klagsbrun M, Eriksson E, Bernfield M (1997) Endothelial cell surface alkaline phosphatase activity is induced by IL-6 released during wound repair. *J Invest Dermatol* 109:597–603
- Gelain DP, Pasquali MA, Caregnato FF, Castro MA, Moreira JC (2012) Retinol induces morphological alterations and proliferative focus formation through free radical-mediated activation of multiple signaling pathways. *Acta Pharmacol Sin* 33:558–567
- Gilchrist BA, Bohr VA (1997) Aging process, DNA damage, and repair. *FASEB J* 11:322–330
- Gilliver SC, Ashworth JJ, Ashcroft GS (2007) The hormonal regulation of cutaneous wound healing. *Clin Dermatol* 25:56–62
- Girona J, Rosales R, Plana N, Saavedra P, Masana L, Vallvé JC (2013) FABP4 induces vascular smooth muscle cell proliferation and migration through a MAPK-dependent pathway. *PLoS ONE* 8:e81914
- Greenhalgh DG, Sprugel KH, Murray MJ, Ross R (1990) PDGF and FGF stimulate wound healing in the genetically diabetic mouse. *Am J Pathol* 136:1235–1246
- Grotheer V, Goergens M, Fuchs PC, Dunda S, Pallua N, Windolf J, Suschek CV (2013) The performance of an orthosilicic acid-releasing silica gel fiber fleece in wound healing. *Biomaterials* 34:7314–7327
- Guo S, DiPietro LA (2010) Factors affecting wound healing. *J Dent Res* 89:219–229
- Hacchou Y, Uematsu T, Ueda O, Usui Y, Uematsu S, Takahashi M, Uchihashi T, Kawazoe Y, Shiba T, Kurihara S, Yamaoka M, Furusawa K (2007) Inorganic polyphosphate: a possible stimulant of bone formation. *J Dent Res* 86:893–897
- Hansen SL, Young DM, Boudreau NJ (2003) HoxD3 expression and collagen synthesis in diabetic fibroblasts. *Wound Repair Regen* 11:474–480
- Harjes U, Bridges E, McIntyre A, Fielding BA, Harris AL (2014) Fatty acid-binding protein 4, a point of convergence for angiogenic and metabolic signaling pathways in endothelial cells. *J Biol Chem* 289:23168–23176
- Hatakeyama N, Kojima T, Iba K, Murata M, Thi MM, Spray DC, Osanai M, Chiba H, Ishiai S, Yamashita T, Sawada N (2008) IGF-I regulates tight-junction protein claudin-1 during differentiation of osteoblast-like MC3T3-E1 cells via a MAP-kinase pathway. *Cell Tissue Res* 334:243–254
- Keleidari B, Mahmoudieh M, Bahrami F, Mortazavi P, Aslani RS, Toliyat SA (2014) The effect of vitamin A and vitamin C on postoperative adhesion formation: a rat model study. *J Res Med Sci* 19:28–32
- Keylock KT, Vieira VJ, Wallig MA, DiPietro LA, Schrementi M, Woods JA (2008) Exercise accelerates cutaneous wound healing and decreases wound inflammation in aged mice. *Am J Physiol Regul Integr Comp Physiol* 294:R179–R184
- Khil MS, Cha DI, Kim HY, Kim IS, Bhattarai N (2003) Electrospun nanofibrous polyurethane membrane as wound dressing. *J Biomed Mater Res B Appl Biomater* 67:675–679
- Kim SE, Heo DN, Lee JB, Kim JR, Park SH, Jeon SH, Kwon IK (2009) Electrospun gelatin/polyurethane blended nanofibers for wound healing. *Biomed Mater* 4:044106
- Krskova-Tybitanclova K, Macejova D, Brtko J, Baculikova M, Krizanova O, Zorad S (2008) Short term 13-*cis*-retinoic acid treatment at therapeutic doses elevates expression of leptin, GLUT4, PPAR gamma and aP2 in rat adipose tissue. *J Physiol Pharmacol* 59:731–743
- Kulaev IS, Vagabov V, Kulakovskaya T (2004) *The biochemistry of inorganic polyphosphates*. Wiley, New York
- Kusakari Y, Ogawa E, Owada Y, Kitanaka N, Watanabe H, Kimura M, Tagami H, Kondo H, Aiba S, Okuyama R (2006) Decreased keratinocyte motility in skin wound on mice lacking the epidermal fatty acid binding protein gene. *Mol Cell Biochem* 284:183–188
- Landis SJ (2008) Chronic wound infection and antimicrobial use. *Adv Skin Wound Care* 21:531–540

- Laplante M, Sabatini DM (2009) mTOR signaling at a glance. *J Cell Sci* 122:3589–3594
- Laverty G, Gorman SP, Gilmore BF (2014) Biomolecular mechanisms of *Pseudomonas aeruginosa* and *Escherichia coli* biofilm formation. *Pathogens* 3:596–632
- Lee MY, Tse HF, Siu CW, Zhu SG, Man RY, Vanhoutte PM (2007) Genomic changes in regenerated porcine coronary arterial endothelial cells. *Arterioscler Thromb Vasc Biol* 27:2443–2449
- Lee D, Stojadinovic O, Krzyzanowska A, Vouthounis C, Blumenberg M, Tomic-Canic M (2009) Retinoid-responsive transcriptional changes in epidermal keratinocytes. *J Cell Physiol* 220:427–439
- Lerman ZO, Galiano RD, Armour M, Levine JP, Gurtner GC (2003) Cellular dysfunction in the diabetic fibroblast. *Am J Pathol* 162:303–312
- Leyhausen G, Lorenz B, Zhu H, Geurtsen W, Böhrensack R, Müller WEG, Schröder HC (1998) Inorganic polyphosphate in human osteoblast-like cells. *J Bone Mineral Res* 13:803–812
- Lionelli GT, Lawrence WT (2003) Wound dressings. *Surg Clin North Am* 83:617–638
- Lorencová E, Vltavská P, Budinský P, Koutný M (2012) Antibacterial effect of phosphates and polyphosphates with different chain length. *J Environ Sci Health A Tox Hazard Subst Environ Eng* 47:2241–2245
- Lorenz B, Müller WEG, Kulaev IS, Schröder HC (1994) Purification and characterization of an exopolyphosphatase activity from *Saccharomyces cerevisiae*. *J Biol Chem* 269:22198–22204
- Lorenz B, Batel R, Bachinski N, Müller WEG, Schröder HC (1995) Purification and characterization of two exopolyphosphatases from the marine sponge *Tethya lyncurium*. *Biochim Biophys Acta* 1245:17–28
- Lorenz B, Schröder HC (2001) Mammalian intestinal alkaline phosphatase acts as highly active exopolyphosphatase. *Biochim Biophys Acta* 1547:254–261
- Low QE, Druzea IA, Duffner LA, Quinn DG, Cook DN, Rollins BJ, Kovacs EJ, DiPietro LA (2001) Wound healing in MIP-1 alpha(-/-) and MCP-1(-/-) mice. *Am J Pathol* 159:457–463
- Lu Y, Huang J, Yu G, Cardenas R, Wei S, Wujcik EK, Guo Z (2016) Coaxial electrospun fibers: applications in drug delivery and tissue engineering. *Wiley Interdiscip Rev Nanomed Nanobiotechnol* 8:654–677
- MacNeil S (2007) Progress and opportunities for tissue-engineered skin. *Nature* 445:874–880
- Mamedov LA, Nikolaev AV, Zakharov VV, Shekhter AB, IuR K (1987) Phosphatase activity of blood leukocytes and wound exudate during the experimental healing of an aseptic wound. *Biull Eksp Biol Med* 104:306–309
- Matarese V, Bernlohr DA (1988) Purification of murine adipocytes lipid-binding protein. Characterization as a fatty acid- and retinoic acid-binding protein. *J Biol Chem* 263:14544–14551
- McCarty SM, Percival SL, Clegg PD, Cochrane CA (2015) The role of polyphosphates in the sequestration of matrix metalloproteinases. *Int Wound J* 12:89–99
- McDougall S, Dallon J, Sherratt J, Maini P (2006) Fibroblast migration and collagen deposition during dermal wound healing: mathematical modelling and clinical implications. *Philos Trans A Math Phys Eng Sci* 364:1385–1405
- Mehr SMH, Dinarvand P, Rezaie AR (2014) Inorganic polyphosphate activates mTOR complexes 1 and 2 in vascular endothelial cells. 56th ASH Annual Meeting in San Francisco, CA, (Session 302, Abstract 1441)
- Menke NB, Ward KR, Witten TM, Bonchev DG, Diegelmann RF (2007) Impaired wound healing. *Clin Dermatol* 25:19–25
- Minematsu T, Nakagami G, Yamamoto Y, Kanazawa T, Huang L, Koyanagi H, Sasaki S, Uchida G, Fujita H, Haga N, Yoshimura K, Nagase T, Sanada H (2013) Wound blotting: A convenient biochemical assessment tool for protein components in exudate of chronic wounds. *Wound Rep Reg* 21:329–334
- Moon JH, Park JH, Lee JY (2011) Antibacterial action of polyphosphate on *Porphyromonas gingivalis*. *Antimicrob Agents Chemother* 55:806–812

- Mukherjee S, Date A, Patravale V, Korting HC, Roeder A, Weindl G (2006) Retinoids in the treatment of skin aging: an overview of clinical efficacy and safety. *Clin Interv Aging* 1:327–348
- Müller WEG, Wang XH, Diehl-Seifert B, Kropf K, Schloßmacher U, Lieberwirth I, Glasser G, Wiens M, Schröder HC (2011) Inorganic polymeric phosphate/polyphosphate is an inducer of alkaline phosphatase and a modulator of intracellular Ca^{2+} level in osteoblasts (SaOS-2 cells) in vitro. *Acta Biomater* 7:2661–2671
- Müller WEG, Schröder HC, Burghard Z, Pisignano D, Wang XH (2013) Silicateins—a novel paradigm in bioinorganic chemistry: enzymatic synthesis of inorganic polymeric silica. *Chemistry* 19:5790–5804
- Müller WEG, Schröder HC, Wang XH (2014a) Enzyme-based biosilica and biocalcite: biomaterials for the future in regenerative medicine. *Trends Biotechnol* 32:441–447
- Müller WEG, Tolba E, Schröder HC, Diehl-Seifert B, Link T, Wang XH (2014b) Biosilica-loaded poly(ϵ -caprolactone) nanofibers mats provide a morphogenetically active surface scaffold for the growth and mineralization of the osteoclast-related SaOS-2 cells. *Biotechnol J* 9:1312–1321
- Müller WEG, Tolba E, Dorweiler B, Schröder HC, Diehl-Seifert B, Wang XH (2015a) Electrospun bioactive mats enriched with Ca-polyphosphate/retinol nanospheres as potential wound dressing. *Biochem Biophys Rep* 3:150–160
- Müller WEG, Tolba E, Feng Q, Schröder HC, Markl JS, Kokkinopoulou M, Wang XH (2015b) Amorphous Ca^{2+} polyphosphate nanoparticles regulate the ATP level in bone-like SaOS-2 cells. *J Cell Sci* 128:2202–2207
- Müller WEG, Tolba E, Schröder HC, Diehl-Seifert B, Wang XH (2015c) Retinol encapsulated into amorphous Ca^{2+} polyphosphate nanospheres acts synergistically in MC3T3-E1 cells. *Eur J Pharm Biopharm* 93:214–223
- Müller WEG, Tolba E, Schröder HC, Neufurth M, Wang SF, Link T, Al-Nawas B, Wang XH (2015d) A new printable and durable N, O-carboxymethyl chitosan- Ca^{2+} —polyphosphate complex with morphogenetic activity. *J Mater Chem B* 3:1722–1730
- Müller WEG, Tolba E, Schröder HC, Wang SF, Glaßer G, Muñoz-Espí R, Link T, Wang XH (2015e) A new polyphosphate calcium material with morphogenetic activity. *Mater Lett* 148:163–166
- Müller WEG, Neufurth M, Wang SF, Tolba E, Schröder HC, Wang XH (2016a) Morphogenetically active scaffold for osteochondral repair (polyphosphate/alginate/N, O-carboxymethyl chitosan). *Eur Cell Mater* 31:174–190
- Müller WEG, Schröder HC, Tolba E, Diehl-Seifert B, Wang XH (2016b) Mineralization of bone-related SaOS-2 cells under physiological hypoxic conditions. *FEBS J* 283:74–87
- Murad A, Nath AK, Cha ST, Demir E, Flores-Riveros J, Sierra-Honigmann MR (2003) Leptin is an autocrine/paracrine regulator of wound healing. *FASEB J* 17:1895–1897
- Neufurth M, Wang XH, Schröder HC, Feng QL, Diehl-Seifert B, Ziebart T, Steffen R, Wang SF, Müller WEG (2014) Engineering a morphogenetically active hydrogel for bioprinting of bioartificial tissue derived from human osteoblast-like SaOS-2 cells. *Biomaterials* 35:8810–8819
- Nurden AT, Nurden P, Sanchez M, Andia I, Anitua E (2008) Platelets and wound healing. *Front Biosci* 13:3532–3548
- Obara K, Ishihara M, Fujita M, Kanatani Y, Hattori H, Matsui T, Takase B, Ozeki Y, Nakamura S, Ishizuka T, Tominaga S, Hiroi S, Kawai T, Maehara T (2005) Acceleration of wound healing in healing impaired db/db mice with a photocrosslinkable chitosan hydrogel containing fibroblast growth factor-2. *Wound Rep Reg* 13:390–397
- Ohtake H, Wu H, Imazu K, Anbe Y, Kato J, Kuroda A (1996) Bacterial phosphonate degradation, phosphite oxidation and polyphosphate accumulation. *Resour Conserv Recycl* 18:125–134
- Ong SY, Wu J, Mochhala SM, Tan MH, Lu J (2008) Development of a chitosan-based wound dressing with improved hemostatic and antimicrobial properties. *Biomaterials* 29:4323–4332
- Pandel R, Poljšak B, Godic A, Dahmane R (2013) Skin photoaging and the role of antioxidants in its prevention. *ISRN Dermatol* 12:930164

- Pasche S, Schyrr B, Wenger B, Scolan E, Ischer R, Voirin G (2013) Smart textiles with biosensing capabilities. *Adv Sci Technol* 80:129–135
- Pilliar RM, Filiaggi MJ, Wells JD, Grynblas MD, Kandel RA (2001) Porous calcium polyphosphate scaffolds for bone substitute applications—in vitro characterization. *Biomaterials* 22:963–972
- Plutzky J (2011) The PPAR-RXR transcriptional complex in the vasculature: energy in the balance. *Circ Res* 108:1002–1016
- Risau W (1990) Angiogenic growth factors. *Prog Growth Factor Res* 2:71–79
- Sawamura D, Meng X, Ina S, Sato M, Tamai K, Hanada K, Hashimoto I (1998) Induction of keratinocyte proliferation and lymphocytic infiltration by in vivo introduction of the IL-6 gene into keratinocytes and possibility of keratinocyte gene therapy for inflammatory skin diseases using IL-6 mutant genes. *J Immunol* 161:5633–5639
- Schröder HC, Lorenz B, Kurz L, Müller WEG (1999) Inorganic polyP in eukaryotes: enzymes, metabolism and function. In: Schröder HC, Müller WEG, (eds) *Inorganic polyphosphates: biochemistry, biology, biotechnology*. *Prog Mol Subcell Biol* 23:45-81
- Schröder HC, Kurz L, Müller WEG, Lorenz B (2000) Polyphosphate in bone. *Biochemistry* 65:296–303 (Moscow)
- Segawa S, Fujiya M, Konishi H, Ueno N, Kobayashi N, Shigyo T, Kohgo Y (2011) Probiotic-derived polyphosphate enhances the epithelial barrier function and maintains intestinal homeostasis through integrin-p38 MAPK pathway. *PLoS ONE* 6:e23278
- Shiba T, Nishimura D, Kawazoe Y, Onodera Y, Tsutsumi K, Nakamura R, Ohshiro M (2003) Modulation of mitogenic activity of fibroblast growth factors by inorganic polyphosphate. *J Biol Chem* 278:26788–26792
- Simbulan-Rosenthal CM, Gaur A, Sanabria VA, Dussan LJ, Saxena R, Schmidt J, Kitani T, Chen YS, Rahim S, Uren A, Crooke E, Rosenthal DS (2015) Inorganic polyphosphates are important for cell survival and motility of human skin keratinocytes. *Exp Dermatol* 24:636–639
- Simmonds RE, Foxwell BM (2008) Signalling, inflammation and arthritis. *Rheumatology* 47:584–590
- Skórkowska-Telichowska K, Czemplik M, Kulma A, Szopa J (2013) The local treatment and available dressings designed for chronic wounds. *J Am Acad Dermatol* 68:e117–e126
- Smith SA, Mutch NJ, Baskar D, Rohloff P, Docampo R, Morrissey JH (2006) Polyphosphate modulates blood coagulation and fibrinolysis. *Proc Natl Acad Sci USA* 103:903–908
- Supaphol P, Chuangchote S (2008) On the electrospinning of poly(vinyl alcohol) nanofiber mats: a revisit. *J Appl Polymer Sci* 108:969–978
- Tabe Y, Konopleva M, Munsell MF, Marini FC, Zompetta C, McQueen T, Tsao T, Zhao S, Pierce S, Igari J, Estey EH, Andreeff M (2004) PML-RAR alpha is associated with leptin-receptor induction: the role of mesenchymal stem cell-derived adipocytes in APL cell survival. *Blood* 103:1815–1822
- Tang M, Zhong M, Shang Y, Lin H, Deng J, Jiang H, Lu H, Zhang Y, Zhang W (2008) Differential regulation of collagen types I and III expression in cardiac fibroblasts by AGES through TRB3/MAPK signaling pathway. *Cell Mol Life Sci* 65:2924–2932
- Thorey IS, Hinz B, Hoeflich A, Kaesler S, Bugnon P, Elmlinger M, Wanke R, Wolf E, Werner S (2004) Transgenic mice reveal novel activities of growth hormone in wound repair, angiogenesis and myofibroblast differentiation. *J Biol Chem* 279:26674–26684
- Tkalčević VI, Cuzić S, Parnham MJ, Pasalić I, Brajsa K (2009) Differential evaluation of excisional non-occluded wound healing in db/db mice. *Toxicol Pathol* 37:183–192
- Tsuchiya H, Ikeda Y, Ebata Y, Kojima C, Katsuma R, Tsuruyama T, Sakabe T, Shomori K, Komeda N, Oshiro S, Okamoto H, Takubo K, Hama S, Shudo K, Kogure K, Shiota G (2012) Retinoids ameliorate insulin resistance in a leptin-dependent manner in mice. *Hepatology* 56:1319–1330
- Uppal R, Ramaswamy GN, Arnold C, Goodband R, Wang Y (2011) Hyaluronic acid nanofiber wound dressing—production, characterization, and in vivo behavior. *J Biomed Mater Res B Appl Biomater* 97:20–29

- Wang L, Fraley CD, Faridi J, Kornberg A, Roth RA (2003) Inorganic polyphosphate stimulates mammalian TOR, a kinase involved in the proliferation of mammary cancer cells. *Proc Natl Acad Sci USA* 100:11249–11254
- Wang L, Tankersley LR, Tang M, Potter JJ, Mezey E (2004) Regulation of alpha 2(I) collagen expression in stellate cells by retinoic acid and retinoid X receptors through interactions with their cofactors. *Arch Biochem Biophys* 428:92–98
- Wang XH, Schröder HC, Wiens M, Ushijima H, Müller WEG (2012) Bio-silica and bio-polyphosphate: applications in biomedicine (bone formation). *Curr Opin Biotechnol* 23:570–578
- Wang XH, Schröder HC, Diehl-Seifert B, Kropf K, Schloßmacher U, Wiens M, Müller WEG (2013a) Dual effect of inorganic polymeric phosphate/polyphosphate on osteoblasts and osteoclasts in vitro. *J Tissue Eng Regen Med* 7:767–776
- Wang XH, Schröder HC, Feng QL, Draenert F, Müller WEG (2013b) The deep-sea natural products, biogenic polyphosphate (Bio-PolyP) and biogenic silica (Bio-Silica), as biomimetic scaffolds for bone tissue engineering: fabrication of a morphogenetically-active polymer. *Mar Drugs* 11:718–746
- Wang XH, Schröder HC, Feng Q, Diehl-Seifert B, Grebenjuk VA, Müller WEG (2014a) Isoquercitrin and polyphosphate co-enhance mineralization of human osteoblast-like SaOS-2 cells via separate activation of two RUNX2 cofactors AFT6 and Ets1. *Biochem Pharmacol* 89:413–421
- Wang XH, Schröder HC, Grebenjuk V, Diehl-Seifert B, Mailänder V, Steffen R, Schloßmacher U, Müller WEG (2014b) The marine sponge-derived inorganic polymers, biosilica and polyphosphate, as morphogenetically active matrices/scaffolds for the differentiation of human multipotent stromal cells: potential application in 3D printing and distraction osteogenesis. *Mar Drugs* 12:1131–1147
- Wang XH, Schröder HC, Müller WEG (2014c) Enzymatically synthesized inorganic polymers as morphogenetically active bone scaffolds: application in regenerative medicine. *Int Rev Cell Mol Biol* 313:27–77
- Wang SF, Wang XH, Draenert FG, Albert O, Schröder HC, Mailänder V, Mitov G, Müller WEG (2014d) Bioactive and biodegradable silica biomaterial for bone regeneration. *Bone* 67:292–304
- Wang XH, Schröder HC, Müller WEG (2016) Polyphosphate as a metabolic fuel in Metazoa: a foundational breakthrough invention for biomedical applications. *Biotechnol J* 11:11–30
- Werner S, Grose R (2003) Regulation of wound healing by growth factors and cytokines. *Physiol Rev* 83:835–870
- Yoshimura K, Uchida G, Okazaki M, Kitano Y, Harii K (2003) Differential expression of heparin-binding EGF-like growth factor (HB-EGF) mRNA in normal human keratinocytes induced by a variety of natural and synthetic retinoids. *Exp Dermatol* 12(Suppl 2):28–34
- Yuan J, Geng J, Xing Z, Shim KJ, Han I, Kim JC, Kang IK, Shen J (2015) Novel wound dressing based on nanofibrous PHBV-keratin mats. *J Tissue Eng Regen Med* 9:1027–1035
- Zhang Y, Lim CT, Ramakrishna S, Huang ZM (2005) Recent development of polymer nanofibers for biomedical and biotechnological applications. *J Mater Sci Mater Med* 16:933–946
- Zhang S, Li J, Lykotrafitis G, Bao G, Suresh S (2009) Size-dependent endocytosis of nanoparticles. *Adv Mater* 21:419–424

Entotheonella Bacteria as Source of Sponge-Derived Natural Products: Opportunities for Biotechnological Production

Agneya Bhushan, Eike E. Peters and Jörn Piel

Abstract Marine sponges belong to the oldest animals existing today. Apart from their role in recycling of carbon and nitrogen in the ocean, they are also an important source of a wide variety of structurally diverse bioactive natural products. Over the past few decades, a multitude of compounds from sponges have been discovered exhibiting diverse, pharmacologically promising activities. However, in many cases the low substance quantities present in the sponge tissue would require the collection of large amounts of sponge material, thus impeding further drug development. Recent research has focused on understanding natural product biosynthesis in sponges and on investigating symbiotic bacteria as possible production sources in order to develop sustainable production systems. This chapter covers research efforts that have taken place over the past few years involving the identification of 'Entotheonella' symbionts responsible for production of sponge compounds, as well as the elucidation of their biosynthetic routes, highlighting future biotechnological applications.

1 Introduction

The ocean and its chemical and biological diversity is far from being understood today, representing a virtually unlimited resource for natural product discovery (Blunt et al. 2015). Within this vast ecosystem, sponges (phylum Porifera) have provided more marine natural products (MNPs) than any other group of marine organisms, contributing more than 30% of all MNPs discovered up to date (Mehbub et al. 2014). Marine sponges are discussed as the most ancient extant metazoans, with fossils dating back over 600 million years (Maloof et al. 2010; Love et al. 2009). They are globally distributed and functionally important members of benthic communities (Van Soest et al. 2012; Bell 2008), due to their important role in the

A. Bhushan · E.E. Peters · J. Piel (✉)
Institute of Microbiology, Eidgenössische Technische Hochschule (ETH) Zurich,
Vladimir-Prelog-Weg 4, 8093 Zurich, Switzerland
e-mail: jpiel@ethz.ch

provision of dissolved inorganic nitrogen (Diaz and Ward 1997). Additionally, they are also important as a sink and source of particulate organic carbon, dissolved organic carbon and nitrogen. These might be reasons that sponges are the most abundant marine organisms in many areas of the ocean, covering, e.g., up to 80% of all surfaces in polar regions (Dayton 1989), and are often the dominant benthic organisms in temperate reefs (Bell and Smith 2004; Pawlik 2011).

Even though sponges can exhibit a huge variety of different morphologies, they exhibit a common basic body plan. The skeletal system of these sessile filter feeders is comprised of spicules that are either made of calcium carbonate, silicon dioxide or spongin, a collagenous protein. Their body does not possess any distinct organs or aquiferous systems for circulation, digestion, and excretion, as found in higher metazoans, but is composed of only a few types of differentiated cells. The outer surface (pinacoderm) of the sponge is built by a layer of pinacocytes, dispersed by some porocyte cells that form a network of channels and chambers throughout the sponge body. Choanocyte cells are found around the so-called choanosome chambers and are flagellated cells generating a water current that flows from the outside through the sponge towards the osculum, where it is expelled. The part between the epidermis and choanocytes—the mesohyl—is composed of gelatinous material in which some archaeocytes (or amoebocytes) migrate. Archaeocytes have several different functions: delivery of food from choanocytes to other cells, giving rise to eggs for sexual reproduction, but they can also differentiate into specialized cells. Examples of such cells are collencytes that produce a collagen-like protein to maintain the mesohyl structure, sclerocytes that generate spicules, or spongocytes producing spongin in most sponges (Leys and Hill 2012; Taylor et al. 2007).

Bacteria and parasites were already present in the ocean when sponges emerge, meaning that sponges evolved while constantly exposed to these microbes. Sponges have developed an impressive arsenal of defenses against microbial pathogens (reviewed in Hentschel et al. 2012), but in addition they also form intimate symbiotic relationships with diverse communities of microorganisms from all domains of life (Taylor et al. 2007), i.e. bacteria, archaea, and unicellular eukaryotes. Viruses (Harrington et al. 2012) and bacteriophages (Lohr et al. 2005) have also been detected in sponge tissue. Such microorganisms can be mainly found in the mesohyl (Imhoff and Stohr 2003) and can constitute up to 35% of the total sponge biomass, yielding densities of up to 10^9 microbial cells per cubic centimeter of sponge tissue (Taylor et al. 2007).

The reason for the high frequency of MNPs in marine sponges is still unclear, but it is generally believed that animals that are permanently attached to surfaces and lack mechanical protection often develop chemical defenses (Paul and Puglisi 2004). These substances have evolved for millions of years to interact efficiently with their targets and hence often show high and selective activity that is of great interest in many drug screening programs (Mayer et al. 2010). To date, there are only few examples for sponge-derived MNPs that made their way into the clinics. For preclinical and clinical trials the supply of sufficient GMP-grade pure compound must be guaranteed, which is in many cases a serious challenge due to the minute concentration of MNPs in their animal sources (sometimes less than $10^{-6}\%$

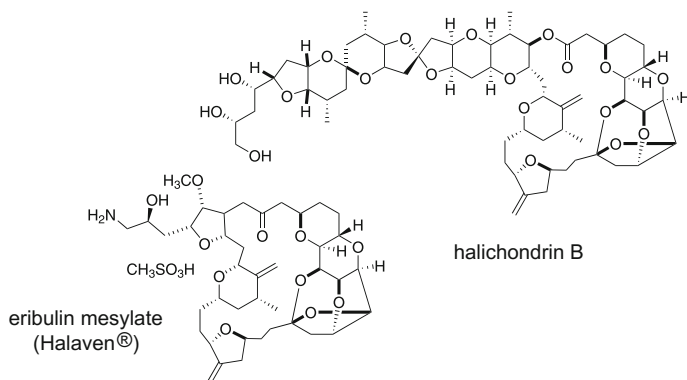


Fig. 1 Halichondrin B and its synthetic analog eribulin mesylate (Halaven[®])

of wet weight (Mendola 2000)). Besides this technical challenge, the collection of tons of sponge material from the natural habitats can have severe ecological implications. Therefore alternative supply strategies have to be developed in order to meet the demands of the pharma industry (Proksch et al. 2002; Sipkema et al. 2005). Some progress has been made with mariculture sponges (Mendola 2003) but so far none of the existing cultivation systems have been commercially implemented for MNP production. For some MNPs, total chemical synthesis or semi-synthetic approaches are feasible to solve the supply issue. One prominent example is Halaven[®] (eribulin mesylate, Fig. 1), a structurally highly complex, yet simplified synthetic analog of the even more complex sponge-derived actin inhibitor halichondrin B that was approved by the FDA for the treatment of late-stage metastatic breast cancer in 2010 (Huyck et al. 2011). The substance has a long history of development that includes several landmark accomplishments: the establishment of a 90-step total synthesis protocol (Aicher et al. 1992), the collection of one metric ton of animal material to isolate 300 mg halichondrin B for preclinical trials (Munro et al. 1999), and the synthesis and testing of a variety of different variants up to the recent development of a more efficient total synthesis protocol (61 steps) of the synthetic analog (Yu et al. 2013). These achievements are impressive, but they also illustrate the challenge of developing drugs from sponge-derived MNPs.

Already for a long time, scientists noticed the structural similarity of some sponge-derived MNPs to those derived from bacteria (Bewley and Faulkner 1998; Moore 1999; Piel 2004). This is, for example, the case for compounds resembling complex polyketides and nonribosomal peptides, which in microorganisms are produced by type I polyketide synthases (PKSs; Rawlings 2001) and nonribosomal peptide synthetases (NRPSs; Finking and Marahiel 2004), respectively. Bacterial type I PKSs are huge multi-domain proteins that consist of repeated functional units, termed modules. Each of these modules incorporates a building block into the nascent polyketide chain. The condensation reaction is catalyzed by a ketosynthase (KS) that is usually present in all modules. In addition, every module contains an

acyl carrier protein (ACP) domain, to which intermediates are covalently attached and an acyltransferase (AT) domain that transfers short CoA-bound building blocks to an ACP domain. The release of the nascent acyl chain is most often catalyzed by a thioesterase (TE) domain by either an attack of an exogenous nucleophile leading to hydrolysis or transesterification or by an intramolecular nucleophile effecting macrolactonization or macrolactamization (Horsman et al. 2016). The structural diversity of PKS-derived MNPs mainly results from the action of additional domains: a ketoreductase (KR) domain reduces the β -keto group to a hydroxyl group, a dehydratase (DH) eliminates water to yield a double bond and an enoylreductase (ER) reduces the double bond to the saturated intermediates. In addition to these textbook PKSs, also known as *cis*-type I PKSs, there also exists another modular type I PKS, in which the AT domain is missing in each module. In these enzymes, the acyl building block is received by a free-standing or *trans*-AT domain (Helfrich and Piel 2016). So far only one to three domains with AT functionality were found to be encoded in the same gene cluster which are either encoded as single domains, as tandem-ATs or fused to an oxidoreductase domain which serves as a *trans*-ER (Bumpus et al. 2008). Hence, the 'same' AT is used in an iterative fashion to build the polyketide (Cheng et al. 2009). Because most *trans*-acting AT domains are specific for one building block (malonyl-CoA), the same building block is usually loaded on each PKS module (Cheng et al. 2003). In contrast to the simpler acyl transfer machinery, the module architecture of *trans*-AT PKSs is more diverse and complex than for *cis*-AT systems and can exhibit a large number of variations regarding domain types, domain combinations, and chemical outputs, many of which are poorly understood. Apart from these enzymatic features, another differentiating feature of *trans*-AT and *cis*-AT PKSs is the correlation of PKS gene sequences to the final product. While *cis*-AT PKSs follow the collinearity principle, where the growing polyketide chain follows the logic of the domain architecture of entire modules, KS domains in *trans*-AT PKSs share a phylogenetic correlation with their substrate specificities required for product elongation (Nguyen et al. 2008). Both correlations permit detailed predictions of polyketide structures from sequences of biosynthetic gene clusters.

The modular organization of NRPSs superficially resembles that of type I PKSs, but each module incorporates one amino acid into the peptide product instead. Each NRPS module comprises at least three domains: the adenylation (A) domain selects, activates and loads the substrate (proteinogenic or non-proteinogenic amino acid); the peptidyl-carrier (PCP) domain covalently attaches the substrate to the synthetase and a condensation (C) domain catalyzes peptide bond formation. As for type I PKSs, most NRPS contain a TE domain that is normally attached to the last module and is in this case responsible for the release of the peptide from the synthetase by either hydrolysis or macrolactonization (Finking and Marahiel 2004).

2 Cell Separation-Based Evidence for ‘Entotheonella’ as Natural Product Source in Sponges

The possibility that MNPs might originate from symbiotic microbes rather than from the sponge host itself would have major implications for drug development, since it could allow for the establishment of bacterial-based production systems. Several early attempts have been made to identify the origin of specific MNPs in sponge tissue using a variety of different methods. These methods were all based on tissue dissociation and subsequent separation of individual cell populations by, e.g., flow-cytometry using either auto-fluorescent properties or physical parameters of the cells (Bewley et al. 1996; Faulkner et al. 1994; Flowers et al. 1998; Garson et al. 1992; Gillor et al. 2000; Müller et al. 1986; Richelle-Maurer et al. 2001; Salomon et al. 2001; Salomon and Faulkner 2002; Turon et al. 2000). For example, cell density gradient centrifugation was used in a series of landmark papers by Bewley, Schmidt, Haygood, and Faulkner on a Palauan chemotype of the sponge *Theonella swinhoei* (Bewley et al. 1996; Schmidt et al. 2000). Here, cell populations were prepared that were enriched in unicellular heterotrophic bacteria, filamentous bacteria, cyanobacteria and sponge cells, respectively (Bewley et al. 1996). Extraction and natural product analysis of each fraction reveal highest concentrations of the antifungal glycopeptide theopalauamide in the filamentous fraction, whereas the cytotoxic polyketide swinholide A (Fig. 2) was mainly present in the heterotrophic unicellular fraction (Bewley et al. 1996). The as-yet uncultivated filamentous bacteria were assigned as δ -proteobacteria by phylogenetic analysis of 16S rRNA gene amplicons, visualized using catalyzed reporter deposition fluorescence in situ hybridization (CARD-FISH), and named ‘*Candidatus Entotheonella palauensis*’ (Schmidt et al. 2000). Schirmer et al. used the same cell separation method for the sponge *Discodermia dissoluta* (Schirmer et al. 2005) in attempts to identify the producer of the highly potent anti-cancer discodermolides (Gunasekera and Wright 2012). Although the genes responsible for discodermolides could not be identified, the authors identified a giant *cis*-AT PKS system and a partial *trans*-AT PKS and in

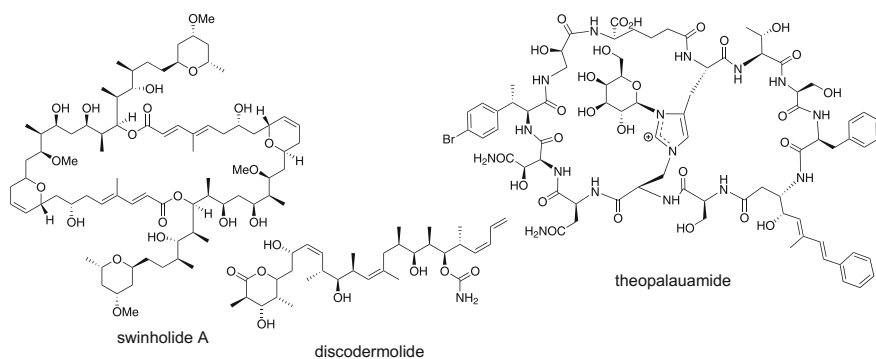


Fig. 2 Examples of NPs isolated from different symbionts of marine sponges

addition detected many NRPS and PKS genes by PCR in the library prepared from the enriched filamentous bacteria. Based on 16S rRNA sequencing, ‘*Candidatus Entotheonella*’ bacteria were the most abundant microorganisms within this fraction, makes them good candidates for the origin of the natural product genes (Schirmer et al. 2005).

3 Assignment of Natural Products in *Theonella swinhoei* to ‘*Entotheonella*’ by Metagenomic and Single-Bacterial Techniques

The lithistid sponge *Theonella swinhoei* is a source of exceptionally diverse natural products (Fig. 3) that occur in distinct chemotypes; with samples collected from different locations having largely distinct metabolic profiles. In addition to the Palauan chemotype mentioned in the last section, a prominent chemotype is *T. swinhoei* Y (Y corresponding to the yellow interior of the sponge), occurring at Hachijo Jima, Japan. This sponge has yielded more than 40 bioactive polyketides and modified peptides (Fusetani and Matsunaga 1993). For almost all of them, ‘*Entotheonella*’ bacteria have been identified as the bacterial source by methods based on metagenomics (i.e., study of all genomes present in a sample) or single-bacterial analysis (Wilson et al. 2014). These studies provided detailed insights into biosynthetic pathways, which often comprise unexpected, new biochemistry. These pathways and their identification are outlined in the following sections.

3.1 *Onnamides and Theopederins*

Onnamides and theopederins (Fig. 3) are part of large group of structurally related, highly cytotoxic polyketides that occur in remarkably diverse macroorganisms. Most members are known from marine sponges, including onnamide A from *T. swinhoei* (Matsunaga et al. 1992; Sakemi et al. 1988), mycalamide A from *Mycale hentscheli* (Perry et al. 1988) and psymberin (irciniastatin A) from *Psammocinia* aff. *bulbosa* (Cichewicz et al. 2004) and *Ircinia ramosa* (Pettit et al. 2004). Additional congeners are e.g. pederin found in rove beetles of the genera *Paederus* and *Paederidus* (Mosey and Floreancig 2012), diaphorin from the psyllid *Diaphorina citri* (Nakabachi et al. 2013) and nosperin from the lichen *Peltigera membranaceae* (Fig. 4; Kampa et al. 2013). Crystallization studies showed that mycalamide A binds to the 60S large ribosomal subunit at the E-site (Gurel et al. 2009). Since mycalamide A, onnamide A, and theopederin A were all shown to displace the ribosome binder 13-deoxytendanolide from the ribosome, it is likely that E-site-binding is a conserved feature for these compounds (Nishimura et al. 2005).

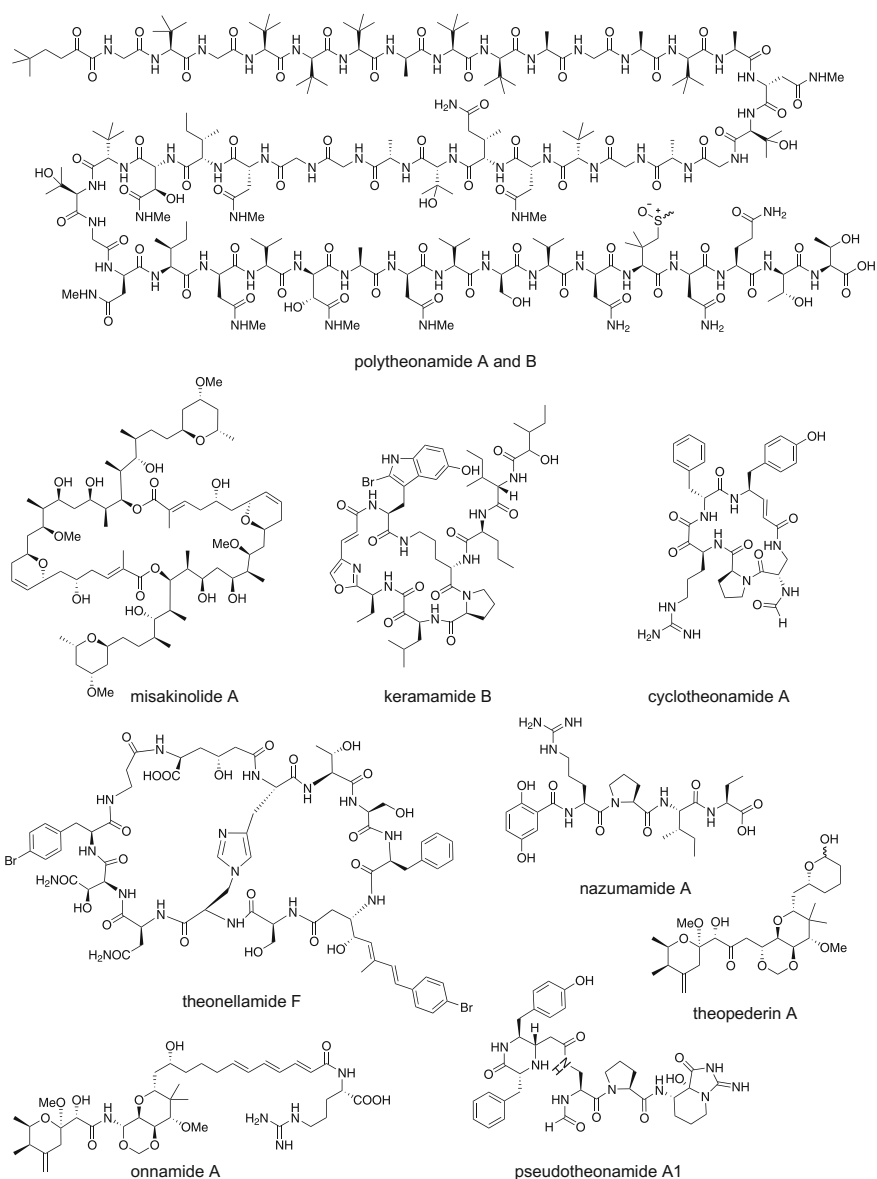


Fig. 3 Examples of the NPs isolated from different chemotypes of the sponge *Theonella swinhoei*

Identification of the onnamide biosynthetic genes in the complex sponge-microbial assemblage of *T. swinhoei* Y was possible by prior isolation of pederin genes in the much less complex metagenome of *Paederus fuscipes* beetles (Kellner 2002; Piel 2002; Piel et al. 2004a, b). In these insects, pederin is produced by a symbiotic *Pseudomonas* sp. bacterium through a *trans*-AT PKS, at the time of

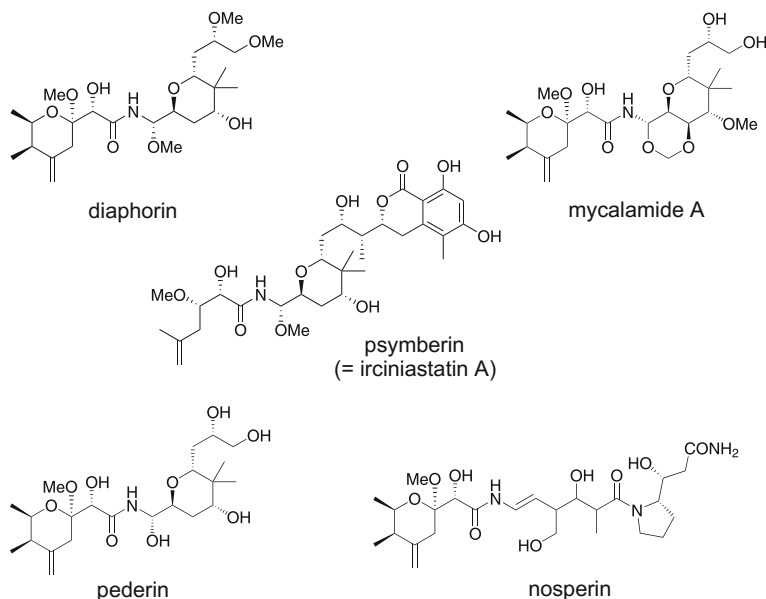


Fig. 4 Group of compounds structurally related to onnamides

discovery a highly unusual PKS system and the first functionally assigned member of this family. Since *trans*-AT PKSs were also assumed to generate the pederin-like onnamides, PCR amplicons of KS gene regions obtained from the metagenome of *T. swinhoei* Y were screened for their phylogenetic affiliation with *trans*-AT PKS sequences (Fisch et al. 2009; Piel et al. 2004a). This strategy revealed candidate amplicons for the onnamide PKS gene cluster, which was subsequently isolated from a metagenomic fosmid library constructed from total sponge DNA.

The onnamide gene cluster (Fig. 5) consists of three main ORFs, *onnBIJ*, encoding PKS proteins responsible for elongation of the polyketide with their domain architecture very similar to that of the pederin PKS enzymes. These similarities include tandem enoyl-CoA hydratases (ECHs) in OnnB which along with a 3-hydroxy-3-methylglutaryl-coenzyme A synthase-(HMGS-)-like enzyme, OnnA, work in conjunction to install an exomethylene group at the β -position, and a pyran synthase (PS) domain in OnnI that is responsible for the closure of the tetrahydropyran ring. The A domain present in the last module of OnnJ is predicted to incorporate an arginine into the polyketide backbone, after which the TE domain releases the chain. This released product needs to undergo hydroxylation and O-methylation to give the final onnamides.

The onnamide gene cluster exhibits features strongly resembling bacterial biosynthetic gene clusters, including the *Pseudomonas*-derived pederin cluster, which suggested a bacterial origin. In a multinational collaborative effort, the onnamide producer was identified in the highly diverse and abundant microbiome of *T. swinhoei* Y (Wilson et al. 2014). Using differential centrifugation, bacteria

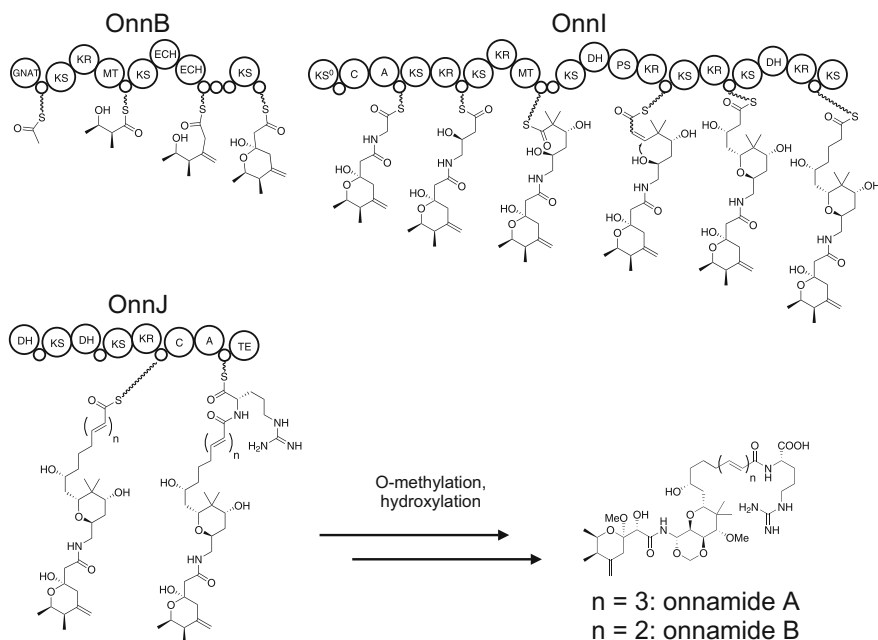


Fig. 5 Biosynthetic model proposed for onnamides on the basis of the isolated PKS gene cluster. Each *large circle* indicates a domain while the *small circle* indicates an acyl carrier protein (ACP) domain. GNAT: acetyl-loading AT of the GCN5-related *N*-acetyl transferase superfamily; MT: methyl transferase; C: condensation domain, KS⁰: non-elongating KS domain

from the sponge were enriched according to their cell densities. A highly enriched population of large filamentous bacteria similar to the ‘*E. palauensis*’ symbiont of the Palauan *T. swinhoei* chemotype described above was observed microscopically. The different bacterial fractions were sorted by fluorescence-assisted cell sorting (FACS), resulting in individual bacterial particles distributed in microtiter plates. Multiple displacement amplification (MDA) of single bacterial genomes was performed from each well, and PCR-based screening of the wells based on onnamide genes and universal regions of 16S rRNA genes indicated the filamentous ‘*Entotheonella*’ bacteria as the producers. Independent metagenomic sequencing of the filamentous fraction confirmed this result, revealing the presence of two distinct ‘*Entotheonella*’ phylotypes, named ‘*Candidatus Entotheonella factor*’ TSY1 and ‘*Candidatus Entotheonella gemini*’ TSY2. Both phylotypes possess similar, unusually large genome sizes of ca. 9 Mb. The onnamide gene cluster was assigned to ‘*E. factor*’, but more surprisingly ‘*E. factor*’ was found to contain many additional gene clusters that were attributed by bioinformatic methods and biochemical studies to almost all polyketide and peptide natural products that had previously been isolated from the sponge host, including polytheonamides (see below), cyclotheonamides, pseudotheonamides, keramamides, and nazumamides. In addition to these clusters, both ‘*E. factor*’ and ‘*E. gemini*’ contain many further PKS,

NRPS, and other natural product gene clusters for as-yet unknown compounds. These findings were unexpected as they set a precedent of uncultivated bacteria as a cornucopia of secondary metabolites on par with metabolically “talented” cultured strains used in drug discovery like filamentous actinomycetes, cyanobacteria, and myxobacteria. A thorough phylogenetic analysis using 38 concatenated, universally conserved single copy marker genes placed these ‘Entotheonella’ phylotypes in a new proposed candidate phylum named ‘Tectomicrobia’ (Wilson et al. 2014).

For the onnamide-type compound psymbirin from the sponge *Psammocinia* aff. *bulbosa*, the gene cluster was isolated from a metagenomic fosmid library using a similar strategy to that applied to onnamides (Fisch et al. 2009). As in the case of onnamide, the genes exhibit typical bacterial features, but the symbiont’s taxonomic identity is to date unknown.

3.2 Polytheonamides

Among the many natural products of *T. swinhoei* Y, the largest and most complex metabolites are the polytheonamides (Fig. 3), previously reported as 48-residue linear peptides exhibiting low-picomolar cytotoxicity towards mammalian cell lines (Hamada et al. 1994a, b). Reported in 1994, polytheonamides A-C belong to the most complex known specialized metabolites. Containing many non-proteinogenic amino acids accompanied with an alternating L- and D-configuration of its residues, the polytheonamides had initially been assumed as products of a nonribosomal peptide synthetase (NRPS). However, using a semi-nested PCR protocol with primers designed on a hypothetical ribosomal precursor peptide, Piel, Matsunaga, and coworkers were able to isolate a gene sequence corresponding to an unprocessed, proteinogenic polytheonamide precursor (Freeman et al. 2012). This information, which was obtained before identifying ‘Entotheonella’ in this sponge, was used to screen a fosmid library of 920,000 clones constructed from total metagenomic DNA of *T. swinhoei* Y to identify and isolate the whole polytheonamide biosynthetic gene cluster (Fig. 6). These results, together with functional experiments described below, confirmed that the polytheonamides, despite their numerous D-amino acids and unusual amino acid modifications, are not products of an NRPS pathway but ribosomally synthesized and posttranslationally modified peptides (RiPPs). In RiPP biosynthesis, a precursor peptide containing in most cases an N-terminal leader and a C-terminal core is synthesized by the ribosome from standard amino acids. The core, corresponding to the final natural product, is modified by maturation enzymes and undergoes proteolytic cleavage from the leader to generate the bioactive natural product.

The polytheonamides are by far the most heavily modified peptides known, requiring 48 posttranslational modifications (PTMs) and far surpassing thiocillin tailoring involving 13 modifications (Brown et al. 2009). Unlike previously characterized RiPPs, which involve short leader regions, the polytheonamide leader of the precursor PoyA is unusually large, bearing homology to the α -subunit of nitrile

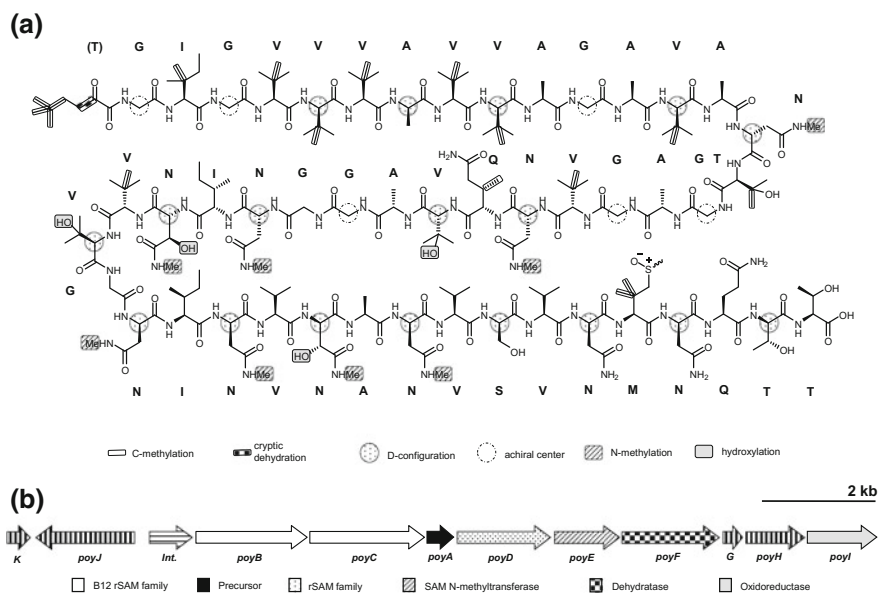


Fig. 6 Structure and biosynthetic gene cluster of polytheonamides. **a** Secondary structures of polytheonamide A and B are shown, differing in the configuration of the methionine sulfoxide. Modifications occurring post-translationally on the canonical proteinogenic amino acids are shown in the legend below. **b** Graphical representation of the isolated polytheonamide gene cluster. Highlighting corresponds to the modifications hypothesized to occur from the encoded ORFs. *Int.* (*horizontal lines*) is an integrase, *K*, *poyJ*, *poyG* and *poyH* (*bold vertical lines*) are thought to be involved in resistance, proteolytic maturation, or regulation

hydratases, but lacking the conserved metal-chelating residues necessary for catalysis. Thus, polytheonamides are the first characterized members of a natural product family, since named proteusins. Interestingly, this family had been previously proposed based on in silico analysis of bacterial genomes and shown to be widespread in prokaryotes (Haft et al. 2010), but except for polytheonamides, no natural product has been identified to date.

The isolated polytheonamide gene cluster has a typical bacterial architecture and contains only 12 putative open reading frames despite numerous posttranslational modifications. To generate polytheonamides, 17 C-methylations, eight N-methylations, four hydroxylations, and unique 18 L-amino acid to D-amino acid epimerizations were proposed to take place (Freeman et al. 2012). In particular, epimerization of multiple residues had not been reported before, suggesting unusual biochemistry. Surprisingly, only six enzyme candidates required for these modifications were identified. These are PoyB, PoyC and PoyD bearing homology to members of the radical S-adenosylmethionine (rSAM) superfamily, PoyE homologous to SAM-dependent methyltransferases, PoyI homologous to Fe(II)/ α -ketoglutarate oxidoreductases, and PoyF homologous to dehydratase domains of

LanM-type lantibiotic synthetases. Functions of polytheonamide genes were subsequently tested by heterologous expression in *E. coli*.

Initial efforts to express *poyA* proved to be unsuccessful; however, coexpression with the rSAM enzyme-encoding gene *poyD* resulted in substantial improvements in yields and solubility of PoyA. HPLC separation following acid hydrolysis of the peptide and Marfey's-type derivatization of the resulting individual amino acids revealed the presence of D-configured asparagine and valine residues within the PoyA core sequence, confirming that PoyD is responsible for most and perhaps all epimerizations (Freeman et al. 2012). Another study (Morinaka et al. 2014), using three cyanobacterial PoyD homologs, provided the first insights into the mechanism of this unprecedented activity. A transaminase knockout mutant of *E. coli* expressing precursor-epimerase pairs were fed with deuterated amino acids. Upon epimerization, each incorporated deuterated amino acid experienced a loss of a deuterium presumably at the α -position, suggesting that the hydrogens are not shuttled within the substrate peptide after initial radical formations. These studies also showed that epimerization is irreversible, indicating considerable biotechnological potential for the generation of peptides containing D-amino acids.

For polytheonamides, other coexpression experiments revealed that PoyE, a SAM-dependent methyltransferase homolog was responsible for the eight N-methylations of the various asparagines residues (Freeman et al. 2012). Another enzyme that was functionally verified was the LanM-like dehydratase, PoyF. Coexpression of the enzyme with *poyA* and *poyD* resulted in mass loss of 18 Da at a threonine in the *poyA* core that was previously believed to be directly upstream of the first core residue. This result suggested that the threonine is part of the core and converted into the unique *N*-acyl moiety of polytheonamides (Freeman et al. 2012). It is hypothesized that the dehydrated threonine residue undergoes a remarkable transformation involving net *tert*-butylation by four consecutive C-methylations, with proteolytic cleavage generating the α -keto function by spontaneous enamine hydrolysis. PoyB and PoyC, two putative C-methyltransferases are thought to be responsible for this and 13 other C-methylations of five different amino acid residues. The remaining PTMs are proposed to be carried out by the Fe(II)/ α -ketoglutarate-dependent hydroxylase PoyI, thought to be responsible for the four β -hydroxylations of two valines and two (N-methyl) asparagine residues.

With the sequencing studies mentioned in Sect. 3.1, the polytheonamide cluster was localized to the 'E. factor' genome, revealing this bacterium as a source of highly unusual metabolic processes.

3.3 *Misakinolide A*

The *T. swinhoei* chemotype WA occurring at Hachijo Jima, Japan, has a distinct natural product profile compared to the Y chemotype counterpart found at the same location and discussed in the previous sections. The two groups of bioactive compounds reported from this sponge are the actin inhibitory polyketide

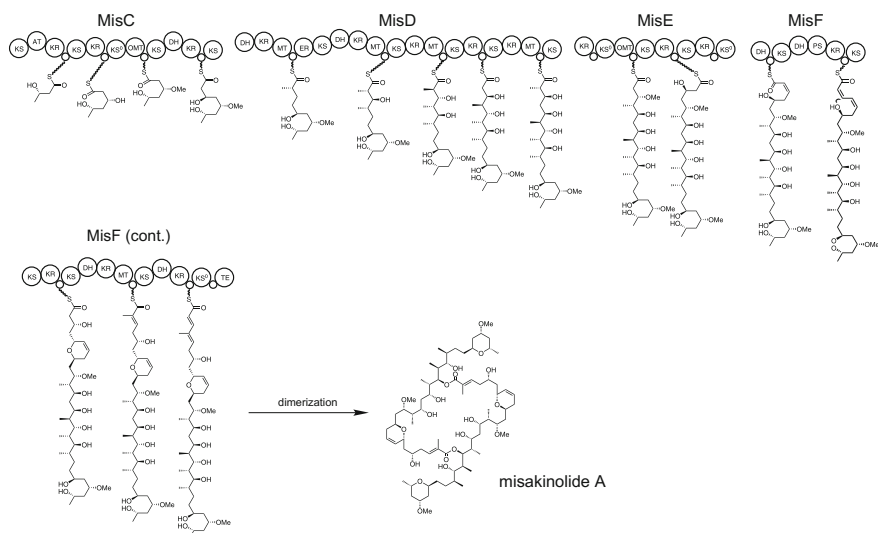


Fig. 7 Biosynthetic model proposed for misakinolide A on the basis of the isolated *mis* locus. OMT: O-methyl transferase

misakinolide A (Allingham et al. 2006; Sakai et al. 1986) and theonellamide-type cytotoxic modified peptides (Fig. 3; Matsunaga et al. 1989), thus more resembling the Palauan chemotype. From a sample of the sponge, an enriched fraction of filamentous bacteria bearing resemblance to ‘Entotheonella’ was prepared (Ueoka et al. 2015). After detecting *trans*-AT PKS-encoding genes using a nested PCR protocol with degenerate primers, an initial attempt to construct a fosmid library from this preparation failed due to DNA instability. Instead, a 350,000 clone library from total sponge DNA was constructed and screened iteratively resulting in the isolation of a 99 kb region containing a large *trans*-AT PKS cluster, termed *mis* cluster (Fig. 7).

The *mis* cluster consists of four large core PKS-encoding genes *misC*, *misD*, *misE*, and *misF* and the AT-encoding gene *misG*. Based on KS phylogeny and domain architecture, the cluster provided an almost perfect match for misakinolide with two exceptions. One is an additional module at the terminus of the PKS assembly line that does not correlate to a further extension in misakinolide, but present in the structurally similar swinholides from the Palauan chemotype discussed in Sect. 2. This architecture suggests that the module is a nonfunctional evolutionary relic derived from a swinholide-like PKS. Upon re-analysis of the sponge extracts by liquid-chromatography-high resolution mass spectrometry (LC-HRMS), only misakinolide A was detected. It is therefore likely that the last module is skipped during biosynthesis. The other exception is the presence of tetrahydropyran rings in the tail regions of misakinolide which has no counterparts in the *mis* gene cluster, suggesting a new ring closure mechanism. Apart from this, misakinolide also contains a dihydropyran ring in each monomer, the suspected

product of the PS domain of MisF. To functionally test this domain, the *mis* PS domain was cloned and expressed in *E. coli* (Ueoka et al. 2015). The purified enzyme was subsequently incubated with the surrogate open-chain *N*-acetylcysteamine (SNAC) precursors, resulting in the formation of cyclized products and verifying the function of the PS. A phylogenetic analysis of KR domains which allows for prediction of OH-bearing stereocentres and double bond geometries was performed and found to be in agreement with the stereochemistry of misakinolide, further supporting the identity of the *mis* cluster.

Surrounding the *mis* locus, extended regions with genes exhibiting >80% nucleotide identity with homologs from ‘E. factor’ and ‘E. gemina’ were also identified. The cluster was unequivocally assigned to ‘Entotheonella’ by amplifying and sequencing DNA from a single isolated bacterial filament, revealing the *mis* cluster on its genome. The genome also contained a 16s rRNA gene with 98.3% identity to the homolog of ‘E. factor’. This result and average nucleotide identity (ANI) calculation supported the existence of a new candidate species named ‘Entotheonella sarta’. Additionally, the location of misakinolide and ‘E. sarta’ filaments within the sponge tissue was also investigated (Ueoka et al. 2015). Using matrix-assisted laser desorption-ionization imaging mass spectrometry (MALDI-IMS) on thin sections of the misakinolide-containing *T. swinhoei* WA sponge, it was found that the distribution of the polyketide is localized to the tissue zones lining pores, chamber and the exterior. In addition, catalyzed reporter deposition fluorescence in situ hybridization (CARD-FISH) using ‘Entotheonella’ specific probes showed a distribution of the bacteria at the same locations as that of the compound, further supporting ‘E. sarta’ as the source of misakinolides.

3.4 Calyculins

The polyketide calyculin A was first isolated in 1986 from the sponge *Discodermia calyx* as major cytotoxic compound (0.15% wet weight, IC50 in picomolar range) and subsequently found to be a specific inhibitor of protein phosphatases 1 and 2A (Ishihara et al. 1989; Kita et al. 2002; Lindvall et al. 1997; Wakimoto et al. 2002). Its unique structure contains a terminal nitrile, a tetraene, a 5,6-spiroacetal system and phosphate, oxazole, and dimethylamino moieties. The compound has drawn a lot of interest amongst synthetic chemists, leading to six total synthetic routes (Fagerholm et al. 2010). In a retrobiosynthetic approach similar to one used to isolate the *mis* locus, a 250,000 clone metagenomic library of *D. kiiensis* was screened for the presence of gene sequences corresponding to KS domains of *trans*-AT PKSs, A domains and HMGS-like enzymes proposed to be involved in β -branching (Wakimoto et al. 2014). These efforts resulted in the isolation of a very large gene cluster, termed *cal* cluster (Fig. 8), measuring over 150 kb. The cluster contains 29 KS and 5 A domains making it one of the largest hybrid PKS/NRPS cluster known to date.

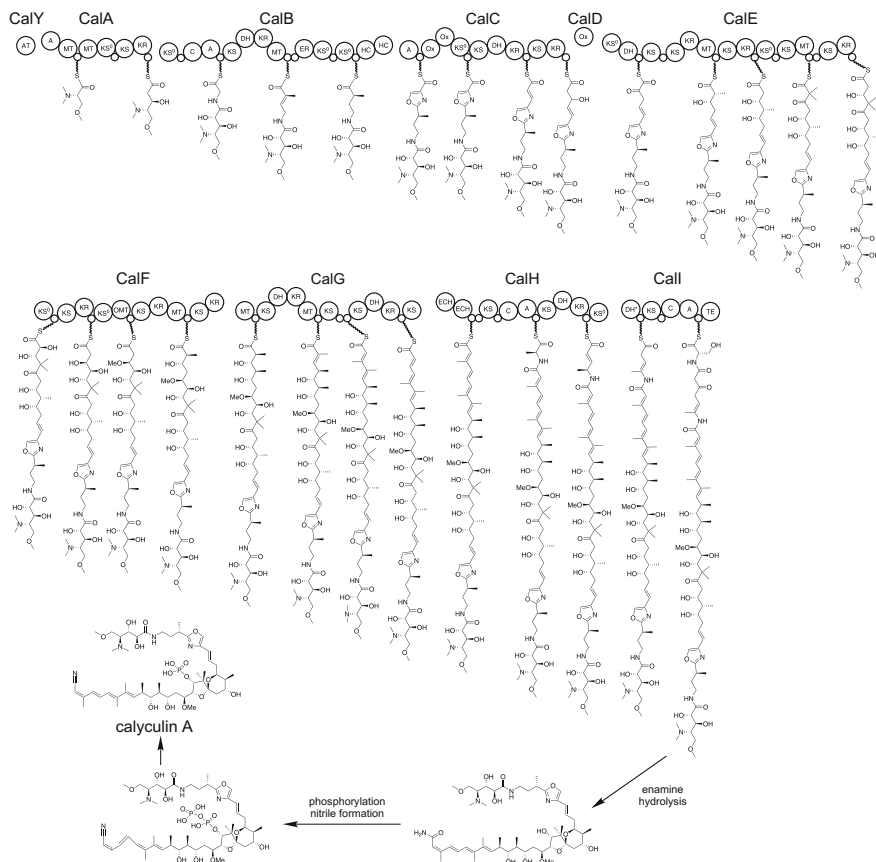


Fig. 8 Model for the biosynthesis of calyculin A on the basis of the isolated *cal* locus. OX: oxidation domain

The starter A domain in CalA is predicted to incorporate serine as the first building block which is proposed to undergo permethylation by the two methyltransferases (MTs) to generate the unusual trimethylseryl starter. The following PKS and NRPS modules are within the framework for the biosynthesis of calyculin A. The A domain in CalB is predicted to be specific for glycine, but a possible inherent flexibility for alanine could explain the occurrence of this residue in calyculin C. Other features include two ECHs in CalH which in conjunction with an HMGS could give rise to a β -branch. An unusual calyculin moiety adjacent to the oxazolylvinyl unit, which seemingly arises from elongation by a C1 rather than a C2 unit, is suggested to involve oxidative cleavage by a flavin-dependent monooxygenase (FMO), CalD. This enzyme is proposed to catalyze α -hydroxylation of a C2-elongated intermediate resulting in a labile α,β -diol (Fig. 9). This intermediate would then be dehydrated by a succeeding DH domain on CalE to yield an enol that might tautomerize to the α -ketoester subunit. Chain

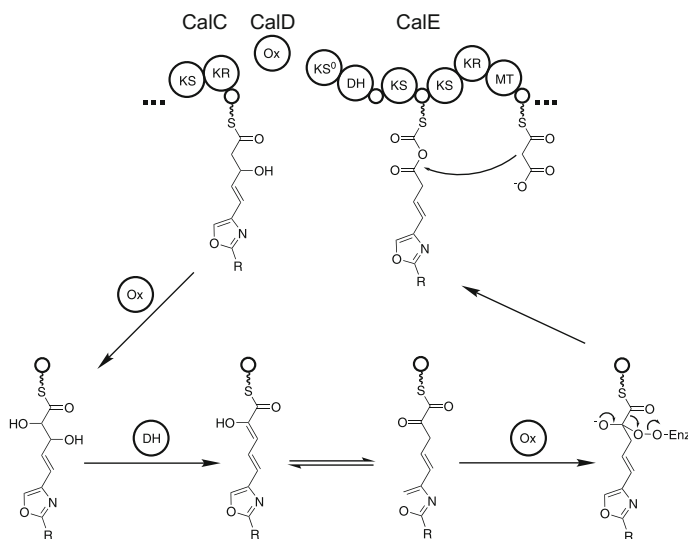


Fig. 9 Proposed mechanism for chain shortening during calyculin biosynthesis

shortening would then occur by conversion of the α -ketoester to an anhydride by Baeyer–Villiger-type oxidation, followed by a Claisen condensation on the ester carbonyl.

Another noncanonical feature is the presence of five seemingly superfluous modules present in CalH and CalI. It is proposed that these modules produce a labile intermediate during the final steps of the biosynthesis before calyculin is released. Incorporation of alanine by the A domain would be followed by formation of a double bond by the following PKS module. Shift of this double bond to the β,γ -position by the following DH domain would yield an enamide intermediate. The enamide functionality, being susceptible to hydrolysis, would be converted to an amide terminus of the calyculin A precursor. This primary amide is then proposed to be converted into the terminal nitrile following an iminophosphate intermediate. This hypothesis is supported by the presence of three genes encoding phosphotransferases (*calM*, *calP*, and *calQ*) in the gene cluster. In vitro functional analysis with the heterologously expressed *calQ* led to the identification of an unexpected new biosynthetic product, phosphocalyculin A, which harbors a pyrophosphate instead of the monophosphate present in calyculin A. On reexamining the sponge extracts, it was found that the highly labile phosphocalyculin A is the actual end product of the pathway and rapidly decomposes to calyculin A (Wakimoto et al. 2014). The cytotoxicity of phosphocalyculin A is 1000 fold less than that of calyculin A. Assuming that phosphocalyculin A enables the sponge to avoid self-toxicity, wounding experiments revealed that phosphocalyculin rapidly undergoes dephosphorylation by an as-yet unidentified phosphatase to yield calyculin A in a process known as activated chemical defense.

A sponge homogenate analyzed by light microscopy, revealed the presence of filamentous bacteria similar to 'Entotheonella' (Wakimoto et al. 2014). Through CARD-FISH experiments targeting genes of the *cal* cluster, the filamentous bacterium was identified as the source of the *cal* locus. Additionally, single filaments were isolated, and PCRs specific for the *cal* cluster and for 16S rRNA confirmed this 'Entotheonella' bacterium as the producer of calyculins.

4 Opportunities for Biotechnological Production Systems for Sponge-Derived Natural Products

As mentioned above, obtaining sufficient quantities of a bioactive sponge compound from the natural resources for clinical testing and ultimate production is generally challenging to impossible. For promising candidates, synthetic routes for the often structurally complex substances involve many steps. Furthermore, even if the bacterial source of the sponge compounds is identified, the symbiotic producers often tend to be difficult to cultivate. It is therefore imperative to find/develop alternative strategies that would allow us to produce these active natural products in reasonable amounts to carry out functional studies and clinical trials. These are outlined in the following sections.

Heterologous expression of gene clusters responsible for production of desired natural products is an attractive method to achieve production. To date, only a few bacterial host strains (*E. coli*, streptomycetes, myxobacteria, pseudomonads and bacilli) were used for heterologous expression of multigene bacterial natural product gene clusters. The organisms are fast growing, genetically amenable and possess cellular machinery required for protein production. *E. coli* has previously been used to produce the cytotoxic patellamides (Fig. 10a; Donia et al. 2006), a RiPP produced by cyanobacterial symbionts of the marine tunicate *Lissoclinum patella* (Schmidt et al. 2005), yet other successful attempts at expressing marine invertebrate-derived natural products have not been reported. This is due to the many challenges that differ from case to case. These include the need to assemble large gene clusters from multiple genomic regions in case of complex polyketides and nonribosomal peptides, promoters and regulators are not recognized by the host, difference of codon usage, and the inability to fold or activate enzymes by the host. For compounds from 'Entotheonella', the distant taxonomic relationship of the producers to any available culturable host (no member of the candidate phylum 'Tectomicrobia' has to date been cultivated), represents a particular challenge. On the other hand, the fact that 'Entotheonella' is the source of a wide range of natural products from different sponges represents significant opportunities, since expression systems tailored for genes from these bacteria might be suited to produce many different compounds. Similarly broad potential could lie in the development of cultivation methods for 'Entotheonella' or other prolific producers in sponges. The available genomes of sequenced 'Entotheonella' variants are unusually large

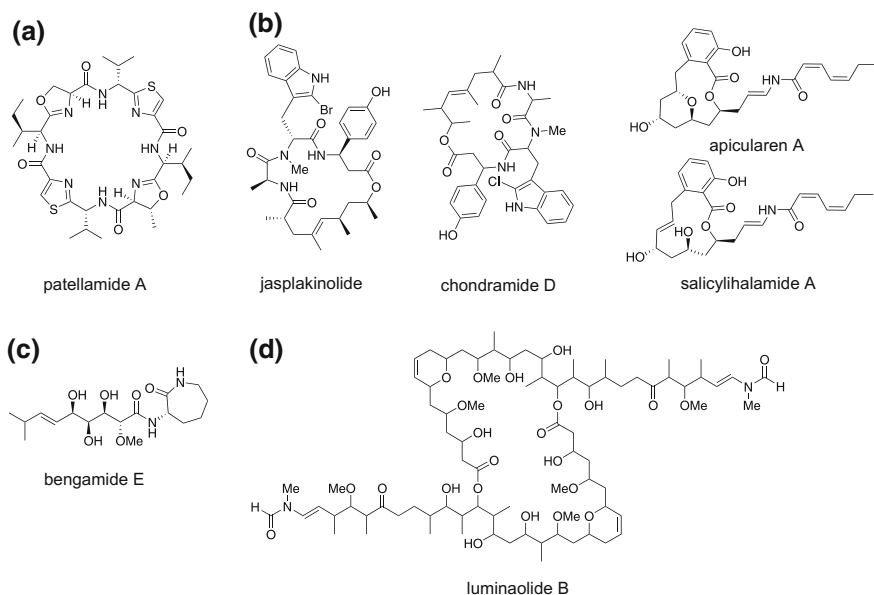


Fig. 10 **a** Structure of patellamide A. **b** Comparison of structurally similar sponge and bacterial compounds. **c** Structure of bengamide E. **d** Structure of luminaolide B

(comparable to, e.g., those of streptomycetes) and do not appear to lack critical genes needed for independent growth. If such cultivation systems can be established, they could provide access to a large diversity of sponge natural products.

Another option for the bacterial production of sponge compounds is to identify structurally identical or similar compounds in free-living, cultivatable bacteria. An example of a “sponge-like” compound found in bacterial cultures (Fig. 10b) is jasplakinolide (Crews et al. 1986), also named jaspamide (Zabriskie et al. 1986), from the sponge *Jaspis splendens* (Waldmann et al. 2008), which is related to chondramide D from the myxobacterium *Chondromyces crocatus* (Kunze et al. 1995). Likewise, the vacuolar ATPase inhibitor salicylihalamide A (Lebreton et al. 2008) from a *Haliclona* sponge (Erickson et al. 1997) is closely similar to apicularen A from the myxobacterium *Chondromyces robustus* (Kunze et al. 1998). A more recent example is the finding that the culturable strain *Myxobacterium virescens* DSM 15898 FD produced the bengamide-type polyketide-peptides (Fig. 10c; Johnson et al. 2012), which were first isolated from the marine sponge *Jaspis* cf. *coraciae* (Quinoa et al. 1986). The bengamides exhibit nanomolar potency in NCI-60 human tumor cell lines screen, which prompted the development of an efficient synthetic route (Xu et al. 2003) to yield LAF389 (Kinder et al. 2001; Thale et al. 2001), leading to phase I clinical trials before further development was halted due to cardiovascular side effects (Dumez et al. 2007).

While these findings of free-living producers were based on serendipity, knowledge on the biosynthetic gene cluster of a symbiont natural product can be

used to detect homologous clusters in other bacteria to identify producers. An example of this strategy is use of information on the onnamide- and pederin-type gene clusters for the discovery of the related compound nosperin (Kampa et al. 2013). In this study, an onnamide-type PKS cluster was found in the metagenome of the lichen *P. membranacea*. After identifying the producer *Nostoc* sp., a cyanobacterial symbiont of the lichen and cultivation of this bacterium, the cytotoxic nosperin was isolated from its cultures. In a similar manner, after the discovery of the misakinolide gene cluster, an architecturally related PKS cluster was detected in the free-living cyanobacterium *Planktothrix paucivesiculata* PCC 9631 (Ueoka et al. 2015). Structural predictions based on KS phylogeny suggested that the cluster is responsible for the production of the misakinolide-like compound luminaolide, a compound previously isolated from a coralline macroalga (Kitamura et al. 2009). This prediction resulted in isolation of a new luminaolide congener, luminaolide B (Fig. 10d). Even though bacterial compounds bearing structural similarity to sponge-derived natural products are found, it is noteworthy that these sponge substances are not more widespread in free-living bacteria, perhaps suggesting ecological functions that are particularly beneficial in sponge-bacterial interactions. However, as more bacterial genomes from diverse sources are becoming sequenced, it is expected that incidences of “sponge-type” gene clusters among culturable prokaryotes will increase. Through genome mining and structure prediction analysis, promising candidates could be cherry picked from large pools to find more sponge-derived NPs.

References

- Aicher TD, Buszek KR, Fang FG, Forsyth CJ, Jung SH, Kishi Y, Matelich MC, Scola PM, Spero DM, Yoon SK (1992) Total synthesis of halichondrin B and norhalichondrin B. *J Am Chem Soc* 114(8):3162–3164. doi:[10.1021/ja00034a086](https://doi.org/10.1021/ja00034a086)
- Allingham JS, Klenchin VA, Rayment I (2006) Actin-targeting natural products: structures, properties and mechanisms of action. *Cell Mol Life Sci* 63(18):2119–2134. doi:[10.1007/s00018-006-6157-9](https://doi.org/10.1007/s00018-006-6157-9)
- Bell JJ (2008) The functional roles of marine sponges. *Estuar Coast Shelf S* 79(3):341–353. doi:[10.1016/j.ecss.2008.05.002](https://doi.org/10.1016/j.ecss.2008.05.002)
- Bell JJ, Smith D (2004) Ecology of sponge assemblages (Porifera) in the Wakatobi region, south-east Sulawesi, Indonesia: richness and abundance. *J Mar Biol Assoc UK* 84(3):581–591. doi:[10.1017/S0025315404009580h](https://doi.org/10.1017/S0025315404009580h)
- Bewley CA, Faulkner DJ (1998) Lithistid sponges: star performers or hosts to the stars. *Angew Chem Int Ed* 37(16):2163–2178
- Bewley CA, Holland ND, Faulkner DJ (1996) Two classes of metabolites from *Theonella swinhoei* are localized in distinct populations of bacterial symbionts. *Experientia* 52(7):716–722. doi:[10.1007/Bf01925581](https://doi.org/10.1007/Bf01925581)
- Blunt JW, Copp BR, Keyzers RA, Munro MH, Prinsep MR (2015) Marine natural products. *Nat Prod Rep* 32(2):116–211. doi:[10.1039/c4np00144c](https://doi.org/10.1039/c4np00144c)
- Brown LCW, Acker MG, Clardy J, Walsh CT, Fischbach MA (2009) Thirteen posttranslational modifications convert a 14-residue peptide into the antibiotic thiocillin. *Proc Natl Acad Sci U S A* 106(8):2549–2553. doi:[10.1073/pnas.0900008106](https://doi.org/10.1073/pnas.0900008106)

- Bumpus SB, Magarvey NA, Kelleher NL, Walsh CT, Calderone CT (2008) Polyunsaturated fatty-acid-like trans-enoyl reductases utilized in polyketide biosynthesis. *J Am Chem Soc* 130 (35):11614–11616. doi:[10.1021/ja8040042](https://doi.org/10.1021/ja8040042)
- Cheng YQ, Coughlin JM, Lim SK, Shen B (2009) Type I polyketide synthases that require discrete acyltransferases. *Methods Enzymol* 459:165–186. doi:[10.1016/S0076-6879\(09\)04608-4](https://doi.org/10.1016/S0076-6879(09)04608-4)
- Cheng YQ, Tang GL, Shen B (2003) Type I polyketide synthase requiring a discrete acyltransferase for polyketide biosynthesis. *Proc Natl Acad Sci U S A* 100(6):3149–3154. doi:[10.1073/pnas.0537286100](https://doi.org/10.1073/pnas.0537286100)
- Cichewicz RH, Valeriote FA, Crews P (2004) Psymberin, a potent sponge-derived cytotoxin from *Psammocinia* distantly related to the pederin family. *Org Lett* 6(12):1951–1954. doi:[10.1021/ol049503q](https://doi.org/10.1021/ol049503q)
- Crews P, Manes LV, Boehler M (1986) Jaspilkinolide, a cyclodepsipeptide from the marine sponge *Jaspis* sp. *Tetrahedron Lett* 27(25):2797–2800. doi:[10.1016/S0040-4039\(00\)84645-6](https://doi.org/10.1016/S0040-4039(00)84645-6)
- Dayton PK (1989) Interdecadal variation in an antarctic sponge and its predators from oceanographic climate shifts. *Science* 245(4925):1484–1486. doi:[10.1126/science.245.4925.1484](https://doi.org/10.1126/science.245.4925.1484)
- Diaz MC, Ward BB (1997) Sponge-mediated nitrification in tropical benthic communities. *Mar Ecol Prog Ser* 156:97–107. doi:[10.3354/meps156097](https://doi.org/10.3354/meps156097)
- Donia MS, Hathaway BJ, Sudek S, Haygood MG, Rosovitz MJ, Ravel J, Schmidt EW (2006) Natural combinatorial peptide libraries in cyanobacterial symbionts of marine ascidians. *Nat Chem Biol* 2(12):729–735. doi:[10.1038/nchembio829](https://doi.org/10.1038/nchembio829)
- Dumez H, Gall H, Capdeville R, Dutreix C, van Oosterom AT, Giaccone G (2007) A phase I and pharmacokinetic study of LAF389 administered to patients with advanced cancer. *Anticancer Drugs* 18(2):219–225. doi:[10.1097/CAD.0b013e328010ef5b](https://doi.org/10.1097/CAD.0b013e328010ef5b)
- Erickson KL, Beutler JA, Cardellina II, Boyd MR (1997) Salicylilalamides A and B, novel cytotoxic macrolides from the marine sponge *Haliclona* sp. *J Org Chem* 62(23):8188–8192
- Fagerholm AE, Habrant D, Koskinen AM (2010) Calyculins and related marine natural products as serine-threonine protein phosphatase PP1 and PP2A inhibitors and total syntheses of calyculin A, B, and C. *Mar Drugs* 8(1):122–172. doi:[10.3390/md80100122](https://doi.org/10.3390/md80100122)
- Faulkner J, Unson MD, Bewley CA (1994) The chemistry of some sponges and their symbionts. *Pure Appl Chem* 66(10–11):1983–1990
- Finking R, Marahiel MA (2004) Biosynthesis of nonribosomal peptides. *Annu Rev Microbiol* 58:453–488. doi:[10.1146/annurev.micro.58.030603.123615](https://doi.org/10.1146/annurev.micro.58.030603.123615)
- Fisch KM, Gurgui C, Heycke N, van der Sar SA, Anderson SA, Webb VL, Taudien S, Platzer M, Rubio BK, Robinson SJ, Crews P, Piel J (2009) Polyketide assembly lines of uncultivated sponge symbionts from structure-based gene targeting. *Nat Chem Biol* 5(7):494–501. doi:[10.1038/nchembio.176](https://doi.org/10.1038/nchembio.176)
- Flowers AE, Garson MJ, Webb RI, Dumdei EJ, Charan RD (1998) Cellular origin of chlorinated diketopiperazines in the dictyoceratid sponge *Dysidea herbacea* (Keller). *Cell Tissue Res* 292 (3):597–607. doi:[10.1007/s004410051089](https://doi.org/10.1007/s004410051089)
- Freeman MF, Gurgui C, Helf MJ, Morinaka BI, Uria AR, Oldham NJ, Sahl HG, Matsunaga S, Piel J (2012) Metagenome mining reveals polytheonamides as posttranslationally modified ribosomal peptides. *Science* 338(6105):387–390. doi:[10.1126/science.1226121](https://doi.org/10.1126/science.1226121)
- Fusetani N, Matsunaga S (1993) Bioactive sponge peptides. *Chem Rev* 93(5):1793–1806. doi:[10.1021/cr00021a007](https://doi.org/10.1021/cr00021a007)
- Garson MJ, Thompson JE, Larsen RM, Battershill CN, Murphy PT, Bergquist PR (1992) Terpenes in sponge cell-membranes—cell-separation and membrane fractionation studies with the Tropical marine sponge *Amphimedon* sp. *Lipids* 27(5):378–388. doi:[10.1007/Bf02536153](https://doi.org/10.1007/Bf02536153)
- Gillor O, Carmeli S, Rahamim Y, Fishelson Z, Ilan M (2000) Immunolocalization of the toxin latrunculin B within the Red Sea sponge *Negombata magnifica* (Demospongiae, Latrunculiidae). *Mar Biotechnol* 2(3):213–223
- Gunasekera SP, Wright AE (2012) Chemistry and biology of the discodermolides, potent mitotic spindle poisons. *Anticancer Agents from Natural Products*, 2nd edn, pp 241–262

- Gurel G, Blaha G, Steitz TA, Moore PB (2009) Structures of Triacetyloleandomycin and methylamide A bind to the large ribosomal subunit of *Haloarcula marismortui*. *Antimicrob Agents Chemother* 53(12):5010–5014. doi:10.1128/Aac.00817-09
- Haft DH, Basu MK, Mitchell DA (2010) Expansion of ribosomally produced natural products: a nitrile hydratase-and Nif11-related precursor family. *BMC Biol* 8. doi:10.1186/1741-7007-8-70
- Hamada T, Sugawara T, Matsunaga S, Fusetani N (1994a) Polytheonamides, unprecedented highly cytotoxic polypeptides from the marine sponge *Theonella swinhoei*: 2. Structure elucidation. *Tetrahedron Lett* 35(4):609–612. doi:10.1016/S0040-4039(00)75851-5
- Hamada T, Sugawara T, Matsunaga S, Fusetani N (1994b) Polytheonamides, unprecedented highly cytotoxic polypeptides, from the marine sponge *Theonella swinhoei*: 1. Isolation and component amino acids. *Tetrahedron Lett* 35(5):719–720. doi:10.1016/S0040-4039(00)75799-6
- Harrington C, Del Casale A, Kennedy J, Neve H, Picton BE, Mooij MJ, O’Gara F, Kulakov LA, Larkin MJ, Dobson AD (2012) Evidence of bacteriophage-mediated horizontal transfer of bacterial 16S rRNA genes in the viral metagenome of the marine sponge *Hymeniacidon perlevis*. *Microbiology* 158(Pt 11):2789–2795. doi:10.1099/mic.0.057943-0
- Helfrich EJ, Piel J (2016) Biosynthesis of polyketides by *trans*-AT polyketide synthases. *Nat Prod Rep* 33(2):231–316. doi:10.1039/c5np00125k
- Hentschel U, Piel J, Degnan SM, Taylor MW (2012) Genomic insights into the marine sponge microbiome. *Nat Rev Microbiol* 10(9):641–U675. doi:10.1038/nrmicro2839
- Horsman ME, Hari TP, Boddy CN (2016) Polyketide synthase and non-ribosomal peptide synthetase thioesterase selectivity: logic gate or a victim of fate? *Nat Prod Rep* 33(2):183–202. doi:10.1039/c4np00148f
- Huyck TK, Gradishar W, Manuguid F, Kirkpatrick P (2011) Eribulin mesylate. *Nat Rev Drug Discov* 10(3):173–174. doi:10.1038/nrd3389
- Imhoff JF, Stohr R (2003) Sponge-associated bacteria: general overview and special aspects of bacteria associated with *Halichondria panicea*. *Prog Mol Subcell Biol* 37:35–57
- Ishihara H, Martin BL, Brautigam DL, Karaki H, Ozaki H, Kato Y, Fusetani N, Watabe S, Hashimoto K, Uemura D et al (1989) Calyculin A and okadaic acid: inhibitors of protein phosphatase activity. *Biochem Biophys Res Commun* 159(3):871–877
- Johnson TA, Sohn J, Vaske YM, White KN, Cohen TL, Vervoort HC, Tenney K, Valeriote FA, Bjeldanes LF, Crews P (2012) Myxobacteria versus sponge-derived alkaloids: the bengamide family identified as potent immune modulating agents by scrutiny of LC-MS/ELSD libraries. *Bioorg Med Chem* 20(14):4348–4355. doi:10.1016/j.bmc.2012.05.043
- Kampa A, Gagunashvili AN, Gulder TAM, Morinaka BI, Daolio C, Godejohann M, Miao VPW, Piel J, Andresson OS (2013) Metagenomic natural product discovery in lichen provides evidence for a family of biosynthetic pathways in diverse symbioses. *Proc Natl Acad Sci U S A* 110(33):E3129–E3137. doi:10.1073/pnas.1305867110
- Kellner RLL (2002) Molecular identification of an endosymbiotic bacterium associated with pederin biosynthesis in *Paederus sabaeus* (Coleoptera:Staphylinidae). *Insect Biochem Mol* 32(4):389–395. doi:10.1016/S0965-1748(01)00115-1
- Kinder FR Jr, Versace RW, Bair KW, Bontempo JM, Cesarz D, Chen S, Crews P, Czuchta AM, Jagoe CT, Mou Y, Nemez R, Phillips PE, Tran LD, Wang RM, Weltchek S, Zabłudoff S (2001) Synthesis and antitumor activity of ester-modified analogues of bengamide B. *J Med Chem* 44(22):3692–3699
- Kita A, Matsunaga S, Takai A, Kataiwa H, Wakimoto T, Fusetani N, Isobe M, Miki K (2002) Crystal structure of the complex between calyculin A and the catalytic subunit of protein phosphatase 1. *Structure* 10(5):715–724
- Kitamura M, Schupp PJ, Nakano Y, Uemura D (2009) Luminaolide, a novel metamorphosis-enhancing macrodiolide for scleractinian coral larvae from crustose coralline algae. *Tetrahedron Lett* 50(47):6606
- Kunze B, Jansen R, Sasse F, Hofle G, Reichenbach H (1995) Chondramides A approximately D, new antifungal and cytostatic depsipeptides from *Chondromyces crocatus* (myxobacteria). Production, physico-chemical and biological properties. *J Antibiot (Tokyo)* 48(11):1262–1266

- Kunze B, Jansen R, Sasse F, Hofle G, Reichenbach H (1998) Apicularens A and B, new cytostatic macrolides from *Chondromyces* species (myxobacteria): production, physico-chemical and biological properties. *J Antibiot (Tokyo)* 51(12):1075–1080
- Lebreton S, Jaunbergs J, Roth MG, Ferguson DA, De Brabander JK (2008) Evaluating the potential of vacuolar ATPase inhibitors as anticancer agents and multigram synthesis of the potent salicylhalamide analog saliphenylhalamide. *Bioorg Med Chem Lett* 18(22):5879–5883. doi:10.1016/j.bmcl.2008.07.003
- Leys SP, Hill A (2012) The physiology and molecular biology of sponge tissues. *Adv Mar Biol* 62:1–56. doi:10.1016/B978-0-12-394283-8.00001-1
- Lindvall MK, Pihko PM, Koskinen AM (1997) The binding mode of calyculin A to protein phosphatase-1. A novel spiroketal vector model. *J Biol Chem* 272(37):23312–23316
- Lohr JE, Chen F, Hill RT (2005) Genomic analysis of bacteriophage PhiJL001: insights into its interaction with a sponge-associated alpha-proteobacterium. *Appl Environ Microbiol* 71(3):1598–1609. doi:10.1128/AEM.71.3.1598-1609.2005
- Love GD, Grosjean E, Stalvies C, Fike DA, Grotzinger JP, Bradley AS, Kelly AE, Bhatia M, Meredith W, Snape CE, Bowring SA, Condon DJ, Summons RE (2009) Fossil steroids record the appearance of Demospongiae during the Cryogenian period. *Nature* 457(7230):718–721. doi:10.1038/nature07673
- Maloo AC, Rose CV, Beach R, Samuels BM, Calmet CC, Erwin DH, Poirier GR, Yao N, Simons FJ (2010) Possible animal-body fossils in pre-Marinoan limestones from South Australia. *Nat Geosci* 3(9):653–659. doi:10.1038/Ngeo934
- Matsunaga S, Fusetani N, Hashimoto K, Walchli M (1989) Bioactive Marine Metabolites. 26. Theonellamide-F - a novel antifungal bicyclic peptide from a marine sponge *Theonella* sp. *J Am Chem Soc* 111(7):2582–2588. doi:10.1021/ja00189a035
- Matsunaga S, Fusetani N, Nakao Y (1992) 8 new cytotoxic metabolites closely related to onnamide A from 2 marine sponges of the genus *Theonella*. *Tetrahedron* 48(39):8369–8376. doi:10.1016/S0040-4020(01)86585-6
- Mayer AM, Glaser KB, Cuevas C, Jacobs RS, Kem W, Little RD, McIntosh JM, Newman DJ, Potts BC, Shuster DE (2010) The odyssey of marine pharmaceuticals: a current pipeline perspective. *Trends Pharmacol Sci* 31(6):255–265. doi:10.1016/j.tips.2010.02.005
- Mehbub MF, Lei J, Franco C, Zhang W (2014) Marine sponge derived natural products between 2001 and 2010: trends and opportunities for discovery of bioactives. *Mar Drugs* 12(8):4539–4577. doi:10.3390/md12084539
- Mendola D (2000) Aquacultural production of bryostatin 1 and ecteinascidin 743. In: Fusetani N (ed) *Drugs from the sea*. Karger, Basel, pp 120–133. doi:10.1159/000062482
- Mendola D (2003) Aquaculture of three phyla of marine invertebrates to yield bioactive metabolites: process developments and economics. *Biomol Eng* 20(4–6):441–458
- Moore BS (1999) Biosynthesis of marine natural products: microorganisms and macroalgae. *Nat Prod Rep* 16(6):653–674
- Morinaka BI, Vagstad AL, Helf MJ, Gugger M, Kegler C, Freeman MF, Bode HB, Piel J (2014) Radical S-adenosyl methionine epimerases: regioselective introduction of diverse D-amino acid patterns into peptide natural products. *Angew Chem Int Ed* 53(32):8503–8507. doi:10.1002/anie.201400478
- Mosey RA, Floreancig PE (2012) Isolation, biological activity, synthesis, and medicinal chemistry of the pederin/mycalamide family of natural products. *Nat Prod Rep* 29(9):980–995. doi:10.1039/c2np20052j
- Müller WEG, Diehlsefert B, Sobel C, Bechtold A, Kljajic Z, Dorn A (1986) Sponge secondary metabolites—biochemical and ultrastructural-localization of the antimetabolic agent Avarol in *Dysidea avara*. *J Histochem Cytochem* 34(12):1687–1690
- Munro MH, Blunt JW, Dumdei EJ, Hickford SJ, Lill RE, Li S, Battershill CN, Duckworth AR (1999) The discovery and development of marine compounds with pharmaceutical potential. *J Biotechnol* 70(1–3):15–25
- Nakabachi A, Ueoka R, Oshima K, Teta R, Mangoni A, Gurgui M, Oldham NJ, van Echten-Deckert G, Okamura K, Yamamoto K, Inoue H, Ohkuma M, Hongoh Y,

- Miyagishima S, Hattori M, Piel J, Fukatsu T (2013) Defensive bacteriome symbiont with a drastically reduced genome. *Curr Biol* 23(15):1478–1484. doi:[10.1016/j.cub.2013.06.027](https://doi.org/10.1016/j.cub.2013.06.027)
- Nguyen T, Ishida K, Jenke-Kodama H, Dittmann E, Gurgui C, Hochmuth T, Taudien S, Platzer M, Hertweck C, Piel J (2008) Exploiting the mosaic structure of *trans*-acyltransferase polyketide synthases for natural product discovery and pathway dissection. *Nat Biotechnol* 26(2): 225–233. doi:[10.1038/nbt1379](https://doi.org/10.1038/nbt1379)
- Nishimura S, Matsunaga S, Yoshida M, Hirota H, Yokoyama S, Fusetani N (2005) 13-Deoxytedanolide, a marine sponge-derived antitumor macrolide, binds to the 60S large ribosomal subunit. *Bioorgan Med Chem* 13(2):449–454. doi:[10.1016/j.bmc.2004.10.012](https://doi.org/10.1016/j.bmc.2004.10.012)
- Paul VJ, Puglisi MP (2004) Chemical mediation of interactions among marine organisms. *Nat Prod Rep* 21(1):189–209. doi:[10.1039/b302334f](https://doi.org/10.1039/b302334f)
- Pawlik JR (2011) The chemical ecology of sponges on Caribbean reefs: natural products shape natural systems. *Bioscience* 61(11):888–898. doi:[10.1525/bio.2011.61.11.8](https://doi.org/10.1525/bio.2011.61.11.8)
- Perry NB, Blunt JW, Munro MHG, Pannell LK (1988) Mycalamide A, an antiviral compound from a New-Zealand sponge of the genus *Mycale*. *J Am Chem Soc* 110(14):4850–4851. doi:[10.1021/ja00222a067](https://doi.org/10.1021/ja00222a067)
- Pettit GR, Xu JP, Chapuis JC, Pettit RK, Tackett LP, Doubek DL, Hooper JNA, Schmidt JM (2004) Antineoplastic agents. 520. Isolation and structure of irciniastatins A and B from the Indo-Pacific marine sponge *Ircinia ramosa*. *J Med Chem* 47(5):1149–1152. doi:[10.1021/jm030207d](https://doi.org/10.1021/jm030207d)
- Piel J (2002) A polyketide synthase-peptide synthetase gene cluster from an uncultured bacterial symbiont of *Paederus* beetles. *Proc Natl Acad Sci U S A* 99(22):14002–14007. doi:[10.1073/pnas.222481399](https://doi.org/10.1073/pnas.222481399)
- Piel J (2004) Metabolites from symbiotic bacteria. *Nat Prod Rep* 21(4):519–538. doi:[10.1039/b310175b](https://doi.org/10.1039/b310175b)
- Piel J, Hui DQ, Wen GP, Butzke D, Platzer M, Fusetani N, Matsunaga S (2004a) Antitumor polyketide biosynthesis by an uncultivated bacterial symbiont of the marine sponge *Theonella swinhoei*. *Proc Natl Acad Sci U S A* 101(46):16222–16227. doi:[10.1073/pnas.0405976101](https://doi.org/10.1073/pnas.0405976101)
- Piel J, Wen GP, Platzer M, Hui DQ (2004b) Unprecedented diversity of catalytic domains in the first four modules of the putative pederin polyketide synthase. *ChemBioChem* 5(1):93–98. doi:[10.1002/cbic.200300782](https://doi.org/10.1002/cbic.200300782)
- Proksch P, Edrada RA, Ebel R (2002) Drugs from the seas—current status and microbiological implications. *Appl Microbiol Biotechnol* 59(2–3):125–134. doi:[10.1007/s00253-002-1006-8](https://doi.org/10.1007/s00253-002-1006-8)
- Quinoa E, Adamczeski M, Crews P, Bakus GJ (1986) Bengamides, heterocyclic anthelmintics from a *Jaspidae* marine sponge. *J Org Chem* 51(23):4494–4497. doi:[10.1021/jo00373a036](https://doi.org/10.1021/jo00373a036)
- Rawlings BJ (2001) Type I polyketide biosynthesis in bacteria (part B). *Nat Prod Rep* 18(3): 231–281
- Richelle-Maurer E, Braekman JC, De Kluijver MJ, Gomez R, Van de Vyver G, Van Soest RW, Devijver C (2001) Cellular location of (2R, 3R, 7Z)-2-aminotetradec-7-ene-1, 3-diol, a potent antimicrobial metabolite produced by the Caribbean sponge *Haliclona vansoesti*. *Cell Tissue Res* 306(1):157–165
- Sakai R, Higa T, Kashman Y (1986) Misakinolide A, an antitumor macrolide from the marine sponge *Theonella* sp. *Chem Lett* 9:1499–1502. doi:[10.1246/cl.1986.1499](https://doi.org/10.1246/cl.1986.1499)
- Sakemi S, Ichiba T, Kohmoto S, Saucy G, Higa T (1988) Isolation and structure elucidation of onnamide A, a new bioactive metabolite of a marine sponge *Theonella* sp. *J Am Chem Soc* 110 (14):4851–4853. doi:[10.1021/ja00222a068](https://doi.org/10.1021/ja00222a068)
- Salomon CE, Deerinck T, Ellisman MH, Faulkner DJ (2001) The cellular localization of dercitamide in the Palauan sponge *Oceanapia sagittaria*. *Mar Biol* 139(2):313–319
- Salomon CE, Faulkner DJ (2002) Localization studies of bioactive cyclic peptides in the ascidian *Lissoclinum patella*. *J Nat Prod* 65(5):689–692. doi:[10.1021/np010556f](https://doi.org/10.1021/np010556f)
- Schirmer A, Gadkari R, Reeves CD, Ibrahim F, DeLong EF, Hutchinson CR (2005) Metagenomic analysis reveals diverse polyketide synthase gene clusters in microorganisms associated with the marine sponge *Discodermia dissoluta*. *Appl Environ Microbiol* 71(8):4840–4849. doi:[10.1128/AEM.71.8.4840-4849.2005](https://doi.org/10.1128/AEM.71.8.4840-4849.2005)

- Schmidt EW, Nelson JT, Rasko DA, Sudek S, Eisen JA, Haygood MG, Ravel J (2005) Patellamide A and C biosynthesis by a microcin-like pathway in *Prochloron didemni*, the cyanobacterial symbiont of *Lissoclinium patella*. Proc Natl Acad Sci U S A 102(20):7315–7320. doi:[10.1073/pnas.0501424102](https://doi.org/10.1073/pnas.0501424102)
- Schmidt EW, Obraztsova AY, Davidson SK, Faulkner DJ, Haygood MG (2000) Identification of the antifungal peptide-containing symbiont of the marine sponge *Theonella swinhoei* as a novel delta-proteobacterium, “*Candidatus Entotheonella palauensis*”. Mar Biol 136(6):969–977. doi:[10.1007/s002270000273](https://doi.org/10.1007/s002270000273)
- Sipkema D, Osinga R, Schatton W, Mendola D, Tramper J, Wijffels RH (2005) Large-scale production of pharmaceuticals by marine sponges: sea, cell, or synthesis? Biotechnol Bioeng 90(2):201–222. doi:[10.1002/bit.20404](https://doi.org/10.1002/bit.20404)
- Taylor MW, Radax R, Steger D, Wagner M (2007) Sponge-associated microorganisms: evolution, ecology, and biotechnological potential. Microbiol Mol Biol Rev 71(2):295–347. doi:[10.1128/MMBR.00040-06](https://doi.org/10.1128/MMBR.00040-06)
- Thale Z, Kinder FR, Bair KW, Bontempo J, Czuchta AM, Versace RW, Phillips PE, Sanders ML, Wattanasin S, Crews P (2001) Bengamides revisited: new structures and antitumor studies. J Org Chem 66(5):1733–1741
- Turon X, Becerro MA, Uriz MJ (2000) Distribution of brominated compounds within the sponge *Aplysina aerophoba*: coupling of X-ray microanalysis with cryofixation techniques. Cell Tissue Res 301(2):311–322. doi:[10.1007/s004410000233](https://doi.org/10.1007/s004410000233)
- Ueoka R, Uria AR, Reiter S, Mori T, Karbaum P, Peters EE, Helfrich EJ, Morinaka BI, Gugger M, Takeyama H, Matsunaga S, Piel J (2015) Metabolic and evolutionary origin of actin-binding polyketides from diverse organisms. Nat Chem Biol 11(9):705–712. doi:[10.1038/nchembio.1870](https://doi.org/10.1038/nchembio.1870)
- Van Soest RW, Boury-Esnault N, Vacelet J, Dohrmann M, Erpenbeck D, De Voogd NJ, Santodomingo N, Vanhoorne B, Kelly M, Hooper JN (2012) Global diversity of sponges (Porifera). PLoS ONE 7(4):e35105. doi:[10.1371/journal.pone.0035105](https://doi.org/10.1371/journal.pone.0035105)
- Wakimoto T, Egami Y, Nakashima Y, Wakimoto Y, Mori T, Awakawa T, Ito T, Kenmoku H, Asakawa Y, Piel J, Abe I (2014) Calyculin biogenesis from a pyrophosphate protoxin produced by a sponge symbiont. Nat Chem Biol 10(8):648–655. doi:[10.1038/nchembio.1573](https://doi.org/10.1038/nchembio.1573)
- Wakimoto T, Matsunaga S, Takai A, Fusetani N (2002) Insight into binding of calyculin A to protein phosphatase 1: isolation of hemicalyculin a and chemical transformation of calyculin A. Chem Biol 9(3):309–319
- Waldmann H, Hu TS, Renner S, Menninger S, Tannert R, Oda T, Arndt HD (2008) Total synthesis of chondramide C and its binding mode to F-actin. Angew Chem Int Ed Engl 47(34):6473–6477. doi:[10.1002/anie.200801010](https://doi.org/10.1002/anie.200801010)
- Wilson MC, Mori T, Ruckert C, Uria AR, Helf MJ, Takada K, Gernert C, Steffens UA, Heycke N, Schmitt S, Rinke C, Helfrich EJ, Brachmann AO, Gurgui C, Wakimoto T, Kracht M, Crüsemann M, Hentschel U, Abe I, Matsunaga S, Kalinowski J, Takeyama H, Piel J (2014) An environmental bacterial taxon with a large and distinct metabolic repertoire. Nature 506(7486):58–62. doi:[10.1038/nature12959](https://doi.org/10.1038/nature12959)
- Xu DD, Waykole L, Calienni JV, Ciszewski L, Lee GT, Liu W, Szweczyk J, Vargas K, Prasad K, Repič O, Blacklock TJ (2003) An expedient synthesis of LAF389, a bengamide B analogue. Org Process Res Dev 7(6):856–865. doi:[10.1021/op0341162](https://doi.org/10.1021/op0341162)
- Yu MJ, Zheng W, Seletsky BM (2013) From micrograms to grams: scale-up synthesis of eribulin mesylate. Nat Prod Rep 30(9):1158–1164. doi:[10.1039/c3np70051h](https://doi.org/10.1039/c3np70051h)
- Zabriskie TM, Klocke JA, Ireland CM, Marcus AH, Molinski TF, Faulkner DJ, Xu CF, Clardy JC (1986) Jaspamide, a modified peptide from a *Jaspis* sponge, with insecticidal and antifungal activity. J Am Chem Soc 108(11):3123–3124. doi:[10.1021/ja00271a062](https://doi.org/10.1021/ja00271a062)